U.S. Department
of Commerce

Volume 91
Number 2
April 1993

Fishery Bulletin

U.S. Department of Commerce
Ronald H. Brown
Secretary

National Oceanic and Atmospheric Administration
D. James Baker
Under Secretary for
Oceans and Atmosphere

National Marine Fisheries Service

Fishery Bulletin

Scientific Editor
Dr. Ronald W. Hardy
Northwest Fisheries Science Center
National Marine Fisheries Service, NOAA
2725 Montlake Boulevard East
Seattle, Washington 98112-2097

Editorial Committee
Dr. Andrew E. Dizon National Marine Fisheries Service
Dr. Linda L. Jones National Marine Fisheries Service
Dr. Richard D. Methot National Marine Fisheries Service
Dr. Theodore W. Pietsch University of Washington
Dr. Joseph E. Powers National Marine Fisheries Service
Dr. Tim D. Smith National Marine Fisheries Service

Managing Editor
Nancy Peacock
National Marine Fisheries Service
Scientific Publications Office
7600 Sand Point Way NE, BIN C15700
Seattle, Washington 98115-0070

The *Fishery Bulletin* (ISSN 0090-0656) is published quarterly by the Scientific Publications Office, National Marine Fisheries Service, NOAA, 7600 Sand Point Way NE, BIN C15700, Seattle, WA 98115-0070. Second class postage is paid in Seattle, Wash., and additional offices. POSTMASTER send address changes for subscriptions to Fishery Bulletin, Superintendent of Documents, Attn: Chief, Mail List Branch, Mail Stop SSOM, Washington, DC 20402-9373.

Although the contents have not been copyrighted and may be reprinted entirely, reference to source is appreciated.

The Secretary of Commerce has determined that the publication of this periodical is necessary in the transaction of the public business required by law of this Department. Use of funds for printing of this periodical has been approved by the Director of the Office of Management and Budget.

For sale by the Superintendent of Documents, U.S. Government Printing Office, Washington, DC 20402. Subscription price per year: $24.00 domestic and $30.00 foreign. Cost per single issue: $12.00 domestic and $15.00 foreign. **See back page for order form.**

The *Fishery Bulletin* carries original research reports and technical notes on investigations in fishery science, engineering, and economics. The Bulletin of the United States Fish Commission was begun in 1881; it became the Bulletin of the Bureau of Fisheries in 1904 and the Fishery Bulletin of the Fish and Wildlife Service in 1941. Separates were issued as documents through volume 46; the last document was No. 1103. Beginning with volume 47 in 1931 and continuing through volume 62 in 1963, each separate appeared as a numbered bulletin. A new system began in 1963 with volume 63 in which papers are bound together in a single issue of the bulletin. Beginning with volume 70, number 1, January 1972, the *Fishery Bulletin* became a periodical, issued quarterly. In this form, it is available by subscription from the Superintendent of Documents, U.S. Government Printing Office, Washington, DC 20402. It is also available free in limited numbers to libraries, research institutions, State and Federal agencies, and in exchange for other scientific publications.

U.S. Department
of Commerce
Seattle, Washington

Volume 91
Number 2
April 1993

Fishery Bulletin

Contents

183 **Anganuzzi, Alejandro A.**
A comparison of tests for detecting trends in abundance indices of dolphins

195 **Choat, J.H., Peter J. Doherty, B.A. Kerrigan, and J.M. Leis**
A comparison of towed nets, purse seine, and light-aggregation devices for sampling larvae and pelagic juveniles of coral reef fishes

210 **Comyns, Bruce H., and George C. Grant**
Identification and distribution of *Urophycis* and *Phycis* (Pisces, Gadidae) larvae and pelagic juveniles in the U.S. Middle Atlantic Bight

224 **Davis, Tim L.O., and Grant J. West**
Maturation, reproductive seasonality, fecundity, and spawning frequency in *Lutjanus vittus* (Quoy and Gaimard) from the North West Shelf of Australia

237 **Ebert, Thomas A., Stephen C. Schroeter, and John D. Dixon**
Inferring demographic processes from size-frequency distributions: Effect of pulsed recruitment on simple models

244 **Fitzhugh, Gary R., Bruce A. Thompson, and Theron G. Snider III**
Ovarian development, fecundity, and spawning frequency of black drum *Pogonias cromis* in Louisiana

254 **Forward, Richard B., Leslie M. McKelvey, William F. Hettler, and Donald E. Hoss**
Swimbladder inflation of the Atlantic menhaden *Brevoortia tyrannus*

260 **Jackson, George D.**
Seasonal variation of reproductive investment of the tropical loliginid squid *Loligo chinensis* and the small tropical sepioid *Idiosepius pygmaeus*

271 **Kimura, Daniel K., Allen M. Shimada, and Sandra A. Lowe**
Estimating von Bertalanffy growth parameters of sablefish *Anoplopoma fimbria* and Pacific cod *Gadus macrocephalus* using tag-recapture data

281 **Lough, R. Gregory, and David C. Potter**
Vertical distribution patterns and diel migrations of larval and juvenile haddock *Melanogrammus aeglefinus* and Atlantic cod *Gadus morhua* on Georges Bank

304 **O'Connell, Victoria M., and David W. Carlile**
Habitat-specific density of adult yelloweye rockfish *Sebastes ruberrimns* in the eastern Gulf of Alaska

310 **Prager, Michael H., and Alec D. MacCall**
Detection of contaminant and climate effects on spawning success of three pelagic fish stocks off southern California: Northern anchovy *Engraulis mordax*, Pacific sardine *Sardinops sagax*, and chub mackerel *Scomber japonicus*

328 **Shepherd, Gary R., and Josef S. Idoine**
Length-based analyses of yield and spawning biomass per recruit for black sea bass *Centropristis striata*, a protogynous hermaphrodite

338 **Smith, Wallace G., and Wallace W. Morse**
Larval distribution patterns: Early signals for the collapse/recovery of Atlantic herring *Clupea harengus* in the Georges Banks area

348 **Squire, James L. Jr.**
Relative abundance of pelagic resources utilized by the California purse-seine fishery: Results of an airborne monitoring program, 1962–90

362 **Tringali, Michael D., and Raymond R. Wilson Jr.**
Differences in haplotype frequencies of mtDNA of the Spanish sardine *Sardinella aurita* between specimens from the eastern Gulf of Mexico and southern Brazil

Notes

371 **Bartoo, Norman, and David Holts**
Estimated drift gillnet selectivity for albacore *Thunnus alalunga*

379 **Haynes, Evan B.**
Stage-I zoeae of laboratory-hatched *Lopholithodes mandtii* (Decapoda, Anomura, Lithodidae)

382 **Lai, Han-Lin**
Optimal sampling design for using the age-length key to estimate age composition of a fish population

389 **McBride, Richard S., Jeffrey L. Ross, and David O. Conover**
Recruitment of bluefish *Pomatomus saltatrix* to estuaries of the U.S. South Atlantic Bight

A comparison of tests for detecting trends in abundance indices of dolphins

Alejandro A. Anganuzzi
Inter-American Tropical Tuna Commission
8604 La Jolla Shores Drive, La Jolla, California 92037-1508

Abstract. – An analysis of alternative methods for detecting trends in a series of abundance indices is carried out through simulation. The alternative procedures explored have been applied to analysis of relative abundance indices of dolphins in the eastern Pacific Ocean. They include a linear test over a moving time-period, and a nonparametric procedure based on smoothing of the time-series of abundance indices. Results indicate that the nonparametric procedure outperforms the linear tests in most of the situations tested.

Manuscript accepted 26 January 1993.
Fishery Bulletin, U.S. 91:183-194 (1993).

An important part of the analysis of any set of abundance indices is the application of an objective procedure or test to determine whether changes in the estimates are due to random fluctuations in conditions of the sampling procedure or to actual changes in the population size. Such a procedure must exhibit certain properties in order to be effective. Among these properties, perhaps most important is the power of the test for a given significance level.

In deriving conclusions about changes in the size of a population, we can fall into two types of error. First, we can erroneously conclude that population size has changed when, in fact, differences in estimates are due to random errors. This is usually known as a Type-I error. A Type-II error occurs when we conclude that the estimates reflect random fluctuations when, in fact, there has been a change in population size. The probability of falling into a Type-I error is usually referred to as the significance level of the test. The power of a test is defined as 1 minus the probability of a Type-II error. An ideal test will minimize the trade-offs between both types of error. Another desirable property of a test is robustness to underlying assumptions about the populations. For example, tests commonly carried out to detect changes in population size are based on specific assumptions about the error structure of the estimates (e.g., normality) and the model that would best describe the population size as a function of time (e.g., linear, exponential; see, for example, Gerrodette 1987).

In the case of dolphin stocks involved in the tuna fishery in the eastern Pacific Ocean (EPO), it has been recommended that their management should include both estimates of absolute abundance, derived from research-vessel data (RVD), and analysis of trends in relative abundance, derived from tuna-vessel observer data (TVOD) (IWC 1992:218). In the case of EPO dolphin stocks, the use of TVOD seems the natural choice for analyzing trends, given the vast amount of low-cost information available from the observer programs. However, for this analysis to be effective, it is necessary to obtain abundance estimates with a constant bias over the years, or, at least, a bias that shows no trend over the years. Procedures developed by the Inter-American Tropical Tuna Commission (IATTC) to analyze the TVOD, described in Buckland & Anganuzzi (1988) and Anganuzzi & Buckland (1989), were specifically aimed at reducing the magnitude of year-to-year fluctuations in the estimates due to changing biases. These procedures were complemented with more specific analyses when there were reasons to suspect that biases might be changing, for example, due to widespread use of high-resolution radar for the detection of birds (Anganuzzi et al. 1991). However, in spite of the robustness of the methods, randomly fluctuating biases (an extra source of

variability) may still affect estimates from year to year. This problem may not be exclusive to the TVOD estimates; interannual variability also seems to affect estimates of relative abundance derived from research-vessel data (Wade & Gerrodette 1992). These biases and imprecise estimates will affect the performance of statistical tests designed to detect trends and, ultimately, our ability to draw conclusions about the status of populations.

For the analysis of trends in the EPO dolphin stocks, Buckland & Anganuzzi (1988) applied a linear test for trends over a moving period of 5 yr, although they expressed concern about the low power of such a test. Edwards & Perkins (1992) extended the moving time-frame to 10 yr to increase the power. However, such a test still shows some undesirable properties. Given the inadequacy of the tests based on linear regressions, Buckland et al. (1992) proposed a different procedure, based on a nonparametric regression, which addresses some of the problems exhibited by the linear test.

In this paper, the characteristics of these tests are discussed and compared by analyzing their performance in a number of simulated scenarios.

Current tests for trends

Linear tests

Buckland & Anganuzzi (1988) tested for linear trends over successive 5 yr periods by carrying out a weighted linear regression of abundance index vs. time. Each individual estimate was weighted by the inverse of its variance, calculated by applying a bootstrap procedure. The null hypothesis for the test is that no change has occurred in the population, i.e., that the slope of the regression is equal to zero. As the authors noted, the test has low power since it estimates precision from the deviations of only five estimates from a straight line. Power can be increased by extending the moving time-period to incorporate more years in the test. Unfortunately, this also increases the probability of violating the assumption of a constant rate of change implicit in the linear model being fitted to the estimates (Edwards & Perkins 1992).

The linear test also fails to consider the precision of estimates adequately. Variances of the estimates are not taken into account except as weights in the regression. As a consequence, only the ratios of the variances between estimates are relevant, and not their absolute values. For example, if for any given series of estimates we double the variance of each individual estimate, the results of the test will remain unchanged.

Weighting by the inverse of the variance can also present other problems. Suppose, for example, that the variance of the estimate is not independent of the estimate itself, but that the variance is correlated with the estimate, i.e., the coefficient of variation (CV=ratio of standard error to point estimate) is constant. In this case, a very low estimate (and especially in the case of an outlier) with a correspondingly small variance will become an influential observation. A linear test for trends will then indicate that there was a decline in the population if that estimate is at the end of the moving period, or a significant increase if it is at the beginning. An example from the EPO dolphin abundance estimation is the case of the 1983 index of relative abundance for the northern stock of offshore spotted dolphin *Stenella attenuata*, which was an anomalous index as a result of a very strong El Niño event (Fig. 1). In such cases, where the error distribution of the estimates seems to be better approximated by a lognormal distribution, it would be more appropriate to apply weights (wt) defined as

$$wt = \ln(1+CV^2)^{-1}. \quad (1)$$

For the comparisons in this paper, two versions of the linear test are applied: the original 5 yr linear test with inverse variance weighting applied by Buckland & Anganuzzi (1988), and a 10 yr linear test with weights as described by Eq. 1.

Smoothed trends

The approach taken by Buckland et al. (1992) differs considerably from the method just described. First, they replaced the assumption of a parametric model for the underlying change in population with a nonparametric model. Among the many possible choices for such a model, they selected the smoothing algorithm known as '4253H, twice' (Velleman & Hoaglin 1981) on the basis of a comparison described by K. L. Cattanach and S. T. Buckland (SASS Environ. Model. Unit, MLURI, Craigiebuckler, Aberdeen, Scotland, unpubl. manuscr.). The adoption of a nonparametric model increases the robustness of the test to model misspecification, a problem that affects the linear test. Furthermore, the procedure, which involves the use of a compound running median, incorporates the information from nearby years into calculation of the smoothed estimate for a particular year, therefore reducing the influence of possible outliers and increasing the precision of each smoothed estimate. The smoothed test also provides a different way of looking at the trend. Instead of the trend being described by a single parameter (the slope of a linear regression), the sequence of smoothed estimates constitutes the best estimate of the underlying trend.

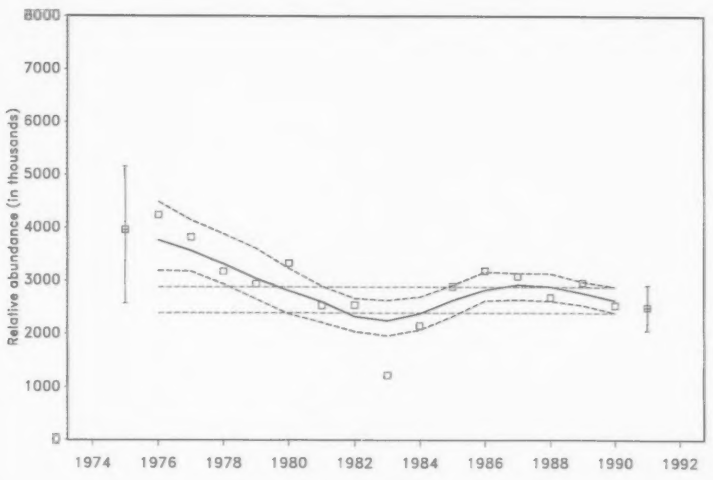

Figure 1

Smoothed trends in abundance of the northern offshore stock of spotted dolphin *Stenella attenuata* in the eastern tropical Pacific Ocean. Broken lines indicate ~85% confidence limits. Horizontal lines correspond to 85% confidence limits for the 1990 estimate. If both the 1990 confidence limits lie above the upper limit for an earlier year, abundance has increased significantly between that year and 1990 ($p<0.05$); if both limits lie below the lower limit for an earlier year, abundance has decreased significantly.

To obtain confidence intervals of the smoothed estimates, Buckland et al. (1992) combined smoothed estimates and bootstrap replication using the following procedure. First, they obtained 79 bootstrap estimates of the abundance index for each year. Next, they built bootstrap replicates of the series of estimates by taking, for example, the first bootstrap estimate for each year to obtain the first replicated series. They smoothed each replicated series, thereby obtaining 79 smoothed estimates for each year. Finally, they sorted the smoothed estimates within each year and obtained 85% confidence intervals based on the percentile method (Buckland 1984). The median of the smoothed bootstrap replicas is considered to be the best smoothed estimate.

The confidence intervals thus calculated allow a direct comparison between estimates. If the confidence intervals for two estimates do not overlap, then they are significantly different at a level of ~5%. An example based on estimates of relative abundance for the northern stock of offshore spotted dolphin is shown in Fig. 1. Since the last and first smoothed estimates are too variable, Buckland et al. (1992) recommend excluding them from the comparisons. The significance level is approximate, since it depends on normality of the estimates, homogeneity of the variances of estimates, and their independence. The second condition is often not met, but it can be shown that results are robust-to-moderate departures from it. The third condition is not met for estimates that are close in time, due to the correlation introduced by smoothing, and the relative importance of this effect is discussed further below.

Simulation comparison between tests

To illustrate the difference in performance between methods, a simulation study was carried out. Series of estimates were simulated by assuming different scenarios of underlying trends in the population over a period of 25 yr. The following scenarios were chosen.

Stable population Population exhibits no trend over the simulated period. This scenario provides us with an estimate of the probability of a Type-I error detecting a trend when, in fact, there is none, or obtaining a "false positive." Under this scenario, a percentage of detected trends close to 5% would be expected for a test based on a significance level of 5%.

Rapid decline Population remains at a constant level for a period of time, and then declines sharply over a period of 3 yr to 50% of its previous level. After the decline, the population recovers at a rate of 5% per yr.

Steady decline Population declines exponentially at an annual rate of 10%.

Steady cycle Population follows a sinusoidal change over the simulated period, completing one cycle over the 25 yr. Amplitude of the cycle is 30% of the original population size.

These scenarios are intended as a means of highlighting properties of the different tests and not as an exhaustive list of possible situations. Each scenario was replicated 100 times for different combinations of sources of variation. Variability in the estimates was assumed as coming from two different sources: (1) **Interannual variability**, resulting in a point estimate for each year t of

$$I_{0t} = N_t e^z,$$

where z is a random variable distributed as N (0, σ^2), and (2) **precision of the estimate**, represented in the distribution of the simulated bootstrap replicas for year t, I_{bt}, as

$$I_{bt} = I_t e^v, \text{ for } b=1, \ldots, 79,$$

where v is a random variable distributed as N (0, ε^2).

The rationale for a setup with independent control of two sources of variation and a lognormal error structure lies in the properties of the estimates and in the fact that the linear and smoothed tests deal differently with both components of variation. The choice of a lognormal error structure can be justified by considering that the abundance estimates are naturally constrained to be positive. The choice of error structure for the simulation can be further justified by an analysis of the available TVOD estimates (Fig. 2), which shows that the main target stocks tend to have constant CV's, particularly in recent years when observer coverage of the tuna fleet increased and more information was available for abundance estimation. There is considerable variability in some stocks, due to changing levels of targeting from the purse-seine fleet that result in unequal sample sizes from year to year.

The argument for including two sources of variation in the estimates is based on the possibility that actual relative abundance indices are affected by random biases from year to year. Under standard assumptions, σ^2 and ε^2 should be equal. However, estimates of dolphin abundance may exhibit an additional variability, represented in this setup as $\sigma^2 > \varepsilon^2$. This can be attributed to randomly-fluctuating biases, such as those introduced by changing environmental conditions or differences in the way the purse-seine fishery operates. It is important to separate these two components since, for example, in the case of the linear test, the results are affected only by the variability represented by σ^2.

Therefore, it was assumed in the simulation that estimates are lognormally distributed around the underlying trend with a constant coefficient of variation. Figure 3 illustrates one simulated series for each of the different scenarios. The simulations were repeated for different combinations of CV_σ and CV_ε, the coefficients of variation for both sources of variation.

To compare the test for trends, two diagnostics were used.

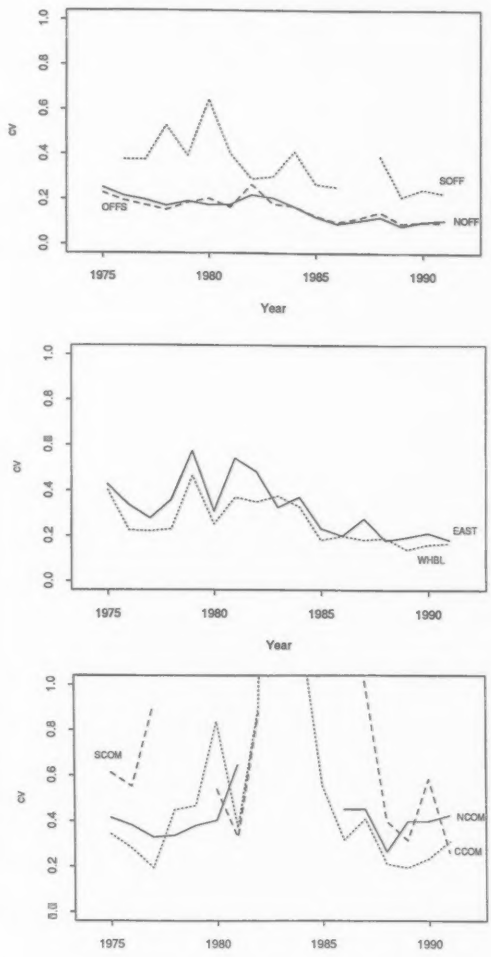

Figure 2

Coefficients of variation in relative abundance estimates of dolphin stocks in the eastern Pacific Ocean as a function of time. **NOFF**=northern stock of the offshore spotted dolphin *Stenella attenuata*; **SOFF**=southern stock of the offshore spotted dolphin; **EAST**=eastern stock of the spinner dolphin *Stenella longirostris*; **WHBL**=whitebelly stock of the spinner dolphin; **NCOM**=northern stock of the common dolphin *Delphinus delphis*; **CCOM**=central stock of the common dolphin; **SCOM**=southern stock of the common dolphin.

Number of detected trends For the linear trends, this is the number of 10 yr periods with slopes significantly different from zero at the 5% significance level. For the smoothed test, it is the number of significant differences between the next-to-last estimate and the estimate 10 yr earlier. In this way, the comparison is based on the same number of tests for each method. Since there are 25 yr simulated in each replica, a total of 1500 tests were carried out in the simulation of each scenario.

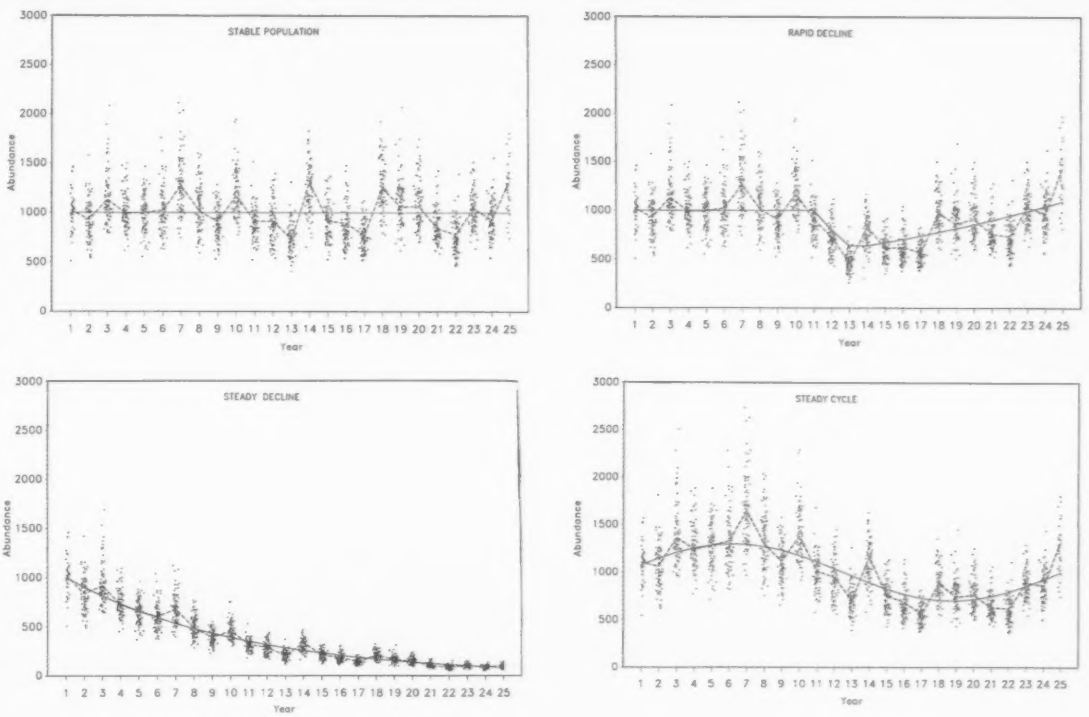

Figure 3

Example of a simulated series of relative abundance estimates for each of four scenarios. Solid line represents true underlying trend in the population. Dashed line connects simulated point estimates. Distribution of simulated bootstrap estimates is represented by the distribution of dots.

Ratio between estimates As a way of assessing how well each method describes the underlying trend in the population, an estimated rate of change was obtained. For the smoothed test, this is the ratio of two smoothed estimates separated by 10 yr. For the linear test, it is the ratio of the corresponding estimates calculated from the linear regression. These estimated rates of change were then compared with the true rates of change and the discrepancies summarized as average absolute error.

Correlation in the smoothed estimates

One of the problems of the smoothed test is that the smoothing procedure induces a correlation between estimates. This lack of independence affects the results of the comparison between estimates close in time, and it is therefore important to assess the magnitude of this correlation and how it is reduced as the separation in time between estimates increases. To investigate this, the following Monte Carlo procedure was carried out on the series of relative abundance estimates for dolphin stocks in the EPO reported by Anganuzzi et al. (1992).

1 For each year, 79 estimates were sampled with replacement from the distribution of bootstrap estimates of relative abundance. The 79 estimates were available from the standard bootstrap procedure used to estimate confidence bounds in the relative abundance estimation (Anganuzzi & Buckland 1989).

2 Each of the 79 trajectories obtained in the previous step were smoothed, and 85% confidence limits for the resulting smoothed estimates were obtained based on the percentile method. This step is essentially the application of the smoothed test.

3 Steps 1 and 2 were repeated 100 times, therefore obtaining 100 estimates of the lower and upper confidence bounds for the smoothed estimates for each year.

4 A correlation matrix between years for both upper and lower limits of the confidence bounds was estimated on the basis of results of the previous step.

5 Estimates of correlation as a function of the distance in time between estimates were obtained. This was done by averaging over all correlation coefficients between estimates separated by a given number of years, that is, by taking the average of elements in the subdiagonals of the correlation matrix obtained in step 4.

Results

Number of detected trends

The results of this analysis are shown in Figs. 4–7, as the number of detected trends each year in 100 simulations for the different scenarios. The underlying trends are shown on an arbitrary scale to relate changes in performance of the tests to changes in population trajectory.

Stable population This scenario can be used to assess the actual level of significance of the tests. An ideal procedure for detecting trends would indicate significant trends in ~5% of the tests under this scenario, given that the significance level is set at 5%. Results from the simulations are shown in Fig. 4. Both linear tests show an actual significance level close to the expected value. These results were relatively robust to the different values of CVs tested. The smoothed test also performs well in all cases, except when interannual variation exceeds the precision of the estimate. For example, for CV_σ=0.2 and CV_ε=0.3, the percentage of detected trends was ~10%.

Rapid decline In this scenario, different trade-offs of the tests are illustrated by their performance along the simulated period (Fig. 5). For CV_σ=CV_ε, at the beginning of the period both the linear and smoothed tests have similar proportions of detected trends, close to the nominal significance level. As the underlying trend in the period included in the tests departs from linearity, the smoothed test tends to outperform both linear tests. For CV_σ=CV_ε=0.2, the smoothed test indicates a maximum of almost 80% significant trends in

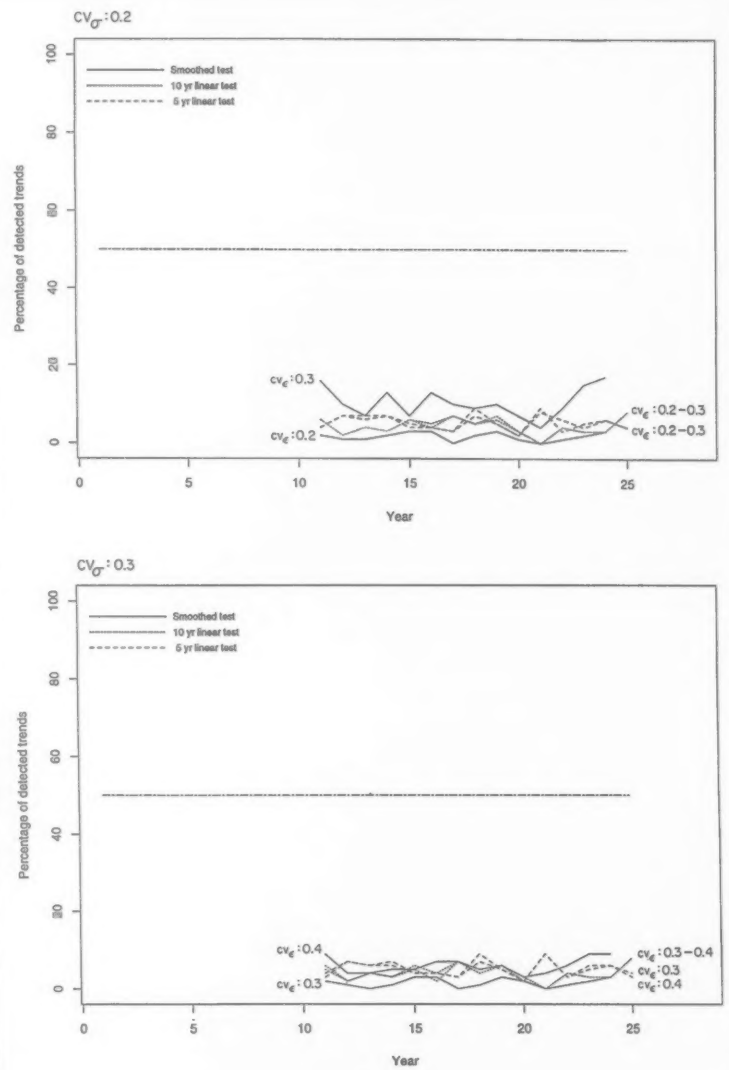

Figure 4

Percentage of trends detected in 100 simulations of the **'stable population'** scenario for two levels of precision: **(top)** CV_σ=0.2, and **(bottom)** CV_σ=0.3. The two lines for each smoothed test represent different levels of interannual variation, CV_ε. Broken line (– – –) represents underlying trend in the population on an arbitrary scale.

comparison with <60% for the linear test. In the recovery phase of the trajectory (starting when the tests cover the period between years 12 and 22), the linear test improves its performance relative to the smoothed test. In absolute terms, the performance of both tests seems to be poor between years 20 and 23, but this is the result of the small difference between the first and last year of the period included in the moving timeframe. After that, the 10 yr linear test performs almost as well as the smoothed test, as the result of an underlying trend that can be approximated well by a linear model. The 5 yr linear test does not perform well, although it detects the decline more frequently than the 10 yr test. In spite of the improvement in the last part of the trajectory, both linear and smoothed tests reach a maximum of only ~70% of significant trends. The performance of all tests degrades quickly for higher amounts of variability; the maximum percentage of detections for the smoothed test falls to around 40% for $CV_\sigma=CV_\varepsilon=0.3$.

In the case of the smoothed test, the number of detections increases when $CV_\sigma>CV_\varepsilon$. This result seems to be a consequence of higher Type-I error probabilities, as suggested by the higher number of detections in years 11 and 12.

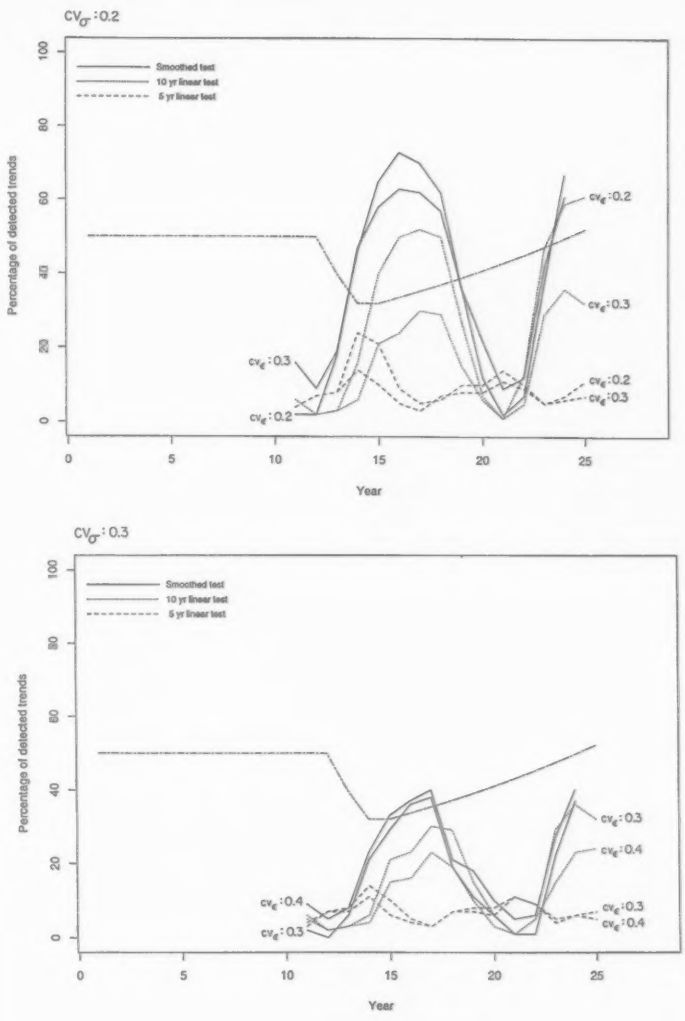

Figure 5

Percentage of trends detected in 100 simulations of the **'rapid decline'** scenario for two levels of precision: **(top)** $CV_\sigma=0.2$, and **(bottom)** $CV_\sigma=0.3$. The two solid lines for each smoothed test represent different levels of interannual variation, CV_ε. Broken line (– – –) represents underlying trend in the population on an arbitrary scale.

Steady decline The power of both types of tests improves under this scenario relative to the previous one, due to the smoother nature of the underlying trend (Fig. 6). For $CV_\sigma=CV_\varepsilon$ the smoothed test outperforms the linear tests for all levels of variability. The percentage of significant trends detected by the smoothed test ranges from over 95% for CV's of 0.20 to ~80% for a CV of 0.30. The power of the 10 yr linear test seems to be more affected by increasing variability in the estimates, falling to ~50% detections for CV=0.40. For $CV_\sigma>CV_\varepsilon$, the power of the smoothed test seems to increase although, as before, this is probably the result of greater Type-I error rates. The 5 yr linear tests show low power for all levels of variability.

Steady cycle The results of this set of simulations are very similar to those from the 'rapid decline' scenario (Fig. 7). Overall performance for both tests im-

proves relative to that scenario, due to the smoother underlying trend, reaching a maximum of 90% for the smoothed test for CV=0.2. This performance falls rapidly, as the amount of variability increases, to a maximum of slightly over 20% when CV=0.40. For $CV_\sigma > CV_\varepsilon$, the smoothed test again shows an apparent increase in power related to high Type-I error probabilities. Once more, the 5 yr linear test shows very low power throughout the series.

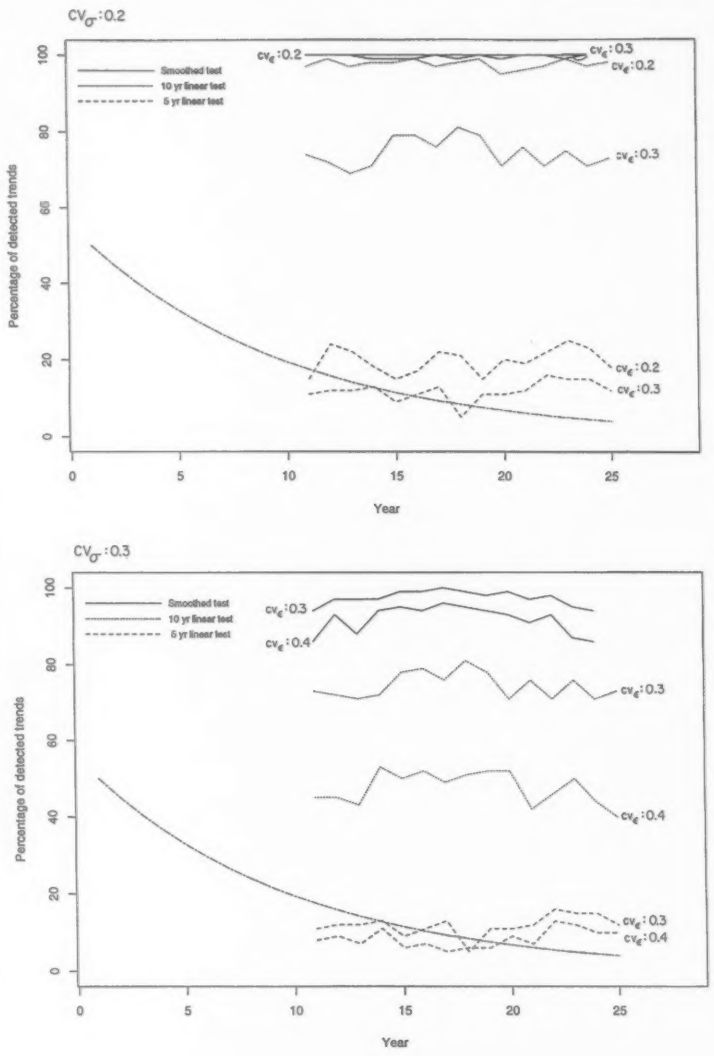

Figure 6

Percentage of trends detected in 100 simulations of the **'steady decline'** scenario for two levels of precision: **(top)** CV_σ=0.2, and **(bottom)** CV_σ=0.3. The two solid lines for each smoothed test represent different levels of interannual variation, CV_ε. Broken line (– – –) represents underlying trend in the population on an arbitrary scale.

Ratio between estimates

The purpose of this analysis is to assess sensitivity of the estimated rates of change, obtained by smoothing or linear procedures, to departures from linearity of the underlying trend. It also measures the ability of the procedures to reconstruct the true underlying population trajectory. The results of this analysis are shown for each of the simulated trajectories in Fig. 8. Results indicate that the estimated rates of change obtained through the smoothing procedures are better, in terms of the average absolute error, than estimates obtained by any of the linear methods, even when the simulated trend is linear ('stable' scenario, Fig. 8, page 192). Estimates from the 5 yr linear regressions are consistently worse than estimates from the 10 yr regressions, as expected due to the greater number of points on which the latter is based. The only exception is for the scenario with cyclic fluctuations, where the 10 yr linear estimates are poorer than the 5 yr estimates. This is a consequence of the period of the sinusoidal cycle in the underlying population that can be better approximated by a linear model over a short period of time. For longer periods in the cycle, 10 yr linear estimate should improve, as suggested by its performance in the scenario with an exponential decline. Results for the smoothed procedure are consistent over the sets of scenarios, indicating its robustness to departures from linearity in the population trajectory.

Correlation between smoothed estimates

Results from this analysis are shown in Figs. 9 and 10 (pages 193, 194), which indicate that the correlation

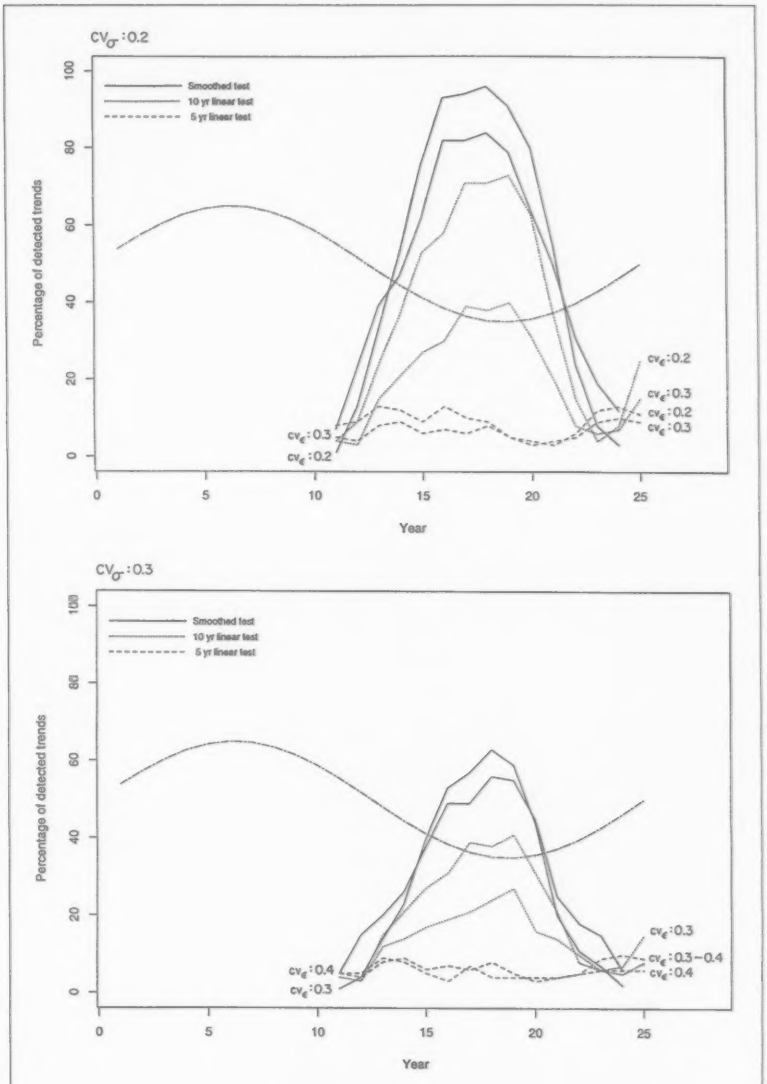

Figure 7

Percentage of trends detected in 100 simulations of the **'steady cycle'** scenario for two levels of precision: **(top)** CV_σ=0.2, and **(bottom)** CV_σ=0.3. The two solid lines for each smoothed test represent different levels of interannual variation, CV_ϵ. Broken line (– – –) represents underlying trend in the population on an arbitrary scale.

declines rapidly as distance between the estimates increases, approaching very low values as the separation between estimates exceeds 4 yr. This suggests that the validity of the test will not be seriously compromised by the correlation induced from the smoothing procedure, when the comparison is carried out on estimates that are separated by at least 4 yr.

A characteristic of the smoothed test is that, while the smoothing procedure induces a correlation between estimates, the correlation across years between fixed percentiles of the distribution of smoothed estimates is lower. This is a result of the (implicit) sorting of estimates that removes some of the dependency. To illustrate this, the average correlation between smoothed estimates obtained before sorting is also shown in Figs. 9 and 10, suggesting that the reduction in correlation due to sorting is ~30% for estimates close in time.

Discussion

In summary, the two types of tests represent different ways of looking at the data, and a comparison between them based on the same criteria only partially reflects these differences. The smoothed test provides more information since it allows a graphic comparison between individual estimates. It is based in a more robust assumption about the underlying trend of the population, since it assumes only that the change has been smooth over a short time-period. It also incorporates the lack of precision of the estimates in a much more effective way than the linear test.

In some cases, however, the linear test might be more suitable. For example, if the amount of interannual variation is low relative to the precision of the estimates, or if changes are closely approximated by a linear function, the linear test should perform better. Also, if large changes in population size occur over a very short time-period, smoothing the series will tend to underestimate the rate of change.

Despite limitations of the comparison, the results from simulations indicated that the smoothed test outperforms the linear test in most situations. The only exception is the tendency to detect spurious trends

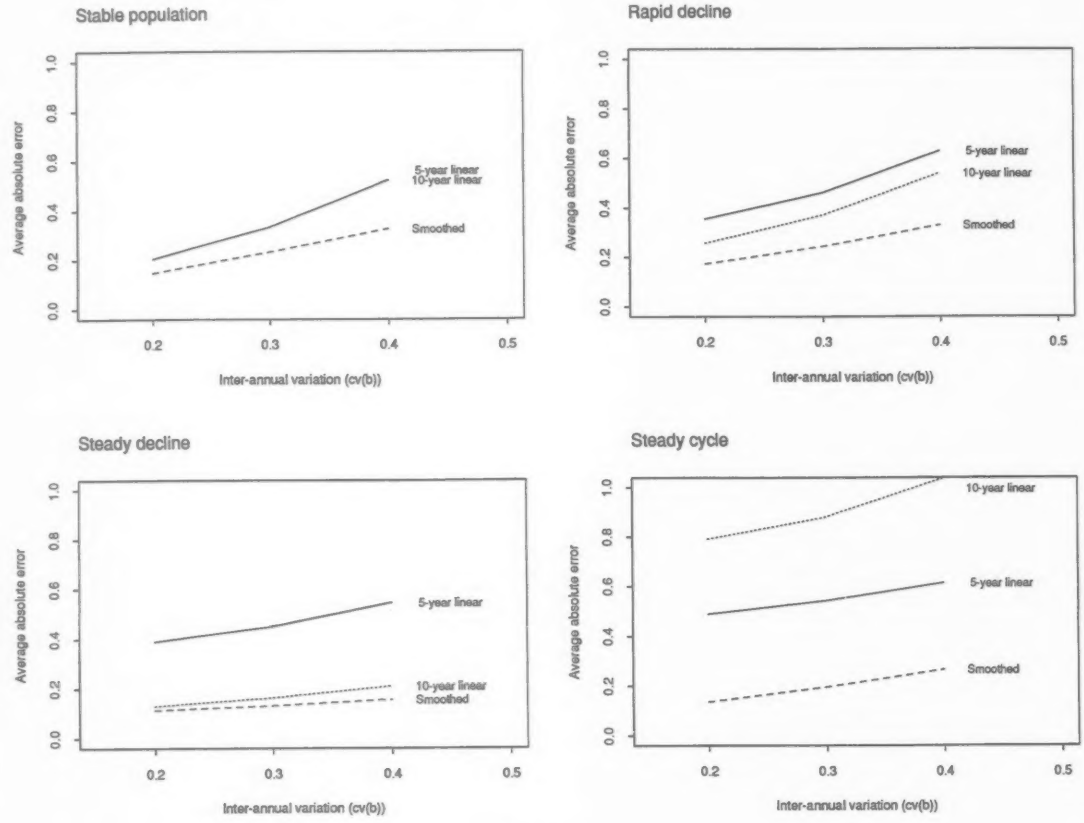

Figure 8

Average absolute error as a function of different degrees of interannual variation, represented by CV_t, for each of the four scenarios simulated.

when the amount of interannual variability exceeds precision of the estimates. In other words, in the inevitable trade-off between Type-I and Type-II errors, the smoothed test has lower Type-II error rates at the expense of an increase in the Type-I error rate. From the management point of view, this is a safer compromise than the one posed by the linear test, since the probability of failing to detect a significant trend is smaller with the smoothed test. The increase in Type-I error rates can be related to the amount of smoothing done by the particular algorithm chosen. An algorithm that would smooth the estimates more would be less prone to this problem, but it would have less power to detect trends in the estimates in certain situations. Such an algorithm would also induce more correlation between smoothed estimates, and the separation in time between them would have to be greater in order not to compromise validity of the comparisons. An alternative would be a smoothing algorithm that can adaptively change the amount of smoothing done on the estimates, either by cross-validation techniques or by controlling the amount of smoothing through incorporating auxiliary information, such as birth and death rates, in the procedure; in other words, by building a model of the population dynamics.

Acknowledgments

I would like to thank Bill Bayliff, Steve Buckland, Martin Hall, and Tim Gerrodette for their valuable comments.

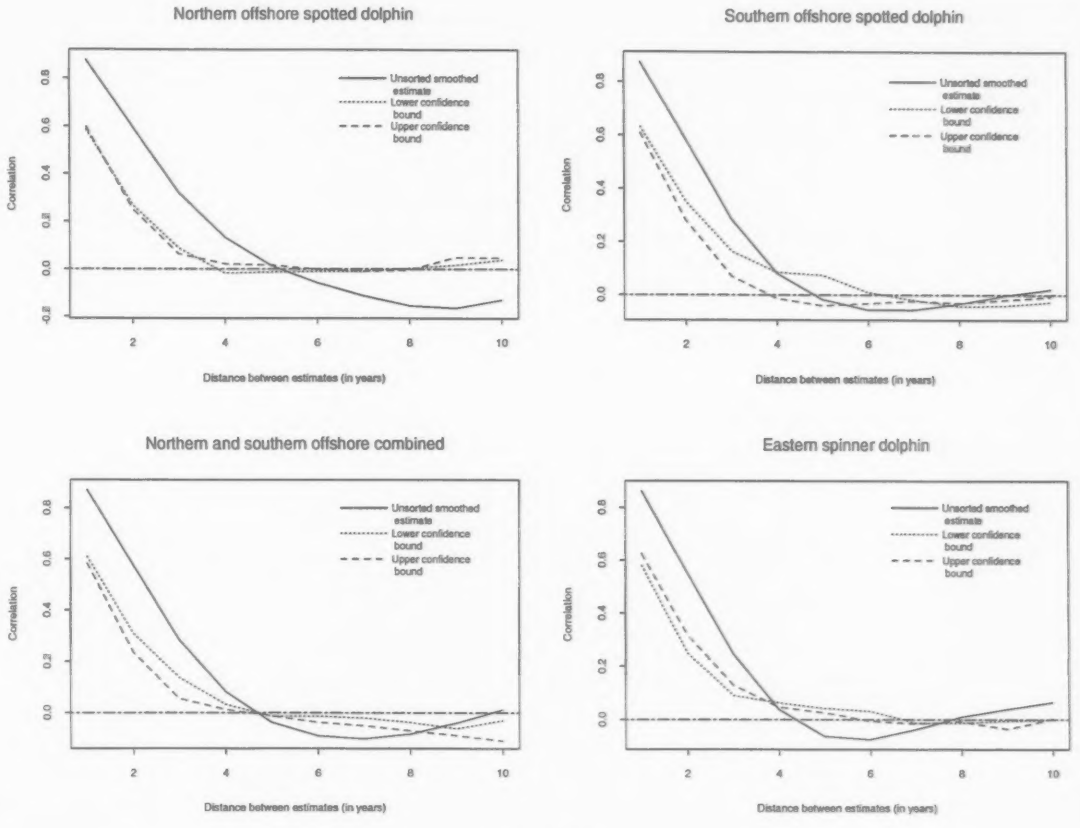

Figure 9

Correlation between smoothed estimates as a function of the separation in years between estimates for four stocks of dolphin in the eastern Pacific Ocean: Offshore spotted *Stenella attenuata* and spinner dolphin *Stenella longirostris*.

Citations

Anganuzzi, A.A., & S.T. Buckland
1989 Reducing bias in estimated trends from dolphin abundance indices derived from tuna vessel data. Rep. Int. Whaling Comm. 39:323–334.

Anganuzzi, A.A., S.T. Buckland, & K.L. Cattanach
1991 Relative abundance of dolphins associated with tuna in the eastern tropical Pacific, estimated from tuna vessel sightings data for 1988 and 1989. Rep. Int. Whaling Comm. 41.

Anganuzzi, A.A., K.L. Cattanach, & S.T. Buckland
1992 Relative abundance of dolphins associated with tuna in the eastern tropical Pacific in 1990 and trends since 1975, estimated from tuna vessel sightings data. Rep. Int. Whaling Comm. 42:541–546.

Buckland, S.T.
1984 Monte Carlo confidence intervals. Biometrics 40:811–817.

Buckland, S.T., & A.A. Anganuzzi
1988 Trends in abundance of dolphins associated with tuna in the eastern tropical Pacific. Rep. Int. Whaling Comm. 38:411–437.

Buckland, S.T., K.L. Cattanach, & A.A. Anganuzzi
1992 Estimating trends in abundance of dolphins associated with tuna in the eastern tropical Pacific Ocean, using sightings data collected on commercial tuna vessels. Fish. Bull., U.S. 90:1–12.

Edwards, E.F., & P.C. Perkins
1992 Power to detect linear trends in dolphin abundance: Estimates from tuna-vessel observer data, 1975–89. Fish. Bull., U.S. 90:625–631.

Gerrodette, T.
1987 A power analysis for detecting trends. Ecology 68:1364–1372.

IWC (International Whaling Commission)
1992 Report of the sub-committee on small cetaceans. Rep. Int. Whaling Comm. 42:178–228.

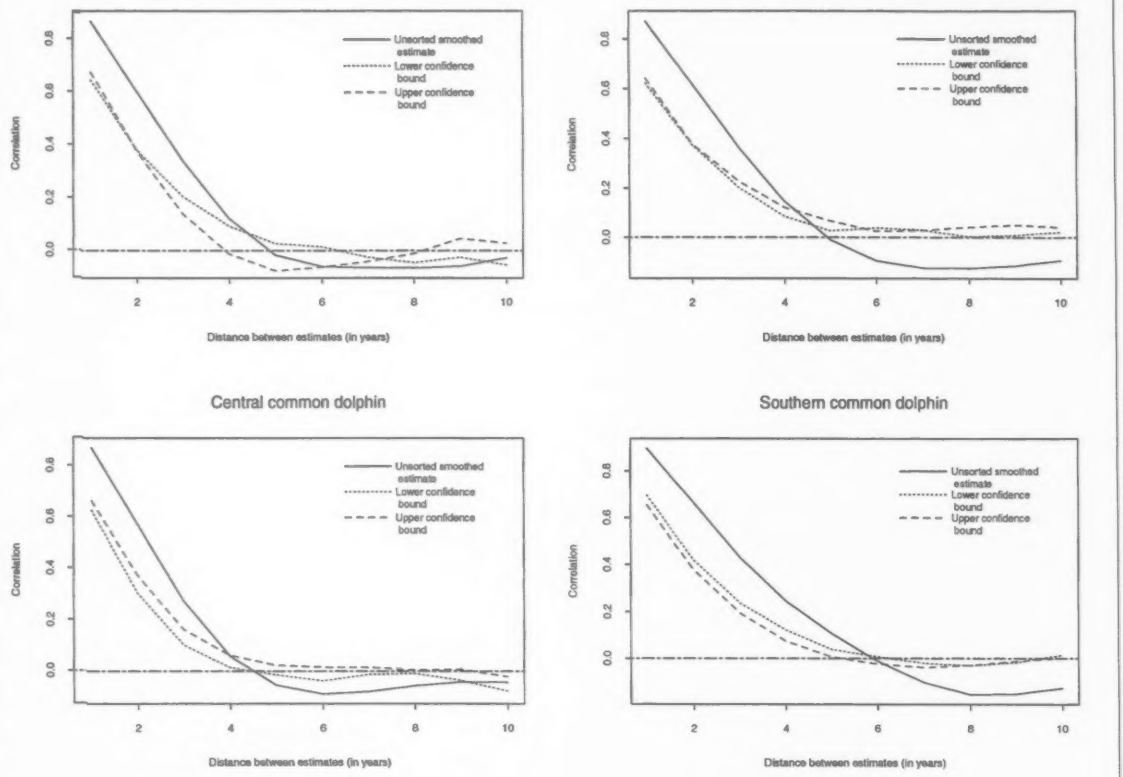

Figure 10

Correlation between smoothed estimates as a function of the separation in years between estimates of four stocks of dolphin in the eastern Pacific Ocean: Spinner dolphin *Stenella longirostris* and common dolphin *Delphinus delphis*.

Velleman, P.F., & D.C. Hoaglin
1981 Applications, basics and computing of exploratory data analysis. Duxbury Press, London.

Wade, P.R., & T. Gerrodette
1992 Estimates of dolphin abundance in the tropical Pacific: Preliminary analysis of five years of data. Rep. Int. Whaling Comm. 42:533–539.

A comparison of towed nets, purse seine, and light-aggregation devices for sampling larvae and pelagic juveniles of coral reef fishes*

John H. Choat
Department of Marine Biology, James Cook University of North Queensland
Townsville, Queensland 4811, Australia

Peter J. Doherty
School of Australian Environmental Studies, Griffith University
Nathan, Queensland 4111, Australia
Present address: Australian Institute of Marine Science, PMB No. 3, Townsville M.C., Queensland 4810, Australia

Brigid A. Kerrigan
Department of Marine Biology, James Cook University of North Queensland,
Townsville, Queensland 4811, Australia

Jeffrey M. Leis
The Australian Museum, P.O. Box A285
Sydney South, N.S.W. 2000, Australia

Abstract. – We compared sampling performance of four nets and two aggregation devices for larval and pelagic juvenile coral-reef fishes. The six sampling devices were deployed simultaneously over three nights near a coral reef at Lizard Island, northern Great Barrier Reef, Australia. The resulting 83 samples captured 57,701 larval and pelagic juvenile fishes of 70 families (excluding clupeoids which were not considered in this analysis). The bongo net took the most families, and the light-trap the fewest. In all methods, a few families dominated the catch. Dominance was least in the Tucker trawl catches and greatest in light-trap catches, where pomacentrids constituted 93% of the catch. Composition of catches was similar for the four nets. Catches from the light-trap were markedly different from those taken by net; catches taken by light-seine showed similarities to those taken by both net and light-trap. For four abundant families (Apogonide, Gobiidae, Lutjanidae, Pomacentridae), the bongo net gave the overall highest density estimates, although those from purse-seine were frequently equivalent to bongo-net estimates. The Tucker trawl provided the lowest density estimates in most cases. Catches of bongo, neuston, and seine nets were similar in size structure and were dominated by small larvae; overall, however, bongo nets collected the greatest size-range of fishes. The Tucker trawl did not collect small larvae well nor did it collect significantly greater densities of large larvae and pelagic juveniles than the bongo net. Fishes collected by aggregation devices were generally larger than those taken by net, and light-traps caught very few fish <5 mm. Light-traps collected greater numbers of large pomacentrids (>6 mm) than other methods. In an extended sampling period of five nights, both aggregation devices showed obvious peaks in the density of large pelagic pomacentrids and mullids; these patterns were not detected by the nets.

Manuscript accepted 24 February 1993.
Fishery Bulletin, U.S. 91:195-209 (1993).

Almost all species of marine teleost fishes have a pelagic phase in the early part of their life history (Moser et al. 1984). Size, morphology, and behavior of larval and pelagic juvenile phases vary greatly (Moser 1981), and this makes accurate sampling of these fishes problematical (Murphy & Clutter 1972, Frank 1988, Suthers & Frank 1989, Brander & Thompson 1989). The problem is exaggerated in tropical waters due to high taxonomic and developmental diversity and the presence of many demersal species with extended pelagic phases (Leis & Rennis 1983, Leis & Trnski 1989, Leis 1991b). Studies of the pelagic phase can provide important information on population biology of reef fishes. Despite its brevity, the high mortality and dispersion characteristic of this phase can have important demographic consequences for many species (Victor 1986). There is now a widespread interest in the process of recruitment in coral reef fishes (Doherty & Williams 1988, Warner & Hughes 1989), and sampling techniques which cover the full size-range of the pelagic phase are needed.

A number of different methods are available to sample this complex assemblage of early-life-history stages, including towed nets, purse-seines, and various types of aggregation devices which attract fish into collection sites or traps. These methods differ in their method of deployment and capture, and each has its own set of advantages and disadvantages. All have biases in number, identity, and sizes of pelagic fishes collected (Clutter & Anraku 1968, Clarke 1983 and 1991). For the pelagic phase of reef fishes, there have been few attempts to evaluate the relative bias of different sampling methods. Recent studies have provided information on the comparative performance

*Contribution of the Lizard Island Research Station. Authorship alphabetical.

of nets and light-traps (Gregory & Powles 1988), nets and plankton pumps (Brander & Thompson 1989), and towed nets and purse-seines (Kingsford & Choat 1985), but have dealt with the less-diverse fauna of temperate waters.

The purpose of this study was to compare several types of towed and seine nets and an automated light-trap (Doherty 1987) in terms of taxa, numbers, and sizes of larvae and pelagic juveniles of coral reef fishes captured. These methods represent the range of sampling devices currently used to collect larval and pelagic juvenile fishes. For the towed nets, we used dimensions and mesh size normally employed to sample larval and pelagic juvenile fishes. We used designs of purse-seine and light-trap which had been subject to thorough field testing (Kingsford & Choat 1985 and 1986, Kingsford et al. 1991, Doherty 1987). For each sampling device we obtained the following information: (1) Taxonomic composition of samples at the level of family; (2) patterns of density and size structure in selected taxa; and (3) temporal patterns in the density of selected taxa over short time-periods. The program also provided information on the logistic constraints associated with each sampling method.

Our findings will be useful to those designing sampling programs for larval and pelagic juvenile stages of demersal fishes in tropical and other areas, and should have some generality because the taxa sampled included a wide variety of body shapes and swimming capabilities. Among the taxa studied are families of great importance in coral reef ecosystems as adults (Apogonidae, Atherinidae, Callionymidae, Gobiidae, Labridae, Pomacentridae), and several are also important in commercial, sport, or subsistence fisheries throughout the tropics (Carangidae, Lethrinidae, Lutjanidae, Mullidae, Nemipteridae, Platycephalidae, Scaridae). All are abundant in ichthyoplankton samples in tropical coastal areas, especially in the Indo-Pacific.

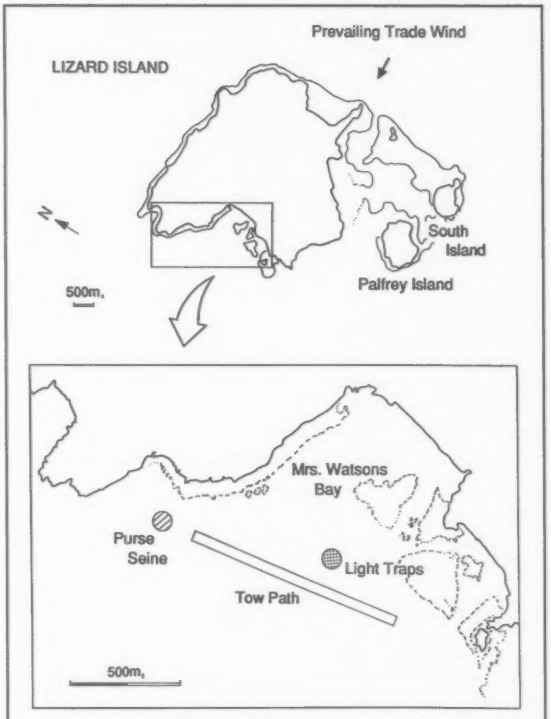

Figure 1

Lizard Island, Great Barrier Reef, Australia, showing location of study area and position of sampling sites for light-traps, towed nets, and purse-seines at Watsons Bay. Coral reefs are shown as broken lines. Lizard Island (145°26'E, 14°40'S) is located 30 km off the eastern coast of mainland Australia.

Materials and methods

Sampling and identification procedures

We sampled at 150–600 m off the fringing reefs at Watsons Bay on the NW side of Lizard Island in the lagoon of the northern Great Barrier Reef, Australia (145°26'E, 14°40'S). Water depth was 20–30 m over a sandy bottom (Fig. 1). This site was chosen for its proximity to the logistic support offered by the Lizard Island Research Station, a base for much work on the pelagic phase of coral reef fishes (Leis 1991b). Also, it offered relatively sheltered conditions from the 15–25 kn southeasterly winds present during the sampling period. This was particularly important for the continuity of sampling over a number of nights.

We sampled on the nights of 2, 3, 5, 6, and 7 December 1986, starting at a minimum of 1.25 h after sunset. Sampling never continued past 0200 h. New moon was on 2 December 1986. Nocturnal sampling reduces potential bias due to vertical distribution because ichthyoplankton show little vertical stratification at night in the study area (Leis 1986, 1991a). In addition, the nets should operate at peak efficiency at night due to lessened visual avoidance. Finally, the aggregation devices are effective only at night because they depend on self-generated light to attract fishes.

We concentrated our analyses on data from 3, 5, and 6 December because we were able to take and process all planned samples from all gears only on these nights. For some gears, it was possible to examine temporal trends over the full sampling period.

Six different sampling devices were deployed each night. Three nets were towed from the 14 m catama-

ran RV *Sunbird* at 1 m/s along a fixed 1 km path. The towed nets were fitted with flowmeters and were washed with pumped seawater. Details of each collection device are as follows.

1 A neuston net of mouth dimensions 1.0×0.3 m with 0.5 mm mesh was rigged to sample water between the bows of the catamaran. Typically, the net sampled to a depth 0.1 m and filtered 187–312 m^3/tow. Four tows were taken per night.

2 A bongo net (McGowan & Brown 1966) of 0.85 m mouth diameter per side, and with 0.5 mm mesh, was towed from an "A"-frame at the stern. The RV *Sunbird* draws 1m, and the net was towed so its top was 1m below surface and on the vessel's centerline in water which had not been disturbed by the passage of its twin hulls. The volume of water filtered for each side of the net was 498–673 m^3/tow. Samples from only the port-side net were analyzed. Four tows were taken per night.

3 A Tucker trawl (Tucker 1951) with nominal mouth dimensions of 2×2 m and of 3 mm mesh was towed in the same position as the bongo net. At a towing speed of 1 m/s, a diver estimated that the bottom bar of the net trailed the top bar by ~0.5 m, so the effective mouth area was ~3.8 m^2. Between 3240 and 4570 m^3 of water were filtered per tow. Four tows were taken per night. Both the bongo net and the Tucker trawl used the same depressor.

Time constraints and the logistics of rigging and deploying each net precluded randomising the order of bongo and Tucker trawl tows, so they were taken in blocks of four, with the order alternating from one night to the next. Neuston net samples were taken during the Tucker trawl tows.

4 A plankton mesh purse-seine of 14×2 m (Kingsford & Choat 1985) of 0.28 mm mesh was used to take samples of ~32 m^3 each. This estimate was based on the ideal cylinder of water enclosed by the net at the beginning of pursing and made no allowance for herding of fishes during deployment or loss during pursing. There was no estimate of variation in the volume enclosed by the net sets. The net was deployed from a 4 m dinghy adjacent to the northern end of the tow path (Fig. 1). Wind conditions precluded effective deployment of this net at greater distances offshore. Two to four samples were taken per night.

5 Two automated light-traps (Doherty 1987) were deployed from an anchored boat adjacent to the center of the tow path and ~700 m from the purse-seine site. Traps were positioned at ~10 m apart. Entries into the trap were at 0.5–1 m below surface. The second trap began to sample 30 min after the first, and both traps sampled for hourly intervals, resulting in continuous sampling in overlapping, 1 h segments. The trap deployment was staggered to allow for clearing and processing of each trap after the 1 h fishing period. Eight to nine 1 h light-trap samples were taken per night.

6 A battery-powered fluorescent light source identical to that in the trap (Doherty 1987) was deployed from a second boat anchored at the purse-seine site. After 1 h in the water, the light was set adrift and the water around it immediately sampled by the same purse-seine used in **(4)** above. Our estimates of what was attracted to the light included only those individuals that were within ~2 m (i.e., radius of the seine at pursing) of the light at the time of seining. Four to five light-seine samples were taken per night. Purse-seine (no light, **(4)** above) and light-seine samples were interspersed during the night.

Our goal was to sample simultaneously using six methods in the same location over several nights, so as to avoid confounding comparisons of methods with temporal or spatial variation. The purse-seine, light-seine, and light-trap samples were taken throughout the nightly sampling period. At the same time, the RV *Sunbird* sampled with the towed nets. Logistic problems required two compromises in this program. Bongo tows and Tucker trawl tows (and simultaneous neuston tows) were done in sequential blocks of four each night as discussed in **(3)** above. The purse-seine and light-trap samples were taken 700 m apart because it was not possible to duplicate these devices and thus randomize their positions. The RV *Sunbird* tow track covered the area between these two.

Fishes from the towed nets, purse-seines, and light-seines were immediately fixed in 10% formalin seawater. Samples from the light-traps were maintained alive until returned to the Research Station where they were subsequently fixed in 100% ethanol or 10% formalin seawater. All fish were transferred to 70% ethanol for at least a month prior to measurement.

For light-traps and light-seines, density is expressed as number per sample. Catches from the towed net and purse-seine collections were standardized to the number of fishes/1000 m^3 on the basis of flowmeter records or purse-seine geometry.

All fishes were removed from samples and identified to family following Leis & Rennis (1983) and Leis & Trnski (1989). Standard lengths were measured to the nearest 0.1 mm using a Bioquant software package that allows for measurement of enlarged *camera lucida* images of fish and accommodates curvature of specimens. The accuracy of electronic measurement was monitored by measuring subsamples manually with calipers and eye-piece micrometers. In a few samples with very large numbers of certain taxa such as gobiids, the catch was subsampled and a minimum of 10% of the sample measured. For some analyses, fishes were divided into small (<6 mm) and large (≥6 mm) size-groups. This was done because, on the basis of results reported here, the light-

trap captures few larvae <6 mm, and we wished to compare density estimates among gears for the sizes of fishes captured by the light-trap. Damaged fish (~3% of total) were excluded from the length analysis.

The terminology of early-life-history stages of fishes is complex and ultimately arbitrary, whether based on morphological or ecological criteria (Kendall et al. 1984, Kingsford 1988, Leis 1991b). We were primarily interested in taxa of which the adults are benthic on coral reefs, but did not want to exclude semipelagic reef-associated taxa by use of an ecological term like 'presettlement', nor did we wish to exclude partially- or fully-transformed but still pelagic individuals of benthic taxa by the use of a morphological term like 'larva'. Therefore, we use the terms 'larvae' and 'pelagic juveniles' for the fishes collected during this study, or refer to them collectively as 'pelagic fishes'.

Larval, transforming, juvenile, and adult clupeoid fishes of several types (including *Spratelloides* spp., *Dussumeria* sp., *Stolephorus* sp., and probably *Herklotsichthys* sp.) were captured in large numbers, mainly by light attraction. These clupeoid fishes represented a distinct assemblage of fishes with a different age and size structure and adult habitat than the reef species of primary interest to us. These clupeoids are not considered here, but will be dealt with in a separate publication.

Reduction of data sets and analytical procedures

Sampling produced a data set comprising 70 families of fishes (exclusive of the Clupeidae and Engraulidae) collected from the sampling nights of 3, 5, and 6 December by six methods. For ease of analysis and unambiguous interpretation, it was necessary to reduce the number of families treated. We initially removed from consideration any family which did not constitute at least 1% of the catch of at least one method. The removal of taxa of this level of rarity would be unlikely to influence the outcome of the analyses (Green 1979). This excluded 51 families, leaving 19 (referred to as 'abundant families') for analysis beyond simple listing of numbers of families sampled (e.g., Table 1). Relative-abundance information obtained by all six sampling methods for the 19 abundant families was subjected to Principal Component Analysis (PCA) using the variance-covariance matrix. As a check, the same analysis was run incorporating the next 10 most-abundant families; this generated identical patterns. Reducing the data set from 29 to 19 families did not change the resulting pattern.

The PCA analysis identified patterns in the complex data set of 19 families sampled by six methods. Many of these 19 families were relatively rare and contributed little to the variation in the data set. A detailed examination of the factors contributing to these patterns required factorial analyses such as multivariate analysis-of-variance (MANOVA). These procedures are best carried out with a reduced number of variables, which allows a clearer interpretation of trends in the data. This called for a further reduction in the number of families analyzed.

To achieve this reduction, the data set of 19 families collected by nets was subjected to a PCA, which identified the taxa that contributed most substantially to the variation in the data set. This PCA identified apogonids, atherinids, gobiids, lethrinids, mullids, and pomacentrids as major contributors (95.2%) to the variation in the data set. These six taxa were used in a MANOVA. This design provided sufficient degrees of freedom for testing and interpreting the significance of method and night of sampling. The analysis was carried out on samples from nets only.

For graphic display of trends in sampling by nets, the eight most-important taxa from the PCA were depicted. These were apogonids, atherinids, gobiids, lethrinids, lutjanids, mullids, pomacentrids, and labrids. Labrids were included in this group at the expense of schindleriids, as they were an abundant reef-associated taxon of considerable interest to reef fish biologists. This substitution did not affect the cumulative variance accounted for by the eight families.

Unlike nets, aggregation devices did not allow for adjustment of fish densities to a common volume. Moreover, aggregation devices collected a different set of fishes. An additional PCA run on light-trap and light-seine data identified atherinids, gobiids, labrids, lethrinids, mullids, and pomacentrids as taxa, which explained over 90% of the variability in the data set. The families selected showed a strong relationship to the overall abundance ranking, although two relatively rare taxa (lethrinids and mullids) were included.

Aggregation devices sample an unknown volume of water. Because catches by aggregation devices could not be standardized to number of fish per unit volume, we made separate comparisons of nets and aggregation devices. The variables used were mean number/1000 m^3 for nets, and mean number/sample for aggregation devices. A factorial analysis was designed to test for differences in sampling method (fixed) and time (random). For factorial analyses, residual analysis was performed (Snedecor & Cochran 1980) to check assumptions of normality and homogeneity of variance. Taylor's Power Law (Taylor 1961) was used to determine the appropriate transformation.

Canonical Discriminant Analysis and Tukey's Studentized Range Test (HSD) were used to display the differences detected. For MANOVA, the multivariate test statistic (Pillai's Trace) was used because it is

less likely to involve Type-I error and is more robust to heterogeneity of variance than comparable tests (Green 1979). All analyses were performed using SAS Version 6 (SAS 1987).

A more subjective procedure was used to select taxa for size-frequency measures. For meaningful comparisons, it was necessary to select taxa that were well represented in the collecting devices and that covered a reasonable size-range (>8 mm) within each method. Apogonids, gobiids, lutjanids, and pomacentrids met these criteria and also accounted for over 95% of the variation in the main data set from net sampling. Catches for nets and aggregation devices were analyzed separately. For net catches, density was expressed as mean number/1000 m^3 within 2 mm size-classes among the different methods and compared by one-way ANOVAs. With aggregation devices, the variable was the number of fish per sample and comparisons were made by *t*-tests.

Results

The 83 samples contained a total of 57,701 fishes of 70 families, excluding clupeoids (Table 1). Table 2 lists families which constituted at least 1% of the individuals taken by any sampling method and records their size-ranges by method. We refer to these as 'abundant families'.

Taxonomic composition and size structure of the samples

There were marked differences in taxonomic composition of the samples among methods. The bongo net collected the largest number of families overall (Table 1), including all of the abundant families and a wide size-range within most families (Table 2). The light-trap collected the fewest families overall and only

Table 1

Number of samples, total individuals, and numbers of families of fishes (clupeoids excluded) taken by six sampling methods on the nights of 3, 5, and 6 December 1986 off Lizard Island, Great Barrier Reef. Volume of water sampled by aggregation devices is unknown.

Sampling method	Number of samples	Number of fish	Volume of water sampled (m^3)	Number of families
Light-trap	26	7624	unknown	20
Seined light	14	2707	unknown	37
Purse-seine	7	812	224	25
Neuston net	12	2418	2861	31
Bongo net	12	43417	6833	63
Tucker trawl	12	723	47100	29
Total	83	57701	—	70

Table 2

Numbers and size ranges of the 19 families of fishes which made up >1% of the catch of at least one method on 3, 5, and 6 December 1986 off Lizard Island, Great Barrier Reef. Clupeoids are excluded. Size-range in mmSL, and total number of individuals within the taxon (*n*).

	Sampling method											
	Light-trap		Light-seine		Bongo net		Purse-seine		Neuston net		Tucker trawl	
Family	SL	*n*	SL	*n*	SL	*n*	SL	*n*	SL	*n*	SL	*n*
Apogonidae	5.4–9.3	4	1.6–9.8	211	1.6–15.5	10295	1.6–6.8	86	1.7–6.2	491	2.3–5.1	99
Atherinidae	6.7–19.1	20	7.6–61.7	135	6.0–25.2	14	6.8–24.7	2	16.0–56.3	110	15.2–39.3	36
Bothidae			3.2–5.3	3	1.4–7.7	76					3.0–10.0	10
Callionymidae			1.3–3.5	35	1.1–4.9	1003	1.3–2.9	11	1.6–3.9	94	1.9–4.5	6
Carangidae			1.9–57.4	19	1.8–7.6	1555	1.9–4.0	7	1.8–4.5	63	2.2–14.2	13
Ephippididae					1.7–8.7	81					5.8–7.5	14
Gobiidae	3.7–10.5	235	1.2–17.7	643	1.1–10.1	8386	1.4–8.6	487	1.4–20.3	1207	1.9–9.0	258
Labridae	5.1–8.8	48	1.5–13.1	47	1.6–6.0	876	1.7–5.9	21	2.0–5.3	27	2.2–4.1	9
Lethrinidae	8.4–16.6	45	1.9–18.0	24	1.8–4.7	380	2.6–3.3	3	1.9–4.4	17	2.6–11.3	9
Lutjanidae			2.1–5.2	76	1.8–6.6	2740	2.1–7.4	33	1.8–4.9	105	2.5–8.4	48
Microdesmidae			1.5–4.8	10	2.0–4.3	100	2.2–3.2	9	3.3–5.4	6	2.9–6.3	7
Monacanthidae	46.6	1	1.5–23.3	13	1.2–4.6	608	1.9–3.3	3	1.8–3.7	11	2.0–6.3	22
Mullidae	11.2–21.9	51	21.5–39.7	54	2.4–4.9	8	5.1–23.6	2	22.4–30.2	10		
Nemipteridae	6.4–9.3	28	1.8–12.3	42	1.5–5.6	1548	1.8–5.2	15	1.6–5.0	75	4.2–4.8	4
Pinguepididae	2.0	1	1.4–6.5	30	1.3–5.6	2838	1.4–4.6	20	1.7–5.5	109	2.3–4.8	9
Platycephalidae			2.1–3.1	6	1.6–8.3	469	2.8–5.5	6	2.4–4.2	3		
Pomacentridae	5.3–14.9	7124	1.8–25.1	1248	1.0–14.6	496	1.9–9.4	22	1.8–11.7	30	6.4–14.6	68
Scaridae			1.6–4.4	30	1.7–4.6	136	2.2–4.0	34	2.5–7.7	10		
Schindleriidae					2.0–16.2	219	3.1–8.3	8	4.1–10.7	25	4.4–17.7	79

the larger individuals of most families. Analysis of the catch by method (Tables 1,2) suggests that the apparent selectivity of the light-trap reflects size-specific rather than taxonomic biases. The absence of certain taxa from the light-trap during the sampling period may mean that few large individuals were in the sampling area. Table 3 shows that, with the exception of bothids, schindleriids and carangids, taxa not caught by the light-trap were represented by relatively small individuals in the catch by other methods. Whether large carangids were present in more than trivial numbers is unclear. A single 57.4 mm carangid was taken by the light-seine, but the next-largest carangid taken by other methods was 14.2mm. The question of selectivity by light-traps must be resolved by more comprehensive sampling.

The light-seine and Tucker trawls captured most of the abundant families in all sizes. The neuston net and purse-seine captured the same abundant taxa, with size-ranges similar to one another. The exceptions were mullids, microdesmids, gobiids, and atherinids, for which the neuston net captured larger individuals. For the mullids and microdesmids, size distributions produced by the two methods overlapped slightly.

Catches by all methods were dominated by a few abundant families of fishes. The first five most-abundant families listed in Table 2 accounted for 80% or more of the catch by all methods. The Tucker trawl was the most equitable in terms of abundance distributions, and the light-trap the least. However, the rank order of abundant families was not the same for all methods (Fig. 2). The dominant families for all towed nets and the purse-seine were gobiids and apogonids. For light-trap and light-seine the dominant families were pomacentrids, followed by gobiids. Small apogonids, although consistently abundant in net samples, were not captured by light-aggregation devices. In light-trap catches, a single family—the Pomacentridae—accounted for 93% of individuals collected.

For most collecting methods, there was a high degree of consistency among samples. Results of PCA (Fig. 3) showed that samples taken by light-trap were

Table 3

Comparison of maximum size of the 19 abundant taxa (Table 2). Maximum size captured by light-trap is compared with maximum size captured by five other methods tested on 3, 5, and 6 December 1986 off Lizard Island, Great Barrier Reef. Taxa listed in increasing order of maximum size captured by 'other methods' (maximum size captured by the next-best 'other method').

	Maximum size (mm) captured by	
Taxon	Light-trap	Other methods
Callionymidae	not caught	4.9(4.5)
Microdesmidae	not caught	6.3(5.4)
Pinguepididae	2.0	6.5(5.6)
Scaridae	not caught	7.7(4.6)
Platycephalidae	not caught	8.3(5.5)
Lutjanidae	not caught	8.4(7.4)
Ephippididae	not caught	8.7(7.5)
Bothidae	not caught	10.0(7.7)
Nemipteridae	9.3	12.3(5.6)
Labridae	8.8	13.1(6.0)
Apogonidae	9.3	15.5(9.8)
Schindleriidae	not caught	17.7(16.2)
Lethrinidae	16.6	18.0(11.3)
Gobiidae	10.5	20.3(17.7)
Monacanthidae	46.6	23.3(6.3)
Pomacentridae	14.9	25.1(14.6)
Mullidae	21.9	39.7(30.2)
Carangidae	not caught	57.4(14.2)
Atherinidae	19.1	61.7(56.3)

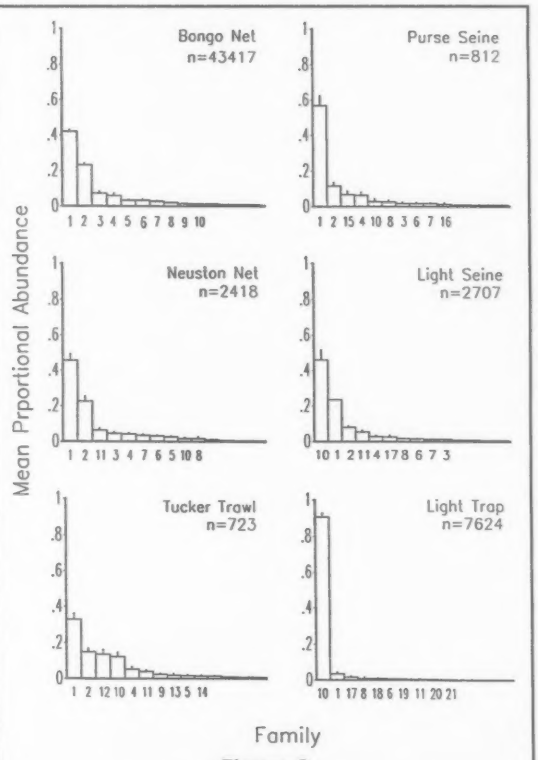

Figure 2

Mean proportional abundance (±1 SE, vertical axis, shown only upward) and ranked taxonomic categories of fishes (clupeoids excluded) collected by six sampling methods off Lizard Island, Great Barrier Reef on 3, 5, and 6 December 1986. Other sample data are given in Table 1. Key to taxa: **1** Gobiidae, **2** Apogonidae, **3** Pinguepididae, **4** Lutjanidae, **5** Carangidae, **6** Nemipteridae, **7** Callionymidae, **8** Labridae, **9** Monocanthidae, **10** Pomacentridae, **11** Atherinidae, **12** Schindleriidae, **13** Ephippididae, **14** Bothidae, **15** Scaridae, **16** Microdesmidae, **17** Mullidae, **18** Lethrinidae, **19** Synodontidae, **20** Scombridae, **21** Blenniidae.

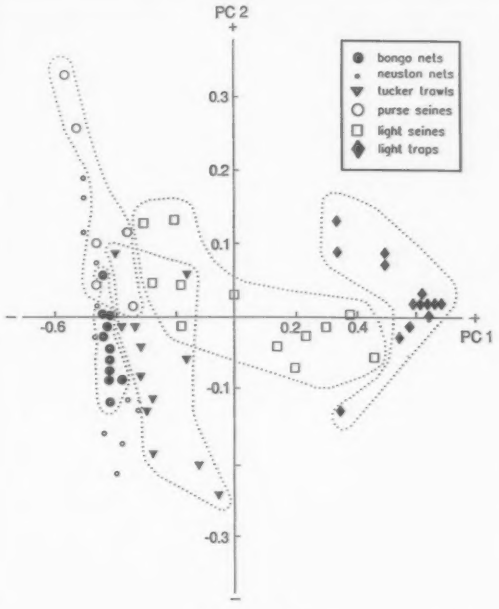

Figure 3

Results of Principal Components Analysis on proportional abundances of 19 families of fishes collected by six sampling methods on 3, 5, and 6 December 1986 off Lizard Island, Great Barrier Reef. Principal Components 1 and 2 are plotted. Differences between number of replicate samples and number of symbols for each method are due to overlap of some symbols.

distinct from net samples, and that samples taken by light-seine were intermediate between net and light-trap samples. Tucker trawl samples were almost completely distinct from bongo, neuston, and seine net samples. Bongo net samples formed a more discrete group than did the neuston and seine net samples.

The data sets for size analysis were heterogenous. Therefore, we attempted only to test for differences in density among methods within selected size-classes using single-factor ANOVA (df 3,39; $p<0.05$). The power of these tests to detect differences among methods was low. For apogonids, gobiids, lutjanids, and pomacentrids, there were sufficient numbers for statistical comparisons across the first three size-classes (i.e., <6 mm, Fig. 4). For all four families, density estimates provided by the bongo net were as high as, and in many cases higher than, those provided by the other nets. The Tucker trawl provided the lowest density estimates.

For the larger sizes (>6 mm), low or zero catches in some size-classes precluded statistical tests in most cases. We compared the Tucker trawl, which is designed to capture such large stages with the bongo net. The few tests that were possible show that in no instance did the Tucker trawl provide higher density estimates than the Bongo net (Fig. 4).

Two taxa, pomacentrids and gobiids, were sufficiently abundant to allow for comparisons of density by 2 mm size-classes between the aggregation devices. For pomacentrids we tested the 7–15 mm size-classes. Light-traps caught significantly higher numbers of pomacentrids in the 7, 9, and 11 mm size-classes than the light-seines (Fig. 4B). The two aggregation devices provided similar estimates of numbers for the 13 and 15 mm size-classes (Fig. 4B). The difference in overall density for pomacentrids sampled by light-traps and light-seines is due to the greater number of pomacentrids in the 7, 9, and 11 mm size-classes in the light-trap catches. Pomacentrid larvae >14 mm were collected by the light-seine on one night only.

Although we did not statistically test the gobiid data, the light-seine appeared to collect greater numbers of smaller (<4 mm), and the light-trap greater numbers of larger (>8 mm), individuals (Fig. 4B). The light-seine collected few gobiids >6 mm and the light-trap almost no gobiids <6 mm. Sizes of apogonid and lutjanid fishes sampled by the light-seine were similar to those of the purse-seine (Fig. 4C). No lutjanids and only four apogonids were collected by the light-traps.

Results of pooled samples from three nights for eight taxa (Materials and methods) by the different nets (Fig. 5) reflect both entry of fish into nets and subsequent extrusion. Most of the fishes taken by all nets were small (Table 2, Fig. 4). Bongo nets consistently provided the highest estimates of density of small fishes, especially gobiids, apogonids, lutjanids, labrids, and lethrinids. This reflects both the low-avoidance and high-retention properties of this fine-mesh net. The purse-seine filtered only small volumes of water, but provided high estimates of density, especially for gobiids, apogonids, and lutjanids (Fig. 4). Extrusion is probably minimal, due to the passive mode of filtering and the very fine mesh of this seine. Neuston nets provided low estimates of density for all families except two that concentrate in the surface layer—atherinids and mullids (Leis 1991a). Density estimates from the Tucker trawl were low for all families, most probably due to the loss of smaller larvae through its large mesh. Both atherinids and mullids, which attained large size (Table 2), were also poorly represented in Tucker trawl catches, possibly because the Tucker trawl did not sample the neustonic habitat of these taxa.

For aggregation devices, we compared densities of the important families identified by PCA, excepting apogonids and lutjanids which were rare or absent from light-traps. Light-traps collect mainly large individuals, so the samples were subdivided by size

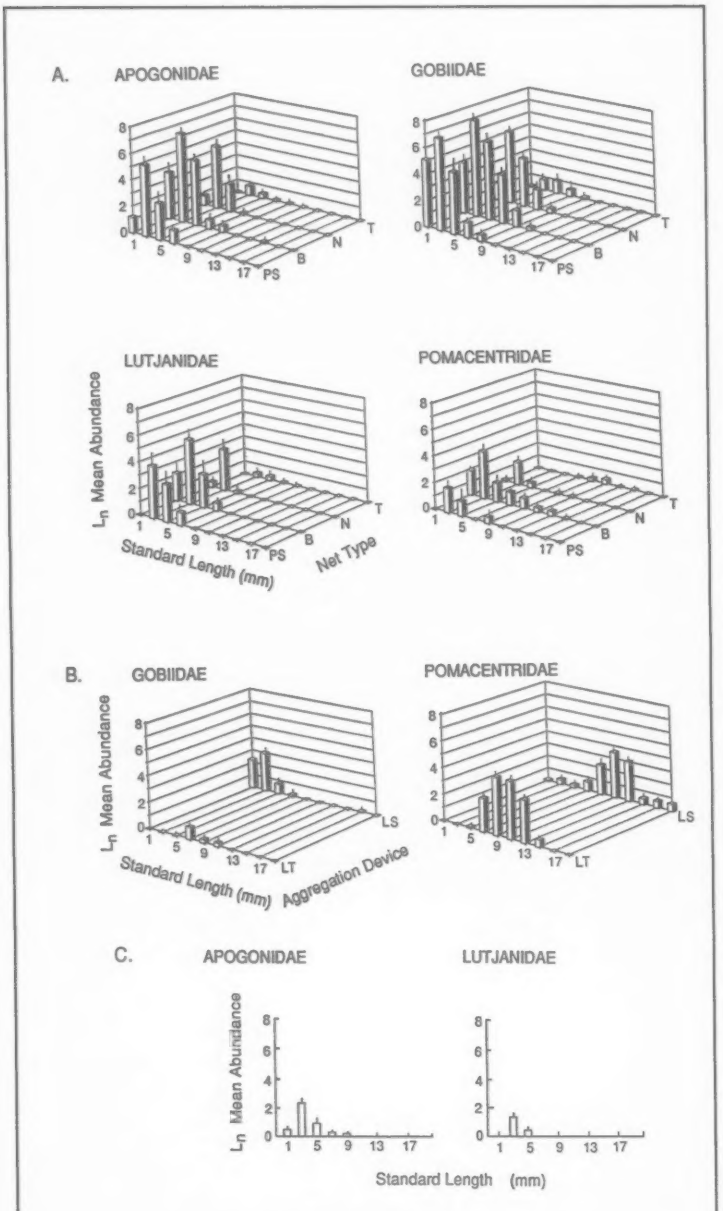

Figure 4

Analysis of size structure in selected families of fishes collected by six sampling methods on 3, 5, and 6 December 1986 off Lizard Island, Great Barrier Reef. **(A)** L_n mean density/1000 m^3 (±SE) of four taxa in each of ten 2 mm size-classes collected by purse seine (PS), bongo net (B), neuston net (N), and Tucker trawl (T). **(B)** L_n mean density per sample (±SE) of gobiids and pomacentrids collected by light-trap (LT) and light-seine (LS). Size-classes as in (A). **(C)** L_n mean density per sample (±SE) of apogonids and lutjanids collected by light-seine. Size-classes as in (A).

(Table 4). Only three significant ($p<0.05$) differences were detected by *t*-tests. The light-trap caught greater numbers of large pomacentrids, the light-seine greater numbers of large atherinids and small gobiids.

Among-night variation

Larval and pelagic juvenile fishes may vary in density at a particular location over short time-periods ranging from hours to days. We examined the among-night variation in two contexts. First, we used factorial analysis to examine the variation attributable to method of sampling and sampling period (nights) in the net collections. Second, we examined the ability of nets and aggregation devices to detect trends in density of large individuals of some families over a longer time-period (five nights).

A multivariate factorial analysis of variance was used to examine trends in mean density in six families: apogonids, atherinids, gobiids, lethrinids, mullids, and pomacentrids. Although both factors were significant (Table 5), the significant interaction between methods and nights (Pillai's Trace $F=1.65$; df 36, 186; $p<0.01$) indicates that differences among methods were not consistent over nights.

Canonical Discriminant Analysis was used to display the relationship between methods and night of sampling. Canonical variates 1 and 2 explained 93% of the variation in the data set (Table 6). Figure 6 illustrates the main conclusions from this analysis. Tucker trawls, and neuston and bongo nets each sampled a distinct fish fauna with little among-night variation. Purse-seine samples overlapped with those of the bongo nets on two nights and were the most variable, both within and among nights, probably reflecting the influence of few samples of small volume. Tucker trawl samples were characterized by consistently low numbers of the

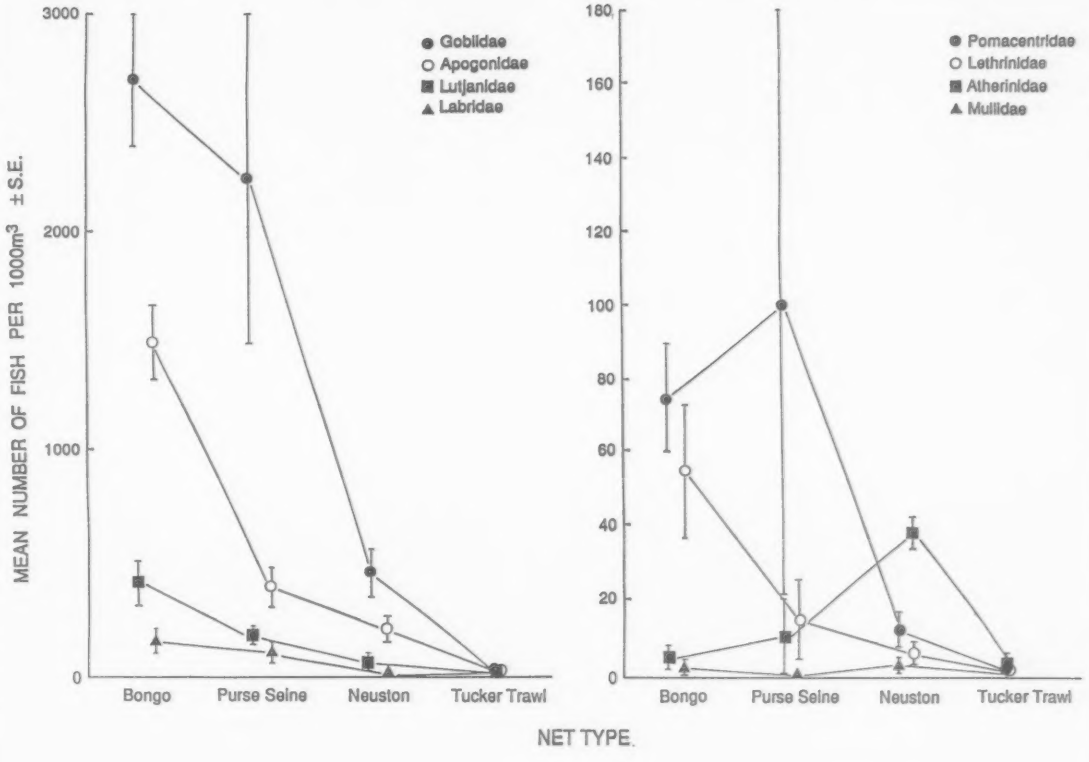

Figure 5

Mean densities of eight selected families (see Materials and methods) collected by four different net types on the nights of 3, 5, and 6 December 1986 off Lizard Island, Great Barrier Reef.

Table 4

Density of six taxa of larval and juvenile fishes collected by aggregation devices on 3, 5, and 6 December 1986 off Lizard Island, Great Barrier Reef. Data are mean densities (with 1SE) of fish per sample pooled over three sampling nights. Fish are divided into two size-classes: <6 mmSL (*S*mall) and >6 mmSL (*L*arge). * $0.05>p>0.01$; NS $p>0.05$.

Family	Size	Light-seine	Light-trap	*p*
Atherinidae	S	0.29± 0.22	0	
	L	9.36± 1.98	0.65± 0.25	*
Gobiidae	S	45.50±10.13	0.12± 0.08	*
	L	0.43± 0.23	8.92± 3.98	ns
Labridae	S	1.57± 0.62	0.04± 0.04	ns
	L	0.21± 0.11	1.54± 0.64	ns
Lethrinidae	S	0.43± 0.23	0	
	L	1.29± 0.34	1.38± 0.77	ns
Mullidae	S	0	0	
	L	3.86± 1.61	1.65± 0.68	ns
Pomacentridae	S	1.36± 0.52	0.27± 0.16	ns
	L	87.79 ±13.10	273.38±32.63	*

Table 5

Multivariate analysis of variance of density data for apogonids, atherinids, gobiids, lethrinids, mullids, and pomacentrids (see Materials and methods) from off Lizard Island, Great Barrier Reef. Factors include sampling methods (purse-seine, bongo net, neuston net, Tucker trawl) and nights (3, 5, and 6 December 1986). Data are ln(x+1) transformed. Test statistic used is Pillai's trace. Significance levels: $**0.01>p>0.001$; $***p<0.001$.

Source	*F*	Numerator df	Denominator df	*p*
Method	11.53	18	9	***
Night	4.05	12	54	***
Method×Night	1.65	36	186	**

dominant families; neuston, by higher numbers of atherinids, a neustonic group. The significant interaction is attributable largely to the purse-seine result.

Table 6

Standardized canonical coefficients from the Canonical Discriminant Analysis of density of fishes over each method by night combination, from samples taken off Lizard Island, Great Barrier Reef on 3, 5, and 6 December 1986. Data were ln(x+1) transformed.

Family	CAN 1	CAN 2
Apogonidae	5.031*	0.675
Atherinidae	−1.129	1.961*
Gobiidae	1.463	0.585
Lethrinidae	−1.005	−1.279
Mullidae	0.177	0.595
Pomacentridae	0.184	−0.736

Canonical variate	Proportion	Cumulative
1	0.793	0.793
2	0.134	0.927

* Consistently high values in total, between and within canonical structure. These variables contribute significantly to the discriminatory power of the canonical variate.

Data from all five nights provided more information on patterns of temporal change for some taxa (Fig. 7). We focused on the comparative ability of the different methods to detect changes over time in numbers of the larger (>6 mm) individuals of some families because we wished to know the best methods for identifying temporal pulses of large larvae and pelagic juveniles of reef fishes. Large pomacentrids and mullids serve as appropriate examples. Although absolute numbers of fishes taken by nets and aggregation devices could not be directly compared, temporal changes in patterns of density could be evaluated among these methods. Comparisons were made using all methods, although bongo net data were available for the nights of 3, 5, and 6 December only.

Data from the two aggregation devices indicated that large pomacentrids increased in density from the 2nd to a peak on the 5th, and decreased over the 6th and 7th (Fig. 7). This pattern was not present in the data from nets, each of which provided a different temporal pattern of density.

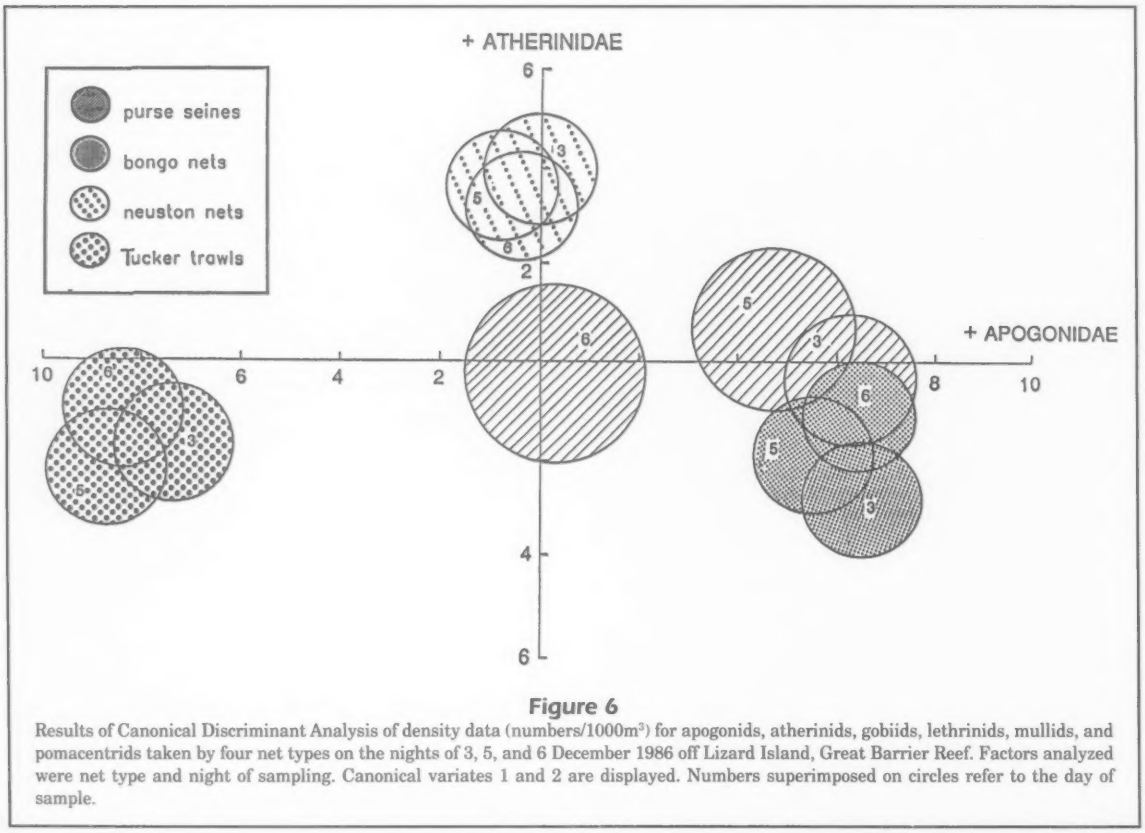

Figure 6

Results of Canonical Discriminant Analysis of density data (numbers/1000m³) for apogonids, atherinids, gobiids, lethrinids, mullids, and pomacentrids taken by four net types on the nights of 3, 5, and 6 December 1986 off Lizard Island, Great Barrier Reef. Factors analyzed were net type and night of sampling. Canonical variates 1 and 2 are displayed. Numbers superimposed on circles refer to the day of sample.

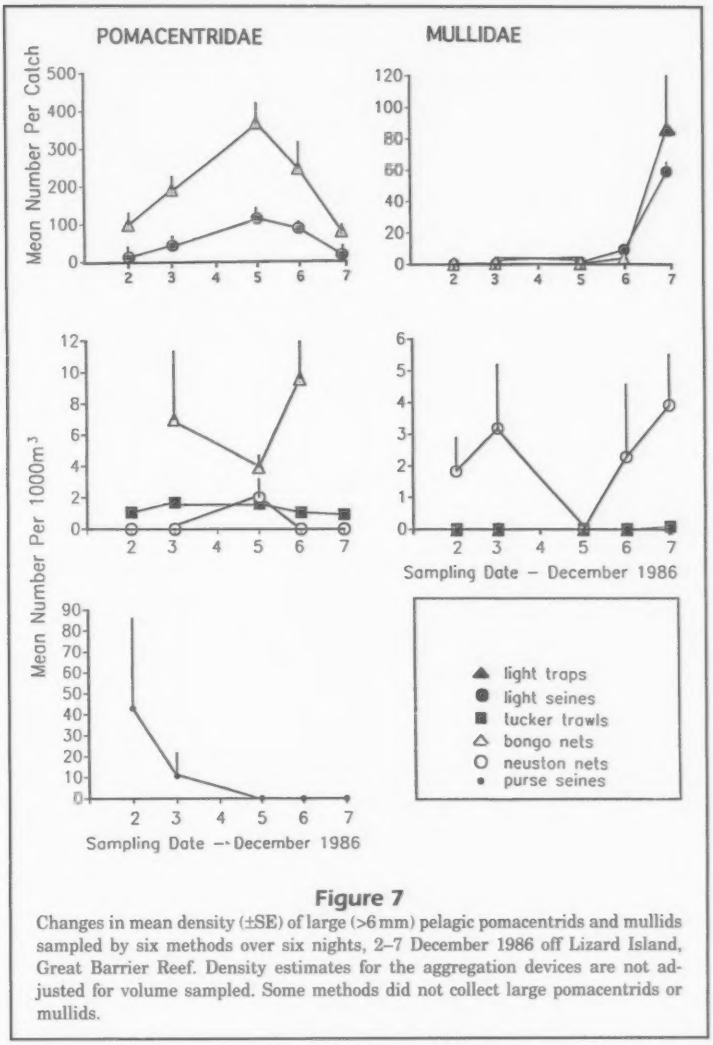

Figure 7

Changes in mean density (±SE) of large (>6 mm) pelagic pomacentrids and mullids sampled by six methods over six nights, 2–7 December 1986 off Lizard Island, Great Barrier Reef. Density estimates for the aggregation devices are not adjusted for volume sampled. Some methods did not collect large pomacentrids or mullids.

The aggregation devices indicated that large mullids were rare or absent until the 5th, and increased greatly in density on the 7th (Fig. 7). This trend was not present in data from the nets. Only the neuston net caught large mullids, but in low and variable numbers.

Discussion

The taxonomic composition obtained when sampling for larval and pelagic fishes is highly method-dependent. The bongo net captured the largest number of families, many of which were rare in the samples. Among abundant taxa, the four nets provided similar estimates of taxonomic composition. The light-trap, however, was more selective, and its catch differed in composition from that of the nets. Taxonomic composition of the light-seine samples was intermediate between the trap and nets, an expected result given its mode of operation.

Our results suggest that capture by the light-trap is dependent on fish size: larger pelagic stages are more likely to be attracted to the light and to swim into the trap than are small stages. However, trap performance may also be time-dependent. For example, apogonids, carangids, lutjanids, and scarids, which were rare or absent in light-trap catches during this study, have been captured during extended light-trap sampling around Lizard Island (M. Milicich, Griffith Univ., Nathan, Queensland, pers. commun.). The absence from light-traps at particular times may simply indicate that large or well-developed individuals of some families were not present at that time.

However, our study provides evidence that pelagic stages of some families may not be photopositive or enter traps, thus indicating some selectivity by the aggregation devices. Schindleriids were present in the net samples to adult size, yet were not captured with either of the light-aggregation methods. The net samples may have included the largest pelagic individuals of callionymids, and perhaps platycephalids and bothids, because they leave the pelagic environment (i.e., settle) at a relatively small size (see Table 3). These families were not present in the light-trap catches.

The size-distribution and density estimates of pelagic fishes captured also differ among nets. The bongo net, neuston net, and purse-seine captured predominantly smaller fishes. For abundant families, density estimates by the bongo net and purse-seine were generally similar, neuston net estimates were somewhat lower, and the Tucker trawl provided still lower estimates. The bongo net provided the highest abundance estimates for most sizes of most families. The Tucker trawl

undersampled smaller individuals, but was no better than the bongo net at capturing larger larvae and pelagic juveniles. This is consistent with the results of Kendall et al. (1987) and Clarke (1991), who compared bongo nets and larger trawls. The light-seine captured a wide size-range of fishes because it combined the sampling characteristics of both a purse-seine and an aggregation device.

Mesh size is an important determinant of catch composition because extrusion varies with mesh size. For a given mesh size, extrusion is a function of body shape and pressure across the net mesh (Clarke 1983 and 1991, Gartner et al. 1989). Body shape is species-specific, which emphasizes the importance of taxon-specific factors in methodological studies. Our results cover a comprehensive range of body shapes, from slender (gobiids) to deep bodied (apogonids and pomacentrids) to moderately deep with elongate fin spines (lutjanids), and should have general application. Purse-seines appear to herd planktonic organisms, while towed nets actively filter, often under considerable pressure; thus extrusion will vary between these two gear types regardless of mesh size. As our primary interest was in comparing a series of sampling devices in their normal working configuration, we did not attempt to test the effects of different mesh sizes within gear types.

Although vertical stratification is minimal at night in the study area (Leis 1986, 1991a), vertical distribution of the fishes could have affected apparent performance of the samplers because each method sampled somewhat differently in the vertical plane. Towed nets were deployed at fixed depths. Experience elsewhere has suggested that light-traps draw their catch from a relatively narrow depth stratum, the upper 5 m (P.J. Doherty, unpubl.). However, only in the neuston net can we confidently attribute greater catches (especially of atherinids) to vertical stratification. For this study, we assumed that vertical distribution of the fishes did not affect our evaluation of the other methods.

Horizontal or temporal variations in density may also have confounded comparisons. A position effect was possible because the aggregation devices were operated at fixed positions about 700 m apart (Fig.1). A temporal effect is possible because the bongo net and Tucker trawl tows were run in blocks and not randomized during each night's sampling, although the order of blocks was alternated among nights.

Absolute sampling efficiency of the nets was not measured. Our estimates of sampling performance were relative, because we did not obtain unbiased estimates of the true densities of small pelagic fishes. We did not attempt to use the methods of Somerton & Kobayashi (1989) to correct our net catches because we felt some of the assumptions required, especially those relating to patch size and consistency through time, were not appropriate in the case of our study. The smaller bongo net seemed to have equal or greater sampling efficiency than the larger Tucker trawl at night for large pomacentrids.

A comprehensive comparison of the six sampling methods would require two things. First, we would need to standardize all results as number of organisms per unit volume of water sampled. Second, we would require an estimate of the sampling precision of each device. For towed nets, both could be obtained because flowmeters provided estimates of the volume filtered for each tow. In the case of the purse-seine, it was not possible to obtain reliable estimates of the volume of water filtered during each deployment of the net. Minor variations in the deployment procedure can modify the dimensions of the volume enclosed by the net. At present, we have no reliable way of estimating this; therefore, for the purse-seine we have a general estimate of water filtered based on idealized dimensions of the deployed net.

Volumes sampled by aggregation devices cannot be estimated at this time, but preliminary calculations (below) suggest they may be large. The bongo net as operated in this study will sample ~4000 m^3/h, the Tucker trawl ~14,000 m^3/h, and we estimate the light-aggregation techniques could sample tens of thousands of m3/h. Therefore, light-aggregation techniques may be the best way to capture sufficient numbers of rarer, larger stages for useful analyses. Aggregation methods may offer considerable advantages in studies of settlement-stage reef fishes, but one must accommodate the characteristic taxonomic selectivity and unknown sample volume.

Two alternatives may explain the apparent disparity in numbers of larger pomacentrids estimated by the bongo net (average 6.9/1000 m^3; Tucker trawl catches averaged 1.49/1000 m^3) and the light-trap (average 273/h): (1) The bongo net undersamples these larger pelagic stages relative to the light-trap, or (2) the light-trap samples larger volumes of water. Assuming the two methods sample large pomacentrids with equal efficiency, the light-traps sample volumes on the order of 40,000m^3/h. This requires the trap to capture, with efficiency equal to that of the net, photopositive stages within a 7–50 m radius (to 5 m depth) of the trap, depending on the current speed (average in the area is 15 cm/s; Leis 1986) and geometry of the light field. It is not possible to choose between alternatives without a better measure of the effective volume swept by traps. Work in progress will help resolve this question.

Short-term temporal variation in the density of particular families was more obvious in the results of some methods than others. For the smaller size-classes, neuston, bongo, and Tucker nets gave consistent results

over short time-periods (Fig. 6). Catches from the purse-seine were more variable within a sampling period and showed greater variability among nights of sampling than did the towed nets. This reflects the localized sampling area and small sample volume of the purse-seine. For larger mullids and pomacentrids, similar trends in density over five nights were identified by the aggregation devices. These trends were not apparent in the data from the towed nets. Thus, the aggregation devices seem particularly suited to studies of short-term temporal variation in the larger (>6 mm) size-classes. The rapid and independent changes in density of the larger individuals of these two families suggest that larger pelagic stages are not present in the water at all times at a location. The alternative, that there are short-term taxon-specific changes in catchability due to changes in behavior of the fishes, seems less likely, but cannot be dismissed without further study.

A number of other studies have compared sampling methods for planktonic and pelagic assemblages. Purse-seines were found to be superior to towed nets for sampling larval anchovies (Murphy & Clutter 1972). Larger, faster, more-transparent nets may minimize net avoidance (Clutter & Anraku 1968). However, Smith & Richardson (1977) suggest that increased net size and towing speed may intensify the disturbance in front of the net and increase net avoidance. All towed nets in these cited studies employed towing bridles, which are a source of water disturbance and, thus, net avoidance by fishes. Towing bridles were not used in the present study, which may be why our conclusions differ from those of Clutter & Anraku (1968) and Murphy & Clutter (1972).

We agree, however, with Clarke (1991) who made detailed comparisons of the effectiveness of two types of bongo nets and a midwater trawl in capturing reef-fish larvae. He suggested that the bongo nets (0.7 m diameter with 0.183 mm mesh, and 1.25 m diameter with 2.5 mm mesh) sampled larvae as well or better than a 3 m Issacs-Kidd trawl (6 mm mesh). Clarke concluded that when densities of larvae were high, 0.7 m and 1.25 m bongo nets were the most effective methods for sampling small and large larvae, respectively. Although larger nets are assumed to capture more and larger fishes due to lessened avoidance (Clarke 1983 and 1991, Methot 1988), this was not true in our study nor is it always true in other pelagic groups (Barnes & Tranter 1965, Sands 1978, Pillar 1984).

One other significant study compared catches from a light-trap with those from a towed net. Gregory & Powles (1988) investigated a relatively simple planktonic assemblage of freshwater fishes. Based on a comparison of taxonomic composition and size of fishes, they concluded that both sampling methods should be used to avoid selectivity biases. An interesting conclusion that differs from our results was that the light-trap provided a better representation of size-classes, including smaller individuals, than did the towed net. This emphasizes the taxon-specific and, perhaps, habitat-specific nature of gear-performance measures.

We agree with Omori & Hamner (1982) that the sampling device and program selected must be question-driven (Kingsford 1988). In order to assist in the choice of appropriate methods, we summarize the performance and sampling properties of the six methods employed in this study (Table 7). Surveys of larval fishes are best accomplished with a bongo net. This will cover a significant portion of the size-range in many important taxa, including larger individuals, at least at night. No extra benefits were apparent from using the larger Tucker trawl. A major advantage of bongo nets is the relative ease with which they may be deployed and retrieved. As expected, neuston nets focused on neustonic fishes.

Surprisingly, the purse-seine provided results comparable to the bongo net despite the small volumes sampled. Among-sample variances were predictably

Table 7

Sampling characteristics of six methods used to collect planktonic and pelagic fishes at the Lizard Island study site, Great Barrier Reef.

Performance criterion	Bongo net	Neuston net	Tucker trawl	Purse seine	Light-trap	Light-seine
Size selectivity	Wide size-range; modal values at lower size.	Samples larger individuals of some taxa; modal values at lower size.	Samples larger sizes; no more effective than bongo net at night.	Primarily small individuals.	Primarily large individuals.	Wide size-range.
Taxonomic selectivity	Least-selective.	Neustonic taxa only.	Slender taxa and small individuals extruded.	Captures only shallow living taxa; undersamples rare taxa.	Selective; dependent on taxon behavior.	Combines light selectivity with characteristics of purse-seine.

higher than those of towed nets. Sampling of local-scale surface features requires the degree of spatial precision and replication provided by small purse-seines (Kingsford & Choat 1985 and 1986, Kingsford et al. 1991), but purse-seines cannot sample deeper than the upper few meters of the water column, and are difficult to operate in any but the best conditions. Localized replicated sampling may also be obtained by free-fall plankton nets (Kobayashi 1989) which, however, obscure vertical patterns and also have a small volume sampled.

Investigation of the patch size of pelagic organisms requires the ability to sample simultaneously over several spatial scales. Large-scale deployment of arrays of automated light-traps will increase replication and allow investigation of phenomena at several spatial scales without risk of temporal confounding, provided the traps can be retrieved over the same time-period. Also, both light-traps and purse-seining with aggregation devices may detect temporal pulses in the density of larger larvae and pelagic juveniles with greater reliability and precision than towed nets.

In addition to the sampling properties of the different devices, there are a number of more pragmatic considerations. Sorting and identification of samples may be a major bottleneck. This will be influenced by the size of the sample, the amount of organic material included, and condition of the fishes themselves. In this context, large samples taken by finer-mesh nets may be particularly difficult to process. Smaller or more selective samples are more readily processed, and those from purse-seines and light-traps yield living fishes suitable for rearing and experimentation. Further, the smaller the larva the more difficult it is to identify; thus, methods like the light-trap, which samples larger fishes, simplify identification.

It is clear that studies of the biology of small pelagic fishes require the use of both nets and aggregation devices either separately or in combination, depending on the type of question posed. No single method can provide a comprehensive picture of the larval and pelagic juvenile fish fauna, and few programs could cover the expense and logistic effort of the simultaneous deployment of a variety of methods. The picture one obtains of the larval and pelagic juvenile fish fauna is highly method-dependent. Which picture or combination of pictures is suitable for answering a given question varies with the question, the taxon, and the size-range of the fishes.

Acknowledgments

This project was supported by funds from the URG Griffith University to PJD, the Australian Marine Sciences and Technology funding panel to JHC and JML, and internal funds from the Australian Museum (JML) and James Cook University (JHC). Field facilities were provided by the Lizard Island Research Station and the Australian Museum. We wish to thank M. and M. Jumelet (RV Sunbird) and M. Milicich, M. Meekan, M. McCormick, N. Preston, and M. Doherty for assistance with the sampling program; D. Furlani, R. Birdsey, S. Reader, and S. Thompson for assistance in the lab; and M. Kingsford and M. Milicich for discussion of the program and critical reading of the manuscript. The manuscript benefited from the comments of anonymous reviewers.

Citations

Barnes, H., & D. J. Tranter
1965 A statistical examination of the catches, numbers, and biomass taken by three commonly used plankton nets. Aust. J. Mar. Freshwater Res. 16:293–306.

Brander, K., & A. B. Thompson
1989 Diel differences in avoidance of three vertical profile sampling gears by herring larvae. J. Plankton Res. 11 (4):775–784.

Clarke, T. A.
1983 Comparison of abundance estimates of small fishes by three towed nets and preliminary results of the use of small purse seines as sampling devices. Biol. Oceanogr. 2:311–340.
1991 Larvae of nearshore fishes in oceanic waters near Oahu, Hawaii. NOAA Tech. Rep. NMFS 101, 19 p.

Clutter, R. I., & M. Anraku
1968 Avoidance of samplers. *In* Zooplankton sampling, p. 57–76. UNESCO Monogr. Oceanogr. Method. 2.

Doherty, P. J.
1987 Light-traps: selective but useful devices for quantifying the distributions and abundances of larval fishes. Bull. Mar. Sci. 41:423–431.

Doherty, P. J., & D. McB. Williams
1988 The replenishment of coral reef fish populations. Oceanogr. Mar. Biol. Annu. Rev. 26:487–551.

Frank, K. T.
1988 Independent distribution of fish larvae and their prey: natural paradox or sampling artifact. Can. J. Fish. Aquat. Sci. 45:48–59.

Gartner, J. V. Jr., W. J. Conley, & T. L. Hopkins
1989 Escapement by fishes from midwater trawls: a case study using lantern fishes. Fish. Bull., U.S. 87:213–222.

Green, R. H.
1979 Sampling design and statistical methods for environmental biologists. Wiley Interscience, NY, 257 p.

Gregory, R. S., & P. M. Powles
1988 Relative selectivities of Miller high-speed samplers and light traps for collecting ichthyoplankton. Can. J. Fish. Aquat. Sci. 45:993–998.

Kendall, A. W. Jr., E. H. Ahlstrom, & H. G. Moser
1984 Early life history stages of fishes and their characters. *In* Moser, H.G., et al. (eds.), Ontogeny and systematics of fish, p. 11–22. Spec. Publ. 1, Am. Soc. Ichthyol. Herpetol. Allen Press, Lawrence KS.

Kendall, A. W. Jr., M. E. Clark, M. M. Yoklavich, & G. W. Boehlert
1987 Distribution, feeding and growth of larval walleye pollock, *Theraga chalcogramma*, from Shelikof Strait, Gulf of Alaska. Fish. Bull., U.S. 85:499–521.

Kingsford, M. J.
1988 The early life history of fish in coastal waters of northern New Zealand: A review. N.Z. J. Mar. Freshwater Res. 22:463–479.

Kingsford, M. J., & J. H. Choat
1985 The fauna associated with drift algae captured with a plankton-mesh purse seine net. Limnol. Oceangr. 30:618–630.
1986 The influence of surface slicks on the distribution and movements of small fish. Mar. Biol. (Berl.) 91:161–171.

Kingsford, M. J., E. Wolanski, & J. H. Choat
1991 Influence of tidally induced fronts and Langmuir circulations on distribution and movements of presettlement fishes around a coral reef. Mar. Biol. (Berl.) 106:167–180.

Kobayashi, D. A.
1989 Fine-scale distribution of larval fishes: Patterns and processes adjacent to coral reefs in Kaneohe Bay, Hawaii. Mar. Biol. (Berl.) 100:285–293.

Leis, J. M.
1986 Vertical and horizontal distribution of fish larvae near coral reefs at Lizard Island, Great Barrier Reef. Mar. Biol. (Berl.) 90:505–516.
1991a Vertical distribution of fish larvae in the Great Barrier Reef Lagoon, Australia. Mar. Biol. (Berl.) 109:157–166.
1991b The pelagic stage of reef fishes: the larval biology of coral reef fishes. *In* Sale, P.F. (ed.), The ecology of fishes on coral reefs, p. 183–230. Academic Press, San Diego.

Leis, J. M., & D. S. Rennis
1983 The larvae of Indo-Pacific coral reef fishes. N.S.W. Univ. Press, Sydney, and Univ. Hawaii Press, Honolulu, 269 p.

Leis, J. M., & T. Trnski
1989 The larvae of Indo-Pacific shore fishes. N.S.W. Univ. Press, Sydney, and Univ. Hawaii Press, Honolulu, 371 p.

McGowan, J. A., & D. M. Brown
1966 A new opening-closing paired zooplankton net. Ref. 66-23, Univ. Calif. Scripps Inst. Oceangr., La Jolla, 56 p.

Methot, R. D.
1988 Frame trawl for sampling pelagic juvenile fish. Calif. Coop. Oceanic Fish. Invest. Rep. 27:267–278.

Moser, H. G.
1981 Morphological and functional aspects of marine fish larvae. *In* Lasker, R. (ed.), Marine fish larvae: morphology, ecology and relation to fisheries, p. 89–131. Univ. Wash. Press, Seattle.

Moser, H. G., W. J. Richards, D. M. Cohen, M. P. Fahay, A. W. Kendall Jr., & S. L. Richardson (editors)
1984 Ontogeny and systematics of fishes. Spec. Publ. 1, Am. Soc. Ichthyol. Herpetol., Allen Press, Lawrence KS, 760 p.

Murphy, G. I., & R. I. Clutter
1972 Sampling anchovy larvae with a plankton purse seine. Fish. Bull., U.S. 70:789–798.

Omori, M., & W. M. Hamner
1982 Patchy distribution of zooplankton: behavior, population assessment and sampling problems. Mar. Biol. (Berl.) 72:193–200.

Pillar, S. C.
1984 A comparison of the performance of four zooplankton samplers. S. Afr. J. Mar. Sci. 2:1–18.

Sands, N. J.
1978 Ecological studies on the deep-water pelagic community of Korsfjorden, western Norway. Comparison of the catch of the more numerous species by two different nets. Sarsia 63:237–246.

SAS
1987 Guide for personal computers, Version 6 ed. SAS Inst., Cary NC.

Smith, P. E., & S. L. Richardson
1977 Standard techniques for pelagic fish eggs and larva surveys. FAO Fish. Tech. Pap. 175, 100 p.

Snedecor, G. W., & W. G. Cochran
1980 Statistical methods, 7th ed. Iowa State Univ. Press, Ames, 593 p.

Somerton, D. A., & D. R. Kobayashi
1989 A method for correcting catches of fish larvae for the size selection of plankton nets. Fish. Bull., U.S. 87:447–455.

Suthers, I. M., & K. T. Frank
1989 Inter-annual distribution of larval and pelagic juvenile cod (*Gadus morhua*) in southwestern Nova Scotia determined with two different gear types. Can. J. Fish. Aquat. Sci. 46:591–602.

Taylor, L. R.
1961 Aggregation, variance and the mean. Nature (Lond.) 189:732–733.

Tucker, G. H.
1951 Relation of fishes and other organisms to the scattering of underwater sound. J. Mar. Res. 10:215–138.

Victor, B. C.
1986 Larval settlement and juvenile mortality in a recruitment-limited coral reef fish population. Ecol. Monogr. 56:145–160.

Warner, R. R., & T. P. Hughes
1989 The population dynamics of reef fishes. Proc. Sixth Int. Coral Reef Symp., Australia, vol. 1:149–155.

Identification and distribution of *Urophycis* and *Phycis* (Pisces, Gadidae) larvae and pelagic juveniles in the U.S. Middle Atlantic Bight*

Bruce H. Comyns
Virginia Institute of Marine Science, The College of William & Mary
Gloucester Point, Virginia 23062
Present address: Gulf Coast Research Laboratory, P.O. Box 7000
Ocean Springs, Mississippi 39564

George C. Grant
Virginia Institute of Marine Science, The College of William & Mary
Gloucester Point, Virginia 23062

Abstract.–Analysis of surface and subsurface plankton collections in the Middle Atlantic Bight (MAB) yielded larvae and juveniles of *Phycis chesteri* and five species of *Urophycis*. Identification was based on numbers of epibranchial gill rakers, abdominal vertebrae, and fin rays (dorsal, caudal, pelvic), patterns of pterygiophore interdigitation, and morphometric characters including body depth at the vent and a ratio between height of the pelvic-fin base and length of the mandible. *Urophycis tenuis* accounted for 99% of the *Urophycis* larvae and pelagic juveniles collected during spring off Virginia and New Jersey and was most abundant offshore. *Urophycis tenuis* larvae were smallest at offshore stations and increased in size as collections proceeded shoreward. *Urophycis chuss* was found in summer and fall collections off the coasts of New Jersey and Virginia, with abundances highest at midshelf stations. *Urophycis chuss* was the only species of hake found during August and early September, and it dominated summer ichthyoplankton collections. *Urophycis regia* was found primarily in midshelf areas off Virginia during fall, but was also collected offshore from both Virginia and New Jersey during winter. *Phycis chesteri*, also found in fall and winter collections, was restricted to offshore stations. Southern species, found exclusively in offshore winter collections, included *U. floridana* and *U. cirrata*.

Manuscript accepted 4 December 1992.
Fishery Bulletin, U.S. 91:210-223 (1993).

Species of the gadid genera *Urophycis* (Gill) and *Phycis* (Artedi), collectively referred to as 'hakes', are abundant on the continental shelf and slope of the northwest Atlantic Ocean. Six species of *Urophycis* and one species of *Phycis* are found in this area (Svetovidov 1948, Wenner 1983): *U. tenuis* (Mitchill), *U. chuss* (Walbaum), *U. regia* (Walbaum), *U. floridana* (Bean and Dresel), *U. earlli* (Bean), *U. cirrata* (Goode and Bean), and *P. chesteri* (Goode and Bean). Larval hake are present at all times of the year in the Middle Atlantic Bight (MAB) and dominate summer plankton collections (Comyns 1987), but persistent taxonomic problems (Dunn & Matarese 1984) have hindered the accumulation of ecological data on these important components of offshore ichthyoplankton communities (Kendall & Naplin 1981, Hermes 1985).

Newly hatched *U. chuss* and *U. regia* of known parentage were described by Hildebrand & Cable (1938), Miller & Marak (1959), Barans & Barans (1972), and Serebryakov (1978). Although these sources describe pigmentation differences between the two species, this information alone is insufficient to positively identify field-caught larvae.

Older larvae and juveniles of *U. chuss*, *U. regia*, *U. floridana*, and a single juvenile specimen of *U. earlli* were described by Hildebrand & Cable (1938). Larvae and juveniles of *U. regia* were collected off Beaufort NC and were identified by the presence of relatively few second dorsal-fin rays and lack of dark ventral-fin pigment. A second larval morph collected off Beaufort was tentatively identified as *U. floridana* because adult *U. floridana* was the only other species of *Urophycis* commonly found in the collection area. These specimens differed from *U. regia* in having darkly-pigmented ventral fins and more second dorsal-fin rays. A single juvenile specimen (37 mm) collected off Beaufort was identified as *U. earlli* because this specimen was darker than *U. regia* and *U. floridana*, and possessed smaller scales. Specimens of a fourth morph, collected off Cape Henry VA were identified as *U. chuss* because they possessed dark ventral-fin pigment, were relatively slender-bodied, and it was assumed that

*Contribution 1799 of the Virginia Institute of Marine Science and School of Marine Science, The College of William & Mary

U. floridana would not be found as far north as Cape Henry.

Methven (1985) presented a size-dependent key to the identification of young *U. chuss*, *U. tenuis*, and *P. chesteri* from the Northwest Atlantic. Identifications were based on body depth, numbers of epibranchial gill rakers (Musick 1973, Wenner 1983), and numbers of caudal-fin rays. Material for Methven's study came primarily from Canadian waters, and he did not encounter *U. cirrata*, *U. earlli*, *U. floridana*, or *U. regia*. As a result, Methven's key is of limited use in more southerly locations where these species occur.

The objective of this paper is to describe additional morphometric and meristic characters that aid in the identification of *Urophycis* and *Phycis* larvae, and to describe the spatial and temporal distribution of these larvae collected 1975–77 off Virginia and New Jersey in the Middle Atlantic Bight.

Materials and methods

Sampling locations and shipboard procedures

Sampling extended from October 1975 until August 1977 and was conducted quarterly at 12 stations off Virginia and New Jersey (Fig. 1, Table 1). Neuston samples were collected with a floating sampler developed at Woods Hole Oceanographic Institution (Bartlett & Haedrich 1968, Craddock 1969). The net, constructed with 505 µm mesh Nitex, was 1 m wide and fished to a depth of 12 cm in calm seas. Tows were of 20 min duration at a ship speed of ~2 kn. The net was deployed from a boom and the towing course followed a widely-circular track to prevent sampling in the ship's wake. A single neuston tow was made at 3 h intervals over a 24 h period at each station, resulting in eight samples per station during each cruise. Two oblique tows between nearsurface and bottom were made at all stations with 60 cm opening-closing bongo systems (McGowan & Brown 1966), the first with paired 202 µm Nitex nets and the second with paired 505 µm nets. To prevent surface contamination, all nets were closed during passage through the surface layer (upper meter). Both bongo and neuston nets were equipped with flowmeters (General Oceanics, Inc.). The flowmeter attached to the underside of the neuston frame provided an estimate of horizontal distance relative to sea surface fished by the net. Estimates of volume filtered by the neuston sampler were determined by multiplying distance fished by net area fished (1 m×12 cm). In calm seas the neuston sampler consistently fished to a depth of 12 cm, but in rough seas the net opening would occasionally be almost completely filled or empty (the flowmeter was always submerged). This variability decreased precision of neuston volume estimates but was not expected to bias volume estimates. Comparisons between neuston and bongo collections were performed only to emphasize the relative importance of the surface layer to larval hakes. Patterns of the spatial and temporal distribution of larvae were based only on comparisons among neuston collections because most specimens were collected with this gear type.

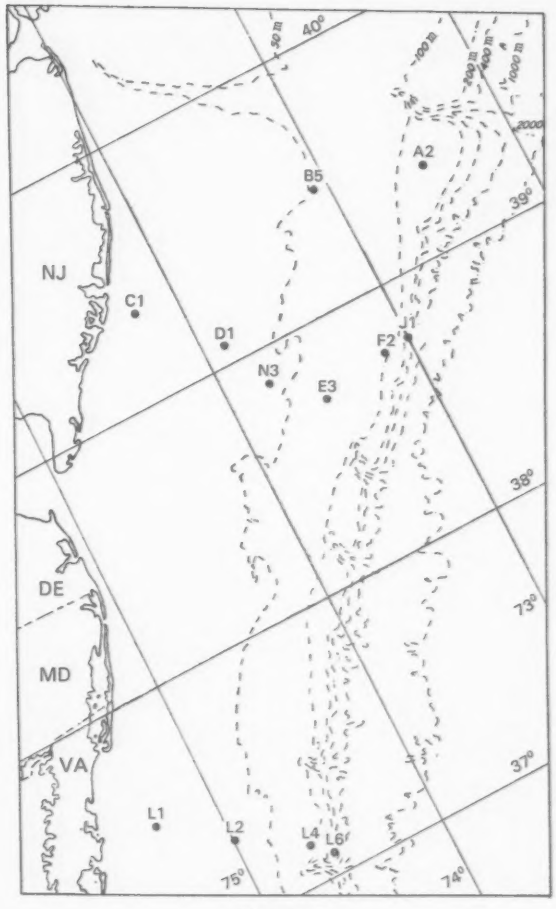

Figure 1
Ichthyoplankton sampling locations off New Jersey and Virginia. Stns. F2, J1, A2, L4, and L6 are considered offshore stations.

Laboratory procedures

Fish larvae were sorted from whole collections. All specimens of *Urophycis* and *Phycis* were cleared and stained (Dingerkus & Uhler 1977, Potthoff 1984, Tay-

Table 1

Sampling schedule for twelve stations occupied off New Jersey (NJ) and Virginia (VA), 1975–77.

	1975	1976				1977		
Stn.	Oct	Feb	Jun	Aug Sep	Nov	Feb Mar	May	Aug
C1 (NJ)	X	X	X	X	X	X	X	X
D1	X	X	X	X	X	X	X	X
N3	X	X	X	X	X	X	X	X
E3	X	X	X	X	X	X	X	X
F2	X	X	X	X	X	X	X	X
J1	X	X	X	X	X	X	X	X
B5 (NJ)					X	X	X	X
A2					X	X	X	X
L1 (VA)					X	X	X	X
L2					X	X	X	X
L4					X	X	X	X
L6					X	X	X	X

lor & Van Dyke 1985), except those occurring in collections taken during August–September 1976 (n>16,000) and August 1977 (n>4000). During these periods of high abundance, subsamples of over 2000 larvae from August–September 1976 and >900 larvae from August 1977 were randomly selected and similarly processed. Herein specimens <18 mmSL are arbitrarily termed larvae, whereas fish ≥18 mm are termed juveniles (Markle et al. 1982). Fish <~12 mm were measured with an ocular micrometer, while lengths of larger specimens were measured with a dial caliper ruler. The largest pelagic juveniles found were ~40 mmSL.

The following morphometric criteria were used in the analysis: (1) height of pelvic fin/vertical distance from base of pelvic fin to ventral margin of body; (2) mandible length/distance from anterior tip of the dentary to posteroventral tip of the angular; and (3) body depth at anus/vertical distance from anterior end of anal-fin base to dorsal surface immediately above. Morphometric measurements were made with an ocular micrometer. The first interneural space was defined as the space anterior to the first neural spine.

Hake larvae and juveniles possessing the adult meristic complement were initially identified using published and unpublished meristic data (Table 2). Meristic observations included epibranchial gill rakers (left side examined), abdominal vertebrae, and fin rays (dorsal, caudal, pelvic). Observations were taken from both cleared and stained material and from radiographs of juvenile and adult museum specimens (App. Table 1).

Identification of smaller larvae was facilitated by using morphometric criteria, patterns of interdigitation between pterygiophores supporting the median fins and the neural or haemal spines, and by defining the size at which larvae attained various stages of fin-ray, vertebral, and gill-raker development. Unfortunately, faded pigmentation caused by specimen storage in formalin and subsequent clearing and staining prevented use and further description of larval pigmentation in the present study.

Table 2

Ranges of meristic characters in *Phycis chesteri* and six species of *Urophycis*. Numbers in parentheses indicate meristic ranges that were extended by the present study. Data sources are (1) Svetovidov 1948, (2) Hildebrand & Cable 1938, (3) Bigelow & Schroeder 1953, (4) Leim & Scott 1966, (5) Miller & Jorgenson 1973, (6) Musick 1973, (7) Hoese & Moore 1977, (8) Markle 1982, (9) Fahay 1983, (10) Wenner 1983, (11) Methven 1985, (12) J.A. Musick, pers. commun., VIMS, Gloucester Point VA 23062.

	U. tenuis	*U. chuss*	*U. regia*	*U. floridana*	*U. earlli*	*U. cirrata*	*P. chesteri*
Caudal-fin rays	33–38(40)	28–34	28–32(34)	28–32(34)	27–30(31)	28–33	28–35(36)
1st dorsal-fin rays	9–10(12)	9–11(12)	8–10	10–13	8–11	9–11(12)	8–11(12)
2nd dorsal-fin rays	50–59(62)	(52)53–64	43–51(52)	54–63	57–63(68)	54–68	50–63
Anal-fin rays	41–52(53)	45–57	41–50(52)	45–54(55)	49–56(60)	46–58	43–54
Vertebrae (total)	47–50(51)	45–50(51)	(44)45–47(48)	44–50(51)	45–47(48)	47–53	45–52
Caudal vertebrae	(32)34–35	33–36	(30)31–33(34)	30–34(35)	31–33(34)	32–37	31–37
Abdominal vertebrae	[a]13–17	14–17	13–15	14–17	14–15	15–17	13–16
Pelvic-fin rays[b]	3	3	3	3	3	3	3
Epibranchial gill Rakers (1st arch)	[c]2	3	3	2	2	3	4–5
Data source	1,3,6,8,11	1,2,4,5,6,8,11	1,2,3,4,5,8	1,7,12	1,5,12	1,12	1,10,11,12

[a] In our material (n=205) *U. tenuis* never possessed <15 abdominal vertebrae.
[b] The third pelvic-fin ray in adult *Urophycis* and *Phycis* is rudimentary.
[c] *Urophycis tenuis* occasionally has three epibranchial gill rakers.

Results

Identification of *Urophycis* and *Phycis* larvae and juveniles

Meristics

Epibranchial gill rakers (Table 3) A complete size-series of all species was not available, but size (mm) at which *U. regia*, *U. chuss*, and *U. tenuis* larvae attain the adult complement of epibranchial gill rakers and other meristic elements is shown in App. Table 2. The following sections are abbreviated to avoid repeating in the text what the tables and figures succinctly show. *Phycis chesteri* does not attain the adult complement of epibranchial gill rakers until 16–18 mm (Methven 1985), but by 13 mm the third gill raker has developed and serves to separate larvae of this species from *U. tenuis*, *U. earlli*, and *U. floridana*. Occasionally *U. chuss* and *U. regia* possess two or four epibranchial gill rakers on one side, but most of these specimens have the normal complement of three gill rakers on the other side. *Urophycis tenuis* occasionally possesses a 3rd epibranchial gill raker, but only very rarely is this third gill raker found on both sides of a specimen.

Caudal-fin rays (Table 3) All but two specimens of *U. tenuis* (n=195) had more caudal-fin rays than all other species of *Urophycis*. Numbers of caudal-fin rays of *U. tenuis* overlapped those of *P. chesteri*, but more than half of our *U. tenuis* were distinct in having >36 rays, and over 40% of *P. chesteri* (n=56) differed from *U. tenuis* in having <34 rays. As few as 28 caudal-fin rays have been reported in *P. chesteri* (Wenner 1983) and *U. cirrata* (J.A. Musick, VA Inst. Mar. Sci., pers. commun.), but this may be because some of the small procurrent rays are not easily seen in radiographs of larger fish.

No *U. earlli* specimens (n=31) possessed >31 caudal-fin rays, while all other hake commonly have >31 rays.

Dorsal-fin rays (Table 3) Despite overlapping extremes, numbers of first dorsal-fin rays helped distinguish *U. floridana* from other species of hake. In our material, *U. regia* and *U. earlli* never possessed >10 and 11 first dorsal-fin rays, respectively, while over 80% of *U. floridana* (n=45) had >11 rays. One-third of *U. floridana* specimens examined possessed 13 first dorsal-fin rays, delimiting these from all other hake taxa.

The relatively low number of second dorsal-fin rays in *U. regia* separated this species from *P. chesteri* and other *Urophycis* species with little overlap. *Urophycis chuss* and *U. regia* with incomplete development of second dorsal-fin rays were delimited by numbers of pterygiophores supporting these rays at sizes as small as 6 mm (Fig. 2). Although extremes in numbers of second dorsal-fin rays overlapped in all other taxa, many of the available specimens of *U. earlli* and *U. cirrata* were distinct in possessing >63 rays.

Abdominal vertebrae (Table 3) Numbers of abdominal vertebrae cannot be used alone to identify individual specimens because of overlapping extremes, but this meristic character is useful when identifying collections comprised entirely of *U. tenuis* or *U. chuss*. *Urophycis tenuis* larvae, identified by numbers of epibranchial gill rakers and caudal-fin rays, were found in the MAB only in spring and accounted for 99% of the *Urophycis* collected at this time (*U. regia* juveniles accounted for the other 1%). *Urophycis* larvae <10 mm (n=154) that were present in spring collections had not yet developed the adult complement of caudal-fin rays, but these larvae (>4 mm) had developed the adult complement of abdominal vertebrae and were identified as *U. tenuis* because their frequency-distribution of numbers of abdominal vertebrae was identical to that found in larger *U. tenuis*; 88% of the larvae had 16 abdominal vertebrae, and no specimens were found with <15. It is unlikely that any of these small larvae were *U. floridana* or *U. cirrata*, two other species with similar numbers of abdominal vertebrae, because these two southern species were found only in offshore winter collections and most specimens were pelagic juveniles.

Urophycis chuss >4 mm (n=448) possessed 14–16 abdominal vertebrae, but the majority of specimens (n=391) had 15. In all other species of *Urophycis* the count of 15 occurred in <20% of the specimens; and although extremes of *U. chuss* and *P. chesteri* were similar, *P. chesteri* commonly had 14 or 16 abdominal vertebrae (17%). Consequently, in the MAB during late summer when *U. chuss* larvae are extremely abundant (and, in this study, were the only species of hake found at this time), complete meristic counts to check for species other than *U. chuss* need be performed only on those specimens that do not have 15 abdominal vertebrae. If species other than *U. chuss* are found in late-summer collections, numbers of abdominal vertebrae are no longer taxonomically useful and complete meristic counts are necessary to identify larvae.

Urophycis regia (n=698) had 13–15 abdominal vertebrae, but only eight specimens had 15, and seven of these specimens had an anomalous 15th abdominal vertebra. This anomalous vertebra possessed one short transverse process characteristic of abdominal vertebrae and one long transverse process typical of caudal vertebrae. Because 99.9% of *U. regia* examined had <15 normal abdominal vertebrae, it was assumed that specimens with ≥15 abdominal vertebrae were not *U. regia*. This meristic character aided in the separation of small (<6 mm) *U. chuss* and *U. regia* in fall collec-

Table 3

Frequency distribution of meristic values recorded in *Phycis chesteri* and six species of *Urophycis*. Asterisks denote that data from juvenile and adult specimens are included. All larvae had attained the adult meristic complement.

Epibranchial gill rakers on left first gill arch. Slash separates numbers on left and right sides.

	2	3/2	3	4/3	4	5
**P. chesteri*					24	8
U. chuss		8	596	8	2	
U. regia		4	631	4	2	
**U. cirrata*			19			
U. tenuis	160	6	1			
**U. floridana*	44					
**U. earlli*	32					

Number of caudal-fin rays

	29	30	31	32	33	34	35	36	37	38	39	40
U. tenuis						2	28	56	65	34	9	1
**P. chesteri*			1	8	15	19	10	3				
U. regia		1	19	34	16	1						
U. chuss	1	1	22	13	10	3						
**U. cirrata*			3	8	2							
**U. floridana*		5	13	21	14	2						
**U. earlli*	12	13	6									

Number of first dorsal-fin rays

	8	9	10	11	12	13
**U. floridana*				8	22	15
**U. cirrata*			2	8	3	
U. chuss		2	33	51	9	
U. tenuis		10	24	26	3	
**P. chesteri*	1	19	38	13	2	
**U. earlli*		6	21	5		
U. regia	14	61	7			

Number of second dorsal-fin rays

	44	45	46	47	48	49	50	51	52	53	54	55	56	57	58	59	60	61	62	63	64	65	66	67	68
**U. cirrata*																1		1	1	1	2	2	5		1
**U. earlli*														1			2	8	8	3	7	1	1		1
U. floridana												6	6	7	9	6	5	3	3						
**P. chesteri*										3	8	5	14	13	5	5	3	1		1					
U. chuss									1	3	4	6	16	16	16	20	9	6	6	3					
U. tenuis								1	3	9	7	8	3	12	5	4	1	1	2						
U. regia	2	1	15	22	30	36	29	16	2																

Number of abdominal vertebrae

	13	14	15	16	17
U. tenuis			20	180	5
**U. cirrata*			2	10	1
**U. floridana*		1	7	38	3
U. chuss		50	391	7	
**P. chesteri*		8	57	4	
**U. earlli*		27	4		
U. regia	66	624	8		

Note: Although 8 specimens of *U. regia* had 15 abdominal vertebrae, in only one of these specimens (0.1%) was the 15th vertebra normally developed.

Number of anal-fin pterygiophores anterior to first haemal spine

	3	4	5	6	7	8	9
**U. earlli*				4	14	8	1
**U. floridana*				11	23	7	1
U. regia			8	156	202	14	
U. chuss			18	173	152	7	
U. tenuis		3	36	25	1		
**U. cirrata*		1	8	2			
**P. chesteri*	3	28	34	5			

Interneural space into which projects the pterygiophore supporting the first ray of the second dorsal fin

	7	8	9	10
U. tenuis		8	52	6
**U. floridana*	1	10	25	6
**P. chesteri*	3	31	20	1
U. chuss	4	203	220	4
U. regia	141	41		
**U. earlli*	15	12		

Note: If pterygiophore was aligned with the tip of a neural spine, it was arbitrarily recorded as pointing into the space posterior to the spine in question.

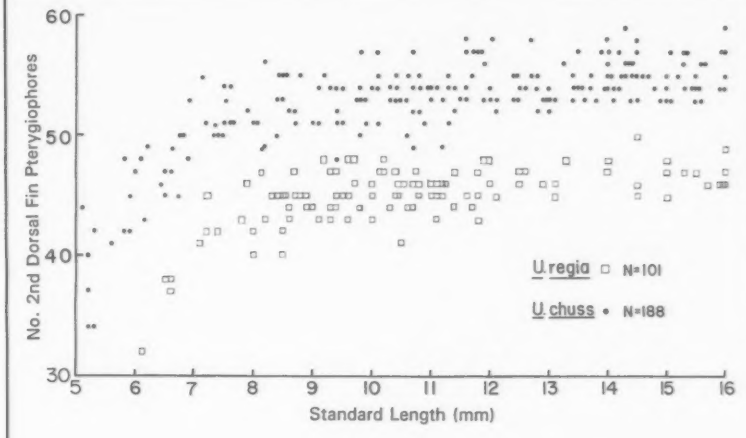

Figure 2
Development of second dorsal-fin pterygiophore number in *Urophycis chuss* and *U. regia*.

tions when numbers of second dorsal-fin pterygiophores were not yet taxonomically useful.

Numbers of abdominal vertebrae may help separate *U. earlli* from *U. floridana* and *U. cirrata*, the other two southern species of *Urophycis*. Over 80% of *U. floridana* and *U. cirrata* possessed 16 or 17 abdominal vertebrae, but *U. earlli* has never been recorded with this many.

Anal-fin pterygiophores (Table 3) The number of anal-fin pterygiophores positioned anterior to the first haemal spine helps distinguish *P. chesteri*, *U. cirrata*, and *U. tenuis* from *U. earlli*, *U. floridana*, *U. regia*, and *U. chuss*. Only one specimen of *U. tenuis* (n=65) and no *U. cirrata* (n=11) or *P. chesteri* (n=70) were found with >7 anal-fin pterygiophores positioned anterior to the first haemal spine, but 45% of *U. chuss* (n=350) and over half of *U. earlli* (n=27), *U. floridana* (n=42), and *U. regia* (n=380) had at least 7 of these pterygiophores. More than 60% of *U. tenuis*, *U. cirrata*, and *P. chesteri* had <6 anterior anal-fin pterygiophores, whereas <2% of *U. regia* and no *U. earlli* or *U. floridana* had this few.

Second dorsal-fin pterygiophores (Table 3) The interneural space into which points the first pterygiophore of the second dorsal fin helped separate *U. chuss* from *U. regia*, and *U. floridana* from *U. earlli*. In over half of *U. chuss* examined (n=431) the first pterygiophore of the second dorsal fin pointed into the 9th or 10th interneural space, whereas in all *U. regia* examined (n=182) this pterygiophore pointed into the 7th or 8th interneural space. In >75% of *U. regia* this pterygiophore pointed into the 7th interneural space, whereas <1% of *U. chuss* showed this pattern.

In >70% of *U. floridana* examined (n=42) the first pterygiophore of the second dorsal fin pointed into the 9th or 10th interneural space, whereas in all juvenile and adult *U. earlli* examined (n=27) this pterygiophore pointed into the 7th or 8th interneural space. In over half of *U. earlli* examined, the first pterygiophore of the second dorsal fin pointed into the 7th interneural space, but in only 2% of *U. floridana* did this pterygiophore project this far forward.

Morphometrics

Body depth at anus (Fig. 3) Body depth at the anus separated some species of hake larvae at sizes >12–13 mm. Extremes of body depth as percent of standard length for cleared and stained *P. chesteri*, *U. tenuis*, and *U. chuss* were 21.0–23.4, 19.0–21.1,

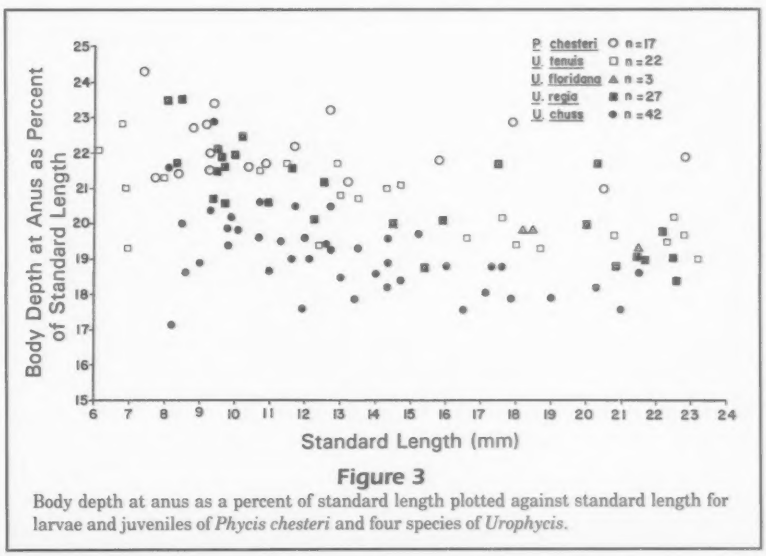
Body Depth at Anus as Percent of Standard Length
Standard Length (mm)
P. chesteri ○ n=17
U. tenuis □ n=22
U. floridana △ n=3
U. regia ■ n=27
U. chuss ● n=42

Figure 3
Body depth at anus as a percent of standard length plotted against standard length for larvae and juveniles of *Phycis chesteri* and four species of *Urophycis*.

Table 4

Ranges of pelvic-fin-base height as percent of mandible length for *Phycis chesteri* and five species of *Urophycis*. Ranges of values are given for different size-intervals of larvae. ND = no data.

		Size-interval (mm)						
		5–9	10–14	15–19	20–24	25–29	30–34	35–45
U. regia	(*n*=31)	21–30	19–33	19–25	16–28	12–17	ND	ND
U. floridana	(*n*=19)	ND	ND	29–36	23–37	23–28	24–29	ND
U. chuss	(*n*=38)	20–39	23–33	24–36	19–22	15–16	16	16
U. cirrata	(*n*=4)	ND	ND	ND	39	31	ND	19–31
P. chesteri	(*n*=29)	44–74	52–61	54–61	46–61	52–64	50–59	26–57
U. tenuis	(*n*=39)	28–42	24–42	33–40	29–37	26–30	32	ND

and 17.6–19.7, respectively. Body depth of *U. floridana*, however, was found to overlap extremes of *U. tenuis* and *U. regia*, while *U. regia* exhibited the greatest variation in this character, overlapping the extremes of *P. chesteri* and all other species of *Urophycis* studied.

Mandible length and height of pelvic fin (Table 4, Fig. 4) Height of the pelvic fin plotted against mandible length separated larval *P. chesteri* from other hake at sizes between ~6 and 35 mm. At sizes > 3 5 m m *P. chesteri* was similar to *Urophycis* with respect to this character because *P. chesteri* became more slender-bodied and the pelvic-fin origin moved closer to the ventral margin of the body. Ranges of pelvic-fin height as percent of mandible length in cleared and stained larvae ranging in length from 6 to 35 mm varied from 44 to 74% in *P. chesteri* (*n*=29), but the highest value of this ratio in five species of *Urophycis* (*n*=131) was only 42%.

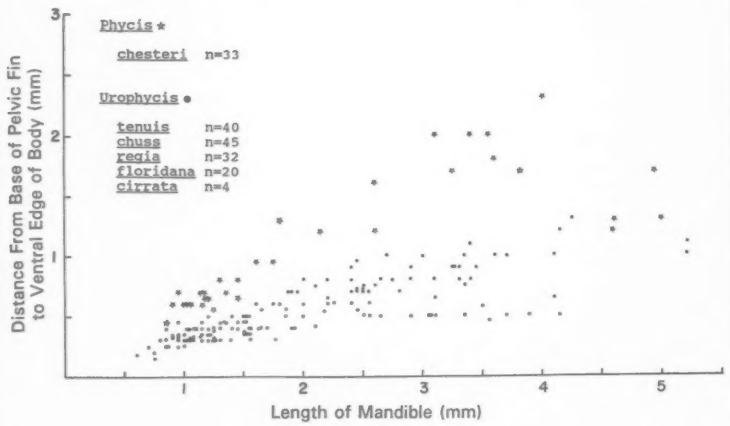

Figure 4

Height of the pelvic fin plotted against mandible length for larvae and juveniles of *Phycis chesteri* and five species of *Urophycis*.

Distribution and abundance of hake larvae

Urophycis chuss *Urophycis chuss* was found only in summer and fall plankton collections from the MAB, and was the only species of larval hake found in August and early September. Densities of *U. chuss* in summer collections off the coast of New Jersey were up to two orders of magnitude greater than densities found off Virginia (Fig. 5). In October 1975 and November 1976, *U. chuss* were still present off both Virginia and New Jersey, but were far less abundant than during summer.

Densities of larval *U. chuss* also varied with distance from shore (Fig. 5), particularly during summer when lowest densities occurred inshore and highest densities were found in midshelf regions in water depths of 40–120 m. Variations in larval density with both latitude and water depth were not well defined in f a l l collections.

An increase in mean size of *U. chuss* was evident in fall collections (Fig. 6). As larval size increased in fall collections, the number of larvae collected with bongo nets decreased greatly. More than 1300 specimens were collected in October 1975 and November 1976, but only 25 of the larvae were collected with bongo gear. Onshore-offshore variation in size of *U. chuss* was most evident in fall collections off both Virginia and New Jersey; size tended to increase with decreasing water depth.

Urophycis regia *Urophycis regia* was collected in the MAB from October until May, with highest densities of larvae occurring in fall collections off the Vir-

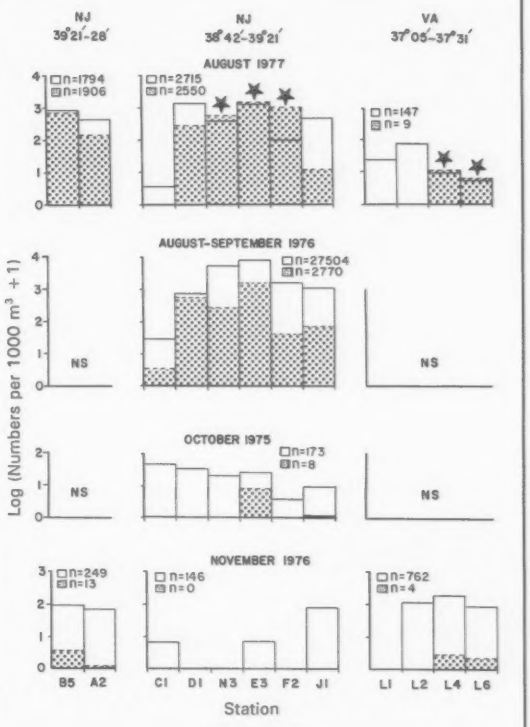

Figure 5

Mean abundance of *Urophycis chuss* in neuston and bongo collections at stations off Virginia and New Jersey, October 1975–August 1977. *n* = number of larvae collected. Neuston catches are denoted by clear histograms; bongo catches by stippled histograms. NS = no samples taken. Star denotes bongo catches exceed neuston catches.

ginia coast at midshelf station L2 (Fig. 7). Densities of *U. regia* were much lower in collections taken in February and March, and most specimens were pelagic juveniles found at offshore stations off both Virginia and New Jersey. By May, *U. regia* was scarce; only seven neustonic juveniles were found at offshore stations.

Urophycis tenuis Apart from an occasional *U. regia* juvenile found at offshore stations, *U. tenuis* was the only species of hake present in spring plankton collections off Virginia and New Jersey. Abundance of *U. tenuis* in May 1977 was up to one order of magnitude greater than abundances in June 1976 (Fig. 8). Larvae were collected at all but inshore stations off both Virginia and New Jersey, but were most abundant at offshore stations. Larvae were smallest at offshore stations and increased in size as collections proceeded inshore (Fig. 9, page 220).

Urophycis floridana and U. cirrata *Urophycis floridana* (*n*=41, 13–32 mmSL) and *U. cirrata* (*n*=5, 20–42 mmSL) were found exclusively in offshore winter collections (Fig. 10, page 221). With the exception of a single juvenile *U. floridana* (23.0 mmSL) captured in a bongo tow, all specimens were found in neuston samples.

Phycis chesteri *Phycis chesteri* larvae first appeared in fall neuston collections from the Middle Atlantic Bight; 16 larvae 6–13 mm in length were collected in November 1976 at offshore stations off Virginia (Fig. 11, page 221). *Phycis chesteri* larvae and pelagic juveniles remained in surface waters during winter and were found in water deeper than ~100 m off both Virginia and New Jersey (*n*=41). All specimens were collected with the neuston net.

Discussion

Because of similarities between larvae of the seven hake species found in the MAB, a dichotomous key is not a practical tool with which to identify hake larvae in this area. However, the specific identification of larval and pelagic juvenile hake is feasible using a suite of diagnostic characters (App. Table 2). Identifications in this study were based on comparison of larval meristics with adult meristics. Further examination of larvae revealed diagnostic characters comprised not only of meristic information, but also morphometric and pterygiophore interdigitation data. Spawning season and capture location were not used as 'characters' to identify larvae in this study.

Methven (1985) had limited success using pigment characters to separate *U. chuss* and *U. tenuis* >7–8 mm. Problems will persist with the identification of small hake larvae until ontogenetic pigment patterns of all species have been described. These ontogenetic pigment patterns, when used in concert with meristic characters, will hopefully enable relatively routine identifications of these taxa.

The only species of *Urophycis* not found in the present study was *U. earlli*. Adult *U. earlli* are rare and larvae remain undescribed, but they are expected to co-occur with *U. floridana* (Hildebrand & Cable 1938). Both species are similar in having two epibranchial gill rakers, but numbers of first dorsal-fin rays, abdominal vertebrae, and caudal-fin rays delimit most specimens of these two species.

Larval and juvenile *Urophycis* or *Phycis* were present in the MAB throughout the year, and patterns of spatial and temporal distribution of larvae were consistent during both years of this study. *Urophycis chuss* larvae were found in summer and fall collections, with greatest abundances occurring during summer in the

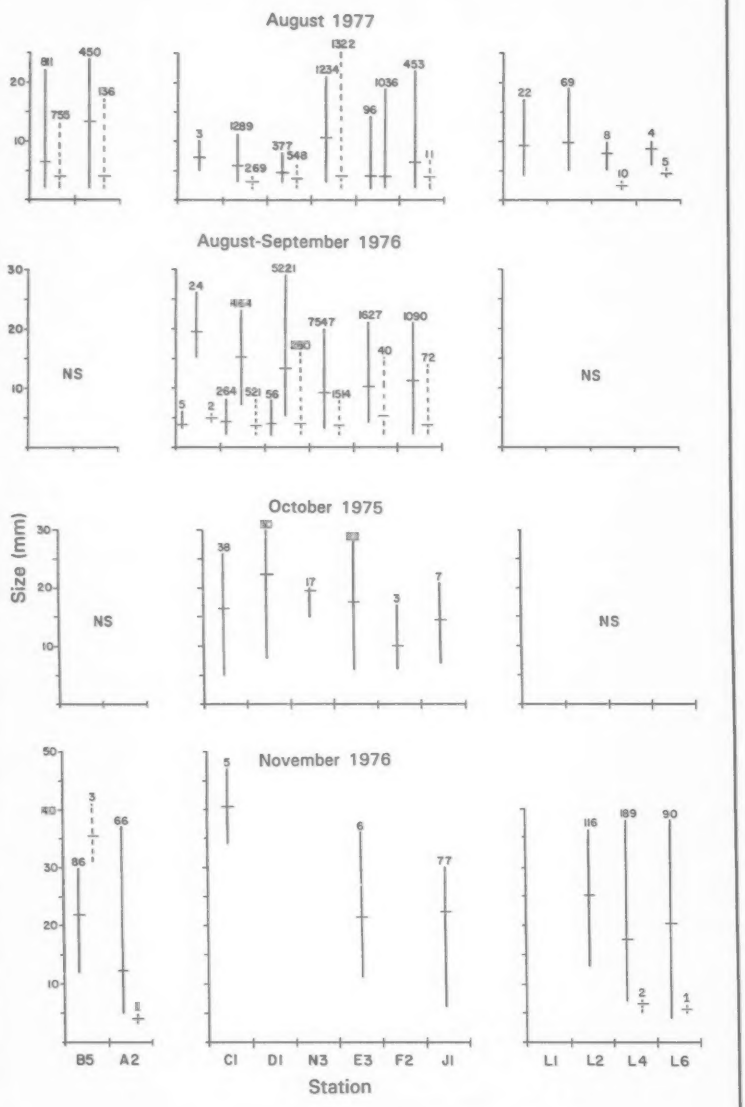

Figure 6

Range and mean size of *Urophycis chuss* in neuston and bongo collections at stations off Virginia and New Jersey. Solid and dashed lines indicate neuston and bongo collections, respectively. Horizontal lines show mean values. Two neuston ranges are shown if more than one size-mode is present. NS = no samples taken; numbers = no. larvae/1000m^3.

central and northern MAB where water depth was 40–60 m. *Urophycis chuss* was the only species of larval hake found in summer collections, and accounted for 80% of all hakes collected during this 2-year study.

Most *U. regia* in the present study were collected in November, but some larvae or neustonic juveniles were collected from October to May. *Urophycis regia* in the MAB is reported to spawn from late September through November, and possibly to February, with peak activity in October (Barans & Barans 1972). *Urophycis regia* was most abundant during fall in the southern MAB in the relatively shallow (41–43 m) midshelf area. Size range of *Urophycis regia* collected in this area was 2–34 mm, and although some of the larger specimens may have drifted from deeper water, small larvae were most likely spawned on the shallower central shelf. Evidence of *U. regia* spawning in shallow water was also found in October 1975 off New Jersey where larvae as small as 4mm were found in water as shallow as 12 m. However, not all specimens off New Jersey originated in shallow water; a second group of larvae 6–23 mm in length was found offshore.

The offshore distribution of *U. regia* became quite distinct in winter collections, with abundances being greatest at offshore stations in February 1976, February–March 1977, and May 1977. These *U. regia* were probably spawned in offshore waters of the MAB or in offshore waters of the South Atlantic Bight and transported northward. Larval *U. regia* have been found in abundance in winter collections from offshore waters off North Carolina in the South Atlantic Bight (Fahay 1975, Powles & Stender 1976).

Late-summer spawning by *U. tenuis* occurs in shallow water of the southern Gulf of St. Lawrence and the Scotian Shelf (Markle et al. 1982). Fahay & Able (1989) suggest the existence of a second stock of *U. tenuis* that spawns in deep water during early spring on the slope of Georges Bank, and probably also along the slopes of the Scotian Shelf, southern New England, and the MAB. The present study found direct evidence of spring spawn-

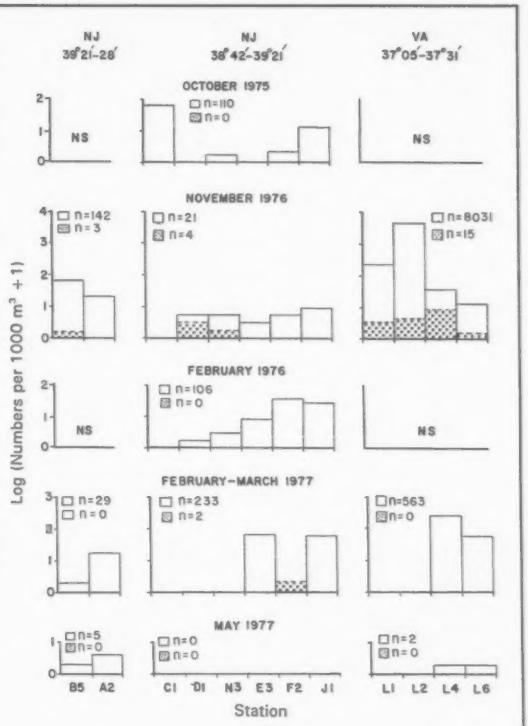

Figure 7

Mean abundance of *Urophycis regia* in neuston and bongo collections at stations off Virginia and New Jersey, October 1975–May 1977. *n* = actual number of larvae collected. Neuston catches denoted by clear histograms, bongo catches denoted by stippled histograms. NS = no samples taken.

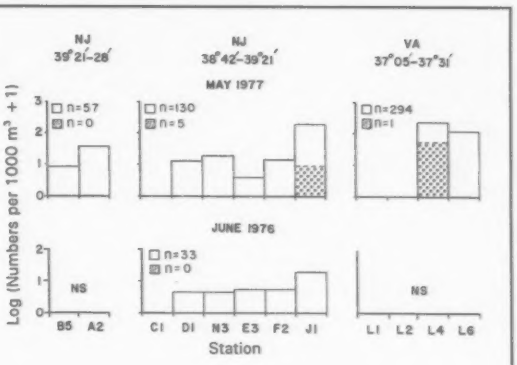

Figure 8

Mean abundance of *Urophycis tenuis* in neuston and bongo collections at stations off Virginia and New Jersey, June 1976 and May 1977. *n* = actual number of larvae collected. Neuston catches denoted by clear histograms, bongo catches denoted by stippled histograms. NS = no samples taken.

ing by *U. tenuis* in deep water of the MAB; in May 1977 *U. tenuis* larvae as small as 3–4 mm were found over the continental break and slope off both New Jersey and Virginia. In June 1976 *U. tenuis* found at offshore stations were 16–38 mm in length. Based on estimated larval and pelagic juvenile growth rates of 10–22 mm/mo (Markle et al. 1982) and demersal juvenile growth rates of ≈30 mm/mo (Fahay & Able 1989), these fish were probably spawned in late April and May.

Fahay & Able (1989), studying young *U. tenuis* in the Georges Bank area, found a shoreward migration with growth. Recruitment to nearshore areas was also indicated in the present study by the increasing size of *U. tenuis* as collections proceeded shoreward. Neustonic juveniles (35–53 mm) were captured in water as shallow as 32 m off the coast of New Jersey.

Urophycis floridana and *U. cirrata*, two southern species of hake, were found off New Jersey and Virginia only in offshore winter collections. The large size and offshore distribution observed for both species suggest that these pelagic juveniles may have been transported northward into the study area. Larvae of *U. earlli*, another species found south of the MAB, are rare and remain undescribed, but this species may also occur occasionally in offshore waters of the MAB during winter. Hildebrand & Cable (1938) expected *U. earlli* to be a winter spawner after collecting three juveniles (37, 75, 103 mm) in March and April off North Carolina, and Fahay (1975) collected a few neustonic *U. earlli* in winter in the South Atlantic Bight.

Phycis chesteri larvae and pelagic juveniles appeared at offshore stations in fall and winter off Virginia and New Jersey. This larval distribution concurs with Wenner (1983) who found adult *P. chesteri* generally at depths >183 m on the continental slope from 36°N to 47°N in the western North Atlantic, and noted that spawning off Virginia took place between late September and April, with peak spawning occurring in December and January. Methven & McKelvie (1986) collected 51 *P. chesteri* larvae and pelagic juveniles along the edge of the continental shelf in the MAB, Grand Bank, and Labrador Shelf, and based on estimated growth rates suggested that most spawning occurs in October.

This study has shown the spatial and temporal distribution of hake larvae in the MAB to be more complex than previously thought. Additional taxonomic characters, particularly ontogenetic pigment patterns, are still needed in order to routinely identify small hake larvae, and more research is needed to explain the observed patterns of larval distribution. Of particular interest is an understanding of the processes that result in the northward transport of larvae and

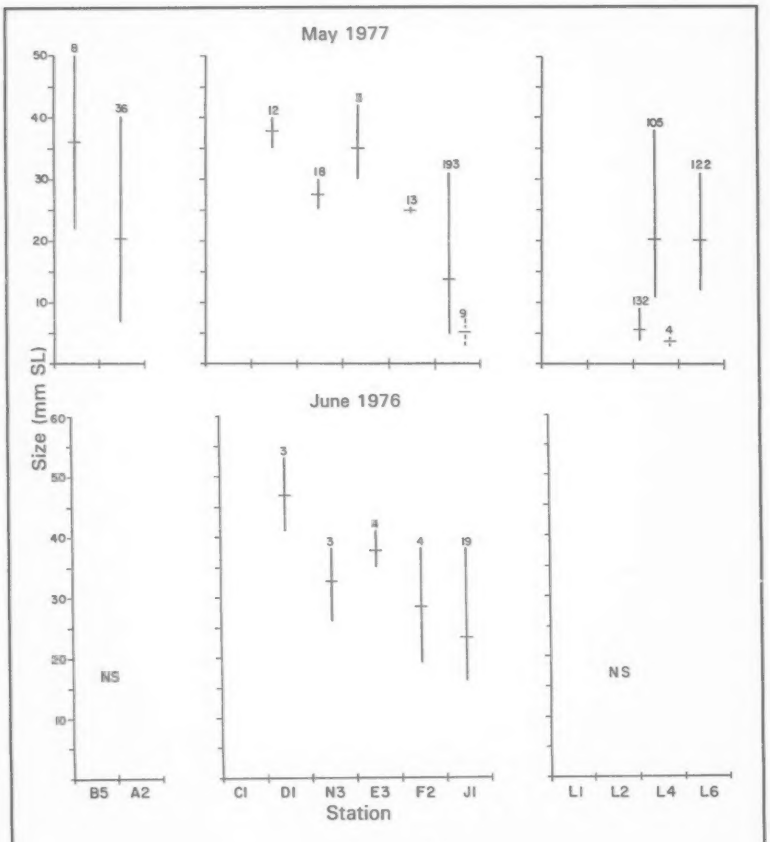

Figure 9

Range and mean size of *Urophycis tenuis* in neuston and bongo collections at stations off Virginia and New Jersey. Solid and dashed lines indicate neuston and bongo collections, respectively. Horizontal bars show mean values. Two neuston ranges are shown if more than one size-class is present. NS = no samples taken; numbers = no. larvae/1000m^3.

pelagic juveniles of southern species into the MAB. Assuming that these individuals are transported northward by the Gulf Stream, it remains to be shown how they leave the influence of this current and move shoreward.

Acknowledgments

Collections serving as the basis of this research were supported by the U.S. Dept. of the Interior, Bureau of Land Management Contracts 08550-CT-5-42 and AA550-CT6-62. We thank J. Musick, J. Olney, C. Baldwin, J. Lyczkowski-Shultz, and especially M. Fahay for reviewing the manuscript. Adult meristic data was provided, in part, by J. Musick and D. Cohen. This work initially comprised a portion of a thesis submitted as partial requirement for the MA degree at the College of William and Mary.

Citations

Barans, C. A., & A. C. Barans
1972 Eggs and early larval stages of the spotted hake, *Urophycis regius*. Copeia 1972 (1):188–190.

Bartlett, M. R., & R. L. Haedrich
1968 Neuston nets and South Atlantic larval blue marlin. Copeia 1968 (3):469–474.

Bigelow, H. B., & W. C. Schroeder
1953 Fishes of the Gulf of Maine. U.S. Fish. Wildl. Serv. Fish. Bull. 74 (vol. 53), 577 p.

Comyns, B. C.
1987 Identification and distribution of *Urophycis* (Gill) and *Phycis* (Artedi) larvae and pelagic juveniles in the Middle Atlantic Bight. M.A. thesis, Va. Inst. Mar. Sci., Coll. William & Mary, Williamsburg, 130 p.

Craddock, J. E.
1969 Neuston fishing. Oceanus 15:10–12.

Dingerkus, G., & L. Uhler
1977 Enzyyme clearing of alcian blue stained small vertebrates for demonstration of cartilage. Stain Technol. 52:229–232.

Dunn, J. R., & A. C. Matarese
1984 Gadidae: Development and relationships. *In* Moser, H.G., et al. (eds.), Ontogeny and systematics of fishes, p.283–289. Spec. publ. 1, Am. Soc. Ichthyol. Herpetol. Allen Press, Lawrence KS.

Fahay, M. P.
1975 An annotated list of larval and juvenile fishes captured with surface-towed meter net in the South Atlantic Bight during four R/V *Dolphin* cruises between May 1967 and February 1968. NOAA Tech. Rep. NMFS SSRF-685, 39 p.
1983 Guide to the early stages of marine fishes occurring in the western North Atlantic Ocean, Cape Hatteras to southern Scotian Shelf. J. Northwest Atl. Fish. Sci. 4, 423 p.

Fahay, M. P., & K. W. Able
1989 White hake, *Urophycis tenuis*, in the Gulf of Maine: spawning seasonality, habitat use, and growth in young of the year and relationships to the Scotian Shelf population. Can. J. Zool. 67:1715–1724.

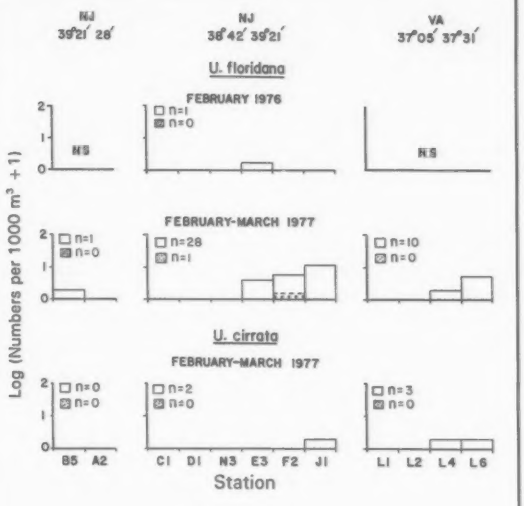

Figure 10

Mean abundance of *Urophycis floridana* and *U. cirrata* in neuston and bongo collections at stations off Virginia and New Jersey, February 1976 and February–March 1977. *n* = actual number of larvae collected. Neuston catches denoted by clear histograms, bongo catches denoted by stippled histograms. NS = no samples taken.

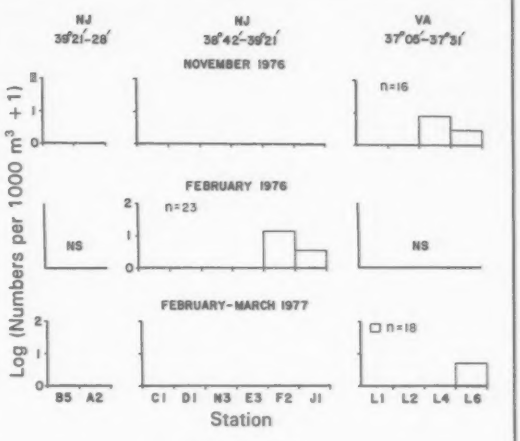

Figure 11

Mean abundance of *Phycis chesteri* in neuston collections at stations off Virginia and New Jersey, during February 1976, November 1976, and February–March 1977. *n* = actual number of larvae collected. Neuston catches denoted by clear histograms, bongo catches denoted by stippled histograms. NS = no samples taken.

Hermes, R.
1985 Distribution of neustonic larvae of hakes *Urophycis* spp. and fourbeard rockling *Enchelyopus cimbrius* in the Georges Bank Area. Trans. Am. Fish. Soc. 114:604–608.

Hildebrand, S. F., & L. E. Cable
1938 Further notes on the development and life history of some teleosts at Beaufort, N.C. Bull. U.S. Bur. Fish. 48:505–642.

Hoese, H. D., & R. H. Moore
1977 Fishes of the Gulf of Mexico, Texas, Louisiana, and adjacent waters. Texas A&M Univ. Press, College Station, 327 p.

Kendall, A. W. Jr., & N. A. Naplin
1981 Diel-depth distribution of summer ichthyoplankton in the Middle Atlantic Bight. Fish. Bull., U.S. 79:705–726.

Leim, A. H., & W. B. Scott
1966 Fishes of the Atlantic Coast of Canada. Fish. Res. Board Can., Bull. 155, 485 p.

Leviton, A. E., R. H. Gibbs Jr., E. Heal, & C. E. Dawson
1985 Standards in herpetology and ichthyology: Part l. Standard symbolic codes for institutional resource collections in herpetology and ichthyology. Copeia 1985 (3):802–832.

Markle, D. F.
1982 Identification of larval and juvenile Canadian Atlantic gadoids with comments on the systematics of gadid subfamilies. Can. J. Zool. 60:3420–3438.

Markle, D. F., D. A. Methven, & L. J. Coates-Markle
1982 Aspects of spatial and temporal cooccurrence in the life history states of the sibling hakes, *Urophycis chuss* (Walbaum 1792) and *Urophycis tenuis* (Mitchill 1815) (Pisces:Gadidae). Can. J. Zool. 60:2057–2078.

McGowan, J. A., & D. M. Brown
1966 A new opening-closing paired zooplankton net. Ref. 66-23, Univ. Calif., Scripps Inst. Oceanogr., La Jolla, 56 p.

Methven, D. A.
1985 Identification and development of larval and juvenile *Urophycis chuss*, *U. tenuis*, and *Phycis chesteri* (Pisces, Gadidae) from the Northwest Atlantic. J. Northwest Atl. Fish. Sci. 6:9–20.

Methven, D. A., & D. S. McKelvie
1986 Distribution of *Phycis chesteri* (Pisces: Gadidae) on the Grand Bank and Labrador Shelf. Copeia 1986 (4):886–891.

Miller, D., & R. R. Marak
1959 The early larval stages of the red hake, *Urophycis chuss*. Copeia 1959 (3):248–250.

Miller, G. L., & S. C. Jorgenson
1973 Meristic characters of some marine fishes of the western Atlantic Ocean. Fish. Bull., U.S. 71:301–312.

Musick, J. A.
1973 A meristic and morphometric comparison of the hakes, *Urophycis chuss* and *Urophycis tenuis* (Pisces, Gadidae). Fish. Bull., U.S. 71:479–488.

Potthoff, T.
1984 Clearing and staining techniques. *In* Moser, H.G., et al. (eds.), Ontogeny and systematics of fishes, p. 35–37. Spec. publ. 1, Am. Soc. Ichthyol. Herpetol. Allen Press, Lawrence KS.

Powles, H., & B. W. Stender
1976 Observations on composition, seasonality and distribution of ichthyoplankton from MARMAP cruises in the South Atlantic Bight in 1973. Tech. Rep. 11, MARMAP Contrib. 118, NMFS MARMAP Prog. Office, Contract 6-35147, and S.C. Wildl. Mar. Resour. Dep., Columbia, 47 p.

Serebryakov, V. P.
1978 Development of the spotted hake, *Urophycis regius*, from the Northwestern Atlantic. J. Ichthyol. [Engl. transl. Vopr. Ikhtiol.] 18:793–799.

Svetovidov, A. N.
1948 Gadiformes. Fauna of the USSR. Vol IX (4), 304 p. [Engl. transl. from Russ. by Israel Prog. Sci. Transl. for Natl. Sci. Found., Wash. DC, 1962.]

Taylor, W. R., & G. C. Van Dyke
1985 Revised procedures for staining and clearing small fishes and other vertebrates for bone and cartilage study. Cybium 9:107–119.

Wenner, C. A.
1983 Biology of the longfin hake, *Phycis chesteri*, in the western North Atlantic. Biol. Oceanogr. 3:41–75.

Appendix Table 1

Sources of material, collection data, and lengths of hakes used in radiographic analyses of meristics and pterygiophore interdigitation. Standard acronyms for resource collections follow Leviton et al. (1985).

Species	Collection #	Location	No. specimens	SL(mm)
U. earlli	USNM 025295	N. Carolina	1	124
	USNM 155746	32°34'N,79°05'W	1	55
	USNM 155747	Wilmington, NC	2	50–60
	USNM 226521	32°29'N,79°42'W	3	88–129
	USNM 226522	32°29'N,79°41'W	3	91–122
	USNM 226523	32°29'N,79°41'W	1	113
	USNM 226524	33°14'N,78°24'W	1	130
	USNM 226525	34°14'N,78°24'W	1	82
	USNM 226526	32°28'N,79°42'W	4	91–132
	USNM 226530	32°29'N,79°40'W	4	96–157
	USNM 226531	32°29'N,79°41'W	5	138–166
	USNM 226543	28°48'N,80°38'W	1	74
	VIMS 06557	Gulf of Mexico	1	195
U. floridana	USNM 073010	Key West, FL	1	63
	USNM 116729	Beaufort, NC	16	35–49
	USNM 131586	26°18'N,83°09'W	1	59
	USNM 155738	Texas	1	77
	USNM 155782	Cape Canaveral, FL	1	86
	USNM 155783	St. Augustine, FL	1	67
	USNM 156146	Pelican-Stn. 120–5	1	94
	USNM 214118	Brickhill Creek, GA	5	64–75
	VIMS 03756	Silver Bay	1	165
	VIMS 04142	Brunswick Sound, GA	5	78–113
	VIMS 04152	Silver Bay	4	52–85
	VIMS 04192	Pensacola, FL	2	81–109
	VIMS 04193	Cumberland Id., GA	2	129–184
	VIMS 04194	N.Cumberland R., GA	2	133–157
	VIMS 04195	Santa Rosa Sound, FL	1	66
	VIMS 04196	Oregon S646	1	185
U. cirrata	GCRL 433	29°09'N,88°33'W	1	281
	GCRL 436	29°22'N,87°30'W	1	290
	GCRL 525	29°11'N,88°07'W	3	318–343
	GCRL 2783	Louisiana	4	109–130
	GCRL 17534	28°27'N,90°38'W	1	145
	USNM 115686	22°23'N,91°45'W	1	141
	USNM 116929	Tortugas, FL	1	140
	USNM 155642	29°04'N,88°44'W	1	114
	USNM 218169	29°18'N,88°51'W	1	108
	USNM 218192	28°58'N,84°44'W	1	109
	USNM uncat.	24°32'N,83°36'W	1	197
	USNM uncat.	28°59'N,88°48'W	1	198
	USNM uncat.	28°35'N,91°12'W	2	186–220
P. chesteri	USNM 025903	Newport, RI	17	73–98
	USNM 026081	Martha's Vineyard, MA	5	68–83
	USNM 026097	No data	1	79
	USNM 028732	No data	9	58–76
	USNM 083821	GA, SC	12	54–65
	USNM uncat.	Atlantic Arctus Exped.	6	105–147
	USNM 092695	No data	1	63
	VIMS 05238	36°43'N,74°39'W	4	67–150

Appendix Table 2

A summary of key meristic, morphometric, and pterygiophore interdigitation characters used to separate *Phycis chesteri* and six species of *Urophycis*. Given for each species: length (mm) at which characters are attained (upper), morphometic or meristic value (middle), and explanatory notes (**bold** letters in parentheses). Percentages indicate proportion of a species that possesses a particular character.

	Epibranchial gill rakers	Caudal-fin rays	2nd dorsal-fin rays	1st dorsal-fin rays	Abdominal vertebrae	Anal-fin pterygiophores anterior to first haemal spine	Interdigitation of second dorsal-fin pterygiophore	Body depth at vent as %SL	Height of pelvic-fin base as percent of mandible length	
U. tenuis	11–13 mm 2 (95%) **(A)**	11 mm ≥35 (99%)	14 mm ≥53 (93%)	15 mm ≤12	4 mm ≥15 **(H)**	8–9 mm >6 (2%) <6 (60%)	≥9 (88%) **(L)**	12 mm 19.0–21.1 **(M)**	6–19 mm 24–42 **(N)**	20–34 mm 26–37
U. chuss	11–13 mm 3 (97%)	8–9 mm <35	14 mm ≥53 **(E)**	14 mm ≤12	4 mm ≥15 (87%) **(I)**	8–9 mm >6 (45%) <6 (5%)	12 mm ≥9 (52%)	12 mm 17.6–19.7	6–19 mm 20–39	20–34 mm 15–22
U. regia	11–13 mm 3 (97%)	8–9 mm <35	14 mm ≤52 **(E)**	13 mm <12 **(G)**	4 mm ≤14 **(J)**	8–9 mm >6 (57%) <6 (2%)	12 mm <9	12 mm 18.4–21.7	6–19 mm 19–33	20–34 mm 12–28
U. floridana	2	<35	≥53	13 (33%)	≥15 (98%) **(K)**	>6 (74%) <6 (0%)	≥9 (73%)	12 mm 17.7–19.8	15–19 mm 29–36	20–34 mm 23–37
U. earlli	2	<35 **(C)**	>53	<12 **(G)**	≤14 (87%) **(K)**	>6 (85%) <6 (0%)	<9			
U. cirrata	3	<35	>53 **(F)**	≤12	≥15 **(K)**	>6 (0%) <6 (82%)				20–34 mm 31–39
P. chesteri	16–18 mm 4–5 **(B)**	<35 (77%) **(D)**	≥53	≤12	≥15 (88%)	>6 (0%)	≥9 (38%)	12 mm 21.0–23.4	6–19 mm 44–74	20–34 mm 46–61 **(O)**

Notes

(A) *U. tenuis* occasionally possessed a third gill raker, but in only one specimen (n=167) were three gill rakers found on both left and right sides.

(B) Three epibranchial gill rakers had developed by 13 mmSL.

(C) *U. earlli* has never been recorded with >31 caudal-fin rays, while all other hake commonly have >31 rays.

(D) Although ranges in *U. tenuis* and *P. chesteri* overlapped, numbers of caudal-fin rays separated over 40% of *P. chesteri* (<34 rays) from more than half of *U. tenuis* (>36 rays).

(E) Numbers of second dorsal-fin pterygiophores separated *U. regia* from *U. chuss* at sizes as small as 6 mmSL. Although not shown here, one specimen of *U. chuss* (n=106) possessed 52 second dorsal-fin rays.

(F) Although ranges overlap, almost 70% of *U. cirrata* had at least 64 second dorsal-fin rays, while *P. chesteri* and other species of *Urophycis* (except *U. earlli*) had <64 rays.

(G) *U. regia* and *U. earlli* have never been found with >10 and 11 first dorsal rays, respectively, while over 80% of *U. floridana* (n=45) possessed >11 rays.

(H) Numbers of abdominal vertebrae helped identify *U. tenuis* larvae <10 mm, the size below which numbers of caudal-fin rays no longer afford confident identifications. See Results.

(I) Numbers of abdominal vertebrae aided in the identification of *U. chuss* in summer collections from the MAB when this was the only species of hake found. See Results.

(J) Only eight specimens of *U. regia* from the Middle Atlantic Bight (n=698) had 15 abdominal vertebrae, and seven of these specimens had an anomalous 15th vertebra.

(K) *U. floridana* and *U. cirrata* commonly possessed 16 or 17 abdominal vertebrae, but *U. earlli* has never been recorded with this many.

(L) Numbers refer to the interneural space into which points the pterygiophore supporting the first ray of the second dorsal fin. The first interneural space was defined as the space anterior to the first haemal spine.

(M) Specimens of all species were cleared and stained.

(N) Size ranges do not define size when character first became useful, but bracket the size-range over which particular morphometric values were found.

(O) At sizes >35 mmSL, *P. chesteri* was similar to *Urophycis* with respect to this character.

Maturation, reproductive seasonality, fecundity, and spawning frequency in *Lutjanus vittus* (Quoy and Gaimard) from the North West Shelf of Australia

Tim L.O. Davis
Grant J. West

CSIRO Division of Fisheries, Marine Laboratories,
GPO Box 1538, Hobart, Tasmania 7001, Australia

Abstract.—The reproductive biology of *Lutjanus vittus*, an important component of the trawl-fishery catch from the North West Shelf of Australia, was determined from random, stratified trawls made every 2 mo during August 1982–October 1983. The smallest mature female was 142 mmFL; half of the females at 154 mm (estimated 1+yr of age) were mature. The major spawning season was from September to April, although some spawning occurred in other months. A semilunar pattern of spawning activity was observed, with peaks in the proportion of spawning females ~3 d after the new moon and 6 d after the full moon. Individuals spawn about 22 times each lunar month. The diel changes in proportion of fish with ripe oocytes and early- and late-stage postovulatory follicles, together with data on maximum oocyte diameter, suggest that most individuals spawn between 11:00 and 15:00 h on peak spawning days. The relationship between batch fecundity (F) and fish fork length (L in mm) was exponential ($F=3.656\times10^{-6}\ L^{4.093}$) and with fish weight (W, g) was linear ($F=124.2\times W-3081$). Unlike gonad weight, batch fecundity did not decline as the spawning season progressed.

Manuscript accepted 17 February 1993.
Fishery Bulletin, U.S. 91:224-236 (1993).

Lutjanids are of great importance in fisheries throughout the tropics and subtropics, and *Lutjanus vittus* distributed throughout the Indo-West Pacific is a highly valued component of the multispecies trawl fishery of the North West Shelf of Australia (NW Shelf), comprising ~4% of the total catch of ~165,000 t between 1972 and 1980 (Jernakoff & Sainsbury 1990). Its early life history has been studied in Japan (Mori 1984); its biology, in New Caledonia (Loubens 1980a,b). Information on growth and mortality of this species on the NW Shelf has recently been published (Davis & West 1992). However, there is no published information on the reproductive biology of *L. vittus* that would pertain to the management of this fishery on the NW Shelf.

Some information on the reproductive biology of over 40 species of lutjanids is available (see review by Grimes 1987). Many studies have indicated that lutjanids are multiple spawners, based on the evidence of multimodal size-frequency distributions of oocytes, but techniques such as the hydrated oocyte and postovulatory follicle methods (Hunter & Goldberg 1980, Hunter & Macewicz 1980), for measuring spawning frequency in marine fishes, have not been applied to lutjanids (Everson et al. 1989). In this paper we present data on oocyte development, size-at-maturity of females, and batch fecundity in *L. vittus* from the NW Shelf. We also demonstrate both diel and semilunar spawning periodicity through an analysis of the temporal distribution of hydrated oocytes and early- and late-stage postovulatory follicles, and provide estimates of spawning frequency and annual fecundity.

Materials and methods

Specimens were obtained from the CSIRO North West Shelf program between August 1982 and October 1983 (Young & Sainsbury 1985). Details of the two-monthly random stratified trawl surveys of shelf waters within latitudes 116°E and 119°E are given in Davis & West (1992). A subsample of 20–40 *Lutjanus vittus*, which approximately represented the size-frequency composition of the total catch (Kimura 1977), was selected from each random trawl. Fork length was measured to the nearest 1 mm and total weight to the nearest 1 g. Fish were sexed and up to 200 ovaries per cruise were fixed in 10% formalin in seawater for histological and whole oocyte examination. Additional biological samples were collected from nonrandom trawls to investigate lunar and diel periodicity in spawn-

ing. Samples were also obtained at 4 h intervals during 6–9 October 1988 to further investigate diel periodicity of spawning.

In the laboratory, ovaries were blotted dry and then weighed to the nearest 0.1 g. Whole oocytes were obtained by cutting a complete cross-section 1–2 mm thick from the middle of the ovary, and teasing the oocytes apart with needles. Oocytes were examined in water under a stereomicroscope using transmitted light and brightfield illumination. We measured maximum oocyte diameter (MOD) as the diameter of the largest oocyte (to the nearest 20 μm) in the sample. Because oocytes were basically spherical, the orientation of oocytes with respect to the line of measurement was random.

The size-frequency distribution of oocytes within ovaries at different stages of maturity was determined. Sections 1–2 mm thick were cut from the middle of one ovary, the oocytes teased apart with needles, and further separated by immersion in an ultrasonic bath for ~5 min. Oocytes were pipetted into grooves on a perspex microscope slide and examined on a moving stage attachment on a stereomicroscope at 50×, using transmitted light. Orientation was random. As well as measuring each oocyte, we also noted its appearance so that the stage of development could be assessed.

We used whole-oocyte staging to assess ovarian maturity (Hilge 1977, Forberg 1983, West 1990). Our three-stage scheme (Table 1) differed from Hilge's (1977) in that we distinguished late-migratory nucleus oocytes (Fig. 1b) from yolked oocytes (Fig. 1a) by the presence of some translucence at the periphery of the vitelline area (West 1990). Ovaries with late-migratory nucleus oocytes or hydrated oocytes were considered ripe (Fig. 1c).

The relative gonadal index (RGI) was used to quantify the reproductive cycle (Erickson et al. 1985). This index is independent of body size and is based on the model, $W=\alpha_i S^{\beta i}$, where W is gonad weight (g), S is ovary-free body weight (kg), and α_i and β_i are parameters estimated for maturity stage i. As β_i did not differ significantly between the three maturity stages (ANCOVA, $F=1.304$, df 2,1046, $p=0.27$), a common β was used.

To study short-term spawning rhythms and to verify whole-oocyte staging, we histologically examined 477 ovaries from one cruise during the height of the spawning season (November–December 1982). Histological sections were 10 μm thick and stained with haematoxylin and eosin. The sequence of oocyte maturation is similar in most teleost species (Wallace & Selman 1981). We used the histological criteria of Yamamoto (1956) for assigning oocytes to developmental stages.

The presence of postovulatory follicles was noted in the histological material. These follicles are readily

Table 1

Whole-oocyte staging scheme in *Lutjanus vittus* based on appearance of the most advanced oocytes (modified from Hilge 1977) and corresponding histological stages (Yamamoto 1956) used to describe ovarian maturity.

Whole-oocyte stage	Histological stage
1 Unyolked	
Transparent with visible nucleus, becoming granular and translucent with increasing size.	**Perinucleolus stage** Cytoplasm purple, outer cell membrane not differentiated at 400×.
Granular, translucent with brownish tinge, becoming darker with increasing size, but not opaque.	**Yolk-vesicle stage** Pale vacuoles (yolk vesicles) and a thin but distinct pink-staining zona radiata both present.
2 Yolked	
Completely opaque except for perivitelline border.	**Yolk-granule stage** Yolk granules appear as pink spheres. Fat vesicles coalesce to form larger vesicles around the central nucleus at the end of this stage.
	Early-migratory nucleus stage Nucleus moves out from center of the cell, being replaced by one or two fat vesicles.
3 Ripe	
Distinguished from Yolked stage when parts of the yolk become translucent.	**Late-migratory nucleus stage** Nucleus moves to the periphery of the cell and some of the yolk granules coalesce.
Oocyte is translucent except for the oil droplet.	**Hydrated-oocyte stage** Yolk granules coalesce to form a uniform pink-staining mass.

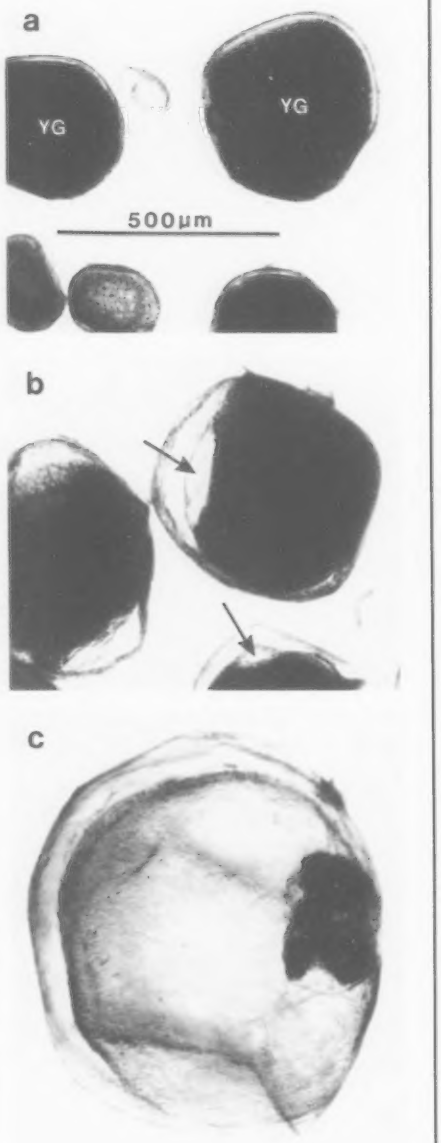

Figure 1
Photomicrographs of whole oocytes of *Lutjanus vittus* representing **(a)** yolk granule (YG) stage, in which the oocyte is completely opaque except for the translucent perivitelline border; **(b)** late-migratory nucleus stage, in which parts of the peripheral yolk have coalesced and become translucent (arrowed); and **(c)** ripe-oocyte stage, in which whole oocyte is translucent, except for the oil droplet. Scale bars 500µm.

identifiable within 12 h after spawning because the folds of the follicle layer are still discrete (Hunter & Goldberg 1980), but they become progressively more compact until they appear as a solid mass of cells. We recorded an early stage where the lumen was open and the wall of the follicle clearly visible (Fig. 2a) and a late stage where the follicle had collapsed and the follicle layer could not be traced around its periphery (Fig. 2b).

Batch fecundity was determined using the gravimetric method (Hunter et al. 1985) to count numbers of hydrated but unovulated oocytes in weighed subsamples of formalin-fixed ovaries. Each subsample consisted of a wedge of tissue extending from the periphery to the lumen of the ovary. In order to estimate the energetic costs of spawning, the dry weight of hydrated oocytes was determined in nine fish. About 100 oocytes were removed from each formalin-fixed ovary. Oocytes

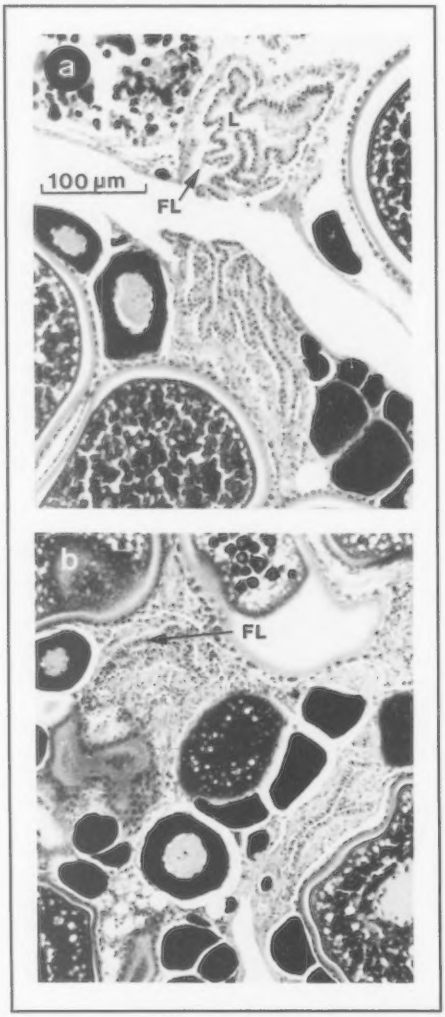

Figure 2
Photomicrographs of transverse section of *Lutjanus vittus* ovary stained with haematoxylin and eosin, showing **(a)** early-stage postovulatory follicles, in which the lumen (L) is open and the folds of the follicle layer (FL) are discrete, and **(b)** late-stage postovulatory follicles, in which the follicle has collapsed and the follicle layer is no longer discrete. FL = follicle layer; L = lumen. Scale bars 100 µm.

were washed in freshwater, counted, dried for at least 24 h at 60°C, and weighed to the nearest 0.1 mg.

Size-at-maturity ($L_{0.50}$) was defined as the smallest length at which half of the fish had yolked or ripe-stage ovaries. Weighted least-squares nonlinear regression was used to select the model (Gompertz curve) that best described the relationship between proportion of mature fish and fish length. The simplest model was chosen in which higher parameter models did not significantly improve the fit using the *F*-ratio statistic (Schnute 1981).

RGI's were log-transformed to stabilize variances, and a 2×2 factorial ANOVA was used to test for differences in RGI's between samples collected in August and October and between consecutive years. Differences in RGI over the four periods sampled during the main spawning season (September 1982–April 1983) were tested using ANOVA, and the period effect was partitioned into a linear component and deviations from a linear component to test for trends.

The log-likelihood ratio χ^2 was used to test for independence in contingency-table data (frequency of fish with and without postovulatory follicles by time of day, month, etc.). Cells with expected frequencies <5 were excluded from statistical tests. Repeated-measures ANOVA was used to test for differences in the numbers of eggs/mg tissue taken from the inner and outer walls, and from anterior, middle, and posterior parts of the ovary of five fish. The relationship between log fecundity and log length at different times of the spawning season was examined using ANCOVA.

Results

Maturation of ovaries

Size-frequency and stage of whole oocytes in ovaries representing the developmental sequence of maturation (Fig. 3) indicated that the size of oocytes is correlated with their stage of development but there is considerable overlap between stages. The pattern of oocyte development is asynchronous. Apart from the inference that *L. vittus* is a multiple spawner, the number of spawnings cannot be inferred from modes in the size-frequency distribution (Hunter & Goldberg 1980).

Size-at-maturity

Ovaries were considered mature if their most advanced oocytes were yolked or ripe, as judged by the appearance of the whole oocyte. To avoid including mature fish that had regressed to an unyolked stage towards the end of the spawning season, only data taken between September and February were used. The smallest ripe female observed was 142 mm long (Fig. 4). All fish >220 mm were mature (Fig. 5). The Gompertz curve was fit to the proportion of mature females by 10 mm length groupings:

$$Y(t) = y_\infty e^{-e^{-g(t-t_0)}}, \quad (1)$$

where $Y(t)$ = proportion mature at length t, and y_∞, g, and t_0 are parameters. This provided the best fit with the least number of parameters. The length at which 50% of females were mature ($L_{0.50}$) was calculated to be 154 mm. $L_{0.50}$ is reached at age-1 (Davis & West 1992), and all females at age-3 and older were mature (Fig. 5).

Spawning season

Only data on fish >200 mm were used to describe seasonal changes. The main spawning season appears to be September–April (Fig. 6). The presence of fish with hydrating oocytes throughout the year indicates the spawning season is protracted, although only four fish with hydrated oocytes were collected in June and August 1983. Some mature fish had only unyolked oocytes in their ovaries during April–August (Fig. 6).

The mean relative gonadal index (RGI) peaked in September–October and then declined gradually, reaching its lowest value in June (Fig. 6). There was a marked and significant increase in mean RGI during August–October (2×2 factorial ANOVA, month effect, F=309, df 1,339, p<0.001), with the same increase in both years (interaction effect not significant: F=2.4, p>0.1), and there was a weak but significant difference between years (F=4.3, p<0.05). There were significant differences in RGI between the four periods sampled during the main spawning season, September 1982–April 1983 (ANOVA, F=50.5, df 3,706, p<0.001), predominantly due to a linear component (F=130.1, df 1,706, p<0.001) caused by a decline in RGI over this period (slope –0.236, SE 0.021). On the other hand, there was no significant difference in proportion of ripe fish throughout this period (likelihood ratio x^2 = 6.3, df 3, p=0.10), nor any indication of a decline in the proportion. This suggests that spawning activity remained at about the same level during the main spawning period but that gonads of individual fish were depleted by successive spawnings.

Lunar periodicity in spawning activity

Ovaries of mature fish (n=374) sampled in November–December 1982 were examined histologically for evidence of spawning activity. Data were grouped into 1 d periods according to moon age. Two measures of spawning were used: proportion of fish with postovulatory

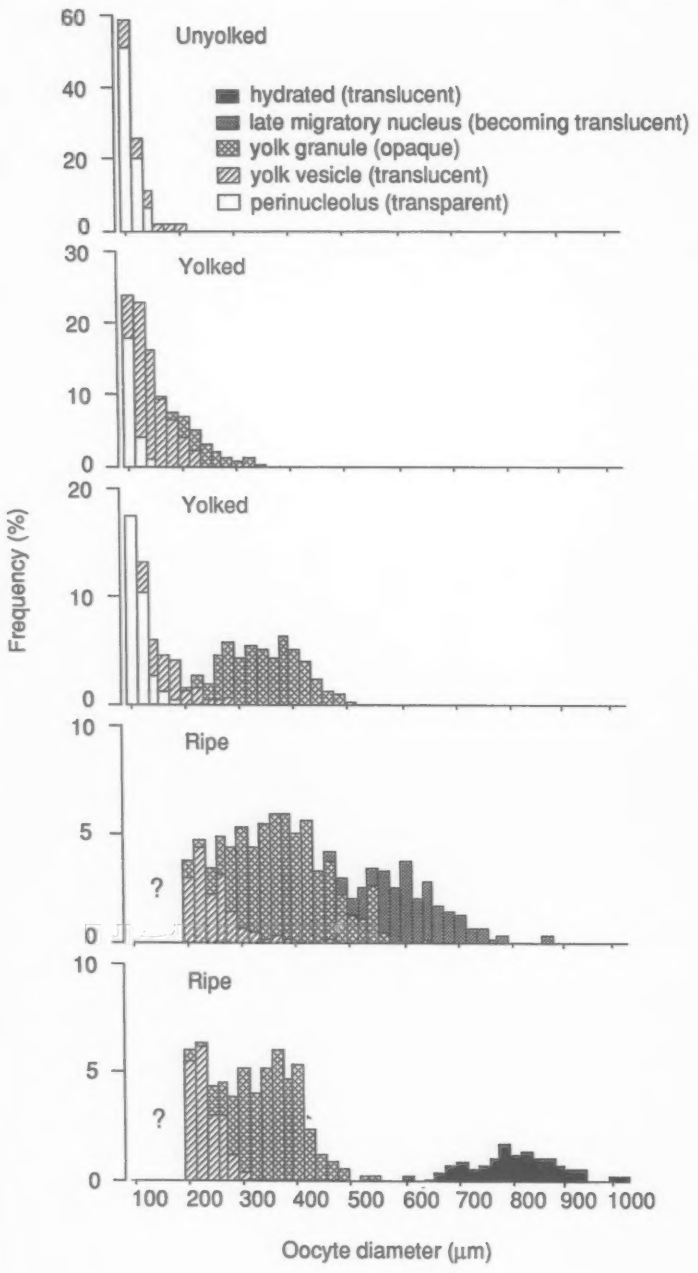

Figure 3

Oocyte size-frequency distribution and oocyte stage, by 20 µm intervals, in *Lutjanus vittus* ovaries representing the developmental sequence of maturation (see Table 1 for details). An ovary classified as Ripe indicates that it contained late-migratory nucleus-stage oocytes or ripe oocytes. Only oocytes >200 µm diameter were measured in Ripe stage-5 ovaries, whereas in other ovaries all oocytes >100 µm were measured.

follicles, and proportion of fish with late-migratory nucleus or hydrated-oocyte stages. The former showed a clear cyclical pattern with two peaks of spawning activity during the month of sampling (Fig. 7). Various sinusoidal curves were fit to the proportion of mature fish with postovulatory follicles sampled each day. The following model, which has a period of 29 d and allows one or two peaks of possibly unequal heights per period, was chosen:

$$y = A+B \sin(x) + C \cos(x) + D \sin(2x) + E \cos(2x), \quad (2)$$

where $t=\frac{1}{29} \times 2\pi$, and t = moon age (d). A regression weighted by the number (n) in each sample was fit to arcsine (angular) root-transformed data. Proportions of 1 were replaced by $n-\frac{1}{4}$ divided by n. The fitted model accounted for 85.9% of variance in the data. The smaller peak occurred 3 d after the new moon, and the larger peak 6 d after the full moon.

No simple pattern of spawning was apparent from the proportion of fish with late migratory nucleus or hydrated oocyte stages captured each day, presumably because such a pattern was confounded by the effects of time of day (see next section). As postovulatory follicles probably persist for a day, and maybe longer in other species (Hunter & Goldberg 1980, Hunter et al. 1986), their detection does not depend on the time of day of sampling.

Diel periodicity in spawning activity

The November–December 1982 samples were also examined for evidence of diel periodicity in spawning. Only mature fish

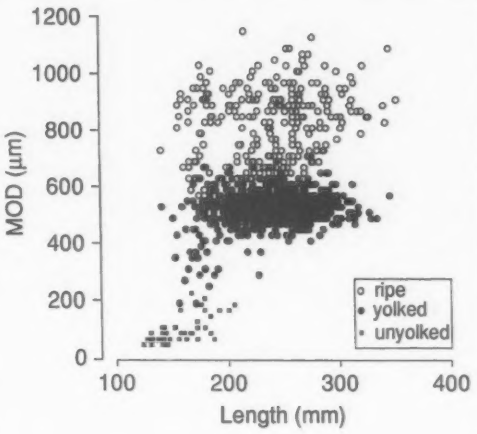

Figure 4

Diameter of the largest oocyte (MOD) of *Lutjanus vittus* by fish length. Ovaries classified as Yolked and Ripe indicate that fish are mature. Data were collected at height of the spawning season (October–February).

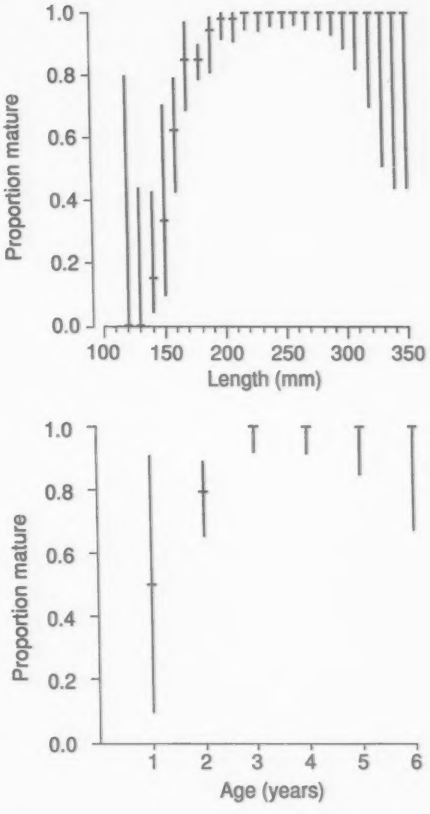

Figure 5

Proportion of total female *Lutjanus vittus* that are mature by 10 mm length-classes and by age-class during the height of the spawning season. Shown are 95% binomial confidence limits. Age data from Davis & West (1992).

caught during days of major spawning activity (lunar days 2–10 and 18–29) were considered. Two measures that proved useful in detecting changes in spawning activity on temporal scales of less than a day were the proportion of mature fish with ripe-stage ovaries based on whole-oocyte staging, and maximum oocyte diameter (MOD).

A clear diel cycle of spawning was evident (Fig. 8). Proportions of ripe-stage fish in samples taken at different times throughout the day were significantly different (likelihood ratio x^2=69, df 7, p<0.001). Proportions of ripe fish were highest between 08:00 and 14:00 h, and no ripe fish were present by 16:00 h. The mixture of ripe and unripe ovaries between 11:00 and 15:00 h could indicate that spawning for that day had already begun and that some of the fish were spent or that only a portion of fish spawned each day. The temporal distribution of MOD showed a similar pattern. Fish about to spawn that day were clearly separable from other fish by MOD at 11:00 h. The MOD's of all but one fish sampled after 15:00 h were the same as nonspawning fish, suggesting that most spawning occurred between 11:00 and 15:00 h on these days, which more or less coincided with rising daytime tides.

Postovulatory follicle data from the same subset of fish also showed a diel pattern (Fig. 9, page 232). The proportion of fish with early- or late-stage postovulatory follicles differed significantly with time of sampling (early-stage likelihood ratio x^2=130, df 7, p<0.001; late-stage likelihood ratio x^2=131, df 7, p<0.001). Fish with early-stage postovulatory follicles were first detected at 12:00 h. By 17:00 h the proportion of fish with early-stage postovulatory follicles had reached its highest level (91%). Thereafter the proportion declined, until by 04:00 h none were present in fish sampled. Late-stage postovulatory follicles followed a similar temporal pattern, with a peak that lagged the early stage by 12–14h. The very few late-stage postovulatory follicles in samples at 17:00 h may have resulted from spawning early that day or late spawn-

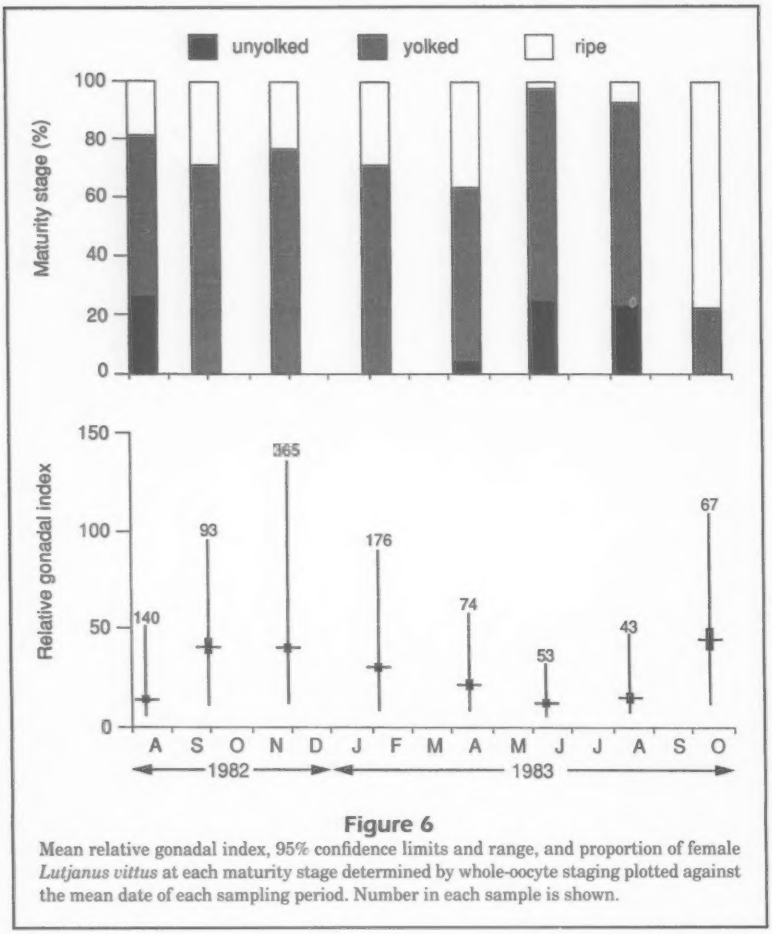

Figure 6

Mean relative gonadal index, 95% confidence limits and range, and proportion of female *Lutjanus vittus* at each maturity stage determined by whole-oocyte staging plotted against the mean date of each sampling period. Number in each sample is shown.

ing on the previous afternoon. In either case, the late stage appears to persist for about 24 h. Only 13% of fish examined from this subset did not have postovulatory follicles, and most of these (74%) were from fish sampled between 09:00 and 15:00 h. This would be consistent with the hypotheses that follicles persist for 24 h or less and that most fish spawn daily during the major periods of spawning activity.

The diel pattern of spawning indicated by data collected in November–December 1982 was supported by further sampling every 4 h over 6–9 October 1988. The proportions of ripe fish in samples taken at different times throughout the day were significantly different (likelihood ratio x^2=110, df 6, p<0.001). Ripe fish were found between 12:00 and 16:00 h (Fig. 10). The temporal distribution of MOD followed the same pattern observed in November–December 1982.

Spawning frequency

As postovulatory follicles in *L. vittus* persist for ~24 h, they provide a good indication of spawning over the previous 24 h and can be used to determine spawning frequency. Parameter A from Eq. 2 provides an estimate of the proportion of females spawning each day averaged over the 29 d lunar cycle. On average, females spawn 21.7 times each lunar cycle (95%CL=19.3–23.9). If we assume that this spawning intensity occurs during October–April, then females spawn at least 150 times each year.

Batch fecundity

In order to determine the most appropriate sites in the ovary from which to take subsamples to determine batch fecundity, the number of eggs/mg tissue was determined for six regions of the ovary of five fish. Wedges of ovary were taken from both inner and outer walls at anterior, middle, and posterior parts of each right-hand ovary. There were no significant differences in numbers of eggs between inside and outside (ANOVA, F=0.016, df 1,4, p=0.91) or anterior, middle, or center (ANOVA, F=1.45, df 2,8, p=0.29) nor any interaction between the effects (ANOVA, F=0.54, df 2,8, p=0.60). A paired t-test indicated that egg counts from a wedge of tissue taken from the middle-outside position did not differ significantly between left and right ovaries (t=–0.008, df 4, p=0.99). Subsequently, batch fecundity was estimated from the mean of three subsamples taken from the anterior, middle, and posterior of either the left or right ovary of 29 fish. The coefficient of variation for estimates from three subsamples was 0.02–0.21, with a mean of 0.11.

The relation between fish length (L, mm) and batch fecundity (F) was best described by the equation

$$F = 3.656 \times 10^{-6} L^{4.093} \quad (F=26.1, \text{ df } 1,27, p<0.001), \qquad \text{(Fig. 11)}$$

and the relation between fish total weight (W, g) and batch fecundity by the equation

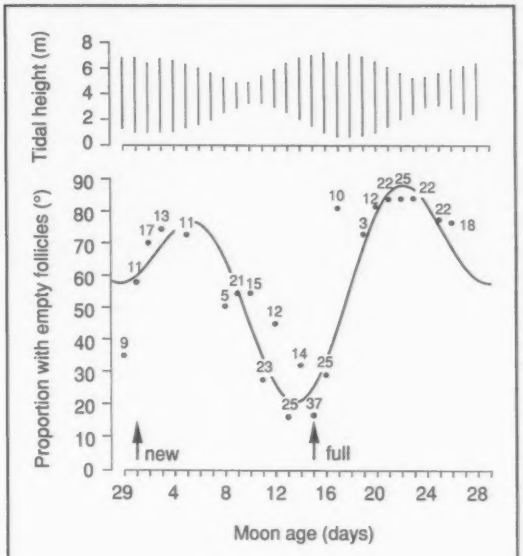

Figure 7

Proportion of mature female *Lutjanus vittus* with early- or late-stage postovulatory follicles plotted against time of sampling (expressed as moon age). A sinusoidal curve with a period of 29 d and two peaks of unequal height were fit to arcsine (angular) root-transformed data. Lunar tide cycle, indicated by maximum and minimum heights of daily tides, has also been plotted, and the number in each sample is shown.

$$F = 124.2 \times W - 3081 \ (F=17.7, \text{df } 1,27, p<0.001).$$

Batch fecundity varied markedly between fish of the same size. As the data were obtained from four different periods during the spawning season, we tested to see whether the different spawning periods could explain some of the variability in batch fecundity. There is some suggestion that batch fecundity might be higher in November and decline over the spawning season, following the seasonal pattern of RGI (Fig. 11). However, in the regression of log fecundity/log length, the test for homogeneity of slopes between sampling periods was found to be not significant (ANCOVA, F=0.318, df 1,2604, p=0.57), and, assuming a common slope, there was no significant difference in the intercepts for the four periods (ANCOVA, F=1.76, df 1,2605, p=0.19).

Oven-dried weights of hydrated oocytes were determined on 9 fish. Egg weight did not vary with fish length (F=0.28, df 1,8, p=0.61) or with maximum oocyte diameter (F=0.88, df 1,8, p=0.37). The mean dry weight of individual hydrated oocytes was 0.012 mg (SE 0.0005).

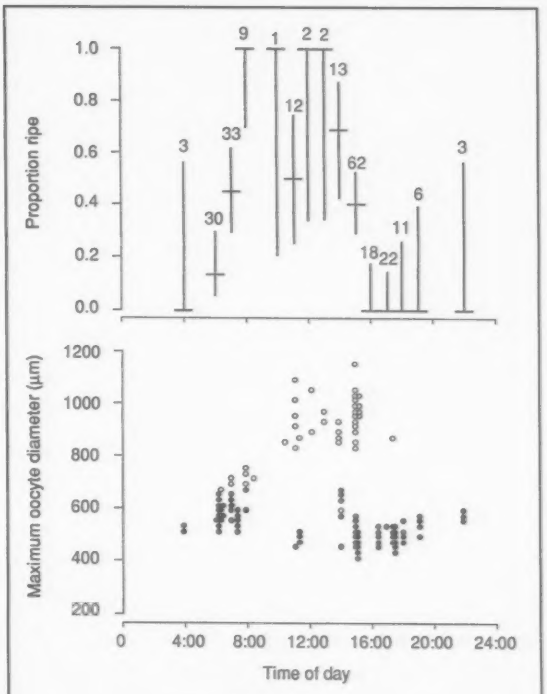

Figure 8

Proportion of mature female *Lutjanus vittus* with ripe-stage ovaries, and maximum oocyte diameter (MOD) in individuals caught at different times of the day. Samples taken during periods of major spawning activity (lunar days 2–10 and 18–29) during November–December 1982. Oocytes have been assigned to ovarian maturity stages: Ripe (○) and Yolked (●). Shown are 95% binomial confidence limits for proportions and number in each sample.

Discussion

The smallest ripe female observed in this study was 142 mm long, which is close to the length-at-first-maturity of female *L. vittus* from New Caledonia (Loubens 1980a). In a review of size-at-first-maturity, Grimes (1987) found consistent differences between insular and continental species of lutjanids and between shallow and deepwater groups in the ratio of length-at-first-maturity to maximum length. Female *L. vittus* clearly fall into the continental shallow group that mature early at ~44% of their maximum length.

The spawning season on the NW Shelf is protracted: While *L. vittus* spawned throughout the year, the major spawning period appeared to be September–April. Loubens (1980a) determined from GSI and visual staging that *L. vittus* spawn during October–February in New Caledonia (Loubens 1980a). *Lutjanus*

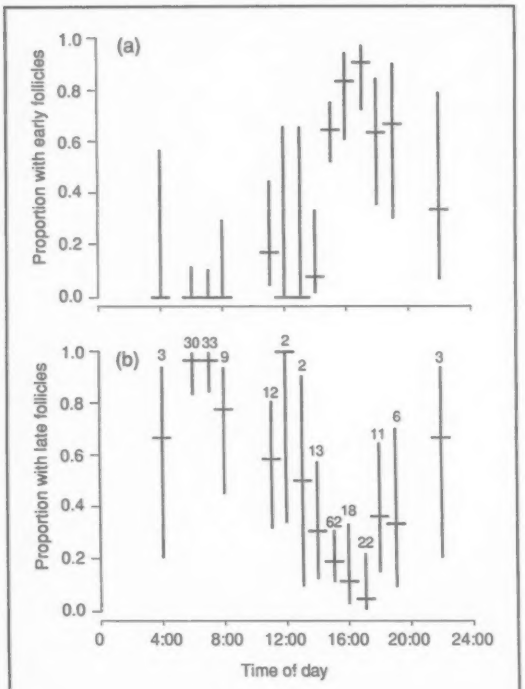

Figure 9

Proportion of mature female *Lutjanus vittus* with **(a)** early and **(b)** late-stage postovulatory follicles plotted against time of sampling. Samples taken during periods of spawning (lunar days 2–10 and 18–29) during November–December 1982. Shown are 95% binomial confidence limits for proportions and number in each sample.

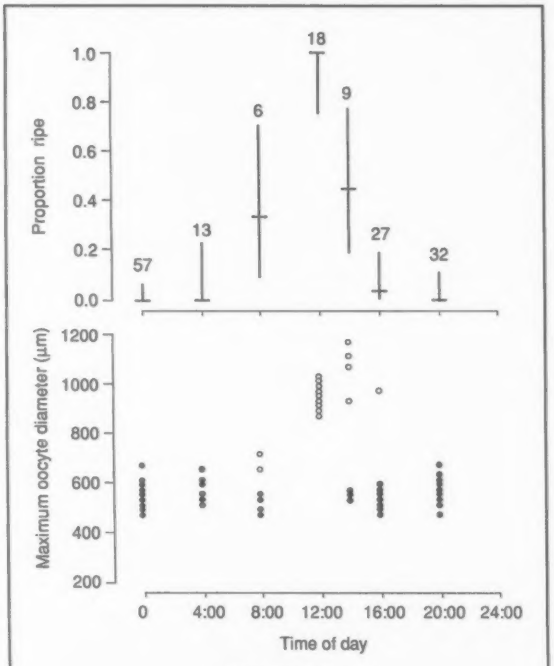

Figure 10

Proportion of mature female *Lutjanus vittus* with ripe ovaries, and maximum oocyte diameter (MOD) of individuals caught at different times of the day. Samples taken during 6–10 October 1988. Oocytes have been assigned to ovarian maturity stages: Ripe (○) and Yolked (●). Shown are 95% binomial confidence limits for proportions and number in each sample.

vittus tends to comply with Grimes' (1987) generalization that continental species, regardless of latitude, have a restricted spawning season.

The pattern of restricted spawning in *L. vittus* may be linked with the production cycle on the NW Shelf, as has been suggested for other continental species of lutjanids (Grimes 1987). The nutrient source is slope-water washing up onto the NW Shelf in summer when the Leeuwin Current is no longer flowing (Holloway et al. 1985, Tranter & Leech 1987). Enrichment is greatest between December and April. In winter the southeast trade winds blow, there is little stratification of the water column, and the plankton are dispersed (Tranter & Leech 1987). These winds abate by late August or early September, enabling the water column to become highly stratified and the plankton more concentrated (Tranter & Leech 1987). This would result in improved feeding conditions for larvae and coincides with the start of major spawning activity.

During the major spawning period, individual *L. vittus* spawn a number of times. Serial spawning has been inferred in a number of lutjanids: *L. purpureus* (De Moraes 1970), *L. kasmira* (Rangarajan 1971), *L. griseus* (Campos & Bashirullah 1975), *L. synagris* (Erhardt 1977), *Pristipomoides multidens* and *P. typus* (Min et al. 1977), *Rhomboplites aurorubens* (Grimes Huntsman 1980), *P. filamentosus* (Ralston 1981), *Etelis carbunculus* (Everson 1984), *E. coruscans* and *Aprion virescens* (Everson et al. 1989). While serial spawning appears to be commonplace in lutjanids, the number of batches of eggs spawned each season has not been determined conclusively for any species (Grimes 1987). Our data suggest that *L. vittus* spawn about 22 times/mo during late November and early December. If this spawning intensity were maintained throughout the whole spawning period (October–April), then most individuals would spawn about 150 times/yr. Even if spawning intensity were half this rate for the remainder of the season, then *L. vittus* would spawn about 90 times/yr.

Greatest spawning activity in *L. vittus* was shortly after the full and new moons. A lunar rhythm in spawn-

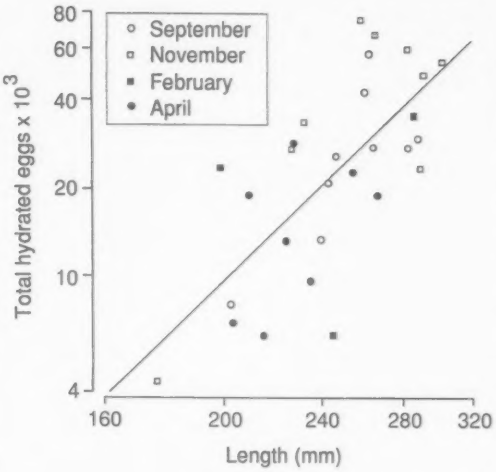

Figure 11
Relation between batch fecundity and fish length of *Lutjanus vittus* at four different spawning periods (scales are logged).

ing has been reported in many teleosts and some lutjanids, with most spawning activity close to the time of the full moon; e.g., *L. vaigiensis* (Randall & Brock 1960), *L. griseus* (Starck 1970), *L. synagris* (Reshetnikov & Claro 1976), *L. kasmira*, *L. rufolineatus*, and *P. multidens* (Mizenko 1984; although aquarium populations of *L. kasmira* spawned at the new and full moon [Suzuki & Hioki 1979]).

Many hypotheses have been proposed to explain why lunar reproductive cycles have developed in fishes (see reviews by Johannes 1978, Thresher 1984, Gladstone & Westoby 1988, Robertson et al. 1990). We cannot adequately explain why *L. vittus* has a well-developed lunar reproductive pattern. Spawning is probably linked to the lunar tidal cycle rather than moonlight per se, as it occurred chiefly after new and full moons and during daylight. The North West Shelf is a region of strong semidiurnal tides which flow predominantly cross-shelf at the shelf break and alongshelf near the coast (Holloway 1983). Spawning during spring tides would therefore disperse the eggs of *L. vittus* alongshelf rather than cross-shelf. There would be a clear advantage for larvae if they were advected to the midshelf or further offshore because these areas have greater productivity (Young et al. 1986). There is, however, no evidence for dispersal offshore; both larvae and adults of *Lutjanus* spp. are primarily found on the inner shelf (Leis 1987).

Frequency of spawning was determined from the proportion of females with postovulatory follicles. Our findings indicate that postovulatory follicles persist for <1 d, whereas studies on other species have found that they persist for <15 h (Takita et al. 1983), <2 d (Hunter & Goldberg 1980, Hunter et al. 1986, Clarke 1987), or slightly longer (Alheit et al. 1984). Our data on postovulatory follicles suggest that females on average spawn about 22 times each lunar month. The proportion of females spawning each day peaks about 3 d after the new moon and 6 d after the full moon.

It seems unusual that *L. vittus* spawns during early afternoon. Thresher (1984) reviewed 22 pelagic egg-producing families, including lutjanids, and found that most spawned around dusk, as did Colin & Clavijo (1988) who examined 26 species associated with coral reefs. Lutjanids produce pelagic eggs (Suzuki & Hioki 1979) and all other reports indicate that they spawn at or after dusk (Wicklund 1969, Starck 1970, Suzuki & Hioki 1979). Possibly spawning is linked to the state of the tide, rather than the time of day per se. In both 1982 and 1988, spawning activity coincided with rising tides; it may have been coincidental that these were during daylight hours.

Batch fecundity increased exponentially with fish length and linearly with fish weight. The variability in batch fecundities did not appear to be due to errors in using the gravimetric method. The mean coefficient of variation of estimates was 0.11, and it never exceeded 0.21. Care was taken to exclude ovaries that had partially spawned (identified by the presence of early-stage postovulatory follicles), and only those ovaries that had a clearly identified mode of partly-hydrated oocytes were used for estimates. Also, batch fecundities did not appear to differ between sampling periods. One might have expected a decline in fecundity as ovary weight declined over the season. Another possible reason for the variability in batch fecundity might have been that samples were taken at different phases of the lunar cycle. However, our data are inadequate to test this hypothesis.

Comparison of the fecundity of *L. vittus* with that of other lutjanids is not particularly useful, due to inconsistencies in methods of estimation and uncertainty as to whether true batch fecundities have been estimated (see review by Grimes 1987). It is, however, useful to consider the energetic costs of spawning by *L. vittus* considering its high annual fecundity. A 300 mm long female *L. vittus* would shed about 7.6 million eggs annually if it spawned 150 times/yr, or 4.5 million eggs if it spawned 90 times/yr. Assuming a calorific content for dried eggs of 25 kJ/g (the mean for a range of gadoids; Hislop & Bell 1987), then the annual energy expended on spawning (not including reproductive behavior) would be ~1300 kJ for 90 spawnings, and 2200 kJ for 150 spawnings. Estimation of reproductive effort or efficiency (egg energy/dietary energy × 100)

requires information on daily ration, which is not available for *L. vittus* and apparently has not been determined for any other lutjanid. *Nemipterous furcosis*, a co-occurring species on the N.W. Shelf, has a daily ration in the wild of 2.3% for 23–29 cm fish (K.J. Sainsbury, CSIRO Div. Fish., pers. commun. 1992). *Epinephalus guttatus* of similar size to *L. vittus* have a daily ration of 4% when fed surplus food once each day in the laboratory (Menzel 1960). Assuming a somewhat generous daily ration of 4% for *L. vittus* and a mean prey energy content of 4.2 kJ /g wet weight (Crisp 1971) would result in an approximate annual reproductive efficiency of 4.8% for 90 spawnings and 8% for 150 spawnings. This is similar to an annual reproductive effort in *Engraulis mordax* of 8–11% (Hunter & Leong 1981), a much smaller, shorter-lived species. The reproductive efficiency of the goby *Pomatoschistus microps* is considered to be among the highest ever calculated (Rogers 1988), although its efficiency was calculated using energy consumed over the 16 wk period of spawning and not the whole year. The reproductive efficiency of *P. microps*, calculated using annual energy intake, would be ~8.7–13.5%. The reproductive efficiency of *L. vittus* is comparatively high considering that this effort is sustained over many years.

Acknowledgments

We thank P. Binni and D. Le for laboratory assistance, and all the people who assisted in the fieldwork on the North West Shelf Program. K. Haskard provided statistical advice and modeled lunar periodicity in spawning activity. S. Blaber, J.S. Gunn, R.E. Johannes, and two anonymous referees reviewed the manuscript and suggested many improvements.

Citations

Alheit, J., V. H. Alarcon, & B. J. Macewicz
1984 Spawning frequency and sex ratio in the Peruvian anchovy, *Engraulis ringens*. Calif. Coop. Oceanic Fish. Invest. Rep. 25:43–52.

Campos, A. G., & A. K. M. Bashirullah
1975 Biología del pargo *Lutjanus griseus* (Linn.) de la Isla de Cubagua, Venezuela. II. Maduración sexual y fecundidad. Bol. Inst. Oceanogr. Univ. Oriente Cumana 14:109–116.

Clarke, T. A.
1987 Fecundity and spawning frequency of the Hawaiian anchovy or nehu, *Encrasicholina purpurea*. Fish. Bull., U.S. 85:127–138.

Colin, P.L., & I.E. Clavijo
1988 Spawning activity of fishes producing pelagic eggs on a shelf edge coral reef, southwestern Puerto Rico. Bull. Mar. Sci. 43:249–279.

Crisp, D. J.
1971 Energy flow measurements. *In* Holmes, N.A., & A.D. McIntyre (eds.), Methods for the study of marine benthos, p. 197–323. IBP (Int. Biol. Prog.) Handb. 16.

Davis, T. L. O., & G. J. West
1992 Growth and mortality of *Lutjanus vittus* (Quoy and Gaimard) from the North West Shelf of Australia. Fish. Bull., U.S. 90:395–404.

De Moraes, N. U. A.
1970 Sobre a desova e a fecundidade do pargo, *Lutjanus purpureus* Poey no nordeste Brasiliero. Bol. Estud. Pesca 10(1):7–20.

Erhardt, H.
1977 Beitrage zur biologie von *Lutjanus synagris* (Linnaeus 1758) an der Kolumbianischen Atlantikkuste. Int. Rev. Gesamten Hydrobiol. 62:161–171.

Erikson, D. L., Hightower, J. E., and G. D. Grossman
1985 The relative gonadal index: an alternative index for quantification of reproductive condition. Comp. Biochem. Physiol. 81A (1):117–120.

Everson, A. R.
1984 Spawning and gonadal maturation of the ehu, *Etelis carbunculus*, in the northwestern Hawaiian Islands. *In* Grigg, R.W., & K.Y. Tanoue (eds.), Proc., Second symposium on resource investigations in the Northwestern Hawaiian Islands, vol. 2, p. 128–148. UNIHI-SEAGRANT-MR-84-01, Univ. Hawaii, Honolulu.

Everson, A. R., H. A. Williams, & B. M. Ito
1989 Maturation and reproduction in two Hawaiian eteline snappers, uku, *Aprion virescens*, and onaga, *Etelis coruscans*. Fish. Bull., U.S. 87:877–888.

Forberg, K.G.
1983 Maturity classification and growth of capelin, *Mallotus villosus* (M.), oocytes. J. Fish. Biol. 22:485–496.

Gladstone, W., & M. Westoby
1988 Growth and reproduction in *Canthigaster valentini* (Pisces, Tetraodontidae): a comparison of a toxic reef fish with other reef fishes. Environ. Biol. Fishes 21:207–221.

Grimes, C. B.
1987 Reproductive biology of the Lutjanidae: a review. *In* Polovina, J.J., & S. Ralston (eds.), Tropical snappers and groupers: biology and fisheries management, p. 239–294. Westview Press, Boulder.

Grimes, C. B., & G. R. Huntsman
1980 Reproductive biology of the vermilion snapper, *Rhomboplites aurorubens* (Cuvier), from North and South Carolina waters. Fish. Bull., U.S. 78:137–146.

Hilge, V.
1977 On the determination of the stage of gonad ripeness in female bony fishes. Meeresforschung 25:149–155.

Hislop, J. R. G., & M. A. Bell
1987 Observations on the size, dry weight and energy content of the eggs of some demersal fish species from British marine waters. J. Fish. Biol. 31:1–20.

Holloway, P. E.
1983 Tides on the Australian North-West Shelf. Aust. J. Mar. Freshwater Res. 34:213–230.

Holloway, P. E., S. E. Humphries, M. Atkinson, & J. Imberger
1985 Mechanisms for nitrogen supply to the Australian North-West Shelf. Aust. J.Mar. Freshwater Res. 36:753–764.

Hunter, J. R., & S. R. Goldberg
1980 Spawning incidence and batch fecundity in northern anchovy, *Engraulis mordax*. Fish. Bull., U.S. 77:641–652.

Hunter, J. R., & R. J. H. Leong
1981 The spawning energetics of female northern anchovy, *Engraulis mordax*. Fish. Bull., U.S. 79:215–230.

Hunter, J. R., & B. J. Macewicz
1980 Sexual maturity, batch fecundity, spawning frequency, and temporal pattern of spawning for the northern anchovy, *Engraulis mordax*, during 1979 spawning season. Calif. Coop. Oceanic Fish. Invest. Rep. 21:139–149.

Hunter, J. R., N. C. H. Lo, & R. J. H. Leong
1985 Batch fecundity in multiple spawning fishes. *In* Lasker, R. (ed.), An egg production method for estimating spawning biomass of pelagic fish: application to the northern anchovy, *Engraulis mordax*, p. 67–77. NOAA Tech. Rep. NMFS 36.

Hunter, J. R., B. J. Macewicz, & J. R. Sibert
1986 The spawning frequency of skipjack tuna, *Katsuwonus pelamis*, from the South Pacific. Fish. Bull., U.S. 84:895–903.

Jernakoff, P., & K. J. Sainsbury
1990 CSIRO's northern demersal finfish stock assessments: 1980 to 1990. Inf. pap. IP/6/90, Bur. Rural Resour., Dep. Primary Ind. & Energy Australia, 169 p.

Johannes, R. E.
1978 Reproductive strategies of coastal marine fishes in the tropics. Environ. Biol. Fishes 3:65–84.

Kimura, D. K.
1977 Statistical assessment of the age-length key. J. Fish. Res. Board Can. 34:317–324.

Leis, J. M.
1987 Review of the early life history of tropical groupers (Serranidae) and snappers (Lutjanidae). *In* Polovina, J.J., & S. Ralston (eds.), Tropical snappers and groupers: biology and fisheries management, p. 189–237. Westview Press, Boulder.

Loubens, G.
1980a Biologie de quelques espèces de poissons du lagon néo-calédonien. II. Sexualité et reproduction. Cah. Indo-Pac. II (1):41–72.
1980b Biologie de quelques espèces de poissons du lagon néo-calédonien. III. Croissance. Cah. Indo-Pac. II (2):101–154.

Menzel, D. W.
1960 Utilization of food by a Bermuda reef fish *Epinephalus guttatus*. J. Cons. Perm. Int. Explor. Mer 25:216–222.

Min, T. S. T., T. Senta, & S. Supongpan
1977 Fisheries biology of *Pristipomoides* spp. (Family Lutjanidae) in the South China Sea and its adjacent waters. Singapore J. Primary Ind. 5(2):96–115.

Mizenko, D.
1984 The biology of the Western Samoan reef-slope snapper populations of: *Lutjanus kasmira*, *Lutjanus rufolineatus*, and *Pristipomoides multidens*. M.S. thesis, School Oceanogr., Univ. Rhode Island, Kingston, 66 p.

Mori, K.
1984 Early life history of *Lutjanus vitta* (Lutjanidae) in Yuya Bay, the Sea of Japan. Jpn. J. Ichthyol. 30(4):374–392.

Ralston, S. V. D.
1981 A study of the Hawaiian deepsea handline fishery with special reference to the population dynamics of opakapaka, *Pristipomoides filamentosus* (Pisces: Lutjanidae). Ph.D. diss., Univ. Wash., Seattle, 204 p.

Randall, J. E., & V. E. Brock
1960 Observations on the ecology of epinephaline and lutjanid fishes of the Society Islands, with emphasis on food habits. Trans. Am. Fish. Soc. 89:9–16.

Rangaragan, K.
1971 Maturity and spawning of the snapper, *Lutjanus kasmira* (Forskal) from the Andaman Sea. Indian J. Fish. 18:114–125.

Reshetnikov, Y. S., & R. M. Claro
1976 Cycles of biological processes in tropical fishes with reference to *Lutjanus synagris*. J. Ichthyol. 16:711–723.

Robertson, D. R., C. W. Peterson, & J. D. Brawn
1990 Lunar reproductive cycles of benthic-brooding reef fishes: reflections of larval biology or adult biology? Ecol. Monogr. 60(3):311–329.

Rogers, S. I.
1988 Reproductive effort and efficiency in the female common goby, *Pomatoschistus microps* (Kroyer) (Teleostei: Gobioidei). J. Fish. Biol. 33:109–119.

Schnute, J.
1981 A versatile growth model with statistically stable parameters. Can. J. Fish. Aquat. Sci. 38:1128–1140.

Starck, W. A. II
1970 Biology of the gray snapper, *Lutjanus griseus*. *In* Starck, W.A. II, & R.E. Schroeder (eds.), Investigations on the gray snapper, *Lutjanus griseus*, p. 1–150. Stud. Trop. Oceanogr. (Miami) 10.

Suzuki, K., & S. Hioki
1979 Spawning behavior, eggs and larvae of the lutjanid fish, *Lutjanus kasmira*, in an aquarium. Jpn. J. Ichthyol. 26:161–166.

Takita, T., T. Iwamoto, S. Kai, & I. Sogabe
1983 Maturation and spawning of the dragonet, *Callionymus enneactis*, in an aquarium. Jpn. J. Ichthyol. 30:221–226.

Thresher, R. E.
1984 Reproduction in reef fishes. T.F.H. Publ., Neptune City NJ, 399 p.

Tranter, D. J., & G. S. Leech
1987 Factors influencing the standing crop of phytoplankton on the Australian Northwest Shelf seaward of the 40 m isobath. Continental Shelf Res. 7(2):115–133.

Wallace, R. A., & K. Selman
1981 Cellular and dynamic aspects of oocyte growth in teleosts. Am. Zool. 21:325–343.
West, G.
1990 Methods of assessing ovarian development in fishes: a review. Aust. J. Mar. Freshwater Res. 41:199–222.
Wicklund, R.
1969 Observations on spawning of the lane snapper. Underwater Nat. 6:40.
Yamamoto, K.
1956 Studies on the formation of fish eggs. Annual cycle in the development of ovarian eggs in the flounder, *Liopsetta obscura*. J. Fac. Sci. Hokkaido Univ. Ser. 6, 12:362–373.
Young, P. C., & K. J. Sainsbury
1985 CSIRO's North West Shelf program indicates changes in fish populations. Aust. Fish. 44(3):16–20.
Young, P. C., J. M. Leis, & H. F. Hausfeld
1986 Seasonal and spatial distribution of fish larvae in waters over the North West Continental Shelf of Western Australia. Mar. Ecol. Prog. Ser. 31:209–222.

Inferring demographic processes from size-frequency distributions: Effect of pulsed recruitment on simple models

Thomas A. Ebert
Stephen C. Schroeter
John D. Dixon
Department of Biology, San Diego State University
San Diego, California 92182-0057

Abstract.—The shape of a size-frequency distribution is the result of age- or size-specific rates of growth and survival, their variability, and seasonal and interannual variation in recruitment. Simulation of size distributions can be used to gain insight into the underlying processes that give rise to observed size structure of organisms in the field, but the utility of this approach depends critically on underlying assumptions. Incorrect judgment of the significance of assumptions can lead to erroneous conclusions concerning the causes of bi- or polymodal distributions.

Using the Brody-Bertalanffy growth model and a constant survival rate, bi- and polymodal distributions can be generated when recruitment is pulsed. Even with as many as 10 recruitment episodes per year, size distributions show several modes. A sampling of the literature indicates that most fish and marine invertebrates have pulsed rather than continuous recruitment; thus, when very little is known about a species, pulsed rather than continuous recruitment would be the better assumption when interpreting the shapes of size distributions.

Our simulations differ from those conducted by Barry & Tegner (1990) who assumed continuous and constant recruitment and focused on changing growth and survival parameters to explain bimodal size structure. These authors also suggested that their analysis was appropriate for interpreting the dynamics of red sea urchins *Strongylocentrotus franciscanus*. We have been documenting settlement of both red and purple (*S. purpuratus*) sea urchins. At La Jolla, California, neither species showed continuous settlement; rather, both species had pulses of settlement in spring 1990 and 1991.

Although age-specific variation in growth or mortality parameters can result in bimodal size distributions, it is more likely that such distributions are caused by seasonal pulses of recruitment.

Manuscript accepted 22 January 1993.
Fishery Bulletin, U.S. 91:237-243 (1993).

For many organisms, size data are easy to gather and size-frequency distributions are common in the literature. In many cases, they provide the only clues to the underlying dynamics of growth, survival, and recruitment. Thus, it is understandable that an extensive literature exists concerning their analysis. One general research approach has focused on the separation of size distributions into components (e.g., Harding 1949, Cassie 1950, Bhattacharya 1967, Young & Skillman 1975, Macdonald & Pitcher 1979). A second approach has attempted to use size data either to estimate mortality when growth parameters are known (e.g., Beverton & Holt 1956, Smith 1972, Van Sickle 1977ab, Ebert 1981 and 1987, Sainsbury 1982) or to estimate both growth and mortality parameters (e.g., Green 1970, Ebert 1973 and 1987, Saila & Lough 1981, Fournier & Breen 1983, Pauly 1987). A third approach has modeled size distributions to gain insight into the underlying processes that give rise to observed distributions (e.g., Craig & Oertel 1966, DeAngelis & Coutant 1982, Barry & Tegner 1990, Hartnoll & Bryant 1990). Simulations of size distributions are metaphors of the dynamic processes that give rise to actual size distributions. The utility of simulation depends critically on the underlying assumptions. If the significance of any of the assumptions is wrongly judged, one may be led to erroneous conclusions concerning underlying dynamics.

As an approach to explaining bimodal size distributions, Barry & Tegner (1990) presented a deterministic model for the development of size distributions that has seven assumptions: (1) Brody-Bertalanffy growth, (2) constant rate of mortality, (3) constant and continuous recruitment, (4) strict determinism for growth, so $\sigma=0$ for all sizes at an age, (5) strict determinism for survival, so $\sigma=0$ for numbers at an age, (6) population growth rate per individual, r, equal to 0, and (7) a stable size distribution equivalent to a stable age distribution. Bimodal size distributions are not possible with these seven assumptions, yet bimodality is commonly observed. Accordingly, one or more of the assumptions must be violated. Barry & Tegner focused on the assumptions concerning growth and survival and concluded that "...bimodality can develop only from an increase in survivorship with age or an increase in the growth coefficient with age, or both." In particular, they argued that size distributions of red sea urchins *Strongylocentrotus franciscanus* required age- or size-specific changes of the growth-rate constant, K, in the Brody-Bertalanffy equation, the mortality coefficient, Z, in an exponential survival curve, or both.

There are three issues that we would like to explore: (1) Possible causes of bimodal size distributions and, in particular, the consequences of pulsed recruitment, (2) applicability of the Barry & Tegner model to sea urchins in California, and (3) general applicability of the Barry & Tegner model.

Size-distribution simulation

We simulated several size distributions to show how the Barry & Tegner model works. Growth was modeled using the Brody-Bertalanffy equation for individual growth:

$$S_t = S_\infty(1-be^{-Kt}) \quad (1)$$

where S_t = size at time t after birth or settlement
S_∞ = asymptotic size
K = growth rate coefficient

$$b = \frac{S_\infty - S_R}{S_\infty} \quad (2)$$

S_R = size at t=0 when organisms begin to grow according to Eq. 1.

Sometimes Eq. 1 is written

$$S_t = S_\infty(1-e^{-K(t-t_0)}) \quad (3)$$

where t_0 = time at which size would be 0

$$b = e^{Kt_0}. \quad (4)$$

Cohort survival was modeled so that the mortality rate was constant:

$$N_t = N_0e^{-Zt} \quad (5)$$

where N_t = number remaining in a cohort at time t
N_0 = initial number in a cohort
Z = mortality rate coefficient.

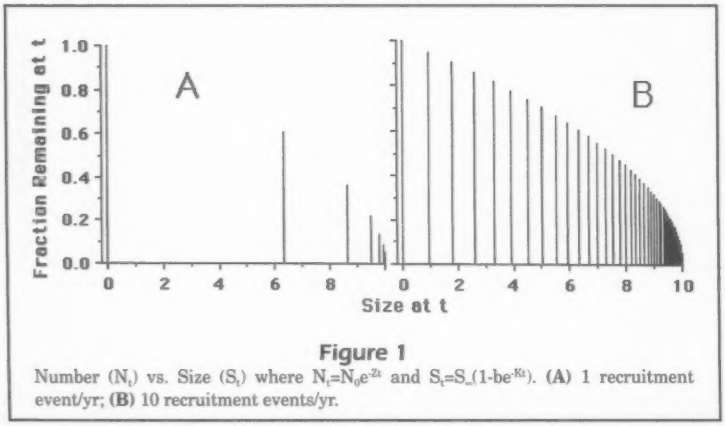

Figure 1
Number (N_t) vs. Size (S_t) where $N_t=N_0e^{-Zt}$ and $S_t=S_\infty(1-be^{-Kt})$. **(A)** 1 recruitment event/yr; **(B)** 10 recruitment events/yr.

Equations 1 and 5 were used to generate a number-density distribution that was integrated over segments of arbitrary size to produce a size-frequency distribution. The first step was to calculate sizes at particular ages (Eq. 1) and then to estimate numbers in a cohort that survived to each age (Eq. 5). The number surviving to a specific size was generated using a constant time-interval and Z<K (Fig. 1). The size-intervals shorten because growth follows Eq. 1. For Fig. 1A, the time-interval between recruitment episodes is 1 unit, which, for purposes of this discussion, we call 1yr. Changing the time-interval for reproduction, that is, the number of evenly-spaced reproductive episodes/yr, changes the number and spacing of lines in the graph. In Fig. 1B we used 10 episodes/yr; that is, an interval of 0.1 yr. In our simulation, we assumed that the population was periodically stable and stationary.

Stable and stationary structure for a population with pulsed recruitment means that demographic structure and number of individuals change between recruitment episodes but are the same across episodes. When the same times after recruitment episodes are compared, the age and size structures of the population are the same (stable structure) and the numbers of individuals are the same (stationary structure). The relationship between density and time would be saw-toothed, with an **average** slope of 0, but with increased numbers-at-recruitment and declining numbers up to the point of another recruitment episode. As the number of recruitment events increases, the height of each tooth becomes smaller until it is smooth when recruitment is continuous. The vertical lines in Fig. 1 represent not only the progression of a single cohort through time, but also cohorts that make up the stable and stationary population.

A size-frequency distribution was constituted by summing all lines within an arbitrary interval of 1.0 size units (Fig. 2). With just one reproductive episode/yr (Fig. 2A), size distribution is polymodal. The overall shape of the size distribution, which is formed by drawing an envelope around the distribution, has a negative slope. Over an increasing range of recruitment frequencies, the polymodal nature is preserved, so that with 10 episodes/yr (Fig. 2C) modes still are evident but the overall shape shows a positive slope. When there are 100 episodes/yr, size distribution approaches the continuous form used by Barry & Tegner:

$$NS = \frac{N_0}{KS_\infty}\left(1-\frac{S_t}{S_\infty}\right)^{\left(\frac{Z}{K}-1\right)}. \quad (6)$$

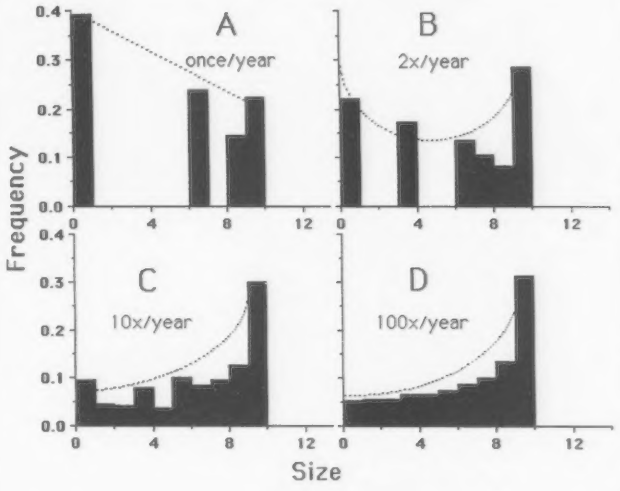

Figure 2

Integration of N_t vs. S_t over intervals of 1.0 size unit. Dotted line emphasizes general shape of the envelope of each distribution. **(A)** 1 recruitment episode/yr; envelope of the distribution has a negative slope. **(B)** 2 recruitment episodes/yr; envelope of the distribution has high points at smallest and largest sizes. **(C)** 10 recruitment episodes/yr; general envelope has a positive slope but has modes at small sizes. **(D)** 100 episodes/yr; envelope has a positive slope.

Simulated size distributions take on an appearance much closer to distributions seen in the field when individual sizes are distributed around mean size-at-age (Fig. 3). A coefficient of variation of 0.1 was used for simulation, so $\sigma=0.1\mu$. Mean sizes were calculated using Eq. 1, and areas under the normal curve were estimated out to 4σ in units of $\sigma/10$. Areas for each size segment were determined by successive subtraction of terms obtained from a polynomial approximation of the area under the normal curve and based on a program for the normal distribution given by Poole & Borchers (1979), who used an algorithm from Hastings (1955) (Function 26.2.16 in Abramowitz & Stegun 1972). P(x) is the area under the normal curve from the mean, μ, to a size, s, given a standard deviation of σ:

$$P(x) = \frac{1}{2} - r(a_1 t + a_2 t^2 + a_3 t^3) + \epsilon(x) \quad (7)$$

$$x = \frac{s-\mu}{\sigma} \quad (8)$$

$$r = \frac{e^{-x^2/2}}{\sqrt{2\pi}} \quad (9)$$

$$t = \frac{1}{1+Px} \quad (10)$$

with $a_1 = 0.4361836$, $a_2 = -0.1201676$, $a_3 = 0.9372980$, $p = 0.33267$, and $\epsilon(x)<10^{-5}$. The area under the normal curve, A, from s to s+Δs is

$$A = P(x)_{s+\Delta s} - P(x)_s. \quad (11)$$

Areas under the normal curve for each cohort were reduced by multiplying each area, A, for a cohort by e^{-Zt} according to Eq. 5. The size-frequency distribution was produced by establishing a 1-unit size-interval and summing parts of all cohorts in each interval.

With one recruitment episode/yr (Fig. 3A), the distribution is polymodal. Because the cluster of individuals that are ≥1 yr is bi-

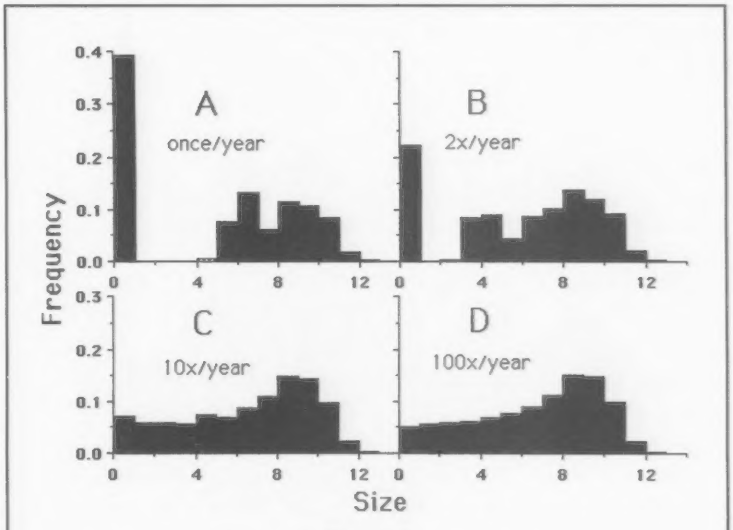

Figure 3

Results of a simulation with Z=0.5, K=1.0, S_∞=10.0, and s=0.1xmean. Simulations differ with respect to number of recruitment episodes/yr (range 1–100/yr). **(A)** polymodal with general envelope with negative slope; **(B)** polymodal with general negative slope; **(C)** polymodality still evident but envelope has a positive slope; **(D)** unimodal with general positive slope.

modal, it is clear that this distribution would always be bi- or polymodal. With two recruitment events/yr (Fig. 3B), the distribution again is polymodal and would always be so. With ten recruitment events/yr (Fig. 3C), the modes begin to disappear but the distribution still is weakly polymodal with modes at 0–1, 4–5, and 8–9 size units. With 100 recruitment events/yr (Fig. 3D), the distribution is unimodal. The general shapes are similar to the distributions in Fig. 2, with slopes that initially are negative (Fig. 3A) switching to positive (Fig. 3C, 3D). A combination of pulsed recruitment, coupled with a decaying exponential growth pattern and low mortality, can lead to size distributions with a wide range of shapes. A panoply of size-distribution shapes can be produced with identical values for Z, K, and S_∞ using different frequencies of recruitment.

Observed settlement of *S. franciscanus* and *S. purpuratus*

Barry & Tegner (1990) used their model specifically to address bimodal size structure in red sea urchins *S. franciscanus*. We disagree with their assumption of continuous recruitment and base this on observed settlement data.

Starting in late February 1990, we deployed settlement collectors at a number of sites along the California coast. Wood-handled scrub brushes (model #0115 National Brush Co., Aurora IL) were used to evaluate temporal and spatial variability in settlement. Brushes were attached as pairs to a line with two pairs per line. The bottom pair of brushes was suspended 1m from the bottom, and the second pair was attached ~20cm farther up the rope. Brushes were tended on a weekly basis at sites within the California Bight and in northern California. One of the sites in southern California was off the end of the pier at Scripps Institution of Oceanography, La Jolla.

Following weekly collection, brushes were placed in a sonic cleaner with seawater for ~3 min to remove animals. Newly-metamorphosed sea urchins have a diameter of ~500 m; thus, following sonication, the water and sediment in the sonicator were strained through 436 m Nitex. Material retained by the screen was then examined using a dissecting microscope, and newly-settled sea urchins were identified and counted.

Settlement at Scripps Pier in San Diego County was confined to a period of about 3 wk starting in late March 1990, and over a longer period in spring 1991 (Fig. 4). Timing of settlement was the same for both *S. purpuratus* and *S. franciscanus*. A few *S. purpuratus* settled in June 1990, but in terms of influencing the structure of a size-frequency distribution, settlement in 1990 can be considered a single event of short duration. Settlement in 1991 began in late February and continued into early June. The important point is that sea urchin settlement at Scripps Pier was seasonal. Settlement at other sites in California, as well as inside and outside kelp beds, all showed seasonal settlement (Ebert et al., in prep.).

Discussion

Bi- or polymodal size distributions and pulsed recruitment are common in the literature. We examined 69 papers that included larval distribution, settlement, or recruitment information for fish, molluscs, annelids, bryozoans, crustaceans, and echinoderms. Out of 216 species, only 8 could be considered to have continuous recruitment, and of these only five spider crab species (Hines 1982) appeared to have constant recruitment; that is, the same number/mo at all seasons. About 98% of the species failed to meet the assumption of constant and continuous recruitment made by Barry & Tegner (1990).

As shown by our simulations, pulsed recruitment produced bimodal distributions that were not transitory in the sense that distributions showed bimodality at all times between recruitment events. However, were a population characterized by pulsed recruitment, sampling could be done in such a manner that the relative magnitude of Z and K could be deduced from a simple

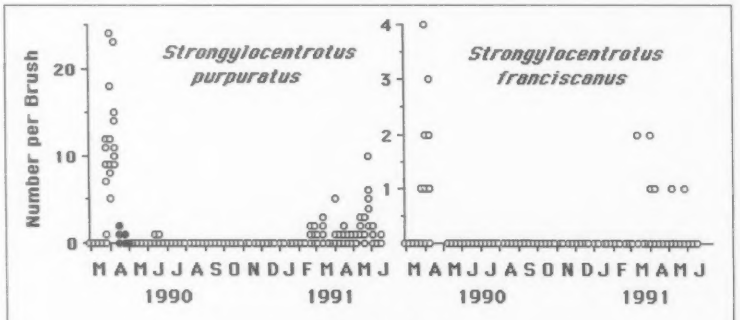

Figure 4

Settlement of purple and red sea urchins, *Strongylocentrotus purpuratus* and *S. franciscanus*, on eight scrub brushes: four suspended 1 m from bottom and four at 1.2 m off bottom at Scripps Pier, Scripps Inst. Oceanogr., La Jolla CA (32°52'N). Solid circles indicate animals not identified to species.

model such as Eq. 6. The changing shapes of the size-frequency distributions for a species with pulsed recruitment could be summed and so be made to approximate the shape that would be obtained with continuous recruitment. To obtain a reasonable approximation, it would be necessary to (1) take many evenly-spaced samples between recruitment events, and (2) weight the samples with the survival rate, e^{-Zt}, from the time of recruitment, t. Weighting could be accomplished if accurate estimates of density were known, which, of course, would be the same as knowing survival. An obvious variant would be the case in which the same area was sampled each time and all individuals were measured. Such a procedure would result in the largest N for the sample immediately following recruitment and the smallest N for the sample just prior to the next recruitment episode. All samples would be pooled before the size-frequency distribution would be constructed.

Approximation of a species with pulsed recruitment to a continuous form could be the same as distributions shown in Figs. 2 and 3. For example, if a species had a single pulse of recruitment and was sampled 10 evenly-spaced times during a year, and each sample was weighted according to the survival rate, then the summed frequency distribution would be C in Figs. 2 and 3. However, if size data were gathered in such a manner that weighting was not automatic, survival rate would have to be obtained by some other technique before size distributions could be summed to approximate continuous recruitment. Techniques for obtaining survival rate, the weighting factor, from size data include those presented by Ebert (1973, 1987), Saila & Lough (1981), Fournier & Breen (1983), and Pauly (1987). It must be noted that analysis of a series of size distributions to obtain the weighting factor would provide information on growth as well as survival, and so there would be scant motivation for constructing a summed distribution.

It is not possible to infer the causes underlying an observed size distribution from a single sample or even from several samples that are widely spaced in time. For example, bimodal size distributions can arise from intra-cohort (e.g., Shelton et al. 1979, Timmons et al. 1980) or inter-cohort (Johnson 1976) competition, and the simple models examined here and in Barry & Tegner (1990) demonstrate that similar size distributions can result from very different mechanisms. In a time-series of size distributions, when the smallest mode shifts through time, the simplest explanation for bimodality is pulsed recruitment (e.g., McPherson 1965, Hickman 1979, Dafni & Tobol 1986/87, Davoult et al. 1990). If sampling is adequate and the smallest mode of a bimodal distribution does not shift during the year (e.g., Gladfelter 1978), the most probable explanation is continuous recruitment coupled with high mortality rates for the smallest animals and improved survival with increased size, which is a case that fits the explanation for bimodality provided by Barry & Tegner (1990). When size distributions are bi- or polymodal and are presented without a time-series (e.g., Tegner & Dayton 1981, Stein & Pearcy 1982, Wilson 1983), reasonable hypotheses can be formulated, but testing requires additional data.

There are numerous examples of pulsed recruitment for sea urchins in California. Size-frequency distributions gathered for purple sea urchins at Papalote Bay, Baja California, Mexico (31°42') (Pearse et al. 1970) may indicate multiple settlement events each year during 1962–69 because samples from January, April, and June–November all had a mode <1.0 cm (Pearse et al. 1970, Ebert 1983). However, if growth was very slow at Papalote Bay, as also indicated by the size-frequency distributions, a single settlement episode would explain the data because individuals with a mode at 0.5 cm were observed only in summer and fall samples.

Published size data for sea urchins at Whites Point (33°43'N) and Point Vicente (33°44'N) during 1966 and 1967 (Pearse et al. 1970) show recruitment pulses for both species of *Strongylocentrotus* and for *Lytechinus*. Recruitment was better in 1966 than in 1967, and small individuals were collected in September 1966 as well as in July and August 1967. Recruitment was not continuous at either Whites Point or at Point Vicente.

Finally, our results showing pulsed settlement for red and purple sea urchins corroborate the observation of a single spike of settlement at Naples Reef (34°25'N) off Santa Barbara in May 1986 (Rowley 1989) and the report by Harrold et al. (1991) of two recruitment events during a year in central California. The pulsed nature of recruitment means that analysis of size-frequency distributions of *Strongylocentrotus* spp. should not be based on a model that explicitly requires continuous and constant recruitment (Eq. 6).

We have demonstrated that by using fixed growth and survival parameters, it is possible to generate a wealth of size-distribution shapes merely by changing the number of recruitment episodes/yr. We have intentionally focused on this aspect of size-distribution shape because we believe that it forms the stumbling block to the application of the Barry & Tegner model. In effect, their model does not provide a convenient way of gaining insight into demographics because, in order to use it to divine the relative magnitude of parameters, it would be necessary to demonstrate the pattern of recruitment for the population being studied. Since the preponderance of field evidence indicates that recruitment generally is pulsed, one cannot "...draw inferences concerning the demographic dynamics of a population...simply by observing the shape of its size-

frequency distribution" (Barry & Tegner 1990). Furthermore, classifying populations as "growth dominated" or "mortality dominated," as these authors have done, introduces terms that obscure rather than illuminate the analysis of size distributions, much in the manner of r- and K-selection comparisons.

Size data should be part of every demographic study because they contain a record of the recent past history of a population. Such data ultimately can be used to estimate parameters, such as Z in Eq. 5, that frequently are difficult to obtain, or to test assumptions concerning annual variability in recruitment or mortality. There currently is no substitute for population studies that include not only size data but also independent estimates of growth and, where possible, survivorship.

Acknowledgments

Support for this work was provided by the National Science Foundation, landing tax funds from commercial sea urchin fishermen administered through the California Department of Fish and Game, and San Diego State University in the form of a sabbatical leave for the senior author.

Citations

Abramowitz, M., & I. A. Stegun (editors)
1972 Handbook of mathematical functions with formulas, graphs, and mathematical tables., 9th ed. U.S. Gov. Printing Off., Wash. DC.

Barry, J. P., & M. J. Tegner
1990 Inferring demographic processes from size-frequency distributions: Simple models indicate specific patterns of growth and mortality. Fish. Bull., U.S. 88:13–19.

Beverton, R. J., & S. J. Holt
1956 A review of methods for estimating mortality rates in exploited fish populations, with special reference to sources of bias in catch sampling. Rapp. P.-V. Cons. Int. Explor. Mer 140:67–83.

Bhattacharya, C. G.
1967 A simple method of resolution of a distribution into Gaussian components. Biometrics 23:115–135.

Cassie, R. M.
1950 The analysis of polymodal frequency distributions by the probability paper method. N.Z. Sci. Rev. 8:90–91.

Craig, G. Y., & G. Oertel
1966 Deterministic models of living and fossil populations of animals. Q. J. Geol. Soc. Lond. 122:315–355.

Dafni, J., & R. Tobol
1986/87 Population structure patterns of a common Red Sea echinoid (*Tripneustes gratilla elatensis*). Isr. J. Zool. 34:191–204 .

Davoult, D., F. Gounin, & A. Richard
1990 Dynamique et reproduction de la population d'*Ophiothrix fragilis* (Abildgaard) du dètroit du Pas-de-Calais (Manche orientale). J. Exp. Mar. Biol. Ecol. 138:201–216.

DeAngelis, D. L., & C. C. Coutant
1982 Genesis of bimodal size distributions in species cohorts. Trans. Am. Fish. Soc. 111:384–388.

Ebert, T. A.
1973 Estimating growth and mortality rates from size data. Oecologia 11:281–298.
1981 Estimating mortality from growth parameters and a size distribution when recruitment is periodic. Limnol. Oceanogr. 26:764 –769.
1983 Recruitment in echinoderms. *In* Jangoux, M., & J.M. Lawrence (eds.), Echinoderm studies 1, p. 169–203. A.A. Balkema, Rotterdam.
1987 Estimating growth and mortality parameters by nonlinear regression using average size in catches. *In* Pauly, D., & G.R. Morgan (eds.), Length-based methods in fisheries research, p. 35–44. ICLARM (Int. Cent. Living Aquat. Resour. Manage.) Conf. Proc. 13, Manila, Philippines, and Kuwait Inst. Sci. Res., Safat, Kuwait.

Fournier, D. A., & P. A. Breen
1983 Estimation of abalone mortality rates with growth analysis. Trans. Am. Fish. Soc. 112:403–411.

Gladfelter, W. B
1978 General ecology of the Cassiduloid urchin *Cassidulus caribbearum*. Mar. Biol. 47:149–160.

Green, R. H.
1970 Graphical estimation of rates of mortality and growth. J. Fish. Res. Board Can. 27:204–208.

Harding, J. P.
1949 The use of probability paper for the graphical analysis of polymodal frequency distributions. J. Mar. Biol. Assoc. U.K. 28:141–153.

Harrold, C., S. Lisin, K. H. Light, & S. Tudor
1991 Isolating settlement from recruitment of sea urchins. J. Exp. Mar. Biol. Ecol. 147:81–94.

Hartnoll, R. G., & A. D. Bryant
1990 Size-frequency distributions in decapod crustacea — The quick, the dead, and the cast-offs. J. Crustacean Biol. 10:14–19.

Hastings, C. Jr.
1955 Approximations for digital computers. Princeton Univ. Press, Princeton.

Hickman, R. W.
1979 Allometry and growth of the green-lipped mussel *Perna canaliculus* in New Zealand. Mar. Biol. 51:311–327.

Hines, A. H.
1982 Coexistence in a kelp forest: size, population dynamics, and resource partitioning in a guild of spider crabs (Brachyura, Majidae). Ecol. Monogr. 52:179–198.

Johnson, L.
1976 Ecology of Arctic populations of lake trout,

Salvelinus namaycush, lake whitefish, *Coregonus clupeaformis*, Arctic char, *S. alpinus*, and associated species in unexploited lakes of the Canadian Northwest Territories. J. Fish. Res. Board Can. 33:2459–2488.

Macdonald, P. D., & T. J. Pitcher
1979 Age-groups from size-frequency data: A versatile and efficient method of analyzing distribution mixtures. J. Fish. Res. Board Can. 36:987–1001.

McPherson, B. F.
1965 Contributions to the biology of the sea urchin *Tripneustes ventricosus*. Bull. Mar. Sci. 15:228–244.

Pauly, D.
1987 A review of the ELEFAN system for analysis of length-frequency data in fish and aquatic invertebrates. *In* Pauly, D., & G.R. Morgan (eds.), Length-based methods in fisheries research. p 7–34. ICLARM (Int. Cent. Living Aquat. Resour. Manage.) Conf. Proc. 13, Manila, Philippines, and Kuwait Inst. Sci. Res., Safat, Kuwait.

Pearse, J. S., M. E. Clark, D. L. Leighton, C. T. Mitchell, & W. J. North
1970 Final report. Marine waste disposal and sea urchin ecology. Appendix. *In* Kelp habitat improvement project, annu. rep. (1 July 1969–30 June 1970) p. 1–93. Calif. Inst. Technol., Pasadena.

Poole, L., & M. Borchers
1979 Some common BASIC programs, 3rd ed. OSBORNE/McGraw-Hill, Berkeley CA.

Rowley, R. J.
1989 Settlement and recruitment of sea urchins (*Strongylocentrotus* spp.) in a sea-urchin barren ground and a kelp bed: Are populations regulated by settlement or post-settlement processes? Mar. Biol. (Berl.) 100:485–494.

Saila, S. B., & R. G. Lough
1981 Mortality and growth estimation from size data—an application to some Atlantic herring larvae. Rapp. P.-V. Reun. Cons. Int. Explor. Mer 178:7–14.

Sainsbury, K. J.
1982 Population dynamics and fishery management of the Paua, *Haliotis iris*. II. Dynamics and management as examined using a size class population model. N.Z. J. Mar. Freshwater Res. 16:163–173

Shelton, W. L., W. D. Davies, T. A. King, & T. J. Timmons
1979 Variation in the growth of the initial year class of largemouth bass in West Point Reservoir, Alabama and Georgia. Trans. Am. Fish. Soc. 108:142–149.

Smith, S. V.
1972 Production of calcium carbonate on the mainland shelf of southern California. Limnol. Oceanogr. 17:28–41.

Stein, D. L., & W. G. Pearcy
1982 Aspects of reproduction, early life history, and biology of macrourid fishes off Oregon, U.S.A. Deep-Sea Res. 29:1313–1329.

Tegner, M. J., & P. K. Dayton
1981 Population structure, recruitment and mortality of two sea urchins (*Strongylocentrotus franciscanus* and *S. purpuratus*) in a kelp forest. Mar. Ecol. Prog. Ser. 5:225–268.

Timmons, T. J., W. L. Shelton, & W. D. Davies
1980 Differential growth of largemouth bass in West Point Reservoir, Alabama-Georgia. Trans. Am. Fish. Soc. 109:176–186.

Van Sickle, J.
1977a Mortality rates from size distributions. The application of a conservation law. Oecologia 27:311–318.
1977b Mortality estimates from size distributions: A critique of Smith's model. Limnol. Oceanogr. 22:774–775.

Wilson, G. D.
1983 Variation in the deep-sea isopod *Eurycope iphthima* (Asellota, Eurycopidae): depth related clines in rostral morphology and in population structure. J. Crustacean Biol. 3:127–140.

Young, M. Y. Y., & R. A. Skillman
1975 A computer program for analysis of polymodal frequency distributions (ENORMSEP), FORTRAN IV. Fish. Bull, U.S. 73:681.

Ovarian development, fecundity, and spawning frequency of black drum *Pogonias cromis* in Louisiana

Gary R. Fitzhugh
Department of Zoology, Box 7617, North Carolina State University
Raleigh, North Carolina 27695-7617

Bruce A. Thompson
Coastal Fisheries Institute, Center for Coastal, Energy and Environmental Resources
Louisiana State University, Baton Rouge, Louisiana 70803-7503

Theron G. Snider III
Department of Veterinary Pathology, School of Veterinary Medicine
Louisiana State University, Baton Rouge, Louisiana 70803-8420

Abstract.—Patterns in oocyte development, batch fecundity, and spawning frequency were assessed for black drum *Pogonias cromis* from Louisiana. We identified histological oocyte stages present throughout a protracted breeding season in 1986–87. We observed vitellogenesis beginning in November, and first postovulatory follicles were detected in February. Atresia of yolked oocytes was complete in May. We detected recruitment of vitellogenic eggs after the onset of spawning, suggesting indeterminant total fecundity. Mean batch fecundity for a 6.1 kg female (mean size sampled with hydrated oocytes) was calculated to be 1.6 million hydrated oocytes. A field estimate of spawning frequency was 0.311, indicating that a female spawns on average once every 3 d during the breeding season. Sex ratios were skewed with respect to sampling gear during the breeding season, suggesting segregation of actively-spawning fish on the spawning grounds.

Manuscript accepted 28 January 1993.
Fishery Bulletin, U.S. 91:244-253 (1993).

The black drum *Pogonias cromis* ranges from Argentina to the Bay of Fundy (Sutter et al. 1986) and is the largest sciaenid, up to 66 kg (Hildebrand & Schroeder 1928). A maximum age of 43 yr was recorded for black drum in the northern Gulf of Mexico (Beckman et al. 1990). Fishing pressure on black drum was historically very low, but has increased with commercial landings in the Gulf of Mexico rising from 1.9 million kg in 1982 to 4.8 million kg in 1987 (NMFS Natl. Fish. Stat. Office, New Orleans LA 70130).

Many temperate fishes are serial spawners with variable production of clutch sizes (Hunter & Goldberg 1980, DeMartini & Fountain 1981, Conover 1985). In particular, large long-lived species may exhibit high variability in reproductive output (Ware 1982). An important management objective with long-lived species is to identify changes in population egg production associated with the harvest loss of older age-classes. For black drum, the potential for exploitation of older age-classes is increased with development of the commercial fishery (NMFS 1986).

Despite the commercial value of black drum, relatively little is known of many life-history aspects of this species (Sutter et al. 1986). In the northern Gulf of Mexico, the spawning season has been reported from late-fall to spring, based upon egg and larval distributions (Jannke 1971, Holt et al. 1985, Ditty 1986) and occurrence of gravid females (Cody et al. 1985). Peters & McMichael (1990) reported peak spawning in March from Tampa Bay, Florida, based on distribution of larvae and juveniles. Murphy & Taylor (1989) computed size-at-maturation to be 590 mm and 650 mmFL for males and females, respectively, although there have been accounts of small females (<350 mmFL) with developing ovaries (Simmons & Breuer 1962, Pearson 1929). Spawning locations have been reported to occur within estuarine bays and in open coastal waters (Pearson 1929, Simmons & Breuer 1962, Jannke 1971, Peters & McMichael 1990). There has been only one estimate of fecundity determined from a single female (Pearson 1929), and no previous estimate of spawning frequency has been made from the adult stock.

Our objective is to provide baseline reproductive information from 1986–87 to be used in assessing popula-

tion changes and potential egg production to maintain future fishing harvests. We characterize ovarian development, seasonal spawning duration, and frequency as determined by ovarian histology and batch fecundity in Louisiana coastal waters.

Materials and methods

We sampled black drum monthly from commercial landings during March, June, July, October, November, and December 1986 and July 1987 to obtain reproductive information. We increased sampling effort during the period of reported peak seasonal reproductive activity and sampled 25 commercial landings during February, March, April, May, and June 1987. We also sampled recreational hook-and-line landings during March and July 1986 and April 1987. Landings sampled from inshore waters (bays and sounds) were primarily taken by gillnet, haul-seine, and hook-and-line. Landings sampled from offshore waters were taken by trawl and purse-seine.

In order to contrast size-at-maturity with other studies, we made gross visual classifications of gonads during sampling. Macroscopic characteristics for classifying gonads as mature correspond to Bagenal (1968) and Nielson & Johnson (1983). Female characteristics included the presence of eggs visible to the naked eye and light-yellow to reddish appearance from increased vascularization of the ovary. Characteristics for mature males included white appearance and relative enlargement of testes within the body cavity. Measurements included fork length (FL), sex, gutted (viscera removed) body weight (BW), and gonad weight (GW; wet weight blotted dry to nearest 0.1 g). We documented reproductive development by expressing gonad weight as a function of body size using the gonosomatic index (GSI) (Htun-Han 1978, Nielson & Johnson 1983).

We held gonads in ice up to 24 h after sampling and then fixed gonads in 10% formalin. One tissue sample was randomly selected from the preserved ovary and placed in an OmniSette tissue cassette. For histological observation, tissue samples were dehydrated, embedded in paraffin, sectioned, stained with Gill's hematoxylin, and counter-stained with eosin*. We classified oocytes from the prepared histology slides following Wallace & Selman (1981), DeVlaming (1983), and Selman & Wallace (1986). These stages include primary growth (PG), cortical alveoli (CA), vitellogenesis (V), and hydration (H).

To determine relative frequency of oocyte stages, we located a random starting point on a histological section and counted and staged all identifiable oocytes within a field before moving to a new microscope field using manual stage drive. Field movement was inward along the ovigerous lamellae, from the outer tunica albuginea toward the center of the ovary, with realignment along a vertical axis. To be counted, >50% of an oocyte must have been within a field of view. We counted and staged a minimum of 200 oocytes from each female and expressed tallies of the four oocyte stages as a percentage of the total count (Htun-Han 1978, Holdway & Beamish 1985). The Bioquant IV image analysis system software, IBM PC, and Houston Instrument digitizing pad (Hipad model DT-11) were used in conjunction with an Olympus microscope (with video attachment) to facilitate counts and measurements.

In addition to relative frequency of developmental stages, we classified each histological section for the presence of postovulatory follicles (POF) and atretic oocytes to aid in determination of spawning frequency. Our atresia classification was modified from that for northern anchovy (Hunter & Macewicz 1985). If no atresia of yolked oocytes was observed, we denoted the ovary as atretic state 0. Tissue sections exhibiting yolked oocytes undergoing atresia at <50%, >50%, and 100% were classed as atretic states 1, 2, and 3, respectively.

To estimate oocyte development rate, we related our histological observations of actively-spawning black drum to published accounts of spawning time of black drum (Mok & Gilmore 1983, Holt et al. 1985) and rates of hydration and postovulatory follicle degeneration in sciaenids (DeMartini & Fountain 1981, Brown-Peterson et al. 1988). With this time-calibrated histological information, we estimated the hours from spawning for females displaying yolk coalescence, hydration, postovulatory follicles, and atresia, and classified day-0, day-1, and nonspawning females. Our estimate of seasonal spawning frequency was determined by taking the average of the fractions of day-0 and day-1 spawning females relative to total females observed histologically with vitellogenic oocytes. Batch fecundity, the number of hydrated oocytes which comprise the leading "batch" of eggs immediately prior to spawning, was determined from formalin-fixed tissue samples taken from each visibly-hydrated ovary. We took replicate ovarian tissue samples (1–2 g) from anterior, mid-, and posterior regions of left and right lobes. In order to obtain 100–300 hydrated oocytes, tissue subsamples of 90–100 mg (weighed to the nearest 0.05 mg) were placed on a slide, glycerin added, and hydrated oocytes counted (Hunter et al. 1985). After observation of histological sections, any ovaries

* Preparation of histological slides, including washing, embedding, sectioning and staining, were completed by the Louisiana State University School for Veterinary Medicine, Department of Pathology.

with postovulatory follicles, indicating onset of spawning and possible shedding of eggs, were eliminated from further analysis of fecundity. To determine the precision of batch fecundity methodology (Hunter et al. 1985), we compared oocyte counts per unit weight within ovaries using a two-way analysis-of-variance model, SAS GLM procedure (SAS 1985).

Results

Sampling, sex ratio, and maturity

We recorded information on length, sex, and gear for 236 male, 108 female, and 36 immature black drum. In addition, we collected capture data, ovarian samples, and measurements, including somatic and gonad weights used for GSI analysis, from 198 males and 296 females. Ovarian histology sections were made from 234 mature females randomly sampled through June 1987, and were used to determine relative frequencies of oocyte stages (Fig. 1). Of these females, 25 were visibly hydrated, possessed no postovulatory follicles, and were used to estimate batch fecundity. Our sample mean length was 761 mmFL, with adults measuring 650–900 mmFL comprising 89% of individuals used in the study.

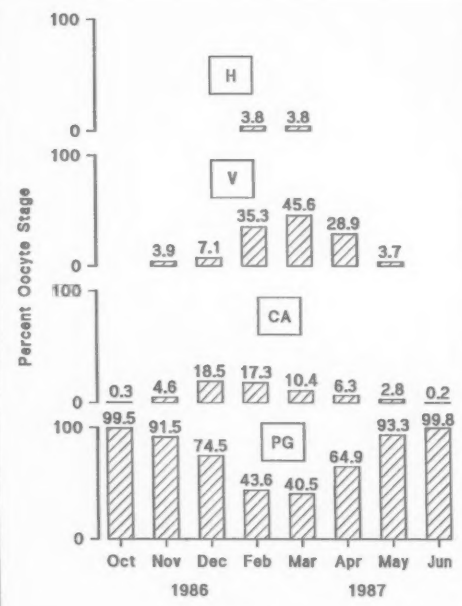

Figure 1

Percent oocyte stage by month for 1986–87 based on point counts of ~200 oocytes/female black drum *Pogonias cromis*. Stages include primary growth **(PG)**, cortical alveolar **(CA)**, vitellogenic **(V)**, and hydrated **(H)**. Number of females examined = 22 Oct, 23 Nov, 23 Dec, 69 Feb, 32 Mar, 24 Apr, 22 May, 19 June.

We found apparent differences in sex ratios from inshore landings (gillnet and haul-seine) and landings from an offshore trawl fishery during the reproductive season (Table 1). Trawl catches were dominated by males, while gillnet and haul-seine samples were dominated by females (Table 1). For months just before and after the reproductive season (October, June, July), females also dominated gillnet and haul-seine landings, but ratios were less divergent. The trawl fishery was not active at these times, but samples of offshore fish were taken from a purse-seine landing (June 1986) and numbers of females and males were nearly equal (0.92:1.0). We applied a χ^2 contingency analysis to test sex ratios by gear type. The χ^2 statistic was significant during the reproductive season (December–May), leading to rejection of the null hypothesis that gear type and sex ratio are independent (Table 1). We assumed that gears were not selective for sex but reflected actual sex ratios in the localities fished. Therefore, the skewed sex ratio suggests a segregation of sexes during the reproductive period. Female: male ratios were more divergent for commercial gears during the months of November–May than October, June, and July (Table 1).

Males and females were first mature at 600–640 mmFL as defined by the size at which individuals exhibit developing and mature gonads from gross visual inspection (Nielsen & Johnson 1983). All black drum >640 mm were mature. All fish <590 mm were immature, but sample size during spawning season was small (n=18 females and 11 males at 460–590 mm).

Table 1

Chi-square contingency analysis of black drum *Pogonias cromis* sex ratios for commercial gears represented by a minimum of 20 individuals.

Gear	Observed			Female:Male ratio
	Male	Female	Total	
Nov, Dec, Feb, Mar, Apr, May (χ^2=79.5, df 2, p<0.001)				
Gillnet	42	105	147	1:0.4
Haul-seine	39	65	104	1:0.6
Trawl	267	126	393	0.47:1
Total	348	296	644	
Oct, June, July (χ^2 =1.18, df 2, 0.9<p<0.5)				
Gillnet	27	42	69	1:0.64
Haul-seine	27	31	58	1:0.87
Purse-seine	13	12	25	0.92:1
Total	67	85	152	

Seasonal oocyte development

Ovaries were characterized by dominance of a single population of primary growth (PG) oocytes year-round, with subsequent appearance of more advanced vitellogenic oocytes during the reproductive season. Cortical alveolar (CA)-stage oocytes, signaling onset of development, were first observed in October 1986 (Fig. 1). By November, CA and vitellogenic (V) stages were common among females and comprised 4.6 and 3.9%, respectively, of the ova counted. We noted increasing proportions of CA and V oocytes relative to counts of PG oocytes by December (Fig. 1). Cortical alveolar-stage oocytes peaked during December, and vitellogenic oocytes lagged in time, exhibiting a peak in March (Fig. 1).

We noted evidence for onset of spawning in 2 females displaying yolk coalescence of vitellogenic oocytes during November 1986. We found conclusive evidence of active spawning on 16 February 1987, when we detected hydrated oocytes (H) and postovulatory follicles (POF). No fish were caught during January 1987 due to bad weather, and there was no evidence of active spawning (i.e., atresia or postovulatory follicles) from samples examined from November, December, or early February (n=61 females). Based on the number of females containing hydrated eggs, spawning peaked in February and March (Fig. 1). Although hydrated oocytes were not detected in April (Fig. 1), presence of postovulatory follicles indicated some spawning was still occurring (Table 2). Coalescence of vitellogenic oocytes, preceding hydration and ovulation, was detected in one female sampled 12 May 1987 (Table 2).

We observed a low proportion of atretic yolked oocytes among females during the development phase prior to onset of spawning. These were similar in appearance to atretic oocytes classified by Hunter & Macewicz (1985) as alpha-stage atresia. A low incidence of atretic yolked oocytes is considered normal during ovarian development in teleosts (DeVlaming 1983). However, we noted an increase in the presence of atretic material as the reproductive season progressed. By 24 April, 13 out of 16 sampled females were classified as atretic state 1, with atretic oocytes <50% of yolked oocytes present. We noted incidence of atretic oocytes >50% of the total yolked oocytes from individuals sampled 12 May 1987, probably signaling a decline in spawning (atretic state 2). By this date, all yolked oocytes were undergoing atresia in 12 out of 22 females examined histologically, and all 22 females exhibited some atretic yolked oocytes. By 12 June, atresia of yolked oocytes was complete for all females examined (n=19), and only gonadotropin-independent PG oocytes remained (atretic state 3).

Table 2

Number of female black drum *Pogonias cromis* in reproductive condition based on histological staging for determination of spawning frequency. Day-0 designated females were actively spawning or close to onset of spawning. Day-1 designated females have been sampled at least 6 h after spawning (see Fig. 3).

Date	Day-0 spawning females	Day-1 spawning females	Total mature females*
11/11/86	2		23
12/16/86	5		23
02/03/87	9		15
02/16/87	19		22
02/20/87	18	5	20
02/24/87			2
02/27/87	6	6	12
03/06/87		4	4
03/23/87	13	12	16
03/27/87	4	10	10
04/06/87		1	8
04/24/87	3	2	16
05/12/87	1		22
Total	80	40	193
Proportion of total	0.415	0.207	
Average proportion of total	0.311		

*Total observed histologically with vitellogenic oocytes

The gonosomatic index (GSI), which is gonad weight expressed as a fraction of body weight, is a common measure of gonad development used to document seasonal changes (Nielson & Johnson 1983). We observed a marked peak in GSI for both males and females in March (Fig. 2). Females exhibited the most dramatic change in gonad weight as the season progressed, with mean gonad weight increasing to >8% of eviscerated body weight. Both sexes followed a similar pattern with respect to time of onset, peak, and decline of GSI (Fig. 2). The gonosomatic index corresponded well with histological observations (Figs. 1, 2). Females exhibited an increase in GSI above "resting" levels in November, when CA and V oocytes were present. Monthly peaks in GSI during February and March resulted from the presence of hydrated oocytes and an increase in the proportion of vitellogenic eggs. Increased atresia of yolked oocytes observed histologically in April and May, associated with decreased spawning, produced a decrease in GSI (Fig. 2). In June, when all yolked oocytes were atretic, female GSI had dropped to 0.87,

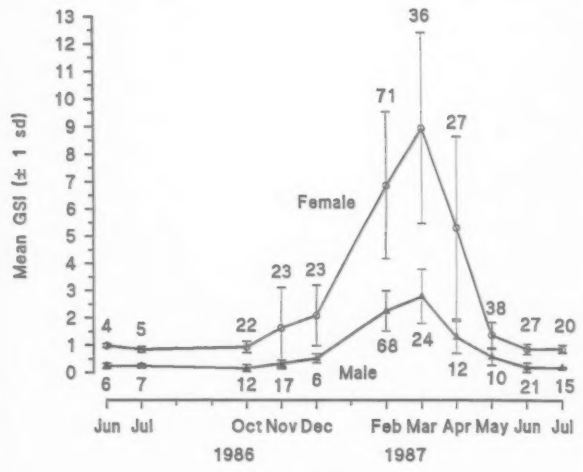

Figure 2
Mean value for gonosomatic index (GSI) for adult black drum *Pogonias cromis* (±1 SD). Sample sizes are indicated by numbers on graph.

and female GSI reached the observed minimum value of 0.84 by July (Fig. 2).

Spawning frequency

In order to estimate proximity to time of spawning and designate females as day-0 and day-1 spawners for spawning frequency calculation (Table 2), we constructed a time-scale of coalescence-stage oocytes, hydrated oocytes, and postovulatory follicles based on literature reports and our observations (Fig. 3). From previous work on related sciaenids, it is known that lipid coalescence, germinal vesicle migration, and yolk coalescence occur beginning in morning samples with hydration becoming evident as the day progresses (DeMartini & Fountain 1981, Fitzhugh et al. 1988, Brown-Peterson et al. 1988). Although exact capture times for some black drum were not known, females exhibiting germinal vesicle migration and yolk coalescence were commonly taken in haul-seine and gillnet sets which were typically landed during morning hours.

A follicle, comprised of an inner layer of epithelial granulosa cells and an outer layer of thecal cells, surrounds each hydrated oocyte. Following ovulation, POFs were present as the evacuated follicle remaining in the ovary. Recent POFs were denoted by linear arrangement of the granulosa cell layer and apical location of very prominent nuclei. These cellular arrangements imparted the appearance of a well-defined lumen and convoluted shape to the POF and were observed from ovaries sampled between 2400 and 0300 h from preliminary samples taken by hook-and-line in March 1986. We concluded that spawning occurred earlier that same night, and used these March 1986 samples as an example of recent POFs. Three females sampled from trawl landings in 1987 with recent POFs also had fully-hydrated eggs in the lumen of their ovaries, indicating active spawning and coinciding with reports of onset of spawning after dusk (Mok & Gilmore 1983, Holt et al. 1985). From interviews of commercial fishermen, capture of black drum in trawls often occurred after dusk and throughout the night, with fish being placed into ice as they were captured. We routinely sampled black drum the morning following their capture, and therefore it is likely that the recent POFs we observed are from fish captured up to 8 h after spawning (Fig. 3).

Over the 1986–87 spawning season, we sampled limited numbers of females bearing POFs (50 females taken from 8 different samples) indicating that duration of POFs may be brief. Hydration-stage oocytes, occurring together with visibly-degenerated POFs, were evident in only 19 females. Additionally, only 1 female contained recent POFs as well as degenerating POFs. Older degenerating POFs were similar in appearance to 24 h-old follicles illustrated in Hunter et al. (1986) from skipjack tuna *Katsuwonus pelamis* spawning at 23–24°C. Therefore, POF duration may be limited to 24–48 h following ovulation (Fig. 3).

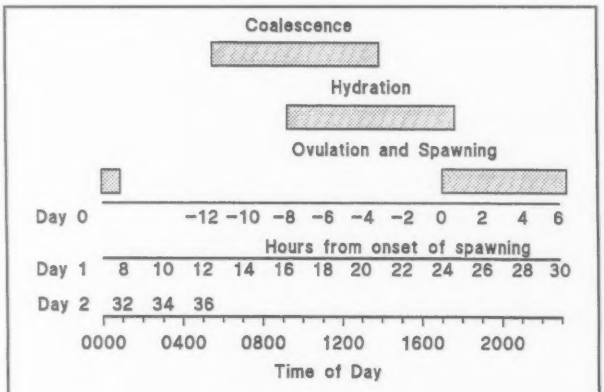

Figure 3
Generalized time-scale of final oocyte maturation and spawning of black drum *Pogonias cromis*, determined from observations and literature reports (see text).

We estimated spawning frequency by examining ovarian tissues of 193 mature females (vitellogenic oocytes present) sampled over the spawning season. We define spawning season as the period during which spawning condition was histologically evident, from first evidence of coalescence of vitellogenic oocytes on 11 November 1986, until atresia of vitellogenic oocytes was occurring in all females encountered on 12 May 1987 (Table 2). The numbers of day-0 and day-1 spawning females was 80 and 40 (frequencies = 0.415 and 0.207) for this period, respectively. This resulted in an overall seasonal frequency of 0.311, or each female spawning on average once every 3 d (Table 2). From November 1986 through May 1987, 50 of 193 females (26%) contained POFs. This method of estimating spawning frequency would correspond to a spawning frequency of once every 4 d, or a total of 46 times, during the spawning season.

Batch fecundity

We determined batch fecundity for 25 visibly-hydrated females which possessed no recent POF in histological sections that would indicate egg shedding. The range in batch fecundity was 7.4×10^5 hydrated oocytes for a 4.3 kg female, to 3.8×10^6 hydrated oocytes for a 4.8 kg female, indicating wide variation in fecundity based on body size (Fig. 4). The number of hydrated oocytes/g of ovary weight ranged from 1046 to 4902. Based on eviscerated body weight, the number of eggs/g ranged from 131 to 793. The mean value for batch fecundity was 1.6×10^6 for a mean eviscerated weight of 6.1 kg.

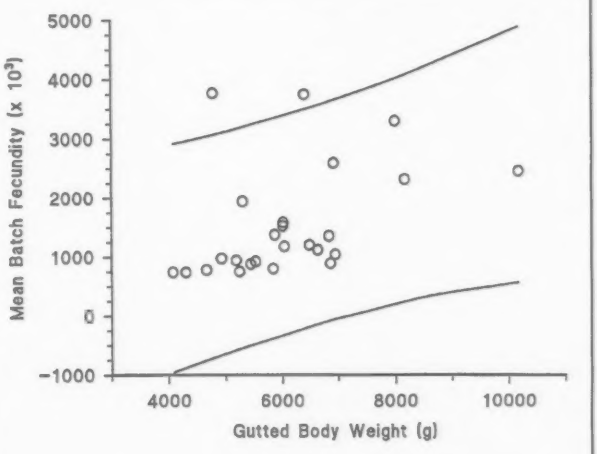

Figure 4
Batch fecundity and eviscerated body weight with 95% confidence interval for hydrated female black drum *Pogonias cromis*, sampled in February and March 1987.

Location of tissue samples

Black drum possess relatively large gonads for teleosts, and we sampled ovaries weighing 0.4–1.6 kg laden with hydrated oocytes. No significant differences were detected between positions within a lobe or between right and left ovarian lobes for number of hydrated oocytes/g of ovarian tissue (Table 3). However, counts of hydrated oocytes/g were lower for the anterior position ($\bar{x}$ 1780) than for either mid- or posterior ovarian regions ($\bar{x}$ 2013 and 1928, respectively) (Table 3).

Discussion

We noted differences in sex ratios between samples collected by various fishing gears during the period of reproductive development and spawning, November–May. Landings by offshore trawlers (where spawning females were found in February and March) were clearly dominated by males. Females dominated in inshore samples from all gears (primarily gillnet and haul-seine landings), but this female dominance was not as prevalent outside the breeding season during October, June, and July. These divergent ratios suggest sexes are spatially segregated for periods during the reproductive season. This difference in sex ratios has been noted in other fisheries where a higher proportion of males attend those females in active spawning condition on the spawning grounds (DeMartini & Fountain 1981, Hunter & Goldberg 1980).

In a synthesis of previous studies, Simmons & Breuer (1962) reported age-at-maturity for black drum to be 2 yr at 320 mm based on scale increments, length frequencies, and gross assessment of ripe females (granular roe observed) in Texas waters. Pearson (1929) found drum as small as 270 mm with developing ovaries. Murphy & Taylor (1989) provide evidence for larger sizes-at-maturity, with males maturing at 590 mm (4–5 yr old) and females maturing at 650 mm (5–6 yr old). Our findings of age-at-maturity agree with Murphy & Taylor's (1989) estimates. Mature females and males occurred at a size-range of 600–640 mmFL, corresponding to ages 3–8 yr (Beckman et al. 1990). A mature female with hydrated eggs was observed as small as 625 mmFL; this indicates that size- or age-at-maturity for northern Gulf of Mexico stocks is greater than previously estimated by Simmons & Breuer

Table 3

Effect of location of tissue samples of black drum *Pogonias cromis* for hydrated oocyte counts per unit of ovary weight (g). Locations are anterior (i), mid (ii), and posterior (iii) of ovarian lobes.

	Mean, SE of oocytes/g, and number of tissue samples								
	Right lobe			Left lobe			Both lobes		
Locations	$\bar{x}$	SE	n	$\bar{x}$	SE	n	$\bar{x}$	SE	n
i	1714	91	25	1846	170	25	1780	96	50
ii	2025	245	25	2000	199	25	2013	156	50
iii	1944	149	25	1911	180	25	1928	116	50
Total	1895	100	75	1919	105	75			

Two-way ANOVA:

Source of variance	df	SS	MS	F	PR>F
Lobe	1	22490	22490	0.03	0.87
Segment	2	1385533	692767	0.87	0.42
Interaction	2	213348	106674	0.13	0.87
Error	144	14701071	796535		
Total	149	116322441			

(1962) and Pearson (1929) for black drum from Texas waters.

Multiple oocyte stages were present throughout the 1986–87 spawning season, including primary growth (PG), cortical alveolar (CA), and vitellogenic (V) stages. Primary-growth oocytes were present year-round and are a gonadotropin-independent stage (Wallace & Selman 1981, DeVlaming 1983). Oocyte recruitment from this PG population and onset of seasonal oogenesis was signaled by the appearance of CA oocytes in October. Vitellogenic oocytes were noted in November, and both CA and V oocytes persisted until May, indicating the potential for a protracted spawning season.

Descriptions of the breeding season for black drum are varied. Gonad development and possible spawning have been reported during the summer (Pearson 1929, Cornelius 1984 cited in Cody et al. 1985). Our June, July, and October samples did not indicate that spawning was evident. By November, reproductive development for two females (yolk coalescence and final oocyte maturation in histological sections) indicated the potential for spawning to occur. Capture of black drum larvae from offshore Louisiana waters has been reported as early as December (Ditty 1986). Pearson (1929) reported the primary spawning season was February to May. Cody et al. (1985) described seasonality of gonad development of black drum in Texas and reported gravid females during November–April, with spawning or spent stages predominant during February–April. From Florida, Murphy & Taylor (1989) and Peters & McMichael (1990) also report the reproductive season ranges from November to April with February–March spawning peaks.

All the changes noted with the onset, peak, and decline of the spawning season were reflected both in histological samples of ovaries and in gonad weight changes relative to body weight (GSI) for females. Increase in proportion of vitellogenic oocytes was associated with GSI increase in November and December. Appearance of hydrated oocytes and postovulatory follicles in February and March coincided with highest values for GSI. Subsequent appearance of atretic vitellogenic oocytes in April, and increase in atresia in May and June, were associated with declines in gonad weights reflected by decreasing GSI. The GSI seasonal pattern for males coincided with the pattern for females, and suggests a synchrony in development of reproductive states for both sexes. However, mean GSI values must be interpreted with caution. For the same stage of oocyte development, a larger individual may exhibit proportionally larger ovaries and a greater GSI value than a smaller individual (DeVlaming et al. 1982). We apply the GSI here only as a relative measure of changes in reproductive condition over the spawning season, and not as a specific measure of reproductive readiness or histological stage.

Black drum spawn in inside (estuarine, bay) as well as in outside (coastal waters seaward of inlets) waters. Pearson (1929) indicated spawning took place in Gulf waters off Texas, although Simmons & Breuer (1962) presented evidence for spawning in estuaries. Osburn & Matlock (1984) present evidence from tagging studies for a "quasi-permanent" movement of black drum >4 yr from bays to the Gulf, where they may act as spawning stock. Jannke (1971) cited evidence of estuarine spawning in the Florida Everglades, but also indicated that spawning occurred outside the estuarine portion of the park. Peters & McMichael (1990) report that spawning in the Tampa Bay region was likely to have occurred both inside and outside the bay. We also noted spawning activity over a gradient from offshore to inshore. Examination of black drum in hydrated condition from trawl landings during February and March indicated spawning was occurring in coastal waters off Louisiana. During late March, however, females in hydrated condition were taken by haul-seine from inshore estuarine waters east of the Mis-

sissippi River. Drumming behavior associated with spawning was noted in Caminada Pass, Louisiana in April, further documenting inshore reproductive activity (Donald Baltz, Coastal Fish. Inst., LA State Univ., Baton Rouge, pers. commun.).

The dynamic of changing spawning locations may have a seasonal component related to water temperature. Mok & Gilmore (1983) analyzed sound production from black drum in Florida waters and noted "loud drumming," which they associated with spawning, occurring at 18–20°C. They also noted cessation of this drumming during a temperature drop to 13–15°C. Peters & McMichael (1990) provided more direct evidence for onset of spawning at 16–20°C. By correlating seasonal water temperature with larval birthdates, peak births were calculated to have occurred in March when temperatures reached 21–24°C. Although we did not have precise locations and temperatures for commercial catches, our samples of hydrated-oocyte and POF-bearing females indicate that spawning may have predominated in outside waters in February (e.g., trawl landings) and moved to inside waters as seasonal temperatures increased (haul-seine and gillnet landings in March and April). Other factors not examined may influence spawning, including moon phase and tidal period (Peters & McMichael 1990).

Postovulatory follicles probably last longer than 24 h at sea temperatures encountered in coastal Louisiana waters in February and March (19–22°C). Hunter & Macewicz (1985) found POFs for 3–4 d from northern and peruvian anchovies (*Engraulis mordax* and *E. ringens*) spawning at 13–19°C. Based on a higher spawning temperature of 23–24°C, Hunter et al. (1986) found 24 h-old follicles in skipjack tuna that appeared similar to those in northern anchovy held 48 h. Our day-1 POFs appeared similar to 24 h POFs for skipjack tuna shown in Hunter et al. (1986). We estimated black drum follicle duration to be at least 32 h old, due to the presence of recent POFs and older-degenerating POFs together in the same histological sections (i.e., 0–8 h plus 24 h, respectively) which is consistent with spawning on successive nights. If follicles are identifiable well past 24 h, our estimate of average duration between spawning would increase.

Our estimates of spawning frequency, once every 3 or 4 d, are similar to other sciaenid species. Tucker & Faulkner (1987) report a daily spawning fraction of 0.35 (once every 3 d) for captive spotted seatrout. Brown-Peterson et al. (1988) calculated an average daily percentage of wild seatrout in ripe condition to be 27.5% (indicating spawning once every 3.6 d) over a 6 mo reproductive season. Red drum have displayed a spawning fraction of 0.68 (once every 1.5 d) in captivity over a 76 d period (Arnold et al. 1977).

The pattern of appearance of vitellogenic oocytes supports our contention that oocyte recruitment continued during the reproductive season. Therefore, the yolked-oocyte population was not deterministic or representative of annual fecundity (Hunter et al. 1985). Of females examined histologically in February, 73% showed evidence of recent spawning (day-0 females), yet the proportion of vitellogenic oocytes from females did not reach a maximum until March. In contrast, a species with a determinant oocyte development pattern could exhibit multiple spawns but the proportion of vitellogenic oocytes would decrease following onset of spawning (Hunter et al. 1985). With continuous recruitment of batches of oocytes, the traditional method to determine fecundity by enumerating vitellogenic oocytes prior to onset of reproduction (e.g., Bagenal 1968) would underestimate potential fecundity. This method necessitates counting of hydrated eggs just prior to ovulation, i.e., determining batch fecundity and number of spawns in the season (Hunter et al. 1985).

Previously, little fecundity information has been reported for black drum (Sutter et al. 1986). Pearson (1929) estimated fecundity at 6 million eggs for one 110 cm gravid female (107cmFL, 16.4 kg eviscerated weight)* based on extrapolation of wet weight for 60 eggs. Our computation of batch fecundity was 1.6 million eggs for a 6.1 kg female (mean eviscerated weight of 25 females). Figure 4 and comparison with Pearson's result suggest that batch fecundity is a function of body size, but we found this relationship to be quite variable (Fig. 4). While these data do not appear to fit a linear relationship as closely as for smaller sciaenids (DeMartini & Fountain 1981, Brown-Peterson et al. 1988), we only sampled hydrated females measuring 660–876 mmFL. Because females >1000 mm are occasionally landed (e.g., Beckman et al. 1990), a broader range of sizes could illuminate the functional relationship between size and fecundity. Batch size may vary also with the reproductive period and may be higher earlier in the spawning season. Our sample size was too small to detect changes in batch fecundity over the breeding season. However, the pattern of vitellogenesis and GSI provides evidence that spawning peaked in March. The proportion of females in spawning condition was also highest in March. Conover (1985) demonstrated a quadratic batch-fecundity relationship for Atlantic silversides during the breeding season. He postulated that this pattern may occur when optimal

* Calculated from TL-FL regression reported in Murphy & Taylor (1989). The relationship between eviscerated body weight (BW) and fork length (FL) is given by the equation: Ln BW = 2.8835 Ln FL - 10.382 (n=100, r^2=0.964, range 459-1122 mmFL).

conditions for reproduction exist at about the same time each year.

The batch fecundity estimate multiplied by the frequency of spawning provides an estimate of annual fecundity (Hunter & Macewicz 1985, Hunter et al. 1985). For example, annual production could be as high as 32 million eggs for a 6.1kg female with an average clutch of 1.6 million eggs over 20 spawns (assuming spawning every 3 d on average during February and March). Although this estimate of annual fecundity is high for wild fish, spawning patterns in captivity for a closely-related sciaenid, red drum *Sciaenops ocellatus*, corroborates this magnitude of egg production. Three captive female red drum produced 6×10^7 eggs over 76 d, or roughly 20 million eggs/female (Arnold et al. 1977).

Although we found no significant differences in hydrated egg counts between ovarian lobes or among locations within a lobe, we observed the maximum number of hydrated oocytes in the mid-region of ovaries. Hydrated eggs per unit of ovary weight were lowest for the anterior region of the ovary, and may have been due to decreased vascularization or the hydration rate (Hunter et al. 1985, Fitzhugh et al. 1988). In future sampling, we recommend multiple samples be taken for accurate batch-fecundity determinations due to the large ovary size and potential for heterogeneity of hydrated oocytes among locations within the ovary.

Acknowledgments

We thank the many fishermen, seafood dealers, and tournament organizations for their efforts and cooperation in obtaining samples. Assistance in data collection was provided by Robby Parker, Dave Nieland, Dan Beckman, Louise Stanley, and David Stanley. This work was supported by the Louisiana Board of Regents' Rockefeller Fund Interest Earnings Grant Program and by the Louisiana State University, Coastal Fisheries Institute.

Citations

Arnold, C. R., W. H. Bailey, J. L. Lasswell, T. D. Williams, & A. Johnson
1977 Laboratory spawning and larval rearing of red drum and southern flounder. Proc., Annu. Conf. Southeast Assoc. Fish Wildl. Agencies 31:347–440.

Bagenal, T. B.
1968 Fecundity. *In* Ricker, W.E. (ed.), Methods for assessment of fish production in freshwaters, p. 160–169. IBP (Int. Biol. Prog.) Handb. 3.

Beckman, D. W., A. L. Stanley, J. H. Render, & C. A. Wilson
1990 Age and growth of black drum in Louisiana waters of the Gulf of Mexico. Trans. Am. Fish. Soc. 119:537–544.

Brown-Peterson, N., P. Thomas, & C. R. Arnold
1988 Reproductive biology of the spotted seatrout, *Cynoscion nebulosus*, in South Texas. Fish. Bull., U.S. 86:373–388.

Cody, T. J., K. W. Rice, & C. E. Bryan
1985 Distribution and gonadal development of black drum in Texas gulf waters. Manage. Data Ser. 72, Tex. Parks Wildl. Dep., Coast. Fish. Branch, 16 p.

Conover, D. O.
1985 Field and laboratory assessment of patterns in fecundity of a multiple spawning fish: The Atlantic silverside *Menidia menidia*. Fish. Bull., U.S. 83:331–341.

Cornelius, S. E.
1984 Contribution to the life history of black drum and analysis of the commercial fishery of Baffin Bay, Vol. II. Tech. Bull. 6, Caesar Kleberg Wildl. Res. Inst., Tex. A&I Univ., Kingsville, 53 p.

DeMartini, E. E., & R. K. Fountain
1981 Ovarian cycling frequency and batch fecundity in the Queenfish, *Seriphus politus*: Attributes representative of serial spawning fishes. Fish. Bull., U.S. 79:547–559.

DeVlaming, V.
1983 Oocyte development patterns and hormonal involvements among teleosts. *In* Rankin, J.C., et al. (eds.), Control processes in fish physiology, p. 176–199. John Wiley, NY.

DeVlaming, V., G. Grossman, & F. Chapman
1982 On the use of the gonosomatic index. Comp. Biochem. Physiol. 73A:31–39.

Ditty, J. G.
1986 Icthyoplankton in neritic waters of the Northern Gulf of Mexico off Louisiana: Composition, relative abundance, and seasonality. Fish. Bull.,U.S. 84:935–946.

Fitzhugh, G. R., T. G. Snider, & B. A. Thompson
1988 Measurement of ovarian development in red drum (*Sciaenops ocellatus*) from offshore stocks. Contrib. Mar. Sci., Suppl. to vol. 30:79–86.

Hildebrand, S. F., & W. C. Schroeder
1928 Fishes of Chesapeake Bay. Bull. U.S. Bur. Fish. 43(1), 388 p.

Holdway, D. A., & F. W. H. Beamish
1985 The effect of growth rate, size, and season on oocyte development and maturity of Atlantic cod (*Gadus morhua* L.). J. Exp. Mar. Biol. Ecol. 85:3–19.

Holt, G. J., S. A. Holt, & C. R. Arnold
1985 Diel periodicity of spawning in Sciaenids. Mar. Ecol. Prog. Ser. 27:1–7.

Htun-Han, M.
1978 The reproductive biology of the dab *Limanda limanda* (L.) in the North Sea: Seasonal changes in the ovary. J. Fish Biol. 13:351–359.

Hunter, J. R., & S. R. Goldberg
1980 Spawning incidence and batch fecundity in Northern Anchovy, *Engraulis mordax*. Fish. Bull., U.S. 77:641–652.

Hunter, J. R., & B. J. Macewicz
1985 Measurement of spawning frequency in multiple spawning fishes. *In* Lasker, R.L. (ed.), An egg production method for estimating spawning biomass of pelagic fish: Application to the northern anchovy, *Engraulis mordax*, p. 79–94. NOAA Tech. Rep. NMFS 36.

Hunter, J. R., N. C. H. Lo, & R. J. H. Leong
1985 Batch fecundity in multiple spawning fishes. *In* Lasker, R.M. (ed.), An egg production method for estimating spawning biomass of pelagic fish: Application to the northern anchovy, *Engraulis mordax*, p. 67–77. NOAA Tech. Rep. NMFS 36.

Hunter, J. R., B. J. Macewicz, & J. R. Sibert
1986 The spawning frequency of Skipjack Tuna, *Katsuwonus pelamis*, from the South Pacific. Fish. Bull.,U.S. 84(4):895–903.

Jannke, T. E.
1971 Abundance of young sciaenid fishes in Everglades National Park, Florida, in relation to season and other variables. Sea Grant Tech. Bull. 11, Univ. Miami Sea Grant Prog., Miami.

Mok, H. K., & R. G. Gilmore
1983 Analysis of sound production in estuarine aggregations of *Pogonias cromis*, *Bardiella chrysoura*, and *Cynoscion nebulosus* (Sciaenidae). Bull. Inst. Zool., Acad. Sin. (Taipei) 22:157–186.

Murphy, M. D., & R. G. Taylor
1989 Reproduction and growth of black drum, *Pogonius cromis*, in northeast Florida. Northeast Gulf Sci. 10(2):127–137.

Nielson, L. A., & D. L. Johnson (editors)
1983 Fisheries techniques. Am. Fish. Soc., Bethesda, 468 p.

NMFS (National Marine Fisheries Service)
1986 Final secretarial Fishery Management Plan, regulatory impact review, initial regulatory flexibility analysis, and final EIS for the red drum fishery of the Gulf of Mexico. Natl. Mar. Fish. Serv., NOAA, Southeast Region, St. Petersburg FL 33702, Dec. 1986.

Osburn, H. R., & G. C. Matlock
1984 Black drum movement in Texas bays. N. Am. J. Fish. Manage. 4:523–530.

Pearson, J. C.
1929 Natural history and conservation of the redfish and the commercial sciaenids on the Texas Coast. Fish. Bull., U.S. 44:129–214.

Peters, K. M., & R. H. McMichael Jr.
1990 Early life history of the black drum *Pogonias cromis* (Pisces:Sciaenidae) in Tampa Bay, Florida. Northeast Gulf Sci. 11(1):39–58.

SAS
1985 SAS user's guide: Statistics. Version 5 ed. SAS Inst. Inc., Cary NC, 956 p.

Selman, K., & R. A. Wallace
1986 Gametogenesis in *Fundulus heteroclitus*. Am. Zool. 26:173–192.

Simmons, E. G., & J. P. Breuer
1962 A study of redfish, *Sciaenops ocellata* Linnaeus, and black drum *Pogonias cromis* Linnaeus. Publ. Inst. Mar. Sci. Univ. Tex. 8:184–211.

Sutter, F. C., R. S. Waller, & T. D. McIlwain
1986 Species profiles: life histories and environmental requirements of coastal fisheries and invertebrates (Gulf of Mexico)-black drum. U.S. Fish Wildl. Serv. Biol. Rep. 82(11.51), U.S. Army Corps of Eng. TR EL-82-4, 10 p.

Tucker, J. W., & B. E. Faulkner
1987 Voluntary spawning patterns of captive spotted seatrout. Northeast Gulf Sci. (1):59–63.

Wallace, R. A., & K. Selman
1981 Cellular and dynamic aspects of oocyte growth in teleosts. Am. Zool. 21:325–343.

Ware, D. M.
1982 Power and the evolutionary fitness of teleosts. Can. J. Fish. Aquat. Sci. 39:1–13.

Swimbladder inflation of the Atlantic menhaden *Brevoortia tyrannus*

Richard B. Forward
Leslie M. McKelvey
Duke University School of the Environment, Marine Laboratory
Pivers Island, Beaufort, North Carolina 28516-9721

William F. Hettler
Donald E. Hoss
Beaufort Laboratory, Southeast Fisheries Science Center
National Marine Fisheries Service, NOAA
Beaufort, North Carolina 28516-9722

Abstract.—Atlantic menhaden *Brevoortia tyrannus* larvae inflate their swimbladders at night and deflate them during the day. The present study considered the relationship of inflation to light intensity, the time-course of inflation, and the presence of an endogenous rhythm in inflation. The percentage of laboratory-reared larvae that inflate their swimbladders increased upon sudden exposure to a decrease in light intensity. Percentage inflation was maximal at an intensity of 10^{13} photons cm^{-2} s^{-1} and lower. For any specific size of larvae, the inflation volume did not vary significantly with light intensity, but volume increased with total larval length. Inflation began within 5 min of introduction into darkness, and maximum percent inflation was evident by 20 min. There was a rhythm in which darkness induced a low percent inflation during the day phase and a high percentage at the beginning of the dark-phase. This dramatic increase in inflation at sunset may function for predator avoidance.

Manuscript accepted 17 February 1993.
Fishery Bulletin, U.S. 91:254-259 (1993).

Diel inflation and deflation of the swimbladder are common to larval clupeoid fishes (Uotani 1973, Hunter & Sanchez 1976, Blaxter & Hunter 1982). Both Atlantic (*Brevoortia tyrannus*; Hoss et al. 1989) and gulf (*Brevoortia patronus*; Hoss & Phonlor 1984) menhaden larvae inflate their swimbladders during the night and deflate them during the day. Inflation occurs by moving to the surface, swallowing air into the alimentary canal, and moving it to the swimbladder through the pneumatic duct (Hoss & Phonlor 1984). Deflation is presumed to take place by diffusion, because menhaden have no open connection between the anal opening and swimbladder (Tracy 1920).

Inflation/deflation by menhaden larvae is clearly related to the light: dark cycle. Field studies of both Atlantic and gulf menhaden found most larvae had deflated swimbladders and low swimbladder volumes during the day, with the reverse conditions at night (Hoss & Phonlor 1984, Hoss et al. 1989). Since inflation is rapid, occurring within 1 h after sunset, Hoss et al. (1989) suggested that change in light intensity may cause the inflation response.

The present study was undertaken to determine (1) the relationship between inflation and light intensity for Atlantic menhaden larvae, (2) the time-course for inflation, and (3) the presence or absence of an endogenous rhythm in inflation.

Materials and methods

Atlantic menhaden *Brevoortia tyrannus* were spawned and reared in the laboratory using methods described by Hettler (1983). After egg hatching, the larvae were held in circular tanks (100 L) at about 20°C on a 12:12 h LD cycle. The dark phase began at 1800 h. Lighting during the light phase was provided by daylight fluorescent tubes at a surface intensity of 1.6×10^{15} photons cm^{-2} s^{-1} (400–700 nm) as measured with a scalar irradiance meter with a 4ii collector (Biospherical Instruments, Inc.). Young larvae were fed rotifers *Brachionus plicatilus* cultured in the laboratory. Older fish (13–15 mm) were fed brine shrimp (*Artemia* sp.) nauplii. Larvae measuring 9–20 mm were used in the experiments.

Inflation was quantified by measuring light-refractive bubbles in the swimbladder and alimentary canal to the nearest 0.02 mm under a microscope. It was assumed that any bubbles in the alimentary canal were being transported to the swimbladder. Gas bubble volume was calculated using the equation of Hunter

& Sanchez (1976): $V = 4/3\ 4ii\ ab^2$, where b = half the bubble width and a = half the bubble length. The total volume of all bubbles was used as the swimbladder volume.

There were three sets of experiments. The first was designed to determine the relationship between light intensity and swimbladder inflation. Larvae were removed from the rearing tanks just before the beginning of the dark phase and maintained under approximately the same light intensity (cool white fluorescent lamps: intensity = 1.7×10^{15} photons cm^{-2} s^{-1}). A control group of the larvae was measured for total length (TL), presence of gas bubbles in the swimbladder and alimentary canal, and size of the bubbles. Similar standard measurements were made on the remaining larvae after being exposed to the test light intensity for 3 h. The light-stimulus source was a 300 W incandescent lamp filtered to the blue region with a Corning 4-96 filter. The transmitted wavelengths encompassed the major spectral-sensitivity maxima of most fish (e.g., Munz 1958, McFarland & Munz 1975). All intensities below the maximum level were controlled by neutral density filters. Each larva was only measured once.

Since the total-length range of larvae was 9–20 mm, an important question is whether all sizes were equally responsive to lighting changes that induce swimbladder inflation. An answer to this question was provided by considering (1) the percentage of different-sized larvae that inflate their swimbladder before and after exposure to new lighting conditions, and (2) the percentage of the total number of larvae sampled in each size-category.

The second set of experiments was designed to determine the time-course for swimbladder inflation. Larvae were again removed from the rearing tank near the end of the light-phase and illuminated at about the intensity used for rearing. Standard measurements were made on a control sample of larvae. The remaining larvae were put into darkness at the beginning of the dark-phase, and standard measurements made on subsamples at various time-intervals (5, 15, 30, 60, 90, 120 min).

The third experiment tested for the presence of an endogenous rhythm in swimbladder inflation. A large group of larvae was removed from the rearing tank at the beginning of the light phase and placed in constant temperature (22°C) and light (cool-white fluorescent lamps: intensity = 1.7×10^{15} photons cm^{-2} s^{-1}) both of which were similar to the light intensity and water temperature of the rearing tanks. Standard measurements were made at 3 h intervals on a subsample of larvae. At the beginning of each of these measurements, a similar subsample was placed in darkness and standard measurements made 2 h later. A change in the percent inflating over the day would suggest the presence of an endogenous rhythm.

The percentage of larvae with inflated swimbladders and the total volume of bubbles in each larva were calculated for each observation within each experiment. Means, standard deviations, and standard errors of percent data were calculated after the data were arcsin-transformed. A Z statistic was used to test differences between two proportions, while a Student's *t*-test was used to compare mean values (Walpole 1974).

Results

Relation of swimbladder inflation to light intensity

The percentage of larvae inflating their swimbladder under all experimental conditions changed with size (Fig. 1). Prior to exposure to new light conditions, the percent of larvae with inflated swimbladders remained relatively low for all sizes of larvae. In contrast, when subjected to a decreased light intensity, the percent response changed dramatically with size. None of the 9 mmTL larvae inflated their swimbladder, and only a low percentage of 10 mmTL larvae showed inflation (Fig 1). Percent inflation increased as size increased, reaching 100% for larvae >17 mmTL. The following study will focus on larvae 11–16 mm in length, because the percent inflation can vary with lighting condition.

Equal numbers of larvae were not sampled in each size-category (Fig. 2), as most larvae were 11–12 mmTL and there were few >15 mmTL. This size distribution

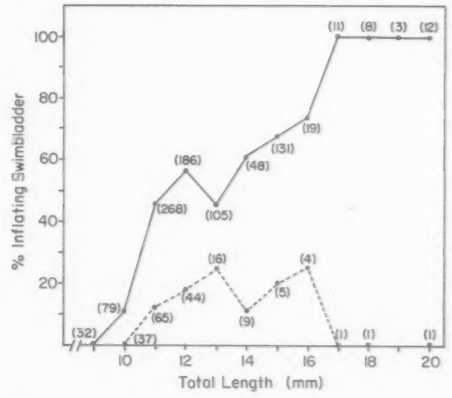

Figure 1

Percentage of larvae inflating their swimbladder versus size for all larvae in the swimbladder inflation versus light intensity experiment (Fig. 3). The dashed line shows the percentages before exposure to different light conditions, and the solid line is the experimental percentages.

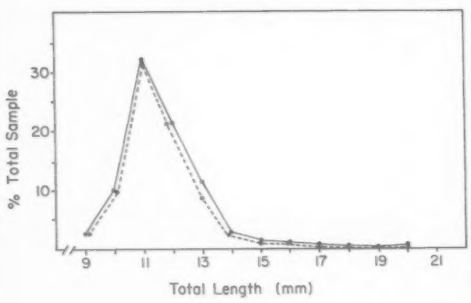

Figure 2

Percentage of the total number of larvae of the different total length sampled for the swimbladder inflation vs. light intensities experiment (Fig 3). Dashed line shows larvae sampled before exposed to different light levels (control; total n=193), whereas the solid line is larvae exposed to different light conditions (experimental; n=834).

was consistent for all experiments. Since the probability of swimbladder inflation was not equal for each size-category (Fig. 1), results will be biased to responses of the most-abundant size if all size-classes are grouped together. Thus, detailed analyses should only consider individual size-classes. The most-abundant size (11 mmTL; Fig. 2) will be used for this purpose.

The percentage of fish inflating their swimbladders increased as they were exposed to lower light intensities (Fig. 3). The highest light intensity to induce a significant increase in the proportion of fish with inflated swimbladders (threshold intensity) varied slightly with fish size. For 11 mmTL larvae (Fig. 3A) the threshold intensity was ~6×10^{13} photons cm^{-2} s^{-1}, whereas for 12–16 mmTL larvae, it was 1 log unit higher (Fig. 3B). For both size-groups, the proportion filling their swimbladders at ~10^{13} photons cm^{-2} s^{-1} and lower light intensities was not significantly different from the proportion in darkness.

The variation in swimbladder volume with light intensity was considered in detail for 11 mmTL larvae (Fig. 4). Mean volume increased as light intensity decreased, but the difference was not significant between the initial mean volume and that in darkness due to large variances (Fig. 4). Similar results were also obtained for 12 and 13 mmTL larvae.

In contrast, swimbladder volume increased proportionately with larvae size (Fig. 5). When the relationship between mean volume (V) in darkness and total length (L) was expressed as the allometric equation ($V=aL^b$), the slope of the regression (b) equaled 5.31 (r^2=0.99, p<0.0001). Means were calculated for larvae of each size in all conditions, because volume did not change with lighting condition (Fig. 4). Since volume changed with larval length, volumes could not be averaged for larvae of different lengths.

Timing of swimbladder inflation

The timing of swimbladder inflation was measured upon transfer from rearing-light intensity to darkness. By producing the maximum rate of intensity change, we assumed the maximum rate of inflation should be evoked. Results were combined for larvae 11–16 mmTL because the proportion inflating in darkness for 11 mm larvae was not statistically different from the proportion of 12–16 mmTL larvae (Fig. 3). A significant increase in the proportion with inflated swimbladders was evident after 5 min in darkness (Fig. 6). The maximum percent inflation was reached within 20 min. The proportion of fish with inflated swimbladders then remained relatively constant for about the next 1.5 h.

Endogenous rhythm in swimbladder inflation

The percent inflating prior to placement in darkness remained low throughout the 24h sampling interval, which

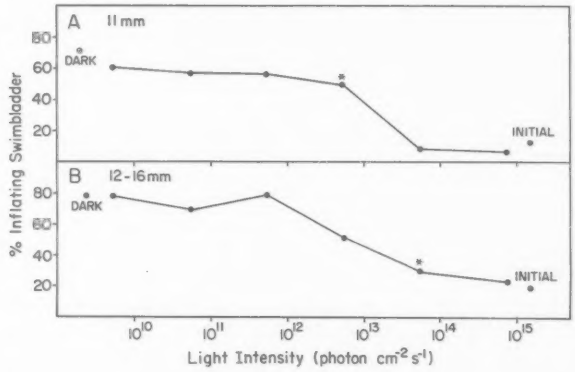

Figure 3

Percentage of larvae 11 mmTL **(A)** and 12–16 mmTL **(B)** inflating their swimbladder when exposed to different light intensities and darkness (dark). "Initial" is the percentage sampled shortly after removal from the rearing tank. Average sample sizes for each condition in A and B are 44 and 58, respectively. Asterisk indicates the highest light intensity to evoke a response that was significantly (p<0.05) greater than the initial response.

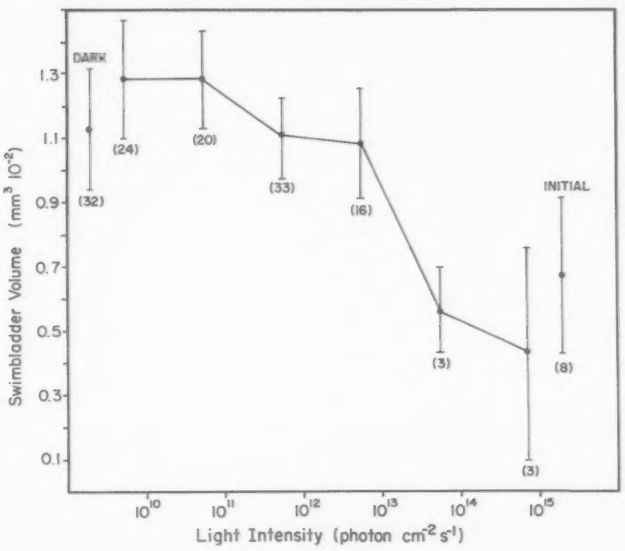

Figure 4

Swimbladder volume of 11 mmTL larvae shortly after removal from the rearing tank (initial) and when exposed to different light levels and darkness (dark). Means and standard errors are shown. Number below each plot is the sample size.

indicates there was no endogenous rhythm in inflation in constant high light conditions (Fig. 7A). Placement in darkness induced inflation in ~40% of the larvae during the normal light-phase. This percentage increased dramatically to 70% at the normal time for the beginning of the dark-phase (Fig. 7A). This response level continued into the time of the next light-phase. Mean swimbladder volume of 11 mmTL larvae varied over time, but the maximum and minimum means over the first solar day were not significantly different due to the large variances (Fig. 7B).

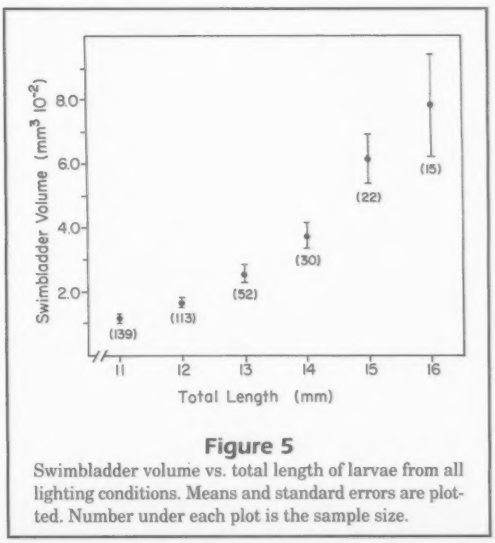

Figure 5

Swimbladder volume vs. total length of larvae from all lighting conditions. Means and standard errors are plotted. Number under each plot is the sample size.

Discussion

Atlantic menhaden inflate their swimbladders in response to a decrease in light intensity. The smallest size observed with an inflated swimbladder was 10 mmTL, which is smaller than the minimum size of 13 mmTL found by Hoss & Blaxter (1982). This difference may result from the large sample size used in the present experiment, since the percentage of 10 mmTL larvae with an inflated swimbladder was ~10%. The percentage of larvae inflating their swimbladder in response to a decrease in light intensity increased with size and reached 100% at 17 mmTL and greater.

Swimbladder volume increased with size, which is not surprising, since larger larvae have larger swimbladders. However, within any fish size, the mean volume did not vary significantly with lighting condition. This result disagrees with the qualitative conclusion of Hoss et al. (1989) and is likely due to the wide variation in volume. Hoss et al. (1989) also found high variances, but failed to compare mean values statistically.

The percentage of larvae inflating their swimbladders increased as the light intensity decreased, which clearly indicates that the decrease in light intensity cued the response. However, a step function was observed, in that once light was below a particular absolute level, maximum inflation occurred. Future experiments are needed to determine whether inflation is cued by exposure to light intensity below an absolute level or to the rate of change in intensity. This information will allow predictions of the time of inflation in the field.

Hoss et al. (1989) failed to find an endogenous rhythm in swimbladder inflation for larvae held under conditions similar to the present experiment. In contrast, our study showed a clear rhythm during the first day for larvae held under constant light. The percent inflation was low in fish introduced to the dark during the time of the light-phase, and nearly doubled at the time the dark-phase began. This high percent response did not return to a low level at the time of the next light-phase. Hoss et al. (1989) did not begin measuring swimbladder inflation until after ~24 h in constant light, which may be why they failed to detect an endog-

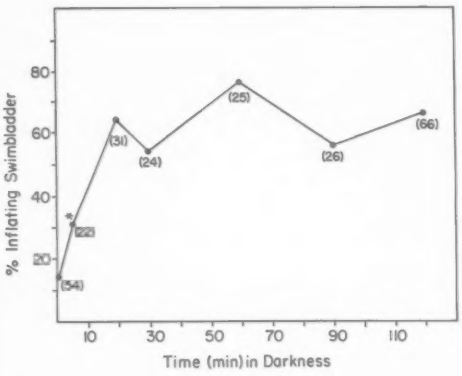

Figure 6

Percentage of larvae 11–16 mmTL filling their swimbladders after different times in darkness. Number under each point is the sample size, and asterisk is the first time that a proportion was significantly greater ($p<0.05$) than the proportion of larvae with inflated swimbladders initially in light, which is plotted at time zero.

enous rhythm. After this time in constant light, variation in inflation after introduction to dark was not evident in the present study. There are two possible explanations for this result. First, the rhythm could fail to continue because larvae were kept in constant light, a condition that frequently suppresses an endogenous rhythm (Hastings et al. 1991). Second, the rhythm could consist of one cycle in which inflation is suppressed during the light-phase and larvae become "ready" to inflate at the beginning of the dark-phase. Readiness then continues until a dark cue is received, which resets the endogenous clock.

Clearly, Atlantic menhaden larvae are adapted for swimbladder inflation at sunset. Their rhythm indicates they are most responsive to a light-intensity decrease at this time and most inflation occurs within 20 min. Such a dramatic response suggests swimbladder inflation has an important functional advantage.

Menhaden larvae are negatively buoyant even with a fully inflated swimbladder. Nevertheless, inflation reduces their sinking rate (Hoss et al. 1989). Past investigators have suggested that swimbladder inflation acts as an energy-saving mechanism, allowing larvae to expend less energy for maintaining their position in the water column at night when they are not feeding (Hunter & Sanchez 1976). During the day, a fully inflated swimbladder may reduce the speed of movement and, thereby, the effectiveness of prey capture and predator avoidance.

In addition, Uotani (1973) proposed that inflation allows larvae to decrease their movement at night, which serves to reduce detection by predators that hunt by vibrations, such as chaetognaths. Field studies show some indication that menhaden larvae undergo reverse diel vertical migration (DVM) in which they descend in the water column near sunset and ascend near sunrise (Hoss et al. 1989). Chaetognaths exhibit the opposite pattern of nocturnal DVM (Pearre 1973, Sweatt & Forward 1985). Reverse DVM is proposed as a mechanism for avoiding zooplankton predators that undergo nocturnal DVM (Ohman et al. 1981, Neill 1990). A slower descent rate at sunset by menhaden larvae due to inflated swimbladders may reduce detection by chaetognaths that are ascending toward the surface. Since the percentage of menhaden larvae with inflated swimbladders increases with size, the importance of reduced sinking rate for predator avoidance may increase with size. The threat of predation to menhaden larvae is probably reduced during their ascent at sunrise because the descending chaetognaths have been feeding all night.

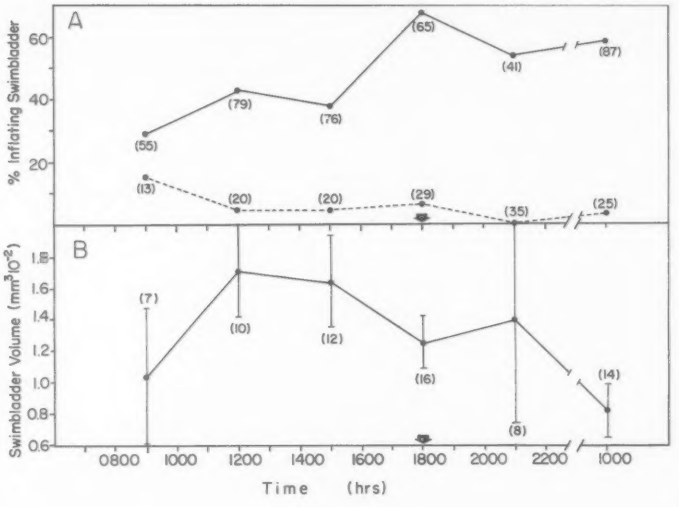

Figure 7

Percentage **(A)** of larvae 11–16 mmTL that filled their swimbladders before (– – –) and after (——) exposure to darkness for 2 h over the solar day. The swimbladder volume of 11 mmTL larvae **(B)** after exposure to darkness is also plotted against time in the solar day. Means and standard errors are plotted. Number near each plot is the sample size. Arrow indicates the times of the beginning of the dark phase of the rearing LD cycle.

Acknowledgments

This research was part of the South Atlantic Bight Recruitment Experiment (SABRE) sponsored by the NOAA Coastal Ocean Program. We thank Dr. R. Tankersley for his technical assistance.

Citations

Blaxter, J. H. S., & J. R. Hunter
1982 The biology of clupeoid fishes. Adv. Mar. Biol. 20:1–223.

Hastings, J. W., B. Rusak, & Z. Boulos
1991 Circadian rhythms: The physiology of biological timing. *In* Prosser, C.L. (ed.), Comparative animal physiology, 4th ed., p. 435–546. Wiley-Liss, NY.

Hettler, W. F.
1983 Transporting adult and larval gulf menhaden and techniques for spawning in the laboratory. Prog. Fish.-Cult. 45:45–48.

Hoss, D. E., & J. H. S. Blaxter
1982 Development and function of the swim bladder-inner-lateral line system in the Atlantic menhaden, *Brevoortia tyrannus* (Latrobe). J. Fish. Biol. 20:131–142.

Hoss, D. E., & G. Phonlor
1984 Field and laboratory observations on dirunal swim bladder inflation-deflation in larvae of gulf menhaden, (*Brevoortia patronus*). Fish. Bull., U.S. 82:513–517.

Hoss, D. E., D. M. Checkley Jr., & L. R. Settle
1989 Diurnal buoyancy changes in larval Atlantic menhaden (*Brevoortia tyrannus*). Rapp. P.-V. Reun. Cons. Int. Explor. Mer 191:105–111.

Hunter, J. R., & C. Sanchez
1976 Diel changes in swim bladder inflation of the larvae of the northern anchovy, *Engraulis mordax*. Fish. Bull., U.S. 74:847–855.

McFarland, W. N., & F. W. Munz
1975 The evolution of photopic visual pigments in fish. Vision Res. 15:1071–1080.

Munz, F. W.
1958 The photosensitive retinal pigments of fish from relatively turbid coastal waters. J. Gen. Physiol. 42:445–459.

Neill, W. E.
1990 Induced vertical migration in copepods as a defense against invertebrate predation. Nature (Lond.) 345:524–526.

Ohman, M. D., B. W. Frost, & E. B. Cohen
1981 Reverse diel vertical migration: an escape from invertebrate predators. Science (Wash. DC) 220:1404–1406.

Pearre, S. Jr.
1973 Vertical migration and feeding in *Sagitta elegans* Verrill. Ecology 54:300–314.

Sweatt, A. J., & R. B. Forward Jr.
1985 Diel vertical migration and photoresponses of the chaetognath *Sagitta hispida* Conant. Biol. Bull. (Woods Hole) 168:18–31.

Tracy, H. C.
1920 The membranous labyrinth and its relation to the precoelomic diverticulum of the swimbladder in clupeoids. J. Comp. Neurol. 31:219–257.

Uotani, I.
1973 Diurnal changes of gas bladder and behavior of postlarval anchovy and other related species. Bull. Jpn. Soc. Sci. Fish. 39:867–876.

Walpole, R. E.
1974 Introduction to statistics. Macmillan, NY.

Seasonal variation in reproductive investment in the tropical loliginid squid *Loligo chinensis* and the small tropical sepioid *Idiosepius pygmaeus*

George D. Jackson

Department of Marine Biology, James Cook University of North Queensland
Townsville 4811, Queensland, Australia
Present address: Department of Zoology, University of Western Australia
Nedlands, Perth, Western Australia 6009

Abstract.—Seasonal variability in gonad growth was investigated for the tropical cephalopods *Loligo chinensis* and *Idiosepius pygmaeus*. Statolith ageing techniques enabled a comparison of gonad growth in relation to both individual size and age. Age analyses revealed that male and female individuals of *L. chinensis* matured earlier during the warmer summer period than in the cooler winter period. These preliminary results suggested that maturity was governed more by individual size rather than age. Analysis of seasonal change in the gonadosomatic index (GSI) revealed that *L. chinensis* gonad tissue accounted for the greatest percentage of body weight in the month of October. The trend in the nidamental gland/mantle length index closely paralleled the trend in GSI values for female individuals of *L. chinensis*, while growth of the nidamental gland and hectocotylus closely paralleled growth of the gonad. The seasonal variation in reproductive investment for *Idiosepius pygmaeus* followed a different pattern compared with *L. chinensis*. Slower growing cool-season (spring) individuals lived longer and had comparatively larger gonads than their warm-season (autumn) counterparts, despite no difference in body size between the two seasons. *Idiosepius pygmaeus* thus appeared to be employing a 'trade-off' in its reproductive strategy by partitioning a greater amount of energy into gonad tissue over a longer lifespan during the cooler period of the year.

Manuscript accepted 10 December 1992.
Fishery Bulletin, U.S. 91:260-270 (1993).

In reviewing cephalopod reproduction, Mangold (1987) has emphasised that there are at least as many open questions as there are established facts, and that there are thus many gaps in our knowledge as well as contradictory statements. Recent research (e.g., Hanlon et al. 1989, Rodhouse & Hatfield 1990, Jackson & Choat 1992) is revealing that cephalopod lifespans are considerably shorter than many estimates made over the last several decades. This past confusion has apparently led to a poor understanding of the reproductive tactics of cephalopods. Clearly, any ideas regarding the lifespan of an organism will influence ideas regarding reproductive events in the individual.

Statolith ageing techniques have the potential for resolving some of the discrepancies in our understanding of the reproductive tactics of squids and sepioids. By analyzing individual age and maturity status, age-at-maturity and time-specific schedules of gonad growth can be constructed. The focus of this study was to consider seasonal variation in age-at-maturity and reproductive investment in the tropical loliginid squid *Loligo chinensis* and the small sepioid *Idiosepius pygmaeus*. Statolith ageing techniques have been applied to both *I. pygmaeus* (Jackson 1989) and *L. chinensis* (Jackson 1990a, Jackson & Choat 1992). Analysis of seasonal samples for both of these species has revealed that there was considerable seasonal variation in growth (Jackson & Choat 1992). This study was therefore undertaken to see if there was any seasonal variation in gonad growth or seasonally-induced variation in age-at-maturity in these two species.

Loligo chinensis is common in North Queensland waters and can be captured by bottom trawls throughout all months of the year. The species is sexually dimorphic, with males growing longer than females. In North Queensland waters, males are commonly encountered up to ~180 mm dorsal mantle length (DML), while females are common up to ~120 mmDML. Hatchling size for *L. chinensis* is ~1.4 mm (unpubl. data). In the summer, *L. chinensis* reaches adult size in ~100 d, while winter growth is slower with adult size reached by 140–170 d (Jackson & Choat 1992).

Idiosepius pygmaeus is a common neritic cephalopod which is found in surface waters in mangrove, estuarine, and breakwater habitats (Jackson 1989). This species, however, is only common in nearshore surface waters between March and November, with few specimens observed over the summer months (December–February) (Jackson 1992). *Idiosepius*

pygmaeus is sexually dimorphic, with females reaching much larger sizes than males. In North Queensland waters, males are commonly encountered up to ~10 mmDML, while females are commonly encountered between 13 and 18 mmDML. Planktonic hatchlings are ~1 mmDML (pers. observ.). This species has a short lifespan, with maturity reached in <80 d (Jackson 1989), and exhibits slower growth during the cooler seasons of the year (Jackson & Choat 1992).

Materials and methods

Loligo chinensis and *I. pygmaeus* were captured from tropical waters off Townsville, North Queensland. Preparation and enumeration of statolith growth increments for both species were similar to techniques used for *Sepioteuthis lessoniana* (Jackson 1990b), although statoliths of *I. pygmaeus* were not ground or polished. Individuals of *L. chinensis* were captured in paired trawl nets (each net had an 11 m gape and 3.8 cm mesh) which were towed for ~20 min. The majority of individuals of *L. chinensis* were captured in Cleveland Bay (19°11'S,146°56'E) in water depth <20 m. Trawling was undertaken generally for one day each month from February 1988 to November 1989, and up to 15 trawls were taken on each sampling date. Individuals of *I. pygmaeus* were captured by dip-netting along a breakwater east of the Townsville harbor (19°15'S,146°50'E; see Jackson 1992). Individuals of *L. chinensis* used in the age analysis were captured on 12 January 1989 (summer, n=37) and 13 July 1989 (winter, n=27). Individuals of *I. pygmaeus* were analyzed from autumn and spring. Individuals (n=41) for the autumn sample were captured during four sampling periods over two years: 22 and 23 March 1988; 21 and 22 March 1989. Individuals (n=38) for the spring sample were from six sampling trips over two months: 10, 23, 24 August 1988; 7, 20, 21 September 1988. The greatest differences in growth rates and population age structure were observed between these two seasonal periods (Jackson & Choat 1992).

Analysis of reproductive structures

Specimens of *L. chinensis* were initially fixed in buffered 10% seawater-formalin to preserve the large tissue mass and later transferred to 70% alcohol to prevent damage to the statoliths. Specimens of *I. pygmaeus* were preserved immediately in 70% alcohol due to their small body size. Gonads were removed, blotted with paper toweling (*L. chinensis*) or filter paper (*I. pygmaeus*), and weighed. Dorsal mantle length (DML) was measured on both species, and nidamental gland length (NGL) and hectocotylus length was measured on female and male individuals of *L. chinensis*, respectively. Measurements were taken with an eyepiece micrometer (*I. pygmaeus*) or with either callipers or a graduated ruler (*L. chinensis*). Maturity was determined by the presence of mature oocytes in the ovary along with large nidamental glands in females, and the presence of spermatophores in males.

To discern the pattern of growth for gonads, the nidamental gland, and the hectocotylus, measurements of gonad weight, nidamental gland length, and hectocotylus length were plotted against both mantle length and age. Due to the large amount of scatter in many of the plots (especially with *I. pygmaeus*) and the complex curvilinear relationship between many of the relationships, regression analyses were not carried out.

Gonadosomatic and NDL/DML indices

The seasonal trend in gonad growth was also examined for *L. chinensis*. Maturity status was determined for 231 individuals from trawl samples between February 1988 and November 1989 (this analysis included data from individuals which were aged from the January 1989 and July 1989 samples). For most samples, all individuals within the adult size-range (>100 mm) were used in the gonad analysis, except for several summer samples in which a very large number of individuals >300 mm were captured.

Parameters measured for each squid were dorsal mantle length, body weight, gonad weight, and nidamental gland length for females. The gonadosomatic index (GSI) was calculated for each specimen as

$$\frac{\text{gonad weight (g)}}{\text{total body weight (g)}} \times 100.$$

For females, the nidamental gland length/dorsal mantle length (NGL/DML) index was also calculated as

$$\frac{\text{nidamental gland length (mm)}}{\text{mantle length (mm)}} \times 100.$$

Analyses of nidamental gland length and hectocotylus length were not carried out for *I. pygnmaeus*.

Results

Loligo chinensis

Gonad growth with age There were differences in the relationship between gonad weight and age for the two samples of *L. chinensis* taken within different seasonal periods (Fig. 1A,B). The relationship between testis weight and age was similar during both sea-

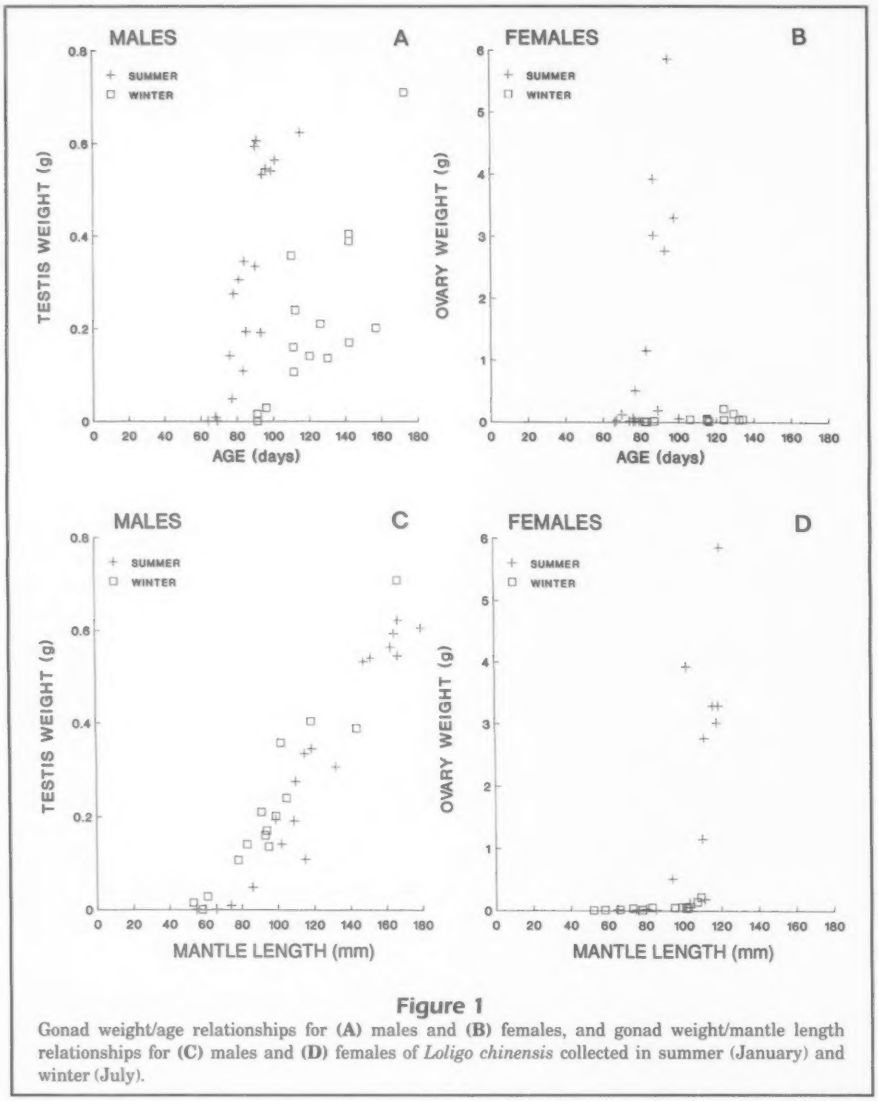

Figure 1

Gonad weight/age relationships for **(A)** males and **(B)** females, and gonad weight/mantle length relationships for **(C)** males and **(D)** females of *Loligo chinensis* collected in summer (January) and winter (July).

sons, with the main difference being the shift in the winter curve to the right (Fig. 1A). Because of seasonally-induced differences in somatic growth (Jackson & Choat 1992), males matured later in winter. The relationship between age and testis weight had greater variability in winter, which suggests that age-at-maturity was less well-defined in the winter, with a slower rate of maturity in some individuals.

In both winter and summer, males with a testis weight >0.1 g had spermatophores present. However, there was variability in age-at-maturity in both seasons, with testis weight in apparent immature males of 0.307–0.335 g. The youngest mature male during summer and winter was 83 d and 111 d, respectively. The oldest immature males for summer and winter were 90 d and 130 d, respectively.

There were also seasonal differences in maturity patterns of females based on ovary weight (Fig. 1B). Females matured in summer at a young age, with the ovary reaching a large size in 65–85 d, although two older specimens were immature. This was especially apparent in the oldest individual (100 d) which also had very undeveloped nidamental glands.

All females in the winter sample had small gonads and nidamental glands, and there were no mature or soon-to-be-mature females. This differed from the pat-

tern observed in males, which had reached maturity in winter, and suggested that female maturity was out of phase with males during this period of the year.

All females aged in summer with an ovary weight >1.161 g were mature, and the ovary filled much of the mantle cavity. The youngest mature female was 83 d, while the oldest immature female was the oldest female aged, 100 d.

Gonad-soma relationships Comparing gonad weight to individual age (Fig. 1A,B) revealed a different pattern than in the gonad weight/mantle length analysis (Fig. 1C,D). Despite the fact that there was a noticeable difference in the testis weight/age scatter plot (Fig. 1A), due to the older winter males, the testis weight/mantle length relationship was similar for both seasons (Fig. 1C). Thus gonad increase was proportional to the squid length rather than its age.

A different pattern emerged when comparing ovary weight/mantle length relationships for female *L. chinensis* (Fig. 1D). Although the lack of maturity was still obvious in winter females, the gonad weight/mantle length relationship for both seasons resulted in a single curvilinear relationship, suggesting that maturity occurred at 100–120 mmDML, regardless of age. Furthermore, although this ageing study indicated that a large proportion of the winter females were older than their summer counterparts, many of the winter immature females were smaller than squids captured in the summer. As with the males, squid size rather than age may be a better indicator of maturity.

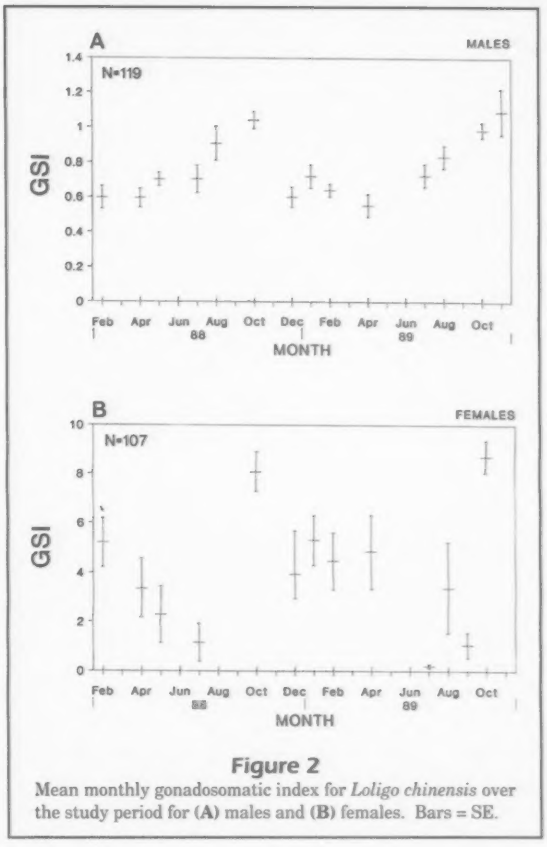

Figure 2
Mean monthly gonadosomatic index for *Loligo chinensis* over the study period for **(A)** males and **(B)** females. Bars = SE.

Reproductive indices Although it was possible to determine the ages of only a small number of individuals in two seasons (n=64), changes in the gonad weight/soma weight relationship throughout the year were examined. For both males and females, a seasonal trend could be detected in the GSI (Fig. 2). In males, GSI values were low, with <1.2% of the total body weight consisting of gonad. In contrast, female GSI values were more variable and generally higher than in males, with the gonad comprising as much as 8% of total body weight.

Mature males were found in all months sampled. However, a regular seasonal oscillation in relative gonad weight was apparent (Fig. 2A). There was an increase in relative gonad weight from April to October in both years. Over the two years, the testis accounted for its greatest percentage (>1%) of body weight in October, while its lowest values were recorded in April.

A similar pattern of fluctuation also existed with the female GSI values (Fig. 2B). In October, females consistently had GSI values that were considerably higher than for other months. Mature females were present in all months except July 1989. As discussed previously, females aged from the 1989 summer sample showed a considerable range in gonad size and level of maturity, despite similarities in both size and age. This range in gonad size was also reflected in the female GSI values, in that the mean values had large standard errors (Fig. 2B) in nearly every month. This was due to the fact that for many months, a proportion of the individuals was immature.

The seasonal trend in the NGL/ML index (Fig. 3) was similar to the trend in the female GSI (Fig. 2B). This index also indicated a greater investment in reproduction during October, with lowest values in July. Furthermore, standard errors were generally less for this index than for the GSI.

The monthly mean mantle lengths for males and females were plotted for the 2 yr period (Fig. 4A,B). Although there was some variation in mantle lengths for the different samples, these could not be related to the seasonal peaks or troughs in the GSI values. For example, the largest females were captured from February to July 1988 (Fig. 4B). However, GSI values dropped considerably over this period. Furthermore, mean mantle length was not highest in October for

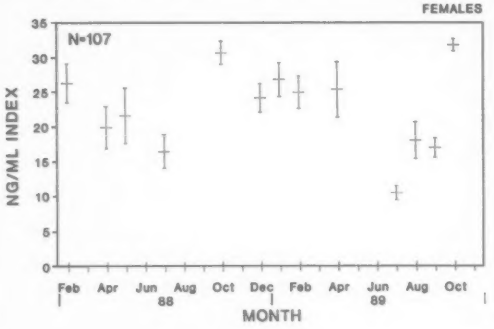

Figure 3
Mean monthly index of nidamental gland/mantle length for female *Loligo chinensis* collected over the study period. Bars = SE.

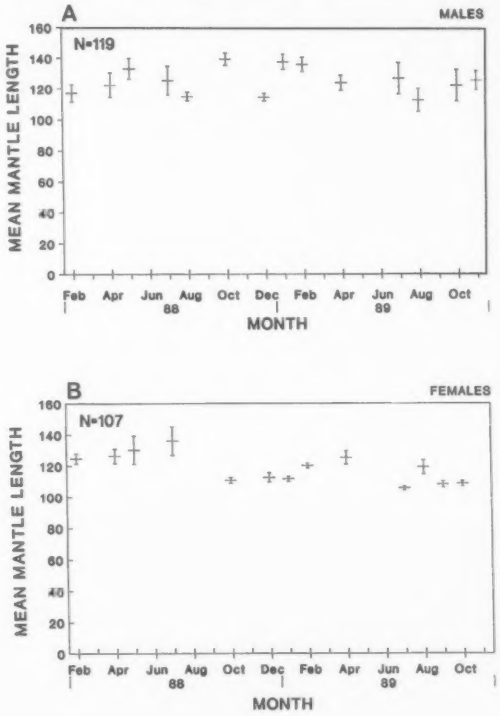

Figure 4
Mean monthly mantle length for **(A)** males and **(B)** females of *Loligo chinensis* used in gonad weight analysis and nidamental gland length analysis (Figs. 2,3).

each year, and although 1989 July values were slightly lower than the other months, the July 1988 values were not. The observed changes in relative gonad weight can thus be considered unbiased by individual size.

Nidamental gland and hectocotylus lengths Nidamental gland length was perhaps the most useful measurement in female squids for obtaining an index of maturity. The relationship of nidamental gland length to mantle length and age of female specimens of *L. chinensis* (Fig. 5) closely resembled the ovary weight/age and mantle length relationships for this species (Fig. 1B,D). For example, two separate relationships were apparent when nidamental gland length was plotted against age, whereas both seasons' data points produced one curvilinear relationship for nidamental gland length vs. mantle length. As with the ovary data, these data suggest that nidamental gland length was more closely related to mantle length than to age.

Similarly for males, hectocotylus length vs. mantle length and age (Fig. 6) exhibited the same pattern observed in the testis weight/age and mantle length relationships (Fig. 1A,C). For example, in winter there was a shift along the age axis, producing a separate correlation for the summer hectocotylus length/age data. However, there was some indication that at large sizes, faster-growing (summer) males had a shorter hectocotylus than slower-growing (winter) males. This relationship was similar to the testis weight/mantle length relationships for *I. pygmaeus* (Fig. 7C,D) seen below.

Idiosepius pygmaeus

Gonad growth with age In contrast to *L. chinensis*, within-season variability in maturity and age-specific trends for *I. pygmaeus* could be determined with a greater degree of accuracy. This was possible because of the greater number of replicate sub-amples taken during each seasonal period (see Methods).

The seasonal pattern of gonad growth was different for *I. pygmaeus* than for *L. chinensis*. The seasonal influence on gonad growth and maturation may have been somewhat less for individuals of *I. pygmaeus* (analyzed for spring and autumn) compared with individuals of *L. chinensis* (analyzed for summer and winter). However, individuals captured in autumn would have grown over the warmer period at the end of summer, while individuals from the spring sample would have grown and matured through the colder period, at the end of winter.

Due to the considerable scatter in age/length relationships for this species (Jackson & Choat 1992), there was also considerable scatter in the gonad weight/age relationship (Fig.7A,B). While gonad weight/age relationships for *L. chinensis* resulted in different scatter plots separated on the age continuum (x axis), the pattern was modified differently for *I. pygmaeus* for

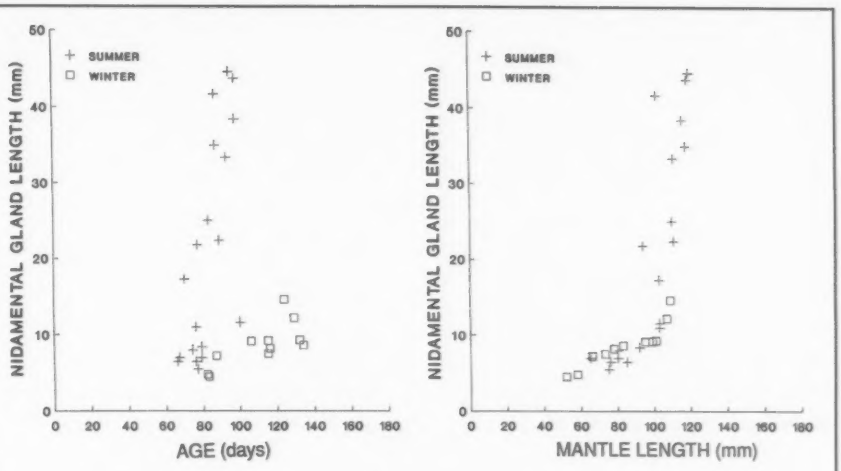

Figure 5

Nidamental gland length/age relationships and nidamental gland length/mantle length relationships for female individuals of *Loligo chinensis* collected during summer (January) and winter (July).

the two seasons (i.e., both seasons' data points fell within the same scatter plot). While individuals of *I. pygmaeus* were older in the spring samples, their gonads reached a proportionally greater weight than did the autumn individuals.

Males The relationship for testis weight vs. age (Fig. 7A) was the same for both seasons, with data points clustering on a single testis weight/age continuum, with the exception of one 41 d individual which fell considerably outside the cluster of data points. The major difference in the seasonal component of the data was a clustering of data points for each season at opposite ends of the testis weight/age continuum, with spring individuals reaching a greater age and possessing proportionally heavier testes than their autumn counterparts.

The youngest mature males in spring and autumn were 22 d and 37 d, respectively, while the oldest im-

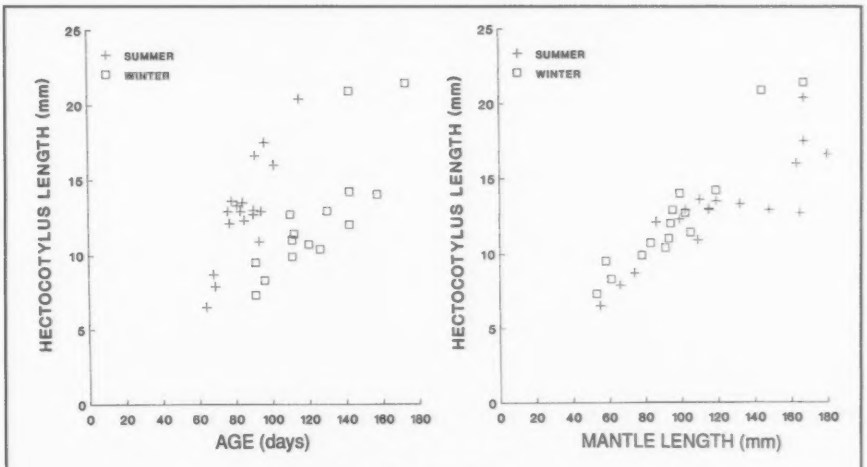

Figure 6

Hectocotylus length/age relationships and hectocotylus length/mantle length relationships for male individuals of *Loligo chinensis* collected during summer (January) and winter (July).

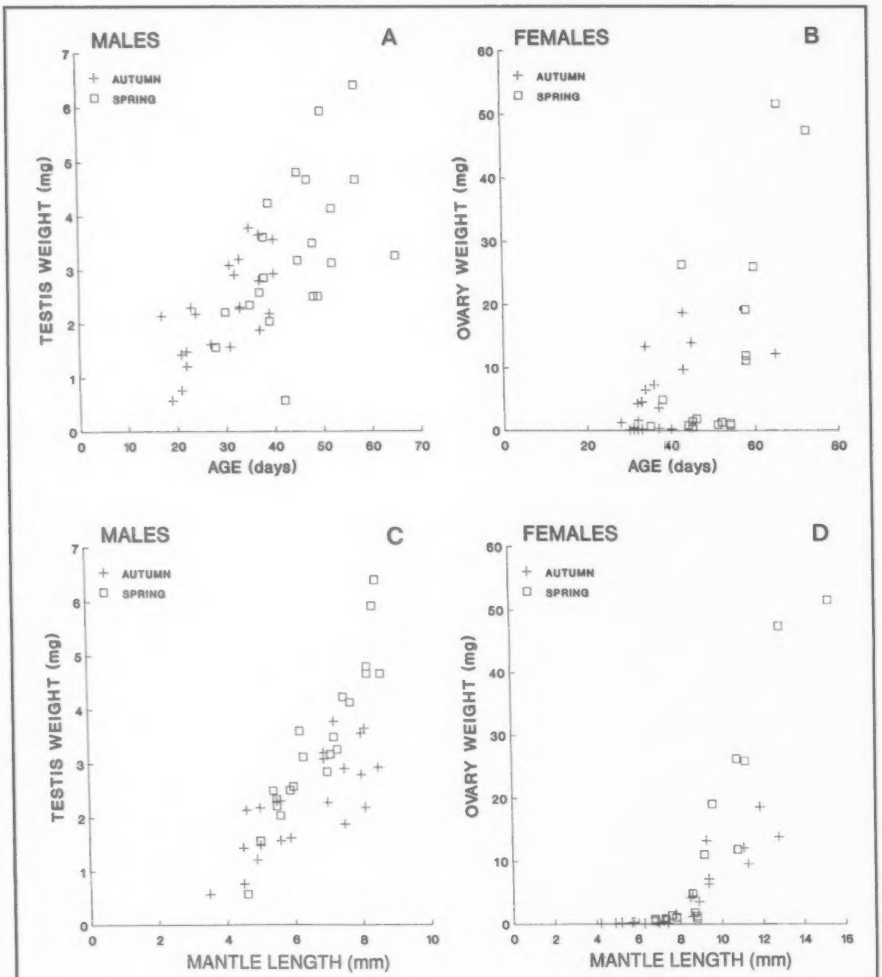

Figure 7

Gonad weight/age relationships for **(A)** males and **(B)** females, and gonad weight/mantle length relationships for **(C)** males and **(D)** females of *Idiosepius pygmaeus* collected in autumn (March) and spring (August/September).

mature males for both seasons were 32 d and 38 d, respectively.

Females A similar relationship to the males also existed in the ovary weight/age relationship, i.e., both seasons' data points tended to cluster along one ovary weight/age continuum (Fig. 7B). However, the scatter was greater than for males, due to the fact that in both seasons there were individuals with very small ovaries. For example, in both seasons, individuals of 40–60 d showed a considerable range in ovary weight. However, as with male testis weight, the spring females also had the heaviest ovaries. Although a number of females had large well-developed ovaries, none of the specimens examined had any mature ova present.

Gonad-soma relationships One possibility for the greater gonad weight in spring vs. autumn could have been due to larger individuals being captured in the spring. However, the plot of gonad weight against mantle length for both sexes (Fig. 7C,D) revealed no size difference in males between seasons and only one spring female slightly larger than the other females. Although there is some overlap in the data for the smaller individuals for both seasons, in the larger sizes,

slower-growing spring individuals did, in fact, eventually produce larger gonads than their autumn counterparts.

Discussion

The biotic and abiotic influences on maturity are complex. Factors such as light (day length), temperature, and food availability can all affect rate and age-at-maturity. Gonad development is directly under hormonal control, and appears to be influenced by the optic gland (Mangold 1987, Boyle 1990). However, the process of maturity is not completely understood and may also be controlled to a certain degree by individual genetic factors, apart from outside influences (Mangold 1983). This study gives preliminary insight into the maturation process in tropical squids and sepioids based on age information. Statolith ageing techniques should prove useful in providing a timescale on the squid maturation process and problems encountered with variation in size-at-maturity.

Loligo chinensis

Variability in size-at-maturity appears to be a common phenomenon with cephalopods. Hixon (1980) found that some immature *Lolliguncula brevis* females were as large as other fully-mature individuals. Considerable variation in maturity has also been shown to exist in *L. opalescens*, with females maturing by 81 mmDML while other females remain immature until 140 mmDML (Hixon 1983). Similar discrepancies in size-at-maturity have also been documented for *Sepia officinalis* (Boletzky 1983) and *Dosidicus gigas* (Nesis 1983). Mangold (1983) has also demonstrated that cultured octopuses reared from the same egg mass reached maturity independent of sibling size or age. The delay in maturity for some *L. chinensis* females for a given length (e.g., Fig. 1B, summer) is similar to observations made for *Lolliguncula brevis* by Hixon (1980). However, in contrast to the other studies cited above, *L. chinensis* females do not show a wide difference in size-at-maturity. The fact that maturity was more closely related to length than to age suggests that there might be some physical or physiological mechanisms controlling maturation apart from age. Some female cephalopods have been shown to develop eggs only when a minimum threshold in body size is achieved (Mangold 1987). The maximum size for individuals of *L. chinensis* obtained in this study is smaller than the maximum size recorded for the species, which is up to 300 mmDML (Roper et al. 1984). This suggests that the squids in Cleveland Bay may be a precocious population which is maturing near the minimum threshold in body size for the species. This could therefore account for the restricted size-range at maturity.

Although male and female *L. chinensis* were mature in the same age-range in summer, a different situation existed in winter, suggesting that maturity in the female winter population was out of phase with the males. This situation has been noted with *Todarodes pacificus* in which males reach maturity 3–6 mo earlier than females (Okutani 1983). This may not be an ecological constraint, considering the reproductive tactics of cephalopods. In many species of cephalopods, males mate with immature females (Mangold 1987) with the females retaining the spermatophores until they spawn. An extended interval between mating and spawning has also been noted in octopods, with up to a 114 d interval between spermatophore transfer and spawning (Boyle 1990).

Alternatively, the apparent absence of mature females in July may have been due to inadequate sampling, since the oldest-aged female captured in winter was 134 d whereas males as old as 173 d were captured. Since maturation was rapid (e.g., females matured in <80 d in summer), it is possible that older mature females existed in winter but that none were captured.

Based on previous work on the effect of temperature on growth rate (e.g., Forsythe & Hanlon 1988 and 1989), seasonal differences in water temperature may also account for the lack of gonad development in *L. chinensis* during winter. As age of field specimens in relation to maturity processes has not previously been considered, only aquarium culture experiments are available for comparison. Richard (1966, cited in Mangold 1987) has shown that males and females of the cuttlefish *Sepia officinalis* from the English Channel, which were raised at 20°C, attained sexual maturity at 7 mo and 140 mmDML, while conspecifics raised at 10°C were totally immature at the same age and were only 50 mm in length. Moreover, Richard (1970, cited in Mangold 1987) also found that females of *S. officinalis* raised at 18°C had a gonad index of 8% at 270 d, while it took 480 d for females raised at 13°C to reach the same value. Other factors, such as seasonal variability in food supply and day length may also influence seasonal differences in maturation rates.

The fluctuations of the GSI and NGL/ML index indicated that ambient environmental conditions (e.g., temperature and food availability) were influencing both the maturity process and the energy *L. chinensis* partitioned into reproduction. Although individuals were often mature (e.g., the majority of males analyzed) there were time-periods when the ovary and testes accounted for a greater percentage of total body weight. This was consistently recorded for both sexes

in the month of October, and would coincide with the spring warming of water in Cleveland Bay after low winter temperatures which begin to rise in August/September (Kenny 1974, Walker 1981). Highest GSI values were also reported for male and female *L. vulgaris* during the spring period in the Mediterranean (Worms 1983).

The interpretation of fluctuations in the GSI and NGL/DML index is complex due to a variety of factors: (1) *L. chinensis* exhibits fast growth and has a short lifespan, therefore annual data sets reflect a number of different generations of squids; (2) because of rapid growth and the observed variability in gonad growth (especially in females), greater sample numbers would be needed to adequately describe gonad growth fluctuations on a smaller scale (e.g., intramonthly variability); (3) due to the tropical nature of the environment, squids (especially males) are mature throughout most months of the year and, therefore, gonad indices are generally reflecting periods of greater investment in reproductive structures rather than periods of immaturity vs. maturity.

The data peaks in October may have been due to the increasing day length in spring, stimulating the optic gland to produce increased hormonal levels which accelerates gonad growth (see Mangold 1987). Since day length would be shortened over the winter period (June–August), the increasing day length during the spring period, along with increasing water temperatures, may produce physiological responses leading to maximal gonad growth. More intensive sampling (e.g., fortnightly) over the late-spring and early-summer period may provide a clearer picture of relative gonad growth over this period. The relationship between mantle length and NGL could constitute a good maturity index for females, since the relationship between NGL and DML is closer than the relationship between DML and gonad weight (Worms 1983). Data for females of *L. chinensis* from this study suggest that the NGL/DML index provides results very similar to GSI values. Maturity parameters based on NGL alone could constitute a more convenient means to determine maturity for tropical squids.

Nidamental gland length The fact that length of the nidamental gland of *L. chinensis* bears a very close resemblance to growth of the gonad highlights the close association this organ has with maturation and egg development. The nidamental gland serves the function of producing a gelatinous matrix which encases the cephalopod egg (Roper et al. 1984). Previous studies have used the NGL/DML ratio as a convenient means to assess maturity. Temperate loliginids have been shown to possess mature oocytes when this ratio is >0.2 (Yang et al. 1986, Hanlon et al. 1989). This relationship generally holds well for females of *L. chinensis*. Out of 112 females (captured throughout the 2 yr sampling period) analyzed for this ratio, all the mature females had an NGL/DML ratio >0.2. Of the immature females analyzed, six individuals (5.4%) had a ratio >0.2 (highest value=0.26). This parameter therefore appears to be useful for tropical loliginids as well. The 0.2 NGL/DML ratio does appear to be the minimum parameter for mature females.

Nidamental gland measurements are thus useful for providing a rapid and convenient means of assessing the level of maturity in tropical loliginids. The nidamental gland can also provide useful information about the past history of a female squid. The fact that some of the larger, older, immature females captured during January had small underdeveloped nidamental glands was one means to ascertain that these females had actually not yet matured and had not regressed from a previously mature condition.

Hectocotylus length The hectocotylus is an important reproductive structure employed by the male to pass spermatophores to the female during copulation. It is also extremely useful for quick sexual identification of preserved specimens. Coelho et al. (1985) carried out a detailed study of the growth of the hectocotylus of *Illex illecebrosus* to determine if the degree of hectocotylization of the fourth arm could be related to maturity. However, no close relationship was found between maturity and the degree of hectocotylization. A partial explanation for this lack of relationship between these parameters was attributed to the fact that the squids examined might have included individuals which hatched at different localities and which had developed under different temperature regimes (e.g., some squids could have been immigrants from a more southerly population exposed to warmer temperatures). This could well account for considerable confusion in the *Illex* data, as individuals of *L. chinensis* from different seasons showed a different relationship between hectocotylus length and mantle length, and hectocotylus length and age. These seasonal growth patterns which were temperature-related did have an influence on the development rate of the hectocotylus, with slower-growing individuals eventually possessing a larger hectocotylus than their faster-growing counterparts. Different-sized hectocotili on similar-sized squids could therefore indicate that the squids had developed under different growth rates. This also suggests that the size ratio of many other structures to body size may also be influenced by the ambient temperature in which the squid develops. Parameter ratios and indices used for taxonomic purposes should therefore be cautiously employed, at least for nearshore squids, and, whenever possible, parameters should be measured in

individuals captured under similar environmental conditions.

Idiosepius pygmaeus

The pattern of gonad maturation in tropical squids and sepioids becomes more complex when the pattern of seasonal maturation of *I. pygmaeus* is also considered. As with *L. chinensis*, individuals of *I. pygmaeus* which grew during a cooler time of the year also reached a greater age. However, gonad maturation was modified in a different way compared with *L. chinensis*. For example, in both seasons males (including mature individuals) had similar-sized testes at an age of 30–40 d suggesting that a minimal gonad size can be reached in just over a month. Nevertheless, as the cooler-season males continued to grow, the gonad continued to reach an appreciably greater size, for the same-sized individual. Thus, environmental constraints (such as temperature, food availability, or light levels) produced a different allometric gonad-soma relationship in this species which was not apparent in *L. chinensis*.

The fact that *I. pygmaeus* has a short lifespan and rapid growth may account for the lack of females with mature ova. It is possible that ovum maturation could take place very rapidly just before egg deposition. Therefore, it could be difficult to capture females with mature oocytes unless it was just prior to egg deposition. Alternatively, females with ripe ova may not have been near the water surface and therefore not available for sampling.

Idiosepius pygmaeus appears to be employing a 'trade-off' in its seasonal reproductive tactics, that is, benefiting from one process bought at the expense of another (Begon et al. 1986). During the cooler period of the year, growth is slowed (presumably as a result of metabolic responses to temperature), therefore lifespan is increased as a necessity, since individuals take longer to reach adult size. As a result, *I. pygmaeus* appears to change its tactics by partitioning a greater amount of energy into gonads over the longer lifespan. Although a longer time-period is taken to reach maturity, there would be a reproductive advantage in that possessing larger gonads would increase reproductive output. A similar situation has been shown to exist with teleost fishes. Stearns (1976) has provided evidence from several species of teleosts, showing that the ratio of ovary weight to body weight (as a measure of reproductive effort) increased with age.

The fact that this phenomenon occurs in *I. pygmaeus* and not the larger *L. chinensis* may be due to the need for *I. pygmaeus* to maximize its reproductive chances because of the greater nearshore habitat variability, or because of the greater constraints this species faces due to its small body size.

Acknowledgments

I would like to thank J.H. Choat for comments throughout this project, C.H. Jackson for critically reading the manuscript and assisting with figures, and the crew of the research vessel *James Kirby* for specimen collection. Manuscript comments by two anonymous reviewers and L.L. Jones were greatly appreciated. This research was supported by grants from the James Cook University of North Queensland Research Funding Panel.

Citations

Begon, M., J. L. Harper, & C. R. Townsend
1986 Ecology. Blackwell Sci. Publ., Oxford, 876 p.

Boletzky, S. V.
1983 *Sepia officinalis*. *In* Boyle, P.R. (ed.), Cephalopod life cycles, vol. I, p. 31–52. Academic Press, London.

Boyle, P. R.
1990 Cephalopod biology in the fisheries context. Fish. Res. (Amst.) 8:303–321.

Coelho, M. L., M. D. Mallet, & R. K. O'Dor
1985 Evaluation of male reproductive features as maturity indices for short-finned squid (*Illex illecebrosus*). NAFO Sci. Counc. Stud. 9:107–115.

Forsythe, J. W., & R. T. Hanlon
1988 Effect of temperature on laboratory growth, reproduction and life span of *Octopus bimaculoides*. Mar. Biol. 98:369–379.
1989 Growth of the eastern Atlantic squid, *Loligo forbesi* Steenstrup (Mollusca: Cephalopoda). Aquacult. Fish. Manage. 20:1–14.

Hanlon, R. T., W. T. Yang, P. E. Turk, P. G. Lee, & R. F. Hixon
1989 Laboratory culture and estimated life span of the eastern Atlantic squid, *Loligo forbesi* Steenstrup, 1856 (Mollusca: Cephalopoda). Aquacult. Fish. Manage. 20:15–34.

Hixon, R. F.
1980 Growth, reproductive biology, distribution and abundance of three species of loliginid squid (Myopsida, Cephalopoda) in the northwest Gulf of Mexico. Ph.D. thesis, Univ. Miami, Coral Gables FL, 233 p.
1983 *Loligo opalescens*. *In* Boyle, P.R. (ed.), Cephalopod life cycles, vol. I, p. 95–114. Academic Press, London.

Jackson, G. D.
1989 The use of statolith microstructures to analyze life-history events in the small tropical cephalopod *Idiosepius pygmaeus*. Fish. Bull., U.S. 87:265–272.
1990a The use of tetracycline staining techniques to determine statolith growth ring periodicity in the tropical loliginid squids *Loliolus noctiluca* and *Loligo chinensis*. Veliger 33:389–393.
1990b Age and growth of the tropical nearshore loliginid squid *Sepioteuthis lessoniana* determined from stato-

lith growth-ring analysis. Fish. Bull., U.S. 88:113–118

1992 Seasonal abundance of the small tropical sepioid *Idiosepius pygmaeus*. Veliger 35:396–397.

Jackson, G. D., & J. H. Choat

1992 Growth in tropical cephalopods: an analysis based on statolith microstructure. Can J. Fish. Aquat. Sci. 49:218–228.

Kenny, R.

1974 Inshore surface sea temperatures at Townsville. Aust. J. Mar. Freshwater Res. 25:1–5.

Mangold, K.

1983 Food, feeding and growth in cephalopods. Mem. Nat. Mus. Vic. 44:81–93.

1987 Reproduction. *In* Boyle, P.R. (ed.), Cephalopod life cycles, vol. II, p. 157–200. Academic Press, London.

Nesis, K. N.

1983 *Dosidicus gigas*. *In* Boyle, P.R. (ed.), Cephalopod life cycles, vol. I, p. 215–231. Academic Press, London.

Okutani, T.

1983 *Todarodes pacificus*. *In* Boyle, P.R. (ed.), Cephalopod life cycles, Vol. I, p. 201–214. Academic Press, London.

Rodhouse, P. G., & E. M. C. Hatfield

1990 Age determination in squid using statolith growth increments. Fish. Res. (Amst.) 8:323–334.

Roper, C. F. E., M. J. Sweeney, & C. E. Nauen

1984 Cephalopods of the world. An annotated and illustrated catalogue of species of interest to fisheries. FAO Fish. Synop. 125(3), 277 p.

Stearns, S. C.

1976 Life-history tactics: a review of the ideas. Q. Rev. Biol. 51:3–47.

Walker, T. A.

1981 Annual temperature cycle in Cleveland Bay Great Barrier Reef province. Aust. J. Mar. Freshwater Res. 32:987–991.

Worms, J.

1983 *Loligo vulgaris*. *In* Boyle, P.R. (ed.), Cephalopod life cycles, vol. I, p. 143–157. Academic Press, London.

Yang, W. T., R. F. Hixon, P. E. Turk, M. E. Krejci, W. H. Hulet, & R. T. Hanlon

1986 Growth, behavior, and sexual maturation of the market squid, *Loligo opalescens*, cultured through the life cycle. Fish. Bull., U.S. 84:771–798.

Estimating von Bertalanffy growth parameters of sablefish *Anoplopoma fimbria* and Pacific cod *Gadus macrocephalus* using tag-recapture data

Daniel K. Kimura
Allen M. Shimada
Sandra A. Lowe

Alaska Fisheries Science Center, National Marine Fisheries Service, NOAA
7600 Sand Point Way NE, Seattle, Washington 98115-0070

Abstract.—Recent papers have provided new insights into the problem of estimating von Bertalanffy growth parameters from tag-recapture data. In particular, the inconsistency and bias of Fabens' (1965) estimates appear to have been addressed by James (1991). Using simulation, we examine the pattern of bias associated with different error assumptions for Fabens' estimates, weighted Fabens' estimates proposed by James, and a robust method also proposed by James. Our results corroborate James' finding that his robust estimates can be significantly less biased than other methods. We then apply these estimators to tag-recapture data obtained for sablefish *Anoplopoma fimbria* found in the Gulf of Alaska and off the U.S. west coast, and Pacific cod *Gadus macrocephalus* found in the eastern Bering Sea. These species are difficult to directly age, so tag-recapture data provide welcomed independent estimates of growth parameters and an indirect method of validating age-determination criteria. The von Bertalanffy parameter estimates using tag-recapture data and James' method were most similar to estimates calculated directly from length-at-age data.

Manuscript accepted 22 January 1993.
Fishery Bulletin, U.S. 91:271-280 (1993).

In its most common form, the von Bertalanffy growth curve has three parameters (L_∞, K, t_0). Conventional interpretation of these parameters is that L_∞ is asymptotic size, K describes the growth rate, and t_0 describes the age at length-0. Fabens (1965) was apparently the first to show how least-squares could be used to estimate two of these parameters (L_∞, K) from tag-recapture data. If at least one additional value of length-at-age was known, then t_0 could be estimated, and hence all values of length-at-age could be estimated directly from recapture data without recourse to direct ages from individual specimens. Besides providing growth-curve estimates, such a procedure would seem to provide an indirect validation of ageing criteria, since estimated growth parameters from length-at-age data and tag-recapture data could be compared.

However, comparisons of growth curves estimated using Fabens' method and ordinary length-at-age data seemed to provide evidence that Fabens' method provided biased parameter estimates. Following the suggestion of Chapman (1961) and others, Sainsbury (1980) showed how individual variability [i.e., the possibility that each fish has different values of (L_∞, K)], could lead to bias in population parameter estimates. Francis (1988a) argued from a sampling point of view that von Bertalanffy parameters calculated from length-at-age and tag-recapture data could be different. He also argued that average growth parameters for individual fish may not describe the population growth curve (Francis 1988b). Maller & deBoer (1988) showed mathematically and with simulation that Fabens' estimates, and related estimates of Kirkwood & Somers (1984), could be inconsistent. Kirkwood (1983) suggested combining length-at-age and tag-recapture data into a single likelihood model, but did not address the problem of bias caused by the interpretation of tag-recapture data.

A recent paper by James (1991) suggests that bias in Fabens' estimates could arise from bias in the estimating functions. James shows how weighted least-squares can be used to derive improved estimates for Fabens' method under the usual "observational error" assumption. James also gives distribution-free estimates for a more general model in which, in addition to the usual observational error, L_∞ itself is allowed to vary among individual fish. Although James' estimates appear to be consistent and less biased than the least-squares estimates, they also appear to be less efficient, usually

having larger standard errors. Nevertheless, James' method provides us with more robust parameter estimates.

This paper illustrates how critical is statistical methodology to the estimation of growth parameters from tag-recapture data. We show, by simulation and through analysis of actual data, that different estimation methods can easily lead to very different parameter estimates. With the help of simulation, we feel that realistic choices can be made among these estimators. For the actual datasets chosen for this paper, we are able to compare growth-curve parameter estimates from tag-recapture data with parameter estimates calculated from length-at-age data, using ages estimated from directly counting annuli. This provides another criterion for choosing among estimators.

Methods

We apply estimators considered by James (1991). The "unweighted Fabens" estimates (Fabens 1965) is the widely used historical method. What we call the "weighted Fabens" estimates, and James' estimates, were derived by James (1991). The weighted Fabens' method weights the residuals by an inverse variance estimate and appears to work well for the observational error model. James' estimators appear to be less prone to bias than the unweighted Fabens' estimators, and more robust to the presence of variability in L_∞ than the weighted Fabens' estimators. A more theoretical description of these estimators can be found in James (1991).

First we present a simulation study that corroborates the main findings of James (1991). Our study is more systematic than that of James (1991), using three estimation methods and error structures and calculating mean square error. Our simulation is based on parameters estimated for a marine teleost, Pacific whiting *Merluccius productus*, while James' simulations dealt with two shellfish species. Nevertheless, these simulations should be considered an addendum to James' original work.

Using notation similar to James (1991), consider a population having von Bertalanffy parameters (L_0, K_0) which we wish to estimate. L_0 refers to the average value of L_∞ in the population, where L_∞ might vary among individual fish. We assume $K=K_0$ does not vary among fish. Also, recall that t_0 cannot be estimated from tag-recapture data alone. To determine t_0 we need the average length of at least one age-group which can be supplied by direct age data (i.e., ages obtained from directly counting annuli), or the modal length-frequency of a dominant year-class of known age.

Suppose we observe the size at release (y_{1i}) and recapture (y_{2i}) of i=1,...,n fish, and the ages at release and recapture are (t_i, t_i+d_i). Suppose also that independent normally-distributed errors (ε_{1i}, ε_{2i}, ε_{3i}) enter into these observations in three possible ways:

$$y_{1i} = (L_0 + \varepsilon_{3i})[1.0 - \exp(-K_0 t_i)] + \varepsilon_{1i}$$

$$y_{2i} = (L_0 + \varepsilon_{3i})[1.0 - \exp(-K_0 (t_i + d_i))] + \varepsilon_{2i}.$$

We refer to ε_{1i} and ε_{2i} as "observational errors" and ε_{3i} as "variability in L_∞."

The three estimators of (L_0, K_0) considered in this paper are all based on the "residuals":

$$\eta_i = y_{2i} - y_{1i} - (L_0 - y_{1i})[1.0 - \exp(-K_0 d_i)].$$

These estimators are:

1 Unweighted Fabens, estimated by minimizing $\Sigma\eta_i^2$
2 Weighted Fabens, estimated by minimizing $\Sigma\,[\eta_i^2/(1.0+\exp(-2K_0 d_i))]$.
3 James, estimated by solving the simultaneous equations $\Sigma\eta_i=0$ and $\Sigma d_i\eta_i=0$.

Unweighted and weighted Fabens' estimates, and their standard errors, were calculated using nonlinear least-squares methods. Define $g_1=\Sigma\eta_i$ and $g_2=\Sigma d_i\eta_i$. James' estimates were calculated as suggested by James (1991) by solving for "L_0 in terms of K_0 from g_1 followed by substitution into g_2" and then applying the bisection method to estimate K_0 (see Press et al. 1986). This method appeared computationally robust and suitable for simulation studies. The variance estimates of these parameter estimates were calculated according to James (1991):

$$\mathrm{cov}(\hat{L}, \hat{K}) = G^{-1} D (G')^{-1},$$

where

$$G = \begin{pmatrix} \frac{\partial g_1}{\partial K_0} & \frac{\partial g_1}{\partial L_0} \\ \frac{\partial g_2}{\partial K_0} & \frac{\partial g_2}{\partial L_0} \end{pmatrix}, \qquad D = \Sigma\eta_i^2 \begin{pmatrix} 1.0 & d_i \\ d_i & d_i^2 \end{pmatrix},$$

and the right-hand expressions are evaluated at the estimated parameters.

Our simulation considered three different error assumptions.

Simulation 1 The observational error model where all fish are assumed to have common growth parameters, with variation due wholly to observational errors ε_{1i}, $\varepsilon_{2i} \sim N(0,\sigma^2)$. Here, all ε_{3i} are assumed to be zero.

Simulation 2 The variation in L_∞ model, where all variation in the observations are due to $\varepsilon_{3i} \sim N(0,\sigma^2)$,

and all observational errors ϵ_{1i} and ϵ_{2i} are assumed to be zero.

Simulation 3 Both observational errors and variation in L_∞ are present in this model, with ϵ_{1i}, ϵ_{2i}, $\epsilon_{3i} \sim N(0,\sigma^2)$.

For these simulations, we assume that the true population parameters are (L_0= 61.23, K_0=0.296), parameters previously estimated for female Pacific whiting (Kimura 1980). Measured in years, t_{1i} and d_i were uniformly and independently distributed over the interval [1, 5], assuming 365 d/yr. New values for t_{1i} and d_i were generated for every replication of the simulation.

Analytic standard errors of parameter estimates were estimated using nonlinear least-squares methods, and the variance estimate described above for James' method. In addition, the sample standard errors (i.e., the sample standard deviation of the replicate parameter estimates) are also provided. The reason for this is that the simulations included variation in t_{1i} and d_i that would not be included in the analytic estimates of standard error, and the probability that the analytic standard errors are themselves biased due to failure of assumptions. For the actual datasets, analytic standard errors were used. For simultaneously considering bias and variance, we include estimates of mean square error (MSE) calculated in the usual way: $\Sigma(\text{estimate} - \text{true})^2/n$.

Following a presentation of simulation results, we analyze tag-recapture data collected for sablefish *Anoplopoma fimbria* from the Gulf of Alaska and off the U.S. west coast, and Pacific cod *Gadus macrocephalus* from the eastern Bering Sea (Fig. 1). Because sablefish and Pacific cod are difficult species to directly age, their growth-curve parameters estimated from tag-recapture data are of special interest. The von Bertalanffy parameters estimated from tag-recapture data were compared with parameters estimated from length-at-age data based on direct ages (i.e., ages from directly counting annuli). For sablefish, we use length-at-age datasets based on break and burn ages (Chilton & Beamish 1982) and parameters estimated using nonlinear least-squares (Kimura 1980). For Pacific cod, we compare tag-recapture results with published von Bertalanffy parameter estimates (Thompson & Bakkala 1990).

Results

Simulation results

For the simulation results given here, the tag-recapture sample size was n=300, simulations were replicated 200 times, and the normal errors (ϵ_{1i}, ϵ_{2i}, ϵ_{3i}) were all independently distributed with σ^2=25. Therefore, the sample size was realistically small and the error variances were substantial. For each estimation method and parameter, simulation results (Table 1) were summarized by four entries: sample mean of the estimated parameter, mean analytic standard error, sample standard error (i.e., the standard deviation of estimated parameters), and mean square error.

The unweighted Fabens' estimate of L_0 is biased low in Simulation 1, biased high in Simulation 2, with biases apparently canceling each other in Simulation 3. For the weighted Fabens' estimates, the L_0 estimate is unbiased for Simulation 1, but biased high for Simulations 2 and 3. James' estimate of L_0 is unbiased in Simulation 2, and only modestly biased in Simulations 1 and 3. Biases in L_0 and K_0 estimates are in the opposite direction, as might be expected from the negative correlation between these parameter estimates.

Standard errors are uniformly smallest for the unweighted Fabens' method, in the middle for the weighted Fabens' method, and largest for James' method.

Performance as measured by mean square error was entirely dependent on the assumptions of the simulation. For Simulation 1 (i.e., observational errors) the weighted Fabens' method MSE was smallest; for Simulation 2

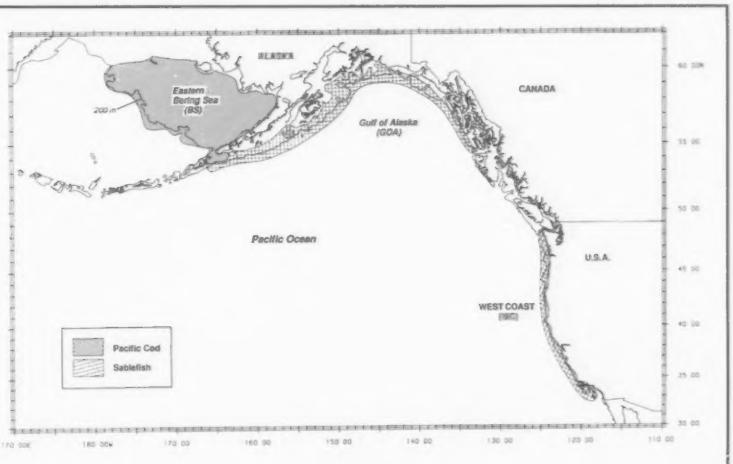

Figure 1
Tag and recovery areas for Pacific cod in eastern Bering Sea **(BS)**, sablefish in Gulf of Alaska **(GOA)**, and sablefish off U.S. west coast **(WC)**.

Table 1

Simulation results using three different methods to estimate von Bertalanffy parameters (L_0=61.23, K_0=0.296) under three different error assumptions: Simulation 1 (observational error), Simulation 2 (variation in L_∞), and Simulation 3 (both observational error and variability in L_∞). For each estimation method and parameter, simulation results are summarized by four entries: sample mean of the estimated parameter, mean analytic standard error, sample standard error (i.e., standard deviation of estimated parameters), and mean square error.

Method	Parameter	Sim. 1	Sim. 2	Sim. 3
Unweighted	mean(L_0)	58.00	65.01	60.39
Fabens	mean(K_0)	0.379	0.238	0.315
	analytic SE(L_0)	1.042	0.981	1.423
	analytic SE(K_0)	0.031	0.011	0.028
	sample SE(L_0)	0.987	0.991	1.370
	sample SE(K_0)	0.030	0.012	0.026
	MSE(L_0)	11.426	15.272	2.576
	MSE(K_0)	0.00775	0.00347	0.00103
Weighted	mean(L_0)	61.24	67.05	67.21
Fabens	mean(K_0)	0.298	0.215	0.216
	analytic SE(L_0)	1.355	1.154	2.347
	analytic SE(K_0)	0.021	0.009	0.018
	sample SE(L_0)	1.542	1.205	2.921
	sample SE(K_0)	0.030	0.012	0.027
	MSE(L_0)	2.365	35.347	44.197
	MSE(K_0)	0.00091	0.00671	0.00714
James	mean (L_0)	62.22	61.23	62.06
	mean (K_0)	0.294	0.299	0.300
	analytic SE(L_0)	4.099	1.588	4.625
	analytic SE(K_0)	0.064	0.028	0.071
	sample SE(L_0)	4.241	1.521	5.332
	sample SE(K_0)	0.066	0.027	0.069
	MSE(L_0)	18.871	2.303	28.986
	MSE(K_0)	0.00432	0.00072	0.00471

(variability in L_∞) the James' method MSE was the smallest; for Simulation 3 (i.e., both observational error and variability in L_∞) the unweighted Fabens' method MSE was the smallest.

It is clear from these simulation results that unweighted or weighted Fabens' estimates of von Bertalanffy parameters can be significantly biased. It is also clear that standard errors for James' estimators tend to be larger than standard errors for the unweighted and weighted Fabens' estimators.

Estimates from sablefish tag-recapture data

Sablefish is a species characterized by rapid growth at young ages followed by extremely slow growth at older ages. In tag-recapture data, it is common for sablefish to show negative growth increments (Figs. 2,3,5,6). The exact reason for this apparent shrinkage is uncertain. However, Sasaki (1985) noted that shrinkage was usually reported for larger male (>60 cm) and female (>70 cm) sablefish. This suggests that such occurrences are due to the combined influence of slow growth and measurement error. Furthermore, Beamish & Chilton (1982) noted that the freezing of commercially-caught fish could cause actual shrinkage. Interestingly, Beamish & Chilton (1982) also noted that data from freshly-caught fish measured by trained biologists occasionally showed shrinkage, indicating that shrinkage can occur in the ocean environment. Considering these factors, all recoveries, including those having negative growth increments, were used in the sablefish data analyses.

Although this species is extremely difficult to age (Kimura & Lyons 1991), age-determination criteria have been validated using oxytetracycline tags (Beamish & Chilton 1982) and radioisotope methods (Kastelle 1991). Because of the difficulty of directly determining ages for sablefish, estimating growth using tag-recapture data is of particular interest.

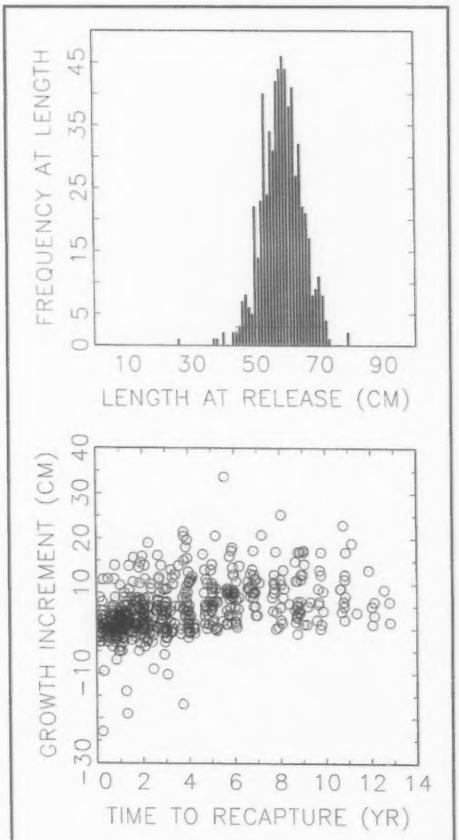
FREQUENCY AT LENGTH
0 5 15 25 35 45
10 30 50 70 90
LENGTH AT RELEASE (CM)
GROWTH INCREMENT (CM)
30 −10 10 20 30 40
0 2 4 6 8 10 12 14
TIME TO RECAPTURE (YR)

Figure 2

Length-frequency at time of release **(top)** and relationship between time at liberty and growth **(bottom)** for male sablefish in Gulf of Alaska.

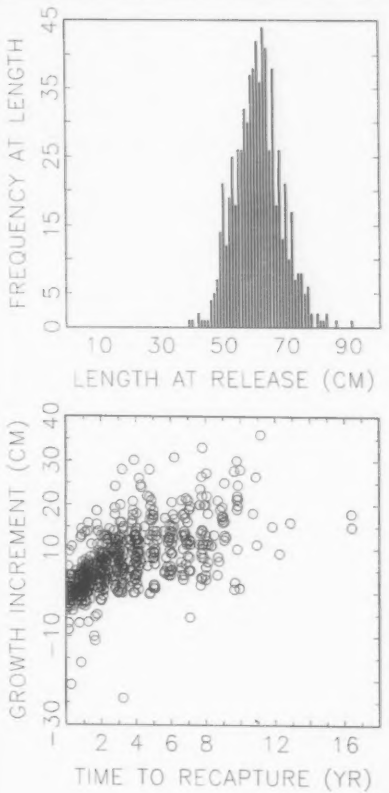
FREQUENCY AT LENGTH
0 5 15 25 35 45
10 30 50 70 90
LENGTH AT RELEASE (CM)
GROWTH INCREMENT (CM)
−30 −10 10 20 30 40
2 4 6 8 12 16
TIME TO RECAPTURE (YR)

Figure 3

Length-frequency at time of release **(top)** and relationship between time at liberty and growth **(bottom)** for female sablefish in Gulf of Alaska.

Sablefish growth differs between regions, so we analyzed tag-recapture data from the Gulf of Alaska and the west coast of the United States separately (Fig. 1). Sablefish growth differs greatly by sex (Sasaki 1985), so it was necessary to estimate growth parameters for each sex.

Because the type of fishing gear used for tagging and recapture might affect the observed growth increments, we include tables of tagging and recapture gears for the usable data for all actual datasets (Table 2). Fish in the Gulf are primarily caught using longline gear, while fish off the west coast are primarily caught by trawl and pot gears.

For Gulf of Alaska sablefish, 133,558 fish were released, with 7946 recoveries between 1972 and 1990. Of these recoveries, 1340 had usable growth-increment information (Figs. 2,3). Longline gear dominated both tag and recovery gears (Table 2).

Table 2

Cross-tabulation of release and recovery fishing gears for Gulf of Alaska sablefish, west coast sablefish, and eastern Bering Sea Pacific cod. Only tag recoveries with usable growth-increment information are included. NA = not available.

		Recovery gear				
		NA	trawl	pot	longline	total
Gulf of Alaska sablefish						
Release	NA		1		2	3
gear	trawl		2	2	28	32
	pot	5	3	17	99	124
	longline	20	81	76	1004	1181
	total	25	87	95	1133	1340
West Coast sablefish						
Release	NA	1				1
gear	trawl	14	36	8	5	63
	pot	66	464	358	68	956
	longline	12	13	31	7	63
	total	93	513	397	80	1083
Eastern Bering Sea Pacific cod						
Release						
gear	trawl	19	175	4	86	284

Estimated von Bertalanffy parameters for sablefish in the Gulf of Alaska based on tag-recapture data can be compared with von Bertalanffy parameters estimated directly from length-at-age data (Table 3) from specimens collected on longline surveys in 1987 and 1989, and aged during 1990 and 1991 (Fig. 4). For this dataset the unweighted Fabens' estimates, the James' estimates, and estimates based on direct ages gave very similar parameter estimates. However, the weighted Fabens' estimates gave estimates quite different from the others.

Table 3

Comparison of von Bertalanffy growth parameters for sablefish in the Gulf of Alaska, estimated from tag-recapture and length-at-age data. Tag-recapture sample sizes: males n=643, females n=697. Direct-ages sample sizes: males n=807, females n=1165.

	L_0	K_0	t_0	SE(L_0)	SE(K_0)	SE(t_0)
Males						
Unweighted Fabens	70.2	0.136		0.83	0.013	
Weighted Fabens	83.0	0.049		3.43	0.007	
James	70.7	0.126		2.84	0.044	
Length-at-age	70.2	0.120	–8.06	0.95	0.014	1.17
Females						
Unweighted Fabens	83.4	0.128		1.36	0.011	
Weighted Fabens	102.8	0.055		5.02	0.007	
James	84.7	0.117		3.53	0.024	
Length-at-age	86.7	0.106	–6.15	1.22	0.008	0.62

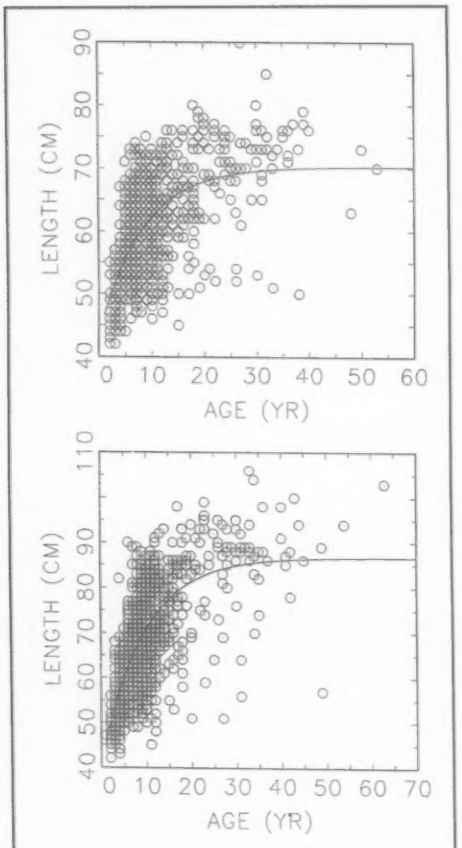

Figure 4
von Bertalanffy growth curves for male **(top)** and female **(bottom)** sablefish in Gulf of Alaska, calculated from length-at-age data.

For west coast sablefish, 52,743 fish were released, with 4220 recoveries between 1971 and 1991. Of these recoveries, 1083 had usable growth-increment information (Figs. 5,6). Pot gear was the dominant release gear, but both trawl and pot were important recovery gears (Table 2).

Estimated von Bertalanffy parameters for west coast sablefish based on tagging data can be compared with von Bertalanffy parameters estimated directly from length-at-age data (Table 4) from specimens collected in trawl and pot surveys in 1983 and 1989, and aged during 1991 and 1992 (Fig. 7). For this dataset, only James' estimates compared well with estimates based on direct ages. If James' estimates were not available, we could not conclude that estimates of growth parameters based on tagging were consistent with length-at-age data generated by age readers. Unexpectedly for the west coast dataset, James' estimates of $SE(L_0)$ were smaller than for the unweighted Fabens' estimates.

Another possible problem when analyzing growth-increment data is that the observed increments may be dependent on the tag or recovery gears that are used. Our west coast sablefish tag-recapture dataset provides an opportunity to examine whether observed growth increments may depend on the fishing gears used for tagging and recapture. From this dataset, we selected only fish with pot gear releases and trawl or pot gear recoveries. We then regressed growth increment against sex, recovery gear, size-at-release, and time at liberty. The analysis showed that fish recovered by pot gear could be expected to have growth increments 3.7 cm larger (significant α=0.0001) than fish recovered by trawl gear after the other independent variables were taken into account. Thus, release and recovery gears can be expected to affect the growth curves estimated from tag-recapture data.

Estimates from Pacific cod tag-recapture data

Pacific cod has also proved to be a very difficult species to directly age (Kimura & Lyons 1990). For eastern Bering Sea (Fig. 1) Pacific cod, 12,396 tagged fish were released, with 375 recoveries between 1982 and 1989. Of these recoveries, 284 had usable growth-increment information (Fig. 8). Bottom trawl was the only release gear, but both trawl and longline were important recovery gears (Table 2). Because of the small tag-recapture sample size available for Pacific cod, we combined male and female data into a single fit.

As with sablefish, Pacific cod tag recaptures can show negative growth increments (Fig. 8). For the complete tag-recapture dataset, unweighted and weighted Fabens' estimates were biased when compared with estimates based on length-at-age data (Table 5). James' estimates did not exist within a reasonable range for K_0 ($0.01<K_0<1.0$). Using recoveries with only positive growth increments allowed James' estimates to be close to those based on length-at-age data (Table 5). After deleting only the larger negative growth increments (i.e., larger in absolute value), data with increments greater than –10 cm gave a standard error for L_0 using James' method of 53.4 cm. These results indicate that for James' estimates, the sample size for Pacific cod was insufficient to overcome variability in the data.

Discussion

Our simulation study confirmed that James' robust estimators for estimating von Bertalanffy parameters from tag-recapture data show little bias when variability can be described by simple observational error and/or variability in L_∞. In contrast, the unweighted and weighted Fabens' estimators sometimes had

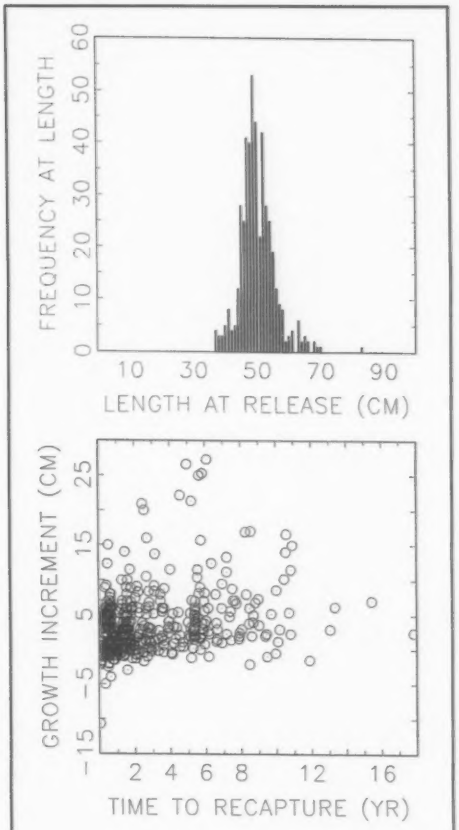
FREQUENCY AT LENGTH
0 10 20 30 40 50 60
10 30 50 70 90
LENGTH AT RELEASE (CM)
GROWTH INCREMENT (CM)
−15 −5 5 15 25
2 4 6 8 12 16
TIME TO RECAPTURE (YR)

Figure 5
Length-frequency at time of release **(top)** and relationship between time at liberty and growth **(bottom)** for male sablefish off U.S. west coast.

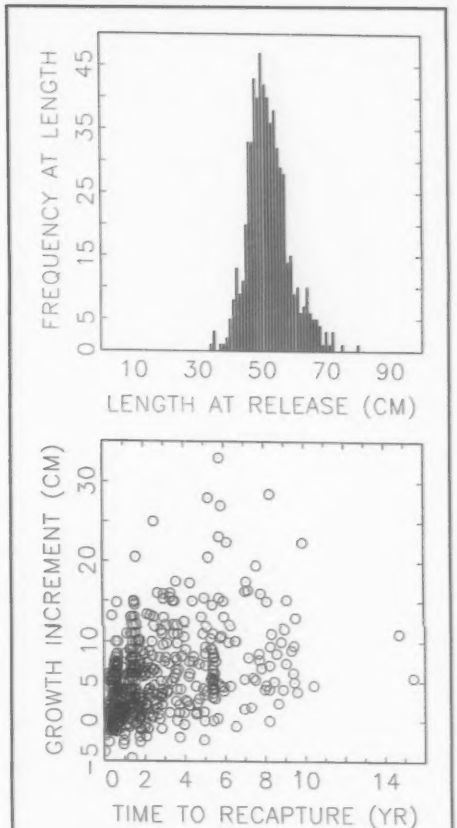
FREQUENCY AT LENGTH
0 5 15 25 35 45
10 30 50 70 90
LENGTH AT RELEASE (CM)
GROWTH INCREMENT (CM)
−5 0 5 10 20 30
0 2 4 6 8 10 14
TIME TO RECAPTURE (YR)

Figure 6
Length-frequency at time of release **(top)** and relationship between time at liberty and growth **(bottom)** for female sablefish off U.S. west coast.

Table 4
Comparison of von Bertalanffy growth parameters for sablefish off the U.S. west coast, estimated from tag-recapture and length-at-age data. Tag-recapture sample sizes: males n=467, females n=616. Direct-ages sample sizes: males n=714, females n=814.

	L_0	K_0	t_0	SE(L_0)	SE(K_0)	SE(t_0)
Males						
Unweighted Fabens	65.4	0.081		2.08	0.014	
Weighted Fabens	144.2	0.009		100.2	0.010	
James	56.6	0.556		0.65	0.108	
Length-at-age	54.7	0.472	−1.82	0.23	0.055	0.51
Females						
Unweighted Fabens	71.5	0.110		1.79	0.013	
Weighted Fabens	130.1	0.020		33.2	0.008	
James	61.4	0.481		0.92	0.085	
Length-at-age	61.0	0.499	−0.81	0.35	0.047	0.32

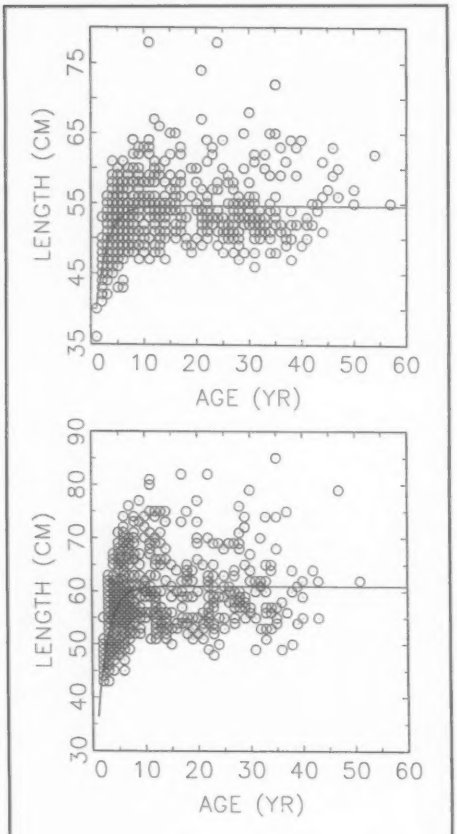

Figure 7
von Bertalanffy growth curves for male **(top)** and female **(bottom)** sablefish off U.S. west coast, calculated from length-at-age data.

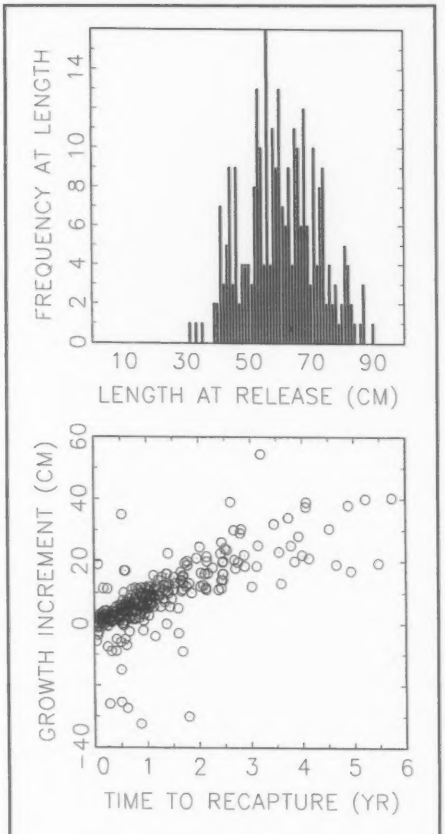

Figure 8
Length-frequency at time of release **(top)** and relationship between time at liberty and growth **(bottom)** for Pacific cod in eastern Bering Sea.

Table 5
Comparison of von Bertalanffy growth parameters for Pacific cod in eastern Bering Sea, estimated from tag-recapture data using all growth increments (n=284), only positive growth increments (n=252), and length-at-age data. Sexes were combined, and von Bertalanffy parameters estimated from length-at-age data were taken from Thompson & Bakkala (1990). NS = no solution, NA = not available.

	L_0	K_0	t_0	SE(L_0)	SE(K_0)	SE(t_0)
All growth increments						
Unweighted Fabens	117.0	0.148		9.69	0.029	
Weighted Fabens	271.0	0.035		147.81	0.024	
James	NS	NS		NS	NS	
Positive growth increments						
Unweighted Fabens	126.3	0.133		8.35	0.020	
Weighted Fabens	175.1	0.070		28.19	0.017	
James	104.3	0.222		10.55	0.065	
Length-at-age	105.4	0.237	1.06	NA	NA	NA

large biases. However, the standard errors for James' estimators tended to be larger, so in terms of mean square error the superior estimation method depended on the assumptions we made concerning variability.

Weighted Fabens' estimators performed well when error was restricted to observational error, but were badly biased when variability in L_∞ was introduced into the simulation. In contrast, James' estimators performed well when there was no observational error and error was due only to variability in L_∞. The unweighted Fabens' estimators were biased when error was solely observational, and biased when variability was due solely to variability in L_∞, but biases apparently canceled when both errors were present.

It is difficult to recommend the unweighted or weighted Fabens' estimators because they are both subject to large biases. It seems difficult to assume biases will cancel, or that there will be no variability in the data due to variability in L_∞.

On the other hand, the James' estimators appeared unbiased but tended to have larger standard errors. Our experience with analyzing the small sample-size dataset available for Pacific cod indicates that James' estimators may require at least moderate sample sizes, the required size depending on variability in the data. If sample sizes are sufficiently large, reducing bias can be far more important than increasing efficiency. Therefore, it seems important that James' estimators be used to at least guard against possible biases. More experience with James' method will probably be needed before researchers can finally decide the correct scope of application for this new method.

In this paper we have used von Bertalanffy parameter estimates based on direct ages as the yardstick by which to measure bias for the three different estimators. Of course, von Bertalanffy parameter estimates based on length-at-age data might themselves be biased. Except for the small sample-size dataset available for Pacific cod, James' estimators compared well with estimates based on direct age data. Unweighted Fabens' estimators compared well with estimates based on direct ages for one dataset. Weighted Fabens' estimators of L_0 appeared to be biased high for all three datasets.

This pattern of bias suggests that the tag-recapture data in these actual datasets contain significant amounts of variability due to variability in L_∞. This is also evidenced by the length-at-age data (see Figs. 4,7). For the three stocks of fish studied in this paper, we conclude that there are no inconsistencies in growth described by direct ages and growth described by tag-recapture data. Without James' estimators, this conclusion could not be made. We feel that James' method represents a significant step forward, and that datasets previously analyzed using Fabens' method might benefit by being reexamined using James' method. However, results may be the same as Fabens' estimates, or quite different, depending upon the nature of variability in the data.

Still, problems remain when evaluating growth from tag-recapture data. McFarlane & Beamish (1990) concluded that external tags could markedly affect the growth of sablefish. We have shown that different fishing gear types may select for slower- or faster-growing individuals. For the west coast sablefish tag-recapture datasets, growth increments appeared larger for fish recovered with pot gear compared with trawl gear. Therefore, sampling gears always play a role in describing the growth parameters we estimate.

Acknowledgments

We thank R.A. Maller, an anonymous referee, and the editorial staff of the journal for comments that greatly facilitated our revision. We thank F.R. Shaw for providing access to the sablefish tag-recovery database. This study was motivated by original insights into tag-recapture growth parameter estimation from I.R. James.

Citations

Beamish, R. J., & D. E. Chilton
1982 Preliminary evaluation of a method to determine the age of sablefish (*Anoplopoma fimbria*). Can. J. Fish. Aquat. Sci. 39:277–287.

Chapman, D. G.
1961 Statistical problems in dynamics of exploited fish populations. Proc. Berkeley Symp. Math. Stat. Probab. 4:153–168.

Chilton, D. E., & R. J. Beamish
1982 Age determination methods for fishes studied by the Groundfish Program at the Pacific Biological Station. Can. Spec. Publ. Fish. Aquat. Sci. 60:1–102.

Fabens, A. J.
1965 Properties and fitting of the von Bertalanffy growth curve. Growth 29:265–289.

Francis, R. I. C. C.
1988a Are growth parameters estimated from tagging and age-length data comparable? Can. J. Fish. Aquat. Sci. 45:936–942.
1988b Maximum likelihood estimation of growth and growth variability from tagging data. N.Z. J. Mar. Freshwater Res. 22:42–51.

James, I. R.
1991 Estimation of von Bertalanffy growth curve parameters from recapture data. Biometrics 47:1519–1530.

Kastelle, C. R.
1991 Radioisotope age validation and an estimate of natural mortality from the gonad to somatic weight index for sablefish (*Anoplopoma fimbria*). M.S. thesis, Univ. Wash., Seattle, 87 p.

Kimura, D. K.
1980 Likelihood estimates for the von Bertalanffy growth curve. Fish. Bull., U.S. 77:765–776.

Kimura, D. K., & J. J. Lyons
1990 Choosing a structure for the production ageing of Pacific cod (*Gadus macrocephalus*). Int. N. Pac. Fish. Comm. Bull. 50:9–23.
1991 Between-reader bias and variability in the age-determination process. Fish. Bull., U.S. 89:53–60.

Kirkwood, G. P.
1983 Estimation of von Bertalanffy growth curve parameters using both length increment and age-length data. Can. J. Fish. Aquat. Sci. 40:1405–1411.

Kirkwood, G. P., & I. F. Somers
1984 Growth of two species of tiger prawn, *Penaeus esculentus* and *P. semisulcatus*, in the western Gulf of Carpentaria. Aust. J. Mar. Freshwater Res. 35:703–712.

Maller, R. A. & E. S. deBoer
1988 An analysis of two methods of fitting the von Bertalanffy curve to capture-recapture data. Aust. J. Mar. Freshwater Res. 39:459–466.

McFarlane, G. A., & R. J. Beamish
1990 Effect of an external tag on growth of sablefish (*Anoplopoma fimbria*) and consequences to mortality and age at maturity. Can. J. Fish. Aquat. Sci. 47:1551–1557.

Press, W. H., B. P. Flannery, S. A. Teukolsky, & W. T. Vetterling
1986 Numerical recipes (the art of scientific computing). Cambridge Univ. Press, 818 p.

Sainsbury, K. J.
1980 Effects of individual variability on the von Bertalanffy growth equation. Can. J. Fish. Aquat. Sci. 37:241–247.

Sasaki, T.
1985 Studies on the sablefish resources in the North Pacific Ocean. Bull. Far Seas Fish. Res. Lab. 22:1–108.

Thompson G. G., & R. G. Bakkala
1990 Assessment of the eastern Bering Sea Pacific cod stock using a catch-at-age model and trawl survey. Int. N. Pac. Fish. Comm. Bull. 50:215–236.

Vertical distribution patterns and diel migrations of larval and juvenile haddock *Melanogrammus aeglefinus* and Atlantic cod *Gadus morhua* on Georges Bank*

R. Gregory Lough
David C. Potter
Northeast Fisheries Science Center, National Marine Fisheries Service, NOAA
Woods Hole, Massachusetts 02543

Abstract.–Vertical distribution patterns of haddock *Melanogrammus aeglefinus* and Atlantic cod *Gadus morhua* are summarized from eight research cruises on Georges Bank, during spring and summer 1981–86. Eggs and larvae were sampled at discrete depths with a 1 m^2 MOCNESS, pelagic juveniles with a 10 m^2 MOCNESS, and recently-settled juveniles with a bottom trawl supplemented with submersible observations. In well-mixed waters during early spring, eggs and larvae were distributed throughout the water column. Upon stratification of waters over the outer margin of Georges Bank in mid-May, the larval population was concentrated in the thermocline; the stronger the stratification, the more larvae were confined to this depth zone. At well-mixed shoal sites, pelagic larvae remained distributed throughout the water column.

Differences in day and night distribution patterns provided evidence to indicate that larvae began migrating as small as 6–8 mm; however, clear sampling differences were evident for larvae only at body lengths of >9–13 mm. Larvae tended to be deeper during the day and shoaler by night; larger larvae had a greater vertical range. Pelagic juveniles (>20 mm) occurred deeper in the water column as they grew. By mid-July most juveniles (~40 mm) were associated with the bottom. The transition from pelagic to demersal life (~40–100 mm) probably occurs over a period of 1–2 mo. Recently-settled juveniles remained demersal by day and migrated upwards 3–5 m at night. Their excursions off-bottom decreased in amplitude with larger sizes. Haddock remained closer to bottom both day and night at a smaller size than cod. The diel vertical behavior of cod may be strongly related to the light-dark cycle, whereas behavior of haddock was more variable. Some differences in vertical distributions between haddock and cod can be attributed to morphology and feeding behavior.

Manuscript accepted 9 February 1993.
Fishery Bulletin, U.S. 91:281-303 (1993).

On Georges Bank off the northeast coast of the United States (Fig. 1, page 293), stocks of haddock *Melanogrammus aeglefinus* L. and Atlantic cod *Gadus morhua* L. historically have been important components of the American and Canadian demersal fishery (Murawski et al. 1983, Overholtz & Tyler 1985). Eggs and larvae of both species are dominant in the spring ichthyoplankton community (O'Boyle et al. 1984, Sherman et al. 1984). Research survey data have shown that the size of a year-class is usually established by the end of the first year of life (Sissenwine 1984). At the Northeast Fisheries Science Center (NEFSC) since 1976, considerable research effort has been focused toward describing the place and time of spawning of haddock and cod, dispersal of eggs and larvae, and survival and recruitment of juveniles on Georges Bank. Field, laboratory, and modeling results were integrated to evaluate important mortality processes during the first year of life. Beginning in spring 1980, a series of interdisciplinary, process-oriented cruises used discrete depth samplers to investigate mortality due to starvation by describing the fine-scale spatio-temporal variability of gadid larvae in relation to their prey during the first few weeks post-hatching (Lough 1984, Laurence & Lough 1985). In 1984, a series of summer and early-fall surveys of juvenile gadids was initiated to document the distribution and abundance of the 0-group fish and their transition to the demersal phase when predation may be a dominant mortality factor (Cohen et al. 1988).

Based on these studies, we now have sufficient information to describe the life history of haddock and cod during the first 6–9 mo. Both species spawn on the northeast part of Georges Bank (Fig. 1). Peak spawning time for cod is late February–early March, and early April for haddock. The egg patches drift southwest a few kilometers per day in the clockwise residual drift and hatch within 2–3 wk (Lough 1984). By May, larval concentrations can be found along the southern edge of Georges Bank between the 60 m and 100 m isobath. In late-spring to fall, a seasonal thermocline develops to a depth of 10–30 m in waters deeper than ~60 m. Water shoaler than 60 m is vertically well-mixed throughout the year by the strong (>60 cm/s) rotary tidal currents. Larvae >30 d can be found shoaler than the 60 m isobath as the patch moves southwest, and by late June some fraction of the population has moved onto the shoals of western Georges Bank (Walford 1938,

*MARMAP Contribution FED/NEFC 90-01, Woods Hole Laboratory, Northeast Fisheries Science Center, National Marine Fisheries Service, NOAA.

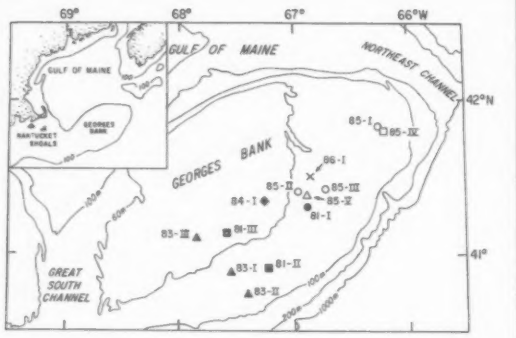

Figure 1
Location of vertical distribution studies, 1981–86, on Georges Bank, designated by year and sampled sites. Sites (Roman numerals) within a cruise have same symbols.

Lough 1984, Smith & Morse 1985, Lough & Bolz 1989). By late July–early August, the highest catches of juvenile gadids are usually found on eastern Georges Bank (Lough et al. 1989).

Haddock and cod undergo typical development and morphological transformation at sizes >20 mm standard length (SL, ~2–3 mo post-hatching) (Fahay 1983, Auditore et al. 1993). Their transition from pelagic to demersal life occurs when they are >25 mm in midsummer (Lough et al. 1989).

Information on larval and juvenile vertical distributions and diel migrations are needed to (a) study their transport by currents, (b) compare vertical distributions of their prey and predators, and (c) make accurate abundance estimates of various stages caught by different sampling gear. In this paper we summarize data on the vertical distribution of 0-group haddock and cod during spring and summer on Georges Bank from 1981 to 1987. The following questions on the early life of haddock and cod were addressed. (1) What is the vertical distribution pattern of larvae and juveniles on Georges Bank? (2) What is the timing and range of diel migratory behavior in relation to development? (3) What is the transition period from pelagic to demersal life for an individual fish? (4) How do light, temperature, salinity, and currents influence vertical distribution and migratory behavior? (5) How does gear selectivity bias vertical distribution patterns?

Methods

Sampling protocol

General cruise objectives and sampling strategy for the larval–juvenile fish studies are described by Lough (1984). A concentration of larvae on Georges Bank was located by a fine-scale grid of stations using standard bongo-net gear. Based upon real-time sample analyses made during the grid survey, sites were selected within well-mixed and stratified waters for the comparative vertical time-series observations. Haddock and cod were collected by three gear types on eight cruises (Table 1). Pelagic larvae and juveniles were sampled with an electronically-controlled, multiple opening/closing net and environmental sensing system (MOCNESS), with a 1 m^2 or 10 m^2 mouth opening (see Wiebe et al. 1976, 1982, 1985). A Yankee 36 bottom trawl was used to sample the recently-settled juvenile fish. The numbers of day, night, and twilight hauls at each site are listed in Table 1.

The MOCNESS used to sample the larval stage has an effective mouth opening of 1 m^2 when towed at a 45° net angle near 3.7 km/h (2 kn). The unit consists of nine 0.333 mm mesh nets that open and close sequentially on command. Temperature (and salinity beginning in 1985) was obtained simultaneously with standard net-sampling parameters such as depth and volume of water filtered. When a concentration of larvae was located, a drogue was deployed at a depth of 15 m to mark the water mass for further sampling. Thereafter, the 1 m^2 MOCNESS was used to sample every 3–6 h at the drogue for a period of 24–48 h. Discrete depths were sampled at 10 m intervals from the surface to within 5 m of the bottom within a 5 min period. Each net filtered ~250 m^3 of water.

The 10 m^2 MOCNESS, used to collect the pelagic juveniles, has five 3.0 mm mesh nets. Because juveniles tend to remain localized for at least 2–4 d, sampling was conducted at fixed sites that were determined to contain high concentrations of juveniles. The vertical distribution of pelagic juveniles was sampled every 6 h. Discrete depth strata ranged 10–30 m from the surface to within 5 m of the bottom; each net filtered between 15,000 and 20,000 m^3 of water during a 30 min tow.

A Yankee 36 bottom trawl was used to catch recently-settled juveniles. Trawl specifications are found in Azarovitz (1981). The opening height and width of the trawl was 3.2×10.4 m. The trawl had graded stretch mesh of 127–13 mm (mouth to cod-end). Standard roller gear (40.6 cm diameter) was used on the *Albatross IV* 86-03 June 1986 cruise; however, rollers were replaced with a sweep chain of rubber disks (11.4 cm diameter) on the *Delaware II* cruises 85-05 of July 1985 and 85-06 of August 1985, to collect fish close to bottom. The standard bottom-trawl set was made at 6.5 km/h (3.5 kn) for 30 min on the bottom. Trawl sampling was conducted for 24 h.

All specimens were initially fixed in either 4% formaldehyde-seawater solution or 90% ethyl alcohol and

then subsequently preserved in 70% ethyl alcohol and water. Temperature and salinity profiles were obtained from the MOCNESS, XBT drop, or CTD cast.

Data analysis

Larvae and pelagic juveniles were measured to the nearest 0.1 mmSL. Demersal juveniles from the bottom trawl were measured to the nearest mm. Length of haddock and cod were corrected for shrinkage to live-length using the method of Bolz & Lough (1983). Catches from the 1 m^2 MOCNESS were initially standardized to n/100 m^3 of water, and 10 m^2 MOCNESS catches to n/10,000 m^3. The fish were grouped into size-classes based on developmental characters (Auditore et al. 1993): 2–5, 6–8, 9–13, 14–19, 20–29, 30–39, 40–49, 50–59, and 60–69 mm.

As an initial step, the percent of a size-class at each depth was plotted with the temperature and salinity profile for each tow (figures not shown). Tows were classified as day, night, or (in a few cases) twilight, i.e., 1 h before and after sunrise and sunset. For each pelagic tow, the mean number of fish within a time-block and size-class was calculated for each depth by summing all hauls at that site. Day and night vertical profiles are plotted from these arithmetic means. Also, abundance of larvae was integrated over the water column, in terms of n/10 m^2 for the 1 m^2 MOCNESS catches and n/1000 m^2 for the 10 m^2 MOCNESS catches. Abundance-weighted mean depth or center of density distributions of size-classes were calculated using the method of Miller et al. (1963). To examine trends, mean depths of selected sites were plotted in time-series with water column thermoclines. Since salinity changes throughout the water column are generally small (<1 psu), temperature usually has a dominant effect on density and stratification of the surface water on Georges Bank (Flagg 1987).

To test for differences in population means between day and night vertical distributions and for interactions among depth, time of day, and size of fish, an unbalanced ANOVA Type-III model was used on all tow data (Dunn & Clark 1974). The linear model is:

$$Y = b_0 + b_1(D) + b_2(T) + b_3(S) + b_4(D\times T) + b_5(D\times S) + b_6(T\times S) + b_7(D\times T\times S) + e, \quad (1)$$

where Y is fish density (n/m^3), D is depth effect (coded depth level), T is time effect (coded night or day), S is size effect (coded size-class), b is a constant, and e is the normally-distributed residual error term. Transformation of the fish density data by $\log_{10}(x+0.1)$ resulted in a normal distribution of the residuals. Although the interpretation of vertical migration based on ANOVA can be difficult, the depth × time interaction is generally considered the most useful factor for detecting diel migrations (Sokal & Rohlf 1969). Summary tables are presented of the factor F-values and their level of significance.

For each station, an average temperature and salinity profile was made by summing all the time-series data across the sampled depth levels and calculating the mean, standard deviation, and 95% confidence limits. At sites where stratification of the water column occurred primarily from solar insolation, upper and lower bounds of the thermocline region were determined by inspection for each tow profile. The thermocline was defined as the region of greatest temperature change. In a well-stratified water column, the zone of greatest temperature change was easily identified between the relatively uniform water above and below this zone. In a weakly-stratified water column, determination of the thermocline zone was more subjective. The distribution of larvae within, above, and below the thermocline was estimated for each size-class within a tow at Sites I&II for May 1983. The mean percentage distribution and standard error of each region were calculated on the angular transformation of the tow percentage data: angle = arcsin $\sqrt{\text{proportion}}$.

Bottom-trawl catches of recently-settled juvenile haddock and cod were standardized to n/30 min haul. Length data were grouped by 1cm size-classes and then grouped by day, night, and twilight catches. Standard statistics ($\bar{x}$, SD, CV) were calculated on the untransformed data. Differences between population means were tested by the Students' t-test on $\log_{10}$ transformed data (Sokal & Rohlf 1969).

Results

Vertical distribution of larvae

Well-mixed water In April 1981, recently-hatched haddock larvae (2–5 mm) and fewer larger larvae (6–8 mm) were distributed throughout the water column (Fig. 2A). Results of the ANOVA for the 2–5 mm haddock (Table 2) showed a significant effect of depth (p<0.05) but not of time of day.

Cod larvae (up to 8 mm) also were distributed through the water column (Fig. 2B). In several vertical profiles the distributions are weakly bimodal. During the day, larger larvae (9–29 mm) were most abundant at mid-depth, 30–40 m, whereas at night they were more abundant above 30 m. Ratios in night-day abundance increased from ~2/10 m^2 or less for the smaller larvae (<14 mm) to 4–6/10 m^2 for the 14–19 mm and 20–29 mm size-classes. ANOVA for cod larvae showed a significant (p<0.05) interaction effect of time × size, which was expected since abundance increases at night as cod get larger (Table 2A). A significant (p<0.05) depth × time interaction occurred only for size-classes >9–13 mm.

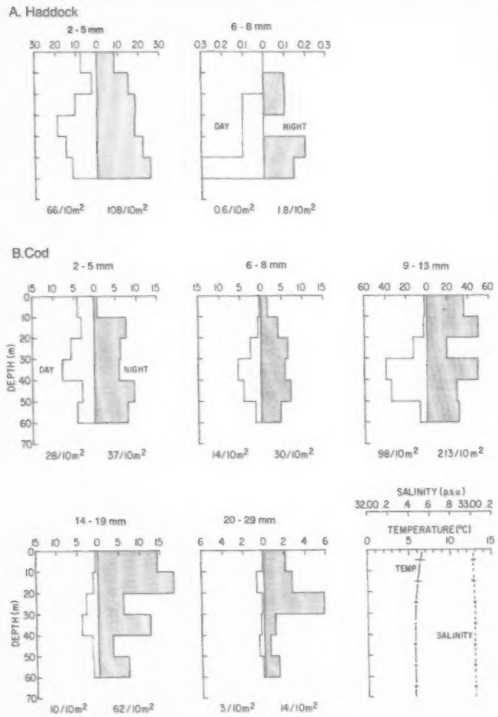

Figure 2

Mean day and night vertical distribution ($\bar{x}$ n/100 m³) of **(A)** haddock *Melanogrammus aeglefinus* and **(B)** cod *Gadus morhua* size-classes of larvae collected by the 1 m² MOCNESS on well-mixed Site 81-I during 27–29 April 1981. Estimated water column abundances (n/10 m²) are included for day-night comparisons at bottom of plots. Composite temperature and salinity profiles are plotted as depth stratum mean (●) and 95% confidence limits (— —).

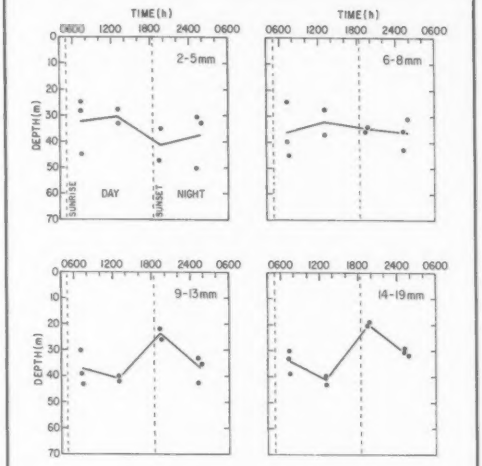

Figure 3

Abundance weighted-mean depths (●) of larval cod *Gadus morhua* size-classes plotted over a 24 h period on well-mixed Site 81-I during 27–29 April 1981. Line connecting replicate points represents the average population trend.

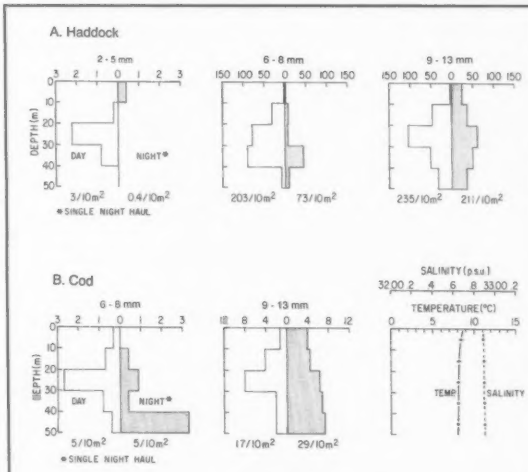

Figure 4

Mean day and night vertical distribution ($\bar{x}$ n/100 m³) of **(A)** haddock *Melanogrammus aeglefinus* and **(B)** cod *Gadus morhua* size-classes of larvae collected by the 1 m² MOCNESS on well-mixed Site 81-III during 27 May 1981. Estimated water column abundances (n/10 m²) are included at bottom of plots. Temperature and salinity profiles are plotted as depth stratum means (●) and 95% confidence limits (— —).

Mean depths of the four smallest cod size-classes are plotted for each tow within a 24 h period over the 2.5 d of sampling at Site 81-I, and a trend line connects the mean depths of abundance (Fig. 3). There appears to be a daily pattern in vertical distribution. The smaller size-classes, 2–5 mm and 6–8 mm, remained at a depth of ~35 m day and night. In contrast, larger size-classes of cod, 9–13 mm and 14–19 mm, showed a consistent diel migration from a mean depth of 40 m at noon to 20–25 m after sunset.

At the well-mixed shoal (35–58 m) Site 81-III on 27 May 1981, 2–13 mm haddock and 6–13 mm cod larvae were distributed through the water column (Fig. 4) with mean depths of abundance generally at 20 m and 40 m. Because of the limited number of tows, a significant difference in day-night patterns could not be determined.

At the well-mixed shoal (34–54 m) Site 83-III on 16–17 May 1983, three size-classes of haddock and cod larvae (6–8, 9–13, 14–19 mm) were distributed through

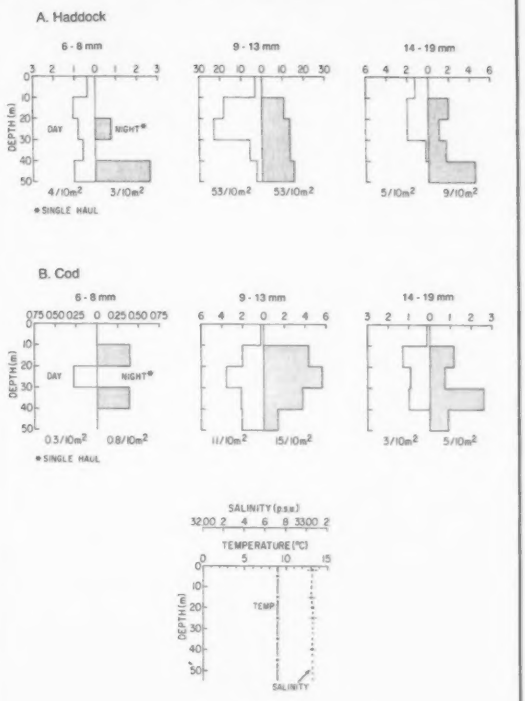

Figure 5

Mean day and night vertical distribution ($\bar{x}$ n/100 m³) of **(A)** haddock *Melanogrammus aeglefinus* and **(B)** cod *Gadus morhua* size-classes of larvae collected by the 1 m² MOCNESS on well-mixed Site 83-III during 16–17 May 1983. Estimated water column abundances (n/10 m²) are included at bottom of plots. Temperature and salinity profiles are plotted as depth stratum means (●) and 95% confidence limits (— —).

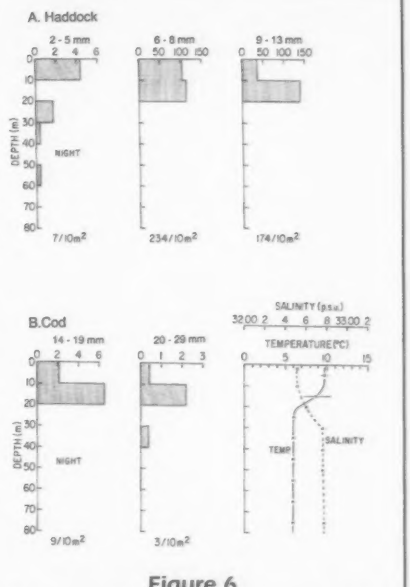

Figure 6

Night vertical distribution ($\bar{x}$ n/100 m³) of **(A)** haddock *Melanogrammus aeglefinus* and **(B)** cod *Gadus morhua* size-classes of larvae collected by a single 1 m² MOCNESS tow on well-stratified Site 81-II before the storm on 21 May 1981. Estimated water column abundances (n/10 m²) are included at bottom of plots. Temperature and salinity profiles are plotted as depth stratum mean (●) and 95% confidence limits (— —).

the water column (Fig. 5). The single night haul and low densities preclude firm conclusions.

Stratified water On 21 May 1981, when the water column at Site 81-II (75–83 m) was strongly stratified, a single 1 m² MOCNESS night tow found haddock and cod larvae 2–13 mm to be confined almost exclusively to the upper 20 m of the water column, and maximum densities usually were within the strong thermocline gradient at 10–20 m depth (Fig. 6). No recently-hatched cod larvae 2–5 mm were caught in this tow. The surface temperature approached 10°C with a strong thermal gradient at 11–21 m, where the temperature decreased to 5.9°C. An intense storm on 21–24 May 1981, with winds up to 18–21 m/s (35–40 kn) and sea wave heights of 3–5 m (10–15 ft), destroyed the strong thermocline shown in Fig. 6. Following the storm, the water column was well mixed and the larvae were distributed broadly (Fig. 7), but about an order of magnitude more abundant relative to the collections made on 21 May. Differences in mean day and night vertical distributions of larvae during the well-mixed period of 24–26 May 1981 indicate a diel shift in distribution patterns of the larger larvae (Fig. 7), with population centers located deeper in the water column by day (40–60 m) and shoaler by night (10–40 m). This diel shift in vertical distribution is supported by the ANOVA (Table 2B), where both haddock and cod have significant (p<0.05) depth × time interaction effects. By 28 May 1981, near-surface insolation warming of the upper 20 m occurred, and larvae reaggregated above 20 m near a weak thermocline (Fig. 8).

Mean depths of larvae captured in tows before and after the storm are plotted in Fig. 9 along with depth bounds of the thermocline region. The weak thermocline deepened after 25 May 1981. Mean depths of larval abundance remained below the weak thermocline until 28 May. Tows made on 26 May showed that the larger larvae were mainly located deeper in the

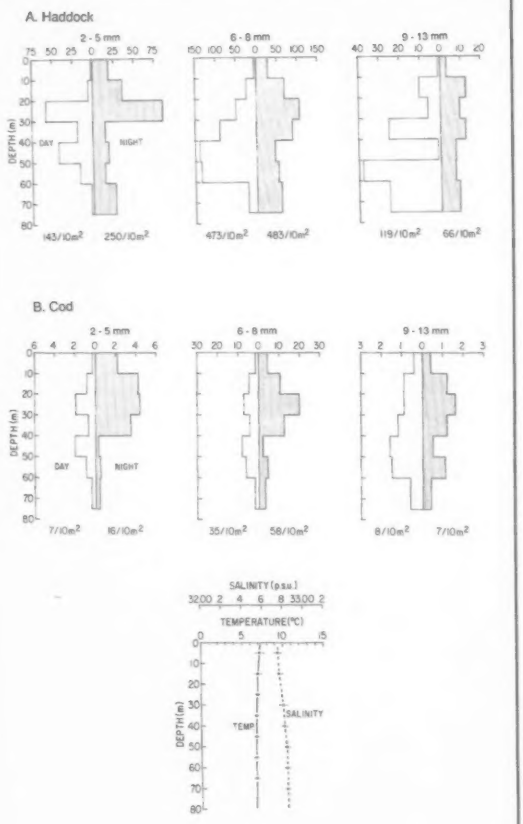

Figure 7

Mean day and night vertical distribution ($\bar{x}$ n/100 m³) of **(A)** haddock *Melanogrammus aeglefinus* and **(B)** cod *Gadus morhua* size-classes of larvae collected by the 1 m² MOCNESS on well-mixed Site 81-II following the storm on 24–26 May 1981. Estimated water column abundances (n/10 m²) are included at bottom of plots. Temperature and salinity profiles are plotted as depth stratum means (●) and 95% confidence limits (— —).

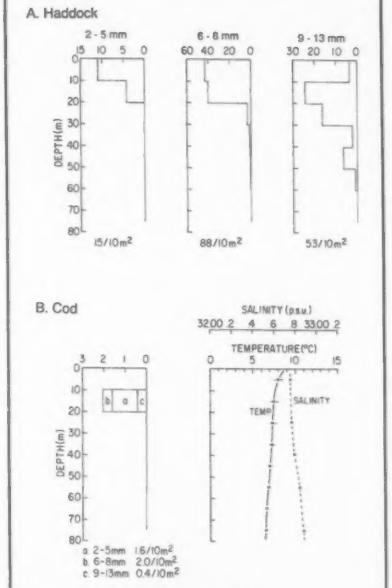

Figure 8

Day vertical distribution ($\bar{x}$ n/100 m³) of size-classes of **(A)** haddock *Melanogrammus aeglefinus* and **(B)** cod *Gadus morhus* larvae collected by a single 1 m² MOCNESS tow on weakly-stratified Site 81-II following the storm on 28 May 1981. Estimated water column abundances (n/10 m²) are included at bottom of plots. Temperature and salinity profiles are plotted as depth stratum means (●) and 95% confidence limits (— —).

water column than smaller larvae. However, when the water column was well-stratified on 21 May and weakly-stratified on 28 May, in both day and night all sizes of larvae were located in or above the thermocline. The single day and night tows were not sufficient to base firm conclusions on diel differences.

In mid-May 1983, two sites were sampled in weakly-stratified waters across the southern margin of Georges Bank. At Site 83-I (Fig. 10), mean day and night vertical distributions show haddock and cod larvae distributed broadly through the water column on 13–14 May, but each of the three size-classes had a different depth distribution. Recently-hatched larvae (2–5 mm) were most abundant at 10–30 m both day and night. The 6–8 mm size-classes of both species were more broadly distributed and most abundant at 10–50 m depths, with haddock tending to be deeper in the water column by day than cod. The 9–13 mm size-class for both haddock and cod had a pronounced diel shift in day-night distribution patterns: most larvae were in the lower half of the water column by day but in the upper half at night. The maximum density for both species was at 10–20 m. There were significant (p<0.05) interactions for each combination of depth, time, and size (ANOVA; Table 2C).

A time-series of larval catches in relation to the thermocline region at Site 83-I is shown in Fig. 11. Although the mean depth of the thermocline centered at ~20 m, its bounds varied between 10 and 40 m, perhaps due to the tides. While the population centers of cod and haddock larvae tended to be associated with

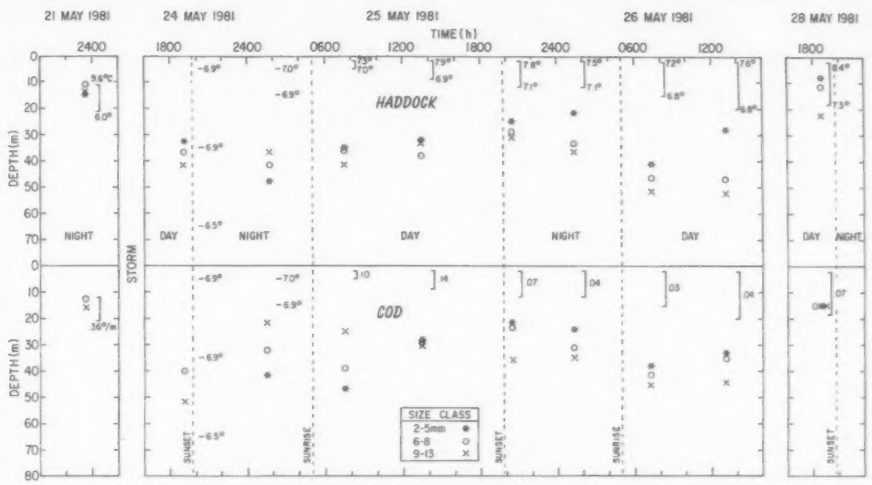

Figure 9

Time-series of abundance weighted-mean depths of larval haddock *Melanogrammus aeglefinus* and cod *Gadus morhua* size-classes on Site 81-II before and after the storm on 21–28 May 1981. Brackets at tow time record upper and lower depth bounds of the thermocline region. In the haddock time-series, boundary temperatures are recorded beside the brackets; for cod, the rate of temperature change ($\delta T/\delta Z$) over the thermocline region is specified. Where no thermocline was evident, temperatures at selected depths are inserted.

the thermocline region, they were not confined exclusively to it, as in May 1981 when the water column was strongly stratified. Larger larvae of both species tended to be found at greater depths during the day, especially the 9–13 mm larvae.

At Site 83-I, >64% of the 9–13 mm size-class for both haddock and cod was found below the thermocline by day, but <28% by night (Table 3A). A significantly ($p<0.05$) greater percentage of the 9–13 mm size-class was found within and above the thermocline at night. For the 2–5 mm size-classes, haddock and cod larvae were found mostly within or above the thermocline; <15% were located below the thermocline, and there was no significant day-night difference in the profile percentages. For the 6–8 mm size-classes of haddock and cod, the highest percentage of larvae were located within the thermocline. Of the haddock larvae, 40% were found below the thermocline by day, but only 18% at night ($p<0.005$). There was no significant change in the day-night percentages for 6–8 mm cod.

On 15–16 May 1983, at Site 83-II (88–93 m) near the shelf/slopewater front, thermocline depth was somewhat deeper with a smaller gradient than at Site 83-I. Most haddock and cod larvae were confined to the upper 40 m, the lower bound of the thermocline (Fig. 12). A small percentage of larger larvae (9–13 mm) were located below the thermocline by day (13% for haddock and 20% for cod) but moved nearer the surface by night (Table 3B). All size-classes of larvae were broadly distributed within the upper part of the water column. There were significant (ANOVA; $p<0.001$) effects of depth, time, and size for haddock; only depth × size interaction was significant ($p<0.01$) for cod (Table 2C). Mean depths of haddock and cod were greater by day for the larger larvae, especially for the 9–13 mm size-classes (Fig. 13), and in all but one night tow the mean depths were located within the confines of the thermocline region.

Vertical distribution of pelagic juveniles

In June 1984, pelagic juvenile haddock and cod were collected at a well-mixed shoal (40–49 m) Site 84-I (Fig. 14). Cod were more abundant than haddock at Site 83-I, and the larger fish (14–29 mm) were caught more abundantly in night tows than day. The three size-classes of haddock were similarly distributed throughout the water column. Few were caught in the upper 10 m; abundance usually peaked near 10–20 m both day and night. Pelagic cod also were caught throughout the water column during the day, with abundance peaks near 10–20 m for the 14–19 mm and 20–29 mm size-classes. They were more abundant in

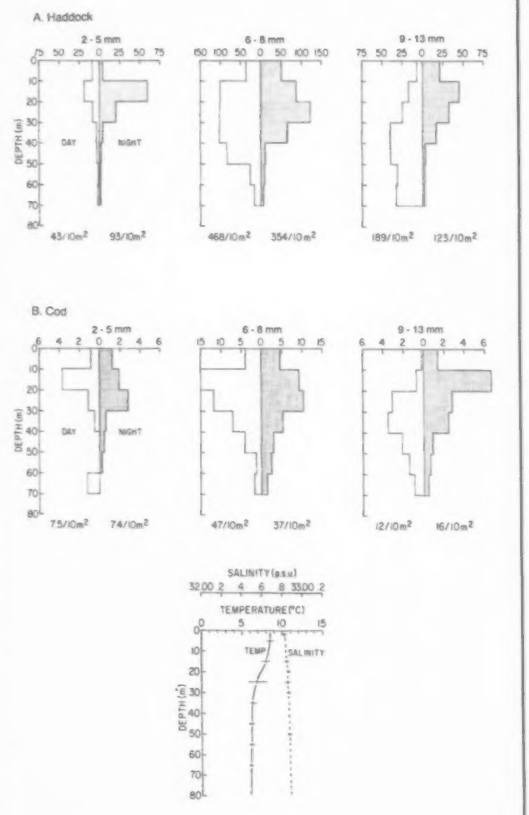

Figure 10

Mean day and night vertical distribution ($\bar{x}$ n/100 m³) of **(A)** haddock *Melanogrammus aeglefinus* and **(B)** cod *Gadus morhua* size-classes of larvae collected by the 1 m² MOCNESS on weakly-stratified Site 83-I during 13–14 May 1983. Estimated water column abundances (n/10 m²) are included at bottom of plots. Temperature and salinity profiles are plotted as depth stratum means (●) and 95% confidence limits (— —).

the upper half of the water column at night, increasing somewhat towards the surface. There were no significant interaction effects in the ANOVA for either cod or haddock (Table 4).

On 18–22 June 1986 at a well-mixed deeper (65–78 m) Site 86-I, cod juveniles 14–49 mm were caught (Fig. 15). Mean day and night vertical distributions show a clear pattern of larger size-classes of cod located progressively deeper in the water column, with the 40–49 mm cod located almost entirely between 50 m and the bottom. Night catches were greater than day catches for all size-classes of cod. Night mean abundance was significantly greater (ANOVA; $p<0.01$) than day mean abundance of the 20–29 mm and 30–39 mm size-classes (Table 4). There was no detectable evidence of diel vertical migrations.

By July, relatively few pelagic haddock and cod juveniles were caught. Highest densities of juvenile gadids were located on eastern Georges Bank (Lough et al. 1989). Three sites were sampled in mid-July 1985 on eastern Georges Bank: Site 85-I (82–87 m), stratified; Site 85-II (64–72 m), weakly stratified; Site 85-III (78–83m), stratified (Fig. 16). The deeper Sites 85-I & 85-III both had a gradual thermocline at 15–30 m depths. Only a few pelagic cod juveniles were caught. Pelagic cod ranging 30–59 mm were caught mostly at night, although a day tow was not made at Site III. Relatively few fish were caught in the upper 30 m, and there was a tendency for the highest densities to be located in the bottom third of the water column. Cod were caught in day tows at Site 85-I in the bottom 60–80 m stratum.

Diel migration of recently-settled juveniles

In 17 bottom trawls (with rollers) at Site 86-I, 25–26 June 1986, demersal cod juveniles with a mean length of 4–5 cm were collected (Table 5). Few were caught in day trawls, but at least an order of magnitude more cod ($\bar{x}$ 103/30 min trawl) were caught in night trawls. During 17–18 July 1985 at Site 85-IV, nine bottom trawls (with rubber disk sweep chain) were made (Table 6; Fig. 17). Both haddock and cod appeared to be caught more abundantly in day trawls than at twilight. Only one haddock juvenile was caught in the single night trawl. The mean length of haddock was 7.1 cm (range 4–10 cm), and 5.5 cm for cod (range 2–12 cm). Mean lengths of both species were the same in day and twilight trawls. The high daylight catches of cod juveniles in this series are in contrast to the high night catches of cod of the same average size, 4–5 cm, in June 1986 using a bottom trawl with rollers. Gear difference (rubber disks vs. rollers) may have been the cause of the different day-night catches, but conclusions cannot be made because in July 1985 only one night trawl was made.

During 16–17 August 1985, 12 bottom trawls (with rubber disk sweep chain) on southeastern Georges Bank (63–71 m), Site 85-V, caught relatively high numbers (210–257/30 min trawl) of 9–19 cm haddock juveniles (Table 7; Fig. 18). The mean number and lengths of fish per trawl were not significantly different ($p>0.05$) by paired t-tests for the night, day, and twilight catches.

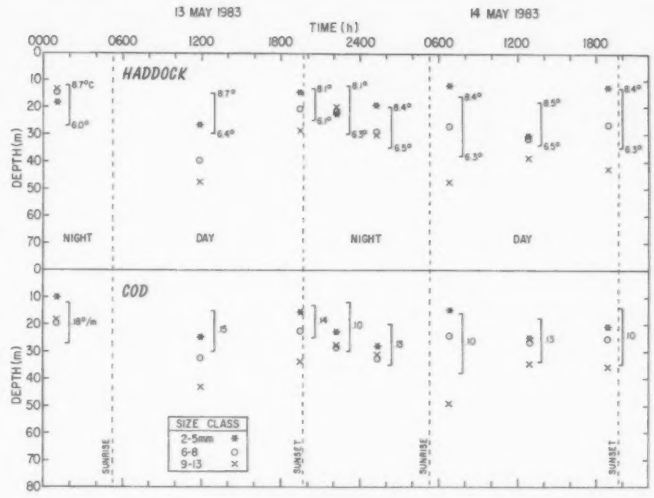

Figure 11

Time-series of weighted-mean depths of **(A)** larval haddock *Melanogrammus aeglefinus* and **(B)** cod *Gadus morhua* size-classes on weakly-stratified Site 83-I during the period 13–14 May 1983. In the haddock time-series, boundary temperatures are recorded beside the brackets; for cod, the rate of temperature change ($\delta T/\delta Z$) over the thermocline region is specified.

Sampler retention and avoidance

The 1 m² MOCNESS sampled effectively on a horizontal scale of 0.2–0.3 km; the 10 m² MOCNESS, 1–2 km; and the bottom trawl, 3–4 km. Minimum length of fish fully retained and not extruded by the various nets was estimated using a model based on the stretch mesh size and a body height-to-length regression (Potter et al. 1990). These estimates indicated that almost all haddock and cod larvae >~4 mmSL are retained by the 1 m² MOCNESS 0.333 mm mesh nets. For the 10 m² MOCNESS, 3.0 mm mesh nets, haddock <17 mm and cod <15–16 mm probably are not fully retained. Minimum size retention of juvenile fish collected by the research bottom trawl is 31–37 mm.

The 1 m² MOCNESS night-day abundance ratios (n/10 m²) are shown in Table 8, page 307 for size-classes of cod and haddock collected in April and May 1981 and May 1983. The total night-day ratios for cod are ~1.2 for the 2–5 mm and 6–8 mm size-classes, near 2.0 for the 9–13 mm size-class, and to ~4.0–6.0 for the 14–19 mm and 20–29 mm size-classes (Fig. 19). An exponential curve fit appears to adequately describe the increase of night-to-day catch ratios with increasing size of fish. Cod appear to visually avoid the 1 m² MOCNESS net by day at all lengths, especially after reaching 9–13 mm. Day abundances of haddock are greater than night for the 6–8 mm and 9–13 mm size-classes, which may indicate a different avoidance behavior at this size.

The 10 m² MOCNESS night-day abundance ratios (n/1000 m²) are shown in Table 9 for size-classes of cod and haddock from study sites in June 1984, 1986, and July 1985. A greater size-range of cod is available than for haddock. For cod, the smallest (9–3 mm) and the largest (50–59 mm) size-classes are not fully vulnerable to the net, due to extrusion of the smallest larvae through the net mesh and distribution of the largest juveniles below the sampling depth. The total night-day ratios for cod are ~2–3 (range 1.49–3.05) for size-classes 14–19 mm through 40–49 mm. Haddock juveniles have night-day ratios of ~3–4 for the 14–19 mm and 20–29 mm size-classes.

Discussion

The difficulty of detecting vertical migration in planktonic organisms, given the high sampling variability and limited resources for replicate time-series of observations as well as gear limitations, has been discussed by Pearre (1979), Shulenberger (1978), Denman & Platt (1978), and others. We are forced to look for repeatable patterns, often in the absence of statistical proof. Because of these difficulties, diverse observations have been reported in the literature. In this study, the vertical distribution patterns and diel migrations of haddock and cod larvae and juveniles have been documented in stratified and well-mixed waters of Georges Bank in greater detail than previously seen because of electronic MOCNESS samplers and the use of submersibles.

Sampler avoidance

Many investigators have reported night-day catch ratios >1. Net avoidance usually is greater for day than night tows because of visual detection of the net (Morse 1989). In another Georges Bank study using the 10 m² MOCNESS, Potter et al. (1990) reported night catches of pelagic cod juveniles averaging 30 mm to be signifi-

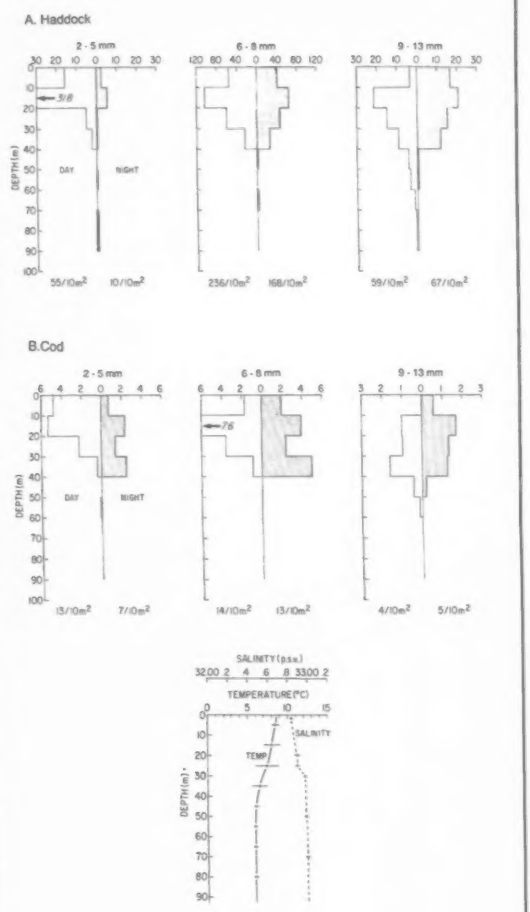

Figure 12

Mean day and night vertical distribution ($\bar{x}$ n/100 m³) of **(A)** haddock *Melanogrammus aeglefinus* and **(B)** cod *Gadus morhua* size-classes of larvae collected by the 1 m² MOCNESS on weakly-stratified Site 83-II during 15–16 May 1983. Estimated water column abundances (n/10 m²) are included at bottom of plots. Temperature and salinity profiles are plotted as depth stratum means (●) and 95% confidence limits (— —).

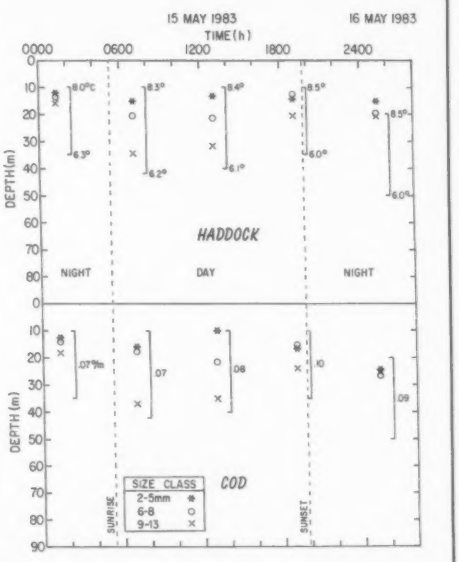

Figure 13

Time-series of abundance weighted-mean depths of larval haddock *Melanogrammus aeglefinus* and cod *Gadus morhua* size-classes on weakly-stratified Site 83-II during the period 15–16 May 1983. In the haddock time-series, boundary temperatures are recorded beside the brackets; for cod, the rate of temperature change (dt/dz) over the thermocline region is specified.

cantly greater than day catches. Their average night-day catch ratio for 16–45 mm cod was 3.0 (range 1.6–4.7), which is similar to the ratios estimated in this study of cod and haddock pelagic juveniles.

In an extensive study of the northeast U.S. continental shelf ichthyoplankton (an 8 yr time-series of data using a 61 cm diameter bongo net, standard MARMAP double-oblique tows), Morse (1989) found larval haddock to be the exception among most taxa in that day catches exceeded night catches for all lengths of larvae in the range 4–15 mm. Day catches were somewhat greater than night catches for 4–12 mm cod, but for the larger fish (13–20 mm) night catches were equal to or greater than day catches.

Haddock larvae, as well as cod, may remain still during the day to evade predator detection by visual or mechano-reception (Zaret 1980). When both haddock and cod reach a larger size and their sensory systems become more developed, they exhibit a startle response and evade the attacking predator (in this case a net) (Blaxter & Fuiman 1990). Flexion and fin ray development is complete for both species at 15–20 mm (Auditore et al. 1993) and they would be more capable of a powerful darting speed. Perhaps at night without visual stimuli, only the larger juveniles exhibit a startle response to the net-mouth pressure stimulus. Light-aided avoidance is expected to decrease with water depth as a function of light attenuation and the fishes' visual threshold (Blaxter & Fuiman 1990). Pressure

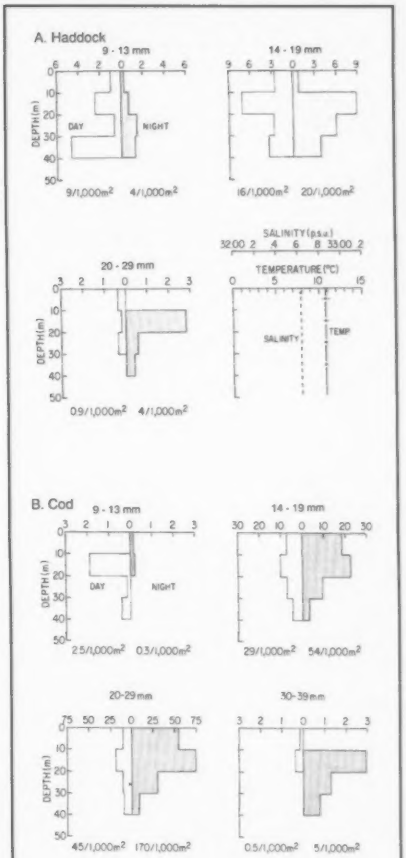

Figure 14

Mean day and night vertical distribution ($\bar{x}$ n/10,000 m³) of **(A)** haddock *Melanogrammus aeglefinus* and **(B)** cod *Gadus morhua* size-classes of pelagic juveniles collected by the 10 m² MOCNESS on well-mixed Site 84-I during 17–19 June 1984. Estimated water column abundances (n/1000 m²) are included at bottom of plots. Temperature and salinity profiles are plotted as depth stratum means (●) and 95% confidence limits (— —).

or sound avoidance are expected to be the same over depth, however.

Therefore, for the three smallest size-classes of haddock and cod <13 mm, light-aided avoidance of the 1 m² MOCNESS sampler may be relatively small (< factor of 2) as a contributing factor in observed day-night vertical distribution patterns. However, in fish >14 mm, night-day catch ratios are expected to increase to >3 because of light-aided avoidance response. Haddock larvae appear to respond differently to light than cod in their avoidance behavior. A correction factor for cod was not applied from the water-column total abundance ratios. The night-day catch ratios are not suitable for correcting depth strata densities, since net avoidance may be a function of light level which decreases with depth. That is, avoidance may be depth-dependent. We do not have the data suitable for making an appropriate depth correction. Applying a constant correction factor to all depth levels of a given size-class would not change the vertical distribution pattern. We need to know the fishes' reaction distance to the net at the different depth light levels.

During the fishes' transition from a pelagic to demersal life at ~30–40 mm, they are not fully vulnerable to either pelagic or demersal sampling gear and this contributes to the sampling variability. Scott (1984) studied diel variations in juvenile haddock catch rates from a 24 h bottom-trawl experiment near Sable Island on the Scotian Shelf in July–August. Haddock >6 cm had a marked vertical migration pattern, moving off the bottom at night and returning by daylight. Based on changes in mean lengths, larger fish moved off the bottom in greater proportions than smaller fish. Colton (1965) examined data from bottom-trawl surveys conducted on Georges Bank and found catch-per-tow of 0-group and 1+ yr haddock to be markedly higher during the night than day. He believed the night-day variability was due to escapement from the net during the day and not to avoidance. Lough et al. (1989) conducted submersible studies on eastern Georges Bank in July 1987 and August 1986 and found recently-settled juvenile gadids (mostly cod) 4–12 cm in length close to the bottom (<0.5 m) during the day and a portion of the population rising 1–5 m off the bottom at sunset, drifting with the current. A comparison of standardized research bottom-trawl (with rollers) catches and submersible transect counts showed the extent of undersampling by the bottom trawl. For 4 cm modal-size cod (1987), daylight trawl abundance estimates were at least an order of magnitude lower than the submersible transects, but not significantly different than the night estimates. For demersally-oriented larger fish (7 cm modal length), few fish were caught by daylight trawls, and night trawl catches were still at least an order of magnitude lower than night submersible counts. The larger fish appeared to stay closer to the bottom both day and night, and consequently they are less vulnerable to the bottom trawl with roller gear which may pass over them. Some preliminary results by Cohen et al. (1985) showed that more cod juveniles of 4–5 cm were caught using the bottom trawl with the smaller rubber disc-covered chain sweep than with the larger roller gear. Thus, the bottom trawl catches of recently-settled cod are known to have a significant sampling bias with more cod collected in night trawls than day, and especially for the larger fish escaping the roller gear.

Vertical distribution patterns

The initial depth distribution of recently-hatched larvae is dependent upon the late-stage egg distribution. Some limited egg profile data

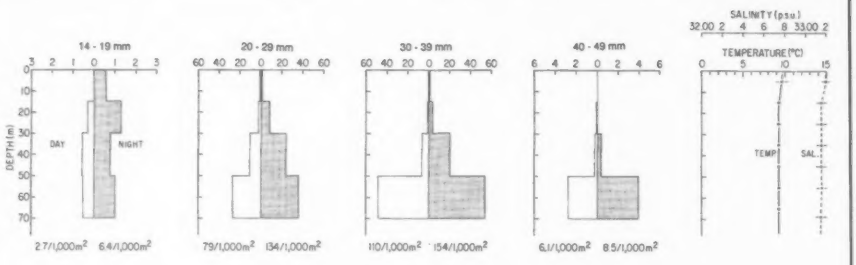

Figure 15

Mean day and night vertical distribution ($\bar{x}$ n/10,000 m³) of cod *Gadus morhua* size-classes of pelagic juveniles collected by the 10 m² MOCNESS on well-mixed Site 86-I during 18–22 June 1986. Water column abundances (n/1000 m²) are included at bottom of figure. Temperature and salinity profiles are plotted as depth stratum means (●) and 95% confidence limits (— —).

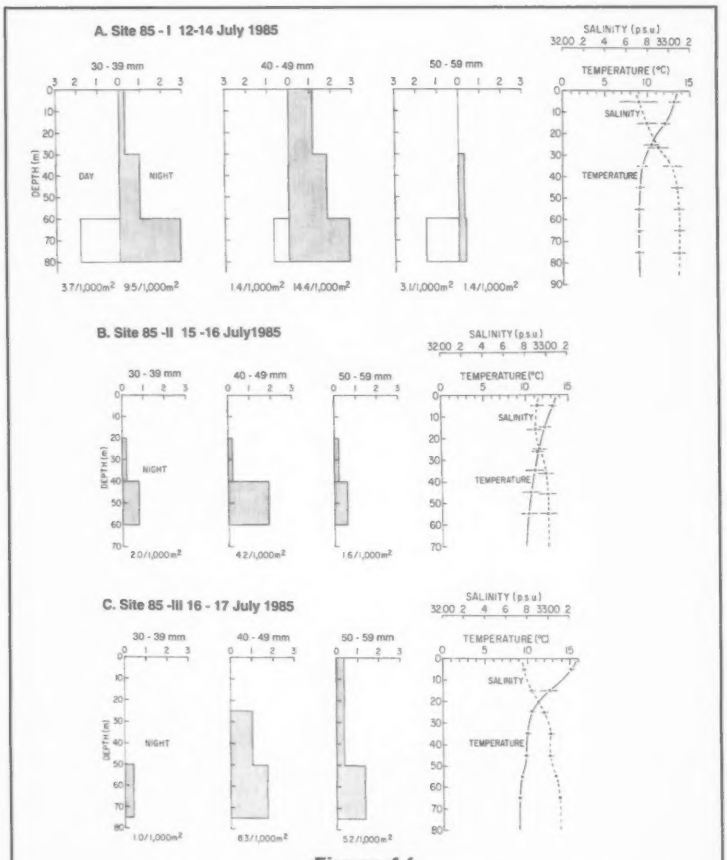

Figure 16

Mean day and night vertical distributions ($\bar{x}$ n/10,000 m³) of cod *Gadus morhua* size-classes of pelagic juveniles collected by the 10 m² MOCNESS on three study sites: **(A)** Site 85-I, stratified, 12–14 July 1985; **(B)** Site 85-II, weakly stratified 15–16 July 1985; **(C)** Site 85-III, stratified, 16–17 July 1985. Estimated water column abundances (n/1000 m²) are included at bottom of plots. Temperature and salinity profiles are plotted as depth stratum means (●) and 95% confidence limits (— —).

was reported by Walford (1938), Colton (1965), and Lough (1984) for haddock on Georges Bank. Their results and other regional studies are reviewed by Frank et al. (1989) and Page et al. (1989) in depth distribution studies of haddock eggs on the Southwestern Scotian Shelf. Because haddock eggs increase their specific gravity with age, newly-hatched larvae were generally found at intermediate depths. Furthermore, these studies found the degree of aggregation for late stage-IV eggs was significantly related to the intensity of stratification.

In the present study, in well-mixed waters during early spring, larval haddock and cod were distributed throughout the water column in the same general pattern as the eggs (Lough 1984), with a mode in abundance at mid-depth, 30–40 m. By mid-May, when the surface water is stratified, larvae resided within the thermocline region; the stronger the stratification, the more closely the abundance centers were confined to the thermocline, especially for the smallest larvae. The larval-thermocline coupling is a dynamic process that is frequently perturbed by strong winds and storms but becomes reestablished with a new thermocline. Even under stratified conditions, larger larvae (>9 mm) tend to be found at greater depths during the day. Day-night shifts in their distribution patterns indicate that diel

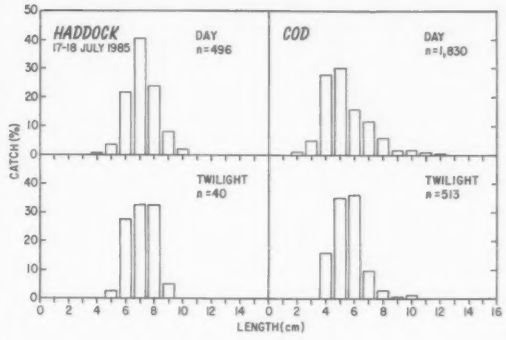

Figure 17

Day and twilight length-frequency distribution of haddock *Melanogrammus aeglefinus* and cod *Gadus morhua* juveniles collected by Yankee 36 bottom trawl on Site 85-IV during a 24 h study, 17–18 July 1985. No fish were caught in night trawls.

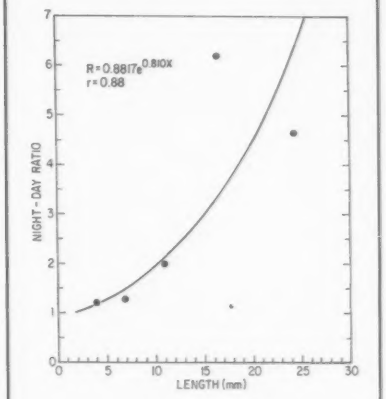

Figure 19

Night-to-day catch ratios for cod, *Gadus morhua*, in tows with 1 m² MOCNESS during April and May 1981 and May 1983. An exponential curve is fitted to the ratios.

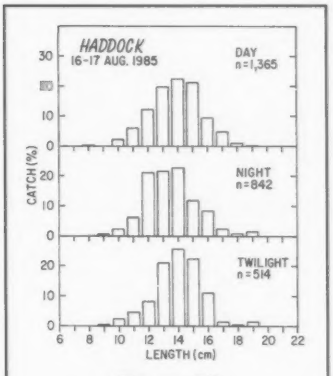

Figure 18

Day, night, and twilight length-frequency distribution of haddock *Melanogrammus aeglefinus* juveniles collected by Yankee 36 bottom trawl on Site 85-V during a 24 h study, 16–17 August 1985.

migrations are fairly well established when larvae reach 9–13 mm length and may be initiated at a smaller size, 6–8 mm, depending on the physical structure of the water column. This pattern of residing deeper by day and shoaler at night continues into the older pelagic juvenile and recently-settled juvenile period.

When larvae reach a length of ~9 mm, the swim bladder may be functionally important in the vertical migration of larvae in both species (Schwartz 1971, Ellertsen et al. 1980, Howell 1984). Haddock and cod have similar developmental patterns; however, there are some important differences (Auditore et al. 1993). At 8–9 mm, haddock have larger and more developed pectoral and pelvic fins than cod. The difference in development is pronounced after 20 mm in length; at 23 mm, the pectoral fins of cod are 1/2 to 3/4 the size of haddock, while the pelvic fins of cod are 1/2 those of haddock. Haddock also possess more total fin rays in the caudal, dorsal, and anal fins than cod. The total number of caudal-fin rays usually determines the overall size of the fin, which is an important means of thrust in gadiform fishes (Cohen 1984). The higher number of caudal- and dorsal-fin rays in haddock, in combination with early paired-fin development, may provide greater maneuverability for haddock. The earlier fin development of haddock larvae compared with cod may allow them to more actively locate high concentrations of prey and stay within these patches. Miller et al. (1963) studied the vertical distribution of larval haddock at three sites on Georges Bank in May 1958. Haddock larvae were found throughout the water column, with maximum concentrations centered at 20–30 m. At all three sites they found periodic changes in the depth distribution of larvae that were related to similar changes in depth of the thermocline. Smaller larvae, 4–8 mm, occurred below the thermocline at each site while >80% of the larger larvae, 9–19 mm, were found in the thermocline. They also found no evidence of diurnal change in the weighted mean depth distribution of larvae, 24 m during the day and 22 m by night. Their observations were in general agreement with those of Frank et al. (1989) for haddock larvae on the Southwestern Scotian Shelf. Frank et al. (1989), using a discrete depth sampler, BIONESS, found recently-hatched haddock larvae in May 1985 and 1986 were concentrated at mid-depth (~30 m) in day and night, and their population centers remained at this level until 20 d post-hatching. The hydrographic conditions were characterized by a density gradient (sigma-*t*) that increased linearly with depth both years. Whereas Miller et al. (1963) and Frank et al. (1989) found had-

dock larvae (<9 mm) below the thermocline, we found both haddock and cod larvae of this size tended to reside mostly within or above the base of the thermocline in May on Georges Bank. Miller et al.'s (1963) ability to discriminate depth changes in larvae was limited because of the small, non-opening/closing samplers (14 cm mouth diameter) that were towed at fixed depth intervals (minimum 9–10 m apart).

Ellertsen et al. (1984) reported on the vertical distribution of cod larvae (4–5 mm) at a strongly-stratified station off the Lofoten Islands, Norway, in May 1982. First-feeding cod larvae were concentrated at 10–20 m depth near the thermocline throughout a 24 h period, but dispersed with the slightest wind mixing. Only under extremely calm conditions were the larvae able to control their vertical distribution and show diurnal migration.

Pelagic juveniles, however, are capable of making extensive migrations through the water column. In our Georges Bank studies, at a well-mixed shoal site in June 1984, pelagic cod juveniles appeared to migrate into the upper half of the water column at night and to remain in the lower water column during the day. Juvenile haddock were much less abundant at this site, and their center of abundance was located at mid-depth with no evidence of day-night migrations like those of cod. The few pelagic cod collected at two stratified sites on eastern Georges Bank in July 1985 were generally found in the lower third of the water column, and few were caught in the thermocline at 15–30 m depth. We have no data on pelagic juvenile haddock at a stratified site for comparison.

Perry & Neilson (1988) studied the vertical distribution of cod and haddock pelagic juveniles in June 1985 on eastern Georges Bank and found a diel migration pattern for both species at a well-mixed shoal site (66 m). At a nearby stratified site in deeper water (80 m), Perry & Neilson (1988) found that juvenile haddock generally remained above 40 m depth with their weighted-mean depth in the thermocline at 20–30 m. In contrast, cod juveniles generally remained deeper than 40 m, below the thermocline, yet still exhibited diel migrations.

Colton (1965) investigated vertical distribution of juvenile haddock using an Isaacs-Kidd midwater trawl in late summer of 1957–58. Over 75% of the pelagic haddock of 27–124 mm occurred between 10 and 40 m depth, with greatest abundance at 20 m at the depth of the thermocline. There was some diel variation in distribution: the weighted-mean abundance was located at 40 m during the day and 30 m at night.

Results from our studies indicate that juvenile haddock and cod change from a pelagic to a demersal existence at a body length of 4–10 cm, and once they reach a demersal stage they stay close to bottom by day and move off bottom into the water column at night. During the transition period the vertical amplitude of these night excursions decreases with size of fish. The data suggest that cod <6 cm make more extensive off-bottom migrations at night than haddock, with some individuals ranging up to the surface. Haddock appear to assume a more complete demersal life at a smaller size (4–6 cm) than cod, which is consistent with older juvenile and adult behavior. Bailey (1975) found that 6.5–13 cm haddock migrated through the water column at night, whereas larger fish were more confined to the seabed in the northern North Sea during August. Beamish (1966) and Woodhead (1966) reported that adult haddock tend to remain associated with the seabed at night, whereas adult cod make extensive vertical migrations. In contrast, Bailey (1975) concluded that cod juveniles remained on or close to the seabed day and night, because fish caught in midwater were never >7 cm, while those on the seabed ranged up to 13 cm.

Juvenile cod and haddock at ~70–90 mm begin feeding on benthic prey such as polychaetes and crustaceans along with planktonic prey, which is consistent with changes in their mouth (Auditore et al. 1993). The time for juvenile cod and haddock to grow from 40 mm to 70 mm is ~30 d, and from 40 to 90 mm is ~48 d (Bolz & Lough 1988). Therefore, in terms of defining the functional transition period for an individual fish, we consider the transition from a wholly pelagic to demersal existence to take ~1–1.5 mo on average.

Other factors influencing vertical distributions

Neilson & Perry (1990) did a recent review of the literature on diel vertical migrations of marine fishes and concluded that the diversity of vertical migration patterns indicated a facultative process significantly influenced by multiple environmental factors. Prey distributions probably play an important role in the vertical distributions of larvae. Based on Georges Bank data (Buckley & Lough 1987) and simulation models (Laurence 1985), haddock larvae are considerably more food-limited than cod. Stable stratified conditions in the spring, which result in the availability of high concentrations of zooplankton prey, favor growth and survival of haddock larvae. Lough (1984) and Buckley & Lough (1987) found that haddock and cod larvae <~13 mm (mode at 7 mm) were generally associated with the planktonic prey biomass that had a maxima in the thermocline during May 1981 and 1983 along the southern margin of Georges Bank. The stronger the water column stratification, the more closely larvae and prey coincided. At the well-mixed sites where larvae were broadly distributed, prey biomass was

lower and more uniformly distributed through the water column.

Frank & McRuer (1989) also found the condition of haddock larvae off Southwestern Nova Scotia in May 1986 consistent with the well-mixed/stratified regime findings of Buckley & Lough (1987). Larvae were in good condition at the deeper stratified sites and in poor condition at the shallow, well-mixed sites. They also found evidence that the buoyancy of starved larvae (4–7 mm) increased, which frequently resulted in a bimodal depth profile, with larvae in poorer condition nearer the surface. Ellertsen et al.'s (1984) study in the Vesteralsfjord of Norway showed that under calm conditions larval cod appeared to concentrate in the surface layers during the night coinciding with the highest density of copepod nauplii, their preferred prey in the study. They also noted that turbulent mixing dispersed the larvae and prey evenly throughout the water column. Therefore, the vertical distribution of larvae and their prey needs to be evaluated in relation to larval buoyancy and water-column turbulence.

Light plays an important role in the diel migrations of cod and haddock larvae, but it is not known whether larvae follow a specific isolume. There may be a critical light intensity at which visual feeding ceases and vertical migration begins. Minimum light-intensity threshold for larval cod feeding was in the range 0.1–0.4 lux, and maximum feeding incidence at 1.4 lux (Ellertsen et al. 1980). Light regime also can affect the swimming activity and buoyancy of yolksac cod larvae by changing their metabolism and utilization of yolk (Solberg & Tilseth 1987).

In Perry & Neilson's (1988) study of pelagic juveniles, the migration pattern of cod appeared to be directly related to the light-dark cycle, whereas that of haddock was more complicated and may have been confounded by periodic changes in the rotary tidal current speed and/or the migratory movements of their preferred mysid prey *Neomysis americana*. Their explanations for the different depth distribution may be related to (1) cod's acclimation to colder waters and haddock's preference for warmer waters, and (2) a possible mechanism for reducing interspecific competition, since their vertical distribution patterns were similar when prey biomass was high and different when prey biomass was low. In our opinion, the differences in vertical distribution between cod and haddock at the stratified site noted by Perry & Neilson (1988) may be attributed to species differences in feeding behavior.

On Georges Bank, planktonic prey selected by both species during settlement at 40–60 mm include copepods, amphipods, euphausiids, and cumaceans (Bowman 1981ab, Koeller et al. 1986, Mahon & Neilson 1987, Lough et al. 1989). Robb (1981) showed that pelagic 0-group gadids in the northern North Sea have a different feeding behavior reflective of the adult lifestyle, i.e., cod fed on larger active pelagic prey, while haddock concentrated on smaller slower-moving or sedentary organisms. Both Robb's (1981) and Perry & Neilson's (1988) feeding results support the view that haddock feed continuously when prey is available.

A complicating factor in understanding vertical distribution patterns in haddock is their commensal association with the large coelenterate *Cyanea* sp. This association has been reported in the literature for fish up to a length of ~10 cm (Colton & Temple 1961, Mansueti 1963, Rees 1966, Bailey 1975, Koeller et al. 1986). Mansueti (1963) stated that jellyfish serve as a source of food and shelter for young fish between the pelagic and demersal stages. The change from a surface to deeper-water habitat by the fish is believed by Mansueti (1963) to be a factor causing the breakup of the commensal relationship. Koeller et al. (1986) showed *Cyanea* sp. to have been most abundant at the surface, decreasing to near zero below 80 m off Nova Scotia in June 1983. Pelagic juvenile haddock, more so than cod, may require contact with some objects such as jellyfish. Whether jellyfish tentacles also serve as a source of food is not known.

The substrate on which the juveniles settle, (i.e., an unsuitable habitat such as sand) may prolong the transition to demersal life. Lough et al. (1989) hypothesized that a large gravel habitat on northeastern Georges Bank favors survival of recently-settled juvenile fish because of predator avoidance through camouflage and/or increased prey abundance. Pelagic juvenile cod were widespread over eastern Georges Bank in June; and in mid-July when they became demersally oriented, they were present on bottom types ranging from sand to gravel. By contrast, in late July to early August, recently-settled juveniles were abundant only on the large gravel deposit on northeastern Georges Bank and were sparse or absent from the large sand and gravelly sand that cover most of eastern Georges Bank (Lough et al. 1989).

To summarize the vertical distribution patterns observed, we developed a generalized day-night mean depth distribution of cod by size-class, from recently-hatched larvae through recently-settled juveniles (Fig. 20). Cod vertical migrations appear to respond primarily to a day-night cycle, whereas haddock migrations respond to other factors such as prey distribution. Depth centers of the smallest larvae (2–8 mm) appear at two levels–15 and 35 m–depending on whether the water column is stratified or well-mixed (Fig. 20). In order for the water column to be considered sufficiently stratified for larvae to initially reside at 15 m, a change of >0.3 sigma-*t* units would have to occur from surface to the base of a pycnocline. Waters around the flank of Georges Bank are typically

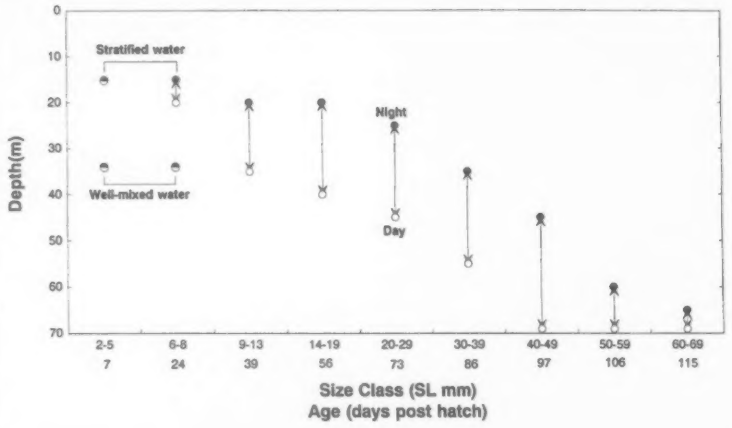

Figure 20

Generalized day-night depth distribution of cod *Gadus morhua* by size-class (mmSL) and age (days post-hatching) from hatched larva through recently-settled juvenile in a 70 m water column. Mean population depth by day (○) and by night (●); vertical range between day and night circles is represented by double arrow. Initial depth centers for the first two size-classes (2–5, 6–8 mm) is largely determined by larval buoyancy and, therefore, whether the water column is well-mixed or stratified.

well-mixed in winter, with a seasonal thermocline developing by mid-May subject to perturbations. When larvae reach a length of 9–13 mm, they appear to make day-night migrations regardless of the water-column structure. There is some uncertainty in the day-night migration range of the pelagic juveniles; however, the 20 m range designated is within their swimming capability at this size. Furthermore, we don't know precisely the transition period from a day to night depth. It probably occurs over a 3–4 h period, but it could be shorter. For example, a 10 mm fish swimming at 1 body length/s could transverse 20 m in 1 h. The vertical distribution pattern presented is sufficiently general to be used as a starting point for both cod and haddock at any bottom depth, even though all situations can be interpreted from the data. These studies highlight the need for investigations of behavior-related sampler avoidance and further time-series of observation on fish distributions in different environmental conditions.

Citations

Auditore, P. J., R. G. Lough, & E. A. Broughton
1993 A review of the comparative development of Atlantic cod and haddock based on an illustrated series of larvae and juveniles from Georges Bank. NAFO Sci. Counc. Stud. (In press).

Azarovitz, T. R.
1981 A brief historical review of the Woods Hole laboratory trawl survey time series. *In* Doubleday, W.G., & D. Rivard (eds.), Bottom trawl surveys. Spec. Publ. Fish. Aquat. Sci. 58:62–67.

Bailey, R. S
1975 Observations on diel behaviour patterns of North Sea gadoids in the pelagic phase. J. Mar. Biol. Assoc. U.K. 55:133–142.

Beamish, F. W. H.
1966 Vertical migration by demersal fish in the Northwest Atlantic. J. Fish. Res. Board Can. 23:109–139.

Blaxter, J. H. S., & L. A. Fuiman
1990 The role of the sensory systems of herring larvae in evading predatory fishes. J. Mar. Biol. Assoc. U.K. 70:413– 427.

Bolz, G. R., & R. G. Lough
1983 Growth of larval Atlantic cod, *Gadus morhua*, and haddock, *Melanogrammus aeglefinus*, on Georges Bank, spring 1981. Fish. Bull., U.S. 81:827–836.
1988 Growth through the first six months of Atlantic cod, *Gadus morhua*, and haddock, *Melanogrammus aeglefinus*, based on daily otolith increments. Fish. Bull., U.S. 86:223–235.

Bowman, R. E.
1981a Food and feeding of 0-group haddock in the Northwest Atlantic. Rapp. P.-V. Reun. Cons. Perm. Int. Explor. Mer 178:322–323.
1981b Food of 10 species of northwest Atlantic juvenile groundfish. Fish. Bull., U.S. 79:200–206.

Buckley, L. J., & R. G. Lough
1987 Recent growth, biochemical composition, and prey field of larval haddock (*Melanogrammus aeglefinus*) and Atlantic cod (*Gadus morhua*) on Georges Bank. Can. J. Fish. Aquat. Sci. 44:14–25.

Cohen, D. M.
1984 Gadidae: Development and relationships. *In* Moser, H.G., et al. (eds.), Ontogeny and systematics of fishes, p. 259–265. Spec. Pub. 1, Am. Soc. Ichthyol. Herpetol. Allen Press, Lawrence KS.

Cohen, E. B., J. R. Green, D. C. Potter, & B. P. Hayden
1985 Some preliminary results of juvenile cod and haddock studies on Georges Bank in 1984 and 1985. Int. Counc. Explor. Sea Comm. Meet. G74:23.

Cohen, E. B., M. P. Sissenwine, & G. C. Laurence
1988 The "recruitment problem" for marine fish populations with emphasis on Georges Bank. *In* Rothschild, B.J. (ed.), Towards a theory on biological-physical interactions in the world ocean, p. 373–392. Kluwer Acad. Publ., Dordrecht.

Colton, J. B. Jr.
1965 The distribution and behavior of pelagic and early demersal stages of haddock in relation to sampling techniques. Int. Comm. Northwest Atl. Fish. Spec. Publ. 6:318–333.

Colton, J. B. Jr., & R. F. Temple
1961 The enigma of Georges Bank spawning. Limnol. Oceanogr. 6:280–291.

Denman, K., & T. Platt
1978 Time series analysis in marine ecosystems. *In* Shugart, H.H. Jr. (ed.), Time series and ecological processes, p. 227–242. SIAM (Soc. Ind. Appl. Math) — SIMS (Siam Inst. Math. Soc.) Conf. Ser., Philadelphia.

Dunn, O. J., & V. A. Clark
1974 Applied statistics: Analysis of variance and regression. John Wiley, NY.

Ellertsen, B., P. Solemdal, T. Stromme, S. Tilseth, & T. Westgard
1980 Some biological aspects of cod larvae. Fiskeridir. Dir. Skr. Ser. Havunders. 17:29–47.

Ellertsen, B., P. Fossum, P. Solemdal, S. Sundby, & S. Tilseth
1984 A case study of the distribution of cod larvae and availability of prey organisms in relation to physical processes in Lofoten. *In* Dahl, E., et al. (eds.), The propagation of cod *Gadus morhua* L., p. 453–477. Flodevigen rapp. 1.

Fahay, M. P.
1983 Guide to the early stages of marine fishes occurring in the western North Atlantic Ocean, Cape Hatteras to the southern Scotian Shelf. J. Northwest Atl. Fish. Sci. 4:1–423.

Flagg, C. N.
1987 Hydrographic structure and variability. *In* Backus, R.H. (ed.), Georges Bank, p.108–124. The MIT Press, Cambridge.

Frank, K. T., & J. K. McRuer
1989 Nutritional status of field-collected haddock (*Melanogrammus aeglefinus*) larvae from Southwestern Nova Scotia: an assessment based on morphometric and vertical distribution data. Can. J. Fish. Aquat. Sci. 46(Suppl. 1): 125–133).

Frank, K. T., F. H. Page, & J. K. McRuer
1989 Hydrographic effects on the vertical distribution of haddock (*Melanogrammus aeglefinus*) eggs and larvae on the Southwestern Scotian Shelf. Can. J. Fish. Aquat. Aci. 46(Suppl. 1):82–92.

Howell, B. R.
1984 The intensive rearing of juvenile cod, *Gadus morhua* L. *In* Dahl, E., et al. (eds.), The propagation of cod *Gadus morhua* L., p. 657–675. Flodevigen rapp. 1.

Koeller, P. A., P. C. F. Hurley, P. Perley, & J. D. Neilson
1986 Juvenile fish surveys on the Scotian Shelf: implications for year-class assessments. J. Cons. Int. Explor. Mer 43:59–76.

Laurence, G. C.
1985 A report on the development of stochastic models of food limited growth and survival of cod and haddock larvae. *In* Laurence, G.C., & R.G. Lough (eds.), Growth and survival of larval fishes in relation to the trophodynamics of Georges Bank cod and haddock, p. 83–150. NOAA Tech. Memo. NMFS-F/NEC-36, Woods Hole MA.

Laurence, G. C., & R. G. Lough
1985 Growth and survival of larval fishes in relation to the trophodynamics of Georges Bank cod and haddock. NOAA Tech. Memo. NMFS-F/NEC-36, Woods Hole MA.

Lough, R. G.
1984 Larval fish trophodynamic studies on Georges Bank: sampling strategy and initial results. *In* Dahl, E., et al. (eds.), The propagation of cod *Gadus morhua* L., p. 395–434. Flodevigen rapp. 1.

Lough, R. G., & G. R. Bolz
1989 The movement of cod and haddock larvae onto the shoals of Georges Bank. J. Fish. Biol. 35:71–79.

Lough, R. G., & D. C. Potter
1983 Rapid shipboard identification and enumeration of zooplankton samples. J. Plankton Res. 5:775–782.

Lough, R. G., P. C. Valentine, D. C. Potter, P. J. Auditore, G. R. Bolz, J.D. Neilson, & R. I. Perry
1989 Ecology and distribution of juvenile cod and haddock in relation to sediment type and bottom currents on eastern Georges Bank. Mar. Ecol. Prog. Ser. 56:1–12.

Mahon, R., & J. D. Neilson
1987 Diet changes in Scotian Shelf haddock during pelagic and demersal phases of the first year of life. Mar. Ecol. Prog. Ser. 37:123–130.

Mansueti, R.
1963 Symbiotic behaviour between small fishes and jelly fishes, with new data on that between the Stromateid *Peprilus alepidotus*, and the Scyphomedusa, *Chrysaora quinquecirrtia*. Copeia 1963:40–80.

Miller, D., J. B. Colton Jr., & R. R. Marak
1963 A study of the vertical distribution of larval haddock. J. Cons. Int. Explor. Mer 28:37–49.

Morse, W. W.
1989 Catchability, growth, and mortality of larval fishes. Fish. Bull., U.S. 87:417–446.

Murawski, S. A., A. M. Lange, M. P. Sissenwine, & R. K. Mayo
1983 Definition and analysis of multispecies otter-trawl fisheries off the northeast coast of the United States. J. Cons. Int. Explor. Mer 41:13–27.

Neilson, J. D., & R. I. Perry
1990 Diel vertical migrations of marine fishes: an obligate or facultative process? Adv. Mar. Biol. 26:115–168.

O'Boyle, R. N., M. Sinclair, R. J. Conover, K. H. Mann, & A. C. Kohler
1984 Temporal and spatial distributions of ichthyoplankton communities of the Scotian Shelf in relation to biological, hydrological, and physiographic features. Rapp. P.-V. Reun. Cons. Perm. Int. Explor. Mer 183:27–40.

Overholtz, W. J., & A. V. Tyler
1985 Long-term responses of the demersal fish assemblages of Georges Bank. Fish. Bull., U.S. 83:507–520.

Page, F. H., K. T. Frank, & K. R. Thompson
1989 Stage dependent vertical distribution of haddock (*Melanogrammus aeglefinus*) eggs in a stratified water column: observations and model. Can. J. Fish. Aquat. Sci. 46(Suppl. 1):55–67.

Pearre, S. Jr.
1979 Problems of detection and interpretation of vertical migration. J. Plankton Res. 1:29–44.

Perry, R. I., & J. D. Neilson
1988 Vertical distributions and trophic interactions of age-0 Atlantic cod and haddock in mixed and stratified waters of Georges Bank. Mar. Ecol. Prog. Ser. 49:199–214.

Potter, D. C., R. G. Lough, R. I. Perry, & J. D. Neilson
1990 Comparison of the MOCNESS and IYGPT pelagic samplers for the capture of 0-group cod (*Gadus morhua*) on Georges Bank. J. Cons. Int. Explor. Mer 46:121–128.

Rees, W. J.
1966 *Cyanea lamarcki* Peron & Lesuer (Scyphozoa) and its association with young *Gadus merlangus* L. (Pisces). Ann. Mag. Nat. Hist. 9:285–287.

Robb, A. P.
1981 Observations on the food and diel feeding behaviour of pelagic 0-group gadoids in the northern North Sea. J. Fish. Biol. 18:183–194.

Schwartz, A.
1971 Swimbladder development and function in the haddock, *Melanogrammus aeglefinus* L. Biol. Bull. (Woods Hole) 141:176–188.

Scott, J. S.
1984 Short-term changes in distribution, size and availability of juvenile haddock around Sable Island off Nova Scotia. J. Northwest Atl. Fish. Sci. 5:109–112.

Sherman, K., W. Smith, W. Morse, M. Berman, J. Green, & L. Ejsymont
1984 Spawning strategies of fishes in relation to circulation, phytoplankton production, and pulses in zooplankton off the northeast United States. Mar. Ecol. Prog. Ser. 18:1–19.

Shulenberger, E.
1978 Vertical distributions, diurnal migrations, and sampling problems of hyperiid amphipods in the North Pacific central gyre. Deep-Sea Res. 25:605–623.

Sissenwine, M. P.
1984 Why do fish populations vary? *In* May, R. (ed.), Exploitation of marine communities, p. 59–94. Springer-Verlag, NY.

Smith, W. G., & W. W. Morse
1985 Retention of larval haddock *Melanogrammus aeglefinus* in the Georges Bank region, a gyre-influenced spawning area. Mar. Ecol. Prog. Ser. 24:1–13.

Sokal, R. R., & F. J. Rohlf
1969 Biometry. W.H. Freeman, San Francisco, 776 p.

Solberg, T. S., & S. Tilseth
1987 Variations in growth patterns among yolk-sac larvae of cod (*Gadus morhua* L.) due to differences in rearing temperature and light regime. Sarsia 72:347–349.

Walford, L. A.
1938 Effect of currents on distribution and survival of the eggs and larvae of haddock (*Melanogrammus aeglefinus*) on Georges Bank. Fish. Bull., U.S. 49:1–73.

Wiebe, P. H., K. H. Burt, S. H. Boyd, & A. W. Morton
1976 A multiple opening/closing net and environmental sensing system for sampling zooplankton. J. Mar. Res. 34:313–326.

Wiebe, P. H., S. H. Boyd, B. M. David, & J. L. Cox
1982 Avoidance of towed nets by the euphausiid *Nematoscelis megalops*. Fish. Bull., U.S. 80:75–91.

Wiebe, P. H., A. W. Morton, A. M. Bradley, R. H. Backus, J. E. Craddock, V. Barber, T. J. Cowles, & G. R. Flierl
1985 New developments in the MOCNESS, an apparatus for sampling zooplankton and micronekton. Mar. Biol. (Berl.) 87:313–323.

Woodhead, P. M. J.
1966 The behavior of fish in relation to light in the sea. Oceanogr. Mar. Biol. Annu. Rev. 4:337–403.

Zaret, T. M.
1980 The effect of prey motion on planktivore choice. *In* Kerfoot, W.C. (ed.), Evaluation and ecology of zooplankton communities. Limnol. Oceanogr. Spec. Symp. 3:594–603.

Table 1
Cruises, sampling sites, and gear used for vertical distribution study on Georges Bank, 1981–86.

Vessel cruise no.	Sampling dates	Site	Bottom depth (m)	Gear	No. depth strata sampled	Tows		
						Night	Day	Twilight
Albatross IV 81-03	27–29 April 1981	81-I	67–70	1m² MOCNESS	6	5	5	0
Albatross IV 81-05	21–27 May 1981	81-II	75–83	1m² MOCNESS	7–8	4	6	0
		81-III	35–58	1m² MOCNESS	7–8	1	3	0
Albatross IV 83-03	13–17 May 1983	83-I	66–79	1m² MOCNESS	7	3	5	0
		83-II	88–93	1m² MOCNESS	8	2	3	0
		83-III	34–54	1m² MOCNESS	5	1	3	0
Albatross IV 84-05	17–19 June 1984	84-I	40–49	10m² MOCNESS	4	3	3	0
Albatross IV 85-06	12–17 July 1985	85-I	80–87	10m² MOCNESS	2–3	4	3	0
		85-II	64–72	10m² MOCNESS	3	3	3	0
		85-III	78–83	10m² MOCNESS	3	2	0	0
Delaware II 85-05	17–18 July 1985	85-IV	80–90	36 Yankee otter trawl with rubber disks	Bottom	1	6	2
Delaware II 85-06	16–17 Aug. 1985	85-V	63–71	36 Yankee otter trawl with rubber disks	Bottom	4	6	2
Albatross IV 86-03	18–22 June 1986	86-I	65–78	10m² MOCNESS	4	5	6	0
	25–26 June 1986			36 Yankee otter trawl with rollers	Bottom	5	11	1

Table 2

Summary of GLM ANOVA for larval haddock and cod abundance on Georges Bank. *F*-values are denoted by their level of significance.

A. 27–29 April 1981	Site 81-I			
Factor	Haddock[a]	Cod[b]	Cod[c]	Cod[d]
Depth (D)	3.15*	8.84***	6.50	8.52
Time (T)	2.07	16.59	39.37	50.92
Size (S)		24.68	31.10	29.09***
D × T	0.49	2.03	3.53***	5.31***
D × S		0.28	1.26	0.93
T × S		3.66*	2.33*	0.14
D × T × S		0.68	0.71	0.76

***$P<0.001$ [a]2–5 mm size-class
**$P<0.01$ [b]2–5, 6–8, 9–13 mm size-class
*$P<0.05$ [c]2–5, 6–8, 9–13, 14–19, 20–29 mm size-class
[d]6–8, 9–13, 14–19 mm size-class

B. 24–26 May 1981	Site 81-II	
Factor	Haddock[a]	Cod[a]
Depth (D)	6.71	3.76
Time (T)	7.72	9.72
Size (S)	18.17	16.36
D × T	3.52**	2.90**
D × S	0.78	0.33
T × S	1.74	0.69
D × T × S	0.20	0.19

***$P<0.01$ [a]2–5 , 6–8, 9–13 mm size-class

C. 13–26 May 1983	Site 83-I		Site 83-II	
Factor	Haddock[a]	Cod[a]	Haddock[a]	Cod[a]
Depth (D)	4.74	8.17	31.97***	23.84
Time (T)	0.35	0.40	12.11***	0.23
Size (S)	39.67	46.52	15.24***	1.77
D × T	3.13**	0.99	0.86	0.09
D × S	1.25	1.13	1.59	2.29**
T × S	5.33**	0.32	0.13	0.46
D × T × S	1.49	2.31**	1.00	0.93

***$P<0.001$ [a]2–5 , 6–8, 9–13 mm size-class
**$P<0.01$

Table 3

Average percentage distribution of haddock and cod larvae in relation to the thermocline at Sites 83-I and 83-II on Georges Bank May 1983. Angular transformation was used on the percentage data: angle = arcsin $\sqrt{\text{proportion}}$. Values are presented as the angular mean ± its standard error followed by a reconverted percentage mean in parentheses.

	Larval size-class					
	2–5 mm		6–8 mm		9–13 mm	
Angle ± SE (%)	Day	Night	Day	Night	Day	Night
A. Site 83-I 13–14 May 1983						
Haddock						
Above thermocline	43.0 ± 12.2 (46.6)	40.7 ± 8.1 (42.6)	22.6 ± 6.4 (14.8)	27.4 ± 9.5 (21.1)	9.9 ± 4.6 (2.9)	25.2 ± 9.5 (18.1)
Within thermocline	32.0 ± 9.3 (28.1)	39.4 ± 4.5 (40.4)	39.5 ± 5.4 (40.5)	49.7 ± 6.2 (58.1)	29.9 ± 4.0 (24.9)	53.4 ± 4.2 (64.4)
Below thermocline	21.7 ± 5.5 (13.6)	22.8 ± 5.8 (15.0)	39.4 ± 6.1 (40.3)	24.9 ± 2.5 (17.7)	56.9 ± 4.8 (70.2)	21.0 ± 5.1 (12.8)
Cod						
Above thermocline	41.0 ± 10.5 (43.0)	29.3 ± 16.9 (23.9)	23.6 ± 6.3 (16.0)	23.5 ± 7.5 (15.9)	6.2 ± 2.8 (1.2)	24.9 ± 2.1 (17.8)
Within thermocline	44.1 ± 14.1 (48.4)	47.5 ± 12.5 (54.4)	45.7 ± 6.9 (51.2)	45.6 ± 4.3 (51.1)	35.8 ± 3.1 (34.3)	46.8 ± 3.4 (53.2)
Below thermocline	18.7 ± 6.4 (10.3)	22.0 ± 3.5 (14.1)	32.6 ± 5.5 (29.1)	39.7 ± 4.8 (40.7)	53.1 ± 3.2 (63.9)	32.0 ± 5.2 (28.1)
B. Site 83-II 15–16 May 1983						
Haddock						
Above thermocline	31.3 ± 2.5 (27.4)	48.0 ± 14.5 (55.1)	23.7 ± 7.3 (16.1)	34.1 ± 9.1 (31.4)	12.1 ± 5.2 (4.4)	31.9 ± 12.3 (27.9)
Within thermocline	58.4 ± 2.4 (72.5)	42.1 ± 14.5 (44.9)	64.8 ± 6.5 (81.9)	55.7 ± 8.9 (68.2)	60.5 ± 2.8 (75.7)	56.0 ± 11.1 (68.7)
Below thermocline	3.5 ± 1.7 (0.1)	1.8 ± 0.0 (0.1)	6.6 ± 1.7 (1.3)	3.1 ± 1.3 (0.3)	21.0 ± 8.0 (12.8)	9.4 ± 2.4 (2.6)
Cod						
Above thermocline	35.6 ± 6.7 (33.9)	33.6 ± 4.7 (30.5)	20.9 ± 1.9 (12.7)	27.2 ± 3.1 (20.9)	1.8 ± 0.0 (0.1)	18.1 ± 16.3 (9.6)
Within thermocline	54.5 ± 6.7 (66.1)	45.0 ± 10.1 (50.0)	69.2 ± 1.9 (87.4)	62.8 ± 3.1 (79.1)	63.6 ± 5.5 (80.3)	72.9 ± 17.1 (91.3)
Below thermocline	8.1 ± 0.0 (0.1)	1.8 ± 0.0 (0.1)	1.8 ± 0.0 (0.1)	1.8 ± 0.0 (0.1)	26.4 ± 5.5 (19.7)	1.8 ± 0.0 (0.1)

Table 4

Summary of GLM ANOVA for juvenile haddock and cod abundance on Georges Bank. *F*-values are denoted by their level of significance.

A. 17–29 June 1984	Site 84-I			
Factor	Haddock[a]	Haddock[b]	Cod[c]	Cod[d]
Depth (D)	1.12	0.59	0.24	0.04
Time (T)	0.48	0.53	0.12	0.06
Size (S)	11.60***		11.46**	0.34
D × T	1.23	0.46	0.34	0.11
D × S	0.37		0.10	0.03
T × S	0.26		0.49	0.02
D × T × S	0.48		0.09	0.03

***$P<0.001$
**$P<0.01$
*$P<0.05$

[a]9–13, 14–19, 20–29 mm size-class
[b]14–19 mm size-class
[c]14–19, 20–29, 30–39 mm size-class
[d]14–19, 20–29 mm size-class

B. 18–22 June 1986	Site 86-I
Factor	Cod[a]
Depth (D)	41.78***
Time (T)	9.98*
Size (S)	4.76*
D × T	0.65
D × S	1.09
T × S	1.91
D × T × S	0.30

***$P<0.001$
**$P<0.01$
*$P<0.05$

[a]20–29, 30–39 mm size-class

Table 5

Number and size of juvenile cod (3–9 cm) collected by time of day in bottom trawls, Site 86-I, 25–26 June 1986, *ALBATROSS IV* 86-03.

	No. trawls	$\bar{x}$ *n*/trawl	SD	CV %	$\bar{x}$ length (cm)	SD	Total no. fish
Night	5	102.8	52.7	51	4.2	0.45	513
Day	11	2.9	1.3	45	4.8	1.48	32
Twilight	1	6.0	—	—	4.4	1.27	6

Table 6

Number and size of juvenile haddock (4–10 cm) and cod (2–12 cm) collected by time of day in bottom trawls, Site 85-IV, 17–18 July 1985, *DELAWARE II* 85-05.

	No. trawls	$\bar{x}$ *n*/trawl	SD	CV %	$\bar{x}$ length (cm)	SD	Total no. fish
Haddock							
Night	1	1.0	—	—	9.0	—	1
Day	6	84.8	64.6	76	7.1	1.1	496
Twilight	2	20.0	9.9	50	7.1	1.0	40
Cod							
Night	1	—	—	—	—	—	—
Day	6	305.0	391.3	128	5.4	1.6	1,830
Twilight	2	256.6	244.0	95	5.5	1.1	513

Table 7

Number and size of juvenile haddock (3–19 cm) collected by time of day in bottom trawls, Site 85-V, 16–17 August 1985, *DELAWARE II* 85-06.

	No. trawls	$\bar{x}$ *n*/trawl	SD	CV %	$\bar{x}$ length (cm)	SD	Total no. fish
Night	4	210.5	143.6	68	13.9	1.68	842
Day	6	227.5	114.4	50	13.5	1.76	1,365
Twilight	2	257.0	4.2	2	14.0	1.68	514

Table 8

Night/day abundance ratios (n/10 m^2) for cod and haddock by length size-classes using the 1 m^2 MOCNESS, April and May 1981 and May 1983.

Size-class (mm)	April 1981 Site 81-I	May 1981 Site 81-II	May 1983 Site 83-I	May 1983 Site 83-II	Total	Ratio
Cod						
2–5	37/28	16/7	7.4/7.5	7/13	67.4/55.5	1.21
6–8	30/14	58/35	37/47	13/14	138/110	1.26
9–13	213/98	7/8	16/12	5/4	241/122	1.98
14–19	62/10				62/10	6.20
20–29	14/3				14/3	4.67
Haddock						
2–5	108/66	250/143	93/43	10/55	461/307	1.50
6–8	0.6/1.8	483/473	354/468	168/236	1006/1179	0.85
9–13		66/119	123/189	67/59	256/367	0.70

Table 9

Night/day abundance ratios (n/1000 m^2) for cod and haddock by length size-classes using the 10 m^2 MOCNESS, June 1984, June 1986, and July 1985.

Size-class (mm)	June 1984 Site 84-I	June 1986 Site 86-I	July 1985 Site 85-I	Total	Ratio
Cod					
9–13	0.3/2.5			0.3/2.5	0.12
14–19	54/29	6.4/2.7		60.4/31.7	1.91
20–29	170/45	134/79		304/124	2.45
30–39	5/0.5	154/110	9.5/3.7	168.5/113.5	1.49
40–49		8.5/6.12	14.4/1.4	22.9/7.5	3.05
50–59			1.4/3.1	1.4/3.1	0.45
Haddock					
9–13	4/9			4/9	0.44
14–19	20/16			20/16	3.33
20–29	4/0.9			4/0.9	4.44

Habitat-specific density of adult yelloweye rockfish *Sebastes ruberrimus* in the eastern Gulf of Alaska*

Victoria M. O'Connell
Alaska Department of Fish and Game, 304 Lake Street, Room 103
Sitka, Alaska 99835

David W. Carlile
Alaska Department of Fish and Game, 802 3rd Street, Box 240020
Douglas, Alaska 99824-0020

Abstract.—Line transects run from a manned submersible were used to estimate the current density of yelloweye rockfish in two areas of the eastern Gulf of Alaska. Yelloweye rockfish were seen in cobble, continuous rock, broken rock, and boulder habitats but were most abundant in broken rock and boulder habitats. The presence of refuge spaces appears to be an important factor affecting occurrence of yelloweye rockfish. Boulder areas in deep water (>108 m) were the most densely-populated habitat, with an estimated density of 9135 adult yelloweye/km^2. Overall density by area and year ranged from 1954 to 2217 adult yelloweye rockfish/km^2. Habitat-specific density estimates were less precise than general area estimates because of smaller sample sizes. For fisheries management, density estimates may be extrapolated to larger areas based on areal estimation of yelloweye habitat from available bathymetric data.

The yelloweye rockfish *Sebastes ruberrimus* is the target species of the commercial longline fishery for Demersal Shelf Rockfishes (DSR) in the eastern Gulf of Alaska (O'Connell & Fujioka 1991). Rockfishes (*Sebastes* spp.) are managed on an assemblage basis in the Gulf of Alaska under the advice of the North Pacific Fishery Management Council (NPFMC). Demersal Shelf Rockfishes comprise eight species of bottom-dwelling rockfishes inhabiting rocky areas of the continental shelf; yelloweye rockfish account for 96% of the landed catch of targeted DSR.

Traditional stock-assessment methods are difficult to apply to DSR because of a combination of behavioral and physiological factors. The close association of DSR with rugged bottom precludes the use of bottom-trawl surveys used for assessing other groundfish in the Gulf of Alaska. Mark-recapture studies are also ineffective because rockfishes incur high embolism mortality when brought to the surface from depth (O'Connell 1991). Consequently, prior to our research, DSR was one of only two assemblages managed under the Gulf of Alaska Fisheries Management Plan for which no biomass estimates were available.

It has been well documented that rockfish tend to be habitat-specific in their distribution (Love & Ebeling 1978, Larson 1980, Richards 1986, Matthews 1991, Love et al. 1991, Matthews & Richards 1991, Rosenthal et al. 1982). Therefore, to estimate their abundance, we initiated a project designed to take advantage of the preference by DSR for rough, rocky habitat. Our approach was based on the assumption that DSR abundance increases with structural habitat complexity (i.e., increased topographic relief and more interstitial space in and between rocks). Our objective was to estimate density of yelloweye rockfish in the Gulf of Alaska for selected habitat and depth categories. We hope to eventually develop a model predicting the relationship between DSR abundance and habitat complexity and to use this model to indirectly estimate the abundance of DSR. If successful, this approach would allow for expansion of abundance estimates to other areas in the eastern Gulf of Alaska without replicating costly surveys.

Methods

Using the submersible *Delta*, we made 20 dives and covered 47 transects during 17–25 August 1990 in two areas off southeastern Alaska (Fig. 1).

*Contribution PP-058 of the Alaska Department of Fish and Game, Division of Commercial Fisheries, Juneau.

Manuscript accepted 28 January 1993.
Fishery Bulletin, U.S. 91:304-309 (1993).

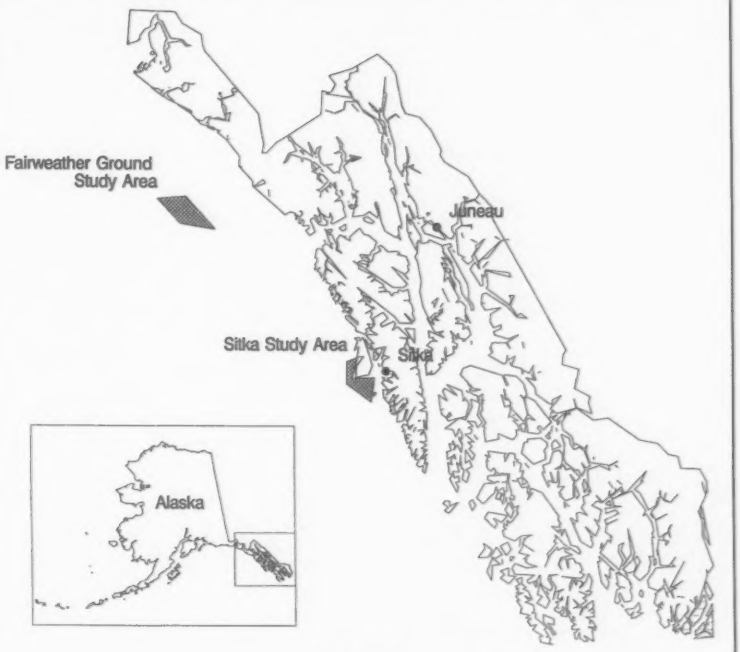

Figure 1

Study sites for submersible survey of yelloweye rockfish, eastern Gulf of Alaska, 1990–1991.

Eleven dives were made on the Fairweather Ground and nine dives were made off Sitka Sound. Eighteen dives and 30 transects were completed off Sitka Sound during 27 May–3 June 1991. One transect was replicated at night to compare day and night effects. Transect locations were chosen systematically to include sites with a range of topographical relief. Bathymetric data from the National Ocean Service Hydrographic and Marine Geophysical databases were used as an aid in site location.

In a typical dive in 1990, three transects were run per dive with each transect lasting 30 min. In 1991, transect durations were extended to 1 h with two transects run per dive. *Delta*'s pilot attempted to maintain a constant speed of 0.5 kn and to remain within 1m of the bottom, terrain permitting. A predetermined compass heading was used to maintain position along a transect line. Periodic locational fixes of *Delta* along each transect were recorded using a TRAK-POINT navigation system aboard the support vessel, in combination with a Loran (1990) or a global positioning system (1991). The length of each transect (l_i) was measured as the sum of distances between locational fixes.

The usual procedure for line-transect sampling entails counting objects on both sides of a transect line. Due to the configuration of the submersible, we only counted fish on the right side of each line. Horizontal visibility was usually good, 5–15 m. All fish observed from the starboard port were individually counted and their perpendicular distance from the line recorded (Buckland 1985). The observer used the lower and middle starboard ports for viewing. An externally-mounted video camera was used to record both habitat and audio observations of species encountered and perpendicular distances to fish. Yelloweye rockfish have distinct coloration differences between juveniles and adults, so observations of the two were recorded separately, and also on a back-up tape recorder. A Pisces Box data-logger recorded depth of the submersible and its distance from the bottom, time of day, and temperature onto the videotape at 1s intervals. These data were later downloaded onto a microcomputer spreadsheet. In addition to the video system, we used a Photosea 35 mm camera with strobe to photograph habitat and fish. Two lamps were mounted externally to provide lighting for the camera systems.

Hand-held sonars were modified to obtain perpendicular distance recordings. Two sonar models were used: Manta and Scubapro. The end of each gun was fit with a tight (rubber) reservoir cinched to the sonar barrel. The reservoir was filled with water, and a syringe used to remove air bubbles. The end of the reservoir was kept damp by resting it on a wet sponge. A digital read-out of the distance from the submersible to its target was obtained by pressing the reservoir end of the gun against the port, aiming the gun, and pressing the trigger. To verify the accuracy of this method, we confirmed readings by positioning a scuba diver at intervals along a marked transect line.

Six habitat categories were used: soft, gravel, cobble, continuous rock, boulder, and broken rock. Other descriptions of habitat were also recorded, including rock type (e.g., basalt), invertebrate cover, and vertical relief. To analyze depth differences, two depth intervals were defined: shallow <108 m, and deep ≥108 m.

Density estimates were obtained for combinations of species, area, depth, and habitat type using the density estimator advanced by Burnham et al. (1980), except that length of transect (l_i) as used in the denominator was not doubled, since we were able to count fishes only on one side of each line transect. Data from all transects were combined, and yelloweye rockfish density was estimated as

$$\hat{D}_{YE} = \frac{n\hat{f}(0)}{L},$$

where n = total yelloweye rockfish adults observed (from all transects), and L = total line length (all transects combined) in meters.

We used the indirect method of estimating variance in density (Burnham et al. 1980:54), and $f(0)$ was estimated from detection functions based on the hazard-rate perpendicular distance model of Hayes & Buckland (1983).

Results

Density estimates

No discernable difference was noted in the occurrence of yelloweye rockfish between day and night replicate transects, and all density estimates are calculated from daytime dives. Estimated densities of yelloweye rockfish in 1990 and 1991 varied from 1954/km² to 2531/km² (Table 1). Estimated probability density functions (pdf) generally exhibited the "shoulder" (i.e., an inflection and asymptote in the pdf for perpendicular distances near 0) that Burnham et al. (1980) discuss as a desirable attribute of the pdf for estimation of f(0) (Fig. 2).

Habitat effects

Boulder fields were the most densely populated habitat type, followed by broken rock (Table 2). Although density was greater in boulder cover regions, the occurrence of this habitat type was relatively infrequent, accounting for only 16% of the total bottom surveyed.

Surveyed habitat ranged from low-relief mud to high-relief pinnacles and cliff faces. The predominant rock type was volcanic, including folded lava flats and columnar basalt. Adult yelloweye rockfish were encountered over all habitats surveyed, but occurred most frequently over broken rock and boulder fields, often observed resting in refuge spaces such as cracks, caves, or overhangs (Fig. 3). They were also observed hovering off cliff faces above cobble or pavement bottoms. Generally, only one yelloweye rockfish was observed per refuge space, but often the hole was co-occupied by a tiger rockfish *Sebastes nigrocinctus*. Frequency-of-occurrence of yelloweye rockfish over soft, cobble, and continuous rock bottom was too low to provide acceptable line-transect density estimates. In both the Sitka Sound and Fairweather areas, there are infrequent abrupt pinnacles overlaid with massive boulders and overhangs. Density of yelloweye and other species was extremely high in these habitats. In the Sitka area we surveyed two adjacent pinnacles: one pinnacle highly dissected with many boulders and overhangs, the other comparatively smooth. Occurrence of yelloweye rockfish on the complex habitat pinnacle was clearly higher than on the smoother pinnacle. Alhough gross vertical relief is similar between the two pinnacles, the number of refuge spaces differed and appeared to be important in the occurrence of yelloweye rockfish.

Depth effects

Depth effects on abundance were difficult to interpret because of the confounding influence of habitat. Depth-related density differences were evaluated by combining the 1990 and 1991 Sitka data and examining two depth zones within the two preferred habitat types: broken rock and boulder. In both habitats, deep zones had higher abundances than shallow zones within the same habitat type. Boulder areas differed the most between shallow and deep zones: The highest estimated density in boulder areas was in the deep zone where 9135 yelloweye rockfish/km² were counted, compared with 6122 yelloweye rockfish/km² in the shallow zone. The deep-zone broken-rock habitat had 2831 yelloweye rockfish/km², compared with 2748/km² for the shallow zone.

Juvenile yelloweye

Abundance of juvenile yelloweye rockfish was too low to obtain reliable habitat-specific density es-

Table 1

Density estimates, CV(D), and 95% CL for adult yelloweye rockfish by area and year.

Year/Area	Density no./km²	n	CV(D)	95% CL Lower	95% CL Upper
1990 Fairweather	2217	221	19.5	1184	3250
1990 Sitka	1954	236	25.3	813	3054
1991 Sitka	2065	352	14.9	1347	3165

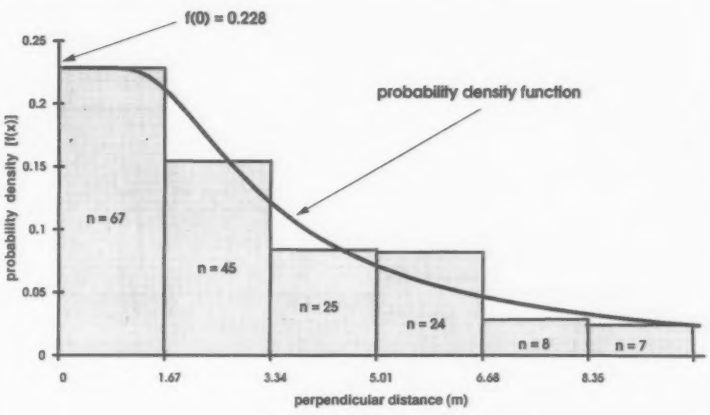

Figure 2

Representative probability density function (pdf) and histogram of relative frequencies ($n_i/(\Delta_i n)$) of yelloweye rockfish observed for 5 distance intervals over boulder habitat in the Sitka study area, 1990. For relative frequencies, n_i = number of fish observed in interval i, Δ_i = size of class interval (in this case, 1.67m), and n = total number of yelloweye observed (in this case, 176).

timates; hence they varied considerably (Table 3). Data on frequency-of-occurrence/meter traversed suggested preference by juvenile yelloweye rockfish for the shallow-zone broken-rock habitat.

Discussion

In addition to confirming the strong association of yelloweye rockfish with rocky habitat noted by Richards (1986), we were able to estimate overall and habitat-specific densities for yelloweye rockfish. The only previously published estimates of yelloweye rockfish densities are from the Strait of Georgia, British Columbia. Richards (1986) used strip transects conducted from the submersible *Pisces VI* to describe spatial distribution patterns of rockfish. Although our results were not directly comparable to hers because of differences in habitat categorization and because juvenile yelloweye rockfish were included in her density estimates, our results were similar. For two depth categories, 21–80 m and 81–140 m, Richards (1986) estimated yelloweye rockfish densities of ~10,000 and 14,000 yelloweye/km^2 in her complex habitat category, including high-relief areas of cobble with large rock, broken rock, and boulder, a category that may encompass our broken-rock and boulder habitat types. In our study, estimated densities in boulder and broken-rock habitats varied from 2405 to 9135 yelloweye rockfish/km^2 depending on depth. Comparison of estimated densities from roughly similar habitat types in the two studies suggests that yelloweye densities in the Strait of Georgia, BC were greater than we estimated for the coast of southeast Alaska.

Use of the submersible allowed collection of qualitative data for assessment of factors contributing to the distribution and abundance of fishes. Occurrence of refuge spaces may be one key to the presence of yelloweye rockfish, which were normally in areas where refuge spaces were available, even if the surrounding habitat was not the preferred habitat of boulder or broken rock. For example, we often encountered yelloweye rockfish under overhangs of large, solitary boulders in cobble flats. Continuous rock bottom was not particularly good habitat in terms of yelloweye density. Additional transects will be needed to increase the precision of habitat-specific estimates and narrow the associated confidence limits. Further refinement of habitat categories (e.g., subcategories of boulders based on average size of boulders and/or interstitial spaces) may also yield more precise habitat-specific estimates for yelloweye.

Differences in density estimates for juvenile yelloweye between the Fairweather and Sitka sites are interesting. The higher density on the Fairweather site may be due to terrain: the Fairweather Ground is a well-defined bank surrounded by large ex-

Table 2

Density estimates for adult yelloweye rockfish by habitat category, area, and year.

Habitat	Year/Area	n	Density no./km^2	CV(D)	95% CL Lower	95% CL Upper
Boulder	1990 Fairweather	59	3660	36.60	792.2	6527.1
	1990 Sitka	52	3712	53.70	0	8015.8
	1991 Sitka	82	5026	30.99	1693.0	8358.9
Broken rock	1990 Fairweather	143	3312	24.50	1575.1	5048.8
	1990 Sitka	175	2515	20.80	1393.2	3637.6
	1991 Sitka	253	2405	40.81	304.84	4505.16

Figure 3
An adult yelloweye rockfish in a typical "refuge space."

Table 3
Density estimates for juvenile yelloweye rockfish by area, eastern Gulf of Alaska, 1990.

Area	Density n	no./km^2	CV(D)	95% CL Lower	95% CL Upper
Fairweather	140	1766	21.34	959.2	2572.7
Sitka	48	497	40.77	63.3	929.7

panses of soft bottom. This topography may cause juveniles to be more closely aggregated than in the Sitka area, where reefs and pinnacles are often linked by hard bottom, e.g., continuous lava flats. Although hard bottom is not ideal habitat, it may promote movement of fish between reefs.

Our ultimate goal is to develop a quantitative predictive model to estimate density of yelloweye rockfish and other DSR species based on one or more parameters reflective of structural habitat complexity. In the interim, the use of line transect-derived density estimates can be directly applied in fisheries management. In the absence of a fishery-independent biomass estimate, the total allowable catch (TAC) currently in use for demersal shelf rockfish had previously been based on historical catch information. In contrast, the transect data allowed us to estimate biomass/km^2 and to expand this estimate to a larger area using an estimate of area of rocky habitat inside the 180 m deep edge of the continental shelf. Allowable biological catch (ABC) and TAC can then be set, using known life-history information including estimates of natural mortality. In 1991, the Gulf of Alaska Plan Team of the NPFMC used this approach in recommending an ABC for the demersal shelf rockfish assemblage in the East Yakutat District (O'Connell et al. 1991).

Acknowledgments

Funding for the submersible and support vessel was provided by NOAA's West Coast National Undersea Research Center, Fairbanks, Alaska. Barry Bracken, Dave Gordon, and Beverly Richardson helped with the field work. Rich Slater and the crews of Delta Oceanographics, the M/V *Wm. A. McGaw*, and the M/V *Privateer* provided invaluable assistance. Thanks also to Ken Krieger and Paul Skvorc for technical advice, and Gordon Kruse and Terry Quinn II for their input regarding line-transect methods and statistical analysis.

Citations

Buckland, S. J.
1985 Perpendicular distance models for line transect sampling. Biometrics 41:177–195.

Burnham, K. P, D. R. Anderson, & J. L. Laake
1980 Estimation of density from line transect sampling of biological populations. Wildl. Monogr. 72, 202 p.

Hayes, R. J., & S. J. Buckland
1983 Radial distance models for the line transect method. Biometrics 39:29–42.

Larson, R. J.
1980 Competition, habitat selection, and the bathymetric segregation of two rockfish (*Sebastes*) species. Ecol. Monogr. 50:221–239.

Love, M. S. & A. W. Ebeling
1978 Food and habitat of three switch-feeding fishes in the kelp forests off Santa Barbara, California. Fish. Bull., U.S. 76:257–271.

Love, M. S., M. H. Carr, & L. J. Haldorson
1991 The ecology of substrate-associated juveniles of the genus *Sebastes*. Environ. Biol. Fishes 30:225–243.

Matthews, K. R.
1991 An experimental study of the habitat preferences and movement patterns of copper, quillback, and brown rockfishes (*Sebastes* spp). Environ. Biol. Fishes 29:161–178.

Matthews, K. R., & L. R. Richards
1991 Rockfish (Scorpaenidae) assemblages of trawlable and untrawlable habitats off Vancouver Island, British Columbia. N. Am. J. Fish. Manage. 11:312–318.

O'Connell, V. M.
1991 A preliminary examination of breakaway tagging for demersal rockfishes. Fish. Res. Bull. 91-06, Alaska Dep. Fish & Game, Div. Commer. Fish., Juneau.

O'Connell, V. M., & J. T. Fujioka
1991 Demersal shelf rockfish. *In* Loh-Lee Low (ed.), Status of living marine resources off Alaska as assessed in 1991, p. 46–47. NOAA Tech. Memo. NMFS F/NWC-211, Northwest Fish. Sci. Cent., Auke Bay AK, 95 p.

O'Connell, V. M., B. E. Bracken, & D. W. Carlile
1991 Demersal shelf rockfish. *In* Stock assessment and fishery evaluation report for the 1992 Gulf of Alaska groundfish fishery. N. Pac. Fish. Manage. Counc., Anchorage AK.

Richards, L. J.
1986 Depth and habitat distributions of three species of rockfish (*Sebastes*) in British Columbia: observations from the submersible *PISCES IV*. Environ. Biol. Fishes 17:13–21.

Rosenthal, R. J., L. J. Halderson, L. J. Field, V. M. O'Connell, M. J. LaRiviere, J. Underwood, & M. C. Murphy
1982 Inshore and shallow offshore bottom fishery sources in the southeastern Gulf of Alaska. Unpubl. rep., Div. Commer. Fish., Alaska Dep. Fish & Game, Junea 99801.

Detection of contaminant and climate effects on spawning success of three pelagic fish stocks off southern California: Northern anchovy *Engraulis mordax*, Pacific sardine *Sardinops sagax*, and chub mackerel *Scomber japonicus**

Michael H. Prager

Southeast Fisheries Science Center, National Marine Fisheries Service, NOAA
75 Virginia Beach Drive, Miami, Florida 33149

Alec D. MacCall

Southwest Fisheries Science Center, National Marine Fisheries Service, NOAA
3150 Paradise Drive, Tiburon, California 94920

Abstract.–We describe a simple biostatistical model of reproductive success (logarithm of recruits/spawner) applied to three coastal pelagic fish stocks off southern California: northern anchovy *Engraulis mordax*, Pacific sardine *Sardinops sagax*, and chub mackerel *Scomber japonicus*. We used the model to detect possible influences of gross climatic conditions and contaminant loadings (particularly of metals and organochlorines) on reproduction in these three stocks. Data included several decades of annual estimates of recruitment and stock size, monthly measures of climate, and annual estimates of contaminant loadings; the model included a compensatory stock-size component before adding environmental effects. The study was meant to generate, rather than test, hypotheses. For the chub mackerel stock, we detected climate influences, but no contaminant influences, on reproductive success, which was usually high during conditions typical of El Niño–Southern Oscillation events. For the northern anchovy stock, we detected no climate or contaminant influences on spawning success; however, the negative results may reflect low statistical power, rather than absence of contaminant influences. For spawning success in the Pacific sardine stock, we detected no consistent climate influences, but we found a strong negative correlation with contaminant loadings. This result is consistent with the hypothesis that contaminant loadings accelerated the collapse of the Pacific sardine stock while it was under stress from severe overfishing. Although many scientific questions about validation of models, mechanisms of action, and identity of specific deleterious contaminants remain to be answered, the observed data are well described by the hypothesis of contaminant-mediated decline.

Manuscript accepted 29 January 1993.
Fishery Bulletin, U.S. 91:310-327 (1993).

In recent years, there has been increasing concern about possible effects of contaminants on the nation's living resources, particularly exploited fish and shellfish populations. Although contaminants such as heavy metals and synthetic organochlorines are commonly detectable in coastal sediments, waters, and organisms (Mearns et al. 1991), it has been difficult, if not impossible, to determine whether sublethal levels of contaminants have influenced the productivity of coastal fish stocks. Mass mortalities and deformities of fish and shellfish have occurred after exposure to high levels of contaminants, but mortality and morbidity in natural populations attributed to chronic low-level exposures is difficult to prove conclusively, even though it may be strongly supported by circumstantial evidence (Sindermann 1978).

In addition, the question of population-level effects has been largely unexplored. For individuals of most species, the physiological effects (if any) of chronic sublethal exposure to contaminants are poorly understood. For populations, the effects of such exposure are not known. Nonetheless, evidence from many studies of individuals suggests that populations should be affected also.

This paper describes exploratory models of the effects of contaminants, climate, and spawning-stock size on three exploited fish populations off southern California. With a rich body of data, this area is unusually well suited to such a study. The waters off southern California contain elevated levels of numerous contaminants, including PCBs, DDT, and several toxic metals (McCain et al. 1988). Estimates of historical contaminant loadings have been made by Summers et al. (1988), and data on climatic conditions are available from public records. Major coastal pelagic fisheries have been monitored by the California Department of Fish and Game since about 1930.

Two main conceptual approaches might be used to model the effects of contaminant exposure on populations. The first approach is a "bottom-up" one: constructing a

*Contribution MIA-91/92-26 of the Miami Laboratory, Southeast Fisheries Science Center, National Marine Fisheries Service, NOAA.

mechanistic population model that somehow extrapolates known effects on individual organisms to effects at the population level. The second approach is entirely at the population level: construction of statistical models that correlate historical changes in population properties (especially properties thought to be sensitive to environmental fluctuation) to changes in contaminant loadings.

Neither of these approaches is completely satisfactory. Weighing against the first approach is the fact that the existing theory of population biology does not allow extrapolation from physiology and behavior of individuals to the net productivity of the population. Indeed, biological populations seem to have emergent properties unknowable from the observable properties of individuals (Mayr 1982). A similar problem is that combinations of contaminants may work in unforeseen ways; one might say that such combinations have their own emergent properties. Thus the biological activity and availability of mixtures of contaminants in the coastal environment are difficult, if not impossible, to extrapolate from laboratory studies of exposure to individual contaminants. Given the seemingly insurmountable barriers to constructing mechanistic bottom-up models of populations chronically exposed to low levels of contaminants, we used the alternative approach: we constructed empirical statistical models of contaminant effects on populations. The empirical approach, of course, also has many limitations; these are discussed at length in later sections.

Model structure

Evidence suggests that the youngest stages of fishes should be most sensitive to the effects of contaminants (Weis & Weis 1989). For that reason, our model of contaminant effects addresses survival from the egg stage to age of recruitment (roughly the first year of life). The model is based on the widely-used Ricker (1954) model of fish recruitment:

$$R = \alpha P e^{-\beta P} \zeta, \qquad (1)$$

where R = recruitment in number of fish or biomass,
P = parent spawning-stock size (usually spawning biomass),
α, β = estimated parameters of the Ricker model,
e = base of natural logarithms, and
ζ = a lognormally-distributed stochastic component with zero mean.

A common interpretation of Eq. 1 is that α represents the net fecundity of a unit of spawning biomass and β reflects the degree of density-dependence in the stock's recruitment.

The Ricker model is often expressed in terms of the natural logarithm of recruits per spawner:

$$\log(R/P) = a + bP + \varepsilon, \qquad (2)$$

where $a = \log(\alpha)$, $b = -\beta$, and $\varepsilon = \log(\zeta)$. (The sign change in b is made merely to simplify the notation; b is negative in a compensatory stock.) Assuming that the total number of eggs spawned is proportional to the spawning biomass P, the quantity R/P is an index of an egg's probability of survival to recruitment. This seems to be a more appropriate quantity to use for detecting exogenous effects than recruitment itself, which is usually held to depend in the first order upon stock size. We refer to the quantity R/P as "spawning success" and to its natural logarithm as "log spawning success." The model of log spawning success (Eq. 2) is linear in the parameters and contains an additive error structure, and thus can be fit by ordinary least-squares (OLS) regression.

Eq. 2 can easily be modified to incorporate external variables, such as climate or contaminant effects, that might affect spawning success. Suppose we have m such variables, $\{x_1, x_2, ..., x_m\}$, for which we wish to estimate parameters $\{\theta_1, \theta_2, ..., \theta_m\}$. Then a model including these variables is

$$\log(R/P) = a + bP + \sum_{i=1}^{m} \theta_i x_i + \varepsilon. \qquad (3)$$

In this expanded model, m explanatory variables and population size affect log spawning success in an additive manner. The application of this linearized model is described in a later section. Other adaptations of the Ricker model to represent contaminant effects were made by Goodyear (1983) and Vaughan et al. (1984).

Data sources and processing

Two main categories of data were used in this study: data on fish abundances, and explanatory data on the environment. Data on fish populations comprised time-series of age-structured abundance estimates from virtual population analyses (VPA). We examined three coastal pelagic stocks off southern California: northern anchovy *Engraulis mordax*, Pacific sardine *Sardinops sagax*, and chub mackerel *Scomber japonicus* (known locally as Pacific mackerel).

These stocks were chosen because they have each supported major fisheries and have been studied sufficiently well so that long time-series of stock and recruitment data are available. These coastal pelagic species also form a conspicuous part of the California Current ecosystem.

Explanatory data (data on the environment) included time-series of two types: variables related to climate, and variables reflecting contaminant loadings or other potential human impacts. These data were subjected to a number of stages of preliminary processing, including two principal component analyses, to compute two sets of derived variables (principal components) from a larger number of potential explanatory variables.

Data on fish abundances

Stock and recruitment data on northern anchovy (Table 1, Fig. 1) were obtained from Table 8 of Methot (1989), who derived his estimates from fishery statistics and research survey data. For spawning-stock size, we used

Table 1

Stock and recruitment data used for modeling effects of contaminants and climate on spawning success of three pelagic fish stocks off southern California. Data on chub mackerel have traditionally been reported, maintained, and analyzed in the English system, and are so reported here.

	Northern anchovy *Engraulis mordax*		Pacific sardine *Sardinax sagax*		Chub mackerel *Scomber japonicus*	
Year	Spawning biomass 10^6t	Recruitment 10^9 fish	Spawning biomass 10^3t	Recruitment 10^6 fish	Spawning biomass 10^6 lbs	Recruitment 10^6 lbs
1946	—	—	566	3875	97.87	20.11
1947	—	—	405	4261	57.91	139.20
1948	—	—	740	3690	28.90	70.92
1949	—	—	793	290	72.43	11.21
1950	—	—	780	397	89.46	3.59
1951	—	—	277	972	72.05	3.80
1952	—	—	136	1197	32.89	55.35
1953	—	—	202	382	10.62	106.48
1954	—	—	239	264	38.58	45.90
1955	—	—	170	588	80.69	91.41
1956	—	—	108	1586	95.00	20.05
1957	—	—	90	905	77.30	28.00
1958	—	—	177	288	36.98	91.81
1959	—	—	122	111	33.59	70.18
1960	—	—	88	74	63.02	128.67
1961	—	—	54	56	81.32	85.60
1962	—	—	27	11	133.10	18.18
1963	—	—	—	—	168.65	9.58
1964	639,210	38.6	—	—	112.05	2.67
1965	531,520	13.4	—	—	44.27	4.21
1966	541,880	13.3	—	—	17.63	5.75
1967	409,170	27.9	—	—	4.11	1.14
1968	396,260	19.8	—	—	2.57	4.08
1969	374,300	33.1	—	—	—	—
1970	321,880	73.1	—	—	—	—
1971	333,600	123.3	—	—	—	—
1972	588,460	154.2	—	—	—	—
1973	1,812,900	114.9	—	—	—	—
1974	1,481,160	32.6	—	—	—	10.15
1975	1,458,430	14.3	—	—	0.63	2.53
1976	1,050,180	57.2	—	—	5.00	138.43
1977	868,890	6.5	—	—	22.68	89.87
1978	435,370	114.3	—	—	95.06	252.20
1979	582,890	82.0	—	—	166.36	35.40
1980	798,280	74.0	—	—	255.27	185.41
1981	782,770	19.7	—	—	332.28	158.58

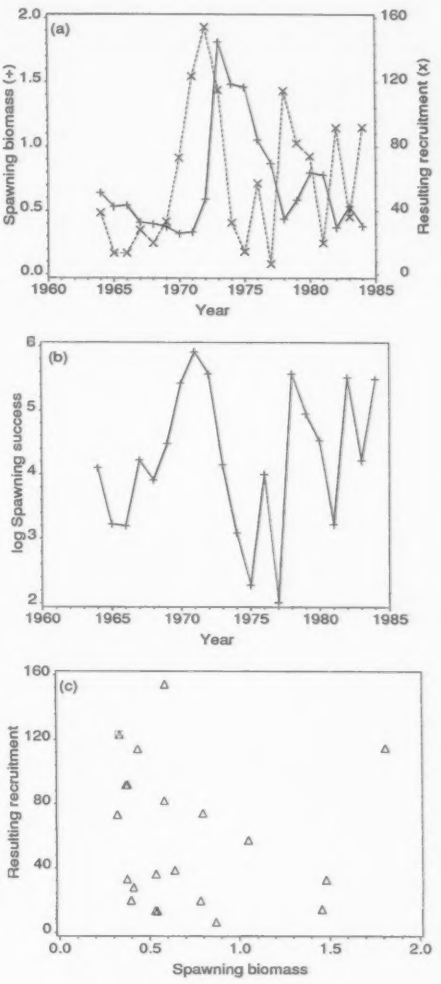

Figure 1

Recruitment of the northern anchovy *Engraulis mordax* stock off southern California. **(a)** Time trajectories of recruitment R (10^9 fish) and spawning biomass P (10^6t); **(b)** time trajectory of log (R/P); **(c)** stock-recruitment scatterplot, in same units as (a).

Methot's estimates of spawning biomass on 15 February of each year. For recruitment, we used Methot's estimates of the number of recruits on 1 July of the same year. Methot stated that his estimates of recruitments before 1964 are much less precise; we used his estimates of 1964 through 81 (the end of the contaminant data series).

Stock and recruitment data on Pacific sardine (Table 1, Fig. 2) are the estimates of MacCall (1979, Table 3), and were derived from fishery statistics. Although the estimates extend through 1964, MacCall (1979) discounted the 1963 and 1964 estimates of recruitment as not sufficiently precise. We used the estimates from 1946 (the beginning of the contaminant series) through 1962.

Stock and recruitment data on chub mackerel (Table 1, Fig. 3) are from Table 1 of Prager & Hoenig (1989), who compiled data from MacCall et al. (1985), Parrish & MacCall (1978), and Prager & MacCall (1988a). The estimates, all derived from fishery statistics, were adjusted by Prager & Hoenig (1989) to a common reporting date. The temporal limits of our analysis, 1946–81, were determined by the limits of the contaminant series. The chub mackerel data span a stock collapse and subsequent closure of the fishery and thus have 6 yr (1969–74) of data missing. Nonetheless, the chub mackerel series (n=30) is the longest of the three stocks. The data encompass at least two distinct epochs in the existence of the population: the pre-collapse epoch of steadily increasing exploitation rate, and the post-collapse epoch of more strictly regulated fishing and the associated population increase.

Explanatory data: Contaminants

Historical contaminant-loadings data were compiled and reconstructed by Summers et al. (1988) according to a mass-balance approach based on manufacturing volume, land use practices, and mobility of particular contaminants. Summers et al. (1988) also compiled more general measures (e.g., wastewater flow) from governmental records. The resulting annual time-series include five major categories: gross indicators, physical-biological factors, nutrient loadings, organochlorine loadings, and metal loadings (Table 2). Prager & MacCall (1990) discussed the loading patterns of individual contaminants and provided time-series plots of each; here, we review major characteristics abstracted from Summers et al. (1988) and Prager & MacCall (1990).

The human population of southern California has increased sharply over the last 50 yr, and this is reflected in many contaminant-loading patterns, particularly in the first three categories (Table 2). For example, loadings of nitrogen, phosphorus, and total organic carbon arise principally from wastewater (sewage) flow, which has increased with population size; power-plant cooling flows, for the most part, also reflect the growing population's use of electricity. While size of the annual kelp harvest is strongly correlated with human population size, the relationship may be noncausal; this is impossible to ascertain statistically. Nonetheless, size of the kelp harvest was included among other potential indicators of environmental stress, as many species are present in kelp-forest habitat during early stages of life history.

With the exception of PCBs, the organochlorines listed in Table 2 were all introduced in the late 1940s. Most fluctuations in individual loadings have followed legal restrictions on use (e.g., of DDT) and subsequent increased use of

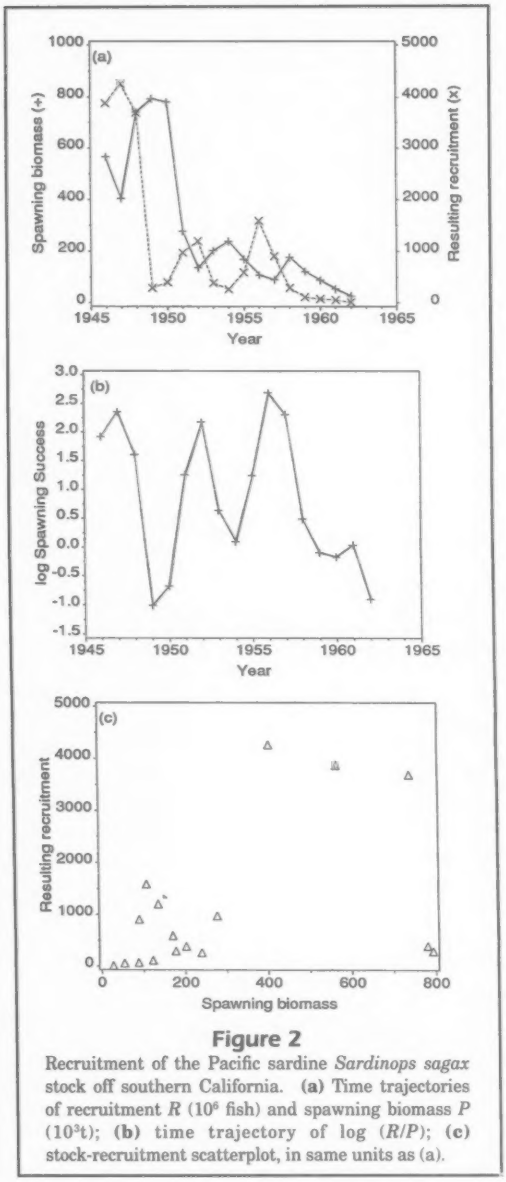

Figure 2

Recruitment of the Pacific sardine *Sardinops sagax* stock off southern California. **(a)** Time trajectories of recruitment R (10^6 fish) and spawning biomass P (10^3t); **(b)** time trajectory of log (R/P); **(c)** stock-recruitment scatterplot, in same units as (a).

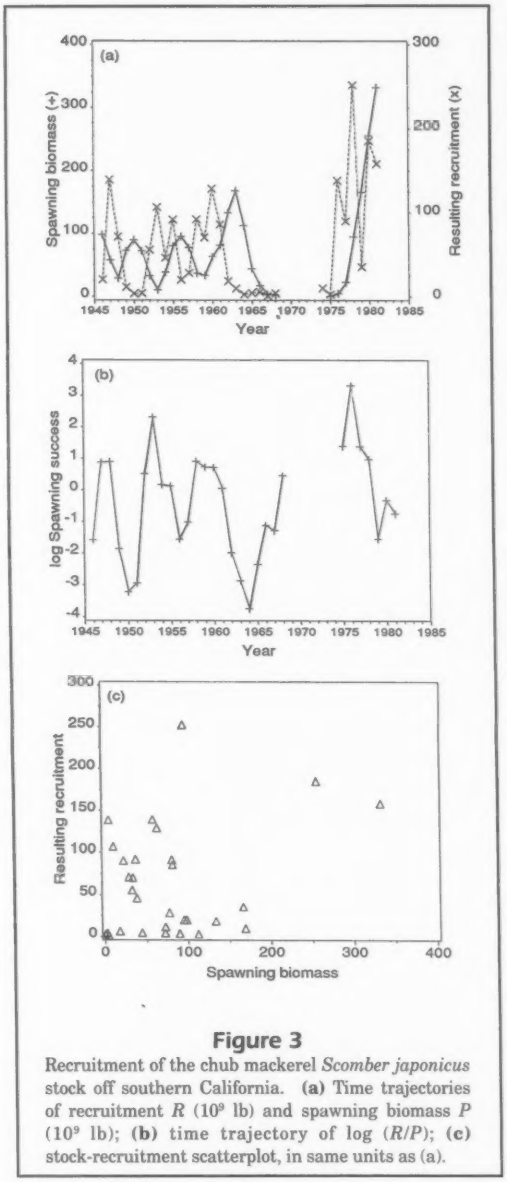

Figure 3

Recruitment of the chub mackerel *Scomber japonicus* stock off southern California. **(a)** Time trajectories of recruitment R (10^9 lb) and spawning biomass P (10^9 lb); **(b)** time trajectory of log (R/P); **(c)** stock-recruitment scatterplot, in same units as (a).

other pesticides. The sharp rise in pesticide use in the 1950s and the subsequent decline in the 1960s and 1970s are similar for many of these compounds, which leads to difficulty in distinguishing their effects statistically. The PCBs, a group of non-pesticide toxic organochlorine compounds, have been used increasingly throughout most of this century, but little is known about the volume of their use and discharge before 1960.

Loadings of metals have varied with growth of the human population and also with fluctuations in patterns of industrial use. Loadings of some particularly toxic metals, such as lead and cadmium, have declined recently because of environmental regulations.

Most of the historical reconstructions of Summers et al. (1988) included values for all years from 1946 through 1981, but some contaminant variables lacked values for 1981. We extrapolated from immediately-

Table 2

Data available on contaminant loadings and other human impacts to the coastal waters of southern California, used for modeling spawning success of three coastal pelagic fish species. Headings indicate major categories. Variables were also assigned to groups (in parentheses) for principal-components analyses, used to reduce the number of variables before modeling. Asterisks (*) indicate variable not used for modeling.

Type of data	Years available
Gross indicators (Indicators group)	
Human population	1890–1980[a]
Municipal wastewater flow*	1890–1985
Physical-biological factors (Indicators group)	
Kelp harvest	1916–1985
Dredging volume	1900–1983
Power-plant cooling flow	1928–1985
Nutrient loadings (Indicators group)	
Nitrogen	1910–1986
Phosphorus	1910–1986
Total organic carbon	1910–1986
Organochlorine loadings (Organochlorines group)	
Aldrin	1945–1982
BHC or Lindane	1945–1982
Chlordane	1945–1982
DDT	1945–1982
Dieldrin	1945–1982
Endrin	1945–1982
Heptachlor	1945–1982
Polychlorinated biphenyls	1929–1986
Toxaphene	1945–1982
Metal loadings (Metals group)	
Cadmium	1920–1980[b]
Chromium	1929–1980[a]
Copper	1929–1980[b]
Mercury	1929–1980[a]
Nickel*	1945–1980[c]
Lead	1929–1980[b]
Zinc	1929–1980[b]

[a] Value for 1981 extrapolated from 1979 and 1980 values.
[b] Value for 1981 set equal to 1980 value.
[c] Time-series contains missing values within this period.

preceding values as necessary (Table 2). The extrapolated 1981 values, although necessary for the principal-component analyses, had very little influence on later calculations.

The reconstructions of Summers et al. (1988) comprise the best available dataset, and the only one on this scale, describing contaminant loadings off southern California in recent decades. Because of this, verification is difficult. Prager & MacCall (1990) found that the reconstructions agreed fairly well with some recent estimates of metals loadings made by the Southern California Coastal Water Resources Project (SCCWRP), which has monitored fluxes of metals from southern California sewage outfalls since 1971 (Konrad 1989). However, only a small portion of total metals loadings are in sewage; this may have caused the discrepancies noted for some metals by Prager & MacCall (1990). We also compared reconstructions with a study of metals deposition in anaerobic sediments in the Santa Barbara basin (H. Schmidt & C. Reimers, Scripps Inst. Oceanogr., La Jolla CA, pers. commun.). However, the sedimentary record, much less precise than the reconstructions, was unable to discern any clear trends or patterns in metals since 1932.

Explanatory data: Climate

A large suite of climate data (Table 3) for the years 1920–84 was compiled by Prager & MacCall (1987a,b,c), who described the data sources and processing in detail. Most of the raw data were provided by Dr. Andrew Bakun (Pac. Fish. Environ. Group, NMFS Southwest Fish. Sci. Cent., Monterey CA).

We detrended most of the sea level (SL) and sea-surface temperature (SST) series to remove rising trends with time. Values for 1983 were not used in computing trend lines, to prevent this extreme El Niño year near the end of the series from distorting the results. Only the series of SST in San Diego did not exhibit a significant trend, and accordingly that series was not detrended.

Seasonal effects were removed by standardizing each variable to zero mean and unit standard deviation (SD) by month of year. For example, the January values (1920–84) of Los Angeles rainfall were standardized as a group to mean 0.0 and SD 1.0. Standardization was performed separately for each month and time-series.

The climate dataset had a few missing values that we replaced with estimates. We used the BMDP procedure AM (Dixon et al. 1983) to estimate these values by stepwise regression on the available data. Reasonableness of the estimates was verified by simulation and by comparison with the nonmissing data (Prager & MacCall 1990).

Principal-component analyses

Many of the explanatory variables contained redundant information. For example, sea-surface temperature and sea level exhibit very similar patterns over time, as both are related to El Niño conditions and the flow of the California Current. Another example, noted above, is that many contaminant time-series are tightly

Table 3

Summary of climate data used for modeling spawning success of three coastal pelagic fish stocks off southern California. Headings indicate major categories. Variables were also assigned to groups (in parentheses) for principal-component analyses used to reduce the number of variables before modeling.

Type of data and station location(s)	Years of monthly data available
Rainfall (Rainfall group)	1920–1984
San Francisco, Oakland	
Los Angeles, Long Beach	
San Diego	
Seawater salinity (Rainfall group)	1920–1984
Scripps Pier: surface	
Scripps Pier: bottom	
Sea-surface temperature (El Niño group)	1920–1984
Farralon Islands	
Pacific Grove	
San Luis Wharf	
San Diego	
Sea level (El Niño group)	1920–1984
San Francisco	
Los Angeles	
San Diego	
Bakun's upwelling index (Upwelling group)	1946–1984
30°N, 119°W	
33°N, 119°W	
36°N, 122°W	
39°N, 122°W	

coupled to human population size, which generates them. This multicollinearity causes problems in fitting and interpreting statistical models such as ours. In extreme cases of multicollinearity, numerical algorithms used for fitting can fail. A more likely problem is that interpretation is not straightforward, because parameter values depend upon the other variables in the model. When sea-surface temperature is included in a model, for example, it may explain a large amount of the variance associated with sea level, so there is little to be gained from including sea level itself in the model. Yet an effect may truly be due to sea level (or to the strength of the California Current), and this relationship may thus be overlooked. Because of this difficulty, any biostatistical study of this nature is inherently unable to isolate the effects of individual causes. An important related practical problem is that a large number of potential explanatory variables makes any fitting procedure unwieldy.

We addressed some of these statistical problems by combining the explanatory data into new composite variables that did not contain duplicate information. These new variables, constructed by principal-component analysis, are linear combinations of the original variables. To reduce the number of variables (initially ~216) to a number more easily analyzed by standard statistical software, data on sea level, sea-surface temperature, and salinity were converted to bimonthly means; also, surface and bottom salinities at Scripps Pier were averaged. Monthly rainfall values were transformed into an annual value of total rainfall (preceding 1 July to current 30 June) and a value representing the median date of the season's rainfall. The explanatory dataset with these changes contained 94 variables before reduction by principal-component analysis.

We constructed two separate sets of principal components. The first set was constructed from physical and climate data (Table 3) but not data on contaminants or general stressors (Table 2). A recruitment model based on this analysis would show how much of the variability in spawning success could be attributed to stock size and climatic variation alone. The second principal-component analysis included all explanatory variables, and was used to reveal how much more variability could be explained by adding contaminant information to the analysis.

Weighting was used in the principal-component analyses to avoid giving undue emphasis to variables (e.g., SST) measured at many locations. To determine weights, each variable was assigned to one of six groups, as shown in Tables 2 and 3. Each group received 1/6 of the total weighting, which was divided equally among the variables within the group.

The results of principal-component analyses are frequently difficult to interpret, as the components are formed on purely statistical grounds. Extensive graphical analysis (presented in Prager & MacCall 1987c, 1990) allowed attaching an interpretation to some, but not all, of the components used in these analyses (Table 4). In interpreting results of the recruitment models, we used a different approach, that of measuring the correlation of the model's explanatory effect with the individual variables, as explained below.

Application of model to three fish stocks

Overview

For each stock, we developed two alternative models: one using the principal components of climate data only, and the second using the principal components of climate and contaminant data. We then examined correlations of each model's estimated explanatory time-series (i.e., the summation on the right side of Eq. 3) to the original climate and contaminant variables. Be-

Table 4

Interpretation of principal components (PCs) used as explanatory variables in models of spawning success in three coastal pelagic fish stocks off southern California. Variables W_1–W_{10} are PCs of data on climate; variables C_1–C_{10} are PCs of data on climate and on contaminant (e.g., metals, organochlorines) loadings. Because interpretation of PCs is difficult, other methods were used to interpret model results (Fig. 4–6; text). SST = sea-surface temperature, SL = sea level.

Variable	Interpretation
W_1	Heavy rainfall; elevated SL and SST; W_1 has peaks in 1958 and 1983 corresponding to El Niño events.
W_2	Very low rainfall, high SST and SL in second half of year.
W_3	Increased upwelling, especially in mid-year.
W_4	Late rainy season with lower-than-average rainfall, decreased SST at northern stations.
W_5	Reduced upwelling at 30°N station, late rainy season.
W_6	Late rainy season in San Francisco.
W_7	Heavy rainfall in San Francisco, high early-year salinity in La Jolla.
W_8	No clear interpretation.
W_9	No clear interpretation.
W_{10}	No clear interpretation.
C_1	Increased upwelling midyear; high loadings of metals, nutrients, and most organochlorines; C_1 is in part a trend component, increasing from 1945 to 1978 and declining slightly thereafter;
C_2	High loadings of organochlorines, Cd, Cr, and Pb; reduced rainfall.
C_3	Elevated SL and SST, heavy rainfall; highest in years of El Niño events.
C_4	Elevated upwelling, especially at 30°N station; high loadings of Cr and BHC; C_4 is high around 1970, lower in other years.
C_5	Early, wet, rainy season, especially in San Francisco.
C_6	High loadings of Hg, early rainy season in southern California.
C_7	No clear interpretation.
C_8	No clear interpretation.
C_9	No clear interpretation.
C_{10}	No clear interpretation.

cause one of the models contained no contaminant data, agreement between the two models on the importance of contaminant variates was considered an indication of severe and troublesome collinearity between relevant climate and contaminant variables. Alternatively, it might simply indicate no contaminant effects. In the presence of strong contaminant effects, and lacking such severe collinearity, one would expect the explanatory effect from the model including contaminants to be more highly correlated with the contaminant variables.

Selection of explanatory variables

It is widely recognized by modelers and statisticians (e.g., Gilchrist 1984:11) that a profound source of uncertainty in statistical modeling is the possibility of error in specifying the model's structure. Such specification error biases parameter estimates and renders most confidence intervals and hypothesis tests invalid (Kennedy 1979, Gilchrist 1984). Unfortunately, the possibilities of specification error and its ramifications are often overlooked when statistical models are used in ecology. The models chosen and presented here were undoubtedly misspecified; they may have included unimportant effects or omitted important ones, and they were limited to a linear functional relationship, which is unlikely to be the true one.

After specifying the linear structure of Eq. 3, choice of variables was the main concern. When no theoretical basis exists to guide it, choice of variables in a regression model must be regarded as heuristic. Neither the theory of the underlying discipline—ecology—nor that of statistics can answer this question unequivocally, so we were forced to use an empirical approach. We started by retaining only the first 10 components from each of the principal-component analyses. (In each case, this retained ~80% of the weighted variance.) To arrive at a parsimonious model, we fit regression models to all combinations of 10 or fewer variables and ranked the many models by C_p, a goodness-of-fit statistic from Mallows (1973). For each combination of stock and data type (climate or combined), we accepted the model with the lowest C_p. However, alternative models of similar fit were similar in structure.

Any method of variable selection in which many candidate explanatory variables and combinations of variables are examined may lead the investigator to accept models which fit well solely through chance. This point has recently been emphasized by Flack & Chang (1987). Although the use of C_p is a relatively conservative approach, the true statistical significance of our results is unknown. Thus we view the modeling exercise as one of hypothesis generation, rather than hypothesis testing. The limitations of inference that come from an empirical choice of model structure are not unique to this study; they pertain to all modeling exercises except those in which

the final model structure and set of explanatory variables are correctly chosen before fitting. Here, we use elements of hypothesis testing, but acknowledge the impossibility of testing the hypotheses rigorously.

Detecting the influence of contaminants

We started with the following null hypothesis: "any apparent influence of contaminants can be explained by random variability alone, including chance correlations of contaminant loadings with climate variability." We imposed three statistical criteria to be met before we would consider rejecting this null hypothesis on the basis of a model including contaminant-loadings data. The first criterion was qualitative: the correlations of the model's explanatory effect with most contaminant variables had to be negative. The other criteria were quantitative: the regression coefficients of the model had to be statistically significant at α=0.05, and the inclusion of contaminant information had to provide more explanatory power than use of climate data alone. If all three criteria were met, we would admit the possibility of contaminant influence on spawning success. The three criteria are described in more detail immediately below.

Sign test Of the variables in Table 3, the metals and organochlorines have been found by bioassay to have deleterious effects on fish (Weis & Weis 1989). (We omitted nickel because of an incomplete time-series and, more importantly, its relatively low toxicity.) Power-plant cooling flow also is generally considered deleterious, but the remaining variables in the indicators group could be favorable as well as unfavorable. The signs of the correlations with the 16 "deleterious" variables were subjected to a (one-tailed) statistical test of the following null hypothesis: "The observed number of negative correlations could arise by chance alone." Under this null hypothesis, the probability of a negative correlation between a contaminant variable and the model's estimated explanatory time-series is 0.5. Assuming independence among the 16 contaminant variables (an assumption that may be violated; see below), the probability of obtaining x negative correlations by chance is given by the binomial probability f(x; n=16, p=0.5). The probability of observing 11 or more negative correlations is 0.105, and of observing ≥12 is 0.038. Thus, the conventional error rate of $\alpha \leq 0.05$ requires ≥12 negative correlations between the 16 deleterious contaminant variables and the explanatory time-series from a model that uses the combined explanatory data.

Such a test concludes that apparent contaminant effects are qualitatively significant if 12 or more negative correlations are found. However, the true probability of Type-I error is >0.038, because many of the contaminant variables are positively correlated with one another, violating the assumption of independence in the binomial probability model and increasing the tail probabilities. While we cannot calculate an exact critical value of x in view of lack of independence, the value would be larger than the nominal value of 12 required for a model to pass this test.

Test of coefficients This test was used to assess whether the coefficients of the chosen model were significantly different from zero. Although we always chose the model with lowest C_p, that criterion does not depend directly on how precisely the regression coefficients are estimated. To test the significance of regression coefficients, we used the standard t-tests (at α=0.05) provided by the statistical software, and required all coefficients to be significant for the model to pass the test.

Improvement-in-fit test Our third criterion required that the model that incorporated contaminant information (i.e., which used the combined explanatory data) had to provide a substantially better fit to the spawning success data than the model using the climate data alone. To judge this, we used the Schwarz criterion (Smith 1988), a statistic for comparing non-nested models. The Schwarz criterion requires an estimate of σ, the true model variance; we used the MSE of the better-fitting model. To pass the test, the model with combined data was required to have a higher value of this statistic than the model with climate data.

Results

Northern anchovy

Not unexpectedly for a short-lived species, the spawning biomass of this northern anchovy stock appears to depend strongly upon the preceding few years' recruitments. A peak in spawning biomass generally follows a corresponding peak in recruitment by 1 or 2yr (Fig. 1a). The stock-recruitment relationship, although noisy, appears density-dependent, in that spawning success improves at lower stock sizes (Fig. 1c), and each model includes a significant compensatory term (the negative stock-size parameter; Table 5). Ricker (1954) and MacCall (1980) have pointed out that cannibalism of eggs or larvae by the adults could cause such compensation.

Neither the climate model nor the combined model explained even half of the variability in log spawning success of northern anchovy (Table 5). Although the model incorporating contaminants had somewhat

Table 5

Summary results of regression models of logarithm of recruits per spawner for three coastal pelagic fish stocks off southern California. Predictor variables were parent stock size (P) and either principal components (W_i, i=1, ..., 10) of climate data (models denoted ○) or principal components (C_i, i=1, ..., 10) of climate data and data on contaminant loadings (models denoted ●). Each model also included an intercept. Variable selection used an all-subsets algorithm with the C_p statistic; thus models may include variables not significant at P<0.05, and all P values are considered nominal.

	Variables included in model (with sign of coefficient) and nominal probabilities of t-statistics for H_0: coefficient = 0.	df of model, error	F statistic	Nominal Prob > F	R^2
	Northern anchovy *Engraulis mordax*				
○	$-P$, 0.025; $-W_5$, 0.13	2, 15	4.20	0.036	0.36
●	$-P$, 0.17; $-C_5$, 0.087; $-C_7$, 0.13	3, 14	4.14	0.027	0.47
	Pacific sardine *Sardinops sagax*				
○	$-W_5$, 0.030	1, 15	5.77	0.030	0.28
●	$-P$, 0.0004; $-C_1$, 0.0001; $-C_5$, 0.002; $+C_{10}$, 0.002	4, 12	14.4	0.0002	0.47
	Chub mackerel *Scomber japonicus*				
○	$-P$, 0.0001; $-W_2$, 0.015; $+W_4$, 0.021; $+W_6$, 0.008; $-W_7$, 0.023; $-W_{10}$, 0.09	6, 23	6.74	0.0003	0.64
●	$-P$, 0.0003; $+C_3$, 0.094; $-C_4$, 0.004	3, 26	8.11	0.0006	0.48

higher R^2 and nominal significance level* than the model including only climate effects, it is impossible to attribute this difference to the effects of contaminants on recruitment. Given the small sample size and relatively small difference in fit, it seems more logical to attribute it to chance.

The two models of anchovy spawning success can be compared by plotting the correlations of the two corresponding explanatory effects with the original explanatory variables (Fig. 4). For some variables (e.g., those related to rainfall), correlations are similar between models; however, many other variables fall into the second and fourth quadrants of the plane, meaning that they are positively associated with spawning success in one model and negatively associated in the other. For example, the two models assign opposite signs to the influence of most upwelling variables. Based on this inconsistent pattern of correlations (Fig. 4) and the lack of nominally significant parameters (except for the stock-size parameters) in Table 5, we conclude that these models identify neither climate- nor contaminant-related variability in the spawning success of this stock.

Indeed, the major determinants of anchovy recruitment strength remain to be discovered. Smith (1985) speculated that recruitment might be controlled in late-larval stages through "plasticity of the interaction between growth rate and survival." Peterman & Bradford (1987) detected a decrease in larval survival associated with episodes of high wind speed; however, Peterman et al. (1988) did not detect significant corre-

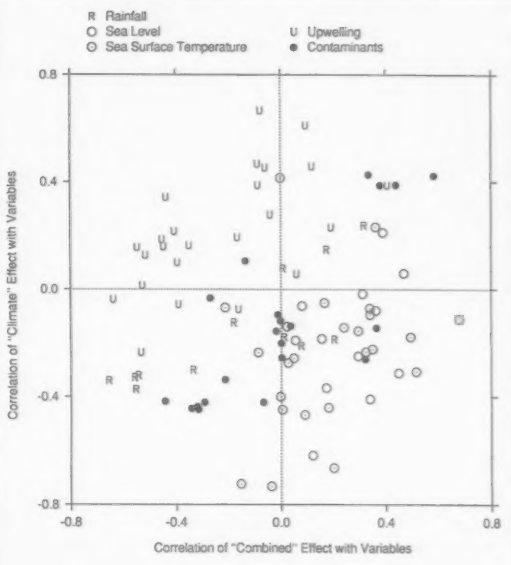

Figure 4

Comparison of two regression models of logarithm of spawning success (recruits/spawner) of northern anchovy *Engraulis mordax* stock off southern California. Models include effects of stock size and environment. Coordinates of a point are the correlations of the models' explanatory effects (see text) with an explanatory variable. For legibility, only category of variable (point) is indicated. Vertical axis: correlations with model estimated on climate data. Horizontal axis: correlations with model estimated on combined climate and contaminant data. Points in first and third quadrants of plane indicate agreement between models as to a variable's effect; points in other quadrants indicate disagreement. Plot suggests that neither model offers a clear explanation of anchovy spawning success.

*To emphasize the impossibility of determining true significance levels, reported significance levels are denoted "nominal."

lation between abundance of larvae and of later early stages or between larval abundance and subsequent recruitment. Because our explanatory data do not include wind speed, we were unable to address this specific question. Cury & Roy (1989) demonstrated that spawning success in coastal pelagic fishes responds nonlinearly to upwelling, but our linearized model could not include this possible relationship.

Methot (1989) has shown that the age of maturity in northern anchovy increases from 1 to 2 when temperatures are below average. Our data already account for this effect, because the spawning-stock estimates of Methot (1989) incorporate this effect of temperature.

The only other likely determinant of anchovy recruitment is spawner abundance itself. This is a straightforward phenomenon in which very low abundance produces very low recruitment. Our stock-recruitment plot (Fig. 1c) does not illustrate this phenomenon; however, the plot begins after the lower abundances of the 1950s, when the effect would have been most pronounced.

Pacific sardine

As in the northern anchovy, the spawning biomass of Pacific sardine depends strongly upon immediately-preceding recruitments, with peaks in recruitment preceding peaks in spawning biomass by about 2 yr (Fig. 2a). Interpretation of the stock-recruitment plot (Fig. 2c) is problematic: If the 2 yr of highest spawning biomass (1949 and 1950) are disregarded, the plot appears biphasic, with small spawning biomasses producing small recruitments and large biomasses producing large recruitments. But if all years are included, recruitment appears to be density-dependent (or strongly influenced by external factors). The stock-size effect estimated by the model with climate effects was not significant (P=0.66); we refit the model without a stock-size effect (Table 5), reducing the R^2 by only 1%. The model with combined climate and contaminant effects identified a statistically significant stock-size effect with the correct sign for compensation (Table 5). This model also fit the data much better.

The two models give quite different pictures of the climatic effects associated with good spawning success in this Pacific sardine stock (Fig. 5). Correlations with rainfall-related signals were mostly negative for both models. Sea level and sea-surface temperatures were estimated to have mostly negative effects in the climate model, but many of these were estimated as positive in the combined model. Correlations with upwelling variables were all positive in the climate model, but were mixed in the combined model.

Most correlations with contaminant variables were negative in both models. In the climate model, correlations ranged from ~0.25 to –0.50. In the model with combined effects, the correlations ranged from ~ –0.25 to ~ –0.95. These strong and consistently negative correlations are consistent with the hypothesis that contaminants affected the dynamics of the Pacific sardine stock, perhaps contributing to its collapse.

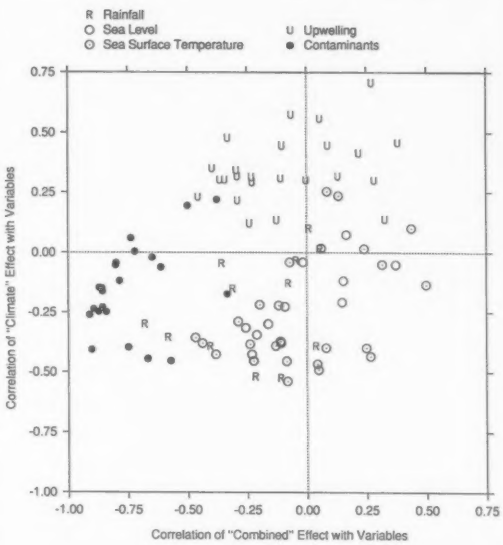

Figure 5

Comparison of two regression models of logarithm of spawning success (recruits/spawner) of Pacific sardine *Sardinops sagax* stock off southern California. Models include effects of stock size and environment. Coordinates of a point are the correlations of the models' explanatory effects (see text) with an explanatory variable. For legibility, only category of variable (point) is indicated. Vertical axis: correlations with model estimated on climate data. Horizontal axis: correlations with model estimated on combined climate and contaminant data. Points in first and third quadrants of plane indicate agreement between models as to a variable's effect; points in other quadrants indicate disagreement. Stronger negative correlations of "combined" model suggest that contaminants have had a negative effect.

Chub mackerel

The models of chub mackerel spawning success included statistically-significant, compensatory stock-size parameters of similar magnitude (Table 5). Compensation has been demonstrated in previous analyses of this stock (Parrish & MacCall 1978, MacCall et al. 1985), and is apparent in Fig. 3b.

Including contaminant variables added little to the model. The climate model had lower MSE than the combined model, and its nominal significance level was more extreme (Table 5). One is left with the impres-

sion that adding the contaminant variables merely muddied the picture.

The two models give similar pictures of the forces that appear to be associated with variability in spawning success of chub mackerel (Fig. 6). We consider the climate variables first. Both models showed moderate-to-strong positive correlations of spawning success with sea-surface temperature early in the year, moderate-to-positive correlations with sea level early in the year, and weak-to-moderate correlations with upwelling later in the year. Correlations with rainfall-related variables were weak.

The models were also similar in correlations with contaminant variables. Correlations with metal loadings were weak-to-moderate, but of different signs for different metals; this suggests chance (noncausal) correlations. Much of the signal in the metal loadings occurred in the late 1960s and beyond, when the chub mackerel stock was declining from overfishing and then recovering (MacCall et al. 1985); this coincidence could have induced noncausal statistical correlations. Correlations with organochlorines were negative. In interpreting this, it is relevant that spawning success in chub mackerel is highly autocorrelated and appears periodic (Fig. 3b). The organochlorine abundances are also very highly autocorrelated, usually consisting of a single peak. This could easily lead to correlations like those observed, even if the observed contaminant levels did not affect spawning success.

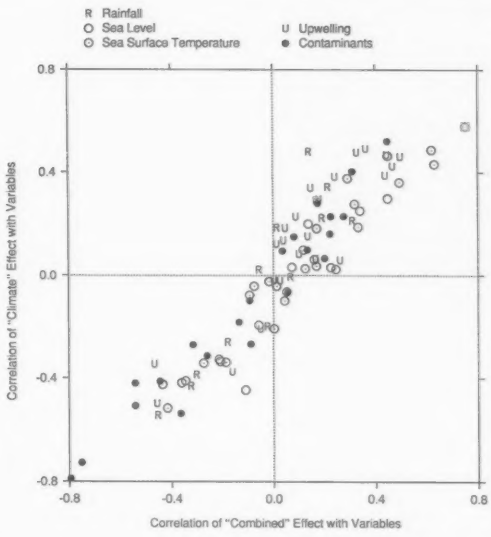

Figure 6

Comparison of two regression models of logarithm of spawning success (recruits/spawner) of chub mackerel *Scomber japonicus* stock off southern California. Models include effects of stock size and environment. Coordinates of a point are the correlations of the models' explanatory effects (see text) with an explanatory variable. For legibility, only category of variable (point) is indicated. Vertical axis: correlations with model estimated on climate data. Horizontal axis: correlations with model estimated on combined climate and contaminant data. Points in first and third quadrants of plane indicate agreement between models as to a variable's effect; points in other quadrants indicate disagreement. Strong agreement between models suggests that addition of contaminant data adds little to this model.

Although several contaminants correlate very highly with spawning success, the correlation patterns are nearly identical for the two models, one of which contains no information on contaminants. We interpret this to indicate that any contaminant effects are indistinguishable from effects of climate variables that fluctuate similarly over time. The strong agreement between the two models also suggests that recruitment-based contaminant analyses of this stock may be exceptionally prone to Type-II error, i.e., failure to detect any contaminant effects that might actually be present.

Parrish & MacCall (1978) also explored the effects of climate on chub mackerel spawning success, but comparison of this work and theirs is difficult for two reasons. Parrish & MacCall (1978) examined many explanatory variables not included in this study. In addition, changes in the estimated maturity schedule and the VPA-based stock and recruitment information (Prager & MacCall 1988) have resulted in a markedly different, as well as considerably extended, stock and recruitment series. Nonetheless, many of our estimated correlations agree with those of Parrish & MacCall (e.g., the positive effects of sea-surface temperature in the south, and the upwelling index at 30°N). Whereas Parrish & MacCall found that spawning success had a negative correlation to sea level at La Jolla, we estimated positive correlations with sea level at La Jolla and Los Angeles from January to June and independence in the later months.

Statistical evaluation of contaminant effects

In a preceding section we developed three statistical criteria for admission of possible contaminant effects. The sign test required 12 negative correlations between 16 "deleterious" contaminant variables and the explanatory effect of a model using the combined explanatory data. Correlations for models of all three stocks were mostly negative. Models of northern anchovy (Fig. 5) and chub mackerel (Fig. 6) each contained 11 negative correlations, but neither result was sufficient to reject

the null hypothesis. However, all 16 correlations were negative for the Pacific sardine (Table 6).

Regression coefficients were significant in models of Pacific sardine and chub mackerel. The model of northern anchovy spawning success fit relatively poorly (Table 5), and although the overall model was statistically significant, the individual regression coefficients were not.

According to the Schwarz criterion S, the models using combined data were marginally preferable to the models using climate data for chub mackerel and northern anchovy (S increased in the third significant figure). For sardine, the combined model was strongly preferable (S in ratio 2:1). Even allowing that the chub mackerel and northern anchovy models passed this test, the only stock to pass all three tests for suspicion of contaminant effects was the Pacific sardine.

Discussion

A somewhat similar biostatistical study was conducted by Martin Marietta Environmental Systems to examine possible effects of contaminants on fishes in five estuaries of the U.S. Atlantic coast, with emphasis on the Hudson-Raritan basin (Summers et al. 1985, 1987). The study used a categorical regression model of historical landings (Rose et al. 1986); the autoregressive model did not attempt biological or demographic realism. After accounting for the effects of hydrographic conditions and previous stock sizes, Summers et al. (1987) detected correlations related to contaminant variables including dissolved oxygen, dredging, and biochemical oxygen demand. The study concluded that there were consistent patterns of anthropogenic influences among similar stocks across different estuaries. In a second categorical regression study, Summers et al. (1990), while expressing some reservations about ultimate causes, concluded that sewage loadings have had a negative effect on white bass *Morone americana* production in the Choptank River, Maryland.

The present study was not undertaken with the expectation of finding clear evidence that contaminants affected fish stocks, nor clear evidence to the contrary. We knew of many reasons that contaminant effects might be difficult to detect, including major theoretical and practical difficulties in the data, shortcomings in biological knowledge, and the limitations of available statistical methodology (for details, see Appendix). As expected, we failed to detect contaminant effects on anchovy or chub mackerel, although we are unable to state whether this reflects a lack of such effects or merely low statistical power. In contrast, the results for Pacific sardine suggest that contaminant stress, at a time of severe overfishing, contributed to the decline and collapse of this stock. Partly because we searched for the best among many possible models, we cannot attach any level of statistical certainty to this suggestion. Our search selected a model of high explanatory power (R^2=83%) in which contaminants were strongly represented, and that, we believe, makes a strong case for further research into the question. Important areas of research would include investigating how such a model of historical events, not formulated a priori, can be statistically validated (or invalidated); which individual contaminants may have contributed to the stock collapse; and by what mechanisms contaminants may have played a role in the decline of Pacific sardine.

An alternative hypothesis about Pacific sardine is that the true spawning-success relationship is depensatory rather than linear, and thus depensation, rather than exogenous influences, mediated the decline of the stock. Consistent with this hypothesis, the stock-size component of our model (Fig. 7a) fits the observed spawning-success data quite well until the mid-1950s (years of very low population size) when the stock-size component predicts higher spawning success than was observed. To examine this alternative hypothesis in more detail, we fit spawning-success models using the following variant of the gamma function:

Table 6

Statistical criteria used to screen models of spawning success of three coastal pelagic fish stocks off southern California. As predictors, models used parent stock-size and principal components derived from measures of climate and of contaminant loadings. Models were required to meet all three criteria in this table before being considered suggestive of contaminant influences on spawning success.

	Fish stock		
Statistical criterion	Northern anchovy	Pacific sardine	Chub mackerel
Number of significant negative correlations with contaminants thought to be deleterious (12 required).	11	16	11
Significance of coefficients in model that included contaminants.	no	yes	yes
Improved fit of model including contaminants, compared with model including only climate. (Improvement judged by Schwarz criterion.)	yes	yes	yes

$$\log(R/P) = \alpha + \gamma \ln P + bP + \sum_{i=1}^{m} \theta_i x_i + \varepsilon. \qquad (4)$$

This differs from our original model, Eq. 3, only in including the term containing the estimated parameter γ. When $\gamma = 0$, this term drops out and the model is equivalent to Eq. 3. When $\gamma < 0$, the model is more strongly compensatory than Eq. 3; when $\gamma > 0$, the model is depensatory. In results of fitting this model, the depensatory effect was estimated as significant only in the absence of climate or combined variables ($\hat{\gamma} = 1.57$, $P < 0.025$ for a one-sided t-test). With the introduction of climate variables, the depensatory effect became smaller and not statistically significant ($\hat{\gamma}=1.02$, $P < 0.19$); with the introduction of the combined variables, the depensatory effect disappeared ($\hat{\gamma} = -0.53$, the wrong sign for depensation). In the model with a depensatory parameter, correlations of the explanatory effect (summation term in Eq. 4) with contaminants were within 2% of those obtained from the model without the depensatory parameter. Of course, the correct specification of spawning-success relationships may be more complex than even Eq. 4. Nonetheless, these results indicate that a simple model including depensation cannot account for the observed decline in spawning success residual to stock-size effects. When this decline, as modeled by our combined variables (Fig. 7b), is combined with Ricker stock-size effects, the resulting model fits well the observed data on Pacific sardine (Fig. 7c).

Are there plausible mechanisms by which contaminants may have contributed to the decline of the sardine population? The high fat content of sardines, anchovy, and mackerel makes them likely to accumulate fat-soluble compounds such as the organochlorines listed in Table 2. It is known that DDT has caused widespread reproductive failures in birds, including those in this geographical area (Anderson et al. 1975). Also, fish have been observed to depurate PCBs by transferring them into eggs (Binder et al. 1984). Since the early stages of many fish species have exhibited reduced survival rates after exposure to toxic compounds (Weis & Weis 1989), plausible mechanisms do exist. The Pacific sardine stock was under severe overfishing pressure at the time of its collapse, and such pressure would increase its susceptibility to environmental stress. The possibility that contaminants may be implicated in the collapse of a major marine fishery is a novel and startling one.

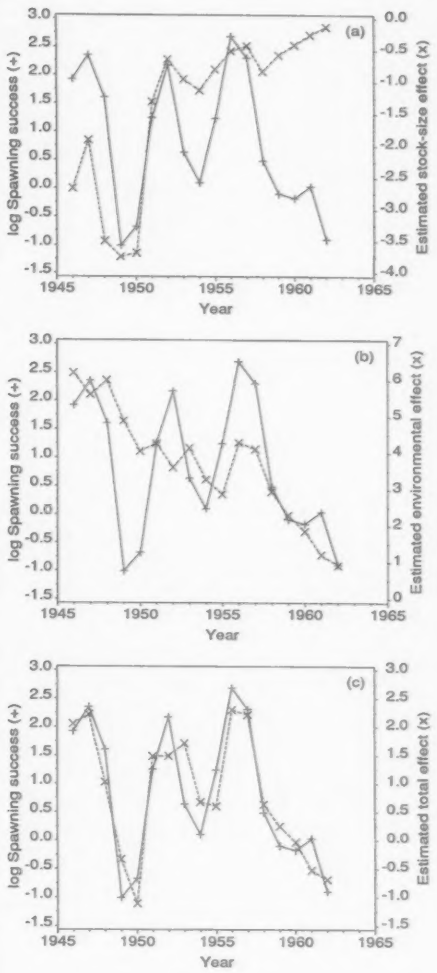

Figure 7

Components (dashed lines) of a model of spawning success (recruits/spawner) of Pacific sardine *Sardinops sagax* stock off southern California. Each panel also shows the observed spawning-success data (solid line) after logarithmic transform. **(a)** Model component associated with estimated stock-size (depensatory) parameter; **(b)** model component associated with estimated parameters corresponding to climate variability and contaminant loadings; **(c)** predicted values from full model (intercept plus stock-size and environmental effects). The environmental component is more influential in the mid-1950s and later, when contaminant loadings generally increased.

Acknowledgments

This work, including the reconstructions by Summers et al. (1988), was funded by the NOAA National Ocean Service, Ocean Assessments Division, Seattle, Washington. We gratefully acknowledge the support of Alan Mearns and Thomas O'Connor of the Ocean Assessments Division. We thank Arnold Mantyla of the Scripps Institution of Oceanography, who corrected some of the climate data and provided additional data to fill several gaps. J. Browder, V. Restrepo, and W. Richards reviewed the manuscript in draft; the work was improved by their suggestions. Two anonymous reviewers also

provided pertinent comments. The Miami Laboratory of the Southeast Fisheries Science Center, NMFS, NOAA, provided support for revisions and publication.

Citations

Anderson, D. W., J. R. Jehl Jr., R. W. Risebrough, L. A. Woods Jr., L. R. DeWeese, & W. G. Edgecomb
1975 Brown pelicans: Improved reproduction off the southern California coast. Science (Wash. DC) 190:806–808.

Binder, R. L., M. J. Melancon, & J. J. Lech
1984 Factors influencing the persistence and metabolism of chemicals in fish. Drug Metab. Rev. 15:697–724.

Cury, P., & C. Roy
1989 Optimal environmental windows and pelagic fish recruitment success in upwelling areas. Can. J. Fish. Aquat. Sci. 46:570–680.

Dixon, W. J., M. B. Brown, L. Engelman, J. W. Frane, M. A. Hill, R. I. Jennrich, & J. D. Toporek
1983 BMDP statistical software, 1985 printing. Univ. Calif. Press, Berkeley, 734 p.

Flack, V. F., & P. C. Chang
1987 Frequency of selecting noise variables in subset regression analysis: a simulation study. Am. Stat. 41:84–86.

Gilchrist, W.
1984 Statistical modeling. John Wiley & Sons, Chichester, 339 p.

Goodyear, C. P.
1983 Measuring effects of contaminant stress on fish populations. *In* Bishop, W.E., R.D. Cardwell, & B.B. Heidolph (eds.), Aquatic toxicology and hazard assessment: Sixth symposium, p. 414–424. Am. Soc. Test. Mat. STP 802.

Goodyear, C. P., & S. W. Christensen
1984 On the ability to detect the influence of spawning stock on recruitment. N. Am. J. Fish. Manage. 4:448–496.

Kennedy, P.
1979 A guide to econometrics. MIT Press, Cambridge MA, 175 p.

Konrad, P. M. (editor)
1989 Recent changes and long term trends in the combined mass emissions discharged into the Southern California Bight, p. 20–28. 1988 Annu. Rep., Southern Calif. Coastal Water Res. Proj. Auth., Long Beach.

MacCall, A. D.
1979 Population estimates for the waning years of the Pacific sardine fishery. Calif. Coop. Oceanic Fish. Invest. Rep. 20:72–82.
1980 The consequences of cannibalism in the stock-recruitment relationship of planktivorous pelagic fishes such as *Engraulis*. *In* Sharp, G.D. (ed.), Workshop on the effects of environmental variation on the survival of larval pelagic fishes, p. 201–220. UNESCO Intergov. Oceanogr. Comm. (IOC), Workshop Rep. 28.

MacCall, A. D., R. A. Klingbeil, & R. D. Methot
1985 Recent increased abundance and potential productivity of Pacific mackerel *(Scomber japonicus)*. Calif. Coop. Oceanic Fish. Invest. Rep. 26:119–129.

Mallows, C. L.
1973 Some comments on C_p. Technometrics 12:661–675.

Mayr, E.
1982 The growth of biological thought. Belknap Press, Cambridge MA, 974 p.

McCain, B. B., D. W. Brown, M. M. Krahn, M. S. Myers, R. C. Clark Jr., S. L. Chan, & D. C. Malins
1988 Marine pollution problems, North American west coast. Aquat. Toxicol. (NY) 11:143–162.

Mearns, A. J., M. Matta, G. Shigenaka, D. MacDonald, M. Buchman, H. Harris, J. Golas, & G. Lauenstein
1991 Contaminant trends in the Southern California Bight: Inventory and assessment. NOAA Tech. Memo. NOS ORCA 62. NOAA, Natl. Ocean Serv., Seattle, WA.

Methot, R. D.
1989 Synthetic estimates of historical abundance and mortality for northern anchovy. *In* Edwards, E.F., & B.A. Megrey (eds.), Mathematical analysis of fish stock dynamics, p. 66–82. Am. Fish. Soc. Symp. 6, Bethesda.

Parrish, R. H., & A. D. MacCall
1978 Climatic variation and exploitation in the Pacific mackerel fishery. Calif. Dep. Fish Game Fish Bull. 167, 110 p.

Peterman, R. M., & M. J. Bradford
1987 Wind speed and mortality rate of a marine fish, the northern anchovy (*Engraulis mordax*). Science (Wash. DC) 235:354–356.

Peterman, R. M., M. J. Bradford, N. C. H.Lo, & R. D. Methot
1988 Contribution of early life stages to interannual variability in recruitment of northern anchovy (*Engraulis mordax*). Can. J. Fish. Aquat. Sci. 45:8–16.

Prager, M. H., & J. M. Hoenig
1989 Superposed epoch analysis: a randomization test of environmental effects on recruitment, with application to chub mackerel. Trans. Am. Fish. Soc. 118:608–618.

Prager, M. H., & A. D. MacCall
1987a An environmental data base describing coastal southern California in the years 1920–1984. Part I: Procedures and summaries. Admin. Rep. LJ-86-31, NMFS Southwest Fish. Sci. Cent., La Jolla CA.
1987b An environmental data base describing coastal southern California in the years 1920–1984. Part II: Data tables. Admin. Rep LJ-86-32, NMFS Southwest Fish. Sci. Cent., La Jolla CA.
1987c An environmental (climatic) data base describing coastal southern California in the years 1920–1984. Part III: Feature extraction. Old Dominion

Univ. Oceanogr. Tech. Rep. 87-9. [Avail. Librarian, NMFS Southwest Fish. Sci. Cent., La Jolla CA.]

1988 Revised estimates of historical spawning biomass of the Pacific mackerel, *Scomber japonicus*. Calif. Coop. Oceanic Fish. Invest. Rep. 29:81–90.

1990 Biostatistical models of contaminant and climate influences on fish populations of the Southern California Bight. Old Dominion Univ. Tech. Rep. 90-04, Rep. to Ocean Assessments Div., U.S. Natl. Ocean Serv. [avail. from the authors].

Ricker, W. E.

1954 Stock and recruitment. J. Fish. Res. Board Can. 11:559–623.

Rose, K. A., J. K. Summers, R. A. Cummins, & D. G. Heimbuch

1986 Analysis of long-term ecological data using categorical time series regression. Can. J. Fish. Aquat. Sci. 43:2418–2426.

Sindermann, C. J.

1978 Pollution-associated diseases and abnormalities of fish and shellfish: a review. Fish. Bull., U.S. 76:717–749.

Smith, A. F. M.

1988 Schwarz criterion. *In* Kotz, S., & N L. Johnson (eds.), Encyclopedia of statistical sciences, vol. 8, p. 289–290. John Wiley & Sons, NY.

Smith, P. E.

1985 Year-class strength and survival of 0-group clupeoids. Can. J. Fish. Aquat. Sci. 42(Suppl. 1):69–82.

Summers, J. K., T. T. Polgar, J. A. Tarr, K. A. Rose, D. G. Heimbuch, J. McCurley, R. A. Cummins, G. F. Johnson, K. T. Yetman, & G. T. DiNardo

1985 Reconstruction of long-term time series for commercial fisheries abundance and estuarine pollution loadings. Estuaries 8:114–124.

Summers, J. K., T. T. Polgar, K. A. Rose, R. A. Cummins, R. N. Ross, & D. G. Heimbuch

1987 Assessment of the relationships among hydrographic conditions, macropollution histories, and fish and shellfish stocks in major northeastern estuaries. NOAA Tech. Memo. NOS-OMA-31. NOAA, Natl. Ocean Serv., Rockville MD, 223 p.

Summers, J. K., C. F. Stroup, V. A. Dickens, & M. Gaughan

1988 A retrospective pollution history of southern California (3 vols). Rep. by Versar Corp. to NMFS Southwest Fish. Sci. Cent., La Jolla CA.

Summers, J. K., W. A. Richkus, C. F. Stroup, & L. J. Rugolo

1990 The influence of natural and anthropogenic environmental change on white perch stock status in the Choptank River, Maryland. Fish. Res. (Amst.) 9:255–268.

Theil, H.

1971 Principles of econometrics. John Wiley & Sons, NY, 736 p.

Vaughan, D. S., R. M. Yoshiyama, J. E. Breck, & D. L. DeAngelis

1984 Modeling approaches for assessing the effects of stress on fish populations. *In* Cairns, V.W., P.V. Hodson, & J.O. Nriagu (eds.), Contaminant effects on fisheries, p. 250–278. John Wiley, NY.

Walters, C. J., & D. Ludwig

1981 Effects of measurement errors on the assessment of stock-recruitment relationships. Can. J. Fish. Aquat. Sci. 38:704–710.

Weis, J.S., & P.Weis

1989 Effects of environmental pollutants on early fish development. Rev. Aquat. Sci. 1:45–74.

Appendix

We encountered many statistical difficulties and uncertainties in our biostatistical approach to detecting contaminant influences. Anyone attempting to interpret our results or to conduct a similar analysis should be cognizant of the following issues concerning data, biological understanding, and statistical methodology.

Difficulties relating to the data

- imprecision in data on stock and recruitment;
- imprecision in measurements of physical (climatic) conditions;
- imprecision in measurements and reconstructions of contaminant loadings;
- lack of residence-time models for contaminants in the water column and sediments, necessitating the use of loading (influx) values, rather than estimated *in situ* concentrations;
- substantial environmental variability that cannot be modeled effectively, and that would thus become "noise";
- strong trends in some resource and contaminant histories that can produce ambiguous correlations between these quantities;
- time-series that are short by statistical standards, although long by comparison with others available;
- multicollinearity: similar patterns over time in different explanatory variables.

Shortcomings in biological understanding

- only rudimentary knowledge of biological response to environmental variability and contaminants;
- poor models of environmental influences on larval production and recruitment;
- poor knowledge of spawning-at-age schedules, especially in light of increased evidence of multiple spawnings within seasons;
- little knowledge of natural mortality rates for most species;
- little or no knowledge of the true form of stock-recruitment relationships for most species.

Problems with statistical methodology

- lack of methods to address the problem of errors-in-variables, except in the simplest cases;
- lack of methods to determine the statistical power of hypothesis tests; and
- lack of methods to identify conclusively a model with the optimum number of parameters, or, for that matter, the correct non-zero parameters;
- possible presence of nonlinear effects, but insufficient data to identify and estimate a nonlinear model.

Similar problems arise in diverse areas of biostatistical analysis of populations and ecosystems, including most studies conducted for fishery management.

We attempted to reduce the effects of collinearity among the explanatory variables by using principal-components analysis. Unfortunately, stock size was at times correlated to other variables. The inability to identify effects of individual climate or contaminant variates is an unavoidable result of collinearity. This problem was accentuated by autocorrelation in the explanatory data and in the stock and recruitment series. Time trends in several explanatory variables, including stock size, compounded the problem of multi-collinearity, as they can lead to spurious (noncausal) correlations.

Even after the principal-component analysis, the suite of possible explanatory variables was large. For parsimony, we chose subset models for each stock. As stated, it is nonetheless probable that our models contain specification error. There are three main forms of specification error: (1) omission of relevant variables or inclusion of irrelevant ones, (2) a wrong functional form for the model (e.g., quadratic response when linear is specified), and (3) changes in the true parameters over time. Consequences of specification error can include biased parameter estimates and biased estimates of variance (Kennedy 1979), which in turn can lead to reduced statistical power. Using principal components, which are biologically arbitrary combinations of variables, may conceivably contribute to specification error (including errors in variables, as defined below).

Most of the recruitment time-series derived from VPA were short and did not coincide exactly with the contaminant data series, themselves not exceptionally long. A major consequence of modeling with a small sample size is low statistical power.

Observation error in explanatory variables causes difficulties in OLS parameter estimates, including inconsistency and, in the bivariate linear case, bias towards zero (Theil 1971, Kennedy 1979). This is known in the field of econometrics as the "errors-in-variables" or "errors-in-predictors" problem, and is sometimes considered a special case of specification error (e.g., Theil 1971). It has been demonstrated that recruitment models used in fisheries are subject to this problem (Walters & Ludwig 1981, Goodyear & Christensen 1984). If one is interested only in a predictive model, the bias is not important. If the parameter estimates are the object, however—as in the present case—the bias is especially problematic because its direction and magnitude are

known only in a few simple cases. By analogy to the results in bivariate linear regression, we suspect that coefficients of our regression models are biased towards zero. The estimated correlations with individual explanatory variates, including contaminants, may also be biased towards zero because of the smearing of the relationship by errors in the predictors.

Further complication is caused by the strong correlations between potential explanatory variables reflecting climate and those reflecting contaminant loadings (Prager & MacCall 1990, Table 6.1). A few examples are the correlations between annual dredging removals and total rainfall in San Diego (r=–0.32), PCBs loadings and July–August SST at San Luis Wharf (r=0.63), and lead loadings and May–June upwelling at 39°N, 122°W (r=0.79). This collinearity makes it nearly impossible to distinguish, by statistical means, the effects of climate from those of contaminants.

Length-based analyses of yield and spawning biomass per recruit for black sea bass *Centropristis striata*, a protogynous hermaphrodite

Gary R. Shepherd
Josef S. Idoine
Woods Hole Laboratory, Northeast Fisheries Science Center
National Marine Fisheries Service, NOAA
Woods Hole, Massachusetts 02543

Abstract.–Dynamic pool models were originally developed to evaluate the effect of exploitation on gonochoristic species of fishes. Consequently, application of these models to hermaphroditic species may lead to erroneous conclusions. The objective of our analysis was to develop an alternative method for estimation of yield-per-recruit and spawning stock biomass-per-recruit that incorporates the effect of sex transformation. Life-history characteristics such as the rate of sex change, growth, and mortality are size-specific; therefore, a length-based model was produced using a series of time-invariant distributed delays. The model incorporates a sequence of length-stages through which the cohort moves, at rates determined from empirical length data. At each length-interval, fish may die, move to the next interval, or switch sex according to a probability distribution of transformation. The model tracks the cohort through time and length categories as an aggregation of individuals rather than a representative average. The estimate of yield-per-recruit for a protogynous hermaphrodite, black sea bass *Centropristis striata*, differed little from traditional models. The distributed delay model with a sex-transformation phase produced considerably lower estimates of spawning stock biomass-per-recruit than the model with traditional assumptions. Potentially erroneous estimates of biological reference points using standard methods for hermaphroditic species may be overcome with use of a distributed delay model, which can incorporate size-specific life-history dynamics.

Manuscript accepted 28 January 1993.
Fishery Bulletin, U.S. 91:328–337 (1993).

Analytical models describing the potential yield of a fisheries resource consist of three basic dynamic elements: population growth, recruitment, and mortality (Russell 1931). Dynamic pool models (e.g., Thompson & Bell 1934, Ricker 1954, Beverton & Holt 1957) are traditionally used to evaluate potential yield-per-recruit (Y/R) and spawning stock biomass-per-recruit (SSB/R) relative to fishing mortality and size-at-recruitment. Potential yield and spawning biomass of a cohort are typically calculated as a summation across discrete age-increments, under specified conditions of growth and natural mortality. Within each age-interval, growth and fishing mortality rates are assumed to apply uniformly to all members of the cohort (Gulland 1977). Not all individuals follow the same growth trajectory, however, and the susceptibility of individual fish to mortality is often a size—rather than age-dependent phenomena (Kirkpatrick 1984). Consequently, length-based models can provide a more precise and accurate depiction of cohort dynamics, in addition to using directly measurable variables that are often linked to management measures.

Traditional age-based models of Y/R and SSB/R may be particularly inappropriate for species with unusual and/or complex life histories. This may be true for hermaphroditic species that have unique reproductive stages that change as a function of fish size. For example, significant growth and mortality changes that occur following sexual transformation would not be accounted for in conventional Y/R models.

Hermaphroditism will also influence estimation of sex-specific mortalities. For example, as transformations occur in a protogynous hermaphrodite, females are lost from the cohort, creating the same effect as increased female mortality. The transformations increase the number of males in the cohort, reducing the apparent mortality of males. Consequently, the mortality estimates for each sex are not independent, and a potential bias may exist in estimating Y/R and SSB/R when sex-specific characteristics are not considered.

Black sea bass *Centropristis striata* is a protogynous hermaphrodite common along the continental shelf of the northwest Atlantic between Massachusetts and Florida. Growth in black sea bass is sexually dimorphic, with faster growth but lower maximum age in females (Lavenda 1949, Mercer 1978, Alexander 1981). Females commonly reach sizes of 38 cm and age 8 yr (Lavenda 1949); however, at sizes of 8–35 cm females may transform into males and enter the male growth regime. Males may grow

to 60 cm and age 20 yr (Lavenda 1949) with greater variability in size-at-age than females. Consequently, a black sea bass has three possible growth rates: female, male, and transitional. These differences in growth rates and variability in size-at-age between the sexes will influence the potential yield from a cohort.

An alternative approach for modeling changes in a cohort over time is use of delay models. Delay models were first developed in the field of industrial dynamics as a technique to monitor movement of individuals through a system of substages (Forrester 1961), and have since been modified to incorporate effects of attrition (mortality) and variability in timing of movements (Manetsch 1976, Vansickle 1977). The subclass of distributed delay models can be a useful tool to describe the movement of any item through a process or, in a biological context, through developmental stages (Manetsch 1976). Extending the model to include a series of consecutive processes, it has been used to simulate growth dynamics in marine crustaceans (Idoine & Finn 1984), insects (Ravlin et al. 1978, Schaub & Baumgartner 1989), and agricultural crops (Gutierrez et al. 1984, 1988). The major advantage of this model type is its focus on the aggregated behavior of individuals rather than a representative mean.

To estimate Y/R and SSB/R in black sea bass, we modeled the growth and mortality of a cohort as a series of distributed delays with an associated mortality, using length categories as individual developmental stages. This approach allowed us to simulate the decline of the cohort while retaining information about variation in size composition and size-specific mortality in the cohort. In addition, we were able to evaluate the influence of additional mortality on the population dynamics of a species with an hermaphroditic life history.

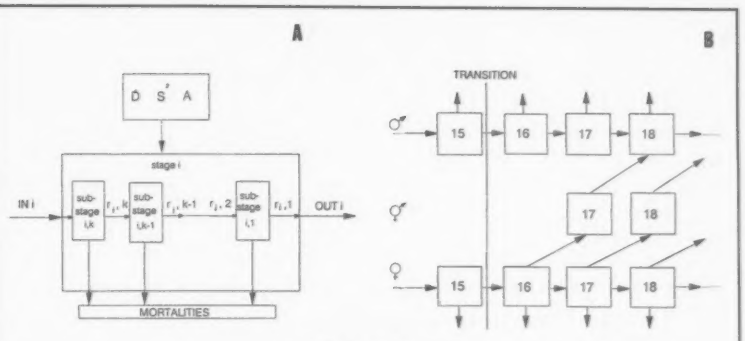

Figure 1

(A) Schematic of intra-stage flow of the distributed delay model: D = delay period defined as mean number of days necessary to move through a stage; S^2 = variance of D; A = instantaneous mortality rate; i = index of stage; INi = number of individuals entering stage i; k = integer value of $D^2/(S^2)$, which defines the number of substages within a stage; r_i = flowrate between substages; OUTi = number of individuals moving into next stage; mortalities = number of individuals removed from stage i through attrition. **(B)** Schematic of flow between cm stages in the model.

Methods

The model structure

Time-invariant distributed delay models with a mortality term (Vansickle 1977) can be characterized as a sequence of stages, with flow through each stage i represented by a series of differential equations (Fig. 1):

$$dr_{i,1}/dt = k/D[(x(t)-r_{i,1}(t))-(A(t)*D/k)]$$
$$dr_{i,2}/dt = k/D[(r_{i,1}(t)-r_{i,2}(t))-(A(t)*D/k)]$$
$$\vdots$$
$$dr_{i,k}/dt = k/D[(r_{i,k-1}(t)-r_{i,k}(t))-(A(t)*D/k)]$$

where $x(t)$ = input rate at time t,
k = integer value of D^2/variance of D (S^2) which defines the number of substages within a stage,
i = index of stage,
j = index of substage from 1 to k, and
$r_{i,j}$ = flowrate between substages j and j-1, stage i;

or

$$r_{i,j} = (k_i / D_i) * Q_{ij}$$

where Q_{ij} = the number of individuals in substage j, stage i,
D = delay period defined as the mean number of days necessary to move through a stage (the value of D at stage i varies by sex), and
$A(t)$ = mortality rate at time t.

All rates in the model are instantaneous. The model was simulated as a series of difference equations with a time step equal to 1 day. The delay model can be expressed either in terms of flows (r_{ij}) or state variables (Q_{ij}) (Vansickle 1977). For simulation purposes, this model utilizes flows within, between, and out of stages representing 1 cm length categories through which a cohort will pass. These flows were converted

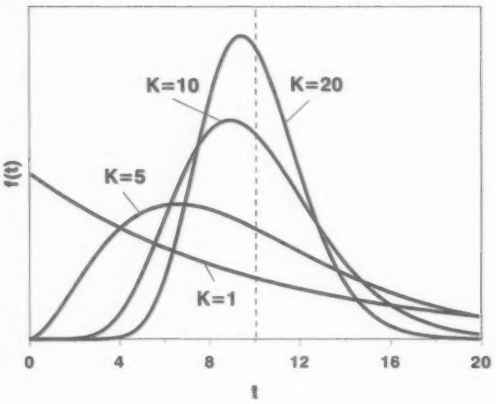

Figure 2
Erlang probability density function for various values of k and a mean t = 10.

to state variables (e.g., numbers of individuals dead due to fishing mortality at a given size) where necessary for analyses. Individuals in the cohort passed through each stage at a rate determined by an Erlang probability density function. The shape, or the order, of the density function was determined by the value of k (Manetsch 1976) (Fig. 2). Transit time of an individual through stage i was a function of the mean delay period (D) and associated variance. The greater the variance relative to the mean, the greater the value of k. This continuous function was approximated, using difference equations, by a series of substages. The number of substages within a stage was equal to the integer value of k, since fractional substages cannot be used in the discrete approximation necessary for the model.

A cohort entered length stage i at time t and moved through the substages at stage-specific rates. At time t+1, fish either moved into length stage i+1, remained in length stage i (at some substage), or were removed from the system at a defined rate of mortality due to fishing and/or natural mortality. At time t+2, some fish were still in stage i, some in i+1, and possibly some in i+2, etc. The biomass of the cohort and mean size changed as the distribution moved through the series of length stages until all individuals reached a maximum size or the cohort was eliminated through mortality. Any individuals moving to a size beyond the maximum were assumed to undergo senescence and were removed from the system at that maximum size. Yield was calculated from the number of individuals removed at each length stage ≥ the size of recruitment to the fishery × the ratio of fishing mortality/total mortality (F/Z). The biomass of fish removed via fishing mortality was calculated using the appropriate sex-specific length-weight equations. Spawning stock was calculated as the sum of the number of females per length remaining in the system at the time of spawning (1 June) × the probability of female maturity-at-length. The number of mature females-at-length was converted to biomass using a length-weight equation.

With this model, hermaphroditism was included by splitting the cohort into three growth regimes and using a size-specific probability of sex transformation. At the initial stage, the cohort was divided into an appropriate number of males and females, then passed through length stages at sex-specific rates. At a designated length-interval, females began transformation by passing through an intermediate transitional stage prior to entering the male growth sequence (Fig. 1).

Input parameters

Input parameters required in the model were mean transit time (D) and its associated variance (S^2) per 1 cm length-category in days and $days^2$, respectively, by sex; maximum potential length for each sex in the population; probability of sex transformation-at-length for females; a range of lengths-at-recruitment (L_c) to the fishery; instantaneous natural mortality rate (specific to length groups and sex if appropriate); a range of instantaneous fishing mortality rates; and the percentage of females mature-at-length. In addition, length-weight equations by sex were necessary for conversion of numbers-at-length to biomass.

Estimates of mean transit times and their associated variances for black sea bass were determined from back-calculation of scale data. Sea bass scales were collected in coastal Long Island during 1979–80, aged, and length-at-age back-calculated (Mark Alexander, Conn. Dep. Environ. Prot., Old Lyme, CT, pers. commun.). Daily time-increments of growth were chosen to provide estimates of k. Transit time (D) by cm-intervals was calculated as

$$D = 365 / \frac{[(S_n - S_{n-1}) * SL]}{S}$$

where S_n = scale annulus n,
S_{n-1} = scale annulus n-1,
S = total scale size,
SL = standard length of fish,

with the assumption of linear growth between annuli (i.e., D equal between cm-intervals $(S_{n-1}/S)*SL$ and $(S_n/S)*SL$). Thus, each individual scale provided estimates of transit times (D) by cm, up to the maximum length of the fish (SL). The means of D and S^2 were

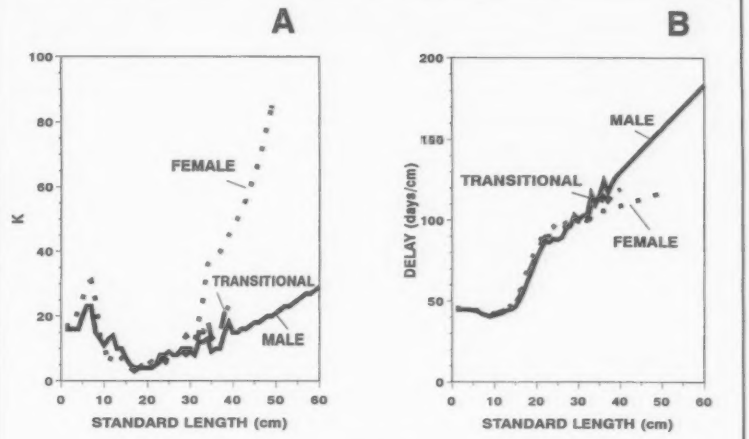

Figure 3

(A) Calculated values of number of substages, k, and **(B)** mean transit times, D, for female, male, and transitional stages of black sea bass *Centropristis striata*.

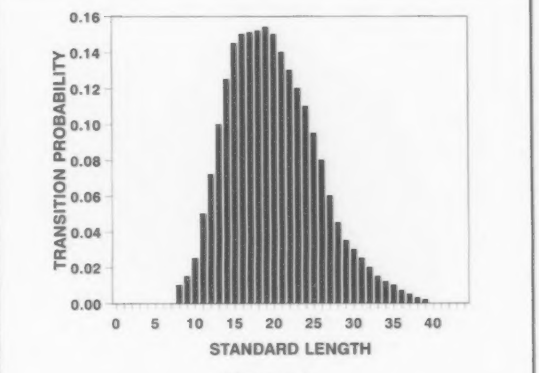

Figure 4

Transformation rates-at-length of female black sea bass *Centropristis striata* used in the delay model.

estimated per length category for each sex, with sex determined at the time of capture. Delay and variance estimates were extrapolated with a linear regression between the largest length categories in the dataset and maximum potential length (Fig. 3). Maximum lengths were 49 cm SL for females, 39 cm SL for transitionals, and 60 cm SL for males. D and S^2 for each length-interval in the transitional category were estimated by using the mean values of females and males. Transformation rates-at-length were estimated from a composite of the frequency of transitional-stage fish recorded in field observations (Fig. 4) (Mercer 1978, Low 1981, Wenner et al. 1986). Transformations began at 8 cm, and individual fish were allowed to exist in a transitional state for 1 cm. Sex-specific length-weight equations (Mercer 1978) used to convert standard length (cm) to weight in grams were

males: $wt=0.01773\ SL^{3.1525}$
females: $wt=0.02810\ SL^{3.0104}$
transitional: $wt=0.02120\ SL^{3.0991}$

Annual instantaneous natural mortality (M) for both the Y/R and SSB/R calculations was modeled as a length-dependent rate equal to 0.3 at lengths 1–10 cm and 0.2 at 11 cm–max. length. Instantaneous fishing mortality (F) was varied between 0.0 and 1.50 in both calculations. Mortality rates were applied over time-intervals of 1d (t=1/365).

Length-at-first-capture (L_c), which was modeled as knife-edge recruitment, varied between 16 and 32 cm SL. Increments were equivalent to annual mean lengths at successive ages, as determined from the delay model. The effect of harvesting was examined by incorporating an additional mortality term at each length category beyond the size-at-recruitment. Maturity-at-length data were collected during NEFSC bottom-trawl surveys between 1982 and 1990 (O'Brien et al. 1993). The initial cohort in the model consisted of 2000 fish divided according to a sex ratio of 99:1 female to male (Mercer 1978, Wenner et al. 1986). Precision of rounded values in the computer program resulted in the net loss of some individuals; therefore, the number of recruits used in the per-recruit calculations was the sum of individuals accounted for at the end of the run rather than the initial input value. The yield model was run for 25 yr or until the number of remaining fish in the cohort was <1; and the spawning biomass model (females only) was run for 11 yr or until the cohort was reduced to <1 fish. The Y/R and SSB/R models were developed as separate computer programs written in ANSI standard FORTRAN.

The Y/R estimates from the distributed delay model were compared with results from a Thompson-Bell (T-B) Y/R model. Lengths-at-annual-intervals for males and females were derived from execution of the delay model without a transitional phase and converted to grams using the appropriate length-weight equations. The mean of the male and female weights-at-age served as input to the T-B Y/R model. M was set equal to 0.3 for age 1, and 0.2 thereafter. The traditional SSB/R

model is a simple extension of the T-B Y/R model (Gabriel et al. 1989) and, consequently, the relationship to the delay models was similar. To avoid redundancy, only the relationship between the T-B Y/R model and the delay models was represented.

The sensitivity of the delay model to changes in the transition rates was examined. The transitional size-range was divided into 8 cm length-intervals and the transition rates within each interval were doubled. Spawning stock biomass-per-recruit was estimated for each interval of increased transition rates over a range of fishing mortalities and a constant size-at-first-capture of 16 cm.

Table 1

Mean length-at-age (cm) and variance from distributed delay model and mean back-calculated lengths-at-age (Mercer 1978) for black sea bass *Centropristis striata*.

Age (yr)	Distributed delay				Back-calculated	
	Male		Female		Male	Female
1	9.6	(0.56)	9.5	(0.45)	8.7	9.0
2	17.7	(0.89)	17.2	(0.96)	16.5	16.3
3	22.5	(1.25)	21.7	(1.20)	21.1	20.4
4	26.5	(1.65)	25.4	(1.64)	24.4	23.6
5	30.1	(1.85)	29.0	(2.20)	27.6	26.1
6	33.5	(1.92)	32.8	(2.35)	31.4	27.9
7	36.6	(1.93)	36.4	(2.17)	34.6	33.6
8	39.5	(1.91)	39.9	(2.11)	36.5	
9	42.3	(1.86)	43.2	(2.02)	38.4	
10	44.9	(1.82)	46.5	(1.84)		
11	47.4	(1.79)	48.4	(0.65)		
12	49.8	(1.76)				
13	52.1	(1.72)				
14	54.3	(1.68)				
15	56.4	(1.64)				
16	58.4	(1.31)				
17	59.5	(0.54)				
18	59.8	(0.18)				

Results

To confirm that the model accurately represented growth in the absence of any harvest mortality, we calculated the mean lengths of the cohort (by sex) at successive 365d periods as generated by the model, and compared the results with independent back-calculated mean lengths-at-age (Mercer 1978) (Table 1). Growth simulated by the delay model was comparable to growth observed from back-calculations, although sizes-at-age tended to diverge in older ages, with slightly higher lengths-at-age produced by the delay model. Under the influence of natural mortality only, a cohort introduced into the delay model was reduced to 0.1% of its initial number by the time the maximum length was attained. The reduction of the cohort using only natural mortality indicated that the model provided an accurate portrayal of the black sea bass growth rate for the stated set of mortality parameters.

To evaluate the effect of harvest mortality in the absence of sex transformation, we calculated Y/R as generated by the delay model without transition and compared the results with those obtained using the T-B model. Under various L_c values, yields-per-recruit from the two models were similar, indicating the basic

Table 2

Estimates of F_{max} for black sea bass *Centropristis striata* from distributed delay model with and without transitional phase and using Thompson-Bell model. Age-at-entry in yr.

Size (age) at entry	Distributed delay		Thompson-Bell
	w/ transition	w/o transition	
16 cm (2)	0.16	0.17	0.17
21 cm (3)	0.20	0.21	0.21
25 cm (4)	0.25	0.27	0.26
28 cm (5)	0.31	0.33	0.33
32 cm (6)	0.45	0.47	0.45
35 cm (7)	0.63	0.64	0.63

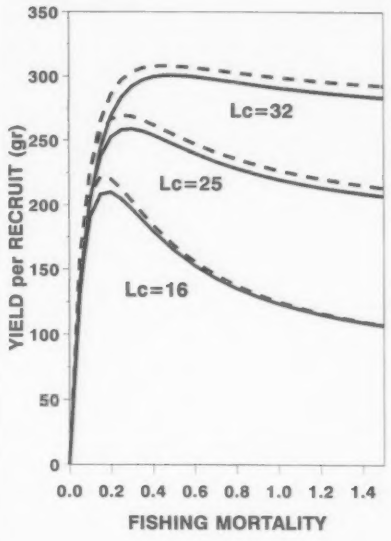

Figure 5

Yield-per-recruit for black sea bass *Centropristis striata* calculated by the distributed delay model without transitions (solid) and with a transitional phase (dash) at various alternative lengths-at-first-capture (L_c). M = 0.3 (1–10cm) and 0.2 (11–max. length).

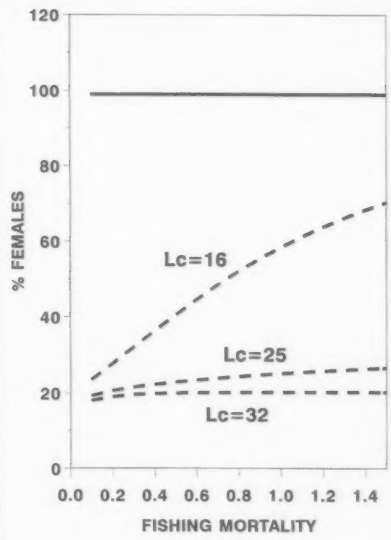

Figure 6

Sex composition of total yield for black sea bass *Centropristis striata* estimated from a distributed delay model with sexual transition (dashed) and without a transitional phase (solid) for varying sizes-at-first-capture (L_c).

delay model was comparable to traditional methods of estimating yield-per-recruit. The calculated biological reference point of F_{max} from both models was nearly identical (Table 2).

The addition of the transitional phase into the model had little effect on the estimates of Y/R. The calculated values of Y/R and F_{max} were similar for each recruitment size and fishing mortality (Fig. 5, Table 2). Although the effect of including the transition phase on the total yield was negligible, the effect on sex composition of that total yield was substantial. With no transition phase, the proportion of females in the yield was dependent upon the initial sex ratio, in this case 99% female (Fig. 6). If the sexual transformation of females to males was included, the percentage of females to the total yield increased as a function of F and decreased as a function of size-at-first-capture (Fig. 6). At a recruitment size of 16 cm SL (age 2), the percentage of female biomass in the yield went from 21.3% at an F=0.05 to 70.4% at F=1.5, whereas a change in recruitment size to 32cm (age 6) decreased the effect of F, resulting in a percentage range of 17.3–20.3% females for F=0.05 and 1.5 respectively.

The addition of a transitional phase had a significant impact on the estimates of SSB/R from the distributed delay model and subsequent estimates of a total female spawning biomass. In the absence of any harvest mortality, maximum SSB/R for a cohort that undergoes a transition was 600.8 g/recruit as compared with 2373.3 g/recruit without transition (Fig. 7). Over the life of the cohort, the spawning biomass-at-age increases similarly for the first 2 yr regardless of the form of the delay model (Fig. 8 for size-at-recruitment of 25 cm), at which point the effect of transition begins. At age 2.5, a cohort undergoing transition approaches the maximum contribution to spawning biomass-at-age, while a cohort that does not undergo transition makes its maximum contribution at age 10.

The inclusion of the transitional term in the model led to lower proportional reductions in SSB/R with increasing F. In a model without the transitional form (e.g., size-at-first-capture of 25 cm [age 4] Fig. 9) at fishing mortality of 1.5, the spawning potential was reduced to 15.2% of maximum spawning potential (%MSP). In a model with the transition term, however, 28.7% of maximum spawning potential was obtained (Fig. 9). The pattern is also obtained at other sizes-at-recruitment. The transitional phase also reduced the sensitivity of SSB/R to changes in F and size-at-recruitment (L_c). Decreasing F from 0.6 to 0.2 (L_c=25) increased SSB/R by 107% in the non-transitional model, but only 60.5% in the delay model with transitions. Similarly, an increase in size-at-first-recruitment from 16 to 32 cm (with F=0.6) increased SSB/R by 201.8% in the transitional model but 368.9% in the non-transitional version. The inclusion of a transitional phase increased the natural reduction in the number of females in the system, which consequently reduced the maximum SSB/R for the cohort and the relative influence of fishing mortality on SSB/R.

The sensitivity of estimates of SSB/R to changes in transformation rates was examined. Doubling the transition rate across all lengths decreased the SSB/R by 71% from 600.8 to 174.6 g/recruit. When the transition rates were doubled over 8 cm length-increments, the impact in SSB/R varied by F and the size-range over which the transformation rate was changed (Fig. 10). Doubling the rate of

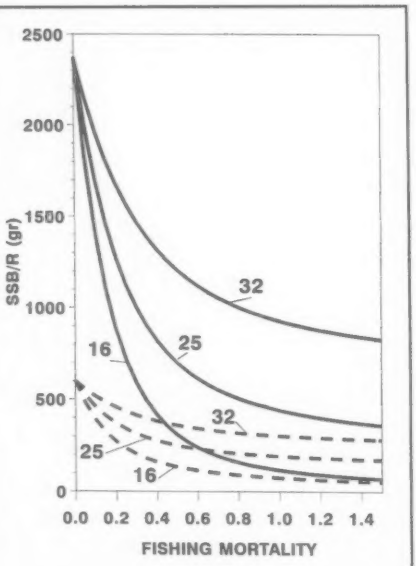

Figure 7

SSB/R for black sea bass *Centropristis striata* estimated from the distributed delay model without transition (solid) and with the transitional phase (dashed). M = 0.3 (1–10 cm) and 0.2 (11–max. length) with varying lengths-at-first-capture (L_c).

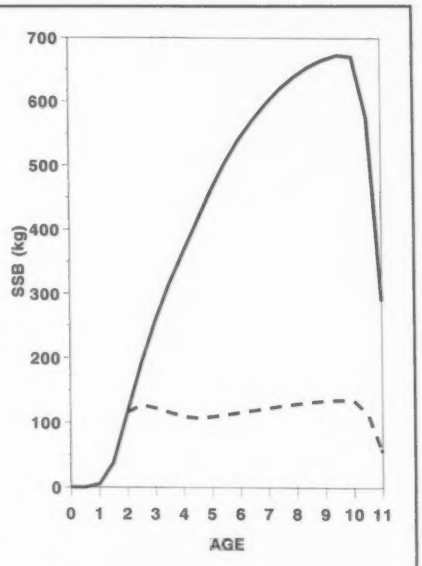

Figure 8

Spawning stock biomass-at-age for black sea bass *Centropristis striata* estimated with a distributed delay model with transitions (dashed) and without transitions (solid) for length-at-recruitment of 25 cm. M = 0.3 (1–10 cm) and 0.2 (11–max. length).

transformation in the 16–23 cm range had the greatest effect, decreasing SSB/R by 39.1% with F=0 (Table 3). Changes in transformation rates in the tails of the transformation probability distribution had little impact. In all cases, increases in F decreased the relative impact of transformation loss and, consequently, the sensitivity to changes in transformation rates decreased.

Discussion

Ignoring the unique population dynamics that may occur in hemaphroditic fishes will increase the risk of incorrectly estimating optimal exploitation levels from yield-per-recruit models (Bannerot et al. 1987). The problems can be compounded by disregarding the increased size variability within the system resulting from sexual transformations. Distributed delay models provide a mechanism for handling length-specific life-history changes, and results can be summarized as an aggregate of individuals and the associated variability rather than a simple mean estimate without error. The consequence is greater flexibility in dealing with changes between length categories without ignoring the size variability inherent within the system.

In the black sea bass example presented, the incorporation of a transitional term in the delay model had little effect on the estimate of yield-per-recruit. Since the sexes were combined to produce total yield, the growth differences between sexes were not large enough to produce significant changes in overall yield. Also, the inclusion of fishing mortality quickly removed any added yield contributed by transformed females. It is likely that the result would diverge further from a traditional model estimate as the differences in longevity or growth rate between the sexes increased.

The effect of modeling length- and sex-specific characteristics with a delay model was more apparent in spawning stock biomass-per-recruit estimates. The removal of female biomass via transformations was similar to increasing natural mortality at each length step, and consequently the spawning potential was reduced more quickly than under typical effects of fishing mortality and a constant M of 0.2. The system was more sensitive to changes in size-at-recruitment to the fishery than reduction in F at a constant size-at-recruitment.

The differences in spawning biomass-per-recruit estimates resulting from the distributed delay model have important management implications. If management

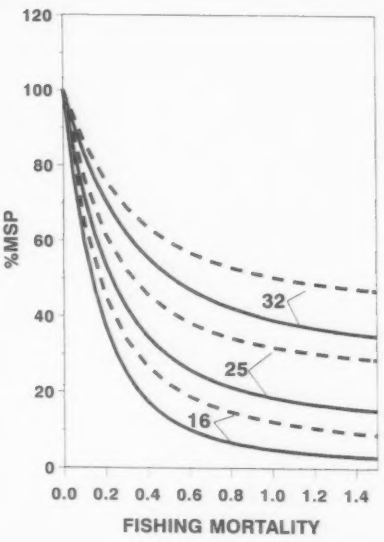

Figure 9

Percentage of maximum potential spawning biomass-per-recruit for black sea bass *Centropristis striata* under various fishing mortalities and lengths-at-first-capture (L_c) using the distributed delay model with transitions (dashed) and without transitions (solid).

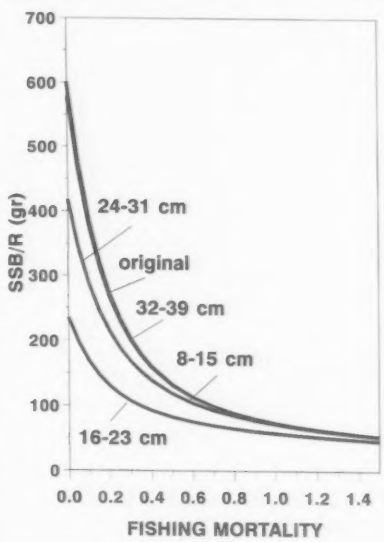

Figure 10

SSB/R for black sea bass *Centropristis striata* estimated under varying transition rates-at-length (L_c = 16 cm). Rates were increased 20% within each length-group indicated.

Table 3

SSB/R for black sea bass *Centropristis striata* as percentage of original values (and L_c=16 cm), where transformation rates have been doubled in differing 8 cm intervals.

F	8–15 cm	16–23 cm	24–31 cm	32–39 cm
0	99.7	39.1	69.5	96.3
0.1	99.7	43.3	74.0	97.2
0.2	99.7	47.9	78.6	98.0
0.3	99.7	52.8	82.9	98.6
0.4	99.7	57.6	86.6	99.1
0.5	99.7	62.1	89.6	99.4
0.6	99.8	66.1	92.0	99.6
0.7	99.8	69.7	93.9	99.8
0.8	99.8	72.9	95.3	99.9
0.9	99.8	75.7	96.4	99.9
1.0	99.8	78.2	97.2	99.9
1.1	99.8	80.4	97.9	100.0
1.2	99.8	82.4	98.4	100.0
1.3	99.8	84.2	98.7	100.0
1.4	99.9	85.8	99.0	100.0
1.5	99.9	87.2	99.2	100.0

were based on a target %MSP, the presence or absence of transition terms in the model would provide dramatically different interpretations. For instance, if the target %MSP were 30% with an F=0.8, and L_c=25 cm, the non-transitional model would indicate the situation was below the target at 22%, whereas the transitional model would place the current conditions above the target at 34%. It would be critical that calculation of SSB in the stock-recruitment relationship used for development of a target SSB/R (and associated %MSP) be made using a framework similar to calculation of SSB/R.

Beyond the issue of the model structure is the appropriateness of using spawning biomass models in general for management of hermaphroditic fishes. The complex social hierarchy of reef fishes (black sea bass can be considered a temperate reef fish) during spawning implies that the number of males may be an important factor limiting reproductive potential (Smith 1982). Recent theoretical studies suggest that males are not limiting in hermaphroditic sea bass populations to the degree that non-dominant males participate in spawning ("streakers") (Peterson 1991). If streakers are abundant, there would be no benefit for a female to transform only to engage in sperm competition with other spawning males. This suggests that under limited exploitation, the reproductive potential of the population is restricted in

terms of egg production. The possibility exists that exploitation could reach a level at which males are eliminated at such a rate that females are forced to transform faster or at an earlier size. The optimal sex ratio, from a behavioral perspective, has not yet been determined for *C. straita*. As suggested by the sensitivity analysis, substantial changes in the transformation rate could significantly alter the contributions of a cohort to the spawning biomass. There is no information currently available to determine the controlling mechanism or degree of plasticity for transformation rates within a population.

Future refinements of this distributed delay model may provide a more detailed picture of the effects of harvest on species such as black sea bass. Density-dependent feedback mechanisms influencing transition rates and age-at-first-transformation will ultimately be incorporated into the model to examine theoretical implications. A time-varying distributed delay model is also possible to account for seasonal changes in growth and mortality. With a minimal amount of growth information, either from back-calculations or tagging data, and some reasonable estimates of other important life-history events, we believe the distributed delay model can provide an effective length-based alternative to traditional dynamic pool models.

Citations

Alexander, M. S.
1981 Population response of the sequential hermaphrodite black sea bass, *Centropristis striata*, to fishing. M.S. thesis, State Univ. New York, Stony Brook, 104 p.

Bannerot, S., W. W. Fox Jr., & J. E. Powers
1987 Reproductive strategies and the management of snappers and groupers in the Gulf of Mexico and Caribbean. *In* Polovina, J. J., & S. Ralston (eds.), Tropical snappers and groupers, biology and fisheries management, p. 561–603. Westview Press, Boulder.

Beverton, R. J. H., & S. H. Holt
1957 On the dynamics of exploited fish populations. Fish. Invest., Ser. II, Mar. Fish., G. B. Minist. Agric. Fish. Food 19, 533 p.

Forrester, J. W.
1961 Industrial dynamics. MIT Press, Cambridge, 464 p.

Gabriel, W. L., M. P. Sissenwine, & W. J. Overholtz
1989 Analysis of spawning on biomass per recruit: an example for Georges Bank haddock. N. Am. J. Fish. Manage. 9:383–391.

Gulland, J.
1977 The analysis of data and development of models. In Gulland, J. (ed.), Fish population dynamics, p. 67–95. John Wiley, NY.

Gutierrez, A. P., M. A. Pizzamiglio, W. J. Dos Santos, R. Tennyson, & A. M. Villacorta
1984 A general distributed delay time varying life table plant population model: cotton (*Gossypium hirsutum* L.) growth and development as an example. Ecolog. Model. 26(1984): 231–249.

Gutierrez, A. P., B. Wermelinger, F. Schulthess, J.U. Baumgaertner, H. R. Herren, C. K. Ellis, & J. S. Yaninek
1988 Analysis of biological control of cassava pests in Africa. I. Simulation of carbon, nitrogen and water dynamics in cassava. J. Appl.Ecol. 25:901–920.

Idoine, J. S., & J. T. Finn
1984 A model of lobster growth. *In* Wade, W. D. (ed.), Proc., 1984 Summer Comput. Simul. Conf., p. 887–891. Soc. Comput. Simul., Boston.

Kirkpatrick, M.
1984 Demographic models based on size, not age, for organisms with indeterminate growth. Ecology 65(6):1874–1884.

Lavenda, N.
1949 Sexual differences and normal protogynous hermaphroditism in the Atlantic sea bass, *Centropristes striatus*. Copeia 3:185–194.

Low, R. A. Jr.
1981 Mortality rates and management strategies for black sea bass off the southeast coast of the United States. N. Am. J. Fish. Manage. 1:93–103.

Manetsch, T. J.
1976 Time-varying distributed delays and their use in aggregative models of large systems. IEEE (Inst. Electr. Electron. Eng.) Trans. Syst. Man Cybern. 6:547–553.

Mercer, L. P.
1978 The reproductive biology and population dybnamics of black sea bass, *Centropristis straita*. Ph.D. thesis, Coll. William & Mary, Williamsburg VA.

O'Brien, L., J. Burnett, & R. K. Mayo
1993 Maturation of nineteen species of finfish off the northeast coast of the United States, 1985–1990. NOAA Techn. Rep. NMFS 113, 67 p.

Petersen, C. W.
1991 Sex allocation in hermaphroditic sea basses. Am. Nat. 138(3):650–667.

Ravlin, F. W., R.I. Carruthers, V. Varadarajan, D. L. Haynes, & R. L. Tummala
1978 Simulation of a natural biological system in which two insect populations are attacked by a common parasite. Proc., Ninth. Annu. Pittsburgh Symp. Model. Simul., p. 117–123. Univ. Pittsburgh, Pittsburgh PA.

Ricker, W. E.
1954 Stock and recruitment. J. Fish. Res. Board Can. 11:559–623.

Russell, E. S.
1931 Some theoretical considerations on the "overfishing problem". J. Cons. Explor. Mer 6:3–27.

Schaub, L. P., & J. U. Baumgartner
1989 Significance of mortality and temperature on the phenology of *Orthotylus marginalis* (Heteroptera: Miridae). Mitt. Schweitz. Entomol. Ges. 62:235–245.

Smith, C. L.
1982 Patterns of reproduction in coral reef fishes. In Huntsman, G. R., W.R. Nicholson, & W. W. Fox Jr. (eds.), The biological bases for reef fishery management, p. 49–66. NOAA Tech. Memo. NMFS-SEC-80, NMFS Southeast Fish. Sci. Cent., Miami FL.

Thompson, W. F., & F. H. Bell
1934 Biological statistics of the Pacific halibut fishery. 2. Effects of changes in intensity upon total yield and yield per unit gear. Rep. Int. Halibut Comm., 49 p.

Vansickle, J.
1977 Attribution in distributed delay models. IEEE (Inst. Electr. Electron. Eng.) Trans. Syst. Man/Cybern. 7(9):635–638

Wenner, C. A., W. A. Roumillat, & C. W. Waltz
1986 Contributions to the life history of black sea bass, *Centropristis striata*, off the southeastern United States. Fish. Bull., U.S. 84:723–741.

Larval distribution patterns: Early signals for the collapse/recovery of Atlantic herring *Clupea harengus* in the Georges Bank area

Wallace G. Smith
Wallace W. Morse
Sandy Hook Laboratory, Northeast Fisheries Science Center
National Marine Fisheries Service, NOAA
Highlands, New Jersey 07732

Abstract.—Changing temporal and spatial distribution patterns of Atlantic herring *Clupea harengus* larvae collected off southern New England over two decades provided early signals of large-scale changes in adult spawning biomass that are now a matter of record. Four contrasting spawning patterns were evident during the 20 yr period. Each pattern covered successive multi-year intervals and reflected the corresponding status of the adult population. In 1971, spawning occurred throughout the Georges Bank/Nantucket Shoals/Massachusetts Bay study area. The principal spawning grounds of herring in the Gulf of Maine region were located on the Northeast Peak of Georges Bank. With the collapse of the Georges Bank fishery in 1976, spawning receded westward to Nantucket Shoals. By 1979, larvae occurred only in the Stellwagen Banks area of Massachusetts Bay, the smallest of the three subareas. After a 6 yr hiatus, spawning beds on Nantucket Shoals were reoccupied in 1985. By 1988 spawning had advanced eastward to Cultivator Shoals on Georges Bank, but through 1990 we found no evidence of renewed spawning activity on the historically-prominent spawning beds on Northeast Peak. The rebuilding process was attributed to recolonization rather than resurgence.

The Atlantic herring *Clupea harengus* has been a target species of broad-scale early-life-history research in the Gulf of Maine since 1956. The initial larval surveys were part of a collaborative study by U.S. and Canadian biologists to define the stock structure of herring in the Northwest Atlantic (Tibbo et al. 1958). This effort continued over two spawning seasons and was followed by annual observations on distribution patterns of herring larvae during 1962–70 (Boyar et al. 1973b). Thereafter, U.S. biologists participated in a multinational field program that represented the starting point of the Northeast Fisheries Science Center's (NEFSC) current database for larval herring. This study, sponsored by the International Commission for the Northwest Atlantic Fisheries (ICNAF), was initiated in 1971 to identify mechanisms that influence survival of larvae (Lough et al. 1985).

With the termination of ICNAF larval herring surveys in 1977, NEFSC began a comprehensive fisheries ecosystem study of the Northeast Shelf Ecosystem (Sherman 1986, Smith 1988). This program, known as Marine Resources Monitoring, Assessment and Prediction (MARMAP), included standardized year-round surveys of fish eggs and larvae to provide baselines against which shifts in species composition and diversity within the finfish community could be observed and evaluated. These surveys continued for 11 years, ending in December 1987.

In 1988, ecosystems research emphasis at NEFSC shifted away from year-round surveys of the entire Northeast Shelf Ecosystem and focused on the Georges Bank area during autumn and winter. The new initiative was designed to document the changing status of herring and investigate density-dependent population regulation between herring and sand lance *Ammodytes* spp., important coastal pelagic species in the western North Atlantic. When combined, the three multi-year research endeavors conducted since 1971 provide an uninterrupted 20 yr database for larval herring in the Georges Bank/Nantucket Shoals/Massachusetts Bay area. During this period, dramatic changes occurred in the herring population.

Spawning biomass was relatively high at the onset of the ICNAF larval herring surveys in 1971, although in decline due to intense foreign fishing pressure that began in the mid 1960s. During the 1960s and continuing through the mid 1970s, biomass of herring on Georges Bank was estimated at 400,000–600,000 t. Annual catches ranged from 150,000 to 374,000 t. Dominating the population during the 1960s were three year-classes, 1956, 1960, 1961, and to a lesser extent 1966, although spawning success was poor in the closing years of the decade. Despite a strong 1970 year-class that entered the Georges Bank fishery in 1973, fishing

Manuscript accepted 8 February 1993.
Fishery Bulletin, U.S. 91:338-347 (1993).

pressure by the large international fleet was so intense that landings declined after 1971. From 1973 to 1975 the principal herring landings shifted from the bank to the vicinity of Great South Channel, just east of Nantucket Shoals. After 15yr of moderate-to-heavy exploitation, and several years of quota management under ICNAF, the Georges Bank herring fishery collapsed in 1976 (Anthony & Waring 1980).

This paper examines the 20yr larval database to look for early signals of the dramatic changes in adult biomass that have occurred since 1971. We evaluate the influence of transport mechanisms on the spatial and temporal distribution patterns of larvae to corroborate the herring stock hypothesis of Iles & Sinclair (1982) and Sinclair & Iles (1985). Finally, we search for supporting evidence that the late-1980s recovery of herring in the Georges Bank area resulted from population resurgence rather than recolonization, a conclusion of Stephenson & Kornfield (1990).

Methods

The 20yr time-series began during the final years of the international fishery. It included a 10yr period when essentially no fishing took place in the study area, and ended with the 1990 spawning season when a limited fishery was again underway. Without a directed fishery after 1976, this dataset, along with NEFSC semi-annual trawl surveys, provided the only source of information to evaluate the status of herring in the Georges Bank area for more than a decade.

Sampling designs

All three larval surveys used the 61cm bongo, fitted with 0.333 and 0.505mm mesh nets. Larval herring catches from the 0.505mm net were analyzed. Net mesh selection was based on recommendations in Smith & Richardson (1977) and on Colton et al. (1980) who found no significant difference in retention rates of herring larvae captured in the two mesh sizes.

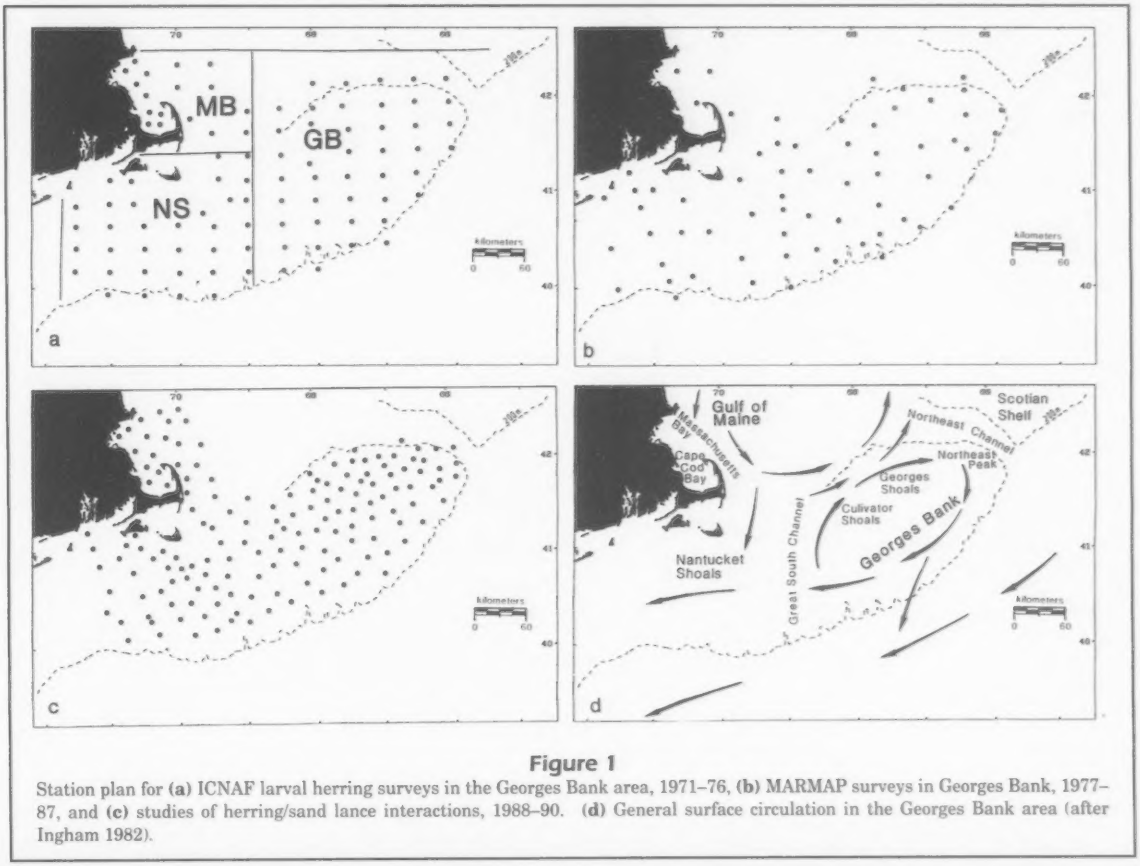

Figure 1

Station plan for **(a)** ICNAF larval herring surveys in the Georges Bank area, 1971–76, **(b)** MARMAP surveys in Georges Bank, 1977–87, and **(c)** studies of herring/sand lance interactions, 1988–90. **(d)** General surface circulation in the Georges Bank area (after Ingham 1982).

The ICNAF larval herring program included the entire Gulf of Maine region but concentrated on the Nantucket Shoals/Georges Bank area (Lough & Bolz 1979a, Lough et al. 1985). The 33 surveys conducted between 1971 and 1976 were used in our analysis. ICNAF participants deployed the bongo at 50 m/min to a maximum depth of 100 m and retrieved it in a smooth oblique profile at 10 m/min. Towing speed was 3.5 kn at stations spaced at 28–37 km intervals on a standard grid pattern (Fig. 1a). Additional stations in areas of high larval abundance were sampled after 1974. Lough & Bolz (1979b) provided a detailed account of sampling operations and cruises for the ICNAF time-series.

MARMAP surveys, conducted at monthly to bimonthly intervals, covered the continental shelf from Cape Hatteras, North Carolina to Cape Sable, Nova Scotia. Cruise activities were described by Sibunka & Silverman (1984, 1989). MARMAP surveys fished the 61cm bongo to a maximum depth of 200 m with payout at 50m/min and retrieval at 20 m/min. Ship speed varied between 1 and 2 kn to maintain a 45° angle in the towing wire. Station intervals ranged from 15 to 45 km (Fig. 1b).

The herring recovery study initiated in 1988 employed MARMAP sampling methods. Cruises were conducted at about monthly intervals and occupied 151 stations in the Nantucket Shoals/Massachusetts Bay/Georges Bank study area (Fig. 1c).

Data analysis

We adjusted the number of larvae caught at each station in the time-series to reflect day/night/twilight catch differences (see Morse 1989). Larvae were partitioned into size-intervals to depict changes in distribution patterns over time. When the partitioned size-intervals of 4.0–7.9 mm, 8.0–12.9 mm, 13.0–17.9 mm, and >17.9 mm were corrected for shrinkage (see Theilacker 1980), they approximated age-groups of <2 wk, 2–5 wk, 5–8 wk, and >8 wk, respectively (Lough et al. 1982). Surveys were grouped by multi-year periods that represented time-intervals between the most apparent changes in spawning patterns during the 20 yr period. Figures showing mean numbers of larvae per 10 m^2 surface area were based on methods recommended for the delta distribution (Pennington 1983). Distributions of larvae grouped by age over time are discussed in relation to circulation patterns shown in Fig. 1 d.

Results

Changes in distribution and abundance of herring larvae during the 20 yr time-series reflected four contrasting spawning patterns that spanned successive multi-year intervals. Larvae were abundant on both Nantucket Shoals and Georges Bank, but not so in Massachusetts Bay, during 1971–75. Conversely, we found low to no measurable numbers of larvae on Nantucket Shoals and Georges Bank during 1976–84, a period when spawning activity increased in Massachusetts Bay. Spawning resumed on Nantucket Shoals in 1985. During 1985–87, larval abundance peaked in Massachusetts Bay but the center of spawning activity shifted to Nantucket Shoals.

Herring were again spawning on the western half of Georges Bank in 1988. The dramatic increase in spawning activity on Nantucket Shoals and renewed spawning on western Georges Bank during 1988–90 elevated larval abundance estimates to their highest levels during the closing years of the time-series (Fig. 2).

When the time-series began in 1971, Georges Bank had been the principal spawning grounds for herring

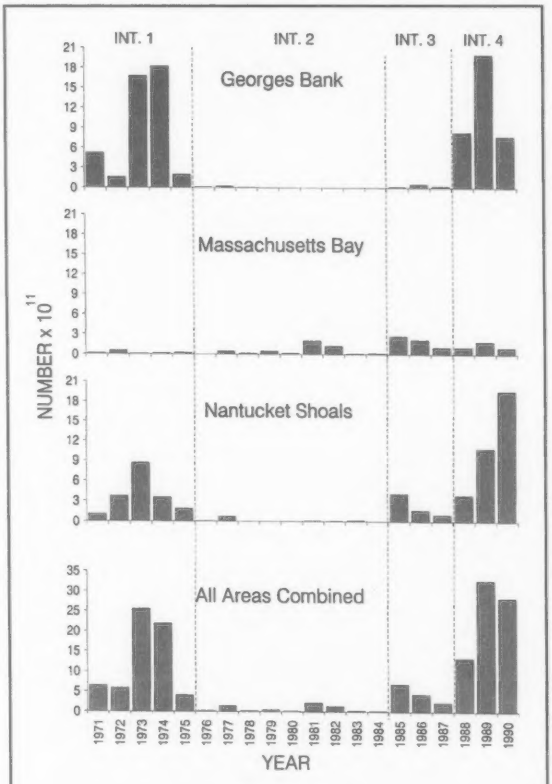

Figure 2

Changes in abundance of Atlantic herring *Clupea harengus* larvae by subarea during the 20yr time-series. Intervals (Int) represent multi-year periods that reflect the most apparent changes in spawning patterns.

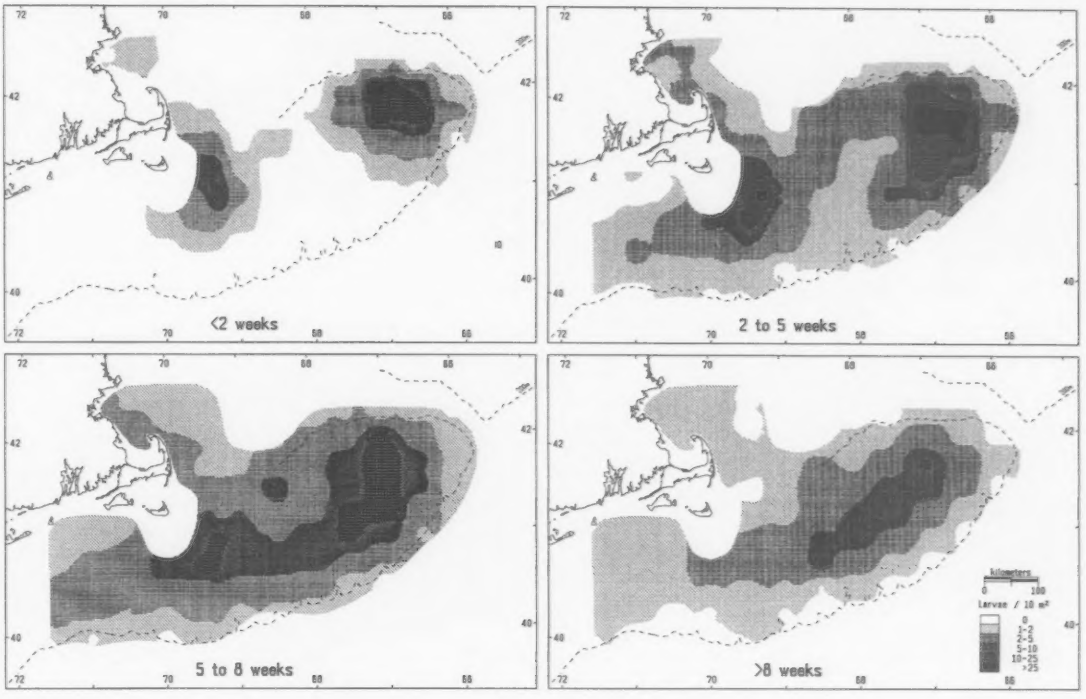

Figure 3
Composite representation of the distribution of Atlantic herring *Clupea harengus* larvae by age in the Georges Bank area, 1971–75.

in the western North Atlantic for at least 15yr (Tibbo et al. 1958, Boyar et al. 1973b, Anthony & Waring 1980, Lough et al. 1985, Grosslein 1987). The magnitude of spawning activity, as measured by the abundance of larvae, was low in 1971 and 1972 but increased sharply in 1973 and continued upward in 1974, the initial spawning years of the strong 1970 year-class. In 1975, larval abundance on Georges Bank declined dramatically and spawning activity on Nantucket Shoals equaled that on the bank. By 1976, when surveys showed only negligible spawning activity east of the 69° meridian, Georges Bank had lost its longstanding status as the principal spawning ground for herring in the western North Atlantic (Fig. 2).

ICNAF surveys of 1971–75 identified two geographically-separate spawning areas: one centered along the eastern edge of Nantucket Shoals, the other on northeastern Georges Bank (Fig. 3). Within 2–5 wk of hatching, larvae began to disperse and the two spawning centers were no longer discrete. At 5–8 wk after hatching, some larvae originating on the Northeast Peak were transported westward across the southern half of Georges Bank by anticyclonic currents. Together with larvae from Nantucket Shoals, their distribution extended over shelf waters from Cape Cod eastward and continued into adjacent slope waters. Although distributions of both Nantucket Shoals and Georges Bank larvae exhibited the influence of known circulation patterns within 5 wk of hatching (Fig. 1d), centers of abundance remained near their points of origin for at least 8 wk. Thereafter, a single center of abundance for larvae >8 wk old emerged over the shallow central part of Georges Bank (Fig. 3).

Herring larvae in all four age-groups occurred largely in coastal waters immediately adjacent to Cape Cod during the 1976–84 time-interval, a distribution pattern that differed significantly from those observed during the first 5yr of the time-series (Fig. 4). We found no larvae <2 wk old on Georges Bank in 1977. In 1978, only a few larvae in the youngest grouping were caught over the once-productive Northeast Peak. For the next decade, we caught no recently-hatched larvae anywhere on Georges Bank. Larvae <2 wk old were essentially absent on Nantucket Shoals during the 1976–84 time-interval as well. The center of larval abundance in each of the four groupings occurred in Massachusetts

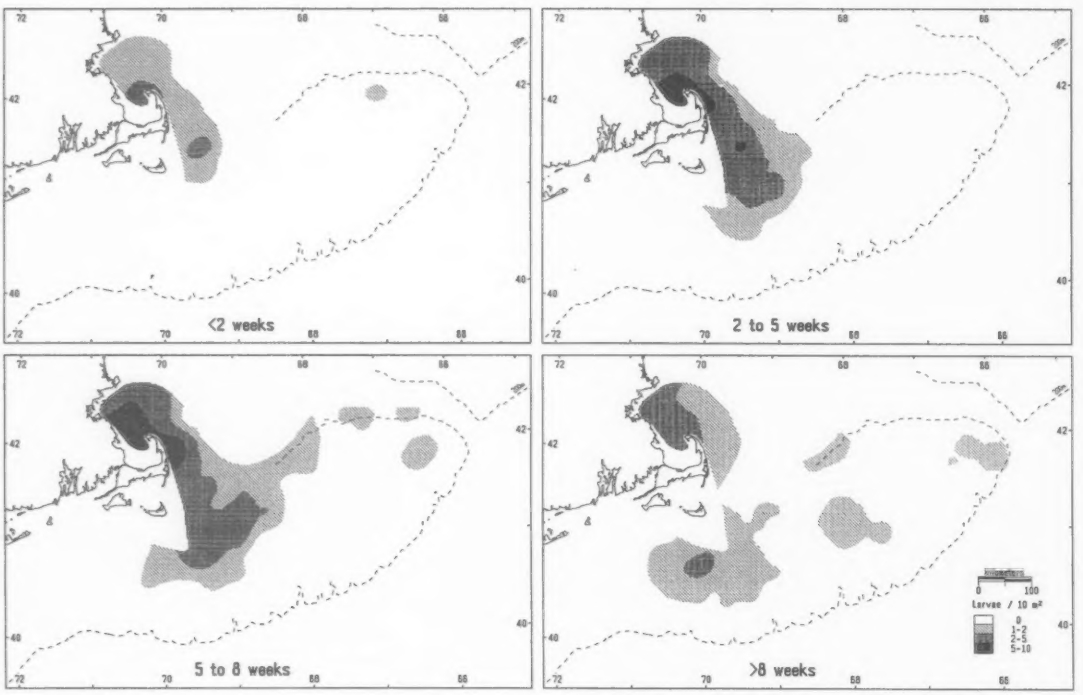

Figure 4
Composite representation of the distribution of Atlantic herring *Clupea harengus* larvae by age in the Georges Bank area, 1976–84.

and Cape Cod bays. As during the 1971–75 interval, larvae partitioned by age exhibited the influence of transport, especially in 1981 and 1982 when distribution patterns expanded from Massachusetts Bay to Nantucket Shoals. Averaging catches over a 9 yr period did not mask the effects of larval transport during the 1981 and 1982 spawning seasons (Fig. 4).

Further change marked the ensuing 3 yr period (1985–87), providing the first evidence that the herring population in the study area was beginning to recover. Spawning beds on Nantucket Shoals were reactivated in 1985, and the center of larval abundance shifted from Massachusetts Bay to Nantucket Shoals (Fig. 5). The influences of advective processes on the distribution of larvae were evident within a month after hatching. Nantucket Shoals larvae 2–5 wk old were transported by the Georges Bank gyre eastward across the northern part of the bank as far as the 68° meridian. The distribution pattern of 5–8 wk old larvae resembled that of 2–5 wk old fish, but exhibited the influence of further drift away from the Nantucket Shoals spawning beds. Larvae >8 wk old were caught in Massachusetts Bay and from Nantucket Shoals eastward onto Georges Bank. As in the 1976–84 period, no recently-hatched larvae occurred over the traditional spawning beds on eastern Georges Bank through 1987 (Fig. 5).

The reoccupation of spawning beds on the western half of Georges Bank and the increasing abundance of larvae on Nantucket Shoals during 1988–90 provided further signals of the changing status of herring in the study area (Fig. 6). Although the principal spawning grounds remained on Nantucket Shoals, the appearance of recently-hatched larvae on Georges and Cultivator shoals in all 3 yr provided the first evidence in a decade of spawning east of the 68° meridian on Georges Bank. Within 5 wk of hatching, larvae were dispersed over all but the eastern tip of the bank. By the time larvae reached 8 wk of age, they occurred throughout the study area (Fig. 6). As with the reactivation of Nantucket Shoals spawning beds in 1985, 3 yr lapsed from the time we first observed larval transport onto Georges Bank until we found evidence of spawning on the bank. Although the recovery of herring in the Georges Bank region was clearly underway during the closing years of the 1980s, we found no evidence in

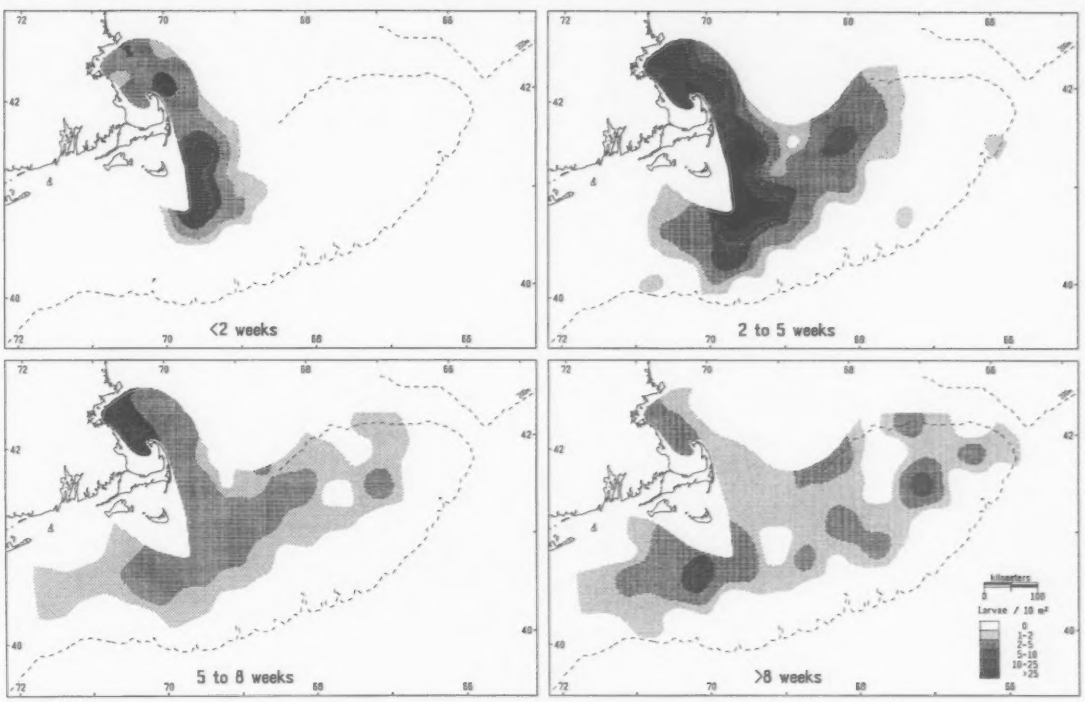

Figure 5

Composite representation of the distribution of Atlantic herring *Clupea harengus* larvae by age in the Georges Bank area, 1985–87.

larval distribution patterns through the 1990 spawning season that the historically prominent spawning beds on eastern Georges Bank had been reoccupied.

Discussion

The literature contains conflicting descriptions of the herring population structure in the western North Atlantic. Iles & Sinclair (1982) hypothesized that the number of Atlantic herring spawning stocks in the Gulf of Maine region is determined by the number of geographically-stable larval retention areas. They recognized four stocks: southwest Nova Scotia, Grand Manan, Georges Bank, and Nantucket Shoals. Sinclair & Iles (1985) revised the stock structure to include Jeffreys Ledge, coastal Gulf of Maine, and Scots Bay. Both Iles & Sinclair (1982) and Sinclair & Iles (1985) further hypothesized that (1) stocks are segregated only during autumn when herring return to their respective spawning grounds, (2) larvae of different stocks do not intermix for several months after hatching, the period when imprinting occurs, and (3) hydrographic conditions create retention areas by isolating larvae in vertically-mixed areas surrounded by stratified waters. Their retention hypothesis recognized that the geographic extent of the retention areas could vary annually and that some horizontal displacement could occur during larval development.

Grosslein (1987) reviewed the stock structure of herring in the Gulf of Maine region using the collective evidence from prior studies. He concluded that the population was composed of three major stocks: Georges Bank, western Nova Scotia, and the Gulf of Maine, with lesser spawning occurring elsewhere around the gulf. Grosslein indicated, however, that this breakdown was speculative and that direct attempts to differentiate between stocks through larval surveys, tagging studies, meristic and morphometric characters, biochemical methods, and parasitology produced inconclusive results.

Smith & Jamieson (1986) argued that no scientific basis existed for the stock concepts of Atlantic herring in either the eastern or western North Atlantic. They viewed the breakdown of herring stocks as transient subdivisions having no taxonomic or evolutionary

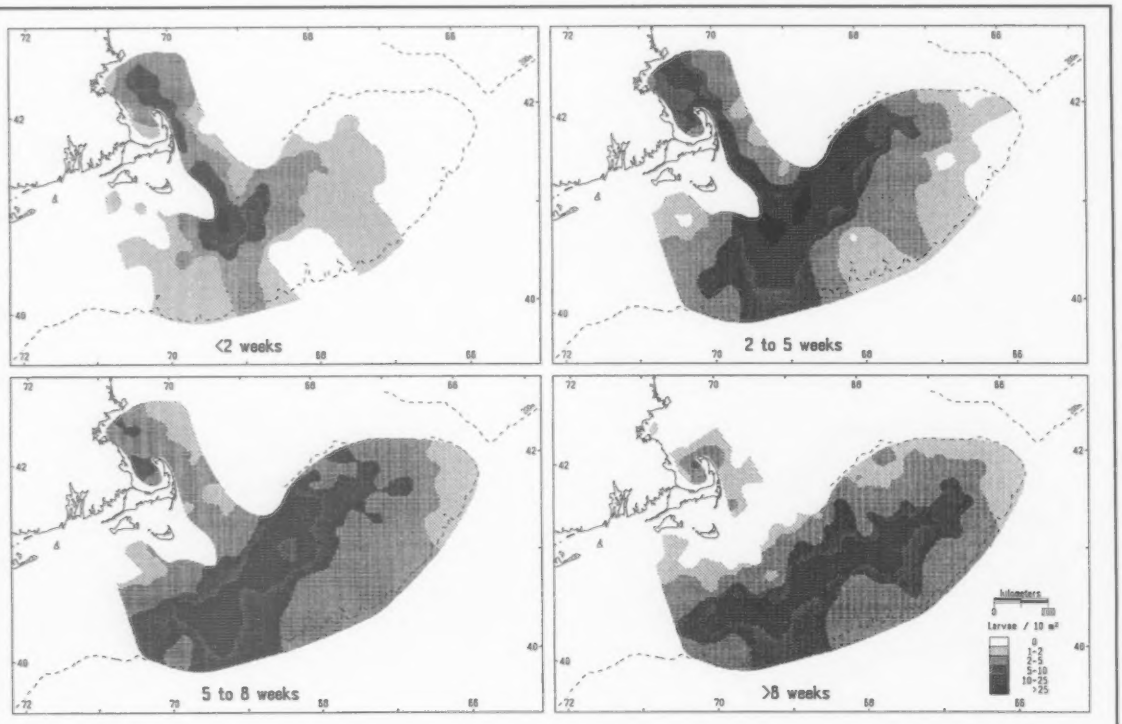

Figure 6
Composite representation of the distribution of Atlantic herring *Clupea harengus* larvae by age in the Georges Bank area, 1988–90.

status. Cushing (1986) also took exception to the retention hypothesis as applied by Iles & Sinclair (1982) to the North Sea area. Cushing (1986) noted that herring do not always spawn in transition zones around the British Isles and, where they do, the fronts brake down within a month after hatching. He further dismissed the retention concept by demonstrating that postlarval metamorphosis takes place near the nursery grounds after prolonged larval drift.

Our analysis of the 20 yr larval time-series supports that segment of the literature showing herring larvae vulnerable to advection after hatching (e.g., Cushing 1986, Bartsch et al. 1989, Heath & Walker 1987). Although transport in our dataset is not extensive, it is not restricted to the retention areas described by Sinclair & Iles (1985). Larvae drift from Massachusetts Bay southward to Nantucket Shoals, and the anticyclonic gyre on Georges Bank mixes larvae originating there with those spawned on the shoals. The direction of transport generally corresponds with reported circulation, a pattern consistent with that of Parrish et al. (1981). Mixing of larvae from the three subareas occurs within weeks after hatching, or earlier in the life cycle than proposed by Sinclair & Tremblay (1984) and Sinclair & Iles (1985).

Drift trajectories of herring larvae from other studies in the Gulf of Maine region agree with our findings in that they correspond to dominant circulation patterns described by Ingham (1982) and Butman & Beardsley (1987). Graham et al. (1972) and Graham (1982) recognized that some herring larvae spawned off eastern Maine drifted westward to mix with larvae originating in central and western Maine waters. Townsend et al. (1986) provided further evidence that herring larvae off Maine are advected from east to west. Although Chenoweth et al. (1989) noted that residual currents do not demonstrate a persistent flow in any direction off eastern Maine, they too observed a westward displacement of herring larvae. Finally, Boyar et al. (1973a) showed herring larvae spawned on Jeffreys Ledge, another of the retention areas of Sinclair & Iles (1985), drifting into Massachusetts Bay where they could mix with larvae originating on and around Stellwagen Bank. Given these reports of drift and mixing in western Gulf of Maine waters near our study area and the demonstrated dispersion and

mixing of early-stage larvae reported here, we see no compelling argument for the separation of herring stocks through larval retention in the western Gulf of Maine and Georges Bank areas.

We consistently found sufficient larval drift and mixing to question the stock structure of Sinclair & Iles (1985) in the Georges Bank region. However, Figs. 3–6 lend some support to the retention hypothesis by showing that a significant portion of the larvae up to 8wk old remained near their points of origin. Campana et al. (1989a, 1989b) reported similar results for haddock *Melanogrammus aeglefinus* and Atlantic cod *Gadus morhua* larvae, respectively, on Browns Bank. Some larvae of the two species were transported shoreward while others remained near the spawning grounds longer than known water residence time. Both of the 1989 studies concluded that the instability of the Browns Bank gyre accounted for the dichotomous distribution patterns. They interpreted the onshore drift as an all-or-none situation for individual larvae. Some readily exited the influence of a weakly established gyre, while most were retained during periods of pronounced gyral circulation. In our view, their theory provides a more plausible explanation for the shifting distribution patterns of herring larvae around Georges Bank, an area also influenced by gyral circulation, than the stock hypothesis proposed by Iles & Sinclair (1982).

Stephenson & Kornfield (1990) attributed the increasing biomass of herring on Georges Bank during the late 1980s to the resurgence of residual fish rather than to recolonization by fish from surrounding areas. Based largely on a 4 yr dataset that excluded Nantucket Shoals and Massachusetts Bay, they concluded that (1) adult herring caught on Georges Bank differed in age composition from herring on Jeffreys Ledge and southwestern Nova Scotia, (2) some of the Georges Bank herring exhibited different isoenzyme characteristics than neighboring herring, and (3) the return of herring to Georges Bank took longer than they expected through recolonization.

In our view, the change in spawning sites on Georges Bank during the 20 yr time-series, coupled with the recession and subsequent expansion of the spawning range over time, makes a convincing case for recolonization rather than resurgence. Larval distribution patterns on Georges Bank during the closing years of the time-series differed markedly from those observed at the outset of the program. Whereas recently-hatched larvae were concentrated on Northeast Peak during the initial survey years, their distribution on the bank progressed eastward only as far as Georges Shoals during the final years of survey activity. If, as proposed by Stephenson & Kornfield (1990), resurgence of residual fish accounted for the recovery of spawning herring on the bank, we would expect little or no change in the location of spawning centers over time. Instead, our 20 yr time-series shows dramatic change.

When the herring population in the study area declined in the early 1970s, its spawning range receded from Georges Bank to Massachusetts Bay. As the population began to grow in the 1980s, the spawning range expanded, initially from Massachusetts Bay to Nantucket Shoals, then from the shoals to Georges Bank. Whether the recovery resulted from an expanding adult population, from fortuitous transport and survival of larvae, or from a combination of the two, is not clear. However, it is worth noting that the reoccupation of spawning beds on both Nantucket Shoals and Georges Bank occurred 3–4 yr after we first observed evidence of larval drift towards these two subareas. This time period, perhaps coincidently, represents the age-at-maturity for Atlantic herring.

Acknowledgments

Although too numerous to mention individually, we herewith acknowledge everyone involved in the collection of the 8590 plankton samples that form the basis of this document; our colleagues at the Polish Sorting Center in Szczecin for their diligence and perseverance in sorting the samples; the technicians and biologists responsible for implementing quality control, data entry, and database management procedures; and those who reviewed earlier drafts of the manuscript and provided constructive comment.

Citations

Anthony V., & G. Waring
1980 The assessment and management of the Georges Bank herring fishery. Rapp. P.-V. Reun. Cons. int. Explor. Mer 177:72–111.

Bartsch, J., K. Brander, M. Heath, P. Munk, K. Richardson, & E. Svendsen
1989 Modelling the advection of herring larvae in the North Sea. Nature (Lond.) 340:632–636.

Boyar, H., R. Cooper, & R. Clifford
1973a A study of the spawning and early life history of herring (*Clupea harengus harengus* L.) on Jeffreys Ledge in 1972. Int. Comm. Northwest Atl. Fish. Res Doc. 73/96, 27p.

Boyar, H., R. Marak, F. Perkins, & R. Clifford
1973b Seasonal distribution and growth of larval herring (*Clupea harengus* L.) in the Georges Bank-Gulf of Maine area from 1962–1970. J. Cons. Cons. Int. Explor Mer 35:36–51.

Butman, B., & R. Beardsley
1987 Physical oceanography. *In* Backus, R., & D. Borne (eds.), Georges Bank, p.88–98. MIT Press, Cambridge.

Campana, S., S. Smith, & P. Hurley
1989a A drift retention dichotomy for larval haddock (*Melanogrammus aeglefinus*) spawned on Browns Bank. Can. J. Fish. Aquat. Sci. 46 (Suppl. 1): 93–102.
1989b An age-structured index of cod larval drift and retention in the waters of southwest Nova Scotia. Rapp.-V Reun. Cons. Int. Explor. Mer 191:50–62.

Chenoweth, S., D. Libby, R. Stephenson, & M. Powers
1989 Origin and dispersion of larval herring (*Clupea harengus*) in coastal waters of eastern Maine and southwestern New Brunswick. Can. J. Fish. Aquat. Sci. 46:624–632.

Cushing, D.
1986 The migration of larval and juvenile fish from spawning grounds to nursery grounds. J. Cons. Cons. Int. Explor. Mer 43:43–49.

Colton, J., J. Green, R. Byron, & J. Frisella
1980 Bongo net retention rates as effected by towing speed and mesh size. Can. J. Fish. Aquat. Sci. 37:606–623.

Graham, J.
1982 Production of larval herring, *Clupea harengus*, along the Maine coast. J. Northwest Atl. Fish. Sci. 3:63–85.

Graham, J., S. Chenoweth, & C. Davis
1972 Abundance, distribution, movements and lengths of larval herring along the western coast of the Gulf of Maine. Fish. Bull., U.S. 70:307–321.

Grosslein, M.
1987 Synopsis of knowledge of the recruitment process for Atlantic herring, *Clupea harengus*, with special reference to Georges Bank. NAFO (Northwest Atl. Fish. Organ.) Sci. Counc. Stud. 11:91–108.

Heath, M., & J. Walker
1987 A preliminary study of the drift of larval herring (*Clupea harengus* L.) using gene-frequency data. J. Cons. Cons. Int. Explor. Mer 43:139–145.

Iles, T., & M. Sinclair
1982 Atlantic herring: stock discreetness and abundance. Science (Wash. DC) 215:627–633.

Ingham, M. (editor)
1982 Summary of the physical oceanographic processes and features pertinent to pollution distribution in the coastal and offshore waters of the northeastern United States, Virginia to Maine. NOAA Tech. Memo. NMFS-F/NEC-17, NMFS Northeast Fish. Sci. Cent., Woods Hole MA, 166 p.

Lough, R., & G. Bolz
1979a Abundance of sea herring (*Clupea harengus* L.) larvae in relation to spawning stock size and recruitment for the Gulf of Maine and Georges Bank, 1968–1978. Ref. Doc. 79–50, NMFS Woods Hole Lab, 13 p.
1979b A description of the sampling methods, and larval herring (*Clupea harengus* L.) data report for surveys conducted from 1968–1978 in the Georges Bank and Gulf of Maine areas. Ref. Doc. 79–60, NMFS Woods Hole Lab., 23 p.

Lough, R., M. Pennington, G. Bolz, & A. A. Rosenberg
1982 Age and growth of larval Atlantic herring, *Clupea harengus* L., in the Gulf of Maine-Georges Bank region based on otolith growth increments. Fish. Bull., U.S. 80:187–199.

Lough, R., G. Bolz, M. Pennington, & M. Grosslein
1985 Larval abundance and mortality of Atlantic herring (*Clupea harengus* L.) spawned in the Georges Bank and Nantucket Shoals areas, 1971–78 seasons, in relation to spawning stock size. J. Northwest Atl. Fish. Sci. 6:21–35.

Morse, W.
1989 Catchability, growth and mortality of larval fishes. Fish. Bull., U.S. 87:417–446.

Parrish, R., C. Nelson, & A. Bakun
1981 Transport mechanisms and reproductive success of fishes in the California Current. Biol. Oceanogr. 1(2):175–203.

Pennington, M.
1983 Efficient estimators of abundance for fish and plankton surveys. Biometrics 39:281–286.

Sherman, K.
1986 Measurement strategies for monitoring and forecasting variability in large marine ecosystems. *In* Sherman, K., & L. Alexander (eds.), Variability and management of large marine ecosystems, p. 203–236. AAAS Sel. Symp. 99.

Sibunka, J., & M. Silverman
1984 MARMAP surveys of the continental shelf from Cape Hatteras, North Carolina to Cape Sable, Nova Scotia (1977–1983). Atlas 1. Summary of operations. NOAA Tech. Memo. NMFS-F/NEC-33, NMFS Northeast Fish. Sci. Cent., Woods Hole MA, 306 p.
1989 MARMAP surveys of the continental shelf from Cape Hatteras, North Carolina to Cape Sable, Nova Scotia (1984–1987). Atlas 3. Summary of operations. NOAA Tech. Memo. NMFS-F/NEC-68, NMFS Northeast Fish. Sci. Cent., Woods Hole MA, 197 p.

Sinclair, M., & T. Iles
1985 Atlantic herring (*Clupea harengus*) distribution in the Gulf of Maine - Scotian Shelf area in relation to hydrographic features. Can. J. Fish. Aquat. Sci. 42:880–887.

Sinclair, M., & M. Tremblay
1984 Timing of spawning of Atlantic herring (*Clupea harengus harengus*) populations and the match-mismatch theory. Can. J. Fish. Aquat. Sci. 41:1055–1065.

Smith, P., & A. Jamieson
1986 Stock discreetness in herring: a conceptual revolution. Fish. Res. (Amst.) 4:223–234.

Smith, P., & S. Richardson
1977 Standard techniques for pelagic fish egg and larval surveys. FAO Fish. Tech. Pap. 175, 100 p.

Smith, W. (editor)
1988 An analysis and evaluation of ichthyoplankton survey data from the Northeast Continental Shelf ecosystems. NOAA Tech. Memo. NMFS-F/NEC-57, NMFS Northeast Fish. Sci. Cent., Woods Hole MA, 132 p.

Stephenson, R., & I. Kornfield
1990 Reappearance of spawning Atlantic herring (*Clupea harengus harengus*) on Georges Bank: population resurgence not recolonization. Can. J. Fish. Aquat. Sci. 47:1060–1064.

Theilacker, G.
1980 Changes in body measurements of larval northern anchovy, *Engraulis mordax*, and other fishes due to handling and preservation. Fish. Bull. U.S. 78:685–692.

Tibbo, S., J. Legare, L. Scattergood, & R. Temple
1958 On the occurrence and distribution of larval herring (*Clupea harengus* L.) in the Bay of Fundy and Gulf of Maine. J. Fish. Res. Board Can. 15:1451–1469.

Townsend, D., J. Graham, & D. Stevenson
1986 Dynamics of larval herring (*Clupea harengus* L.) production in tidally mixed waters of the eastern coastal Gulf of Maine. *In* Bowman, J., C. Yentsch, & W.T. Peterson (eds.), Tidal mixing plankton dynamics, p. 253–277. Springer-Verlag, Berlin.

Relative abundance of pelagic resources utilized by the California purse-seine fishery: Results of an airborne monitoring program, 1962–90

James L. Squire, Jr.

Southwest Fisheries Science Center
National Marine Fisheries Service, NOAA
8604 La Jolla Shores Drive, La Jolla, California 92038

Abstract. – During the period 1962–90, an aerial monitoring program conducted in cooperation with aerial spotters searching for pelagic fishes off California and Baja California, Mexico resulted in the development of an index of apparent abundance for six species of fishes: the northern anchovy *Engraulis mordax*, Pacific sardine *Sardinops sagax*, Pacific bonito *Sarda chiliensis*, Chub mackerel *Scomber japonicus*, jack mackerel *Trachurus symmetricus*, and bluefin tuna *Thunnus thynnus*. Northern anchovy was the dominant species observed, accounting for 89.7% of tonnage recorded during 1962–90. Chub mackerel comprised 6.1% of the total tonnage, jack mackerel 2.1%, Pacific sardine 1.0%, Pacific bonito 0.6%, and bluefin tuna 0.5%.

Apparent abundance indices were computed by dividing the tonnage observed by the number of "block areas" (10' lat. × 10" long.) searched, expressed as tons/block area flown (T/BAF). Indices were calculated for the total area and for the core area of distribution and abundance for each species. All species exhibited large fluctuations in apparent abundance over time. The apparent abundance index for Pacific sardine declined to a very low level during 1966–83. A substantial increase in abundance occurred during the mid- to late-1980s, with the 1990 index value 58 times that observed during the early 1960s. The chub mackerel abundance index declined to a very low level during 1966–76, then increased to a record high value in 1978 and has since declined. The northern anchovy abundance index increased in the early 1970s, with high abundance levels recorded during 1972–81, and then declined sharply to very low levels in the 1980s. The Pacific bonito abundance index was high during 1965–67 and 1983–85, with current levels well below the long-term mean. Very high abundance index levels for jack mackerel were recorded during 1975–79, then declining to very low levels in the 1980s. The bluefin tuna abundance index increased during 1972–80, declining to very low index values since. Based on these data, several species appear to be fluctuating unpredictably with respect to species abundance over time.

Aerial indices were compared with available total, spawning, and larval biomass estimates developed for several species. The most significant correlation of the aerial index was between the northern anchovy and Pacific sardine larval indices.

The rapid decline of the Pacific sardine *Sardinops sagax* fishery in the late 1940s resulted in increased research by the State of California Department of Fish and Game (CDF&G), Federal Government, and other institutions to determine the underlying principles that govern the sardine's behavior, availability to the fishery, and total abundance (Clark & Marr 1955, Sette 1969, Radovich 1982). Catch-per-unit-effort (CPUE) studies of the sardine purse-seine fishery off California did not indicate a significant decline in abundance until just prior to the fishery collapse (Fox 1974). Fisheries tend to target their fishing effort in areas of high densities of fishes (Radovich 1982, Squire & Au 1990), hence CPUE may not accurately reflect resource abundance (de La Mare 1984; J.B. Phillips, CDF&G, pers. commun., 1954). Clark & Marr (1955) concluded that, in addition to other information needs, better information is needed on changes in availability of sardine to the fishery. Related to this is the need for better real-time measures of trends in apparent abundance for successful management of pelagic schooling resources.

In the mid-1950s, the use of aircraft in searching and fishing operations of the California purse-seine fleet had become well established, as was the case in many other U.S. fisheries (Squire 1961). Having had experience in conducting commercial aerial fish spotting and several aerial fish-resource surveys, I initiated a pelagic monitoring program in the fall of 1962, with the cooperation of aerial fish-spotter pilots searching for fish for the commercial purse-seine fishery off central and southern California. The purpose of the program was to develop an effective method of measuring apparent abundance and monitoring changes in abundance. In the case of aerial observations, the concentrations of fish observed may or may not be subjected to fishing.

This paper updates the analysis of apparent abundance data collected by the aerial monitoring program from the first full year of data, 1963–90, using different analytical methods than used in earlier papers (Squire 1972, 1983). It also reviews the trends in apparent abundance during the period 1963–90 for six pelagic species by geographical area and compares the relation of the aerial abundance estimates to other independent biomass estimates made for the same species. The term "apparent abundance" (Marr 1951) refers to that portion of total abundance that is available to the fishery.

Manuscript accepted 28 January 1993.
Fishery Bulletin, U.S. 93:348-361 (1993).

Species included in this study are the northern anchovy *Engraulis mordax*, Pacific sardine *Sardinops sagax*, Pacific bonito *Sarda chiliensis*, chub mackerel *Scomber japonicus*, jack mackerel *Trachurus symmetricus*, and bluefin tuna *Thunnus thynnus*. These species, along with market squid *Loligo opalescens*, are the primary targets of the commercial purse-seine fleet based in San Pedro, California. Most are also fished by the southern California sportfishing fleet. The species are members of a complex interacting coastal and oceanic ecosystem that crosses international boundaries (Sette 1969).

Methods

Procedures for collection and tabulation of data

Since the fall of 1962, fish-spotter pilots have been directed to complete a flight logchart at the termination of each spotting flight. These pilots were instructed to draw their flight track on the chart and record the locations of all schools of fish species observed, along with their best estimates of tonnage observed. These data were recorded either as total tonnage of fish in

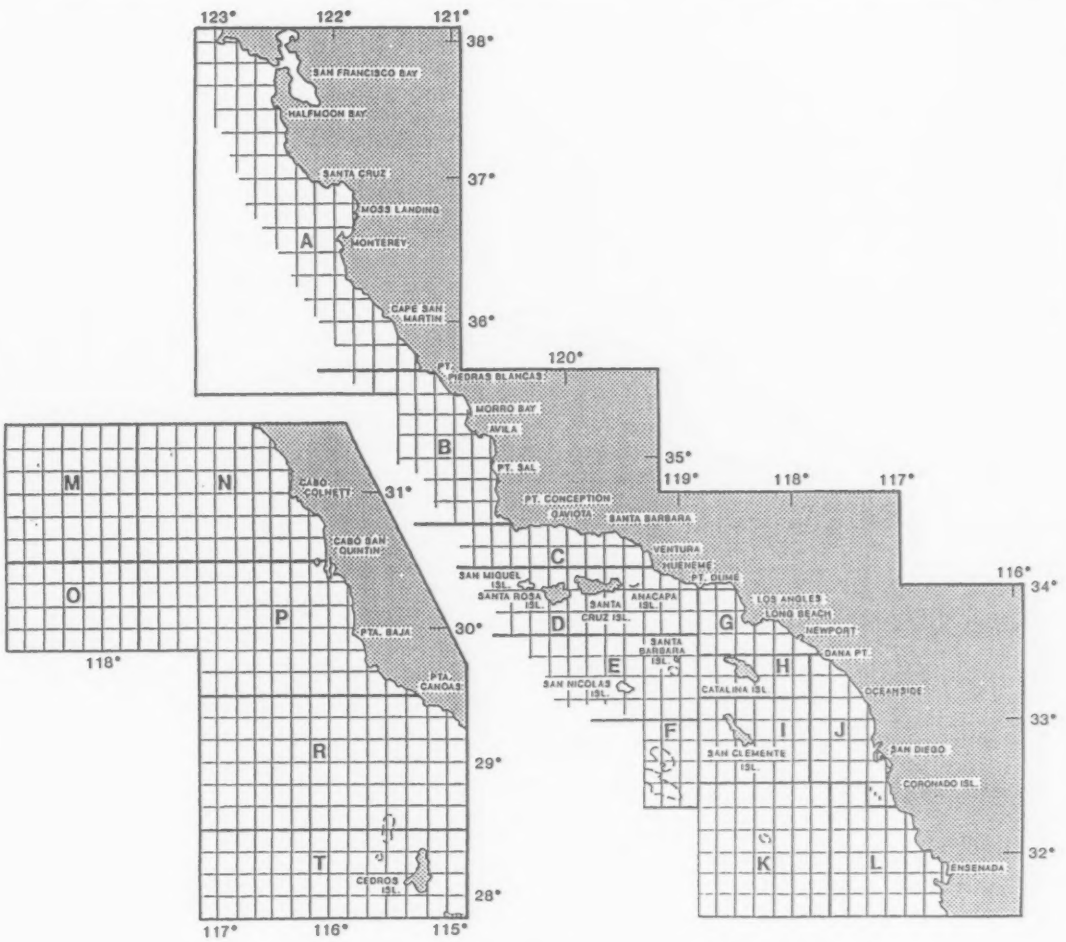

Figure 1

Block areas designated for sampling from off central California to Mexico, grouped in 18 zones, A to T. (Zones Q and S were originally used on flight logs; however, no flights were recorded for these zones.)

the area or numbers of schools with an estimate of the tonnage of each school. Procedures for recording species observations and survey effort have not changed since 1962. Other information such as time of flight (day or night) and flight duration also are recorded on the flight log. Flight logs are submitted quarterly and data from each log are entered into the computer after editing.

Spotter pilots' income is derived from the commercial fishery at a current rate of ~6% of the vessel's gross income. Spotter pilots are paid a nominal fee by the National Marine Fisheries Service (NMFS) to maintain a flight log record of their observations. Pilots in the program averaged ~600h flight time/yr and, with 4–6 pilots, the total number of hours flown was ~3000/yr.

From 1963, the first full year of operation, to 1990, annual indices of abundance for each species were calculated for the total area (from northern Baja California, Mexico to San Francisco, California) and for selected groups of 10" lat. × 10" long. block areas, similar to the "block area" statistical system used by CDF&G (Anon. 1935). These groups of block areas are referred to in this paper as "zones" and were designed to encompass important commercial fishing areas (Fig. 1).

Flight effort for the total area and each zone was determined by counting the number of times the aerial spotter's flight track entered a block area, termed a "block area flight" (BAF). Species abundance was recorded as the tonnage estimate (and hence approximates biomass) for the area observed. Also recorded on the flight log was time of the observation (day or night), pilot, and, since 1988, the target species of the commercial operation.

The procedure to measure effort has not changed from previous studies; however, the computation of species abundance has been modified. In previous analyses (Squire 1972, 1983), abundance was estimated as a rank index according to discrete incremental values of tonnage (tonnage range values). For example, for the northern anchovy, an observation within a block area estimated to be 0–100t was recorded as 1, 100–200t was recorded as 2, etc. Each species had different tonnage range values, since the amount of tonnage observed varied greatly between species. Therefore, the abundance index values for each species are not directly comparable. For this analysis, actual tonnage values as recorded by the spotter pilot and a modification of the index used by Squire (1972) are used, which allows for direct comparison of abundance index values between species.

The apparent abundance index is T/BAF, where T = tonnage estimate, and BAF = total number of block area flights (day plus night, all zones).

Results and discussion

Observation effort and sightings

During the period 1963–90, a total of 24 aerial fish-spotter pilots participated in the program and reported flight operations totaling over 67,000h, searching a total of 376,446 block areas. Table 1 gives the annual search effort (BAF/yr), day and night, during the period 1962–90. From 1963 to 1990, a total of 253,239 BAF were made during day operations (67%) and 123,207 BAF during the night. Pilots have searched an average of 13,444 BAF/yr; however, the variation in annual spotting effort is considerable. There was reduced effort in early 1970. Abundance data for 1970

Table 1

Search effort in block area flights (BAF), day and night, 1963–90, from off Baja California, Mexico to central California. Asterisk indicates <1/2 yr of operation.

	Block area flights		
Year	Day	Night	Total
1962*	362	512	874
1963	3,541	3,279	6,820
1964	5,245	3,415	8,660
1965	5,086	4,367	9,453
1966	7,708	3,781	11,489
1967	7,632	3,495	11,127
1968	7,823	3,835	11,658
1969	9,745	5,896	15,641
1970	4,646	1,853	6,499
1971	12,308	5,181	17,489
1972	7,402	4,448	11,850
1973	12,450	5,031	17,481
1974	8,356	3,887	12,243
1975	7,923	3,398	11,321
1976	14,782	3,781	18,563
1977	7,795	7,788	15,583
1978	6,517	4,415	10,932
1979	10,727	4,767	15,494
1980	3,624	3,403	7,027
1981	9,237	3,781	13,018
1982	9,597	5,754	15,351
1983	13,904	4,571	18,475
1984	9,144	1,063	10,207
1985	15,243	4,031	19,274
1986	12,300	5,684	17,984
1987	8,474	6,348	14,822
1988	7,185	3,335	10,520
1989	8,744	4,116	12,860
1990	16,101	8,504	24,605
Total 1963–90	253,239 = 67%	123,207 = 33%	376,446

Avg. = 13,444 BAF/yr, 1963–90

Table 2

Sighting estimates of total tonnage by species and percentage and by zones, for the period 1962–90.

Zone	Northern anchovy	Pacific sardine	Pacific bonito	Chub mackerel	Jack mackerel	Bluefin tuna
A	25,147,498	19,157	674	108,345	56,158	0
B	865,308	2,739	4,690	216,873	98,035	0
C	11,633,297	*614,595*	*233,330*	*1,386,548*	104,949	333
D	5,126,158	345,360	86,860	639,099	268,823	1,938
E	467,400	22,454	3,688	203,190	45,937	2,934
F	358,614	50,130	250	701,416	*789,877*	22,773
G	*28,519,793*	99,587	37,176	521,732	361,180	3,154
H	5,292,980	183,500	26,363	1,145,839	222,005	1,785
I	1,578,398	33,165	26,231	1,292,866	256,731	27,938
J	10,453,074	68,243	205,553	130,471	30,855	26,494
K	242,164	1,200	2,045	525	910	79,846
L	1,215,269	0	28,418	1,365	50	86,521
M	500	0	0	0	0	9,603
N	2,495,734	4,200	13,881	24,650	0	*143,625*
O	0	0	0	0	0	0
P	123,305	0	2,313	400	0	64,423
R	1,110	0	0	0	0	8,652
T	0	0	0	0	0	0
	93,520,602	1,444,321	671,472	6,373,169	2,235,510	480,019
%	89.7	1.0	0.6	6.1	2.1	0.5

Table 3

Day/night sighting estimates for northern anchovy, Pacific sardine, Pacific bonito, Pacific mackerel, jack mackerel and bluefin tuna, 1962–90.

	Day	Night
Northern anchovy *Engraulis mordax*		
Tonnage	30,140,974	63,379,618
% day/night	32.3	67.7
Pacific sardine *Sardinops sagax*		
Tonnage	361,548	1,082,498
% day/night	25.1	74.9
Pacific bonito *Sarda chiliensis*		
Tonnage	521,302	151,169
% day/night	77.5	22.5
Pacific mackerel *Scomber japonicus*		
Tonnage	2,534,780	3,837,366
% day/night	39.8	60.2
Jack mackerel *Trachurus symmetricus*		
Tonnage	746,827	1,488,683
% day/night	33.5	66.5
Bluefin tuna *Thunnus thynnus*		
Tonnage	462,262	17,756
% day/night	96.3	3.7

are thus not directly comparable to other years, although most search effort was during a period of high abundance levels. Through the years, the center of search effort was off southern California, with search activity off northwestern Baja California, Mexico during the summer for bluefin tuna. There was considerable search effort north of Point Conception into the Monterey Bay area for chub mackerel and Pacific sardine during the early years of the program and less so since the decline in those species' abundances in the mid-1960s.

Estimates of total tonnage sighted by species by zone are given in Table 2. The tonnage estimated for northern anchovy far exceeds that of all other species, totaling 89.7%. The greatest tonnage of northern anchovy was observed in zone G; Pacific sardine, Pacific bonito, and chub mackerel in zone C; jack mackerel in zone F; and bluefin tuna in zone N.

Most spotting effort was carried out during summer to fall, with 49% of BAFs accounted for during the months of July, August, and September (1980–90). During any one year, the amount of effort expended in any one month was highly variable due to fluctuations in abundance, weather, and fleet operations. In summer months, a substantial portion of the increase in spotting effort is related to searching for bluefin tuna, or other species such as albacore *Thunnus alalunga* and yellowfin tuna *Thunnus albacares*.

Differences in tonnage sighted between day and night (Table 3) are similar to that reported by Squire (1972). Northern anchovy, Pacific sardine, chub mackerel, and jack mackerel were more commonly observed at night, while Pacific bonito and bluefin tuna were more commonly observed during the day.

Table 4

Total area index values in T/BAF, day plus night. Dash indicates an abundance level <0.01 T/BAF.

Year	Total area	Year	Total area
Northern anchovy *Engraulis mordax*			
1962	0.66	1977	713.80
1963	141.38	1978	340.19
1964	80.66	1979	382.83
1965	153.45	1980	322.01
1966	83.26	1981	89.87
1967	163.63	1982	42.78
1968	72.20	1983	4.17
1969	195.82	1984	4.54
1970	608.43	1985	27.24
1971	195.63	1986	7.55
1972	81.05	1987	20.67
1973	745.98	1988	42.90
1974	354.25	1989	16.05
1975	819.93	1990	11.96
1976	293.77		
Pacific sardine *Sardinops sagax*			
1962	—	1977	—
1963	0.77	1978	—
1964	0.90	1979	—
1965	0.04	1980	—
1966	0.02	1981	0.01
1967	—	1982	0.12
1968	—	1983	0.15
1969	—	1984	1.88
1970	—	1985	34.37
1971	—	1986	19.87
1972	—	1987	11.76
1973	—	1988	77.11
1974	—	1989	6.23
1975	—	1990	11.83
1976	—		
Pacific bonito *Sarda chiliensis*			
1962	1.18	1977	0.14
1963	6.28	1978	4.35
1964	2.32	1979	0.31
1965	3.47	1980	0.33
1966	10.16	1981	1.73
1967	5.34	1982	0.38
1968	3.06	1983	0.96
1969	1.50	1984	8.17
1970	0.87	1985	3.22
1971	2.93	1986	0.22
1972	2.28	1987	1.55
1973	2.98	1988	1.55
1974	1.40	1989	0.98
1975	0.48	1990	0.76
1976	0.43		
Pacific mackerel *Scomber japonicus*			
1962	2.74	1977	72.30
1963	6.62	1978	142.26
1964	1.06	1979	63.75
1965	0.41	1980	39.10
1966	0.23	1981	31.59
1967	—	1982	26.71
1968	—	1983	8.89
Pacific mackerel *Scomber japonicus* (continued)			
1969	0.03	1984	72.44
1970	0.83	1985	88.73
1971	0.13	1986	41.77
1972	0.03	1987	17.38
1973	0.18	1988	21.66
1974	—	1989	3.53
1975	0.02	1990	3.18
1976	0.47		
Jack mackerel *Trachurus symmetricus*			
1962	5.04	1977	60.40
1963	13.73	1978	82.54
1964	11.56	1979	19.13
1965	9.97	1980	9.23
1966	2.70	1981	4.42
1967	6.61	1982	6.15
1968	11.41	1983	1.56
1969	3.55	1984	1.82
1970	1.87	1985	1.61
1971	5.91	1986	1.44
1972	6.27	1987	1.01
1973	0.21	1988	0.47
1974	1.88	1989	1.37
1975	5.69	1990	0.23
1976	3.89		
Bluefin tuna *Thunnus thynnus*			
1962	4.40	1977	7.12
1963	6.81	1978	30.07
1964	6.81	1979	12.32
1965	0.90	1980	0.69
1966	9.46	1981	0.80
1967	3.42	1982	0.80
1968	6.03	1983	0.20
1969	0.39	1984	0.66
1970	0.02	1985	2.57
1971	0.42	1986	3.03
1972	2.75	1987	0.55
1973	16.45	1988	0.56
1974	17.28	1989	0.48
1975	2.54	1990	0.35
1976	13.20		

Indices of apparent abundance

Abundance index levels in tons/block area flight (T/BAF) were calculated for the total area by species for day plus night observations for the years 1962–90 (Table 4). From the total area index, the general trend of species abundance can be obtained. However, an index designed to better represent abundance change of each species is needed; therefore, a second set of abundance index values was calculated using only data from a core area of abundance as determined for each species by day or night, depending upon which period best represented the abundance of the species (Squire 1972). With the exception of data from one aerial spotter pilot (computer file 26), all data collected during 1962–90 was used in this analysis.

Data reflecting number of sightings and tonnage observed and its geographical distribution were used to define the geographical limits of the core area for each species. The core area for each species was determined to include all or portions of the following zones: northern anchovy, zones C,D,G,H; Pacific sardine, zones C,D,G,H; Pacific bonito, zones C,D,G,J; chub mackerel, zones C,D,G,H,I; jack mackerel, zones D,F,G,H,I; bluefin tuna, zones I,K,L,N,P (Fig. 1). For each species, the number of block areas in each zone comprising its core area and the total number of block areas in its core area are given in Table 5.

The core-area index is the mean of the T/BAF weighted to account for differences in size of core area within the zone to obtain a stratified mean (Cochran 1966). For each zone, the weight factor was the ratio of the total number of block areas having high species density in the zone to the total number of block areas

Table 5

Areas of high density determining core-area abundance, by species.

Core area determined for		
Northern anchovy	Zone G =	10 block areas
Engraulis mordax	D =	11 " "
	C =	10 " "
	H =	6 " "
		37 block areas comprising the anchovy core area
Pacific sardine	Zone C =	6 block areas
Sardinops sagax	D =	5 " "
	G =	5 " "
	H =	4 " "
		20 block areas comprising the Pacific bonito core area
Pacific bonito	Zone C =	6 block areas
Sarda chiliensis	D =	8 " "
	G =	8 " "
	J =	7 " "
		29 block areas comprising the Pacific bonito area
Chub mackerel	Zone G =	6 block areas
Scomber japonicus	H =	3 " "
	I =	3 " "
	D =	5 " "
	C =	4
		21 block areas comprising the Pacific mackerel core area
Jack mackerel	Zone D =	8 block areas
Trachurus symmetricus	G =	7 " "
	H =	3 " "
	I =	3 " "
	F =	4 " "
		25 block areas comprising the jack mackerel core area
Bluefin tuna	Zone I =	20 block areas
Thunnus thynnus	L =	20 " "
	K =	15 " "
	N =	18 " "
	P =	8 " "
		81 block areas comprising the bluefin tuna core area

with high density comprising the entire core area. Core-area abundance (weighted T/BAF) is

$$\sum w_i\,(t/BAF)_i,$$

where W_i – weight for zone i = a/b

a = blocks in core area from zone i

b = total blocks in core area, all zones

$(T/BAF)_i$ = T/BAF for zone i.

Abundance trends by species

Core-area index values in Figs. 2–7 are presented as a weighted mean index and as a running average of three to better illustrate trends in abundance. Core-area abundance index values are given in Table 6.

Table 6

Core-area index values in T/BAF, day or night in T/BAF. Dash indicates an abundance level <0.01 T/BAF.

Year	Core area	Year	Core area
Northern anchovy *Engraulis mordax*			
1962	0.09	1977	858.73
1963	250.98	1978	263.89
1964	160.55	1979	624.80
1965	253.85	1980	578.68
1966	116.92	1981	236.71
1967	225.70	1982	67.86
1968	173.41	1983	7.72
1969	309.84	1984	6.76
1970	629.03	1985	47.88
1971	362.59	1986	13.39
1972	54.55	1987	33.28
1973	1143.55	1988	69.20
1974	494.29	1989	7.24
1975	1010.70	1990	31.45
1976	456.10		
Pacific sardine *Sardinops sagax*			
1962	—	1977	—
1963	1.38	1978	—
1964	1.31	1979	—
1965	0.02	1980	—
1966	0.03	1981	—
1967	225.70	1982	0.24
1968	0.01	1983	0.33
1969	—	1984	2.77
1970	—	1985	97.36
1971	—	1986	32.35
1972	—	1987	20.12
1973	—	1988	145.75
1974	—	1989	34.84
1975	—	1990	39.03
1976	—		
Pacific bonito *Sarda chiliensis*			
1962	2.20	1977	0.23
1963	2.29	1978	0.96
Pacific bonito *Sarda chiliensis* (continued)			
1964	3.39	1979	0.38
1965	5.88	1980	0.38
1966	14.84	1981	1.78
1967	7.20	1982	0.56
1968	3.35	1983	1.31
1969	1.58	1984	9.93
1970	—	1985	3.98
1971	3.47	1986	0.30
1972	2.83	1987	1.05
1973	3.34	1988	2.42
1974	1.76	1989	1.23
1975	0.74	1990	1.15
1976	0.59		
Chub mackerel *Scomber japonicus*			
1962	4.04	1977	104.80
1963	3.36	1978	198.72
1964	1.63	1979	85.27
1965	0.80	1980	58.78
1966	0.51	1981	41.74
1967	0.01	1982	29.24
1968	0.01	1983	19.00
1969	0.07	1984	59.91
1970	2.95	1985	148.18
1971	0.33	1986	85.48
1972	0.10	1987	36.06
1973	0.48	1988	43.55
1974	—	1989	7.83
1975	—	1990	3.19
1976	0.05		
Jack mackerel *Trachurus symmetricus*			
1962	5.28	1977	91.41
1963	23.10	1978	74.90
1964	14.69	1979	20.13
1965	14.58	1980	12.25
1966	4.49	1981	7.77
1967	15.26	1982	10.14
1968	24.21	1983	2.20
1969	5.68	1984	7.47
1970	2.91	1985	6.23
1971	12.55	1986	2.63
1972	11.65	1987	1.69
1973	0.39	1988	1.03
1974	3.41	1989	2.86
1975	13.17	1990	0.81
1976	11.59		
Bluefin tuna *Thunnus thynnus*			
1962	6.57	1977	8.71
1963	6.97	1978	34.52
1964	6.97	1979	12.87
1965	1.28	1980	0.89
1966	13.03	1981	0.95
1967	4.51	1982	1.37
1968	9.45	1983	0.05
1969	0.59	1984	0.62
1970	—	1985	2.32
1971	0.87	1986	1.98
1972	6.94	1987	0.77
1973	17.38	1988	1.23
1974	18.32	1989	1.02
1975	2.60	1990	0.73
1976	13.73		

Northern anchovy (Fig. 2) The core area index (night index) was near 180 T/BAF in the mid- to late-1960s. The index increased in the early 1970s, and during 1972–80 remained in the range of 450–700 T/BAF. The index began to decline in 1980 and reached a low level of abundance by 1983 (<50 T/BAF), a level considerably below that observed in the mid-1960s.

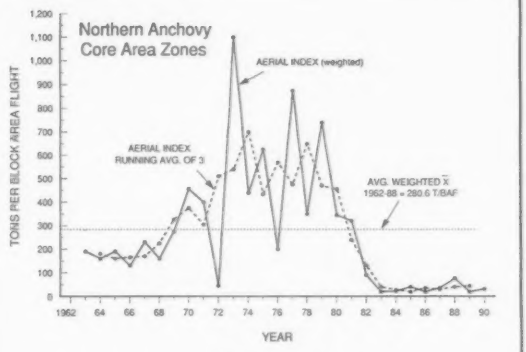

Figure 2
Abundance index levels in T/BAF for northern anchovy *Engraulis mordax* core area, night index, weighted $\bar{x}$, and running average (×3).

Pacific sardine (Fig. 3) The Pacific sardine resource was in a state of decline at the time the aerial spotter program was started. Average tonnage calculated for the 1963–66 period for the core-area index was 1.03 T/BAF. Very low abundance indices were recorded from 1967 until the early 1980s with some years reporting zero sightings of sardine schools. The core-area running mean index (night index) increased to 60 T/BAF by 1988.

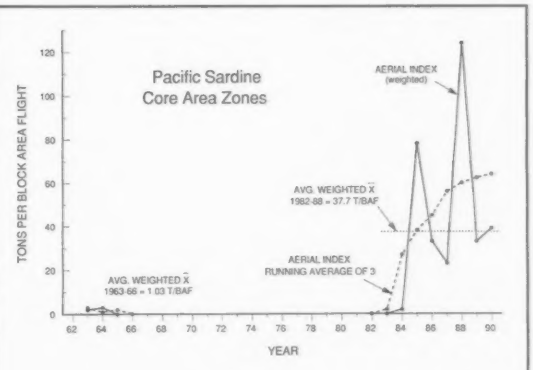

Figure 3
Abundance index levels in T/BAF for Pacific sardine *Sardinops sagax* core area, night index, weighted $\bar{x}$, and running average (×3).

Pacific bonito (Fig. 4) Abundance levels for Pacific bonito show considerable fluctuation. Bonito were rarely taken off southern California prior to the strong El Niño of 1957–58 (Radovich 1960). They were common in southern California waters after this event and were intensively fished starting in about 1963. The increase in fishing effort redirected to this species was the result of decreased abundance of Pacific sardine and chub mackerel.

The core-area index value (day index) reached a high in 1966 of 10.5 T/BAF. This is the highest index value recorded for bonito during 1962–90. The index then declined, increased slightly in 1972 to 3.2 T/BAF, and substantially increased in 1984 to 5.5 T/BAF.

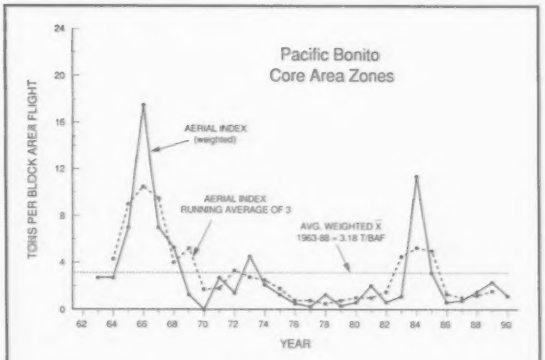

Figure 4
Abundance index levels in T/BAF for Pacific bonito *Sarda chiliensis* core area, day index, weighted $\bar{x}$, and running average (×3).

Chub mackerel (Fig. 5) Declining abundance levels noted in the early to mid-1960s matched the collapse of the fishery, with extremely low index levels (>5 T/BAF) noted for the core-area index (night index) in 1967–75. After 1976, the abundance index rose rapidly to a peak of 170 T/BAF in 1978, then declined to a range of 15–55 T/BAF in 1981–89.

Jack mackerel (Fig. 6) Abundance was high during the mid 1970s. The core-area index (night index) increased to 234 T/BAF in 1976 and declined to <10 T/BAF after 1979.

Bluefin tuna (Fig. 7) For the core area, there were three peaks in the index (day index) of abundance: 1967, 1973, and 1978. The index for recent years is well below the 1963–88 average of 10.8 T/BAF.

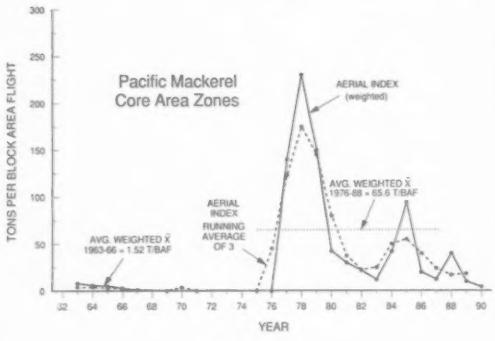

Figure 5

Abundance index levels in T/BAF for chub mackerel *Scomber japonicus* core area, night index, weighted $\bar{x}$, and running average (×3).

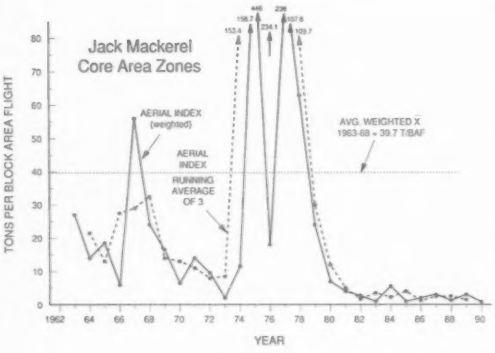

Figure 6

Abundance index levels in T/BAF for jack mackerel *Trachurus symmetricus* core area, night index, weighted $\bar{x}$, and running average (×3).

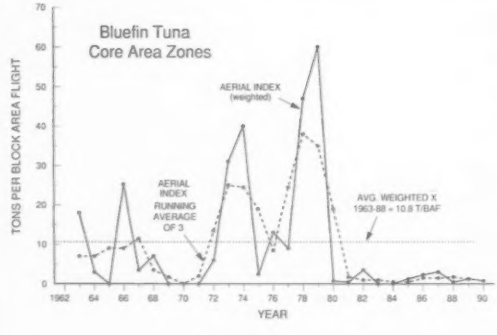

Figure 7

Abundance index levels in T/BAF for bluefish tuna *Thunnus thynnus* core area, night index, weighted $\bar{x}$, and running average (×3).

Interaction between species

To compare periods of high and low abundance of the six species, the logarithm of the moving weighted averages of core-area abundance indices (day or night, dependent upon which time the species was observed more frequently and in greater quantity) were plotted (Fig. 8). The dominant feature of Fig. 8 is the abundance index for the northern anchovy. High index levels of 200–500 T/BAF were recorded during 1962–82, a 21 yr period. The index declined sharply in 1983 and 1984, increasing since. The northern anchovy is the more stable species in terms of less annual percentage change in abundance than any of the other five species. During 1966 and 1967, jack mackerel, bluefin tuna, and Pacific bonito were at higher levels of abundance than those observed in the early 1970s. The Pacific sardine and chub mackerel resources were low in abundance by 1965, and declined to extremely low levels by 1970. The northern anchovy, jack mackerel, chub mackerel, and bluefin tuna increased in abundance in 1974–79. Exceptions were the Pacific bonito and sardine.

The very strong El Niño condition of 1982–83 (Quinn et al. 1987) had a significant effect on the distribution of coastal pelagic species (Fluharty 1984, Squire 1987). This period saw declines in abundance for all species, except Pacific bonito and chub mackerel. These two species showed significant declines in 1986–87. A rapid increase in Pacific sardine abundance was evident in 1984, immediately following the El Niño event and continuing into the late 1980s.

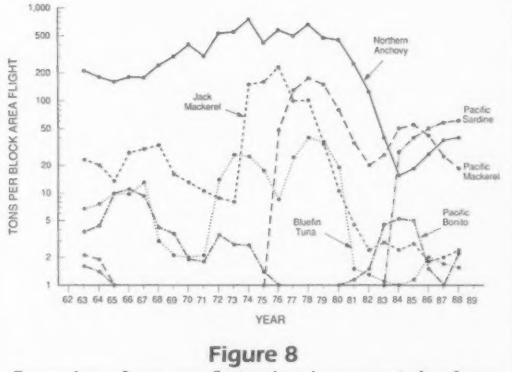

Figure 8

Comparison of core-area fluctuations in apparent abundance index levels for northern anchovy *Engraulis mordax*, Pacific sardine *Sardinops sagax*, chub mackerel *Scomber japonicus*, Pacific bonito *Sarda chiliensis*, jack mackerel *Trachurus symmetricus*, and bluefin tuna *Thunnus thynnus*. Data plotted on a semi-logarithmic scale, in weighted $\bar{x}$, T/BAF, by moving average (×3).

From inspection of core-area fluctuations (Fig. 8), it is difficult to draw any conclusions regarding interaction among most of the species included in this study. The annual abundance values that appear to be more closely related are those of the northern anchovy and bluefin tuna which were significantly correlated ($y=0.76$, $P<0.1$).

Pilot estimation of tonnage

Differences between pilots' ability to estimate school or group size are difficult to evaluate using the type of data recorded in flight logs. Computer recording of flight track and species tonnage observed did not include details of what portion of the block was searched, or where the species were sighted. Aerial spotters entering the block area (an 8×10 nm area) may have observed fish schools of the same species in two geographically different locations. Only the sum of the school sizes was coded.

The time of observation is probably the most critical factor in comparisons of pilot sightings because near-surface fish abundance may be highly variable over a short period of time. Therefore, unless pilots are searching the same area at the same time, different levels of abundance are likely to be observed.

Williams (1981) in surveys of pelagic fish resources off southeast Australia indicated that the professional fish spotters were extremely accurate in tonnage estimates of individual schools. In tests conducted by NMFS and CDF&G to determine northern anchovy school size using acoustic gear, a purse seiner and aerial spotter were used. The aerial spotter had a more accurate estimate of school tonnage than obtained from acoustic gear (P. Mardesich, Flying Fishermen, Inc., pers. commun. 1978).

MacCall (1975), using the NMFS computer database, investigated variation in anchovy abundance estimates (comparison of data collected during the same 10d period in 1973 and 1975) and found considerable differences among spotters. The differences were consistent for individual pilots for day and night observations. Variability in reported tonnage was large, but it could be reduced by long-term averaging. MacCall (1975) further suggested that corrections for pilots estimating efficiency be incorporated in calculations of the abundance index to avoid biasing the result toward the spotter with the highest tonnage. The accuracy of fish-spotter estimates of tonnage was approached statistically by Lo et al. (In press) using a delta-lognormal model. All aerial spotter data were used in this analysis. However, until spotter-pilot estimating efficiency is measured in field experiments, correction factors are unknown. It is possible that these differences between spotters may be due more to differences in numbers of schools seen than to differences in size estimates.

Comparison of aerial index to other abundance indices

The problem of variability among spotter pilots complicates comparisons; however, pilots are paid relative to the amount of tonnage caught. Therefore, the aerial spotter needs to have a reasonable estimate of school size to compare with the amount of fish caught by the seiner. The aerial spotter is continually obtaining "ground truth" from the purse-seine vessel relative to species composition and size of the school caught.

Since the decline of the Pacific sardine resource in 1984, considerable effort has been expended on surveys, using various techniques to collect apparent abundance data that could be modeled to produce an estimate of biomass. Acoustic, egg and larva, and aerial-spotter surveys have been conducted. Each survey measures a different component of the population and, therefore, comparisons of abundance estimates from different methods and models must be viewed with caution.

The aerial-spotter program measures apparent abundance of adults and subadults of epi-pelagic schooling fishes, and assumes that most adults in the population are available to the spotters at some time during the year. The aerial index is a direct calculation (T/BAF). It is a non-random type survey, but is not time-restricted.

The operational procedures used by aerial spotters affect the results. Although they do work closely with the fleet in locating and sometimes directing the setting of the purse seine, much of their time is spent searching large areas of the ocean for fishable resources. Many times, the aerial spotter will conduct flight operations in a general survey mode for the fleet, but does not work directly with the fleet. Even though aerial monitoring is conducted throughout the year, most observation effort is in the summer and early fall (49% of BAF during July, August, and September) when concentrations of commercial species are more common in the nearshore areas.

Quantitative apparent-abundance data derived from field surveys (egg and larvae, and acoustic) are statistically treated under various biological assumptions to ultimately obtain an estimate of biomass or tonnage: spawning biomass and total biomass in the case of egg and larva surveys (Lo 1985), and schooled biomass in the case of acoustic surveys (Mais 1974). Although some biomass estimates have been made for other species, such as the chub mackerel and Pacific

sardine, most biomass studies and modeling for the California region have involved the northern anchovy (Methot 1989).

Over the past 35 yr, studies by fishery biologists have produced a wide range of population estimates for a number of the pelagic species, in particular, the northern anchovy, Pacific sardine, and chub mackerel. The following describes the results of these and others in relation to aerial abundance indices.

Northern anchovy A review of the many abundance estimates for the northern anchovy over the years 1940–66 was given by Messersmith et al. (1969). For the early years of the aerial program, MacCall et al. (1974) compared anchovy biomass estimates from egg and larva surveys with the night aerial index, resulting in a correlation of +0.30 (1962–69). They also compared the aerial night index with the acoustic estimate (1966–72) producing a negative correlation (r=–0.47).

In a review of egg production of the northern anchovy central stock, Lo (1985) presented a correlation between various indices of anchovy spawning biomass. The biomass index from the aerial surveys had a high correlation (r=0.818) with egg production, and there was a similar correlation (r=0.807) between biomass egg production and acoustic surveys.

Correlation plots of normalized data (standard deviates; Snedecor 1959) were used to compare northern anchovy abundance data presented by Lo (1988) with aerial index values. The aerial index (day plus night) for the core area was compared with Lo's (1988) estimate of spawner biomass, determined from a combination of various estimates from the egg production method and the results of the 1969–85 sonar or acoustic surveys (Lo 1988), giving a correlation of r=0.61, df=14, P<0.05%. The aerial index was also compared with the estimate of schooled biomass based on results of acoustic surveys presented by Lo (1988), giving a correlation of r=0.51, df=13, P<0.05%.

MacCall & Prager (1988) presented anchovy larval-abundance indices for 1963–85. These indices, which are a measure of spawning population, were compared with the core-area aerial index for the same set of years. There was statistically significant correlation between the two indices (aerial/larva) (r=0.82, df=13, P<0.1).

Pacific sardine MacCall & Prager (1988) also reviewed the historical trend of sardine larval abundance, 1951–85. A comparison was made between their arithmetic scale of larval abundance (standard index) and the aerial index during the period 1963–85. Indications of a resurgence of the Pacific sardine resource began in 1978, and for the 1963–85 period MacCall & Prager's (1988) estimate of larval abundance correlates well with the aerial index (r=0.98, df=8, P<0.01).

Pacific bonito Pacific bonito, a species whose seasonal abundance off California is more closely associated with environmental conditions (El Niño effects) than the other species (Squire 1987), has not been subjected to detailed assessment. MacCall et al. (1974) used recreational partyboat CPUE data in yearly time-lag periods and compared this with the aerial index. The recreational partyboat fleet generally fishes nearshore and catches younger fish than the offshore commercial purse-seine fleet. The highest correlation (r=0.69) between the recreational fleet CPUE and the aerial index was for a 3 yr lag period (aerial index lags the recreational CPUE). No other independent estimates of Pacific bonito biomass are available for comparison.

Chub mackerel Assessment of the chub mackerel resource has used both standard population-dynamics techniques and methods that utilize egg and larva surveys. For comparison of changes in population over time, Squire (1983) plotted the trend of the aerial index against the spawning biomass index and the larva index of Smith & Richardson (1977). The limited data (1963–67) precluded any long-term comparison; however, all three indices showed a similar decrease. The aerial index was significantly correlated (P<0.05) with both spawning biomass (r=0.99) and the larva index (r=0.94).

The chub mackerel biomass declined to very low levels in the mid-1960s and remained very low until the mid-1970s. A sharp increase in biomass was noted starting in 1976. MacCall & Prager (1988) presented data on chub mackerel larval abundance through 1985. A correlation of the aerial index (core area) with the larva index for 1963–81 was statistically insignificant (r=0.205). A comparison made between the aerial index (core area) and estimated biomass of MacCall et al. (1985) for 1963–84 gave what would appear to be a good fit for the early years, but comparison of later years' estimates was not significant (r=0.26).

Jack mackerel Various indices of abundance for jack mackerel, including the aerial index, show that the resource tends to be highly variable in apparent abundance. Egg and larva surveys have shown the stock to be extremely widespread. Based on tagging data, Knaggs (1973) estimated between 700,000 and 1,500,000 t were available to the fishery in 1973. MacCall et al. (1974) stated that these estimates are in agreement with trends in aerial survey index (Squire

1972). MacCall & Prager (1988) presented graphics on a time-series of abundance indices for jack mackerel larva off southern California. They noted that the index did not correspond well with other larval indices that included samples from central California. An examination of the MacCall & Prager (1988) larva index vs. the aerial index indicated a poor correlation (r=0.16, not significant), particularly for the years 1977–78, a period of marked increase in jack mackerel abundance off southern California.

Bluefin tuna No biomass estimates are available for bluefin tuna in the northeast Pacific, which is part of a Pacific-wide resource. Young year-classes (1–3 yr) are common in the northeast Pacific with some catches of fish up to 6 yr of age (Bayliff 1980). CPUE estimates presented by Calkins (1982) of catch/boat-day (C/BD) for the U.S. purse-seine fishery operating off California and Baja California, Mexico for the years 1963–80 in the area north of 29° N lat. were compared with the aerial core-area mean index. Although both indices (C/BD and T/BAF) show a decline prior to 1980, the correlation was not significant (r=0.033). Calkins (1982) stated that "total catch may be the best indicator of bluefin abundance." Total catch (north of 29° N lat.) as given by Calkins (1982) was compared with the core-area index, and the correlation was again not significant (r=0.147).

Summary and conclusions

The aerial monitoring program has produced information on the trend of apparent abundance for six species of pelagic near-surface schooling species. The program in operation since 1962 utilizes information provided by commercial aerial fish spotters. Spotter pilots operate under strong incentive to estimate tonnage accurately, since their compensation is based on actual tonnage caught. The cost of the program is a small fraction of the cost of other field assessment methods currently used to develop apparent abundance data, such as egg and larva surveys and acoustic surveys.

Data are presented in a relatively simple and understandable index format of tons observed/block area searched (T/BAF). Annual indices (T/BAF) of apparent abundance are calculated for the major species of importance to the commercial purse-seine fleet operating off southern California and northwestern Baja California, Mexico.

All species have shown a fluctuating pattern of apparent abundance over the 29 yr survey period (1962–90). The northern anchovy is the dominant species observed, accounting for 89.7% of all tonnage observed; chub mackerel is second with 6.1%; followed by jack mackerel with 2.1%, and Pacific sardine, Pacific bonito, and bluefin tuna with 2.1%.

From inspection of abundance data, peak periods of higher abundance for four of the six species (chub mackerel, jack mackerel, northern anchovy, and bluefin tuna) occurred in 1977–79. Analysis indicated that species more closely related in abundance over time are the northern anchovy and bluefin tuna, both being at higher levels of abundance during 1972–80. A regression was calculated for 1963–88, giving a significant correlation (r=0.76, P<0.1).

A number of comparisons were made between estimates of biomass (spawning or total biomass) and the aerial abundance indices for the northern anchovy, Pacific sardine, and chub mackerel, and the apparent abundance of bluefin tuna based on CPUE data. There is a significant correlation with the aerial index, the anchovy total biomass estimate, and the historical egg-production index. Also, there was a slightly less but significant correlation with the acoustic survey estimates. The more significant correlations were found in comparing the aerial index with the northern anchovy larva index and the Pacific sardine larva index. For the chub mackerel, a species recognized as having a highly fluctuating record of abundance, the correlations during the early years (1963–66) were very good (aerial index vs. larva index and spawning biomass index); in later years, correlations between the larva index and the estimates of total biomass and the aerial index were not significant. There is a lack of good data relative to the abundance for other species of interest (Pacific bonito, jack mackerel, bluefin tuna) although some comparisons with the aerial data have been made for Pacific bonito, giving a reasonable correlation using a 3 yr lag period. Bluefin tuna C/BD (catch/boat-day) and total catch for the northwest Mexico–southern California fishery were compared with the aerial core index and gave no significant correlation.

Trends of aerial indices indicate that the pelagic resources studied can be described in a state of chaotic fluctuations (Jensen 1987) relative to apparent abundance. The fluctuating record indicates that even short-term predictions of abundance appear not to be feasible. Management must rely on near real-time estimates based on a measurement of a small fraction of the resource, and what is important is the development and use of more than one method or approach in evaluating population status. None of the survey results appear in complete agreement; however, utilizing several approaches to provide "triangles of agreement" (from a method used in navigation) can provide a consensus for management action.

Acknowledgments

The assistance of Dr. David Au in making the statistical comparisons between various methods of measuring apparent abundance and other editorial suggestions is greatly appreciated. The assistance of Dr. Nancy Lo, Dr. Larry Jacobsen, Cindy Meyer, Richard Tauber, Lorraine Prescott, and Karen Handschuh of NMFS, and of Gordon Broadhead and Tom Barnes of Living Marine Resources, Inc., for their review and contribution to the development of this paper is appreciated. To the aerial fish spotters who have provided at least 67,000 flight hours of observation to the aerial program, I express my thanks.

Citations

Anonymous
1935 Commercial fish catch of California for the years 1930–1934 inclusive. Calif. Div. Fish & Game, Bur. Commer. Fish., Fish. Bull. 44, 126 p.

Bayliff, W.H.
1980 Synopsis of biological data on the northern bluefin tuna, *Thunnus thynnus* (Linneaus 1758) in the Pacific Ocean. Inter-Am. Trop. Tuna Comm. Spec. Rep. 2:261–294.

Calkins, T.P.
1982 Observations on the purse-seine fishery for northern bluefin tuna (*Thunnus thynnus*) in the eastern Pacific Ocean. Inter-Am. Trop. Tuna Comm. Bull. 18(2), 225 p.

Clark, F.N., & J.C. Marr
1955 Population dynamics of the Pacific sardine. Calif. Coop. Oceanic Fish. Invest. Prog. Rep., 1 July 1953–30 March 1955, p. 11–48.

Cochran, W.G.
1966 Sampling techniques. John Wiley, NY, 413 p.

de la Mare, W.K.
1984 On the power of catch per unit effort to detect declines in whale stocks. Rep. Int. Whaling Comm. 34:655–661.

Fluharty, D. (coordinator)
1984 1982–1983 El Niño task force summary. Inst. Mar. Stud., Univ. Wash., Seattle, 25 p.

Fox, W.W.
1974 An overview of production modeling. Admin. Rep. LJ-74-10, NMFS Southwest Fish. Sci. Cent., La Jolla CA, 20 p.

Jensen, R.V.
1987 Classical chaos. Am. Sci. 95:168–181.

Knaggs, E.H.
1973 Status of jack mackerel resource and its management. *In* Proceedings of the State-Federal marine fisheries research program planning workshop, March 12–15, 1973, San Clemente, p. 150–156. Calif. Dep. Fish Game, NMFS Southwest Fish. Sci. Cent., La Jolla CA.

Lo, N.C.H.
1985 Egg production of the central stock of northern anchovy, *Engraulis mordax*, 1951–82. Fish. Bull., U.S. 83:137–150.
1988 Preliminary spawning biomass estimate of the northern anchovy in 1988. Admin. Rep. LJ-88-17, NMFS Southwest Fish. Sci. Cent., La Jolla CA, 15 p.

Lo, N.C.H., L. Jacobsen, & J. Squire
In Press Indices of relative abundance from fish spotter data. Can. J. Fish. Aquat. Sci.

MacCall, A.
1975 Investigation of aerial spotter variation in reported abundance of anchovies. Contrib. 19, Anchovy Workshop Meet., 21–22 July 1975. NMFS Southwest Fish. Sci. Cent., La Jolla CA, 3 p.

MacCall, A., & M. Prager
1988 Historical changes in abundance of six fish species off southern California, based on CalCOFI egg and larva samples. Calif. Coop. Oceanic Fish. Invest. Rep. 29:91–101.

MacCall, A., G. Stauffer, & J. Troadec
1974 Stock assessment, fishery evaluation, and fishery management of southern California recreational and commercial fisheries. Admin Rep. LJ-74–24, NMFS Southwest Fish. Sci. Cent., La Jolla CA, 144 p.

MacCall, A., R. Klingbeil, & R. Methot
1985 Recent increased abundance and potential productivity of Pacific mackerel (*Scomber japonicus*). Calif. Coop. Oceanic Fish. Invest. Rep. 16:119–129.

Mais, K.
1974 Pelagic fish surveys in the California Current. Calif. Dep. Fish Game, Fish. Bull. 162, 79 p.

Marr, J.
1951 On the use of the terms abundance, availability and apparent abundance in fishery biology. Copeia 1951:163–169.

Messersmith, J.D., J. Baxter, & P. Roedel
1969 The anchovy resources of the California Current region of California and Baja California. Calif. Coop. Oceanic Fish. Invest. Rep. 12:32–38.

Methot, R.D.
1989 Synthetic estimates of historical abundance and mortality for the northern anchovy. *In* Edwards, E.F., & B.A. Megrey (eds.), Mathematical analysis of fish stock dynamics, p. 66–82. Am. Fish. Soc. Symp. 6, Bethesda.

Quinn, W.H., V.T. Neal, & S.E. Antunez de Mayola
1987 El Niño occurrences over the past four and a half centuries. J. Geophys. Res. 92(C13):14,449–14,461.

Radovich, J.
1960 Redistribution in the eastern north Pacific Ocean, 1957and 1985. Calif. Coop. Oceanic Fish. Invest. Rep. 7:163–171.
1982 Collapse of the California sardine fishery. Calif. Coop. Oceanic Fish. Invest. Rep. 23:56–78.

Sette, O.E.
1969 A perspective of a multi-species fishery. Calif. Coop Oceanic Fish. Invest. Rep. 13:81–87.

Smith, P., & S. Richardson
1977 Standard techniques for pelagic fish egg and larvae surveys. FAO Fish. Tech. Pap. 175, 100 p.

Snedecor, G.W.
1959 Statistical methods. Iowa State Coll. Press, 334 p.

Squire, J.L.
1961 Aerial fish spotting in the United States commercial fisheries. U.S. Fish. Wildl. Serv., Commer. Fish. Rev. 23(12):1–7.

1972 Apparent abundance of some pelagic marine fishes off the southern and central California coast as surveyed by an airborne monitoring program. Fish. Bull., U.S. 70:1005–1019.

1983 Abundance of pelagic resources off California, 1963–78 as measured by an airborne fish monitoring program. NOAA Tech. Rep. NMFS SSRF-762, 75 p.

1987 Relation of sea surface temperature changes during the 1983 El Niño to the geographical distribution of some important recreational pelagic species and their catch temperature parameters. Mar. Fish. Rev. 49(2):44–57.

Squire, J.L., & D.W.K. Au
1990 Striped marlin in the northeast Pacific - A case for local depletion and core area management. *In* Planning the future of billfishes; Proc. 2d Int. Billfish Symp., Pt. 2 Marine recreational fisheries, p. 199–214. Natl. Coalition for Mar. Conserv., Savannah GA.

Williams, K.
1981 Aerial surveys of pelagic fish resources off southeast Australia 1973–1977. CSIRO, Div. Fish. Ocean., Rep. 130.

Differences in haplotype frequencies of mtDNA of the Spanish sardine *Sardinella aurita* between specimens from the eastern Gulf of Mexico and southern Brazil

Michael D. Tringali
Department of Marine Science, University of South Florida
140 Seventh Avenue South, St. Petersburg, Florida 33701
Present address: Florida Marine Research Institute
Department of Natural Resources
100 Eighth Avenue SE, St. Petersburg, Florida 33701-5095

Raymond R. Wilson, Jr.
Department of Marine Science, University of South Florida
140 Seventh Avenue South, St. Petersburg, Florida 33701

Abstract. – Analysis of restriction-site polymorphisms of mtDNA and Monte Carlo statistics were used to test the hypothesis that at least two genetic stocks of Spanish sardine *Sardinella aurita* are present in the eastern Gulf of Mexico, with one occurring at each of the two main fishery locations off Florida. Also included for comparison were specimens of Spanish sardine collected off southern Brazil. No significant heterogeneity of mtDNA haplotype frequencies was detected among specimens from the two locations within the Gulf of Mexico after analysis of 57 individuals (28 from Tampa Bay and 29 from the Florida Panhandle) using 9 informative restriction enzymes. However, highly-significant differences were observed between the specimens from the Gulf of Mexico and 16 specimens from southern Brazil. Based on counts of gill rakers of all specimens from both regions and the results of the mtDNA analysis, it is suggested that *Sardinella brasiliensis*, the Brazilian sardine, is conspecific with *S. aurita*, and that *S. aurita* is probably represented by genetically-identifiable populations in the western North and South Atlantic.

Manuscript accepted 17 February 1993.
Fishery Bulletin, U.S. 91:362-370 (1993).

Spanish sardine *Sardinella aurita* (Valenciennes) ranges in the western Atlantic from Cape Cod, throughout the Gulf of Mexico and Caribbean Sea, to southern Brazil (Whitehead 1973). It is also present in the Mediterranean Sea and in the eastern Atlantic off the African coast (Fisher 1978, Whitehead 1985). A second sardine species, *Sardinella brasiliensis* (Steindachner), reportedly occurs within the range of *S. aurita* between the Gulf of Mexico and southern Brazil (Whitehead 1973 and 1985, Johnson & Vaught 1986), but there have been no studies successful in fully differentiating the two species within the eastern Gulf of Mexico (Wilson & Alberdi 1991). There has traditionally been a small but important baitfish fishery for Spanish sardine off Florida with an annual landing of over 1500 t as recently as 1988. However, this fishery closed abruptly in 1989 after landings dropped sharply between 1988 and 1989. The closure was partly a response to uncertainty about the number of species or stocks being fished (Sutter & Mahmoudi 1992).

Management concerns about the sardine fishery in the eastern Gulf of Mexico involve the possibility of local stock depletion or collapse from increased fishing pressure at the two primary fishing areas in the eastern Gulf of Mexico, the Florida Panhandle and Tampa Bay. There is also concern over the possibility of overfishing one of the two species supposedly present. The first concern has arisen from the observation that Spanish sardines caught by the fisheries operating at these two locations appear to consistently differ morphometrically (Johnson & Vaught 1986), suggesting the possibility of separate genetic stocks or species. In response to these concerns, Wilson & Alberdi (1991) electrophoretically compared more than 300 specimens from the two areas at 41 presumptive genetic loci and found no important differences in allele frequencies, nor any fixed differences. They concluded that stock differences were only weakly indicated, and that no genetic evidence of two species of Spanish sardine in the eastern Gulf of Mexico had appeared.

Analysis of restriction-site polymorphisms of mitochondrial DNA (mtDNA) is generally regarded as offering a higher degree of resolution than protein electrophoresis in population genetic studies (e.g., Ferris & Berg 1987), and has recently become important in studies of potential fishery stocks. The most direct analytical approach is to compare the frequency distributions of composite mtDNA haplotypes among the sample populations, testing (x^2) whether the distributions are homogeneous and, therefore, indicative of stock mixing (Bentzen et al. 1989). However, the usually skewed distribution toward a common haplotype(s) coupled with the common occurrence of several rare haplotypes (Billington & Hebert 1991) in a population sample usually results in low sample numbers per cell in contingency tables, and tabulated values of x^2 cannot be used properly. This problem can be avoided, however, by using a Monte Carlo method of computing the exact x^2 expected from the observed haplotype frequencies among sample populations (Roff & Bentzen 1989, Bernatchez & Dodson 1990).

In this study we employ analysis of restriction-site polymorphisms of mtDNA and Monte Carlo statistics to test the hypothesis that the two main fisheries in the eastern Gulf of Mexico are comprised of at least two genetic stocks of *S. aurita*. We have included specimens of *S. aurita* collected off southern Brazil under an *a priori* expectation that stronger differences in mtDNA haplotype frequencies should exist between specimens from the Gulf of Mexico and southern Brazil. Considering the geographic proximity of our sample populations in the eastern Gulf of Mexico, and recognizing the fact that inadequate sampling of the mitochondrial genome (as evidenced by the number of restriction enzymes used) can bias the outcome in the direction of "no significant differences," inclusion of the Brazilian specimens allows us to objectively gauge the power of our methods to address the stated hypothesis.

Materials and methods

Specimens of *S. aurita* from the eastern Gulf of Mexico were obtained from the two main commercial fisheries along Florida's west coast, one near Tampa Bay and the other off the Panhandle. Individuals were collected fresh from both sites during the summer of 1989 (Fig. 1). Ripe ovaries were excised soon after capture and held on ice or in refrigerated buffer (MSB-Ca^{++} of Lansman et al. 1981) for up to 10d prior to purification of mtDNA; some ovaries from the Tampa Bay sample were stored frozen at –86°C until processing. The timing of specimen collections was structured to avoid resampling a single migrating school. Two samples were taken concurrently from Port St. Joe, Florida (n=10) and Destin, Florida (n=13) in May 1989, and a third sample was taken from Destin (n=6) in September 1989, for a total of 29 specimens (Fig. 1). In the Tampa Bay region a total of 28 individuals were taken during three collection times: February (n=12), May (n=10), and August (n=6) of 1989.

Whole fish specimens obtained from off Santos, Brazil were collected from the fishery and hand-carried frozen on dry ice to St. Petersburg, Florida within 2d and were stored at –86°C for several months without removing the ovaries. Because these specimens were

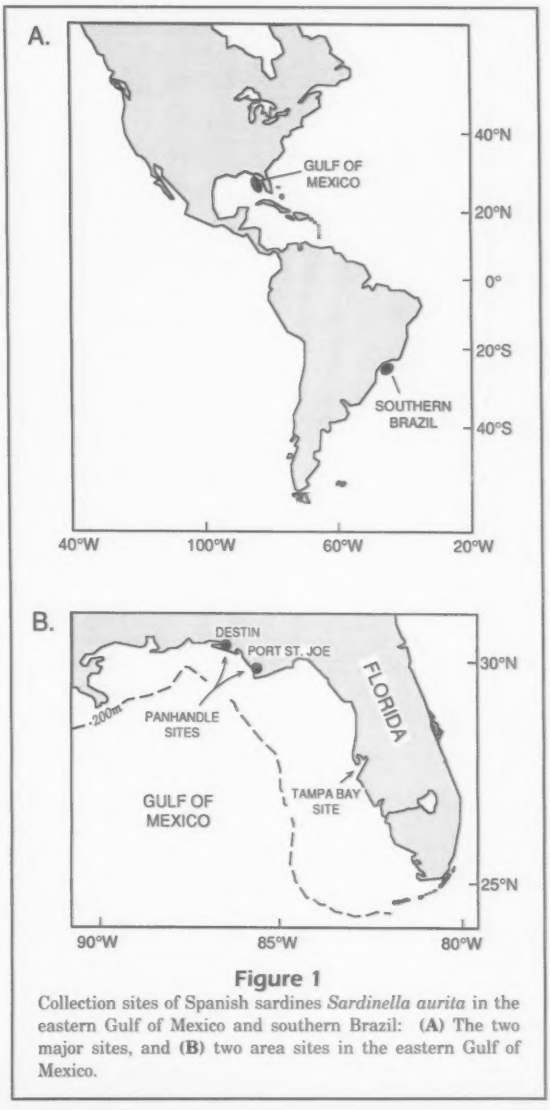

Figure 1

Collection sites of Spanish sardines *Sardinella aurita* in the eastern Gulf of Mexico and southern Brazil: **(A)** The two major sites, and **(B)** two area sites in the eastern Gulf of Mexico.

also used in the electrophoretic study of Wilson & Alberdi (1991), one thaw/refreeze cycle occurred prior to use in the present study. All specimens were identified to nominal species using the criteria of Whitehead (1973, 1985). That is, we counted the number of gill rakers on the lower limb of the first gill arch and related the count to standard length (SL), and we examined the condition (curled or flattened) of the anterior rakers of the lower limb of the first arch.

Mitochondrial DNA was purified from the ripe ovaries of the specimens taken from the Gulf of Mexico as in Wilson & Tringali (1990), except that the mtDNA collected after density-gradient ultracentrifugation was extracted in n-butanol which was not saturated with NaCl. This removed most of the salts, allowing greater precision over the molar concentration of the DNA-containing solution during the ethanol precipitation. The lower yield of mtDNA caused by thawing and refreezing of the Brazilian specimens necessitated use of a modification of the Chapman & Powers (1984) method of extraction (Tringali 1991).

Restriction digests were carried out as specified by the manufacturers using the following enzymes: *Apa*-I, *Bam*H-I, *Dra*-I, *Eco*R-I, *Hin*d-III, *Pst*-I, *Pvu*-II, *Sac*-I, *Xba*-I, and *Xho*-I. Fragments were separated by horizontal agarose gel electrophoresis and visualized in most cases using the gel-incorporated Hoechst 33258 (CalBiochem #SR5A03-0388) fluorochrome dye as in Deflaun & Paul (1986). However, some poor yields of mtDNA during purification made visualization of the smaller restriction fragments difficult using the fluorochrome, thus requiring application of an mtDNA hybridization probe to southern blots of the agarose gels (Tringali 1991). The non-radioactive hybridization probe was made from cesium-purified mtDNA of *S. aurita* using a commercial kit (Genius Kit of Boehringer Mannheim, Cat. #1093657). Hybridization and immunological detection of the probe was performed as specified by the manufacturer with the following modifications. The concentration of the blocking reagent in the prehybridization and hybridization solutions was doubled to 1.0% weight/volume to reduce background coloring of the hybridization filter (Zeta-Probe). The prehybridization period was extended to a minimum of 2h and the volume of the probe-containing hybridization solution was increased to 10 m L/100 cm^2 of filter. The ELISA reaction period was increased to 2 h. Under these modifications, the mtDNA restriction fragments were usually visible on the filter ~15 min into the color reaction.

Molecular weights (in base pairs) of the restriction fragments were estimated by the global form of the reciprocal method as described in Elder & Southern (1987). Restriction-fragment length polymorphisms (RFLPs) were expressed as two data types: restriction-site data and composite mtDNA haplotypes. The restriction-site composition of each individual was inferred from fragment profiles and intraspecific sequence diversity (Nei & Miller 1990) was calculated using the RESTSITE v1.2 algorithm. Composite mtDNA haplotypes were constructed for each individual from their restriction profiles with haplotypes grouped by sample location and time of collection. The frequency distribution of mtDNA haplotypes was tested for heterogeneity, with respect to location and time, by the log-likelihood G-test for independence (Sokal & Rohlf 1981). G-tests were also performed on selected samples following generation of 100 randomized data sets from the observed data, using the Monte Carlo technique described by Roff & Bentzen (1989) where the probability, P, of obtaining a randomized G_H value greater than the original observed value is given by

$$P = n / N_r \quad (1)$$

where n equals the number of outcomes in which the randomized G_H value is greater than the actual G_H value, and N_r represents the number of randomizations performed. The standard error of P was taken as

$$[P(1 - P)/N_r]^{1/2}. \quad (2)$$

The frequency of the most common haplotype was tested, after arcsine square-root transformation (Freeman & Tukey 1950), using the "V" statistic (Desalle et al. 1987) for heterogeneity between sampling locations.

Results

Counts of gill rakers identified 72 of 73 sample specimens as *S. aurita*; one specimen from Brazil had gill-raker counts expected for *S. brasiliensis*. Counts were lowest for the Panhandle specimens while specimens from Tampa Bay and southern Brazil were the most similar, having higher counts (Table 1). Specimens from the Florida Panhandle were of larger average size than those from Tampa Bay and southern Brazil, which were more similar in size (Table 1). A one-way analysis of variance revealed significant heterogeneity ($P<0.05$) in gill-raker counts between the specimens taken from the Panhandle and Tampa Bay, but not between those taken from Tampa Bay and southern Brazil. One Brazilian specimen had a gill-raker count of 154 at 150 mm SL, nearly identical to that reported for the lectotype of *S. brasiliensis* (155 at 148.3 mm SL; Whitehead 1973). However, we could detect no differences in the appearance of the anterior rakers (curled vs. flattened) for this or other specimens. The overall appearance of the rakers of all specimens most closely resembled Whitehead's (1985) diagrammatic drawing

Table 1
Data for Spanish sardines *Sardinella aurita* used in mtDNA analysis.

Location	Number counted	Size range[1] (mmSL)	gill-raker count Mean[2]	gill-raker count Range
Port St. Joe (Panhandle)	10	162–189	113±11SD	102–127
Destin (Panhandle)	19	159–189	114±9	99–128
Tampa Bay	28	149–171	134±7	121–145
Santos, Brazil	16	149–181	132±9	122–154

[1] Mean length of pooled specimens from the Panhandle is significantly larger than that of specimens from the other two regions (ANOVA, $P<0.05$).
[2] Mean number of gill rakers of pooled specimens from the Panhandle is significantly lower than that of specimens from the other two regions (ANOVA, $P<0.05$).

of *S. brasiliensis*, curling anteriorly downward. However, use of this character was extremely problematic for us because, other than the drawing, we found no published taxonomic account of the discovery of this character, no photographic evidence nor written description detailing the character, nor reference of this character to [any] catalogued or type material.

The combination of mtDNA purification and visualization techniques used here provided well-resolved digestion patterns that could be consistently and unambiguously scored for all individuals. Of the 10 restriction endonucleases used, only *Bam*H-I was not informative. This enzyme had but one restriction site in all samples and was used only in probe construction to linearize template mtDNA prior to labeling. Polymorphic digestion patterns occurred for the remaining nine enzymes, with *Pst*-I and *Pvu*-II highly variable (Table 2). The mean mtDNA genome size, calculated from the sums of all digestion patterns, was 16,304 base pairs (bp) ± 71 bp (SD). No size variation was detected between specimens or within the mtDNAs of individual specimens.

The nine informative enzymes sampled 52 unique restriction sites over all individuals (Table 3) with a mean of 43 sites per individual. All RFLPs were consistent with the assumption of a single nucleotide substitution between variant digestion patterns. Intraspecific sequence diversity (Nei & Miller 1990) over all individuals was 0.00525±0.00204 (bootstrapped SE) substitutions per nucleotide, a value consistent among all three sampling locations ($\bar{x}$=0.00509±0.00054, range 0.00452–0.00561). Twenty-four composite mtDNA haplotypes were generated from polymorphic restriction-fragment profiles of the 73 completely characterized Spanish sardines (Table 4). The composite mtDNA haplotype (BAABAAAAA) of the one putative *S. brasiliensis* specimen with a gill raker count close to the lectotype's (Whitehead 1970, 1973) was identical to that of another Brazilian specimen having the low gill raker count indicative of *S. aurita* (126 at 169 mm SL), as well as to that of seven specimens from the Gulf of Mexico (Table 4). The mtDNA haplotype most common in the Gulf of Mexico, AAAAAAAAA, occurred in very low frequency among the Brazilian specimens. The frequency of this haplotype was significantly different between specimens of the Gulf of Mexico and Brazil (V=10.90, $P<0.001$), but not among specimens from the different regions within the Gulf of Mexico (Table 5).

Ten composite haplotypes were unique to the Panhandle region, four to the Tampa Bay region, and five to Brazil. Four were observed in all three locations. G-tests of mtDNA haplotype frequencies for temporal and geographical heterogeneity among specimens from within the Gulf of Mexico did not allow rejection of the null hypothesis of population homogeneity ($P>0.05$). Pooling the Gulf specimens by location and testing for heterogeneity between locations using Monte Carlo statistics (100 randomizations) generated 35 G_H values exceeding the initial value of 25.774, again indicating that the null hypothesis of homogeneity for specimens taken within the Gulf of Mexico cannot be rejected ($P>0.35$, 2SE=0.09). Pooling all Gulf specimens and testing against the Brazilian specimens using Monte Carlo statistics resulted in a G_H value of 44.282 which was not exceeded by any of the 100 randomizations, indicating significant heterogeneity between specimens from those locations ($P<0.01$).

Discussion

Our results indicate an evident lack of genetic stock structuring between the commercially-fished populations of Spanish sardine in the eastern Gulf of Mexico, even though there is a significant difference in the average number of gill rakers between locations, in addition to the morphometric differences reported by Johnson & Vaught (1986). This significant variation in gill-raker counts relative to SL appears to confirm Whitehead's (1973) reference to two rates of increase in the number of gill rakers with increasing standard length among Spanish sardines of the western Atlantic, although the lowest counts (Panhandle) were lower than those Whitehead (1973) mentioned. Whitehead (1973) thought this variation in gill-raker counts indicative of the presence of two valid species of Spanish sardines in the western Atlantic, but our mtDNA analysis does not support his suggestion.

Table 2

Approximate sizes (base pairs) of restriction fragments from mtDNA of *Sardinella aurita*. Letters designate genotypes observed with each enzyme. "A" genotype was the most common for each enzyme.

Apa-I		*Bam*H-I	*Dra*-I		*Eco*R-I		*Hin*d-III		
A	B	A	A	B	A	B	A	B	C
6457	6457	16356	10233	8434	5621	5621	4169	3342	6607
7405	7405		5623	5623	4069	4069	3342	3296	4169
1948	1948		438	1798	3436	3436	3296	2661	2661
360	460			438	1318	1318	2661	2251	2104
107					665	1147	2104	2104	436
					620	665	436	1929	331
					525		331	436	
								331	
16277	16270	16356	16294	16293	16254	16256	16339	16350	16308

Pst-I							*Xho*-I		
A	B	C	D	E	F	G	A	B	C
4880	7100	7100	4360	4880	8184	4880	10965	9593	16274
4360	4360	4880	4200	4360	4880	4360	5309	5309	
3850	4200	4360	3850	3800	3150	3850		1372	
3150	564		3150	3000		2350			
			564	150		750			
16249	16224	16340	16124	16190	16214	16190	16274	16274	16274

Pvu-II								*Sac*-I	
A	B	C	D	E	F	G	H	A	B
6461	6461	10133	10133	6461	6461	6461	10753	7786	15230
4265	3672	2238	2238	3672	4770	3672	2238	7444	912
2238	2238	1779	1779	2238	2238	1878	1778	912	
1778	1778	1188	912	1779	1779	1778	912		
912	1188	912	690	912	912	1188	505		
505	912	230	505	690	230	912	230		
230	230		230	505		360			
				230		230			
16389	16479	16480	16487	16487	16390	16479	16416	16142	16142

Xba-I	
A	B
8317	6905
4809	4809
	2248
2248	1402
685	685
335	335
16394	16384

The intraspecific sequence variability of mtDNA of *S. aurita* is comparable to that observed in most other marine fishes. With a mean sequence divergence of about p=0.51 (Nei & Li 1979), the mtDNAs of Spanish sardines of the Gulf of Mexico fall within the range of mean values observed among other clupeids, i.e., between 0.37% for shad (Bentzen et al. 1989) and 2.4% for menhaden (Avise et al. 1989). In both shad (Roff & Bentzen 1989) and menhaden (Bowen & Avise 1990), population-level mtDNA variability was observed

Table 3

Site matrices inferred from RFLPs of *Sardinella aurita*. Letters denote restriction patterns. Column numbers are the restriction sites observed over all individuals for the given enzyme. Inside the matrices: 1=site presence, 0=site absence.

	Pst-I							*Xba*-I						*Hind*-III							
	1	2	3	4	5	6	7	8	9	10	11	12	13	14	15	16	17	18	19	20	21
A	1	0	1	1	1	0	0	1	0	1	1	1	1	1	0	1	1	1	1	1	1
B	1	1	1	1	0	0	0	1	1	1	1	1	1	1	1	1	1	1	1	1	1
C	1	0	1	1	0	0	0							1	0	1	0	1	1	1	1
D	1	1	1	1	1	0	0														
E	1	0	1	1	1	0	1														
F	1	0	1	0	1	0	0														
G	1	0	1	1	1	1	0														

	Pvu-II									*Dra*-I				*Apa*-I				
	22	23	24	25	26	27	28	29	30	31	32	33	34	35	36	37	38	39
A	1	1	0	1	1	1	1	1	0	1	0	1	1	1	1	1	1	1
B	1	1	1	0	1	1	1	1	0	1	1	1	1	1	1	1	1	0
C	1	0	1	0	1	1	1	1	0									
D	1	0	1	1	1	1	1	1	0									
E	1	1	1	1	1	1	1	1	0									
F	1	1	0	0	1	1	1	1	0									
G	1	1	1	0	1	1	1	1	1									
H	1	0	0	1	1	1	1	1	0									

	EcoR-I							*Xho*-I			*Sac*-I		
	40	41	42	43	44	45	46	47	48	49	50	51	52
A	1	1	1	1	1	1	1	1	0	1	1	1	1
B	1	1	1	1	1	0	1	1	1	1	1	0	1
C								1	0	0			

within the geographic regions sampled. Thus, the evident lack of significant heterogeneity in mtDNA haplotype frequencies among the Gulf specimens of *S. aurita* is probably not due to an inadequate level of mtDNA genome sampling relative to the sequence variability present.

Accepting that the mtDNA variability among sample locations of *S. aurita* was sufficiently characterized, at least two possibilities could account for the observed genetic homogeneity between our sample locations in eastern Gulf of Mexico. This lack of genetic structuring is the result of recent or ongoing genetic exchange between the sampled locations, or there may have been insufficient time for discrete Gulf populations, if they do exist, to diverge through mtDNA lineage sorting. The first explanation seems the more likely one, considering the life history of the species. *S. aurita* is known to be highly migratory (Hildebrand 1963, Simpson & Gonzalez 1967) and to spawn repeatedly throughout much of the year (Grall 1984). Although the pattern of adult migration of *S. aurita* in the eastern Gulf is still poorly understood, spawning occurs continuously between the Panhandle and Tampa Bay with no apparent geographic partitioning in either the distribution or abundance of eggs or larvae (Houde 1976). There are no known physical barriers to dispersal or migration in this region.

Significant geographic variation in mtDNA haplotype frequencies does exist between Spanish sardines in the eastern Gulf of Mexico and waters off southern Brazil, based upon the results of goodness-of-fit testing. This variation is due to two related factors. One is that the haplotype most common among the pooled specimens from the eastern Gulf of Mexico, AAAAAAAAA, possessed by 46% of the specimens, has a much lower occurrence (6%) among the specimens from southern Brazil. The other is the difference in the distribution of the *Pst*-I digestion pattern. Whereas 5 of 16 (31%) of the Brazilian specimens possessed the G-type pattern (Table 2), this pattern was absent in the Gulf specimens (n=57). Relative to the common A-type pattern of *Pst*-I present among the Gulf specimens, this G-type pattern represents a site gain at *Pst*-I.

Table 4

Frequency distribution of the 24 composite haplotypes from 73 *Sardinella aurita* from the western Atlantic. Restriction enzymes are in the following order: *Pst*-I, *Xba*-I, *Hin*d-III, *Pvu*-II, *Dra*-I, *Apa*-I, *Eco*R-I, *Xho*-I, and *Sac*-I. Frequency distribution of pooled haplotypes from the Gulf of Mexico differ from the Brazilian at $P<0.01$ ($G_H=44.282$).

Haplotype number	Composite digestion profile	Panhandle Florida	Tampa Bay Florida	Santos Brazil
1	AAAAAAAAA	14	12	1
2	BAABAAAAA	1	6	2*
3	AAADABAAA	1		
4	AABAAAAAA	1		
5	BAACBAABA	1		
6	BBABAAAAA	1		
7	BAACAAAAA	2	1	
8	CAAAAAAAA	1		
9	DAAAAABAA	1		
10	BAAFAAAAA	1		
11	CAABAAAAA	1	4	3
12	AAAAAAACA	1		
13	AAAEAAAAA	1	1	1
14	EAAAAAABA	1		
15	AAAEABBAA	1		
16	BAABAAAAB		1	
17	FAAAAAAAA		1	
18	BAAGAAAAA		1	
19	AAAFAAAAA		1	
20	AAAHAAAAA			2
21	GACAAAAAA			2
22	GAAAAAAAA			3
23	BAAAAAAAA			1
24	AAAAABAAA			1
		29	28	16

*Including specimen identified as *S. brasiliensis* by gill-raker count.

Table 5

Tests for temporal and geographic heterogeneity of *Sardinella aurita* mtDNA haplotypes. G_H values were generated by comparing the complete distribution of mtDNA haplotypes for each group. "V" statistics were calculated by comparing the frequency of angular-transformed Haplotype 1 between regions.

Sample	G_H	df	V	df
Tampa Bay vs. Panhandle	24.278	17	0.01	1
Tampa Bay vs. Brazil	29.302*	12	9.68*	1
Panhandle vs. Brazil	39.386*	19	11.49**	1
Pooled Gulf of Mexico vs. Brazil	44.282*	23	10.90**	1

* $P<0.05$, ** $P<0.001$ (from tabulated critical values of the x^2 distribution).

We interpret the significant heterogeneity in haplotype frequencies between specimens from the eastern Gulf of Mexico and southern Brazil as genetic stock differences between Spanish sardines of the western North and South Atlantic, rather than as species differences as, for example, between *S. aurita* and *S. brasiliensis*. The one specimen of this study referable to *S. brasiliensis*, with a gill-raker count of 154 at 150 mmSL, came from southern Brazil, but it had one of the mtDNA composite haplotypes (haplotype 2; Table 4) present among specimens from the eastern Gulf of Mexico. All other specimens from both Gulf and Brazilian waters possessed the lower gill-raker counts typical of *S. aurita*.

This interpretation also agrees with results of the electrophoretic study of Wilson & Alberdi (1991). After comparing 350 specimens from the eastern Gulf of Mexico with 41 specimens of Spanish sardine from off southern Brazil at 36 presumptive gene loci, they found no genetic evidence of more than one species of Spanish sardine in those two areas. That is, there were no fixed allelic differences that would suggest the presence of fully segregated gene pools, as in two species. Neither in the present study nor in that of Wilson & Alberdi (1991), which used the same Brazilian specimens as here, was our nominal *S. brasiliensis* distinguishable from *S. aurita* by electrophoretic genotype or mtDNA haplotype.

We think it likely that *S. brasiliensis* is conspecific with *S. aurita*. Whitehead (1970) removed *S. brasiliensis* from the synonymy of *S. aurita* on the observation that the syntypes of *S. brasiliensis* from off Brazil had both high and low gill-raker counts at similar lengths. That is, he concluded that the syntypes with low gill-raker counts were *S. aurita* and that the others with high gill-raker counts were *S. brasiliensis* of Steindachner. Whitehead (1973) again proposed the specificity of *S. brasiliensis* on this character based on his review of published data on gill-raker counts of western Atlantic *Sardinella*, but he did not report data from any additional specimens. Whitehead (1985) proposed that *S. brasiliensis* might be distinguished from *S. aurita* based on the shape of the gill rakers forming the branchial basket, i.e., flattened in *S. aurita* vs. curled in *S. brasiliensis*, but he did not specifically connect this character to catalogued specimens which he examined. No mention was made of this character in his prior discussion of the syntypes (Whitehead 1970).

To our knowledge, no thorough quantitative study of variation in gill-raker counts with SL among Brazilian sardines has been published. Montero & Perez

(1981) conducted a protein electrophoretic comparison at 24 presumptive loci of Brazilian *Sardinella* which had been first identified as either *S. brasiliensis* or *S. aurita* by high or low gill-raker counts, respectively. They reported no electrophoretic differences between the two putative species, which is consistent with our finding of significant variation in gill-raker counts between specimens from the Florida Panhandle and Tampa Bay in the apparent absence of any genetic differences (Table 1). Thus, the higher gill-raker counts which supposedly distinguish *S. brasiliensis* from *S. aurita* are probably due to non-genetic causes, and are of no greater taxonomic importance than the intraspecific variation in gill-raker counts observed between *S. aurita* inhabiting the Panhandle and Tampa Bay locations of the eastern Gulf of Mexico (Table 1). Until the present classification of Western Atlantic *Sardinella* is supported by a thorough study of variation in the characters on which it is based, the validity of *S. brasiliensis* as a species is in question.

Given the non-reticulate nature of mtDNA transmission, it is not difficult to understand intraspecific divergence when there is a mechanism between populations affecting the balance between gene flow and genetic drift. There are a number of potential barriers to gene flow within the trans-equatorial range of *S. aurita*, including diverging oceanic currents (e.g., the North Equatorial current) and the major river plume of the Orinoco which can extend far out into the Caribbean. Even without discrete physical barriers, the stochastic process of mtDNA lineage survival or extinction might in itself be enough to alter haplotype frequencies in this continuously-distributed species if the effective gene flow is low relative to the sizes of the populations or their geographic ranges (Neigel & Avise 1986). However, the mtDNA variability among *S. aurita* might be a product of differential selective forces because the species is distributed over so great a latitudinal (environmental) gradient. For the Spanish sardine of the western Atlantic, there are not yet enough data to choose between the alternative hypotheses of drift vs. selection in accounting for the evident genetic structuring.

To our knowledge, this report represents the first substantiated case of a holopelagic teleost with a supposedly continuous distribution between sample regions (Gulf of Mexico to southern Brazil) exhibiting significant heterogeneity in mtDNA haplotype frequencies. Whereas other studies (e.g., Graves & Dizon 1989) have compared sample populations of holopelagic fishes removed by great longitudinal distances, or on opposite sides of land masses (Ovenden et al. 1989), ours is the first to compare specimens at near-opposite ends of a trans-equatorial distribution spanning many degrees of latitude (30°N to 26°S). Not only do these results further confirm the potential usefulness of mtDNA in studies of hypothesized fishery stocks, but also suggest the need for additional studies on fishes having similar distributions.

Acknowledgments

We thank Dan Woodsen, Harry Mofield, and all those who assisted in the collection of *S. aurita* specimens from the Gulf of Mexico. We also thank Drs. Y. Matsuura (Instituto Oceanographi, Sao Paulo, Brazil) and Frank Müller-Karger (University of South Florida) for help in obtaining the Brazilian specimens. Joyce C. Miller kindly provided the Restsite v.1.2 computer program.

Partial support for this research came from an Aylesworth Marine Scholarship (Florida Sea Grant) and from grants-in-aid-of-research to MDT from Sigma-Xi, Cortez Chapter of the Organized Fishermen of Florida, the USF Department of Marine Science, and by NOAA Grant #NA89WC-H-MF028 (MARFIN) to RRW.

Citations

Avise, J. C., B. W. Bowen, & T. Lamb
1989 DNA fingerprints from hypervariable mitochondrial genotypes. Mol. Biol. Evol. 6(3):258–269.

Bentzen, P., W. C. Leggett, & G.C. Brown
1989 Mitochondrial DNA polymorphism, population structure, and life history variation in American shad *Alosa sapidissima*. Can. J. Fish. Aquat. Sci. 46:1446–1454.

Bernatchez, L., & J. J. Dodson
1990 Mitochondrial DNA variation among anadromous populations of cisco, *Coregonus artedii*, as revealed by restriction analysis. Can. J. Fish. Aquat. Sci. 47:533–543.

Billington, N., & P. D. Hebert
1991 Mitochondrial DNA diversity in fishes and its implications for introductions. Can. J. Fish. Aquat. Sci. 48 (Suppl. 1):80–94.

Bowen, B. W., & J. C. Avise
1990 Genetic structure of Atlantic and Gulf of Mexico populations of sea bass, menhaden, and sturgeon: Influence of zoogeographic factors and life-history patterns. Mar. Biol. (Berl.) 107:371–381.

Chapman, R. W., & D. A. Powers
1984 A method for the rapid isolation of mitochondrial DNA from fishes. Tech. Rep. UM-SG-TS-84-05, Maryland Sea Grant Coll., Univ. Maryland, College Park, 11 p.

DeFlaun, M. F., & J. H. Paul
1986 Hoechst 33258 staining of DNA in agarose gel electrophoresis. J. Microbiol. Methods 5:265–270.

Desalle, R., A. Templeton, I. Mori, S. Pletscher, &d J. S. Johnston
1987 Temporal and spatial heterogeneity of mtDNA polymorphisms in natural populations of *Drosophila mercatorum*. Genetics 116:215–223.

Elder, J. K., & E. M. Southern
1987 Computer-aided analysis of one dimensional restriction fragment gels. *In* Bishop, M.J., & C.J. Rawlings (eds.), Nucleic acid and protein sequence analysis: A practical approach, p. 165–172. IRL Press Ltd., Oxford, Wash DC.

Ferris, S. D., & W. J. Berg
1987 The utility of mitochondrial DNA in fish genetics and fishery management. *In* Ryman, N., & F. J. Utter (eds.), Population genetics and fishery management, p. 277–299. Univ. Wash. Press, Seattle.

Fisher, W.
1978 FAO species identification sheets for fishery purposes (Fishing area 31), vol. II. FAO, Rome.

Freeman, M. F., & J.W. Tukey
1950 Transformations related to the angular and the square root. Ann. Math. Stat. 21:607–611.

Grall, C.
1984 A study of the biology of the Spanish sardine, *S. aurita*, in Florida waters. Master's thesis, Univ. Miami, Miami FL, 107 p.

Graves, J. E., & A. E. Dizon
1989 Mitochondrial DNA sequence similarity of Atlantic and Pacific albacore tuna, *Thunnus alalunga*. Can. J. Fish. Aquat. Sci. 46:870–873.

Hildebrand, S. F.
1963 Genus *Sardinella* Cuvier and Valenciennes 1847, Spanish sardines. *In* Bigelow, H.B. (ed.), Fishes of the western North Atlantic. Mem. Sears Found. Mar. Res., Yale Univ. 1 (3):397–410.

Houde, E. D.
1976 Abundance and potential for fisheries development of some sardine-like fishes in the eastern Gulf of Mexico. Proc. Gulf Caribb. Fish. Inst. 28:73–82.

Johnson, A. G., & R. N. Vaught
1986 Species profile of Spanish Sardine (*Sardinella aurita*). NOAA Tech. Memo. NMFS-SEFC-187, NMFS Southeast Fish. Sci. Cent., Miami, p. 142–153.

Lansman, R. A., R. O. Shade, J. F. Shapina, & J. C. Avise
1981 The use of restriction endonucleases to measure mitochondrial DNA sequence relatedness in natural populations. III. Techniques and potential applications. J. Mol. Evol. 17:214–226.

Montero, G. V., & J. E. Perez
1981 Relaciones taxonomicas entre algunas especies de la familia Clupeidae (Pisces). Biol. Inst. Oceanogr. Venez. Univ. Oriente 20 (1&2):79–84.

Nei, M., & W. H. Li
1979 Mathematical model for studying genetic variation in terms of restriction endonucleases. Proc. Natl. Acad. Sci. USA 76:5269–5273.

Nei, M., & J. C. Miller
1990 A simple method for estimating average number of nucleotide substitutions within and between populations from restriction data. Genetics 125:873–879.

Neigel, J. E., & J. C. Avise
1986 Phylogenetic relationships of mitochondrial DNA under various demographic models of speciation. *In* Karlin, S., & E. Nevo (eds.), Evolutionary processes and theory, p. 515–534. Academic Press, NY.

Ovenden, J. R., A. J. Smolenski, & R.G. White
1989 Mitochondrial DNA restriction site variation in Tasmanian populations of Orange Roughy (*Hoplostethus atlanticus*), a deep-water marine teleost. Aust. J. Mar. Freshwater Res. 40:1–9.

Roff, D. A., & P. Bentzen
1989 The statistical analysis of mitochondrial DNA polymorphisms: Chi-square and the problem of small samples. Mol. Biol. Evol. 6:539–545.

Simpson, J. G., & G. G. Gonzalez
1967 Some aspects of the early life history and environment of the sardine, *Sardinella anchovia*, in eastern Venezuela. Minist. Agric. Cria, Invest. Pesq. Serv. Rec. Explor. Pesq. 1 (2):38–93.

Sokal, R. R., & F. J. Rohlf
1981 Biometry, p. 691–767. W.H. Freeman, NY.

Sutter, F. C., & B. M. Mahmoudi
1992 Investigations of inshore and offshore population dynamics of Spanish sardines along the central west coast of Florida. Unpubl. final rep., NMFS/MARFIN, Award NA90AA-H-MF749, NMFS Southeast Fish. Sci. Cent., Miami FL, 59 p.

Tringali, M. D.
1991 Intraspecific divergence of mitochondrial DNA within the continuous western Atlantic range of the Spanish sardine, *Sardinella aurita*. Master's thesis, Univ. South Florida, Tampa, 43 p.

Whitehead, P. J.
1970 The clupeoid fishes described by Steindachner. Bull. Br. Mus. Nat. Hist. (Zool.) 20 (I):1–46.
1973 The clupeoid fishes of the Guianas. Bull. Br. Mus. Nat. Hist. (Zool.), Suppl. 5:1–219.
1985 Clupeoid fishes of the world (suborder clupeoidei). FAO Fish. Synop. 125 (7):1–303.

Wilson, R. R. Jr., & M. D. Tringali
1990 Improved methods for isolation of fish mtDNA by ultracentrifugation and visualization of restriction fragments using fluorochrome dye: Results from Gulf of Mexico clupeids. Fish. Bull., US 88:611–615.

Wilson, R. R. Jr., & P. D. Alberdi Jr.
1991 An electrophoretic study of Spanish sardine suggests a single predominant species in the eastern Gulf of Mexico, *Sardinella aurita*. Can. J. Fish. Aquat. Sci. 48(5):792–798.

Estimated drift gillnet selectivity for albacore *Thunnus alalunga*

Norman Bartoo
David Holts
La Jolla Laboratory, Southwest Fisheries Science Center
National Marine Fisheries Service, NOAA
P.O. Box 271, La Jolla, California 92038-0271

Drift gillnet (DGN) fisheries, some directed toward albacore *Thunnus alalunga* and some toward other species, have operated in the north and south Pacific Ocean. These fisheries, some of which had their beginnings decades ago, expanded in the early 1980s and exerted a substantial, but as yet unknown, mortality on Pacific albacore populations. Knowledge of the selectivity of DGNs is useful for applying complex population-dynamics techniques to the albacore population.

Several DGN experimental surveys conducted in the north and south Pacific Ocean have produced data on albacore distribution and gear selectivity. In 1984–85 the Southwest Fisheries Science Center of the National Marine Fisheries Service (NMFS) undertook an experiment to quantify DGN mesh-size selectivity for albacore. The experiment produced size-selectivity data for a single mesh size used in the U.S. DGN commercial fishery for albacore (184 mm; all mesh sizes referred to are stretch mesh measurements), in the eastern North Pacific Ocean. Other experiments designed to sample albacore were conducted by the Japan Marine Fishery Resource Center in 1980 (JAMARC 1983), 1982 (JAMARC 1985), and 1983 (JAMARC 1986). These experiments used other mesh sizes which produced complimentary data used in this study. The objective of this analysis was to quantify drift gillnet mesh-size selectivity for albacore, using existing data collected from various experiments and surveys in the Pacific Ocean.

Methods

Various experiments providing data have been conducted independently at different times and in different areas (Fig. 1). Consequently, some assumptions had to be made concerning comparability of nets used and availability and vulnerability of fish sizes to be sampled. However, there was enough information to provide insights into net selectivity for albacore. The nets used in all the experiments were similar to typical Japanese commercial drift nets. All nets had similar mesh-hanging ratios, twine/mesh-size ratios, and were of multifilament construction (Table 1). These are the most important factors affecting the selectivity curve for a given mesh size (Hamley 1975).

Detailed descriptions for the JAMARC experiments, including set locations, timing, mesh size placement, etc, are contained in the JAMARC references. These experiments were designed to obtain information on resource distribution and catch rates for possible future commercial fisheries. In brief, the JAMARC North Pacific experiment was a 1yr survey beginning in the spring of 1980 (Fig. 1). It targeted albacore using nets with mesh sizes of 130–250mm. The JAMARC 1982 and 1983 experiments in the South Pacific were conducted in the area shown in Fig. 1 and targeted all tuna-like species, using 180 mm mesh nets in 1982, and 118 mm and 160–180 mm mesh nets in 1983.

The NMFS experiment targeted albacore. A total of 27 night sets was made: 12 sets in waters south of Point Conception and within 300 mi of shore; 7 sets in the vicinity of the Guide Seamount south of the Farallon Islands; and 8 sets approximately 1000 mi west of Oregon near 142°W long. and 45°N lat. (Fig. 1). All sets used 184 mm mesh nets.

In all the experiments using mesh sizes of >130 mm, the amount of gear fished during each set ranged from 2760 m to 10,800 m, and the number of sets ranged from 11 to 176 (Table 1). Nets in each experiment were deployed and retrieved as in typical commercial operations. Nets were deployed at dusk, and retrieval began at first light often extending into midmorning. Soak times were ~10–16 h/set.

Data collected

Data published by JAMARC are limited to fork length (FL) frequencies by mesh size by set. The NMFS data include fork length-frequencies, maximum or largest body girth, and opercular girths for each fish, and notation on the mode of capture for each fish (tangled, wedged, or gilled). Fish were described as wedged or gilled when inserted into a mesh so that the entire perimeter of the mesh held the fish. This occurred at locations on the body from the snout to the point of maximum body girth. Fish were described as tangled when snared or tangled by fins or tail. Length-frequencies for U.S. troll-caught fish from the same time and areas are available for

Manuscript accepted 9 February 1993.
Fishery Bulletin, U.S. 92:371-378 (1993).

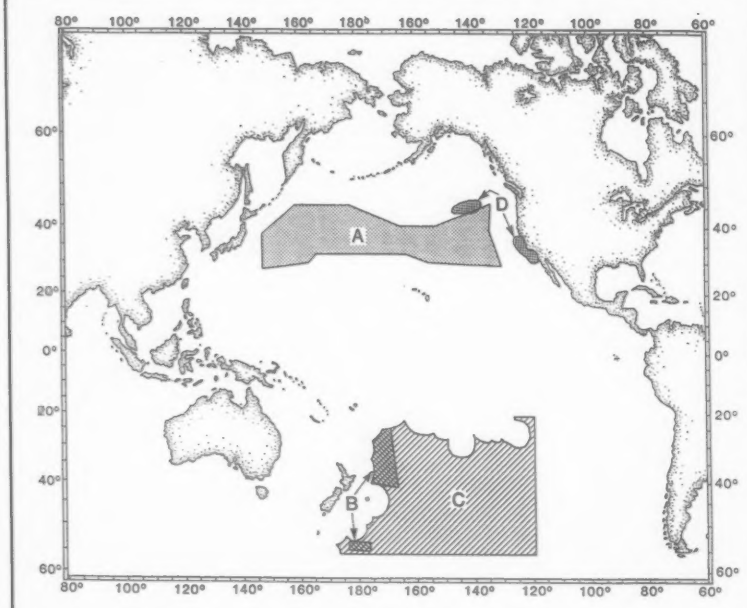

Figure 1

Areas sampled for albacore *Thunnus alalunga* by drift gillnets. **(A)** JAMARC 1980 survey (JAMARC 1983); **(B)** JAMARC 1982 survey (JAMARC 1985); **(C)** JAMARC 1983 survey (JAMARC 1986); **(D)** NMFS 1985 experiment.

Table 1

Characteristics of drift gillnets used, amount of gear fished, and alalunga caught for selected stretch mesh sizes.

Survey	Mesh size	Twine size (dinier/ strand)	Net material	Hang-in-ratio (% stretch mesh Distance/ hanging)	No. set
JAMARC 1980	130	210/21	Nylon	56.1	
(JAMARC 1983)	150	210/24	Nylon	56.1	
North Pacific	160	210/27	Nylon	56.1	
	170	210/30	Nylon	55.5	
	180	210/33	Nylon	56.1	
	200	210/36	Nylon	56.1	
	All				178
JAMARC 1982 (JAMARC 1985) South Pacific	180	210/30	Nylon	55.3	38
JAMARC 1983 (JAMARC 1986) South Pacific	118	210/10	Nylon		11
NMFS 1985 North Pacific	184	210/18	Polyester	50.0	27

comparison. Sample sizes of albacore caught by mesh size for each experiment, as well as the quantity of gear fished, are shown in Table 1.

Results

JAMARC 1980 data

Gear selectivity can only be estimated because there is no information on the actual size structure of the North Pacific albacore population (Hamley 1975). Data from several mesh sizes fished simultaneously and assumptions about shape, variance, and efficiency of the selectivity curves are required. The JAMARC 1980 experiment provided the only published dataset containing this information. Length-frequencies obtained in the 1980 experiment for mesh sizes 130, 150, 160, 170, 180, and 200 mm are shown in Fig. 2 (A–F). In all these mesh sizes, albacore captured had size modes at 53, 62, and 78 cmFL.

Two options are available for calculating an indirect selectivity curve: (1) Fitting a predetermined distribution function to data, using a method similar to that of Ishida (1962); or (2) estimating the selectivity of different meshes to one common size-class (mode) of fish and extrapolating to other mesh sizes (Regier & Robson 1966). Lack of an objective mathematical function in determining the shape of the selectivity curve in the first method, and the need for fitting the selectivity curve "by eye," required that a combination approach was employed.

A basic assumption of gillnet selectivity analysis is that selectivity is the same for those combinations of length interval L(i) and mesh size M(j) where the ratios of L(i)/M(j) are equal (Regier

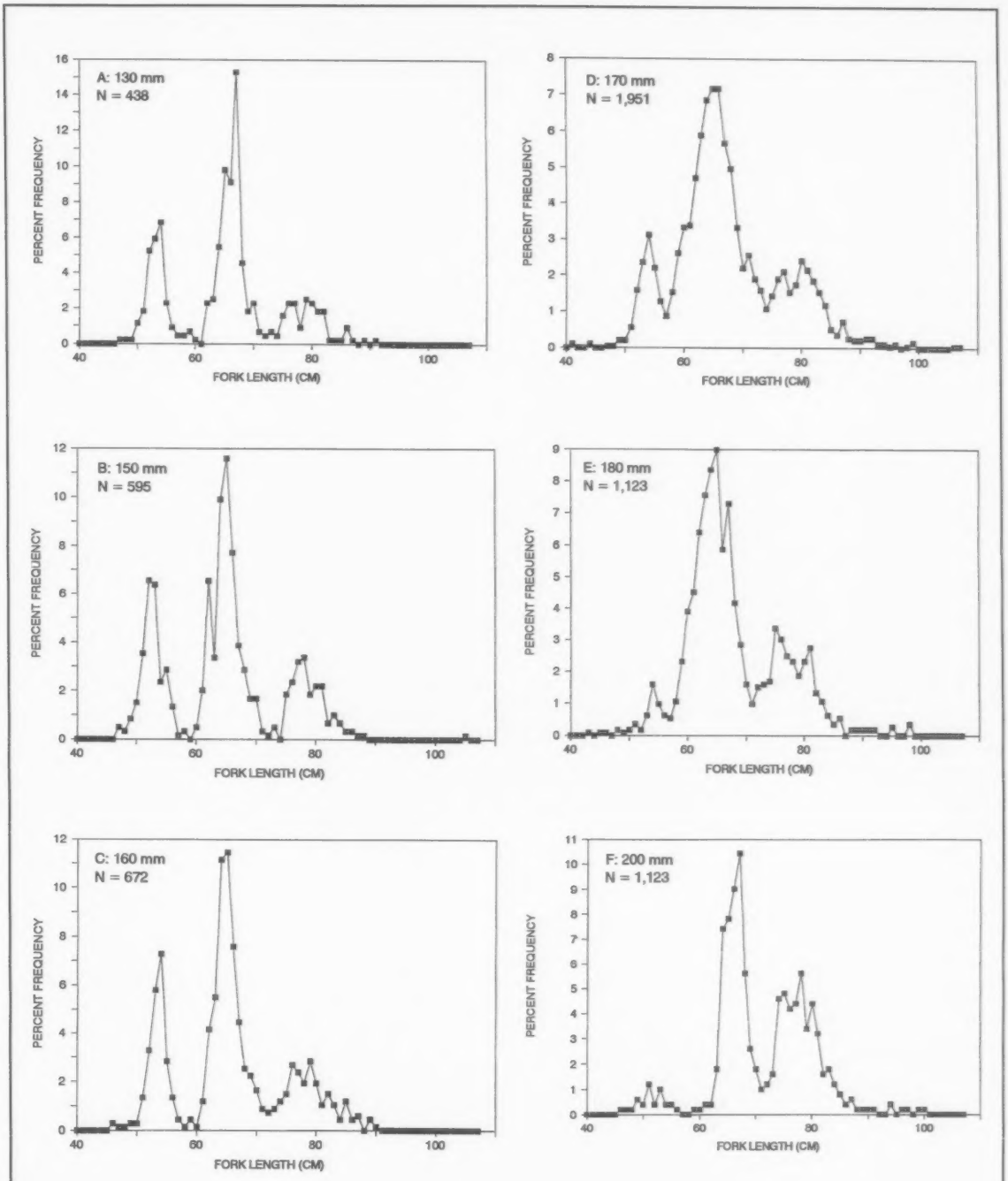

Figure 2

Percent frequency-of-occurrence of albacore *Thunnus alalunga* by fork-length interval by stretch-mesh size. Data from the 1980 JAMARC survey (JAMARC 1983). **(A)** 130mm mesh; **(B)** 150mm mesh; **(C)** 160mm mesh; **(D)** 170mm mesh; **(E)** 180mm mesh; **(F)** 200mm mesh.

& Robson 1966). This assumes that the length:girth ratio is the same for all fish. Each fork-length interval was divided by the appropriate mesh size of capture, and then multiplied by the appropriate observed frequency. This produced "generic" size-frequencies by mesh size. Each resulting size-frequency interval, by mesh size, was normalized to the greatest frequency. The resulting frequencies, one for each mesh size, were then scaled to an assumed 100% efficiency at the peak frequency sampled (the mid-60 cm mode); thus, differential sample sizes by mesh are taken into account. If all mesh sizes have the same selectivity curve, and no sampling variance, they would all be the same.

Rather than using the method of Ishida to describe a common selectivity curve (Regier & Robson 1966), the "mean" shape of the selectivity curve was estimated from the selectivity of the different mesh sizes for the largest (78 cmFL) and smallest (53 cmFL) modes captured by all mesh sizes. The curve obtained for the 53 cm mode described the left or ascending limb of the selectivity curve, and the curve for the 78 cm mode described the right or descending limb. Lengths between these two limbs were assumed to be sampled at 100%. This included some lengths with very low percent-frequencies (i.e., we assumed few fish were available) as well as the size mode near 62 cm. There was no assumption that the left and right limbs have the same shape.

For the 78 cm mode, the cumulative percent-frequency of capture vs. length of fish caught for all mesh sizes are shown in Fig. 3. When plotted on normal probability scales, cumulative percent-frequencies

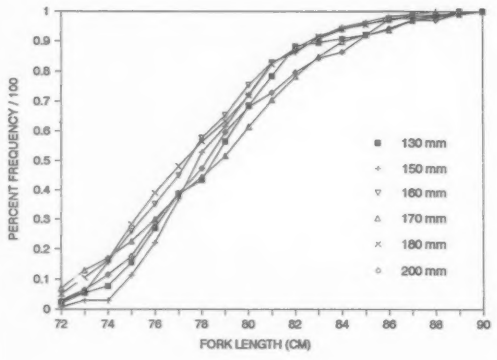

Figure 3

Cumulative percent frequency-of-occurrence by fork-length interval for 130 mm, 150 mm, 160 mm, 170 mm, 180 mm, and 200 mm stretch mesh sizes for the 78 cmFL mode of albacore *Thunnus alalunga* sampled in the 1980 JAMARC survey (JAMARC 1983).

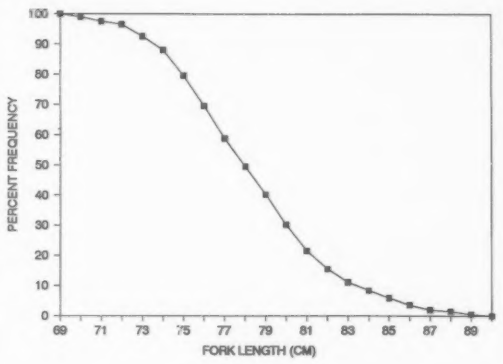

Figure 4

Mean selectivity-curve right limb for albacore *Thunnus alalunga* from the 78 cmFL mode sampled in the 1980 JAMARC survey (JAMARC 1983).

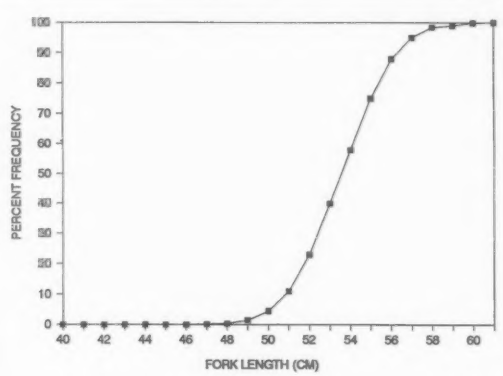

Figure 5

Mean selectivity-curve left limb for albacore *Thunnus alalunga* from the 53 cmFL mode sampled in the 1980 JAMARC survey (JAMARC 1983).

formed straight lines with virtually the same slopes. An average cumulative percent-frequency (subtracted from 100) provided the shape of the right limb (Fig. 4). This introduced the assumption of a constant variance and normal distribution (Hamley 1975). The same procedure provided the left limb of the selectivity curve which increased more rapidly or had a greater slope (Fig. 5).

These two limbs must now be placed appropriately on the X axis for each mesh size. This is accomplished separately for each limb by mesh size. The sampling efficiency at 53.5 cmFL for each mesh size was estimated by linear regression. The observed maximum

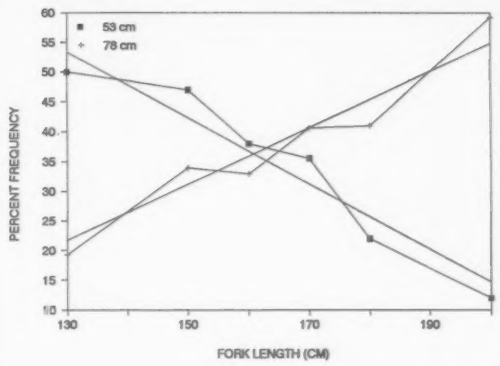

Figure 6

Linear regressions of observed maximum percent sampling efficiency at 53 cm and 78 cmFL against stretch-mesh size for albacore Thunnus alalunga.

Table 2

Estimated percent sampling efficiency for albacore *Thunnus alalunga* at fork lengths of 53 cm and 78 cm for various stretch mesh sizes.

Mesh size (mm)	Fork length (% efficiency)	
	53cm	78cm
130	53.3	21.7
150	42.3	31.2
160	36.8	35.9
170	31.3	40.7
180	25.7	45.4
184	23.5	47.3
200	14.7	54.8

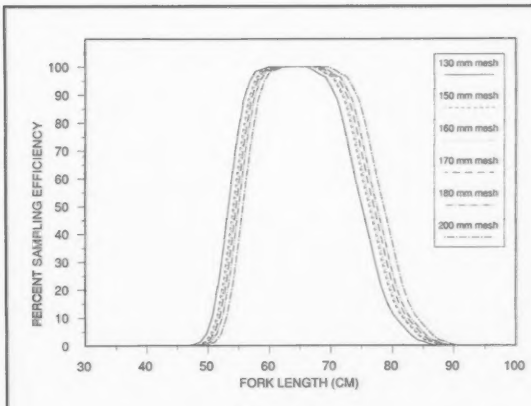

Figure 7

Selectivity curves (%) for albacore *Thunnus alalunga* for 130 mm, 150 mm, 160 mm, 170 mm, 180 mm, and 200 mm stretch-mesh sizes.

percent efficiency of sampling at the 53 cmFL peak was regressed against mesh size for all mesh sizes (Fig. 6). The estimated percent sampling efficiency at 53 cmFL for each mesh size is shown in Table 2. Using the same method, the percent sampling efficiency was estimated for 78 cmFL for each mesh size (Fig. 6, Table 2).

The family of selectivity curves by mesh size is shown in Fig. 7. These were determined by shifting the mean selectivity-curve limbs to the left or right so that sampling efficiencies at 53 and 78 cmFL matched the values in Table 2 for each mesh size. Fork lengths between the two limbs were assumed to be sampled with maximum efficiency, consistent with theory associated with unimodal selectivity curves (Hamley 1975).

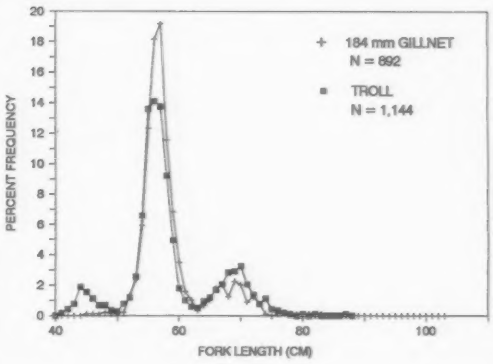

Figure 8

Percent frequency-of-occurrence by fork-length interval for albacore *Thunnus alalunga* sampled in the 1985 NMFS experiment by 184mm stretch mesh and by trolling.

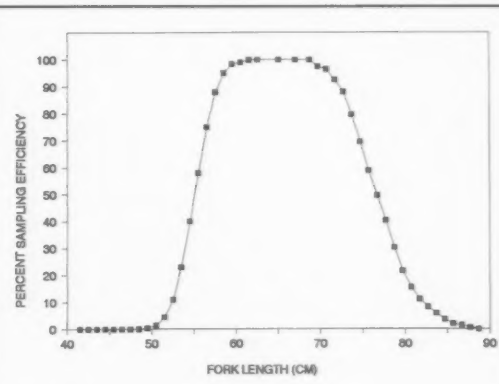

Figure 9

Selectivity curve for albacore *Thunnus alalunga* for 184 mm stretch-mesh size.

NMFS 1985 experiment

Length-frequency data for albacore collected in the 184 mm mesh during the 1985 NMFS experiment are shown in Fig. 8. The estimated selectivity curve is shown in Fig. 9 and, as expected, is almost identical to the 180 mm mesh selectivity curve (Fig. 7). For comparison, length-frequencies from the NMFS experiment taken by both trolling jigs and drift netting in the same area are shown in Fig. 8. As predicted by the selectivity curve (Fig. 9), few fish <50 cm length were sampled by the 184 mm mesh even though the fish were assumed available to the net, as indicated by the size-frequency sampled by the trolling gear fished in the same area and time.

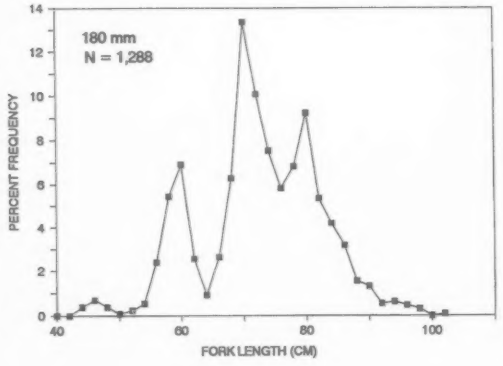

Figure 10
Percent frequency-of-occurrence by fork-length interval for albacore *Thunnus alalunga* for 180mm stretch mesh sampled by the 1982 JAMARC survey (JAMARC 1985).

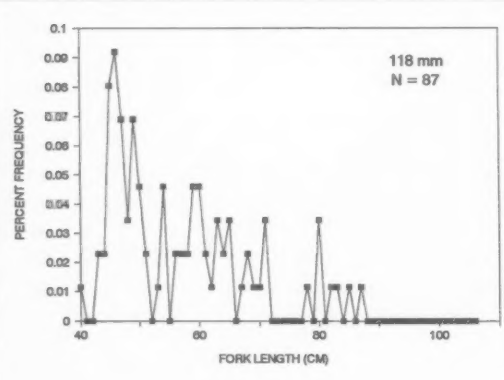

Figure 11
Percent frequency-of-occurrence by fork-length interval for albacore *Thunnus alalunga* for 118mm stretch mesh sampled by the 1983 JAMARC survey (JAMARC 1986).

JAMARC 1982 experiment

The 1982 JAMARC South Pacific experiment collected data for a 180 mm mesh size. Length-frequency data obtained are shown in Fig. 10. The estimated selectivity curve for this mesh is the same as shown for the 180 mm mesh in Fig. 7. From inspection of the length-frequencies for 180 mm and 184 mm mesh sizes from the North Pacific, it was apparent that the South Pacific experiment sampled an albacore population with a different size structure. The results show a much greater proportion of fish in the 70–80 cmFL range than in the North Pacific sampling. This is also seen in samples taken from the U.S. troll fishery that operated in the South Pacific (Rensink 1991)

JAMARC 1983 experiment

Length-frequency data obtained from the 1983 JAMARC South Pacific experiment using 118 mm mesh are shown in Fig. 11. The selectivity relationships developed from the North Pacific data do not accurately predict the expected selectivity curve for the 118 mm mesh. This is a result of small sample sizes and an observed peak size mode well below the sizes of albacore captured in the mesh sizes used to derive the selectivity curves.

Discussion

Selectivity curves derived from the JAMARC 1980 experimental data appear similar in shape to selectivity curves presented for salmon *Onchorynchus nerka* and *O. keta*, slender tuna *Allothunnus fallai*, and mackerel *Scomberomorus niphonius*, and other fusiform fishes (Taguchi 1961, Ishida 1964, Shimazaki et al. 1984). The asymmetry of each selectivity curve (i.e., steeper on the left limb and flatter on the right limb) is similar to that observed for selectivity curves of other fusiform fishes (Hamley 1975) and is explained by the mechanics of capture. The smallest fish, retained by the net at some particular girth/mesh-perimeter ratio, tend to be caught near maximum girth. Also, the range of sizes providing the ratio is relatively narrow. For larger fish, the same ratio can be found over a larger range of fish sizes because the point of capture may be anywhere from the maximum girth forward to the snout tip. For example, maximum girth of albacore increases more rapidly than opercular girth as a function of length (Fig. 12) which extends or skews the

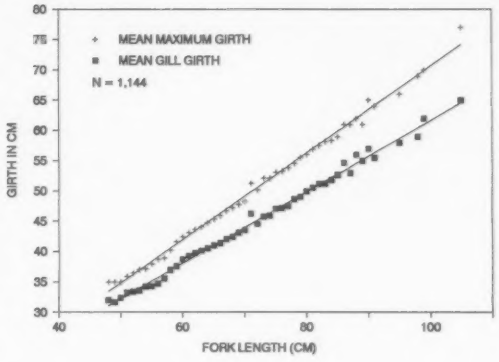

Figure 12
Relationship of albacore *Thunnus alalunga* maximum and opercular girths to fork length for 1144 fish sampled by the 1985 NMFS experiment.

right limb of the selectivity curve. This skewing can be troublesome when symmetrical or pre-determined selectivity curves are fit to data. The method used in this study minimizes this problem.

Assumptions that selectivity curves estimated from the 1980 JAMARC experiment applied to similar nets, such as the NMFS 184 mm mesh and the JAMARC-1982 180 mm mesh, appear acceptable from the data available. The principal factor limiting the application of these selectivity curves to other albacore populations is the girth/length relationships discussed above (Fig. 12). Significant changes in this relationship will change the steepness of the selectivity-curve limbs and the skewness.

Extrapolation of the mean selectivity curve to smaller mesh sizes than those providing the initial data may be improper based on the data observed for the 118 mm mesh. Although the sample size was relatively small, the apparent increase in tangling of larger fish caught in smaller mesh sizes compared with larger mesh sizes suggests that the right portion of selectivity curves for meshes <130 mm are more skewed. Tangled fish did not appear to be a problem in the NMFS or JAMARC 1980 datasets, presumably because all mesh sizes either gilled or wedged fish in the largest mode. Additionally, there may have been fewer larger fish available in the survey areas, as shown by troll-caught samples.

The absence of larger, tangled fish in both net-caught and troll-caught samples could result from reduced availability or vulnerability of larger fish in the areas sampled. Surface fisheries (i.e., drift net, troll, and pole-and-line) for albacore in the North Pacific produce catches with similar length-frequencies in the same areas (Bartoo & Foreman In press). However, albacore taken by subsurface longline gear at the same time and area are generally larger in length than those taken in the surface fisheries. This indicates albacore show differential availability or vulnerability between surface and subsurface gears. This could be due to spatial separation or behavior which may change with fish size. The results presented here assume that vulnerability to DGNs is relatively static over time.

Acknowledgments

We acknowledge contributions to this work by several individuals. Thanks to Tony West and the crew of the F/V Steelfin II for their assistance during the cruises. Thanks to Earl Weber for helping conduct the NMFS drift gillnet experiment, Sonee Sonu for providing Japanese-English translations, and to the many reviewers for constructive comments on the manuscript. Finally, thanks to Karen Handschuh for production of the manuscript.

Citations

Bartoo, N., & T. J. Foreman
In Press A synopsis of the biology and fisheries for north Pacific albacore tuna. *In* Shomura, R. (ed), Report of the FAO Expert Consultation on Interactions of Pacific Ocean Tuna Fisheries. FAO Fish. Tech Pap.

Hamley, J. M.
1975 Review of gillnet selectivity. J. Fish. Res. Board Can. 32(11):1943–1969.

Ishida, T.
1962 On the gill-net mesh selectivity curve. Bull. Hokkaido Reg. Fish. Res. Lab. 25(1):20–25 [Engl. transl. by Fish. Res. Board Can Transl. Ser. 1338].
1964 Gillnet mesh selectivity curves for sardine and herring. Bull. Hokkaido Reg. Fish. Res. Lab. 29(1): 1–9 [Engl. transl. by Fish. Res. Board Can. Transl. Ser. 1284].

JAMARC (Japan Marine Fishery Resource Center)
1983 Newly developing resources survey report, north and west Pacific. Rep. 16 (1980), Jpn. Mar. Fish. Resour. Cent., 187 p. [in Jpn.].
1985 Newly developing resources survey report, eastern south Pacific-high latitudes. Rep. 15 (1982), Jpn. Mar. Fish. Resour. Cent. 73 p. [in Jpn.].
1986 Newly developing resources survey report, eastern south Pacific-high latitudes. Rep. 14 (1983), Jpn. Mar. Fish. Resour. Cent., 98 p. [in Jpn.].

Regier, H. A., & D. S. Robson
1966 Selectivity of gill nets, especially to lake whitefish. J. Fish. Res. Board Can. 23:423–454.

Rensink, G.
1991 Summary of the 1989–90 U.S. south Pacific albacore fisheries data. Admin. Rep. LJ-91-14, NMFS Southwest Fish. Sci. Cent., La Jolla CA.

Shimazaki, K., S. Yamamoto, & T. Meguro
1984 A non-selective drift gill net for pelagic fish on the high sea. Bull. Fac. Fish. Hokkaido Univ. 35(1):17–27 [in Jpn, Engl. summ.].

Taguchi, K.
1961 On the suitable mesh size on salmon gillnets inferred from the relationship between body weight of salmon caught by gillnets and its mesh size. Bull. Jpn. Soc. Sci. Fish. 27:645–649 [in Jpn., Engl. summ.].

Stage-I zoeae of laboratory-hatched *Lopholithodes mandtii* (Decapoda, Anomura, Lithodidae)

Evan B. Haynes
Auke Bay Laboratory, Alaska Fisheries Science Center
National Marine Fisheries Service, NOAA
11305 Glacier Highway, Juneau Alaska 99801–8626

Of the approximately 25 species of Lithodidae of the northern North Pacific Ocean, larvae have been described, at least in part, for 11 species: *Dermaturus mandtii* Brandt, *Cryptolithodes typicus* Brandt, *Hapalogaster grebnitzkii* Schalfeew, *H. mertensii* Brandt, *Lithodes aequispina* Benedict, *Paralithodes brevipes* (Milne Edwards and Lucas), *P. camtschaticus* (Tilesius), *P. platypus* Brandt, *Placetron wosnessenskii* Schalfeew, *Rhinolithodes wosnessenskii* Brandt, and *Hapalogaster dentata* (De Haan). A review of the published descriptions of these larvae, except *H. dentata*, has been given by Haynes (1984). In this paper I describe and illustrate Stage-I zoeae of *Lopholithodes mandtii* Brandt and compare its morphology with the larvae reviewed by Haynes and with the published description of *H. dentata*.

Methods

Zoeae were hatched in the laboratory by an ovigerous female collected 4 April 1989 at Little Port Walter, southern Baranof Island, Alaska. The female was transported to the Auke Bay Laboratory 14 April 1989 and kept in an aquarium with running seawater. The zoeae began hatching about 2 wk later and were active swimmers, congregating near the surface of the aquarium. About 25 of the hatched zoeae were preserved every 2 or 3 d during 2–31 May 1989, until no zoeae remained alive in the aquarium. No attempt was made to rear the zoeae. Water temperatures in the aquarium were 5.6–6.5°C during collection of the larvae. No prezoeae were seen. None of the zoeae collected had molted to Stage II and no morphological differences were noted among the zoeae studied.

Methods of measuring zoeae and their appendages and techniques of illustrations follow Haynes (1984). Processes on the telson are numbered from the outermost to innermost (medial) pair. For clarity in the illustrations, setules on plumose setae and spinules on telsonal spines are omitted, but spinulose setae are shown. At least 5 zoeae were used to verify segmentation and setation; 10 zoeae were used for carapace and total length measurements.

Description of zoeae

Carapace (Fig. 1A,B) Mean carapace length, 1.3 mm (range 1.1–1.5mm); mean total length (excluding telsonal processes), 5.7mm (range 5.1–6.0 mm). Carapace with medially curved, long (>1/4 carapace length) posterolateral spines, and pronounced dorsal ridge. No supraorbital spines. Eyes sessile.

Antennule (Fig. 1C) First antenna (antennule) with unsegmented tubular portion (peduncle) and distal conical projection. Peduncle with ventral plumose seta. Conical projection with 5–6 aesthetascs and a simple seta terminally and two aesthetascs subterminally.

Antenna (Fig. 1D) Antenna with endopod and scale. Endopod slightly shorter than scale, and tipped with two hook-like projections. Antennal scale unsegmented, with fringe of 9 heavily plumose setae along terminal inner margin and prominent spine on distal outer margin. Ventral surface of protopodite with spinulose spine at base of endopod and naked spine at base of antennal scale.

Mandibles (Fig. 1E) Incisor process of right and left mandibles tooth-like with minute serrations. Right mandible: anterior margin with small teeth and denticulated projection; dorsal margin of molar with two denticular ridges; posterior margin with two denticulated projections. Left mandible: anterior margin with premolar denticles. Mandibles without subterminal processes, movable premolar denticle, palp, or palp bud.

Maxillule (Fig. 1F) Endopod 3-segmented, with 3 setae terminally, long distal seta on second segment, and short distal seta on 1st segment; coxal endite unsegmented with 4 plumodenticulate setae and 3 setae subterminally that sometimes have either a few minute spinules or setules; basal endite with 2 elongate, spinelike teeth armed with small denticles and 2 naked setae subterminally; no fine hairs on maxillule.

Maxilla (Fig. 1G) Endopod bilobed, setation formula 3,1,3; basal and coxal endites bilobed; coxal endite with 7 (sometimes 6) terminal and 1 subterminal setae on proximal lobe, 3 terminal and 1 subterminal setae on distal lobe, basal endite with 4 terminal and 1 subterminal setae on proximal lobe and 3 terminal and 1 subterminal setae on distal lobe; scaphognathite with 4 long, marginal plumose setae; fine

Manuscript accepted 2 February 1993.
Fishery Bulletin, U.S. 91:379-381 (1993).

hairs on outer margin of endopod and proximal lobe of coxal endite.

Maxilliped 1 (Fig. 1H) No coxal setae, setation formula of basipod 2,2,3,3; endopod 5-segmented, setation formula 3,2,1,2,4+I (Roman numeral denoting subterminal seta); exopod partially segmented with 4 plumose natatory setae; endopod barely longer than exopod.

Maxilliped 2 (Fig. 1I) No coxal setae; basipod with 1 distal thin spine, armed with marginal spinules plus 1 naked seta and a naked seta in proximal half; endopod 4-segmented, first 3 segments each with distal thin spine armed with marginal spinules plus 1 plumose seta, fourth with 4+I plumose setae; exopod incompletely 2-segmented, 4 plumose natatory setae.

Maxilliped 3 (Fig. 1J) Exopod and endopod undeveloped; exopod partially segmented, with 3 undeveloped setae terminally; endopod with undeveloped seta terminally.

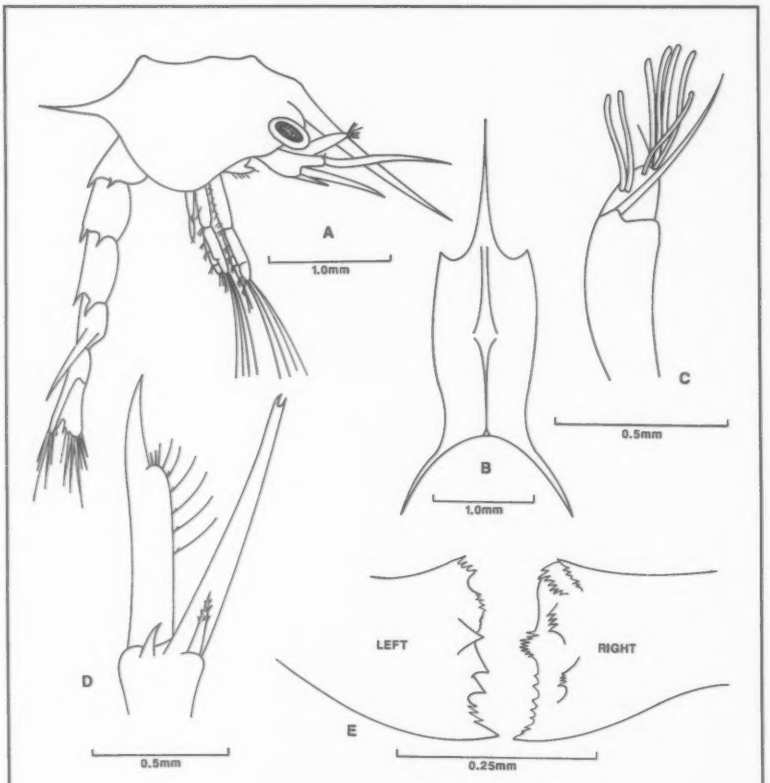

Figure 1
Stage-I zoea of *Lopholithodes mandtii*: **(A)** whole animal, right side; **(B)** carapace, dorsal; **(C)** antennule, ventral; **(D)** antenna, ventral; **(E)** mandibles (left and right), posterior;

Pereopods (Fig. 1K) Poorly developed, without exopods; 1st pereopod bilobed; 5th pereopod arises medially between 1st and 2nd pereopods.

Abdomen and telson (Fig. 1L) Abdomen with 5 somites and telson (somite 6 fused with telson); somites 2–4 each with 3 pairs of spines, 2 pairs posterodorsal, 1 pair lateral, lateral pair longest; posterodorsal spines of somite 2 generally equal-sized; median pair of somites 2–4 strongest; lateral pair on somite 5 long (~1.4 times somite width), pointed, somewhat sinuate; telson margin convex with median cleft and 8+8 processes (1,i,3–8), 1st an articulated simple spine, 2nd an anomuran hair (i), 3rd–8th denticulate spines, 4th pair longest, about equal to maximum telson width; all articulated with telson; no uropods or anal spine.

Distinction between *L. mandtii* and other lithodid zoeae

Stage-I zoeae of *L. mandtii* are typical of Stage-I lithodid larvae of the northern North Pacific Ocean as characterized by Haynes (1984). The morphological characteristics of Stage-I lithodid larvae are: sessile eyes and 4 natatory setae each on maxillipeds 1 and 2, maxilliped 3 undeveloped and without natatory setae, pleopods and uropods absent, telson and 6th abdominal somite fused. Lithodid species with typical Stage-I zoeae have 4 zoeal stages. Thus, *L. mandtii* probably has 4 zoeal stages also.

Since the review of lithodid larvae of the northern North Pacific Ocean by Haynes (1984), larvae of *Hapalogaster dentata* have been described by Konishi (1986) who noted that zoeae of *H. dentata* are most similar to those of *Dermaturus mandtii* and can be distinguished from the latter by setation of the antennal scale (7 vs. 10 setae) and the absence of a minute subterminal spine on the antennal endopod in *D. mandtii*. Stage-I zoeae of *H. dentata* are readily distinguished from Stage-I *L. mandtii* by the short (≤1/4 carapace length) posterolateral spines on the carapace and 7+7 telsonal processes.

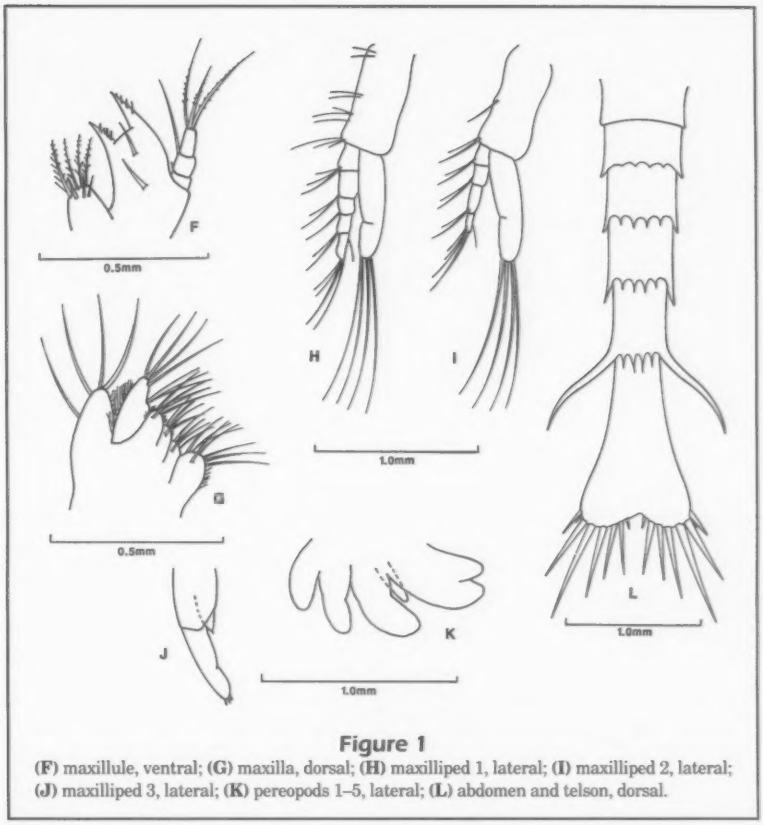

Figure 1
(F) maxillule, ventral; **(G)** maxilla, dorsal; **(H)** maxilliped 1, lateral; **(I)** maxilliped 2, lateral; **(J)** maxilliped 3, lateral; **(K)** pereopods 1–5, lateral; **(L)** abdomen and telson, dorsal.

Comparing Stage-I *L. mandtii* with published descriptions of Stage-I lithodid larvae of the northern North Pacific, they are most similar to Stage-I *Paralithodes camtschaticus*, *P. platypus*, and *Placetron wosnessenskii*. These four species are characterized by a relatively long, pointed rostrum and by relatively long posterolateral spines on the carapace (Sato 1958, Kurata 1964, Makarov 1967, Haynes 1984).

Stage I of *L. mandtii* can be distinguished from *Paralithodes camtschaticus* and *P. platypus* by the shape of the posterolateral spines on the carapace and on somite 5 of the abdomen. In *L. mandtii*, the posterolateral spines on the carapace are slightly longer and have more outward curvature, and the posterolateral spines on somite 5 are longer and more sinuous than in *P. camtschaticus* or *P. platypus*. Also, Stage-I *P. camtschaticus* has fewer plumose setae on the antennal scale than Stage-I *L. mandtii* (5 vs. 9), and Stage-I *P. platypus* has 9+9 telsonal processes rather than 8+8.

Stage-I *L. mandtii* can be distinguished from Stage-I *Placetron wosnessenskii* by general appearance and spination of the abdomen and telson. Individuals of the latter species are noticeably more rugose; the carapace is more heavily ridged and the rostrum is deeper than in Stage-I *L. mandtii*. In Stage-I *P. wosnessenskii* the abdominal spines are relatively long (those of abdominal somite 2 are one-half the length of abdominal somite 3), wide, and blunt, whereas in Stage-I *L. mandtii* the abdominal spines are short (those of somite 2 about one-third the length of somite 3), narrow, and pointed. Also, the telson of *P. wosnessenskii* has 7+7 terminal processes whereas the telson of *L. mandtii* has 8+8 terminal processes.

Citations

Haynes, E. B.
1984 Early zoeal stages of *Placetron wosnessenskii* and *Rhinolithodes wosnessenskii* (Decapoda, Anomura, Lithodidae) and review of lithodid larvae of the northern North Pacific Ocean. Fish. Bull., U.S. 82:315–324.

Konishi, K.
1986 Larval development of the stone crab, *Hapalogaster dentata* (De Haan, 1984) (Crustacea: Anomura: Lithodidae) reared in the laboratory. J. Fac. Sci. Hokkaido Univ. 24:155–172.

Kurata, H.
1964 Larvae of decapod Crustacea of Hokkaido. 6. Lithodidae (Anomura). Bull. Hokkaido Reg. Fish. Res. Lab. 29:49–65 [in Jpn., Engl. summ.].

Makarov, R.R.
1967 Larvae of the shrimps and crabs of the West Kamchatkan Shelf and their distribution (Lichinki krevetov, rakov-otshel'nikov i krabov zapadnokamchatskogo shel'fa i ikh reprendelenie). Transl. Natl. Lending Library Sci. Technol., Boston Spa, Yorkshire, England, 199 p.

Sato, S.
1958 Studies on larval development and fishery biology of king crab, *Paralithodes camtschatica* (Tilesius). Bull. Hokkaido Reg. Fish. Res. Lab. 17:1–102 [in Jpn., Engl. summ.].

Optimal sampling design for using the age-length key to estimate age composition of a fish population

Han-Lin Lai
Washington State Department of Fisheries
1111 Washington Street SE, P.O. Box 43144
Olympia, Washington 98504-3144

An age-length key (ALK) is the traditional method for estimating age composition of an application of fish population. Tanaka (1953) showed that the ALK method is a double-sampling technique (Cochran 1977). The first stage uses simple random sampling to collect a very large, but relatively inexpensive, length sample. The second stage subsamples a small number of fish from the first-stage length samples for relatively costly age determination (age subsample). Age subsampling in the second stage can be taken in two fundamental ways, one in which age subsamples are randomly taken from the entire first-stage length samples (random-age subsampling; Kimura 1977) and another in which age subsamples are taken from each stratified length-stratum (stratified-age subsampling; Tanaka 1953). In stratified-age subsampling, fixed-age subsampling (a constant number of age specimens is taken at each length-stratum) and proportional age subsampling (age specimens is proportional to the random length-frequency) are the most popular (Ketchen 1949). However, a general stratified-age subsampling (number of age specimens varied at each length-stratum) can also be used. Stratified-age subsampling is the major focus of this paper. The similarities in results obtained from proportional and random-age subsamplings are given in the Discussion.

This paper was motivated by two articles, Lai (1987) and Jinn et al. (1987), using optimal sampling designs to estimate age composition of a fish population using ALK. The two articles differ significantly. Lai (1987) was based on the classic double-sampling technique and derived the optimal allocation of length samples and age subsamples using Kimura's Vartot (Kimura 1977) and the Cauchy-Schwartz inequality (Kendall & Stuart 1977) for fixed-age subsampling and proportional-age subsampling. Lai (1987) incorrectly used random-age subsampling for proportional-age subsampling. In contrast, Jinn et al. (1987) used a Bayesian approach to estimate age composition, variance, and covariance for a general stratified-age subsampling. They used the iterative method of Roa & Ghangurde (1972) to obtain the optimal allocation of length samples and age subsamples for each length-stratum, with a set of known per-unit costs for ageing a fish in each stratum.

The length-based optimal sampling design of Jinn et al. (1987) has advantages. Because the age of a fish can be expressed as a function of its length (e.g., a von Bertalanffy growth relationship) and because older fish are more difficult to age, the per-unit cost of ageing a fish can be used to estimate the difficulty of ageing older (larger) fish. In addition, the covariance components are important statistics because the sum of all age proportions equals 1, indicating that the estimates of age composition are not mutually independent. The disadvantage of the Bayesian approach of Jinn et al. (1987) is that their method is mathematically complicated and does not provide explicit expressions for the optimal allocations of length and age samples for an ALK, and thus requires substantial computing effort.

The purpose of this paper is to derive a length-based optimal sampling design for an ALK using a classic double-sampling technique. The covariance of age composition also is derived using the method of Kimura (1977). This paper also provides answers to the question many fishery scientists have asked me: What is the explicit solution to a length-based optimal sampling design for an ALK? A discussion on the general applicability of ALK in the sampling program with complexity of fishery-time-areal stratification and tows/trips clusterization is also provided.

Methods

I use the following notation for an ALK with a general stratified-age subsampling:

- N = total number of length samples;
- N_i = number of fish in the ith length-stratum, i=1,...,L;
- l_i = proportion of fish in the ith length-stratum, ($\hat{l}_i = N_i/N$);
- n_i = number of age sub-samples randomly taken from the ith length-stratum;
- n_{ij} = number of fish from n_i assigned to the jth age-class;
- q_{ij} = proportion of fish in the ith length-stratum that fall into the jth age-class ($\hat{q}_{ij} = n_{ij}/n_i$);
- A = number of age-classes;
- L = number of length-strata;
- p_j = proportion of population in the jth age-class;

Manuscript accepted 10 December 1992.
Fishery Bulletin, U.S. 92:382-388 (1993).

$\mathrm{Var}(p_j)$ = variance of p_j ;
$\mathrm{Cov}(p_j,p_k)$ = covariance between p_j and p_k.
A caret denotes the estimate of each variable.

The unbiased estimate of p_j (Tanaka 1953) from an ALK is

$$\hat{p}_j = \sum_{i=1}^{L} \hat{l}_i \hat{q}_{ij} \,. \tag{1}$$

The variance of $\hat{p}_j$ has been derived by Tanaka (1953) and Kimura (1977); however, the approximate form of variance is more frequently used (Kutkuhn 1963, Southward 1963, Doubleday & Rivard 1983, Lai 1987):

$$Var(\hat{p}_j) \approx \sum_{i=1}^{L} \left[\frac{\hat{l}_i^2 \hat{q}_{ij}(1-\hat{q}_{ij})}{n_i} + \frac{\hat{l}_i (\hat{q}_{ij}-\hat{p}_j)^2}{N} \right]. \tag{2}$$

The terms in the right-hand side of Eq. 2 represent the portion of the total variance due to variation within length-strata and that due to variation between strata, respectively.

The covariance of $\hat{p}_j$ and $\hat{p}_k$ is derived using the method of Kimura (1977):

$$\begin{aligned} Cov(\hat{p}_j,\hat{p}_k) &= \sum_{i=1}^{L} \frac{-\hat{l}_i(1-\hat{l}_i)\hat{q}_{ij}\hat{q}_{ik}}{Nn_i} + \sum_{i=1}^{L} \frac{-\hat{l}_i^2 \hat{q}_{ij}\hat{q}_{ik}}{n_i} + \sum_{i=1}^{L} \frac{\hat{l}_i \hat{q}_{ij}\hat{q}_{ik}}{N} - \frac{\hat{p}_j \hat{p}_k}{N} \\ &\approx \sum_{i=1}^{L} \frac{-\hat{l}_i^2 \hat{q}_{ij}\hat{q}_{ik}}{n_i} + \sum_{i=1}^{L} \frac{\hat{l}_i \hat{q}_{ij}\hat{q}_{ik}}{N} - \frac{\hat{p}_j \hat{p}_k}{N} \,. \end{aligned} \tag{3}$$

The approximate form of covariance omits the first term because this term is small compared with the sum of the other two terms. A quadratic loss function (Jinn et al. 1987) is used to infer the precision of the estimated age composition $\hat{\mathbf{p}}'=(\hat{p}_1,\hat{p}_2,...,\hat{p}_A)$:

$$\begin{aligned} \mathcal{L}(\hat{\boldsymbol{p}},\boldsymbol{p}) &= (\hat{\boldsymbol{p}}-\boldsymbol{p})'\boldsymbol{W}(\hat{\boldsymbol{p}}-\boldsymbol{p}) \\ &= \sum_{j=1}^{A} w_{jj} Var(\hat{p}_j) + \sum_{j\neq k}^{A} w_{jk} Cov(\hat{p}_j,\hat{p}_k) \\ &= E\left[\sum_{j=1}^{A} w_{jj} (\hat{p}_j - p_j)^2 \right] + E\left[\sum_{j\neq k}^{A} w_{jk} (\hat{p}_j - p_j)(\hat{p}_k - p_k) \right]. \end{aligned} \tag{4}$$

The loss function presented in Eq. 4 is identical to Kimura's Vartot provided that $\mathbf{W}$ is an identity matrix, i.e., $w_{jj}=1$ and $w_{jk}=0$ for $j\neq k$.

Substituting Eq. 2 and the approximate form of Eq. 3 into Eq. 4 and collecting terms, we obtain:

$$\mathcal{L} = \sum_{i=1}^{L} \left(\frac{a_i - u_i}{n_i} \right) + \frac{b+v-m}{N}, \tag{5}$$

where $a_i = \sum_{j=1}^{A} w_{jj} \hat{l}_i^2 \hat{q}_{ij}(1-\hat{q}_{ij})$,

$u_i = \sum_{j\neq 1}^{A} w_{jk} \hat{l}_i^2 \hat{q}_{ij} \hat{q}_{ik}$,

$b = \sum_{i=1}^{L} \sum_{j=1}^{A} w_{jj} \hat{l}_i (\hat{q}_{ij} - \hat{p}_{ij})^2$,

$v = \sum_{i=1}^{L} \sum_{j\neq k}^{A} w_{jk} \hat{l}_i \hat{q}_{ij} \hat{q}_{ik}$.

$m = \sum_{j\neq k}^{A} w_{jk} \hat{p}_j \hat{p}_k$,

and where a_i, u_i, b, m, and v are all positive.

A linear cost function is used for the optimal sampling design:

$$C = c_1 N + \sum_{i=1}^{L} c_{2i} n_i, \tag{6}$$

where C is total cost, c_1 is per-unit cost of collecting a random length sample, and c_{2i} is per-unit cost for ageing a fish in the ith length-stratum.

Survey designs generally are based on two constraints: (i) a fixed total cost, i.e., minimize the loss function in Eq. 4 at a fixed cost; or (ii) a desired precision of the estimators, i.e., minimize the total cost at a given level of the loss function. Therefore, the problem for optimal allocation becomes one of determining the optimal set of N^* and n_i^*'s which minimizes L at a given total cost or which minimizes total cost at a desired precision level of L (N^* and n_i^* are the optimal sample sizes of length and age samples, respectively). Kendall & Stuart (1977, Sect. 39.20) and Cochran (1977, Sect. 5.5) show that choosing the optimal set of N^* and n_i^*'s to minimize L for a fixed C or to minimize C for a fixed L are both equivalent to minimizing the product of L and C:

$$\mathcal{L}C = \left[\sum_{i=1}^{L} \frac{a_i - u_i}{n_i} + \frac{b+v-m}{N} \right] \left[c_1 N + \sum_{i=1}^{L} c_{2i} n_i \right]. \tag{7}$$

Applying the Cauchy-Schwarz inequality to Eq. 7, the product LC is

$$\begin{aligned} \mathcal{L}C &= \left[\sum_{i=1}^{L} \left(\sqrt{\frac{a_i-u_i}{n_i}} \right)^2 + \left(\sqrt{\frac{b+v-m}{N}} \right)^2 \right] \left[(\sqrt{c_1 N})^2 + \sum_{i=1}^{L} (\sqrt{c_{2i} n_i})^2 \right] \\ &\geq \left[\sum_{i=1}^{L} \sqrt{c_{2i}(a_i-u_i)} + \sqrt{b+v-m} \right]^2. \end{aligned}$$

Kendall & Stuart (1977) showed that the minimum value of the product LC occurs when

$$\frac{\sqrt{c_{21} n_1}}{\sqrt{\frac{a_1-u_1}{n_1}}} = \ldots = \frac{\sqrt{c_{2i} n_i}}{\sqrt{\frac{a_i-u_i}{n_i}}} = \ldots = \frac{\sqrt{c_{2L} n_L}}{\sqrt{\frac{a_L-u_L}{n_L}}} = \frac{\sqrt{c_1 N}}{\sqrt{\frac{b+v-m}{N}}} = \text{constant} > 0 \tag{8}$$

Use the terms of the equality between the ith and the (L+1)th terms and rearrange the variables to obtain $r_i^* = n_i^*/N^*$, the optimal subsampling ratio between age subsamples and length samples in the ith length stratum. The solution of r_i^* is:

$$r_i^* = \sqrt{\frac{c_1(a_i - u_i)}{c_{2i}(b+v-m)}}. \quad (9)$$

For a survey design subject to a given total cost C, r_i^* is the optimal subsampling ratio required to reach the minimum loss function value (min. $\mathcal{L}$). Thus, substitute Eq. 9 into Eq. 6 and solve for the optimal set of N^* and n_i^*:

$$N^* = \frac{C}{c_1 + \sum_{i=1}^{L} c_{2i} r_i^*},$$

$$n_i^* = r_i^* N^*,$$

$$\text{min. } \mathcal{L} = \sum_{i=1}^{L}\left(\frac{a_i - u_i}{n_i^*}\right) + \frac{b+v-m}{N^*}. \quad (10)$$

For a survey design subject to a desired precision level of $\mathcal{L}$, r_i^* is the optimal subsampling ratio to reach the minimum total cost (min. C). The optimal set of N^* and n_i^* can be obtained by substituting Eq. 9 into Eq. 5:

$$N^* = \frac{1}{\mathcal{L}}\left[\sum_{i=1}^{L}\left(\frac{a_i - u_i}{r_i^*}\right) + b+v-m\right],$$

$$n_i^* = r_i^* N^*, \quad (11)$$

$$\text{min. } C = c_1 N^* + \sum_{i=1}^{L} c_{2i} n_i^*.$$

Similarly, the above derivation can be extended to the traditional fixed- and proportional-age subsampling schemes. For these age subsampling schemes, the per-unit cost for ageing a fish is not length-specified (i.e., $c_{2i} = c_2$ for all i's). The loss and cost functions in Eq. 5 and 6 are modified according to the definition of the two age subsampling schemes: (1) $n_i = n/L$ for fixed-age subsampling, and (2) $n_i = n\, l_i$ for proportional-age subsampling, where $n = \Sigma n_i$. The loss function for fixed-age subsampling is

$$\mathcal{L} = \frac{\sum_{i=1}^{L} L\,(a_i - u_i)}{n} + \frac{b+v-m}{N} \quad (12)$$

and that for a proportional-age subsampling is

$$\mathcal{L} = \frac{\sum_{i=1}^{L} L\,(a_i - u_i)/\hat{l}_i}{n} + \frac{b+v-m}{N}. \quad (13)$$

The cost function for both age subsampling schemes is:

$$C = c_1 N^* + c_2 n \quad (14)$$

Using the Cauchy-Schwarz inequality, the optimal subsampling ratio (r*) for either minimizing $\mathcal{L}$ at a fixed total cost C or minimizing total cost C at a desired precision level of $\mathcal{L}$ for a fixed-age subsampling is:

$$r^* = \frac{n^*}{N^*} = \sqrt{\frac{c_1 \sum_{i=1}^{L} L\,(a_i - u_i)}{c_2\,(b+v-m)}} \quad (15)$$

The optimal set of N^* and n^* and min. $\mathcal{L}$ subject to fixed cost is:

$$N^* = c_1 + c_2 r^*,$$

$$n^* = r^* N^*, \quad (16)$$

$$\text{min. } \mathcal{L} = \frac{\sum_{i=1}^{L} L\,(a_i - u_i)}{n} + \frac{b+v-m}{N}.$$

and the optimal set of N^* and n^* and min. C subject to a desired precision level of $\mathcal{L}$ is

$$N^* = \frac{1}{\mathcal{L}}\left[\frac{\sum_{i=1}^{L}(a_i - u_i)}{r^*} + b+v-m\right],$$

$$n^* = r^* N^*, \quad (17)$$

$$\text{min. } C = c_1 N^* + c_2 n^*.$$

For proportional-age subsampling, the optimal subsampling ratio (r^*) for either minimizing $\mathcal{L}$ at a given total cost C, or minimizing total cost C at a desired precision level of $\mathcal{L}$, is:

$$r^* = \sqrt{\frac{c_1 \sum_{i=1}^{L} (a_i - u_i)/\hat{l}_i}{c_2\,(b+v-m)}} \quad (18)$$

The optimal set of N^* and n^* and min. $\mathcal{L}$ subject to a given total cost C is

$$N^* = c_1 + c_2 r^*,$$

$$n^* = r^* N^*, \quad (19)$$

$$\text{min. } \mathcal{L} = \frac{\sum_{i=1}^{L}(a_i - u_i)/\hat{l}_i}{n^*} + \frac{b+v-m}{N^*}.$$

and the optimal set of N^* and n^* and min. C subject to a desired precision level of $\mathcal{L}$ is:

$$n^* = \frac{1}{\mathcal{L}}\left[\frac{\sum_{i=1}^{k}(a_i - u_i)\hat{l}_i}{r^*} + (b+v-m)\right],$$

$$n^* = r^* N^*, \qquad (20)$$

$$\text{min. } C = c_1 N^* + c_2 n^* .$$

The solutions given in Eq. 16–20 are similar to that of Lai (1987), provided that the matrix **W** is an identity matrix.

Example

The lemon sole (= English sole *Pleuronectes vetulus*) example of Jinn et al. (1987) is used to illustrate the length-based optimal sampling design. The ALK and per-unit costs are summarized in Table 1. The total cost is C=$229.15, and the per-unit cost for collecting a length of fish is c_1=$0.15. For simplicity without loss of generality, consider the special case: w_{jk}=0 for j≠k. Three different sets of w_{jj} are used to reflect different aspects of interest:

Table 1

Age-length key and length-frequency distribution of male lemon sole (= English sole, *Pleuronectes vetulus*) collected from Strait of Georgia, British Columbia. Original dataset is from Ricker (1975:68), and per-unit cost for ageing is from Jinn et al. (1987).

Length stratum (cm)	Number of age subsamples	Age						Number of length samples	Per-unit cost of ageing
		4	5	6	7	8	9		
27	6	5	1					6	1.0
28	9	3	4	2				9	1.2
29	10	4	4	1	1			30	1.4
30	10	1	5	4				51	1.6
31	10		8	2				54	1.8
32	10	1	7	1	1			48	2.0
33	10	1	3	3	2	1		41	2.2
34	10		2	6	1	1		27	2.4
35	10		1	4	3		2	13	2.6
36	6			1	3	2		6	2.8
37	3			1	1	1		3	3.0
38	1					1		1	3.2
Age proportion		0.12	0.48	0.26	0.09	0.04	0.01		
Variance ($\times 10^{-3}$)		1.09	2.98	2.46	0.88	0.33	0.04		

Case 1 {1,1,1,1,1,1}: equal interest in estimating all $\hat{p}_i$'s;

Case 2 {10,30,30,10,1,1}: increase precision of four major age-classes with larger Var($\hat{p}_i$);

Case 3 {1,1,1,1,10,60}: interest in older but rare age-classes.

The results obtained from length-based design are compared with those from fixed- and proportional-age subsampling schemes. The average per-unit cost for ageing a fish (c_2) is calculated as the weighted mean of c_{2i}, which is c_2=$1.96. The optimal set of {N^*, n_i^*} and min. $\mathcal{L}$ subject to the given total cost of $229.15 are computed using Eq. 9 and 10 for length-based age subsampling, Eq. 15 and 16 for fixed-age subsampling, and Eq. 18 and 19 for proportional-age subsampling.

Precision improves substantially when length-based age subsampling rather than fixed-age subsampling is used in all three cases (Table 2). In the first two cases, however, precision improves marginally by using length-based age rather than proportional-age subsamplings. When rare and older fish (ages 8 and 9, Case 3) are of interest, precision is substantially improved by using length-based age instead of proportional-age subsampling. This is due to the fact that proportional-age subsampling is not designed to increase age subsamples from length-strata consisting of older age-classes.

The optimal set of {N^*, n_i^*} and min. C subject to a desired precision level of $\mathcal{L}^*$=0.01 are computed from Eq. 9 and 11 for length-based age subsampling, Eq. 15 and 17 for fixed-age subsampling, and Eq. 18 and 20 for proportional-age subsampling. Tables 2 and 3 show similar trends. The cost efficiency of length-based age subsampling is superior to fixed-age subsampling in all cases. However, cost efficiency is only marginally

Table 2

Optimal sample sizes of length and age samples and min. $\mathcal{L}$ ($\mathcal{L}$: loss function) subject to fixed total cost, C=$229.15, for three different age subsampling schemes. Age-length key dataset is listed in Table 1. Per-unit cost of observing a length sample, c_1=$0.15. Case 1 $\{w_i\}$={1,1,1,1,1,1}; Case 2 $\{w_i\}$={10,30,30,10,1,1}; and Case 3 $\{w_i\}$={1,1,1,1,10,60}.

Length (cm)		Case 1	Case 2	Case 3
27		2	2	2
28		4	5	3
29		14	13	10
30		21	23	15
31		15	18	11
32		16	16	12
33		17	16	18
34		9	9	11
35		5	4	13
36		2	1	3
37		1	1	1
38		1	1	1
Length-based	n*	107	109	100
sampling	N*	183	182	204
design	min. $\mathcal{L}$	0.0058	0.1312	0.0110
Improvement of precision (%)[1] vs.				
Fixed-age subsampling		36.26	39.15	28.57
Proportional-age subsampling		4.92	4.23	19.12
Fixed-age	n*	106	106	104
subsampling	N*	146	141	172
	min. $\mathcal{L}$	0.0091	0.2156	0.0154
Proportional-age	n*	103	103	103
subsampling	N*	179	177	183
	min. $\mathcal{L}$	0.0061	0.1370	0.0136

[1] % = percent difference of min. $\mathcal{L}$ between length-based sampling design and fixed or proportional-age subsampling.

Table 3

Optimal sample sizes of length and age samples and minimum total cost (min. C) subject to a desired precision level of loss function, $\mathcal{L}$=0.01 for the three different age subsampling schemes. Age-length key dataset is listed in Table 1. Per-unit cost of observing a length sample, c_1=$0.15. $\{w_i\}$ for each case are the same as that in Table 2.

Length (cm)		Case 1	Case 2	Case 3
27		1	3	2
28		3	6	4
29		8	17	11
30		12	30	17
31		9	23	12
32		9	21	13
33		10	21	20
34		5	12	12
35		3	5	14
36		1	2	3
37		1	1	2
38		1	1	1
Length-based	n*	63	142	111
sampling	N*	106	236	223
design	min. C	135.98	300.6	257.25
Cost efficiency (%)[1] vs.				
Fixed-age subsampling		35.14	39.09	27.06
Proportional-age subsampling		1.08	3.68	17.33
Fixed-age	n*	97	229	160
subsampling	N*	133	304	265
	min. C	209.66	493.48	352.68
Proportional-age	n*	62	141	140
subsampling	N*	108	242	249
	min. C	137.46	312.07	311.16

[1] % = percent difference of min. C between length-based sampling design and fixed- or proportional-age subsampling.

different between length-based age and proportional age subsamplings in Cases 1 and 2. In Case 3, the cost efficiency of length-based age subsampling increases subtantially over proportional-age subsampling.

Discussion

To draw a general conclusion, many different sets of w_{ij}'s and full matrices of **W** also were investigated. The results from these additional analyses were similar to that of Tables 2 and 3. In general, the length-based age subsampling is superior to either fixed- or proportional-age subsampling. However, precision improvement and cost efficiency depend on the weights placed on particular age-classes. Total cost will change in accord with the different weights and desired precision. A higher total cost should be allowed for cases where sampling is designed to improve the precision of highly variable estimates, usually young and old age-classes.

A larger budget will increase precision of the estimates, especially for highly variable age-classes; however, as Lai (1987) showed, there is a point of diminishing returns as the budget increases (Fig. 1). For the examples used in this paper, precision improvement is marginal when total cost (C) increased beyond $40 for Cases 1 and 3, and beyond $120 for Case 2. Kimura (1989) showed that satisfactory results from cohort analysis can be obtained at low sampling levels (i.e., total cost) provided that the representativeness of the samples can be maintained.

It is difficult to compare the methods of Jinn et al. (1987) with those of this paper because the Bayesian approach and classic sampling techniques are derived from different theoretical backgrounds. Nontheless, the results obtained from this paper are similar to that of

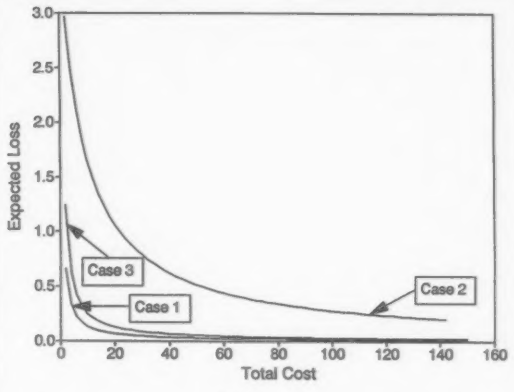

Figure 1

Relationship between minimum loss function value and total cost for the lemon sole (= English sole *Pleuronectes vetulus*) example. The relationship can be obtained from substituting N^* and n_i^* in Eq. 10 into the third equation in Eq. 10.

Jinn et al. (1987) although the values of N^* and n_i^* are different. An advantage of the classic double-sampling technique is the explicit solutions of the optimal set of N^* and n_i^*, which reduces computational effort.

In this paper, the optimal sampling design is for stratified-age subsampling. For random-age subsampling in which the number of age subsamples (n) is randomly taken from the entire length sample of size N, the estimated variance and covariance (Kimura 1977) are

$$Var\,(\hat{p}_j) = \sum_{i=1}^{L}\left[\frac{\hat{l}_i\hat{q}_{ij}\,(1-\hat{q}_{ij})}{n} + \frac{\hat{l}_i(\hat{q}_{ij}-\hat{p}_j)^2}{N}\right]$$

and

$$Cov\,(\hat{p}_j,\hat{p}_k) = \sum_{i=1}^{L}\frac{-\hat{l}_i\hat{q}_{ij}\hat{q}_{ik}}{n} + \sum_{i=1}^{L}\frac{\hat{l}_i\hat{q}_{ij}\hat{q}_{ik}}{N} - \frac{p_j\hat{p}_k}{N}.$$

These two equations are similar to that of proportional-age subsampling in which $n_i = n\hat{l}_i$ is substituted into Eq. 2 and 3. However, the estimated variance and covariance for proportional-age subsampling are approximate, and those for random-age subsampling are not. The similarities of random- and proportional-age subsamplings can be anticipated because N is a random sample from a population so that $E(\hat{l}_i)=E(N_i/N)=l_i$, and n is randomly taken from N so that $E(n_i/n)=N_i/N$. This indicates that the size of each n_i will be approximately proportional to l_i, i.e., $n_i/n \approx N_i/N \approx \hat{l}_i$ and $n_i \approx n \cdot l_i$ (Kutkuhn 1963).

An ALK requires a large random sample of fish from which a length-stratified subsample is collected for ageing. Most fishery data are collected either from surveys in which fish from different tows are sampled or from commercial catches in which fish from different vessel-trips are sampled. Pooling data over such clusters is necessary because of the cost of data gathering. In addition to cluster sampling, fisheries data are frequently stratified into time-area, fisheries (or gears), and sex strata (Kimura 1989). The question is how to make the optimal sampling design of ALK generally applicable. To address this, the following factors must be considered: (1) Need of stratification, (2) ALK sampling within stratum, and (3) combined-strata estimation.

Westrheim & Ricker (1978) showed the need for stratification. An ALK obtained from a population at a time-interval should not be universally applied to length-frequency datasets from other populations or other time-intervals if growth and survival rates are different among the populations and time-intervals. Therefore, the factors that may result in differences in growth and survival rates should be evaluated, and stratification should account for these factors.

Current sampling programs (e.g., Doubleday & Rivard 1983, Quinn et al. 1983, Kimura 1989) adopted the strategy in which length-frequency data collected from clustered sampling units (e.g., tows or vessel-trips) within a stratum are pooled, from which a length-stratified subsample is collected for ageing. Southward (1963) evaluated an old method (Southward 1963:12) in which a set of length and age data is collected from each landing of a vessel-trip. Because this old method is not developed from a probability sampling design, the within-vessel variability in fish lengths is assumed to be less than between-vessel variability. Southward (1963) showed that this assumption is not valid and the estimated variances of age composition from this old method are so large that little confidence can be placed in it.

The length-frequency data pooled over clusters should be a representative sampling of that stratum. Therefore, the weighting factor of each sample should be included in the pooling. Ignoring the weighting factor will bias the estimated age composition (Kimura 1989). Quinn et al. (1983) described a sampling-rate method in which a fixed proportion of halibut were sampled from landings >1000 lbs for length data, and then age data were subsampled from the pooled length samples from these landings. All length samples are self-weighted and can be pooled directly.

Quinn et al. (1983) evaluated the methods of combined-strata estimation and found that the "project-and-add" method (total catch-at-age is estimated for each stratum and then the estimates are added over

strata; see Quinn et al. 1983) produces unbiased estimators if all strata are sampled. The project-and-add method uses the concept of a stratified, random sampling technique (Cochran 1977). Therefore, Cochran's rules (Cochran 1977:98) of optimal allocation for stratified random sampling can be applied. In a given stratum, take larger length and age samples if (1) the stratum is larger, (2) the stratum is more variable internally, and (3) sampling is cheaper in the stratum. The first two rules are the basis of the Neyman allocation (Cochran 1977:99). The sampling-rate method proposed by Quinn et al. (1983) built upon the first rule and can easily incorporate other rules in the sampling program.

It is clear that the number of strata and variability (vartot or loss function) of each stratum should be evaluated first for designing ALK sampling. Then, the total cost is allocated into various strata according to Cochran's rules. Once the total cost for each stratum is determined, an optimal sampling design for ALK can be applied. The sampling rate method of Quinn et al. (1983) can be used to collect the optimal length sample size from clusters. After pooling the length samples, a length-stratified subsample is collected for ageing.

Acknowledgments

I thank D.K. Kimura for his help with derivation of the covariance. Thanks to M. Sigler for his constructive comments on an earlier draft. This paper is partially supported by the U.S. Agency for International Development, Fisheries Stock Assessment CRSP (DAN-4146-G-SS-5071-00).

Citations

Cochran, W.G.
1977 Sampling techniques, 3rd ed. John Wiley, NY.

Doubleday, W. G., & D. Rivard (editors)
1983 Sampling commercial catches of marine fish and invertebrates. Can. Spec. Publ. Fish. Aquat. Sci. 66, 290 p.

Jinn, J. H., J. Sedransk, & P. Smith
1987 Optimum two-phase stratified sampling for estimation of the age composition of a fish population. Biometrics 43:343–353.

Kendall, M., & A. Stuart
1977 The advanced theory of statistics, vol. 3, 3rd ed. Griffin & Co., London, 585 p.

Ketchen, K. S.
1949 Stratified subsampling for determining age distributions. Trans. Am. Fish. Soc. 79:205–212.

Kimura, D. K.
1977 Statistical assessment of age-length key. J. Fish. Res. Board Can. 31:317–324.
1989 Variability in estimating catch-in-numbers-at-age and its impact on cohort analysis. *In* Beamish, J. R., & G. A. McFarlane (eds.), Effects of ocean variability on recruitment and an evaluation of parameters used in stock assessment models, p.57–66. Can. Spec. Publ. Fish. Aquat. Sci. 108.

Kutkuhn, J. H.
1963 Estimating absolute age composition of California salmon landings. Calif. Fish Game Fish. Bull. 120, 29 p.

Lai, H. L.
1987 Optimum allocation for estimation age composition using age-length key. Fish. Bull., U.S. 85:179–185.

Quinn, T. J. II, E. A. Best, L. Bijsterveld, & I. R. McGregor
1983 Port sampling for age composition of Pacific halibut landings. *In* Doubleday, W. G., & D. Rivard (eds.), Sampling commercial catches of marine fish and invertebrates, p. 194–205. Can. Spec. Publ. Fish. Aquat. Sci. 66.

Rao, J. N. K., & P. D. Ghangurde
1972 Bayesian optimization in sampling finite populations. J. Am. Stat. Assoc. 67:439–443.

Ricker, W. E.
1975 Computation and interpretation of biological statistics of fish populations. Fish. Res. Board Can. Bull. 191, 382 p.

Southward, G. M.
1963 Sampling landings of halibut for age composition. Int. Pac. Halibut Comm. Sci. Rep. 58, 31 p.

Tanaka, S.
1953 Precision of age-composition of fish estimated by double sampling method using the length for stratification. Bull. Jpn. Soc. Sci. Fish. 19:657–670.

Westrheim, S. J., & W. E. Ricker
1978 Bias in using an age-length key to estimate age-frequency distributions. J. Fish. Res. Board Can. 35:184–189.

Recruitment of bluefish *Pomatomus saltatrix* to estuaries of the U.S. South Atlantic Bight*

Richard S. McBride
Rutgers University Marine Field Station
Institute of Marine and Coastal Sciences
P.O. Box 278, Tuckerton, New Jersey 08087

Jeffrey L. Ross
North Carolina Division of Marine Fisheries
P.O. Box 1550, Manteo, North Carolina 27954

David O. Conover
Marine Sciences Research Center
State University of New York
Stony Brook, New York 11794–5000

The bluefish *Pomatomus saltatrix* is a pelagic species that is distributed circumtropically (Briggs 1960, Richards 1965, van der Elst 1976, Fable et al. 1981, Pollock 1984, Lenanton & Potter 1987). Ichthyoplankton surveys off the U.S. east coast indicate three separate spawning concentrations of bluefish, namely (1) a spring-spawned cohort produced between March and May in the South Atlantic Bight (SAB), (2) a summer-spawned cohort originating between June and August in the Middle Atlantic Bight (MAB), and (3) a fall-spawned cohort produced in the SAB between September and January (Norcross et al. 1974, Kendall & Walford 1979, Powles 1981, Collins & Stender 1987).

The abundance of bluefish has fluctuated widely along the Atlantic coast during the past century (Baird 1873, Bigelow & Schroeder 1953). Recently, population abundance increased steadily from the early 1960s to the late 1970s (Gilmore 1985) and remained relatively high during the 1980s (NMFS 1987, 1988). Chiarella & Conover (1990) speculated that increased recruitment success of the spring-spawned cohort is largely responsible for this recent increase in overall bluefish abundance. They demonstrated that bluefish off the New York coast during the 1980s were primarily spring-spawned fish, and this contrasts with a more equal proportion of spring-spawned and summer-spawned fish observed by Lassiter (1962) in the late 1950s, when overall bluefish abundance was lower.

Our understanding of how these three intra-annual cohorts contribute to the overall year-class strength of bluefish along the U.S. Atlantic coast, however, is still unclear. For example, Kendall & Walford (1979) hypothesized that spring-spawned bluefish were transported from the SAB northward into the MAB estuaries, but Collins & Stender (1987) postulated that spring-spawned fish were transported directly inshore to estuaries of the SAB. Otolith analyses of young recruits have confirmed the northerly dispersal of spring-spawned fish as proposed by Kendall & Walford (Nyman & Conover 1988, McBride & Conover 1991), but similar studies of recruitment to SAB estuaries are nonexistent. Length-frequency data for bluefish from SAB estuaries is also sparse, thus it has been difficult to evaluate if bluefish use estuaries in the SAB as nursery grounds. Here we present evidence of recruitment by three cohorts of young-of-the-year (YOY) bluefish to estuaries and nearshore habitats of the SAB.

Materials and methods

Field sampling

Bluefish <360mm fork length (FL) were collected from estuarine pound-net (a summer fishery) and oceanic trawl (a winter fishery) samples taken in North Carolina (Table 1). The upper limit of 360mmFL represents the largest size attained by young bluefish in their first year of life (Lassiter 1962). Additional data were also obtained from a variety of fishery-independent sources of sampling from North Carolina to Florida (Table 1).

Otolith aging

To avoid dissolution, sagittal otoliths were extracted directly in the field, or from frozen or preserved (95% ETOH) fish. Nyman & Conover (1988) validated that daily increments are present in otolith microstructure, and we followed their methods of preparation. Sagittae were chosen randomly from YOY specimens of the large fishery collections. Eight of the total 51 sagittae prepared were determined to be yearling fish and were excluded from further analysis. Daily sagittal increments were counted independently three times, and a mean count was considered valid if the range was <10% of the mean count. If the range was greater (11% of the time), then a fourth count was made and the outlier was discarded.

Manuscript accepted 22 January 1993.
Fishery Bulletin, U.S. 91:389-395 (1993)

* Contribution 867 of the Marine Sciences Research Center, State University of New York at Stony Brook.

Table 1

Sources of bluefish *Pomatomus saltatrix* samples examined in this study. Size range is given as mmFL. Larger datasets (n>500) were used to compile length-frequency distributions, and some fish from 1987–88 were used for otolith analyses. Other samples ($n \leq 13$) were obtained specifically for otolith analyses.

Sampling location	*Gear (size & mesh)*	*Sampling period*	*Sample size*	Bluefish *Length range*	*Source**
N.C. estuaries Pamlico and Core Sounds	Otter trawls (3.2 & 6.1m headrope)	March–November 1979–90	547	21–320	NCDMF (Phalen & Stephan 1984)
N.C. estuaries Pamlico Sound Oliver's Reef	Pound-net fishery (Lead 150mm mesh, Tunnel 50mm mesh)	May–November 1982–85	4484	100–360**	NCDMF
N.C. coast Oregon—Beaufort Inlets 4.5–18.5m depths	Trawl fishery (27–33m headrope 400–1400mm wing mesh 50mm cod end mesh)	November–April 1982–85	4466	150–360**	NCDMF
S.C. coast Stono Inlet	Otter trawl (6.1m headrope)	2 November 1988	1	101	NCDMF
S.C. coast Breech Inlet	1×2m neuston net (2 mm mesh)	April–June 1988	9	39–68	SCWMRD
S.C. North Inlet (Town Creek)	Surface trawl	26 July 1988	13	101–123	USC
Nearshore continental shelf Capes Hatteras—Canaveral 4.9–9.1m depths	Falcon trawl (9.1m Mongoose type, 39–45mm stretch mesh)	May–November 1987–88	2276	80–360**	SEAMAP (Wenner 1989)

* Most data and specimens supplied by the N.C. Dep. Mar. Fish. (NCDMF); additional material from S.C. Wildl. Mar. Resour. Dep. (SCWMRD), Univ. South Carolina (USC) Belle Baruch Lab., and the Southeast Area Monitoring and Assessment Program (SEAMAP).

** Data from these sources were truncated at 360mmFL.

Mean ring count (= daily age) was subtracted from date of capture to estimate birthdate, assuming no lag between birthdate and date of first ring deposition. Average growth rate was calculated as ([FL-2mm]/daily age); a 2mm constant represents the size-at-hatching (Deuel et al. 1966). Growth rate was also calculated using least-squares regression of FL on daily age.

Results

Evidence of spring-spawned juveniles Small bluefish (21–60mmFL) entered North Carolina estuaries in March and April (Fig. 1A). These fish were similar in size to spring-spawned bluefish collected by neuston nets on incoming tides at Breech Inlet (South Carolina) as early as 29 April 1988, and as late as 16 June 1988 (Table 2).

This spring-spawned cohort grew rapidly and recruited to the North Carolina pound-net fishery in July (Fig. 1B). These fish became progressively larger until the fishery ended in October. A July recruitment of spring-spawned fish was also evident in SEAMAP trawling (Fig. 1C).

Bluefish <175mmFL in July were YOY that had been spawned primarily in April (Table 2, Fig. 2). For example, a sample from 29 July 1987 had a mean birthdate of 19 April ± 13d (±1SD), and a sample for 26 July 1988 had a mean birthdate of 26 April ± 12d (Table 2). Bluefish observed in July, but >200mmFL, showed evidence of an overwinter growth mark on their otoliths. Very few specimens of 175–200mm were available for otolith analysis, which precluded a more precise separation of age from size modes. Bluefish juveniles were larger and older in August samples (Table 2). Spring-spawned YOY bluefish grew 1.2–1.9mm/d during this time-period (Fig. 3).

Evidence of summer-spawned juveniles Small bluefish (<150–170mmFL) appeared in North Carolina estuaries and in nearshore continental shelf waters of the SAB in October (Fig. 1). Small bluefish (<150mm) collected near Bogue and Stono Inlets in October and November 1988 had a mid-July birthdate (Table 2,

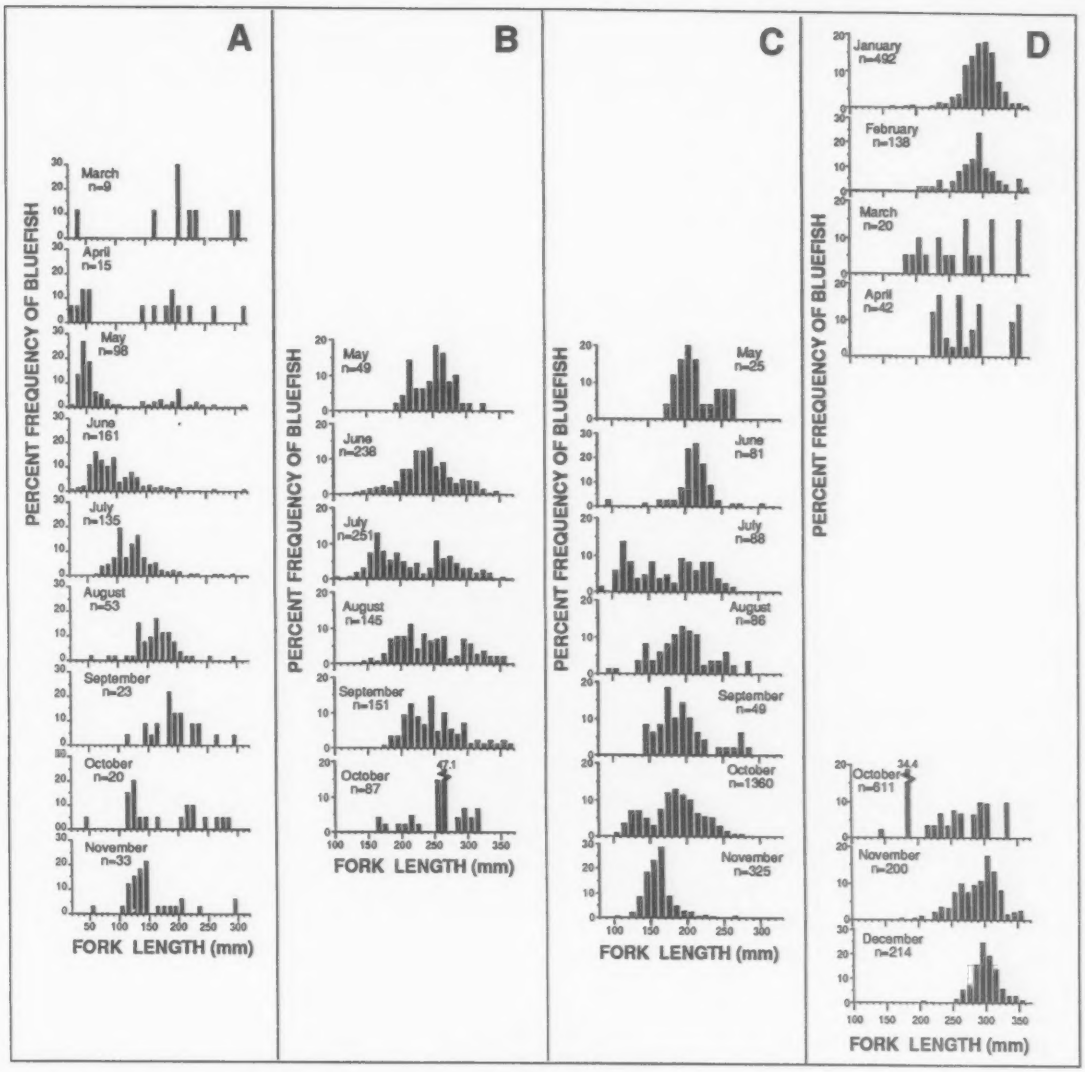

Figure 1

Length-frequency histograms of bluefish *Pomatomus saltatrix* <360mmFL for **(A)** monthly data pooled over the years 1979–90 from a N.C. Dep. Mar. Fish. trawl survey; **(B)** 1984 monthly data from the N.C. summer estuarine pound-net fishery; **(C)** 1988 monthly data from the SEAMAP nearshore trawl survey between N.C. and Florida; and **(D)** 1984–85 monthly data from the N.C. winter oceanic trawl fishery. Years plotted for the last three data sets are representative of data from other years. Ordinates are either 20 or 30%.

Fig. 2). These summer-spawned fish appeared to reach a size similar to that of spring-spawned fish at a common age (Fig. 3), but because they were spawned 2mo later (on average), they were smaller on common sampling dates (Fig. 1A,B,C).

Evidence of fall-spawned juveniles Winter trawl collections did not contain small juveniles between October and January, despite the expectation of an additional length-mode representing fall-spawned fish (Fig. 1D). There was very little evidence of fall-spawned fish in any of the length-frequency data, except possibly two fish (~40–60mmFL) collected in October and November in North Carolina estuaries (Fig. 1A). Based on otolith ageing, a single specimen collected in August was determined to be 206d old (i.e., with a corresponding birthdate of 9 January) which was unique in relation to all other estimated birthdates in this study

Table 2

Descriptive statistics for 43 aged specimens of juvenile bluefish *Pomatomus saltatrix* collected in North and South Carolina (NC and SC). Fork length (mmFL), age (d), and growth rate (GR; mm/d) are given as means. One standard deviation (SD) is provided where more than one specimen was measured.

Collection date	Location	Mean FL	SD	Mean Age	SD	Mean GR	SD	n
			1987					
15 Jun	Pamlico Sound NC	75		74.0		0.986		1
29 Jul	Pamlico River NC	119.6	14.5	101.3	13.1	1.169	0.134	5
13 Aug	Pamlico Sound NC	208		142.0		1.456		1
17 Aug	Pamlico Sound NC	192		125.3		1.516		1
			1988					
29 Apr	Breech Inlet SC	50.7	3.05	62.4	1.21	0.779	1.147	3
17 May	Breech Inlet SC	40		51.3		0.740		1
16 Jun	Breech Inlet SC	57.8	11.9	51.4	7.53	1.079	0.128	5
26 Jul	North Inlet SC	112.7	6.74	91.8	12.0	1.216	0.102	10
2 Aug	Pamlico Sound NC	159.5	37.0	143.6	8.94	1.088	0.206	4
2 Aug	Pamlico Sound NC	220		206		1.058		1
25 Oct	Bogue Inlet NC	118.2	31.3	103.2	12.3	1.128	0.064	10
2 Nov	Stono Inlet SC	101		110.0		0.900		1

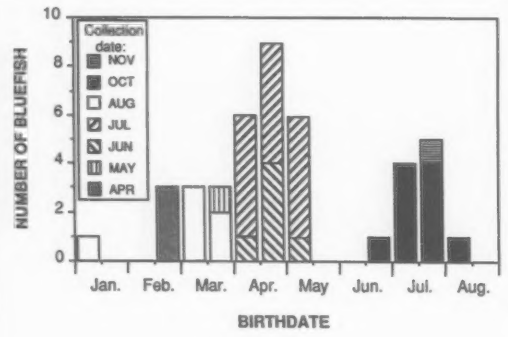

Figure 2

Back-calculated birthdate for 43 YOY bluefish *Pomatomus saltatrix* examined in this study. Date of collection is also shown by month.

(Table 2, Fig. 2) and may have been produced at the tail end of the "fall-spawning" period.

Discussion

Spring-spawned YOY bluefish This cohort recruited to the estuaries of North and South Carolina as early as April and as young as 40d old, and continued to ingress as late as mid-June. Spring-spawned bluefish grew rapidly and appeared in the North Carolina pound-net fishery and in trawls over the nearshore continental shelf in July. Spring-spawned bluefish arrived in SAB estuaries at about the same age (i.e., 40–60d old) but at an earlier first date of estuarine recruitment than in northern estuaries such as New York and New Jersey. Spring-spawned bluefish arrive to the New York Bight no earlier than late May and approximately 60d after hatching (Nyman & Conover 1988, McBride & Conover 1991).

Our findings support Collins & Stender's (1987) hypothesis that at least some spring-spawned YOY bluefish are transported directly inshore and enter estuaries south of Cape Fear. Combined with previous evidence of dispersal north of Cape Hatteras (Nyman & Conover 1988, McBride & Conover 1991), spring-spawned bluefish appear to recruit to estuaries within a broad geographic region encompassing both the SAB and the MAB.

Summer-spawned YOY bluefish This cohort also appeared in estuaries and in nearshore habitats within the SAB. Summer-spawned fish arrived in October at ~100–150mmFL and were generally older than 100d. The presence of these summer-spawned fish in the SAB demonstrates that this cohort migrates from their MAB spawning/nursery grounds into the SAB in the fall. Lund and Maltezos (1970) demonstrated that YOY bluefish tagged in New York migrated to the SAB, but these tagged fish were the larger spring-spawned fish.

Fall-spawned YOY bluefish This cohort was not clearly observed in length-frequency data and, at most,

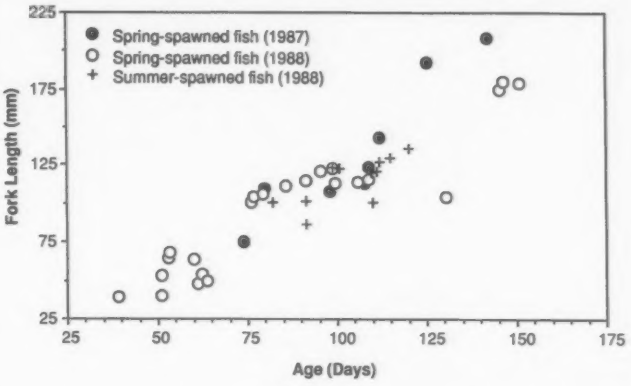

Figure 3

Fork length (FL) as related to daily age of bluefish *Pomatomus saltatrix*, based on samples collected near inlets and within estuaries. Linear regression equations for spring-spawned YOY bluefish were FL= -62.8+1.86(Age) [r^2=0.85] for 1987, and FL= -6.67+1.20(Age) [r^2=0.87] for 1988.

one specimen appeared in our otolith analysis. The winter data used in our study may be inappropriate for sampling fall-spawned bluefish because the trawl fishery uses a large mesh size and fishes in deep water (Table 1). Presumptive fall-spawned YOY fish were uncommon in previous surveys between North Carolina and Florida (Table 3). Wenner & Sedberry (1989) speculated that they had collected fall-spawned fish during January and May trawl collections in nearshore habitat of the SAB, but their interpretation may have been confounded by use of age-length relationships from Wilk (1977). Wilk's growth estimates do not account for intercohort differences in size-at-first-annulus or in growth rates (Lassiter 1962, McBride & Conover 1991). Future analysis of age structure of young bluefish in the SAB should focus on this cohort.

Implications for relative contribution of each cohort We observed polymodal length distributions that represented the size difference between spring- and summer-spawned YOY bluefish cohorts during the fall. Barger (1990) reported that bluefish collected in the SAB had a backcalculated mean FL at Annulus-I of 290mm. This size matches the mean FL at Annulus-I reported for spring-spawned fish from North Carolina in the late 1950s (Lassiter 1962). This observation supports the conclusion that the spring-spawned cohort is of dominant abundance relative to the other cohorts, as interpreted by Chiarella & Conover (1990).

Table 3

Total number of young-of-the-year bluefish *Pomatomus saltatrix* collected in various seining studies from North Carolina to Florida. Number of bluefish is given by month, "Years" refers to the duration of each study, and size range is given in parentheses as mmFL (either as reported or as converted using regressions from McBride 1989). Asterisk indicates that length-frequencies were given as 5mm class-intervals. nd = no data. Sampling frequency ranged from biweekly to bimonthly; seine sizes 12.2–21.3m in length. References: (1) Tagatz & Dudley 1961, (2) Anderson et al. 1977, (3) Cupka 1972, (4) Miller & Jorgenson 1969, (5) Futch & Dwinell 1977.

Location (Ref.)	Jan	Feb	Mar	Apr	May	Jun	Jul	Aug	Sep	Oct	Nov	Dec	Years
Beaufort NC (1)	0	0	0	0	1	0	1	0	0	7	12	0	1957–60
Ocean Beach					(46)		(100)			(65–79)	(40–55)		
Beaufort NC (1)	0	0	0	0	0	0	1	0	0	0	0	0	1957–60
Salt Marsh							(136)						
Beaufort NC (1)	0	0	1	0	4	1	1	0	0	0	0	0	1957–60
River			(120)		(66–77)	(86)	(123)						
Folly Beach SC (2)	0	0	0	0	0	1	1	0	0	0	0	0	1969–71
Ocean Beach						(104)	(137)						
Murrells Inlet—	0	0	0	0	0	44	0	0	0	0	0	0	1971
Edisto beaches SC (3)						(69–124)							
St. Simons I. GA	0	3	2	1	7	9	6	3	0	2	0	0	1953–61
Ocean Beach (4)*		(66–85)	(96–125)	(46–50)	(36–90)	(36–95)	(46–70)	(96–125)		(51–60)			
Hutchinson I. FL	2	nd	0	nd	4	nd	3	nd	0	nd	2	nd	1971–73
Ocean Beach (5)	(325–366)				(273–317)		(42–51)				(70–367)		

Fall-spawned fish are the least represented cohort among juveniles and are known mostly from larval surveys (e.g., Kendall & Walford 1979, Collins & Stender 1987). Collins & Stender (1987) reported bluefish larvae <4mm in the SAB to be more abundant in the spring compared with the fall. Other estuarine surveys have collected small bluefish (<100mm) from October–March in the SAB (Table 3) which strongly suggests that at least some fall-spawned fish do recruit to estuaries.

We suggest that the fall-spawned cohort contributes the least, the summer-spawned cohort contributes somewhat more, and the spring-spawned cohort contributes the most to the Atlantic coast bluefish population, at least in recent years. It is not clear why such differences in abundance among cohorts occur nor for how long such differences persist. The spring-spawned cohort may be more abundant because it is spawned at a place and time enabling invasion of estuaries within the SAB, as well as to estuaries as far north as Maine (Targett & McCleave 1974). The fall-spawned cohort may be less abundant, on average, as it is likely to experience colder temperatures and lower food supplies relative to the other cohorts.

Estuaries of the MAB may be more important as nursery grounds for bluefish than are those of the SAB. Summer abundances of spring- and summer-spawned YOY bluefish in New York Bight estuaries are apparently much higher (0.2–6.3 fish/30m seine haul; McBride & Conover 1991) than in the SAB, based on small numbers of bluefish collected during year-long studies in the south (Table 3). Rountree & Able (1992) also found YOY bluefish to be very common (sixth most abundant fish of 63 spp.) in New Jersey marsh creeks, in contrast to much lower relative abundances in similar polyhaline creeks in the SAB (e.g., Cain & Dean 1976). The wide latitudinal distribution and movements of young bluefish, within and between the Middle and South Atlantic Bights, demonstrate the need to monitor and manage bluefish on a large geographic scale (i.e., nearly the entire U.S. Atlantic coast).

Acknowledgments

We thank E. Day, P. Kenny, V. Ogburn-Matthews, and B. Stender for their help in collecting samples and arranging collecting trips in South Carolina. J. Hare, W. Morse, and R. Rountree offered helpful suggestions on the manuscript. This project was partially funded by grants to D.O.C. from the Office of Sea Grant, National Oceanic and Atmospheric Administration, under grant NA86AA-D-SG045 to the New York Sea Grant Institute and from the New York State Department of Environmental Conservation.

Citations

Anderson, W. D. Jr., J. K. Dias, R. K. Dias, D. M. Cupka, & N. A. Chamberlain
1977 The macrofauna of the surf zone off Folly Beach, South Carolina. U.S. Fish. Wildl. Serv., Spec. Sci. Rep. Fish., 23 p.

Baird, S. F.
1873 Natural history of some of the more important food fishes of the south shore of New England. Rep. U.S. Comm. Fish Fish. for 1871–1872, p. 228–252.

Barger, L. E.
1990 Age and growth of bluefish, *Pomatomus saltatrix*, from the northern Gulf of Mexico and U.S. South Atlantic coast. Fish. Bull., U.S. 88:805–810.

Bigelow, H. B., & W. C. Schroeder
1953 Fishes of the Gulf of Maine. U.S. Fish. Wildl. Serv., Fish. Bull. U.S. 53:383–389.

Briggs, J. C.
1960 Fishes of worldwide (Circumtropical) distribution. Copeia 1960(3):171–180.

Cain, R. L., & J. M. Dean
1976 Annual occurrence, abundance and diversity of fish in a South Carolina intertidal creek. Mar. Biol. (Berl.) 36:369–379.

Chiarella, L. A., and D. O. Conover
1990 Spawning season and first-year growth of adult bluefish from the New York Bight. Trans. Am. Fish. Soc. 119:455–462.

Collins, M. R., & B. W. Stender
1987 Larval king mackerel (*Scomberomorus cavalla*), Spanish mackerel (*S. maculatus*), and bluefish (*Pomatomus saltatrix*) off the southeast coast of the United States, 1973–1980. Bull. Mar. Sci. 41:822–834.

Cupka, D. M.
1972 A survey of the ichthyofauna of the surf zone in South Carolina. Tech. Rep. 4, S.C. Wildl. Mar. Resour. Dep., Charleston.

Deuel, D. G., J. R. Clark, & A. J. Mansuetti
1966 Description of embryonic and early larval stages of bluefish, *Pomatomus saltatrix*. Trans. Am. Fish. Soc. 95:264–271.

Fable, W. A. Jr., H. A. Brusher, L. Trent, & J. Finnegan Jr.
1981 Possible temperature effects on charter boat catches of king mackerel and other coastal pelagic species in Northwest Florida. Mar. Fish. Rev. 43(8):21–26.

Futch, C. R., & S. E. Dwinell
1977 Nearshore marine ecology at Hutchinson Island, Florida: 1971–1974. IV. Lancelets and fishes. Fla. Mar. Res. Publ. 24, 23 p.

Gilmore, J. J.
1985 Oceanic distribution, abundance and migration of bluefish (*Pomatomus saltatrix*) along the east coast of the United States. M.S. thesis, State Univ. New York, Stony Brook, 60 p.

Kendall, A. W. Jr., & L. A. Walford
1979 Sources and distribution of bluefish, *Pomatomus saltatrix*, larvae and juveniles off the east coast of the United States. Fish. Bull., U.S. 77:213–227.

Lassiter, R. R.
1962 Life history aspects of the bluefish, *Pomatomus saltatrix* (Linnaeus), from the coast of North Carolina. M.S. thesis, N. Carolina State Coll., Raleigh, 103 p.

Lenanton, R. C. J., & I. C. Potter
1987 Contribution of estuaries to commercial fisheries in temperate western Australia and the concept of estuarine dependence. Estuaries 10(1):28–35.

Lund, W. A., & G. C. Maltezos
1970 Movements and migrations of the bluefish, *Pomatomus saltatrix*, tagged in waters of New York and southern New England. Trans. Am. Fish. Soc. 99:719–725.

McBride, R. S.
1989 Comparative growth and abundance of spring- versus summer-spawned young-of-year bluefish, *Pomatomus saltatrix*, recruiting to the New York Bight. M.S. thesis, State Univ. New York, Stony Brook, 92 p.

McBride, R. S., & D. O. Conover
1991 Recruitment of young-of-the-year bluefish (*Pomatomus saltatrix*) to the New York Bight: Variation in abundance and growth of spring and summer-spawned cohorts. Mar. Ecol. Prog. Ser. 78:205–216.

Miller, G. L., & S. C. Jorgenson
1969 Seasonal abundance and length frequency distribution of some marine fishes in coastal Georgia. Data Rep. 35, U.S. Fish Wildl. Serv., 103 p. [microfiche].

NMFS (National Marine Fisheries Service)
1987 Status of the fishery resources off the northeastern United States for 1987. NOAA Tech. Memo. NMFS-F/NEC-50, NMFS Northeast Fish. Sci. Cent., Woods Hole MA.
1988 Status of the fishery resources off the northeastern United States for 1988. NOAA Tech. Memo. NMFS-F/NEC-63, NMFS Northeast Fish. Sci. Cent., Woods Hole MA.

Norcross, J. J., S. L. Richardson, W. H. Massmann & E. B. Joseph
1974 Development of young bluefish (*Pomatomus saltatrix*) and distribution of eggs and young in Virginian coastal waters. Trans. Am. Fish. Soc. 103:477–497.

Nyman, R. M., & D. O. Conover
1988 The relation between spawning season and the recruitment of young-of-the-year bluefish, *Pomatomus saltatrix*, to New York. Fish. Bull., U.S. 66:237–250.

Phalen, P. S., & D. C. Stephan
1989 North Carolina marine fisheries trawl surveys. *In* Azarovitz, T.R., J. McGurrin, & R. Seagraves (eds.), Proceedings of a workshop on bottom trawl surveys, p. 59–62. Spec. Rep. 17, Atl. States Mar. Fish. Comm.

Pollock, B. R.
1984 The tailor (*Pomatomus saltatrix*) fishery at Fraser Island and its relation to the life-history of the fish. Proc. R. Soc. Queensl. 95:23–28.

Powles, H.
1981 Distribution and movements of neustonic young of estuarine dependent (*Mugil* spp., *Pomatomus saltatrix*) and estuarine independent (*Coryphaena* spp.) fishes off the southeastern United States. Rapp. P.-V. Reun. Cons. int. Explor. Mer 178:207–209.

Richards, C. E.
1965 Availability patterns of marine fishes caught by charter boats operating off Virginia's Eastern Shore, 1955–1962. Chesapeake Sci. 6(2):96–108.

Rountree, R. A., & K. W. Able
1992 Fauna of high salinity subtidal marsh creeks in southern New Jersey: composition, abundance and biomass. Estuaries 15(2):171–185.

Tagatz, M. E., & D. L. Dudley
1961 Seasonal occurrence of marine fishes in four shore habitats near Beaufort, N.C., 1957–60. U.S. Fish Wildl. Serv., Spec. Sci. Rep. Fish. 390, 19 p.

Targett, T. E., & J. D. McCleave
1974 Summer abundance of fishes in a Maine tidal cove with special reference to temperature. Trans. Am. Fish. Soc. 103:325–330.

van der Elst, R.
1976 Game fish of the east coast of southern Africa. I. The biology of the elf, *Pomatomus saltatrix* (Linnaeus), in the coastal waters of Natal. Invest. Rep. 44, Oceanogr. Res. Inst., S. Afr.

Wenner, C. A., & G. R. Sedberry
1989 Species composition, distribution, and relative abundance of fishes in the coastal habitat off the southeastern United States. NOAA Tech. Rep. NMFS 79, 49 p.

Wenner, E.
1989 Southeast Area Monitoring and Assessment Program (SEAMAP). *In* Azarovitz, T. R., J. McGurrin, & R. Seagraves (eds.), Proceedings of a workshop on bottom trawl surveys, p. 23–26. Spec. Rep. 17, Atl. States Mar. Fish. Comm.

Wilk, S. J.
1977 Biological and fisheries data on bluefish *Pomatomus saltatrix* (Linnaeus). Tech. Ser. Rep. 11, Sandy Hook Lab., NMFS Northeast Fish. Sci. Cent., Highlands NJ, 56 p.

Superintendent of Documents **Subscriptions** Order Form

Order Processing Code:
*

S3

Charge your order. It's Easy!

To fax your orders (202) 512–2233

☐ **YES,** enter my subscription(s) as follows:

____ subscriptions to **FISHERY BULLETIN (FB)** for $24.00 per year ($30.00 foreign).

The total cost of my order is $_____. Prices include regular domestic postage and handling and are subject to change.

_____
(Company or Personal Name) (Please type or print)

_____
(Additional address/attention line)

_____
(Street address)

_____
(City, State, ZIP Code)

_____
(Daytime phone including area code)

_____
(Purchase Order No.)

For privacy protection, check the box below:

☐ Do not make my name available to other mailers

Please choose method of payment:

☐ Check Payable to the Superintendent of Documents

☐ GPO Deposit Account ☐☐☐☐☐☐ – ☐

☐ VISA or MasterCard Account

☐☐☐☐☐☐☐☐☐☐☐☐☐☐☐☐

☐☐☐☐ (Credit card expiration date)

Thank you for your order!

_____
(Authorizing Signature)

Mail To: Superintendent of Documents
P.O. Box 371954, Pittsburgh, PA 15250–7954

The National Marine Fisheries Service (NMFS) does not approve, recommend or endorse any proprietary product or proprietary material mentioned in this publication. No reference shall be made to NMFS, or to this publication furnished by NMFS, in any advertising or sales promotion which would indicate or imply that NMFS approves, recommends or endorses any proprietary product or proprietary material mentioned herein, or which has as its purpose an intent to cause directly or indirectly the advertised product to be used or purchased because of this NMFS publication.

Fishery Bulletin

Guidelines for Contributors

Form of manuscript

The document should be in the following sequence: Title Page, Abstract (not required for Note), Text, Acknowledgments, Citations, Text footnotes, Appendices, Tables, Figure legends, and Figures.

Title page should include authors' full names and mailing addresses and the senior author's telephone and FAX numbers.

Abstract Not to exceed one double-spaced typed page. Should include a sentence or two explaining to the general reader why the research was undertaken and why the results should be viewed as important. Abstract should convey the main point of the paper and outline the results or conclusions. No footnotes or references.

Text A brief introduction should portray the broad significance of the paper. The entire text should be intelligible to readers from different disciplines. All technical terms should be defined, as well as all abbreviations, acronyms, and symbols in text, equations, or formulae. Abbreviate units of measure only when used with numerals or in tables and figures to conserve space. Measurements should be expressed in metric units, with other equivalent units given in parentheses. Follow the *U.S. Government Printing Office Style Manual*, 1984 ed., and the *CBE Style Manual*, 5th ed. Fishery and invertebrate nomenclature should follow the *American Fisheries Society Special Publication 12* (for fishes), *16* (for mollusks), and *17* (for decapod crustaceans).

Text footnotes should be numbered in Arabic numerals and typed on a separate sheet from the text. Footnotes are not used for reference material or personal communications, but rather to explain or define terms in the text and for contribution numbers on the title page.

Informal sources Personal communications, unpublished data, and untitled manuscripts in preparation are noted parenthetically in the text (full name, affiliation, brief address including zip code, and month and year when appropriate).

Acknowledgments Gather all acknowledgments into a brief statement at the end of the text. Give credit only for exceptional contributions and not to those whose contributions are part of their normal duties.

Citations All titled sources should be listed in the Citations section, including unpublished and processed material. In text, cite as Smith and Jones (1977) or (Smith and Jones 1977); if more than one citation, list chronologically (Smith 1936, Jones 1975, Doe In press). All sources cited in the text should be listed alphabetically by the senior authors' surnames under the heading CITATIONS. Abbreviations of periodicals and serials should conform to *Serial Sources for the BIOSIS Data Base™*. Indicate whether sources are in a language other than English. For informal literature, include address of author or publisher. Authors are responsible for the accuracy of all citations.

Tables should supplement, not duplicate, the text. Each table should be numbered and cited consecutively, with headings short but amply descriptive so that the reader need not refer to the text. For values less than one, zeros should precede all decimal points. Indicate units of measure in column headings; do not deviate from the unit of measure within a column. Table footnotes should be noted consecutively in Roman letters across the page from left to right and then down. Since all tables are typeset, they need not be submitted camera-ready.

Figures Photographs and line drawings should be of professional quality—clear and concise—and reducible to 42 picas for full-page width or to 20 picas for a single-column width, and to a maximum 55 picas high. All graphic elements in illustrations must be proportioned to insure legibility when reduced to fit the page format. Line weight and lettering should be sharp and even. Lettering should be upper and lower case, and vertical lettering should be avoided whenever possible (except for vertical, y, axis). Zeros should precede all decimal points for values less than one. Reproductions of line artwork are accepted in the form of high-quality photographic prints from negatives or photomechanical transfer (PMT). Halftones should be sharply focused with good contrast. Micron rules should be inserted on electron micrographs, even when magnification is included in the figure legend. There should be clear distinction between identifying letters (press-on or overlay) and background of photograph. Label each figure in pencil on the back. Send only xerox copies of figures to the Scientific Editor; originals or photographic prints will be requested later when the manuscript is accepted for publication.

Copyright Government publications are in the public domain, i.e., they are not protected by copyright.

Submission of manuscript

Disks Authors are encouraged to retain manuscripts on word-processing storage media (diskettes, floppy disks) and submit a double-spaced hardcopy run from the storage media. Submit disks as MS-DOS "print" or "nondocument" files (often called "ASCII files"). If a disk cannot be converted to an ASCII file, the author should indicate on the disk the source computer and software language along with the file name. Either 5¼-inch or 3½-inch disks from IBM-compatible or Apple/MacIntosh systems (non-graphics only) can be submitted, double-sided/double-density or high-density, limiting each file to 300 kilobytes. All 8-inch word-processing disks (e.g., Wang or NBI) must be converted onto 5¼- or 3½-inch MS-DOS print disks.

Send original hardcopy and two duplicated copies to:

Dr. Ronald W. Hardy, Scientific Editor
Northwest Fisheries Science Center
National Marine Fisheries Service, NOAA
2725 Montlake Boulevard East
Seattle, WA 98112-2097

Copies of published articles and notes The senior author and his/her organization each receive 50 separates free-of-charge. Additional copies may be purchased in lots of 100.